POLITECNICO DI TORINO
Repository ISTITUZIONALE

A LIGHTWEIGHT THERMAL MODELLING APPROACH FOR EMBEDDING WATER QUALITY IN MULTI-OBJECTIVE RESERVOIR OPERATION

Original
A LIGHTWEIGHT THERMAL MODELLING APPROACH FOR EMBEDDING WATER QUALITY IN MULTI-OBJECTIVE RESERVOIR OPERATION / Alfano, M.E., Zaniolo, M., Bosio, R., Savoldi, L., Poggi, D.. - 16:(2026), pp. 343-346. (16th International Symposium on Ecohydraulics Ecole Polytechnique Federale De Lausanne (EPFL), Lausanne, Switzerland June 14 to 18, 2026) [10.64697/iahr.proc.ise2026.abs].

Availability:
This version is available at: 11583/3016048 since: 2026-09-29T08:15:02Z

Publisher:
IAHR

Published
DOI:10.64697/iahr.proc.ise2026.abs

Terms of use:

This article is made available under terms and conditions as specified in the corresponding bibliographic description in the repository

Publisher copyright

(Article begins on next page)

28 November 2026

Book of abstracts:

XVI INTERNATIONAL SYMPOSIUM ON ECOHYDRAULICS

Challenges and solutions in the time of global changes

Lausanne, Switzerland, 16-20 August 2026

Editors: Paolo Perona, Azin Amini, Giulio Calvani, Giovanni De Cesare & Christophe Reymond



iahr.org



Book of Abstracts 16th International Symposium on Ecohydraulics
Challenges and solutions in the time of global changes
August 16–20, 2026
Hosted by: Ecole Polytechnique Federale De Lausanne (EPFL), Lausanne, Switzerland
Website: ise2026.epfl.ch
Cover photo: Credits to Lausanne Tourism Office @LT/Régis Colombo

EDITORS

Paolo Perona, *EPFL, Switzerland*
Azin Amini, *EPFL, Switzerland*
Giulio Calvani, *EPFL, Switzerland*
Giovanni De Cesare, *EPFL, Switzerland*
Christophe Reymond, *EPFL, Switzerland*

PUBLISHED BY

© 2026 IAHR. CC BY-NC-ND 4.0
ISBN 978-90-837233-9-6
ISSN 2790-2420
DOI [10.64697/iahr.proc.ise2026.abs]

*Typeset by **LODE Publishing** in LaTeX.*

Martina Marín Dobrincic, *IAHR Publications & Knowledge Products Manager*
martina.marin@iahr.org

The International Association for Hydro-Environment Engineering and Research (IAHR), founded in 1935, is a worldwide independent organisation of engineers and water specialists working in fields related to the hydro-environmental sciences and their practical application.
Hosted by Federal Polytechnical School of Lausanne, Switzerland.

IAHR Madrid Office
Paseo Bajo Virgen del Puerto 3, 28005, Madrid, SPAIN
Tel: +34 913357908

IAHR Beijing Office
A-1 Fuxing Road, Haidian District, 100038, Beijing, CHINA
Tel: +86 1068781128

Prologue

Dear colleagues, dear friends,

Welcome to the IAHR XVI International Symposium on Ecohydraulics, ISE 2026, Welcome to Lausanne and EPFL!

Ecohydraulics has been the inspiration engine of science and practice and related research has produced unprecedented results linking hydraulics, biological and ecological processes. The intimacy of such links also appears in processes of everyday life, but only careful eyes capture their evidence and importance for the people and the planet. In recognising and studying them, ecohydraulic scientists mimic the art of poets in embedding the essential!

New understanding of ecohydraulic processes also profoundly changed engineering and water management approaches of river streams and riparian corridor dynamics. Ecohydraulics has also inspired bio- and eco-morphodynamics thus favouring stream restoration and rehabilitation to be on main international political agendas. This achievement would have been unconceivable without cornerstone results of ecohydraulic research.

Thirty-two years after its first edition in Trondheim, the International Symposium on Ecohydraulics will for the first time reach Switzerland, the so-called “water-tower of Europe”, Lausanne and EPFL, in particular!

Thanks to your commitment and participation, the conference on Ecohydraulics will explore cutting-edge developments in the field—with contributions from wet, semiarid and arid regions targeting either perennial or ephemeral streams. By this means, the Symposium will also emphasise sustainable and nature-based solutions for aquatic ecosystems in the light of global changes. Session A will highlight innovations in experimental, numerical, and theoretical approaches, enhancing our scientific fundamental understanding of ecohydraulic processes. Session B introduces a novel, interdisciplinary perspective for future interactions and collaborations by integrating social, architectural, and engineering aspects to address the societal challenges posed by environmental change. Sessions C and D will focus on practical applications of ecohydraulics in inland and coastal water systems, respectively, showcasing sustainable management strategies that balance ecological integrity with human needs. Advances in monitoring techniques (Session E) will be discussed to improve data collection and decision-making for resilient water systems. Finally, the Swiss Ecohydraulics Day (Session F) will provide a platform for regional expertise and collaboration. By bridging science, practice, and society, the conference will foster sustainable ecohydraulic solutions that ensure the long-term health of aquatic environments worldwide.

The Symposium will offer master classes and workshops, scientific excursions to field sites and the city, social events as well as an exclusive Diversity, Equity and Inclusion session. Several awards will also be assigned, including the career award to a highly celebrated and renowned scientist in the field.

While acknowledging the invaluable help of the Scientific Committee as well as the financial support of sponsors, exhibitors and EPFL, we truly hope you’ll enjoy the Symposium of which this collection of extended abstracts represents your precious work and commitment to ecohydraulics over the years.

Thank you and wish you all a very nice conference!

The ISE 2026 Organizing Committee

Conference Themes

Session A — Fundamental Ecohydraulics

- A1: Interactions between flow, natural elements, and structures
- A2: Organism-flow interactions — movement, transport, and sensing
- A3: Ecomorphodynamics — linking flow, sediment, and biota instabilities
- A4: Ecohydraulics across space and time — from habitats to catchments
- A5: Global change impact — biogeochemical cycles, biodiversity loss

Session B — Interdisciplinary Perspectives

- B1: Urban, suburban, and periurban streams
- B3: Ecohydraulics meets landscape architecture
- B4: Governance, socio-environmental benefits, and areas of conflict

Session C — Inland Water Applications

- C1: Peaking regimes and environmental flows
- C2: Fish passage — design, modelling, and assessment
- C3: Bioengineering approaches and nature-based solutions (rivers)
- C4: Sediment transport and connectivity
- C5: Ecohydraulics of the hyporheic zone

Session D — Coastal Applications

- D1: Impact and mitigation measures of coastal structures
- D3: Bioengineering approaches and nature-based solutions (coastal)

Session E — Monitoring and Data

- E1: Remote sensing
- E2: Real-time monitoring
- E3: AI approaches

Session F — Swiss Ecohydraulics Day

Poster Session

Local Organising Committee

Prof. Dr. Eng. Paolo Perona
PL-LCH, EPFL

Dr. Eng. Giovanni De Cesare
PL-LCH, EPFL

Dr. Eng. Azin Amini
PL-LCH, EPFL

Dr. Eng. Giulio Calvani
PL-LCH, EPFL

Dr. Hannes Peter
RIVER, EPFL

Prof. Sara Bonetti
CHANGE, EPFL

Prof. Mirko Musa
STREEM, EPFL

Dr. Luiz G. M. Silva
IfU, ETH Zurich

Dr. David Vetsch
VAW, ETH Zurich

Administrative Team: Séverine Sudre, Christophe Reymond

Peer Review

All submissions were peer-reviewed by at least two members of the Scientific Committee. The review process was single-blind.

Scientific Committee

Alp Maria
INRAE Lyon

Ana Margarida Bento
CIIMAR, Porto

Angeloudis Athanasios
University of Edinburgh

Arborino Tony
Independent

Asaeda Takashi
Saitama University, Japan

Bätz Nico
EAWAG (EPFL)

Baki Abul Basar
Clarkson University, USA

Bertuzzo Enrico
University of Venice

Binh Doan Van
Vietnamese-German University

Boavida Isabel
Técnico Lisbon

Boes Robert
ETH Zurich

Cotel Aline
University of Michigan, USA

Czuba Jonathan
Virginia Tech

D'Alpaos Andrea
University of Padua

Dolores Bejarano Maria
Universidad Politécnica de Madrid

Edmaier Katharina
FOEN

Fink Sabine
WSL

Follet Elizabeth
Cardiff University

Franca Mario
KIT

Franklin Paul
NIWA, New Zealand

Gitai Ben
EPFL

Gouraud Véronique
Hydro-ecology, EdF France

Gorla Lorenzo
FOEN

Guala Michele
University of Minnesota

Habit Evelyn
University of Concepcion, Chile

Hauer Christoph
BOKU, Vienna

Hoerner Stefan
Grenoble INP

Hondzo Miki
University of Minnesota

Kantoush Sameh
Kyoto University

Karimpour Shooka
York University

Lamouroux Nicolas
INRAE, Lyon

Manes Costantino
Politecnico di Torino

Mathers Kate
Loughborough University

Martinez-Capel Francesco
Univ. Politécnica de València

Matson Paul
OAK Ridge Laboratories

McLelland Stuart
University of Hull

Molnar Peter
ETH Zurich

Mossa Michele
Politecnico di Bari

Muñoz-Mas Rafael
Institute of Aquatic Ecology, Univ. Girona

Semadeni Nadia
Abteilung Umwelt AXPO

Nepf Heidi
MIT

Ouellet Val
Atlantic Salmon Federation

Pasternack Gregory
University of California, Davis

Piégay Hervé
University of Lyon

Piton Guillaume
Univ. Grenoble Alpes, INRAE

Rey Freddy
Univ. Grenoble Alpes, INRAE

Ruiz-Villanueva Virginia
Uni Bern

San Juan Blanco Jorge
NC State University

Sangalli Paola
EFIB

Santos Hersília
CEFET-MG, Brazil

Schwindt Sebastian

Selz Oliver
FOEN

Schalko Isabella
WSL

Sukhodolov Alexander
IGB Berlin

Temmerman Stijn
Univ. of Antwerp

Termini Donatella
University of Palermo

Tinoco Raphael
University of Illinois

Tonina Daniele
University of Idaho

Tseng Chien-Yung
CSU

Tuhtan Jeffrey
Tallinn University of Technology

Uijttewaal Wim
TU Delft

Vanzo Davide
Karlsruhe Institute of Technology

Vargas Luna Andrés
Universitat Pontificia Javieriana

Vettori Davide
Politecnico di Torino

Vezza Paolo
Politecnico di Torino

Vigano Paola
EPFL

Weber Christine
EAWAG

White Daniel
CSU

Yang Judi
University of Minnesota

Zolezzi Guido
University of Trento

Keynote Speakers



Christine Weber

Eawag, Swiss Federal Institute of Aquatic Science and Technology, Switzerland

Shifting a paradigm: From anecdotal to systematic learning in river restoration

Learning from doing is common in river restoration and is typically based on data or individual experiences gathered at the level of a single project. Project-level learning is flexible and efficient. However, insights are rarely published, synthesised, or compared across contexts, which leaves valuable knowledge isolated and underused. In contrast, a programmatic approach builds on systematic evidence gathered across multiple projects using standardised methods. Replication and cross-project comparison foster collaborative learning and strengthen evidence-based restoration.
In 2020, Switzerland implemented a programmatic monitoring and evaluation for river restoration at the national scale, with the aim to provide a sound evidence base to support the country's ambition to restore 5% (4,000 km) of its hydrographic network by 2090. In this plenary lecture, I will synthesise the lessons learned during the development phase (2015–2019) and the first five years of implementation to illustrate the opportunities and challenges of programmatic monitoring and evaluation at the national scale.



Elowyn Yager

Center for Ecohydraulics Research, Department of Civil and Environmental Engineering, University of Idaho, USA

Predicting seedling removal by the flow: the importance of sediment scour, plant structure, and bed grain size

Riparian vegetation impacts flow hydraulics, sediment transport, and resulting channel morphodynamics. These physical processes, in turn, affect the initial recruitment, stability, and fitness of individual plants, as well as the diversity of riparian ecosystems. Some of these complex feedback mechanisms between riparian vegetation and physical processes are included in 1D and 2D morphodynamic models. However, uncertainties remain on how to best capture these feedback mechanisms, particularly for flow and sediment scour induced removal of seedlings. This can be critical in river restoration projects, where planted seedlings are often used to increase bank strength, augment future channel shading, and restore native vegetation populations. We develop mechanistic predictive equations for seedling removal and identify controlling processes for removal that may need to be included in morphodynamic models and river restoration planning.



Guido Zolezzi

Department of Civil, Environmental and Mechanical Engineering,
University of Trento, Italy

Ecohydraulics and river morphodynamics: an expanding research interface

The early development of ecohydraulics focused on understanding how hydraulic conditions influence ecological and biological processes in aquatic systems, with channel morphology recognized as a fundamental control but generally treated as static. The keynote will explore the recent expansion of this interface between hydraulics and ecology towards sediment transport, river morphodynamics, and fluvial geomorphology, highlighting the emergence of a more integrated framework for understanding and managing riverine systems.
The talk will mainly refer to the classical topic of river habitat modelling, and how such habitat is structured and affected by morphodynamic processes at multiple scales, to highlight our present process understanding and unresolved gaps. It will discuss the role of different channel morphologies on habitat properties, and the possible effects of decadal-scale changes. In such respect, it will refer to the related interdisciplinary field of eco-morphodynamics, which focused on the trilateral interplay among flow, sediment transport and riparian vegetation dynamics in shaping fluvial landforms and related habitats. The talk will conclude by exploring possible integrations at relevant scales between (morpho)dynamic habitat modelling and river eco-morphodynamics, to discuss open directions on topics that have mainly received separate investigation efforts so far.



Gregory Pasternack

Department of Land, Air and Water Resources, University of California,
Davis, USA

Ecohydraulics Can Contribute to A More Equitable And Resilient Civilization

Ecohydraulics spans many research disciplines and applied problems but is best known for use on regulated rivers requiring instream flows and fish passage. In recent years, cities and their surrounding communities have been hit with more extreme flash floods, growing unhoused human populations living in streamside camps, new threats to water quality, and continued declines in riparian and aquatic species' populations. Classic river restoration concepts and engineering technologies are being added to with "low-tech" and "nature-based" methods. Socio-economic understand of coupled human-nature systems has also been growing. Now is the time for ecohydraulics to be incorporated into urban river management, but also for ecohydraulics to be changed by the needs arising from this new application and important developments regarding environmental justice. For example, how can ecohydraulic products be merged with those generated from socio-economic, flash-flood, water-quality, and sustainable-agriculture methods to obtain a systemic understanding of stream network functioning? Beginning in 2023, an interdisciplinary, transdisciplinary team has been conducting research and outreach about urban-stream ecohydraulics using the San Francisco Bay Area as a testbed. This 16,900 km^2 region with >8,000 km of streams supports >7 million people across >100 towns. It also is home to diverse anadromous fish, riparian plants, and wildlife. I will showcase how ecohydraulics has been used to address complex human-nature interactions, opening new future directions for our community.



Paola Vigano

EPFL, Lausanne, Switzerland

Water Designs

"Water designs" are of major importance today. The number of projects dealing with water-related issues is so pervasive that it plays the role of connector, among coalitions of different players, disciplines, performances and ways of thinking.
Water itself "designs", according to its rationalities, logics and behaviours. The water project is the one that shapes territories and living spaces over the longue durée. Water is the subject and the agent that we simply reveal, rediscover, accompany and follow, through design, with projects that listen to its voice and intentions.
Cities and territories are the "water laboratory" where to shape the socio-ecological transition and water, one of the many weak subjects of Modernity — modified, hidden, violated — is the pervasive 'weak structure', capable of organising the contemporary city-territory: beyond its heterogeneity, fragmentation and separation of spaces and function. Water is about life, space and power relations. "Water designs" is biopolitical.



Piotr Parasiewicz

Warsaw University of Life Sciences (SGGW), Poland; Rushing Rivers Institute, USA

From micro to macro: applying the principles of habitat modelling across the scales

Habitat models are built and validated at the scale of an individual organism, yet river management decisions are taken at the scale of reaches, basins and continents. This keynote asks what makes such scale-crossing legitimate. Ecological scale theory — grain and extent, nested hierarchies, orders of selection, riverscape connectivity and scale mismatch — frames upscaling as three distinct problems: spatial, biological and temporal. Each is illustrated with work spanning nine orders of magnitude: multiplex modelling for an endangered mussel in the Upper Delaware River; habitat-use guilds applied on the Niobrara, Ramganga and Polish rivers; conditional suitability criteria validated on bullhead; mesoscale hydraulic transfer on the Oder; and a Fish Community Macrohabitat Typology and Conceptual Habitat Alteration Model quantifying 203,100 km of altered free-flowing habitat across Europe. Temporal upscaling, the dimension most often skipped, is addressed through duration-and-frequency thresholds under a shifting baseline. Legitimate scale-crossing, it is argued, is a discipline of validation at every rung.



Roman Stocker

Department of Civil, Environmental and Geomatic Engineering, ETH Zurich, Switzerland

Movement behavior in ecohydraulics, from bacteria to fish

Movement behavior is a defining process in ecology, shaping how organisms find resources, avoid hazards, interact with one another, and ultimately shape ecosystems. I will explore how advances in single-organism imaging and tracking allow quantification of movement behavior in aquatic ecosystems across scales, from bacteria to fish. I will discuss recent results showing how bacteria can utilize rapid motility and exquisite chemical sensing to aggregate around and exploit ephemeral nutrient hotspots, thereby influencing carbon cycling, and how juvenile trout exposed to hydropeaking can swim to seek hydraulic shelter in low-velocity refugia. I will also briefly introduce the Riverine Organism Drift Imager (RODI), a minimally invasive field technology we have developed to couple imaging with artificial intelligence and thereby massively increase the throughput of sampling small aquatic organisms in the field, from invertebrates to fish larvae. These examples show how high-resolution measurements of movement and movement behavior can improve the understanding of ecohydraulic processes across scales and reveal mechanisms that are often invisible to population-scale approaches, yet critically shape transport, habitat use, survival, and ecosystem functioning.



Teresa Ferreira

School of Agriculture, University of Lisbon, Portugal

Ecohydraulics at the heart of river restoration in a changing world

Rivers worldwide are increasingly pressured by damming, channel alteration, sediment deficits, and the growing presence of in-stream infrastructures. These changes and increased human demands for water, are driving a progressive degradation of river habitats, ecological processes, and aquatic communities. In response, major efforts are underway to restore river ecosystems and biodiversity, in Europe particularly at WFD's River Basin Management Plans and the new Nature Restoration Regulation.

Ecohydraulics occupies a central and increasingly strategic role in providing the scientific and technical foundations needed to understand river processes and support effective management and restoration. Applications such as habitat modelling, fish passage design, environmental flows and sediment management, demonstrate the breadth and relevance of the field in addressing ongoing contemporary river rehabilitation. An important challenge remains: how to scale up often localized restoration actions to achieve measurable ecological recovery at catchment and basin scales.

This keynote will address the foundational role of ecohydraulics in the restoration process, explore how it contributes to diagnosing river degradation and recovery, supporting restoration planning, and evaluating ecological outcomes across scales. It will highlight the growing need for interdisciplinary approaches capable of linking physical processes with ecological responses in dynamic and uncertain environments. Ultimately, the talk will argue that ecohydraulics is not only a tool for mitigating impacts, but a key enabling discipline for delivering resilient, adaptive, and nature-positive solutions for restoring and managing river systems.

Sponsors

Platinum Sponsor

Hydro Québec

Silver Sponsors

FLOW-3D HYDRO

hydrosuisse

wsp

Supporting Sponsors

ALPIQ

ecorisQ

gruner

Helveos

HOLINGER the art of engineering

hydrique.

KWO

Lombardi

MHYD

patscheiderpartner ENGINEERS

ROMANDE ENERGIE

WATERTRACKS

Exhibitors

EFIB

frontiers in Environmental Science

SCALGO

Published by IAHR, © 2026 IAHR. CC BY-NC-ND 4.0| DOI: [10.64697/iahr.proc.ise2026.abs]

Contents

Session A1: Interactions between flow, natural elements, and structures 1

LOCAL SCOUR AROUND A SINGLE PIER ON A TRANSVERSALLY INCLINED BED 3
BOMBAR, Gokcen; GUMGUM, Firat; CARDOSO, Antonio Heleno

LEAF-TO-STEM FLEXIBILITY RATIO MODULATES FLOW IMPEDANCE BY FOLIAGE 7
DICKINSON, Rufus E.; MATSUMOTO, Kazumasa; MARJORIBANKS, Timothy I.; SANJOU, Michio; KEYLOCK, Christopher J.; OKAMOTO, Takaaki

ANTICIPATED CFD MODELING FOR HABITAT SCALE HYDRODYNAMIC COMPLEXITY METRICS IN BOULDER DOMINATED CHANNELS 11
REGGAD, Naima; BAKI, Abul BM; KATOPODIS, Christos; GHAMRY, Haitham; ZOBEYER, Hasan

EFFECTS OF A HIGH-HEAD HYDROPOWER SYSTEM ON THE HYDROLOGY AND PHYSICAL ENVIRONMENT IN A RIVER SYSTEM 15
ALFREDSEN, Knut Tore

RIVER RESTORATION: THE ROLE OF HABITAT HETEROGENEITY AND FLOOD REFUGIA 19
HISCHIER, Chantal Mariette; BÄTZ, Nico; RACHELLY, Cristina; DEMUTH, Paul; WEITBRECHT, Volker; VETSCH, David Florian; DINKEL, Christian; WEBER, Christine

FLOW RESISTANCE CHARACTERISTICS AND FLOW STRUCTURE OF OPEN CHANNELS DUE TO DIFFERENCES IN VEGETATION ARRANGEMENT AND DENSITY 23
TANAKA, Takayuki; SUGIURA, Kanta

FLOW DRAG PARAMETERISATION OF LEAKY BARRIERS FOR NATURAL FLOOD MANAGEMENT . 27
BRADBROOK, Kate; FOLLETT, Elizabeth; HANKIN, Barry

THREE DIMENSIONAL NUMERICAL SIMULATION OF TURBULENT FLOW WITH BRIDGE OVERTOPPING 31
KWON, Yongjun; KIM, Hyung-Suk

IN-STREAM MESOHABITAT MODELLING BASED ON HYDROACOUSTIC DATA AND HIERARCHICAL CLUSTERING 33
SCHLOBIES, Kerstin; VAN ROOIJEN, Erik; VANZO, Davide; LOTSARI, Eliisa Selina

SCALE RESOLVED NUMERICAL SIMULATIONS OF A NOVEL EDDY BASED FISH GUIDANCE SYSTEM (EGS) 37
LILLBERG, Eric; LARSSON, Mikaela; VETSCH, David Florian; PANDEY, Kamal Prasad; SOLEMSLIE, Bjørn Winther; ALBAYRAK, Ismail; PETER, Armin; FORSETH, Torbjørn; DAHLHAUG, Ole Gunnar; BOES, Robert M; SILVA, Ana T.

APPLYING TESLA VALVE PRINCIPLES TO OPEN-CHANNEL CONDITIONS FOR ECOHYDRAULIC BARRIERS 41
KLEINEWIETFELD, Inga; KLOPRIES, Elena-Maria

PREDICTING FISH HABITAT SUITABILITY USING HABITAT-SCALE HYDRODYNAMIC COMPLEXITY METRICS INTEGRATED INTO THE RIVER2D MODEL 45
BAKI, Abul BM; ZOBEYER, Hasan; SHAGOR, Md Aminul Islam; GHAMRY, Haitham; KATOPODIS, Christos; LANGEN, Tom A.

ENVIRONMENTAL AND HYDRAULIC EFFECTS OF PILOT RIVERBANK PROTECTION WORKS ON THE MANU RIVER: A DECADAL POST-PROJECT EVALUATION 49
MURAOKA, Kazumitsu; MATSUKAWA, Minako

IMPROVING FISH RECEPTION CONDITIONS AT THE OUTLET OF DOWNSTREAM MIGRATION DEVICES AND SPILLWAYS USING FIELD MEASUREMENTS AND URANS-VOF MODELING . . 53
ECORCE, Antoine; COURRET, Dominique; CHATELLIER, Ludovic; DAVID, Laurent

FIELD-SCALE FLOW CONDITIONS AROUND ENGINEERED LOGJAMS: INSIGHTS FROM LARGE-SCALE PIV 57
BROSS, Felix; SCHALKO, Isabella

QUANTIFYING LATERAL BEDLOAD TRANSPORT FROM BATHYMETRIC SCANS: EXPERIMENTS WITH A YAWED SUBMERGED VANE ARRAY 61
MUSA, Mirko; TSENG, Chien-Yung; LEE, Jiyong; GUALA, Michele

INSIGHTS INTO THE SETTLING AND INTERACTION BEHAVIOUR OF SPHERICAL MICROPLASTICS 65
RAMEZANI, Mohammadmehdi; SEYFI, Siamak; DE CASTRO, Camillo; KARIMPOUR, Shooka

Session A2: Organism-flow interactions: movement, transport, and sensing 69

FISH PATHWAYS IN BOULDER-DOMINATED NATURE-LIKE FISHWAYS: LINKING SPATIAL VARIABILITY AND ENERGY EXPENDITURE 71
SHAGOR, Md Aminul Islam; TUSHER, Md. Sajjad Hossain; LANGEN, Tom A.; GHAMRY, Haitham; KATOPODIS, Christos; BAKI, Abul B.M.

THE PATCH SCALE MATTERS: HABITAT-SPECIFIC RESPONSE OF MACROINVERTEBRATE DRIFT TO FLOW PULSES 75
FRIESE, Nathalie; MATHERS, Kate L.; WEBER, Christine; TONOLLA, Diego; BÄTZ, Nico

IMPACT OF ANTHROPIZED RIVER HYDRODYNAMIC CONDITIONS ON SILVER EEL MIGRATION SPEEDS 79
CIRAANE, Utashi; SONNY, Damien; FALGAS, Gaia; PIERRE, Archambeau; BENJAMIN, Dewals; PIROTTON, Michel; ERPICUM, Sébastien

WIND-POWERED AERATION SYSTEM FOR EFFECTIVE CYANOBACTERIA CONTROL IN RESERVOIRS 83
ELÇI, Sebnem; HAZAR, Oguz; TUNEY KIZILKAYA, Inci

A WOOD-SHAPED SENSOR FOR LARGE WOOD MOTION DETECTION 87
YANG, Jiangtao; SEIDEL, Frank; J. FRANCA, Mário

THE EFFECT OF DIFFERENT FLOW PULSES ON THE BIOMASS PERIPHYTON IN AN EXPERIMENTAL FLUME 91
SUN, LongFei; WU, LeiXiang; HUANG, Wei

HYDRODYNAMIC CUES AND MOVEMENT BEHAVIOUR OF SEA LAMPREY: INSIGHTS FOR CONTROL AND CONSERVATION 95
ZIELINSKI, Daniel

HYDRODYNAMIC THRESHOLDS FOR RESUSPENSION OF DRIFTING FISH EGGS IN BOTTOM VORTEX STRUCTURES 99
GAO, Yiheng; HAN, Rui; YANG, Hongyi; FU, Miaoran

A PREDICTIVE MODEL FOR ASSESSING FISH LARVAL DRIFT UNDER VARIABLE HYDROLOGICAL CONDITIONS 103
CUDNA, Wiktoria; PARASIEWICZ, Piotr

SEASONAL, NOCTURNAL AND SPATIAL DYNAMICS OF ICHTHYOPLANKTON DRIFT NEAR THE POŁANIEC POWER PLANT, VISTULA RIVER, POLAND 107
PREKURAT, Wojciech; PARASIEWICZ, Piotr

USING FIELD AND FLUME STUDIES PAIRED WITH HYDRODYNAMIC MODELING TO INFORM A FRESHWATER MUSSEL REINTRODUCTION 111
DINICOLA, Megan; LANE, Belize

PREFERENTIAL PATHS OF GRASS CARP LARVAE SWIMMING THROUGH PATCHES OF FLOATING VEGETATION: INSIGHTS FROM LABORATORY EXPERIMENTS 115
TINOCO, Rafael; PRASAD, Vindhyawasini

PATHWAYS: AN ALGORITHM FOR MODELING MULTIPLE SWIMMING PATHS BETWEEN HABITATS AND THEIR ENERGETIC COSTS IN A 2D FLOW FIELD 117
HOLZAPFEL, Patrick; WILDT, Daniel; SCHMALFUSS, Lisa; PASTERNACK, Gregory; HAUER, Christoph

Session A3: Ecomorphodynamics: linking flow, sediment and biota, instabilities, and patterns' formation 123

FROM STOCKPILE EROSION TO CHANNEL ADJUSTMENT: INVESTIGATING THE HYDRO-MORPHOLOGICAL IMPACTS OF SEDIMENT REPLENISHMENT VIA NUMERICAL SIMULATION 125
LIN, Jiaqi; A. KANTOUSH, Sameh; SUMI, Tetsuya

GENERATING SYNTHETIC TERRAIN MODELS FROM SPARSE HISTORIC DATASETS FOR ECOHYDRAULIC ASSESSMENT 131
STIEVE, Jared; LANE, Belize; LEE, Anzy

CURRENT FLOW AND RIVERBED CONDITIONS FOR BENTHIC INVERTEBRATES AND EFFECTS OF SEDIMENT REPLENISHMENT ON ECOLOGICAL RESTORATION IN THE UJI RIVER, KYOTO, JAPAN 135
KOBAYASHI, Sohei; CAI, Boyuan; KANTOUSH, Sameh

ANALYSES OF RIPARIAN VEGETATION ESTABLISHMENT DUE TO FLOW REGIME CHANGES FOCUSED ON VEGETATION RECRUITMENT AND FLOOD RISK – A CASE OF THE UPPER-MIDDLE NAKDONG-GANG RIVER IN KOREA 139
WOO, Hyo Seop; JANG, Chang-Rae; CHOI, Sung-Uk

INUNDATION DYNAMICS AND CHANNEL NETWORK CHANGES IN RESPONSE TO FLOODS IN AN ALPINE BRAIDED RIVER 143
OMER MAHMOUD AWADALLAH, Mahmoud; VANZO, Davide; VETSCH, David Florian; BOES, Robert Michael; CAPONI, Francesco

MODELLING THE ROLE OF HYDROPEAKING ON VEGETATION ESTABLISHMENT DYNAMICS ON GRAVEL BARS 147
CAPONI, Francesco; VETSCH, David F.; VANZO, Davide

LANDSCAPE METRICS AS INDICATORS FOR HABITAT COMPLEXITY IN RESTORED RIVER REACHES 151
DEMUTH, Paul; WEITBRECHT, Volker; HISCHIER, Chantal M.; WEBER, Christine; BOES, Robert M.; VETSCH, David F.

DISCHARGE-DEPENDENT BRAIDED RIVER NETWORKS: PROPERTIES AND IMPLICATIONS FOR DISPERSION PROCESSES 155
VENDRUSCOLO, Margherita; CAMPOREALE, Carlo; RIDOLFI, Luca

NUMERICAL MODELLING OF BIOMORPHODYNAMICS: A COMPARISON OF EXISTING CLOSURES FOR BEDLOAD TRANSPORT IN VEGETATED FLOWS 159
DALLMEIER, Antonia; CAPONI, Francesco; VANZO, Davide; SCHWEDHELM, Hannah; KOPMANN, Rebekka; RÜTHER, Nils

PARTIALLY VEGETATED MEANDERING FLUME: PRELIMINARY RESULTS ON FLOW VELOCITY DISTRIBUTION IN THE BEND APEX AREA 163
TERMINI, Donatella

FLOOPLAIN VEGETATION CONTROLS ON IN-CHANNEL HABITAT AVAILABILITY AND REFUGE IN A MEANDERING MORPHOLOGY 167
VANZO, Davide; PAVA, Nicolas; TRANMER, Andrew; WHITE, Daniel

A MULTI-STAGE DISCHARGE FRAMEWORK FOR DIAGNOSING SEDIMENT TRANSPORT REGIMES AND BED DISTURBANCE IN DAM-INFLUENCED RIVER REACHES USING FIXED-BED 2D HYDRODYNAMIC MODELLING 171
HARADA, Morihiro

HYDROLOGY DRIVEN WETLANDS MORPHOLOGY AND ITS ROLE IN THE WATER-CARBON BUDGET 175
MIELE, Filippo; KARGERE, Benjamin; AEPPLI, Meret; BONETTI, Sara

RIVER FLOW VARIABILITY AS A CATALYST FOR VEGETATION GROWTH AND CARBON PUMPING . 179
SALERNO, Luca; BERTAGNI, Matteo; CAMPOREALE, Carlo

DEVELOPMENT PATTERNS OF MANGROVES IN ARTIFICIAL COASTAL ZONES AND THEIR IMPACTS ON INVERTEBRATE POPULATIONS 183
SUN, Bangjie; WANG, Zhaoyin; XU, Mengzhen; YANAN JIANG, Sabrina; ZHOU, Yi

Session A4: Ecohydraulics Across Space and Time: from habitats to catchments, instants to decades, and individuals to communities 187

FROM CROSS-SECTION AVERAGES TO IMMERSIVE, AGENT-BASED COMPUTATIONAL ECOHYDRAULICS 189
SCHWINDT, Sebastian; KEMMLER, Benjamin; SCOLARI, Federica; PASTERNACK, Gregory B.

EXTENDING ECO-HYDRAULICS INTO ECO-EVO-HYDRAULICS THROUGH HYDRO-EVOLUTIONARY FEEDBACKS 193
CAI, Xiatong; RENNIE, Colin D.; BLANCHET, Simon; BOLNICK, Daniel I.; CALBOLI, Federico C.F.; DEFLEM, Io S.; HELLEMANS, Bart; HENDRY, Andrew P.; DE MEESTER, Joke; MOHAMMADIAN, Abdolmajid; VOLCKAERT, Filip A.M.; WILLEMS, Patrick; RAEYMAEKERS, Joost A.M.

WAKE TURBULENCE AT LOW SUBMERGENCE: INTEGRAL LENGTH SCALES AND LINKS TO FISH BODY SIZE 197
NILSSON, Dan; ANDERSSON, Anders; LARSSON, Sofia; ANDERSSON, Robin; BILLSTEIN, Mats

A TOOLBOX FOR ASSESSING PATCH-SCALE HABITAT DYNAMICS FOR MACROINVERTEBRATES IN FLOW-ALTERED RIVERS 201
LECRIVAIN, Aude; DE CESARE, Giovanni; WEBER, Christine; BÄTZ, Nico

MODELLING FISH HABITAT CHANGES DUE TO THE PRESENCE OF LARGE WOOD IN RIVERS . . 205
SANZ RAMOS, Marcos; RUIZ-VILLANUEVA, Virginia; BLADÉ, Ernest

NEW TOOLS AND DATABASES FOR RIVER MESOHABITAT MODELING 209
VEZZA, Paolo; NEGRO, Giovanni; FARÒ, David; PINNA, Beatrice; FORTE, Simone; ZOLEZZI, Guido

REFINING THE FLOW-T MESOSCALE MODEL FOR RIVER MACROINVERTEBRATE COMMUNITIES 213
PINNA, Beatrice; LAINI, Alex; BURGAZZI, Gemma; GUARESCHI, Simone; VEZZA, Paolo

ZOOPLANKTON MODULE INDICATES TOP-DOWN EFFECTS ON EUTROPHICATION: IMPLICATIONS FOR LAKE RESTORATION BY BIOMANIPULATION 217
ZHANG, Chen; YU, Ruolan

IDENTIFYING FISH MACROHABITATS IN EUROPEAN RIVERS 221
CHAUHAN, Geetika; BELKA, Kamila; PARASIEWICZ, Piotr

INTEGRATED FUNCTIONAL HABITAT AND FISH POPULATION DYNAMICS MODELLING FOR IMPROVED RIVER RESTORATION 225
FARÒ, David; WOLTER, Christian

APPLICATION OF INSTREAM FLOW INCREMENTAL METHODOLOGY TO CHECK THE IMPACT OF FLOOD PROTECT MEASURES ON FISH MICROHABITATS 229
HUNG, Meng-Chi; HUANG, Chuan-Yi; HSU, Chang-An

EFFECTS OF RELATIVE FLOODPLAIN WIDTH ON HYDRAULIC VARIABILITY AND AQUATIC HABITAT 233
BENJANKAR, Rohan; TONINA, Daniele

HOW ECOHYDRAULIC PRINCIPLES AND TOOLS CONTRIBUTES TO SUSTAINABLE HYDROPOWER REFURBISHMENT 237
HARBY, Atle; CAROLLI, Mauro; FOERST, Markus Peter; SABIL, Sahra Naima; SUNDT, Håkon

MESOHYDRAULICS: MODELLING HABITAT SUITABILITY ON THE ODER RIVER AT THE MESOSCALE 241
PARASIEWICZ, Piotr; SABOLEK, Jura; KICZKO, Adam; MIROSŁAW-ŚWIĄTEK, Dorota; WÓJTOWICZ, Jan

PHYSICAL HABITAT SIMULATION OF SCHIZOTHORAX PRENANTI SPAWNING GROUNDS BASED ON INDOOR FLUME EXPERIMENTS 245
CHEN, Min

Session A5: Global change impact, biogeochemical cycles, biodiversity losses, and ecosystem resilience 249

INFLUENCE OF GLOBAL WARMING ON URBAN STORMWATER QUALITY: IMPLICATION FOR EFFECTIVE MANAGEMENT 251
LIU, An; WIJESIRI, Buddhi; GOONETILLEKE, Ashantha

A STUDY OF POTENTIAL MITIGATION MEASURES FOR STORÅNE, A HYDROPEAKED RIVER IN NORWAY 255
GRAF, Magnus Simon; ALFREDSEN, Knut Tore; BOCQUILLON, Noé; DØNNUM, Bjørn Otto

THE IMPACT OF CLIMATE CHANGE ON RIPARIAN VEGETATION IN BOREAL CONDITIONS 259
HÖLLER, J. Bastian; ANDERSSON, Anders G.; HELLSTRÖM, J. Gunnar I.

TOTAL DISSOLVED GAS IN NEOTROPICAL SYSTEMS AND ITS EFFECTS ON THE FISH FAUNA . . 263
NOGUEIRA, Lorena B; VIEIRA, Higor A A G; MAGALHÃES, Breno A; RIBEIRO, Dieimys S; ROSA, Liandro; MAFRA, Juliano; FERRAZ, Guilherme; DE CASTRO, Andrey L F; MARTINEZ, Carlos B; SILVA, Luiz G M

ASSESSMENT OF ECOSYSTEM REGULATION ON WATERSHED ECOHYDRAULIC VARIABLES UNDER CLIMATE AND LAND USE CHANGE IN SOUTHERN CHINA 267
XIONG, Jianxiang; KONG, Lingqiao; OUYANG, Zhiyun

HABITAT MODELLING OF FISH COMMUNITIES IN THE ODER RIVER: APPLICATION OF THE MESOHABSIM MODEL UNDER ENVRIOMENTAL STRESS CONDITIONS 271
CUDNA, Wiktoria; SUSKA, Katarzyna; PARASIEWICZ, Piotr

WHEN THE RIVER MEETS ENERGY DEMAND: BALANCING ENERGY, CLIMATE, AND NATURE . . . 275
FOERST, Markus; HARBY, Atle

CLASSIFYING HYDROMORPHOLOGICAL CONDITIONS FOR IMPACT ASSESSMENTS IN PROTECTED WATERCOURSES IN NORWAY USING A REMOTE SENSING APPROACH 279
SUNDT, Håkon; CAROLLI, Mauro; HARBY, Atle

ADVANCING LIMNOLOGICAL RESEARCH IN CENTRAL ASIA: CONTRIBUTIONS TO FRESHWATER BIODIVERSITY AND ECOLOGY FROM THE HYDRO4U PROJECT 283
HAYES, Daniel S.; KARIMOV, Erkin; VERHELST, Pieterjan; OMONOV, Otabek; FUNK, Andrea; KOPECKI, Ianina; COECK, Johan; KARIMOV, Bakhtiyor K.; DE KEYSER, Jan; MUHAMMADIYEV, Fazliddin; SCHNEIDER, Matthias; ZEIRINGER, Bernhard; ALAPFY, Bertalan; CAREY, Justine; SELIGER, Carina; WAGNER, Falko; ROESSGER, Tom; SCHLETTERER, Martin

FROM PHOSPHORUS CONTROL TO HABITAT RESPONSE: WATER COLUMN RECOVERY AND LEGACY SEDIMENT EFFECTS IN A CHALK STREAM 287
TRINCI, Giuditta; WHARTON, Geraldene; HEPPELL, Kate; KELLY, Thomas

Session B1: Urban, suburban, and periurban streams 291

PREDICTING EUTROPHICATION POTENTIAL OF AN URBAN WETLAND IN BRAHMAPUTRA VALLEY, INDIA: APPLICATION OF A 1D-2D HYDRODYNAMIC AND WATER QUALITY MODEL 293
KOCH, Daisy; SEN, Dhrubajyoti; GUPTA, Ashok Kumar

HYDRO-ECOLOGICAL PERFORMANCE OF THE ARVE–DRIZE FISHWAY: ASSESSING SEDIMENT CLOGGING AND SELF-SCOURING PROCESSES 297
DUPARC, Nicolas; GARCIA, Anthony; ANDREINI, Nicolas; CERESETTI, Davide

THE SHIFTING SANDS OF GRAVEL STREAMBEDS: CYCLIC TRENDS IN EMBEDDEDNESS FLUCTUATION IN AN URBANZIED STREAM 301
HARGETT, Justus; CZUBA, Jon

SOIL AND WATER BIOENGINEERING AS RIVER HEAT PERIOD MITIGATION IN AN URBAN STREAM 303
MUELLER, Helene; LUDWICZEK, Anna; VON DER THANNEN, Magdalena; RAUCH, Hans Peter

SOLUTIONS TO FLOODING OF THE ESTEPONA RIVER IN THE URBAN CENTER OF BAKIO (BIZKAIA, SPAIN) 307
SANGALLI, Paola; SANGALLI, Sergio; TARDÍO, Guillermo

WATER QUALITY DYNAMICS IN COMBINED WASTEWATER–STORMWATER CHANNELS AND A TIDAL RECEIVING RIVER: A 1D-2D MODELLING STUDY OF KOLKATA, INDIA 311
DAS, Ronak Prakash; DAS, Manas Kumar; BARMAN, Bibhas Chandra; SEN, Dhrubajyoti

Session B3: Ecohydraulics meets landscape architecture 315

MAPPING 360° TRANSITIONAL LANDSCAPES: HYDRAULICS FOR ECOLOGICAL ECOSYSTEM CONNECTIVITY IN THE ORBE–CHAVORNAY REGION 317
GITAI, Ben; LOMBARDI DELLAMONICA, Chiara; JESSEL, Beate

LA MARJAL AND GRØNNINGEN BISPEPARKEN FLOODABLE PARKS, TWO DIFFERENT DESIGNS, ONE SINGLE AIM 321
MARTIN MUÑOZ, Silvia

ECOHYDRAULIC ASSESSMENT OF WATERSHED HYDROLOGICAL SERVICES USING THE VIC MODEL: A CASE STUDY OF THE LUAN RIVER BASIN, NORTH CHINA 325
YANG, Yuze; LI, Ruonan; ZHENG, Hua

DESIGNING THE WATER MACHINE: INTERDISCIPLINARY APPROACHES TO THE DENDER VALLEY 329
ZHANG, Qinyi; FREDRICK, Nathan

DESIGNING A TECHNONATURE: INTEGREATED WATER SYSTEM IN THE FUTURE RINGPARKS IN ANTWERP 333
ZHANG, Qinyi; FREDRICK, Nathan

RENATURATION OF THE DRIZE AND AIRE RIVERS IN GENEVA'S PAV DISTRICT: AN INTEGRATED APPROACH TO URBAN ECOHYDRAULICS AND LANDSCAPE ARCHITECTURE 337
BOURQUI, Pierre; LAUNAY, Marina; RAMPINI, Marco; BACH, Yves; GERBER, François; EHRENSPERGER, Kim

Session B4: Governance, socio-environmental benefits, and areas of conflict 341

A LIGHTWEIGHT THERMAL MODELLING APPROACH FOR EMBEDDING WATER QUALITY IN MULTI-OBJECTIVE RESERVOIR OPERATION 343
ALFANO, Maria Elena; ZANIOLO, Marta; POGGI, Davide; BOSIO, Roberto; SAVOLDI, Laura

THE FUTURE OF ECOHYDRAULICS: A COMMUNITY PERSPECTIVE 347
BASILIO HAZAS, Mónica; WITTMANN, Joël; VANZO, Davide; DE KEYSER, Jan; SATTELMEIER, Melina; SCHWEDHELM, Hannah; MERL, Kevin; PADOAN, Francesca; ADEVA-BUSTOS, Ana; VETTORI, Davide; CHABAL, Mathias; SABIL, Sahra N.; TONINA, Daniele; HAYES, Daniel S.

BUILDING POLISH DATABASE OF FREE-FLOWING RIVERS TOWARDS PRIORITIZATION OF RESTORATION EFFORTS 351
BELKA, Kamila; BRACH, Michał; CHAUHAN, Geetika; GĄSIOR, Mariusz; JUSIK, Szymon; KARPIO, Krzysztof; KONECKI, Paweł; NADOLNY, Adam; NATORF, Włodzimierz; NAWROCKI, Przemysław; BURY, Sławomir; PARASIEWICZ, Piotr

WHO GIVES AND WHO GETS ROOM FOR THE RIVER? NEGOTIATING THE FRONTIER OF FLOOD RISK AND RIVERBANK INFORMAL SETTLEMENTS IN KATHMANDU'S ECOLOGICAL URBAN RENEWAL 355
GOMEZ TEJERA, Alejandro

PROCESSES AND INTERNATIONAL COLLABORATION ON SEDIMENT MANAGEMENT IN THE RHÔNE : TOWARD SUSTAINABLE SEDIMENT CONTINUITY 359
GIRARD, Charlotte; PRESSIAT, Franck; CHERRAK, Marion; DIOUF, Seydina; PINET, Laurent

Session C1: Peaking regimes and environmental flows 361

ECOLOGICAL CONSEQUENCES OF FLOW REGIME ALTERATION FROM HYDROPOWER REGULATION: A COMPARATIVE ASSESSMENT OF THE RHÔNE AND ÇORUH RIVERS 363
DEMIREL, Ibrahim Halil; DE CESARE, Giovanni

ECOLOGICAL PORTRAIT OF THE KIPAWA RIVER IN LIGHT OF A POTENTIAL HYDROELECTRIC DEVELOPMENT 367
ENDERS, Eva; JACQUES, William; FOULON, Etienne; ST-HILAIRE, André

IMAGING ORGANISM DRIFT CONTINUOUSLY AT 1-SECOND RESOLUTION: A 10 WEEK CASE STUDY 371
WITTMANN, Joël R.; GRAF, Levi; FERRERO, Vittorio; KUSTER, Lea; WIGGER, Anaïs; ZAMBOTTO, Giulia; DE SCHAETZEN, Frédéric; GIACOMUZZI, Sandro; STOCKER, Roman; SILVA, Luiz G. M.

DISCHARGE MODIFICATIONS BY FLOOD DAMPENING FROM HYDROPOWER RESERVOIRS: SURNA CASE STUDY 375
SABIL, Sahra Naima; BULLE ARIAS, Keilly; BAKKEN, Tor Haakon; ALFREDSEN, Knut

ASSESSING HYDROPEAKING IMPLICATIONS ON BROWN TROUT (SALMO TRUTTA) POPULATIONS ON THE NORTH BRANCH OF THE POTOMAC RIVER 379
DYE, Benjamin; CZUBA, Jonathan

USING GENETIC TOOLS TO ASSESS FISH POPULATION ABUNDANCE AND CONNECTIVITY IN A REGULATED RIVER 383
DI PANE, Julien; PRUNIER, Jérôme; DUBUT, Vincent; LEPAIS, Olivier; GOURAUD, Véronique; TISSOT, Laurence; PIFFADY, Jeremy; BOMPARD, Pierre

ECOLOGICAL FLOWS AS A DRIVER FOR FUTURE HYDROPOWER DEVELOPMENT 387
NEGRO, Giovanni; VIALE, Sara; GUGLIELMETTO, Alessandro; VEZZA, Paolo

EVALUATING YOUNG-OF-THE-YEAR FISH RESPONSE TO A HYDROPEAKING MITIGATION MEASURE TROUGH A DIVERSION HYDROPOWER PLANT 391
MERL, Kevin; ZEIRINGER, Bernhard; HAYES, Daniel; HOLZAPFEL, Patrick; HAUER, Christoph; SCHLETTERER, Martin; SCHMUTZ, Stefan; GREIMEL, Franz

ASSESSING ECOLOGICAL GAINS OF HYDROPEAKING MITIGATION MEASURES IN A CLIMATE CHANGE CONTEXT 395
GOURAUD, Véronique; TARENA, Fabio; BARILLIER, Agnès; DI PANE, Julien; LAMOUR, Marie; HARBY, Atle; CAPRA, Hervé; BECHE, Leah; LAMOUROUX, Nicolas

HYDRAULIC AND ECOLOGICAL CHARACTERIZATION OF TWO ADJACENT RIVER REACHES WITH DIFFERENT REGULATED STREAMFLOW 399
QUADRONI, Silvia; SERVANZI, Livia; ESPA, Paolo

FROM MULTI-SCALE MONITORING TO 2D HYDRO-THERMAL MODELING: ASSESSING SEASONAL SPATIO-TEMPORAL TEMPERATURE VARIABILITY IN A REGULATED RIVER 403
GAMARRA, Nicolas Francisco; CASAS-MULET, Roser; RÜTHER, Nils

E-FLOW GUIDELINE FOR HYDROPOWER PROJECTS IN THE ROYAL KINGDOM OF BHUTAN, ECOHYDRAULIC ELEMENTS 407
SCHNEIDER, Matthias; JORDE, Klaus; PETER, Armin; KOPECKI, Ianina; DORJI, Chhimi; KHORLO, Tenzin

APPLICATION OF THE FUNCTIONAL FLOWS APPROACH IN A HIGHLY REGULATED MEDITERRANEAN BASIN (JÚCAR RIVER BASIN, SPAIN) 411
MARTÍNEZ-CAPEL, Francisco; GRANTHAM, Ted E.; SANTIAGO-BAZAN, Frank; MACIAN-SORRIBES, Hector; MUÑOZ-MAS, Rafael; PULIDO-VELAZQUEZ, Manuel A.

PHYSIOLOGICAL RESPONSES OF IBERIAN RIPARIAN WOODY SPECIES TO HYDROPOWER OPERATION: A STABLE ISOTOPE ASSESSMENT IN A CONTROLLED FLUME EXPERIMENT 413
AZNAR, Ignacio; BALADRÓN, Alejandro; BEJARANO, María D.

IMPLEMENTATION OF ENVIRONMENTAL FLOWS: REALITIES, CONSTRAINTS AND WAY FORWARD 417
GOSSELIN, Marie-Pierre; CAROLLI, Mauro; DA SILVA, Luiz; HAYES, Daniel; SCHLETTERER, Martin; SCHWEIZER, Steffen; MCCOSEY, Dana

Session C2: Fish passage: design, modelling, and assessment 421

EFFECT OF TOE LOCATION OF ASSEMBLED BOULDERS ON LEADING FLOW DOWNSTREAM OF FISH PASSAGE 423
YASUDA, Youichi; AONO, Yuuichi

FROM FLUME TO FIELD: FULL-SCALE VALIDATION OF A MODIFIED BAR RACK FISH-GUIDANCE SYSTEM 427
KJÆRÅS, Halvor; BAKTOFT, Henrik; SILVA, Ana T.; GJELLAND, Karl Ø.; ØKLAND, Finn; MADDAHI, Mohammadreza; ALBAYRAK, Ismail; LIA, Leif; BOES, Robert M.; FORSETH, Torbjørn

FLOW DYNAMICS AND HYDRAULIC EFFICIENCY IN FISHWAY BED CONFIGURATIONS 431
KANTOUSH, Sameh; SOHRABZADEH-ANZANI, Hossein; KOBAYASHI, Sohei

DOWNSTREAM MOVEMENT OF JUVENILE ATLANTIC SALMON (Salmo salar) IN NATURE-LIKE FISHWAYS 435
TUSHER, Md. Sajjad Hossain; SCHUCKERS, Christopher; ISLAM, Md. Shoriful; LANGEN, Tom A.; GHAMRY, Haitham; KATOPODIS, Christos; BAKI, Abul BM

FISH PASSAGE SOLUTIONS IN HIGHLY REGULATED CATCHMENTS: AN INDIVIDUAL-BASED FRAMEWORK FOR ADAPTIVE WATER MANAGEMENT IN FLANDERS 439
JASPAERT, Hanna; VERHELST, Pieterjan; BAETENS, Jan

DIFFERENTIAL PASSAGE SUCCESS AND FLOW CUES: UPSTREAM MIGRATION OF EUROPEAN EEL AT A TURBINE-WEIR-FISH PASSAGE COMPLEX ON THE DIJLE RIVER, BELGIUM 443
BRUNEEL, Stijn; VANDAMME, Lore; VERHELST, Pieterjan; BUYSSE, David; PAUWELS, Ine; COECK, Johan; THIENPONT, Kaat; DE VISSCHER, Sam

ASSESSMENT OF ATTRACTION FLOW EFFECT ON FISHWAY ENTRANCE FLOWS: A CASE STUDY FROM SWITZERLAND 447
ALBAYRAK, Ismail; WYSS, Andris; LAIS, Adriano; MADDAHI, Mohammadreza; SCHERNGELL, Alfredo; SUTTER, Roland; ROBER M., Boes

DEVELOPMENT OF A NOVEL EDDY-BASED FISH GUIDANCE SYSTEM (EGS) (PART-1) 451
PANDEY, Kamal Prasad; ALBAYRAK, Ismail; PETER, Armin; FORSETH, Torbjørn; LILLBERG, Eric; VETSCH, David Florian; LARSSON, Mikaela; BOES, Robert Michael; SILVA, Ana Teixeira

HEAD LOSSES ON FISH-FRIENDLY ANGLED BAR RACKS SUBJECTED TO CLOGGING: AN EXPERIMENTAL STUDY 455
BON, Guillaume; MBA-ASSOUMOU, Baba; CHATELLIER, Ludovic; DAVID, Laurent

LIMITS OF ELECTROFISHING AS A TOOL FOR MULTISPECIES FISHWAY EVALUATION 459
NIJSSEN, David; ODE, Torsten; SONNY, Damien; SCHMIDT, Daniel; SCHEIFHACKEN, Nicole; SCHOLTEN, Matthias; SCHÜTZ, Cornelia

EVALUATING PASSAGE EFFICIENCY OF MULTIPLE FISH SPECIES IN A LARINIER SUPER ACTIVE BAFFLE FISHWAY 463
SCHIAVON, Alfredo; ALDERIGHI, Ambra; SPAIRANI, Michele; CANDIOTTO, Alessandro; NYQVIST, Daniel; BONETTO, Davide; PINI PRATO, Enrico; COMOGLIO, Claudio

3D-NUMERICAL INVESTIGATION OF FISH PASSAGE STRUCTURE 467
FEURICH, Robert; MAYRHOFER, Bernhard; TEBBEN, Heiko

INNOVATIVE BYPASS SYSTEM: HYDRAULIC PERFORMANCE AND ATLANTIC SALMON (Salmo salar) PASSAGE EFFICIENCY 471
YAN, Yuhao; ALDVÉN, David; MÜLLER, Stephanie; SILVA, Luiz G. M.; ANDREASSON, Patrik; VETSCH, David F.; FREI, Seline; LILLBERG, Eric; SILVA, Ana T.; BOES, Robert M.; ALBAYRAK, Ismail

CONTRASTING SWIMMING CHARACTERISTICS OF PASSING AND FAILING ROACH (RUTILUS RUTILUS) DOWNSTREAM OF A VERTICAL SLOT 475
FOCHT, Lina; HENEKA, Patrick; HENNING, Martin; NOSS, Christian; ABERLE, Jochen

DOWNSTREAM ROUTE SELECTION OF ATLANTIC SALMON AT HYDROPOWER FACILITIES EXPLAINED BY HYDRAULIC AND SITE CONFIGURATION METRICS 479
ZIMMER, Emilie; TOMANOVA, Sylvie; TISSOT, Laurence; COURRET, Dominique; ROY, Romain; LAGARRIGUE, Thierry; FREY, Aurélien; BEGUIN, Jérémy; LERQUET, Marc; COLSON, Dylan; SONNY, Damien; OVIDIO, Michaël

BRIDGING THE CONNECTIVITY CONUNDRUM: A REVIEW OF FISH SORTING TECHNOLOGIES FOR SELECTIVE FISH PASSAGE 483
ASHRAF, Muhammad Usama; ZIELINSKI, Daniel P.; SWANSON, Reid G.; MUIR, Andrew M.; MCLAUGHLIN, Robert L.; PRATT, Thomas C.; GOODWIN, R. Andrew; COTEL, Aline J.; HRODEY, Peter J.; WAGNER, C. Michael; EICKHOLT, Jesse; COMOGLIO, Claudio; BOLLAND, Jonathan D.

THE KUDENSEE PROJECT: DEVELOPMENT OF A LESS-DAMAGING REPLACEMENT PUMP FOR SUSTAINABLE WATER MANAGEMENT 487
HOERNER, Stefan; POWALLA, Dennis; ABDELGHAFAR, Islam; KERIKOUS, Emeel; WAGNER, Falko; TUHTAN, Jeffrey; SCHUMACHER, Roland

OPTIMIZATION OF FISH BYPASS ENTRANCES: THE OPTIPASS APPROACH 491
KOPECKI, Ianina; ROESSGER, Tom; WAGNER, Falko

LARGE SCALE PERFORMANCE EVALUATION OF NOVEL EDDY BASED FISH GUIDANCE SYSTEM (EGS) (PART-2) 497
SILVA, Ana T.; ALDVEN, David; MÜLLER, Stephanie Muller; LILLEBERG, Eric; PANDEY, Kamal; VETSCH, David F.; CALLES, Olle; BOES, Robert M.; FORSETH, Torbjørn; ALBAYRAK, Ismail

DEVELOPMENT OF AN IMAGE ANALYSIS-BASED METHOD FOR TRACKING FISH BEHAVIOR IN VERTICAL SLOT FISHWAYS 501
RABU, Corentin; TREMBLAIS, Benoit; PETERI, Renaud; MASCARILLA, Laurent; DAVID, Laurent; CALLUAUD, Damien

STATUS OF UPSTREAM FISHWAYS IN NORWAY 505
STRANZL, Sebastian Franz; TEIXEIRA DA SILVA, Ana Margarida Ferreira; PULG, Ulrich

DOWNSTREAM FISH PASSAGE EVALUATION USING BAROTRAUMA DETECTION SENSORS: COMPARATIVE INSIGHTS FROM NORWEGIAN AND SWEDISH HYDROPOWER PLANTS 509
CAROLLI, Mauro; SUNDT, Håkon; SABIL, Sahra; HARBY, Atle; TUTHAN, Jeffrey; MUSETH, Jon; CALLES, Olle; FÖRST, Markus P.

DESIGN OF A COMBINED FISH LADDER AND VERTICAL LIFT FOR RESTORING FISH MIGRATION AT THE AIROLO RESERVOIR 513
MAZZOCCHI, Eugenio; TOGNOLA, Fabio; CAMPARADA, Federico; MONAI, Bernhard

FROM REGULATION TO REALITY: ECOHYDRAULIC CHALLENGES OF FISH PASSAGE DESIGN FOR SMALL HYDROPOWER IN ALPINE AND CENTRAL EUROPEAN RIVERS 517
BALZARINI, Alex; HOCHSCHWAZER, Mathias; GOSTNER, Walter

Session C3: Bioengineering approaches and Nature-Based Solutions (river) 521

REHABILITATING MACROPHYTE COMMUNITIES IN REGULATED LAKES AND RESERVOIRS USING A LAKE-IN-RESERVOIR 523
RÖJNING, Linda; WIDÉN, Åsa; HOLMGREN, Kerstin; ÖSTERGREN, Johan

SMALL SCALE EXPERIMENTAL INVESTIGATION OF LARGE WOOD REGULATION EFFECTS DUE TO ARTIFICIAL LOG JAMS AND BEAVER DAMS ANALOGS 527
DELTOMBE, Zoé; PITON, Guillaume; FRUCTUS, Natacha; PINJON, Samuel; BORGNIET, Laurent; EVETTE, André

HYDRAULICS OF MACRO-ROUGHNESS ELEMENTS FOR RIVER RESTORATION: LABORATORY EXPERIMENTS 531
SPELTONI, Simone; WEITBRECHT, Volker; BOES, Robert M.; SCHALKO, Isabella

MECHANICS OF ASYMMETRIC AND SYMMETRIC ROOTS UNDER PULL-OUT FORCE 535
KANG, Junjia; CALVANI, Giulio; DE CESARE, Giovanni; PERONA, Paolo

SOIL AND WATER BIOENGINEERING FOR RIVERBANK STABILIZATION: IMPLEMENTING MORE ROBUST STRUCTURES BASED ON A BETTER UNDERSTANDING OF FAILURE PROCESSES. 537
LEBLOIS, Solange; PITON, Guillaume; EVETTE, André

MODERNIZATION AND LEGACY: ECOHYDRAULIC EVOLUTION OF THE BEAUHARNOIS–LES CÈDRES COMPLEX, BUILT LONG BEFORE TODAY'S ENVIRONMENTAL REQUIREMENTS 541
ALFARO, Carola; NG, Karen; SADOCH, Nicolas; GUAY, Jean-Christophe; LANGLOIS, Simon; CHEVRIER-BÉDARD, Yannick; MEHRABI JIRANDEHI, Parisa

Session C4: Sediment transport and connectivity 545

AI-ENHANCED PREDICTION SYSTEM FOR TURBIDITY AND ECOLOGICAL STRESS MANAGEMENT UNDER EXTREME RAINFALL 547
CHUNG, Sewoong; KWON, Hyunhan; CHO, Honglae; KIM, Sungjin; KIM, Dongmin

NUMERICAL ANALYSIS OF MORPHOLOGICAL RESPONSES TO FLOOD EVENTS IN THE GEUM RIVER, KOREA 551
JANG, Chang-Lae; BAEK, Tae Hye

LAGRANGIAN MODELING OF PASSIVE PARTICLE TRANSPORT IN ANASTOMOSING RIVERS: LINKING CHANNEL GEOMETRY AND SEDIMENT PROCESSES USING RANDOM WALK ALGORITHMS – A CASE STUDY OF THE UPPER NAREW RIVER 555
KICZKO, Adam; KRAJEWSKI, Adam; MARCINKOWSKI, Paweł

MODELLING BRAIDED RIVERS IN DATA-SCARCE REGIONS: DATA COLLECTION AND MODEL SETUP 559
SCHWEDHELM, Hannah; SCHMID, Hannah; DALLMEIER, Antonia; RÜTHER, Nils

IMPACT OF FLOODS ON SEDIMENT DYNAMICS: LABORATORY-SCALE EXPERIMENTS TO ENHANCE SPAWNING HABITAT RESTORATION 563
GRATTEPANCHE, Florent; GOMIT, Guillaume; CALLUAUD, Damien; COURRET, Dominique; SAGNES, Pierre

BENTHIC SEDIMENT TRANSPORT PROCESSES UNDER ENERGETIC RIVER FLOW REGIMES: PART I, A NEW MULTIFREQUENCY ACVP INSTRUMENTATION FOR TWO-PHASE LIGHT-WEIGHT PARTICLE EXPERIMENTS 567
YON-CAMPANER, Oriana; LERNOULD, Maxime; BARRAUD, Pierre-Alain; FROMANT, Guillaume; HURTHER, David

BENTHIC SEDIMENT TRANSPORT PROCESSES UNDER ENERGETIC RIVER FLOW REGIMES: PART II, NOVEL SAND-LADEN OPENCHANNEL FLOWS 571
REYMOND, Christophe; HUTHER, David; DE CESARE, Giovanni

MORPHODYNAMICS AND CONNECTIVITY IN RIVER WIDENING TRANSITIONS 575
VAN MOL, Romain; DE CESARE, Giovanni

SUSPENDED SEDIMENT TRANSPORT DURING EXPERIMENTAL FLOODS IN THE SPÖL: MONITORING AND POTENTIAL DOWNSTREAM CONSEQUENCES 579
DEMMEL, Sophia; AGOSTINI, Ludovico; DROUJKO, Jessica; MOLNAR, Peter

Session C5: Ecohydraulics of the hyporheic Zone 583

HYPORHEIC MACROINVERTEBRATE COMMUNITIES AND PHYSICOCHEMICAL CONDITIONS REFLECT REACH SCALE SUBSTRATE COMPOSITION 585
MATHERS, Kate; MCKENZIE, Morwenna; WOOD, Paul

PERMEABILITY CONTROLS ON SALMON REDD HYPORHEIC HYDRAULICS 589
MONSALVE, Angel; HILLIARD, Brandon; TONINA, Daniele

SPATIAL DISTRIBUTION OF FINE SEDIMENT AND JUVENILE FRESHWATER MUSSEL SETTLING IN THE GRAVEL BEDDED DAN RIVER, NORTH CAROLINA 593
BUEHRER, Ellie; SHACHERI, Fatemeh; ALIF, Muhammad; CZUBA, Jonathan

ASSESSING THE INTEGRATION OF HYPORHEIC EXCHANGES INTO SALMONID SPAWNING HABITAT MODELS 597
RONCORONI, Matteo; GILLIS, Carole-Anne; BECK, Allen; THERRIEN, René; BERGERON, Normand

Session D1: Impact and mitigation measures of coastal structures 601

DESIGNATION OF ENVIRONMENTAL DEGRADATION ZONES WITHIN THE COASTAL AREA 603
HUANG, Wei-Po; CHIANG, Chorng-Yeu; YE, Chun-Jhen; HSU, Jui-Chan

INFLUENCE OF SHIP WAKE DYNAMICS ON SURFACE AND INTERIOR CIRCULATION IN THE HOUSTON SHIP CHANNEL 607
BHEEROO, Vivek; LEE, Mu-Jung; SOCOLOFSKY, Scott; CHANG, Kuang-An

PREDICTING PROPAGULE DISPERSAL IN COASTAL WETLAND 611
BOSSAER, Laura; FIVASH, Gregory; SCHOUTENS, Ken; VAN DER STOCKEN, Tom; VAN DE KOPPEL, Johan; BOUMA, Tjeerd; TEMMERMAN, Stijn

A STOCHASTIC APPROACH FOR RECOVERY TIMES OF COASTAL DUNE VEGETATION 615
DEMICHELE, Davide; CAMPOREALE, Carlo

Session D3: Bioengineering approaches and Nature-Based Solutions (coast) 619

COMPARATIVE ANALYSIS OF NATURAL AND ARTIFICIAL WAVE ATTENUATION: EFFECTS OF BAYS AND WAVE FENCES ON WIND- AND BOAT-INDUCED WAVES 621
SCHERBAUM, Susanne; FUCHS, Yannic; SCHNEIDER, Josef

NUMERICAL MODELLING APPROACHES FOR WAVE ATTENUATION USING SEAGRASS AND OYSTER REEFS: A SYSTEMATIC LITERATURE REVIEW 625
GHASEMI, Hani; DASTGHEIB, Ali; O'SULLIVAN, John; SALAUDDIN, Md

NEW INSIGHTS ON THE EFFECT OF A CURRENT ON THE WAVE ATTENUATION INDUCED BY A SUBMERGED FLEXIBLE CANOPY 629
VETTORI, Davide

APPLICATION OF ENVIRONMENTAL DNA IN THE ECOLOGICAL STUDY OF ARTIFICIAL WETLANDS IN MACAO 633
ZHOU, Yi; WANG, Zhao-yin; XU, Meng-zhen; JIANG, Sabrina Yanan; SUN, Bang-jie

Session E1: Remote sensing 637

DECADAL RIVER TEMPERATURE DYNAMICS IN A MEANDERING SYSTEM 639
GHAHRAMAN, Kaveh; NONES, Michael

A REMOTE AND DATA-DRIVEN APPROACH FOR IDENTIFYING POTENTIAL REPLACEMENT WETLANDS USING SATELLITE AND REANALYSIS DATA: A CASE STUDY OF THE KOREAN PENINSULA . 643
SUNG, Jeemi; HWANG, Seunghyun; KU, Seoyeong; BAIK, Jongjin; JUN, Changhyun

EVALUATION OF A RIVER-SCALE FLOW MODEL WITH LIDAR BATHYMETRY FOR SALMONID CONSERVATION IN THE HEDDØLA RIVER, SOUTHWESTERN NORWAY 647
WEBER, Arnaud; ALFREDSEN, Knut; STICKLER, Morten; DE CESARE, Giovanni

USING UNMANNED AERIAL SYSTEMS FOR MEASUREMENTS OF WAVES, NEAR-SURFACE CURRENTS AND BATHYMETRY IN COASTAL ENVIRONMENTS 651
CHANG, Kuang-An; BHEEROO, Vivek; LEE, Mu-Jung; WU, Ting-Chu; TORRES-FREYERMUTH, Alec; SOCOLOFSKY, Scott

SPATIAL DISTRIBUTION OF THE PROBABILITY OF PRYMNESIUM PARVUM OCCURRENCE IN THE ODER RIVER 655
SUSKA, Katarzyna; KOPEĆ, Dominik; NIEDZIELKO, Janek; CHARYTON, Jakub; ŁAWNICZAK, Karol; NAPIÓRKOWSKA-KRZEBIETKE, Agnieszka; PARASIEWICZ, Piotr

AUTOMATING DTM BATHYMETRIC CORRECTION FROM GAUGING STATION DATA: A METHODOLOGICAL ASSESSMENT 659
CACCAMO, Elisa; CAMPOREALE, Carlo Vincenzo

Session E2: Real time monitoring 663

A NOVEL SENSOR-BASED APPROACH TO QUANTIFY FISH PASSAGE DELAY DYNAMICS IN ARCHIMEDEAN SCREWS. 665
BROOS, Sarah; PAUWELS, Ine S.; BUYSSE, David; BRUNEEL, Stijn; DE MULDER, Tom; TOMING, Gert; TUHTAN, Jeffrey A.

GAS SUPERSATURATION: FROM RISK ASSESSMENTS TO FIELD MONITORING IN NORWAY AND SWEDEN 669
VARTIA, Ida; PULG, Ulrich; ENQVIST, Martin; HAMPER, Rowan; STRANZL, Sebastian

THE IMPACT OF HYDROPOWER ON DEEP RIVER HABITAT HETEROGENEITY 673
HABERSETZER, Luis Philipp; SILVA, Luiz G. M.; STOCKER, Roman; BRODERSEN, Jakob

LOW-COST SENSORS IN ALPINE HEADWATERS : FONCTIONALITY AND PERFORMANCE 677
PIRLOT, Pascal; FIKENTSCHER, Nils; NOACK, Markus

RETRACE: A MODULAR FRAMEWORK FOR EVENT-BASED DISCHARGE AND SUSPENDED SEDIMENT ANALYSIS 681
AGOSTINI, Ludovico; MOLNAR, Peter

Session E3: AI approaches 685

A MODELING AND MACHINE LEARNING FRAMEWORK FOR PREDICTING SEDIMENT SPILL DEPOSITION 687
WANG, Binbin; XU, Ruichen; SUN, Qingqing; DENG, Baolin

MONOCULAR FISH LENGTH ESTIMATION FOR VIDEO TUNNELS IN EUROPEAN RIVERS 691
IVANOV, Aleksandr; KOLOSOVA, Alexandra; TUHTAN, Jeffrey Andrew; MOCKENHAUPT, Bernd; SCHEIFHACKEN, Nicole

IDENTIFICATION OF INLAND WETLAND BIODIVERSITY DRIVERS USING EXPLAINABLE ARTIFICIAL INTELLIGENCE AND SATELLITE-BASED REMOTE SENSING DATABASE 695
HWANG, Seunghyun; SUNG, Jeemi; KU, Seoyeong; BAIK, Jongjin; JUN, Changhyun

MACHINE LEARNING–BASED PREDICTION OF SUSPENDED SEDIMENT TRANSPORT IN CHILEAN RIVERS UNDER PROLONGED DROUGHT CONDITIONS 699
CID VARGAS, María José; CAAMAÑO AVENDAÑO, Diego; GAMBOA MÉNDEZ, Maribet

RIVER.FEATURES: AN OPEN ANNOTATED UAV IMAGE DATASET FOR RIVER MONITORING AND MACHINE LEARNING 703
SOTO PARRA, Tulio; ČEHOVIN ZAJC, Luka

REDUCING HUMAN ANNOTATION EFFORT FOR AI FISH COUNTERS USING CONFORMAL PREDICTION 707
KOLOSOVA, Alexandra; TUHTAN, Jeffrey A.

AN AI-BASED EULERIAN–LAGRANGIAN MODEL FOR FISH MOVEMENT NEAR A FISHWAY ENTRANCE 711
EL HACHEM, Abbas; HENNING, Martin; NOSS, Christian

DEEP LEARNING BASED VEGETATION HEIGHT ESTIMATION- CASE STUDIES IN ITALY AND POLAND 715
GUO, Yiwei; NONES, Michael; QI, Yitian

ESTIMATING LABORATORY RELATIVE BLADE STRIKE VELOCITIES WITH A RIGID CYLINDRICAL PLASTIC SENSOR 719
TUHTAN, Jeffrey A.; KÖSTERS, Iring Wolf; TOMING, Gert; ABBASZADEH, Shokoofeh; HOERNER, Stefan

ANOMALY DETECTION AND AUTOMATIC DATA CORRECTION FOR HYDROMETRIC STATIONS . . 723
PIROOZMAND, Pasha; FARSHI, Davood

Session F: Swiss Ecohydraulics Day 727

"BRI: BIOENGINEERED RIVER ISLAND" A PROMISING CONSTRUCTION TYPE FOR RIVER RESTORATION. CONSTRUCTIVE APPROACHES AND PRACTICE-BASED EXPERIENCES. 729
NEUHAUS, Vasco; RACHELLY, Cristina; MEIER, Luzia

RISK OF FISH INJURIES WHEN INTERACTING WITH ELECTRIFIED BAR RACKS 733
MOLDENHAUER-ROTH, Anita; SÜSS, Gabor; SILVA, Luiz G.M.; MOECKLI, Celine; DISERENS, Nicolas; ALBAYRAK, Ismail; BOES, Robert M.

LABORATORY PROOF OF WATER RETENTION AND BANK STORAGE BY THE IMPLEMENTATION OF BEAVER DAM ANALOGS (BDA'S) 737
JENZER ALTHAUS, Jolanda; WEBER, Matthias; FLEPP, Gianluca; GRÜNIG, Dominic; WIRTH, Stefanie

TECHNO-ECONOMIC AND ENVIRONMENTALASSESSMENT OF THE APPLICATIONS OF BATTERYENERGY STORAGE SYSTEMS (BESS) IN STORAGEHYDROPOWER PLANTS FOR FLEXIBLE POWER REGULATIONAND HYDROPEAKING MITIGATION 741
COURTOIS, Marc-Antoine; MANSO, Pedro; DE CESARE, Giovanni; DEHAIL, Vincent

SMOLTCAMERA: DEVELOPMENT OF A NON-INVASIVE, AI-ASSISTED CAMERA TECHNOLOGY FOR MONITORING MIGRATION LAKE-RUN BROWN TROUT SMOLTS 745
DE SCHAETZEN, Frederic; G.M. SILVA, Luiz; MEYER, Matthias; SCHWEIZER, Steffen

Session PS: Poster Session 749

STABILISING RIVERBANK TOE USING SOIL AND WATER BIOENGINEERING AND LARGE WOOD STRUCTURES : PRELIMINARY FINDINGS OF PHYSICAL MODEL EXPERIMENTS 751
FRUCTUS, Natacha; DELTOMBE, Zoé; EVETTE, André; DELAYE, Julie; RECKING, Alain

EXPERIMENTAL STUDY ON AERATION CHARACTERISTICS OF HIGH-SPEED OPEN CHANNEL FLOW UNDER DIFFERENT ATMOSPHERIC PRESSURE 755
LIANG, Haoran; WEI, Wangru; QIU, Yuxuan; DENG, Ju; LIU, Mingjiang; RAN, Yubo; LONG, Qiang

FROM DATA TO DESIGN: HYDRAULIC STAGES FOR FISH PASS DEVELOPMENT IN SMALL HYDROPOWER PLANTS ON THE RHÔNE RIVER 759
GUDOT, Aurélien; CORRALES LALINDE, Emilio; BARTHOUT, Théo

VALIDATING A 2D NUMERICAL MODEL OF FLOW IN VERTICAL SLOT FISHWAYS: THE ARTO-BLANCA CASE STUDY 763
BOMBAČ, Martin; RAK, Gašper

EVALUATING REMOTE SENSING-ENABLED MACHINE LEARNING FOR SALINITY PREDICTION IN THE VIETNAMESE MEKONG DELTA 767
SANG, Ngo Tran; BINH, Doan Van; THY, Pham Thi Mai; KANTOUSH, Sameh Ahmed; AN, Tran Thi; VUONG, Nguyen Dinh

MORPHOLOGICAL EVOLUTION OF THE PRÉVERENGES BIRD ISLAND AND TOMBOLO FORMATION 771
GIL, Thomas; AMINI, Azin; DE CESARE, Giovanni

ECO-HYDRAULICS SOLUTIONS FOR WAVE ATTENUATION: THEORETICAL, NUMERICAL AND EXPERIMENTAL ANALYSIS 775
DE PADOVA, Diana; BEN MEFTAH, Mouldi; DE SERIO, Francesca; MOSSA, Michele

HORIZONTAL SCREENS FOR FISH PROTECTION AND GUIDANCE – SYNOPSIS OF EFFICIENCY EVALUATION 779
GEIGER, Franz; CUCHET, Mathilde

PHENOMENOLOGICAL MODELLING OF SPACE-TIME EJECTION-SWEEP SEQUENCES 783
SPOLETINI, Nicola; PERONA, Paolo

PREDICTING BROWN TROUT DISPERSAL PATTERN UNDER DIFFERENT FLOW REGIMES USING A HABITAT-SUITABILITY-DRIVEN METAPOPULATION MODEL 787
PADOAN, Francesca; CALVANI, Giulio; KNOBLAUCH, Alexandra E.; WAGNER, William; DECESARE, Giovanni; PERONA, Paolo

INTEGRATED MANAGEMENT OF LOW-FLOW HYDRAULICS: A METHODOLOGICAL FRAMEWORK APPLIED TO THE AIRE AND DRIZE 791
SALAMIN, Brian; ARBORINO, Tony; GRAZIOLI, Jacopo; PIDOUX, Franck; PERONA, Paolo

AVERAGE LIFETIME OF RIPARIAN VEGETATION FROM STOCHASTIC EROSION AND DETERMINISTIC RECOVERY 795
CALVANI, Giulio; PERONA, Paolo

ECOHYDRAULIC MANAGEMENT OF SATURATION-EXCESS BRACKISH WATER PONDING IN NOUAKCHOTT, MAURITANIA 799
PRAPLAN, Elouan; ABIDINE, Mohamed Mahmoud; TALEB, Moustapha; DUBOIS, Emmanuel; SALECK, Maimouna; BOUKHREISS, Fatimetouh; BRUNNER, Philip; PERONA, Paolo

LAB EXPERIMENTS TO UNRAVEL DYNAMOTROPISM IN RIPARIAN PLANT ROOTS 803
ELIYAHU-YAKIR, Yahel; DE CESARE, Giovanni; PERONA, Paolo

MODELLING FREE-SURFACE FLOW CONSTRUCTED WETLANDS TO IMPROVE SEDIMENT FILTERING EFFICIENCY: THE CASE OF THE SKUTERUD WETLAND, NORWAY 807
LIU, Jiaqi; BREGOLI, Francesco; UIJTTEWAAL, Wim; CALVANI, Giulio; KRZEMINSKA, Dominika; BLANKENBERG, Anne-Grete B.; MCCLAIN, Michael

A PROCESS-BASED ECOHYDRAULIC FRAMEWORK FOR VADOSE-ZONE RESPONSES TO SALINITY FORCING INDUCED BY SALTWATER INTRUSION 811
AGHAEI, Yasamin; PERONA, Paolo

COMPARISON OF LIDAR TECHNOLOGIES FOR MONITORING OF STREAM BANK MORPHOLOGY . 815
STIHL, Elia; GÜNTER, Mark; SCHWARZ, Massimiliano

SYNTHESIS OF LONG-TERM ECOHYDRAULIC OBSERVATIONS UNDER REGULATED AND SPRING-FED FLOW REGIMES IN PERI-URBAN TOKYO 819
FUKUDA, Shinji

SPH MODELING OF SALINITY TRANSPORT PHENOMENA IN NAVIGATION LOCKS 823
CALVO, Lucas; SERRANO, Noé; FABREGA, José

Session A1

Interactions between flow, natural elements, and structures

Book of Abstracts of the *16th International Symposium on Ecohydraulics*
Challenges and solutions in the time of global changes
August 16–20, 2026, Lausanne, Switzerland
ISSN: 2790-2420 | ISBN: 978-90-837233-9-6 | doi:[10.64697/iahr.proc.ise2026.abs]
© 2026 IAHR. CC BY-NC-ND 4.0

LOCAL SCOUR AROUND A SINGLE PIER ON A TRANSVERSALLY INCLINED BED

Gokcen BOMBAR[1], Firat GUMGUM[2] , António Heleno CARDOSO[3]

[1] Professor, Department of Civil Engineering, İzmir Katip Çelebi University, Izmir, Turkey.
email: gokcen.bombar@ikcu.edu.tr

[2] Asst. Professor, Department of Civil Engineering, Dicle University, Diyarbakir, Turkey.
email: firat.gumgum@dicle.edu.tr

[3] Professor, Departamento de Engenharia Civil, Arquitetura e Ambiente, Civil Engineering Research and Innovation for Sustainability, Instituto Superior Técnico, Universidade de Lisboa, Lisboa 1049-001, Portugal.
email: antonio.cardoso@tecnico.ulisboa.pt

ABSTRACT

This study examines the effect of a 25% transverse bed slope on local scour around a circular pier. The experiment was performed under clear-water conditions with uniform sediment. Scour development was monitored continuously using an Acoustic Doppler Velocimeter, and the final bed and water surface elevations were measured after seven days. Results showed rapid scour in the first 12 hours, followed by gradual deepening. A six-parameter polynomial accurately represented the time evolution, predicting an equilibrium depth of 15.23 cm, approximately 11% higher than the final depth. The scour hole exhibited strong asymmetry: a steeper, deeper side slope formed on the shallow side of the pier, whereas the deep side displayed a gentler slope and a smaller scour depth. Excavated sediment from the scour hole was deposited at the deep side of the bank.

Keywords: Local scour; bridge piers; transverse slope; transverse inclination.

1. Introduction

Local scour around bridge piers has long been of interest to researchers, and the role of geometric conditions have been extensively studied. One conditions that is not much considered is the transverse slope of the bed. Beds in natural streams are often transversely inclined near the banks, where the flow features and the critical velocity for incipient sediment motion change with the inclination, causing the scour holes to be different from those commonly reported in literature (Bombar and Cardoso, 2024). This study aims at investigating the effect of transverse bed inclination on the scouring process at a circular bridge pier to contribute for the proper design of bridge piers and the associated scour countermeasures. The analysis is based on a clear-water scour experiment conducted with uniform sediment. The temporal evolution of the scour depth and the changes in the bed topography were analyzed.

2. Experimental Setup

The experiment was carried out in a 9 m long and 1 m wide open channel. A schematic of the experimental setup, with all dimensions in centimeters, is shown in Figure 1. A 1.6 m long and 11 cm deep recess box existed at the channel bottom, starting 5.4 m from the upstream end. The entire channel bottom, defined as $z = 0$, and the recess were covered with uniform sand ($\sigma_g = 1.35$) of median grain size $d_{50} = 0.86$ mm. The sand thickness was 1.5 cm at the deep side of the bank (simulated as an inclined bed) and 26.5 cm at the shallow side, providing a transverse slope of 25%. A circular pier with diameter $b = 11$ cm was positioned within the recess, with its center located 39 cm from the deep side wall and 6.2 m from the upstream channel end.

A constant discharge $Q = 32$ ℓ/s was supplied, corresponding to an approach flow depth $d = 15.3$ cm at the pier centerline. The discharge was measured using an electromagnetic flowmeter with an accuracy equal to ± 0.5 ℓ/s. The experiment lasted approximately seven days. At the end of the test, bed elevations were densely surveyed using an UltraLab UWS Miniature Echo Sounder (± 1 mm), while water levels were also profusely recorded with a Baumer Ultrasonic Distance Measurement Sensor (± 5 mm). Both probes were mounted on a

robotic arm capable of three-axis movement. The temporal evolution of scour depth at the leading edge of the pier was continuously monitored with a down-looking Nortek Vectrino Acoustic Doppler Velocimeter (ADV).

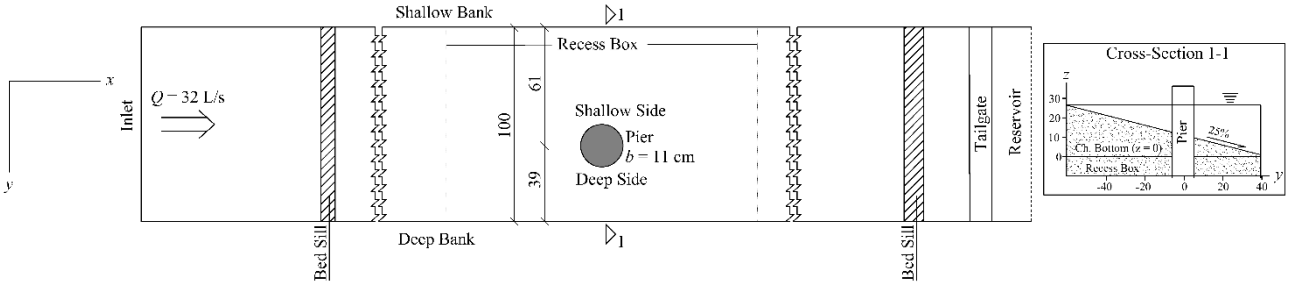

Fig. 1. The general view of the experimental setup.

3. Results and Conclusions

The temporal evolution of the scour depth at the leading edge of the pier is shown in Figure 2. The scour depth, d_s, increased quite rapidly during the first 12 hours, and then exhibited a slight yet sustained increase.

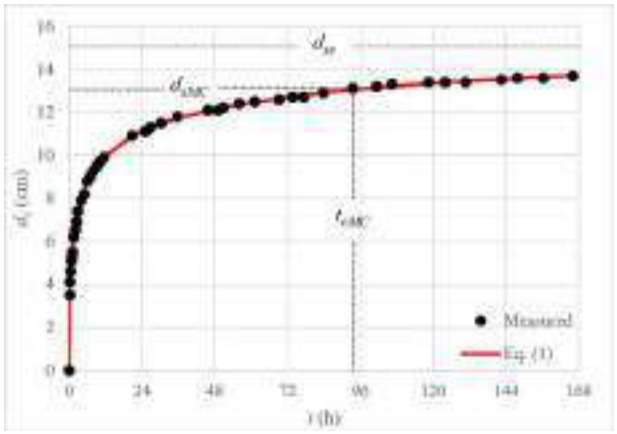

Fig. 2. The temporal evolution of the scour depth at the leading edge of the pier

Some researchers (e.g., Kothyari et al. 1992, Oliveto and Hager 2002, Lança et al. 2010) suggested that the scour depth continues to increase over time and that the equilibrium can only be achieved at $t = \infty$. Since it is not possible to continue an experiment that long, Lança et al. (2010) modified the polynomial of Bertoldi and Jones (1998) and adjusted it to long time-registers of the scour depth to estimate its equilibrium value at $t = \infty$. Their six parameters polynomial reads

$$d_s(t) = \ell_1 \frac{t/\tau_1}{1 + t/\tau_1} + \ell_2 \frac{t/\tau_2}{1 + t/\tau_2} + \ell_3 \frac{t/\tau_3}{1 + t/\tau_3} \tag{1}$$

where ℓ_i and τ_i are coefficients obtained by minimizing the root mean square error (RMSE) of the adjustment. For $t = \infty$, $d_s(t)$ becomes the equilibrium scour depth, $d_{se} = \ell_1 + \ell_2 + \ell_3$. Figure 2 shows that the curve obtained from Eq. (1) displays an excellent fit to the measurement points, yielding a d_{se} value of 15.23 cm at $t = \infty$. This value is 1.11 times greater than that read at the end of the experiment after 7 days. According to Melville and Chiew (1999), the equilibrium scour depth, d_{sMC}, is reached when the scour depth increases no more than 5% of the pier diameter in the preceding 24 hours. The value of d_{sMC} and the associated time duration, t_{eMC}, as defined by Melville and Chiew (1999) were also indicated in Figure 2. It can be seen that the experiment continued for almost 3 days after t_{eMC}; d_{sMC} was found to be almost 4% and 14% smaller than the final and the equilibrium scour depth values, respectively.

Figure 3a and Figure 3b illustrate, respectively, the transverse and longitudinal profiles of the bed defined at the center of the pier. In the figure, z_0 denotes the initial bed level and z_f the final bed level. The greatest scour depth was registered close to the leading edge of the pier, slightly shifted toward the shallow side. The scour hole was markedly more extensive on the shallow side of the pier in comparison to the deep side. At the leading edge and on the shallow side of the pier, the slope of the scour hole slightly exceeded the tangent of the bed material's internal friction angle, θ_r, whereas on the deep side it was noticeably gentler. As expected, the smallest scour depth was observed near the trailing edge. Unlike the horizontal bed case, where the excavated material accumulates symmetrically along the x-axis in the wake, the excavated sediment was deposited mostly at the deep side of the bank.

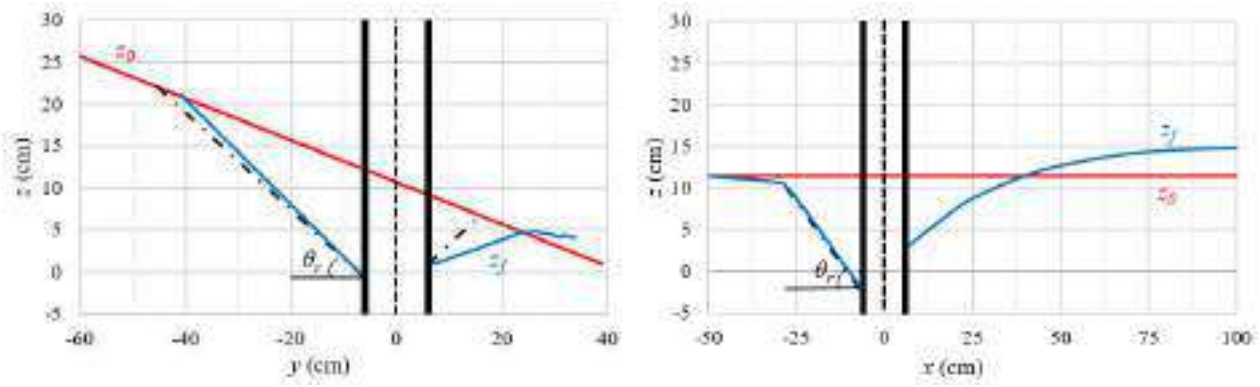

Fig. 3. a) transverse and, **b)** longitudinal profiles of the bed defined at the center of the pier.

References

Bombar G, Cardoso AH (2024) Effect of transversal bed slope on the equilibrium scour depth at bridge piers, Journal of Hydraulic Engineering, 150(4), 04024015.

Bertoldi DA, Jones JS (1998) Time to scour experiments as an indirect measure of stream power around bridge piers, In: Water Resources Engineering '98, ASCE, 264–269.

Kothyari UC, Garde RCJ, Ranga Raju KG (1992) Temporal variation of scour around circular bridge piers, Journal of Hydraulic Engineering, 118(8), 1091–1106.

Melville BW, Chiew YM (1999) Time scale for local scour at bridge piers, Journal of Hydraulic Engineering, 125(1), 59–65.

Oliveto G, Hager WH (2002) Temporal evolution of clear-water pier and abutment scour, Journal of Hydraulic Engineering, 128(9), 811–820.

Lança RM, Fael CS, Maia RJ, Pêgo JP, Cardoso AH (2013) Clear-water scour at comparatively large cylindrical piers, Journal of Hydraulic Engineering, 139(11), 1117–1125.

Book of Abstracts of the *16th International Symposium on Ecohydraulics*
Challenges and solutions in the time of global changes
August 16–20, 2026, Lausanne, Switzerland
ISSN: 2790-2420 | ISBN: 978-90-837233-9-6 | doi:[10.64697/iahr.proc.ise2026.abs]
© 2026 IAHR. CC BY-NC-ND 4.0

LEAF-TO-STEM FLEXIBILITY RATIO MODULATES FLOW IMPEDANCE BY FOLIAGE

Rufus E. DICKINSON[1,2], Kazumasa MATSUMOTO[3], Timothy I. MARJORIBANKS[1], Michio SANJOU[3], Christopher J. KEYLOCK[1], Takaaki OKAMOTO[4]

[1] Loughborough University, United Kingdom
email: R.Dickinson@lboro.ac.uk
email: T.I.Marjoribanks@lboro.ac.uk
email: C.J.Keylock@lboro.ac.uk

[2] JSPS International Research Fellow (Graduate Kyoto University)

[3] Kyoto University, Japan
email: Matsumoto.Kazumasa.3z@kyoto-u.ac.jp
email: Sanjou.Michio.6c@kyoto-u.ac.jp

[4] Meijo University, Japan
email: OkamotoT@meijo-u.ac.jp

ABSTRACT

For many types of flexible vegetation which block waterways, collect sediment, and provide shelter to fauna, foliage, rather than stems and branches, is the main source of plant surface area that has the potential to disrupt flow. Despite the variation in leaf flexibility across species, and the prevalent theory of flow-induced reconfiguration for plant stems, there is an imbalance in understanding regarding leaves and foliage, focusing on simple quantification of foliage density rather than flexibility. Seeking to correct this, we apply a recently developed theoretical perspective on leafy stems to experimentally study their behaviour in submerged patches spanning an open channel flow. We vary the ratio of leaf-to-stem flexibility, and control for vegetation density, testing over a range of flow velocities. Our results from Particle Image Velocimetry show differences in time and depth-averaged velocity and turbulent kinetic energy in the near and intermediate wake, suggesting that the applied theoretical perspective should be used to modulate understanding of foliage density.

Keywords: Foliated Flow, Flexible Reconfiguration, Particle Image Velocimetry, Physical Theory

1. Introduction

It is widely understood that patches and canopies of flexible vegetation provide a unique obstruction to flow, and that their effects span many topics of Ecohydraulics, as they shelter fauna (Baladrón *et al.*, 2021), alter sediment deposition (Matsumoto *et al.*, 2025), drive nutrient mixing (Field *et al.*, 2023), and impede flow. Much of the vegetation that is of interest to Ecohydraulics is foliated - river weeds, saltmarsh grasses, kelp, and mangrove shrubs – but there is still a need for strong theories to explain the effects of foliage (Maio *et al.*, 2025), and complex morphology in general (Boothroyd *et al.*, 2016; Marjoribanks, 2023). Zhang and Nepf (2021) modelled a collection of leafy saltmarsh plants, but their method benefits from the similarity of biomechanical properties between the stem and leaves, so cannot be generally descriptive. In one recent work (Hang *et al.*, 2025), the principles of flow-induced reconfiguration (Luhar and Nepf, 2011) were applied to model the flexible leaves of *Kandelia obavata*, but since that plant's stems are effectively fully rigid, this is also an isolated special case. One reason for the lack of theoretical underpinning is the complexity of foliated reconfiguration; it has long been known that the percentage contribution to drag by foliage depends on the fluid speed (Aberle and Järvelä, 2013), which presents difficulty in making any extension of leafless theory.

However, recent theoretical and computational work (Dickinson *et al.*, 2026) has provided the broadest theory to-date of flow-induced reconfiguration of leafy plant stems. The principle of "Isoanemeity", a term which

describes the relative reconfiguration of leaves and stem, predicts that most leafy stems undergo two stages of reconfiguration. Plants can therefore be classified by the order in which they progress through these stages (See Fig. 1), thus allowing well-reasoned application of different models. This framework is rooted in the theory of flow-induced reconfiguration (Luhar and Nepf, 2011), which states that the ratio of the drag force to stem rigidity (Given by the Cauchy number, Ca) is the dimensionless driver of reconfiguration of homogenous, neutrally buoyant plant stems. While Ca considers the drag force on a leafless stem, we may extend it to $\mathrm{Ca}^\star$ for a leafy plant, which accounts for the total drag, on the stem *and* leaves. One may also conceptualize of $\mathrm{Ca}_{\mathrm{leaf}}$, applying the single-stem reasoning to a single leaf (Zhang and Nepf, 2021), and then proceed with the ratio $\mathrm{Ia} = \mathrm{Ca}_{\mathrm{leaf}}/\mathrm{Ca}^\star$ which is the isoanemeity. A low value of Ia predicts stem-then-leaf reconfigurations (as the flow speed increases), and a high value predicts leaf-then-stem. The ability of this value to classify plant species based on their reconfigurations is valuable, as it has been concluded that a species-by-species approach seems inefficient (De Langre, 2012).

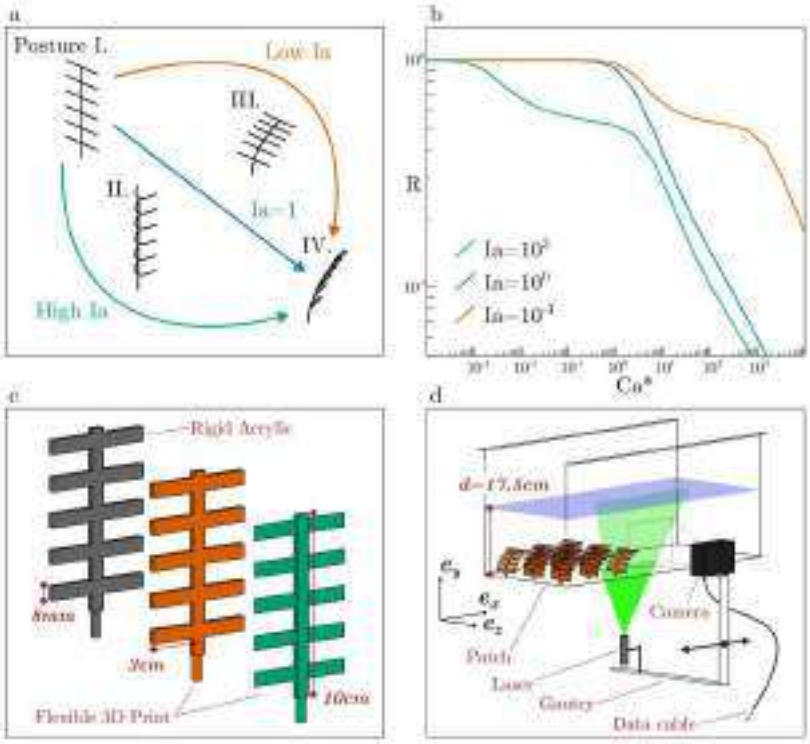

Fig. 1. (a) The varied stages of reconfiguration of leafy stems, as controlled by isoanemeity. (b) Reproduced results showing the degree of streamlining by different leafy stems, in terms of R = drag felt by flexible plant / drag felt by rigid equivalent plant (From Dickinson *et al.*, 2026). (c) Sketches of the three plant model types used. (d) Schematic of the flume experiment.

There have been several recent publications regarding hydraulic flume experiments with patches of foliated vegetation. Cornacchia *et al.* (2022) studied patches of different species of live plants, but their conclusions focused primarily on patch dimensions and population density, which varied across the species, but do not assist understanding of the foliage. Artini *et al.* (2024) and Liu *et al.* (2024) both studied bed-load transport under foliated canopies, considering the distribution of surface area along the main stem, but did not focus on the reconfiguration process. Caroppi *et al.* (2022) studied the wakes of foliated and then defoliated patches, demonstrating that seasonal defoliation strongly reduces impedance of flow. Results from Maio *et al.* (2025) corroborate this, but their additional tests varying leaf shape, to mimic species variance, did not see similarly significant results.

In summary, experimental research suggests that both the abundance and the distribution of foliage affect issues of ecohydraulics. Leaf flexibility has not so far been studied, however it impacts isoanemeity ($\mathrm{Ia} \propto EI_{\mathrm{stem}}/EI_{\mathrm{leaf}}$ where EI is flexural rigidity), and therefore reconfiguration mechanics; so it may potentially impact patch-scale processes. In light of this knowledge gap, and the new theoretical provisions relating to isoanemeity, the current work studies the ratio of leaf-to-stem flexibility at the patch scale, via hydraulic flume experiments.

2. Methodology

To study the wakes behind 3 patches of plants, 90 plant models were constructed with height h = 10 cm, so 30 of each type shown in Fig. 1c. The first type, the control, were made with 12mm laser-cut acrylic plastic, and

thus were rigid. The second and third types were flexible; 3D printed with NinjaTek NinjaFlex filament, which has a documented Young's modulus E = 12 MPa. The second ("flexible leaf") plant type was printed with leaves of 0.4 mm thickness and a stem 5 mm thick (EI = 5.1e-7 and 1e-3 Nm^2 respectively), and the third ("flexible stem") type with uniform 3 mm thickness (EI = 2e-4 Nm^2). Respectively, these correspond to rigidity ratios of 1950 and 1, or values of Ia = 13 and 0.0068.

The experiments were carried out in a 10 m hydraulic flume in the Katsura Turbulent Flow Laboratory at Kyoto University, Japan. The flume was reduced in width to 30 cm with weighted blocks, and two flow rates were picked to study the wakes before and after plant reconfiguration, yielding bulk velocities of U_0 = [10.5, 42.0] cms^{-1}. A schematic of the experiment is displayed in Fig. 2b. The plants were placed at the bottom of the flume: 10 mm thick boards of clear acrylic plastic were laid along the bottom, with 30x 10 mm holes drilled to hold the plant model roots. These were arranged in a staggered arrangement – alternating in streamwise rows 2-3-2-3… with 9 cm longitudinal gaps and 6 cm lateral – giving a patch length of 81 cm and thus surface area per-unit-volume of 3.95 m^{-1}. Particle Image Velocimetry (PIV) was used to study the flow dynamics in the wake of the patch, recording 2 ms separated image pairs at 30 Hz. The laser light sheet and high-speed camera used for this were mounted to a gantry which could be moved along the flume, allowing approximately 1 m of the wake to be studied by taking 1 minute recordings at 14 progressively downstream locations. Using the PIV datasets, we calculated time and depth-averaged streamwise velocity and two-axis turbulent kinetic energy in the vertical range $y < 0.8h$, to evaluate (1) the recovery of the wake in terms of transport of streamwise momentum to the wake zone and (2) the turbulence produced by each plant type.

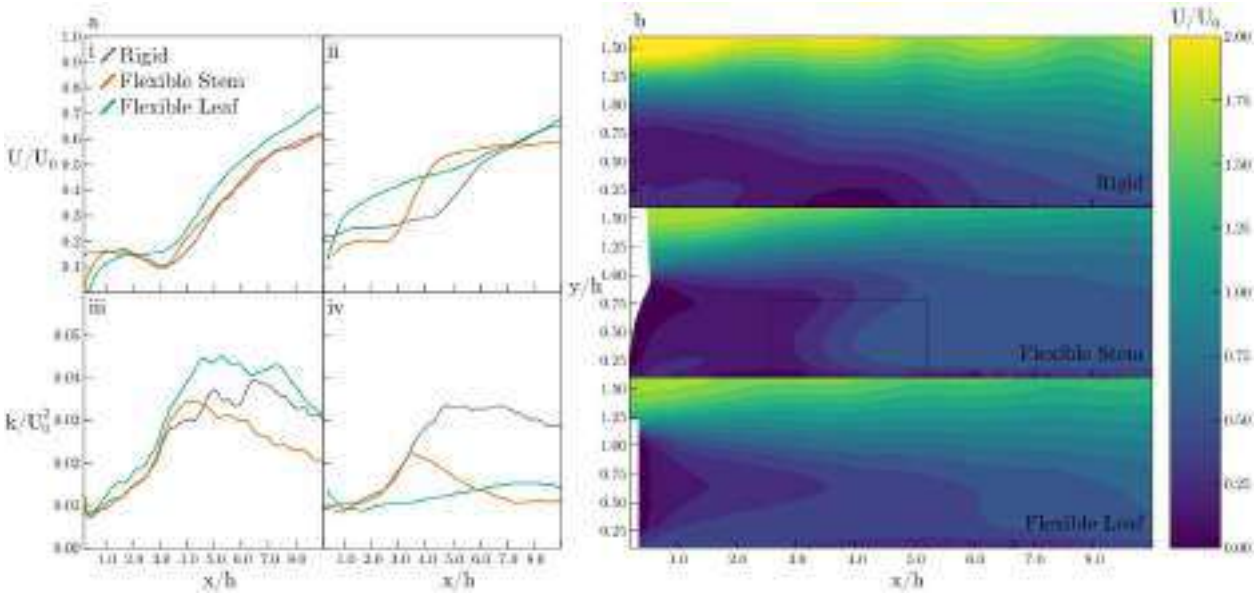

Fig. 2. Results of PIV analysis downstream of the plant patch (a) Streamwise-profiles of averaged velocity and turbulent kinetic energy in the wakes of each patch type: (i) and (iii) show results for U_0 = 10.5 cms^{-1}, and (ii) and (iv) for U_0 = 42.0 cms^{-1}. (b) Heatmaps of Reynolds-averaged velocity for the flexible leaf, flexible stem, and rigid plant patches.

3. Results

At the highest flow rate, both types of flexible plant exhibited significant reconfiguration. The flexible leaf plant reconfigured from posture I (See Fig.1a) to II, and the flexible stem plant to posture III. Time and depth-averaged velocities and turbulences are shown in Fig. 2a. At U_0 = 10.5 cms^{-1}, there was negligible deformation by any of the plants, and as such there is little difference, between plant types, in the profiles of velocity and turbulence. At U_0 = 42.0 cms^{-1} however, the plants had deformed to postures II and III, and this appears to produce different wake dynamics. Both flexible plant types, deforming either in their leaves or stems, appear to have shorter immediate wakes, and produce less turbulent kinetic energy, compared to the rigid plant type. While the average streamwise velocity behind the rigid patch recovers to $0.3U_0$ by $x = 4.4h$, this recovery is achieved behind the flexible stem by $x = 3.2h$ and by $x = 1h$ behind the flexible leaves. Interestingly, by $x = 7.2h$, all three wakes have recovered to $\sim 0.58U_0$, though the accordance is short-lived. In Fig. 2b, heatmaps of the Reynolds-averaged velocity are shown for the highest flow rate, and the differing shapes of the wakes suggest that different effects drive each one's recovery. For example, the immediate vertical profile of velocity behind the flexible leaf patch is the least pronounced, suggesting that it redirected less flow vertically, and is

therefore a less significant flow blockage. On the other hand, the flexible stem patch contains a surge in momentum between $x = 3h$ and $4h$ (dashed region in Fig. 2b), suggesting the presence of a secondary flow, which may be similar to that found by Matsumoto *et al.* (2025) downstream of a canopy of flexible grass.

4. Conclusion

Our experimental results are the first that investigate the ratio of leaf-to-stem flexibility as a standalone independent variable, and they demonstrate that it has an effect on near and intermediate wake dynamics. Whilst many recent experimental works have strived to use at least semi-realistic plant morphologies, our plants are novelly idealized. While this limits direct application of our findings to any specific species, we argue that it has allowed clarity in our results, by avoiding unwanted covariances, making it possible to study a single, key parameter. Due to the connection between the flexibility ratio and the recently theorized isoanemeity (Dickinson *et al.*, 2026), we suggest that isoanemeity is driving the differences we see between the flexible leaf / stem plant types. Further, since we have controlled foliage density, e.g. via leaf area index (Jalonen *et al.*, 2013), we suggest that isoanemeity specifically acts to modulate the impact of foliage density; since a patch with relatively flexible leaves appears to impede flow less efficiently, in terms of the loss in momentum and production of turbulence. Practically speaking, this means that vegetation patches of different plant species can impede flow differently even when they are of equal density, which could for example influence the value of different species in aquatic reforestation projects.

Acknowledgements

The experiments reported in this work were gratefully funded by the Japan Society for the Promotion of Science Summer Program, and by EPSRC grants EPP/R513088/1 and EP/W524487/1. The authors owe thanks to Jonathon Hales at Loughborough University, for manufacturing the vegetation models; to Mikihiro Nakamoto and Yasuto Tatsuyama at the DPRI Labs at Kyoto University, for manufacturing further experimental apparatus; and to Ryoji Ogawa, for assisting with the experiments and data processing.

References

Aberle, J. and Järvelä, J. (2013) 'Flow resistance of emergent rigid and flexible floodplain vegetation', Journal of Hydraulic Research, 51(1), pp. 33–45.
Artini, G. et al. (2024) 'Effects of Leafy Flexible Vegetation on Bed-Load Transport and Dune Geometry', Water Resources Research, 60(10).
Baladrón, A. et al. (2021) 'Can vegetation provide shelter to cyprinid species under hydropeaking?', Science of The Total Environment, 769.
Boothroyd, R.J. et al. (2016) 'The importance of accurately representing submerged vegetation morphology in the numerical prediction of complex river flow', Earth Surface Processes and Landforms, 41(4), pp. 567–576.
Caroppi, G. et al. (2022) 'Flow and wake characteristics associated with riparian vegetation patches: Results from field-scale experiments', Hydrological Processes, 36(2).
Cornacchia, L. et al. (2022) 'Flow and Wake Length Downstream of Live Submerged Vegetation Patches: How Do Different Species and Patch Configurations Create Sheltering in Stressful Habitats?', Water Resources Research, 58(3).
De Langre, E. (2012) 'Methodological advances in predicting flow-induced dynamics of plants using mechanical-engineering theory', Journal of Experimental Biology, 215(6), pp. 914–921.
Dickinson, R. *et al.* (2026) 'Isoanemeity Predicts the Combined Effects of Leaf versus Stem Flexure on Plant Drag', submitted to Geophysical Research Letters.
Field, H.R. et al. (2023) 'Importance of Dense Aquatic Vegetation in Seasonal Phosphate and Particle Transport in an Agricultural Headwater Stream', Water Resources Research, 59(9).
Hang, C. et al. (2025) 'A numerical simulation on wave attenuation by Kandelia obovata mangroves with flexible canopies', Ocean Engineering, 342.
Jalonen, J. *et al.* (2013) 'Leaf Area Index as Vegetation Density Measure for Hydraulic Analyses', Journal of Hydraulic Engineering, 139(5), pp. 461–469.
Liu, C. et al. (2024) 'Plant Morphology Impacts Bedload Sediment Transport', Geophysical Research Letters, 51(12).
Luhar, M. and Nepf, H. (2011) 'Flow-induced reconfiguration of buoyant and flexible aquatic vegetation', Limnology and Oceanography, 56(6), pp. 2003–2017.
Maio, M. *et al.* (2025) 'The role of seasonality and plant morphology on wake characteristics behind a patch of natural-like riparian vegetation', Advances in Water Resources, 204.
Marjoribanks, T.I. (2023) 'Numerical Modelling of Flow-Vegetation Interactions in Rivers and Coastal Environments: Recent Trends and Future Research Directions', in S. Dutta and V. Chembolu (eds) Recent Development in River Corridor Management. Springer Nature Singapore, pp. 81–93.
Matsumoto, K. et al. (2025) 'Secondary flow structure and sediment deposition around flexible and rigid vegetation patches', Physics of Fluids, 37(2).
Zhang, X. and Nepf, H. (2021) 'Wave-induced reconfiguration of and drag on marsh plants', Journal of Fluids and Structures, 100.

Book of Abstracts of the *16th International Symposium on Ecohydraulics*
Challenges and solutions in the time of global changes
August 16–20, 2026, Lausanne, Switzerland
ISSN: 2790-2420 | ISBN: 978-90-837233-9-6 | doi:[10.64697/iahr.proc.ise2026.abs]
© 2026 IAHR. CC BY-NC-ND 4.0

ANTICIPATED CFD MODELING FOR HABITAT SCALE HYDRODYNAMIC COMPLEXITY METRICS IN BOULDER DOMINATED CHANNELS

Naima REGGAD[1], Abul B. M. BAKI[1*], Christos KATOPODIS[2], Haitham GHAMRY[3], and Hasan ZOBEYER[4]
[1]Department of Civil and Environmental Engineering, Clarkson University, Potsdam, NY, USA
Email: abaki@clarkson.edu
[2]Katopodis Ecohydraulics Ltd., 122 Valence Avenue, Winnipeg, MB, CANADA
Email: katopodisecohydraulics@live.ca
[3]Freshwater Institute, Fisheries and Oceans Canada, 501 University Cres, Winnipeg, MB, CANADA
Email: Haitham.Ghamry@dfo-mpo.gc.ca
[4]Department of Water Resources Engineering, Bangladesh University of Engineering and Technology, Dhaka 1000, BANGLADESH
Email: zobeyer@wre.buet.ac.bd
*Corresponding author: Abul B.M. Baki; abaki@clarkson.edu

ABSTRACT

Instream boulder placement is a common river restoration technique that significantly alters wake zones, mean and turbulent flow characteristics, and sediment transport processes, thereby shaping instream habitat quality and availability. This study applied Computational Fluid Dynamics (CFD) modeling to investigate the mean and turbulent flow fields and their corresponding habitat-scale hydrodynamic complexity metrics (HHCMs) within a boulder-dominated channel under varying flow regimes. The CFD model is developed and validated using controlled laboratory experiments in the Ecohydraulics Flume at Clarkson University, where high-resolution Digital Elevation Models (DEMs) of the channel geometry were generated through the Structure-from-Motion (SfM) photogrammetry technique. A detailed sensitivity analysis comparing multiple turbulence closure models (k–ε, k–ω , and RSM) against ADV measurements of velocity magnitude and turbulent kinetic energy (TKE) was performed to identify the most reliable turbulence formulation. The k–ω model was selected for the mean flow, while the Reynolds Stress Model (RSM) was selected for turbulence due to its superior predictive capability. Analyses focused on patterns and variability in HHCMs, including energy gradients, turbulent kinetic energy, turbulent energy dissipation rates, Reynolds shear stresses, and vorticity, reveal distinctive patterns across different arrangements of boulders and lead to novel relationships between HHCMs and flow regimes. These findings highlight the role of boulder-induced flow complexity in driving habitat diversity, offering predictive tools for ecohydraulic stream restoration. The integration of CFD with high-resolution bathymetry advances the design of restoration interventions that balance hydraulic and ecological goals.

Keywords: *Instream boulders; Stream restoration, Computational Fluid Dynamics (CFD); Habitat complexity metrics.*

1. Introduction

Instream boulder placement is a widely implemented river restoration strategy designed to enhance hydraulic complexity and restore ecological function in degraded systems. The introduction of boulders as large roughness elements (LREs) fundamentally modifies near-bed hydrodynamics by altering both the mean and turbulent flow fields, generating complex wake structures, vortices, and recirculation zones that govern sediment transport, nutrient mixing, and habitat heterogeneity (Shamloo et al., 2001; Katopodis & Aadland, 2006; Papanicolaou et al., 2011). Turbulence generated by boulder-induced flow structures regulates energy dissipation, flow resistance, and sediment entrainment, enhancing bed stability, hydraulic roughness, and habitat diversity, thereby shaping channel morphology and supporting ecosystem resilience and biodiversity

(Nepf, 2012; Brayshaw, 1984; Van Zyll de Jong & Cows, 1997). Previous work by Golpira et al. (2022) experimentally examined how boulder placement affects mean-flow habitat complexity metrics, but it was limited to two flow conditions and lacked insight into turbulence-driven habitat complexity metrics. The subsequent study by Reggad et al. (2025) advanced this understanding by introducing turbulent-flow-based habitat complexity metrics, yet remained confined to controlled flume experiments. To address these limitations, the present study integrates CFD modeling with high-resolution SfM-derived bathymetry to analyze both mean and turbulent flow structures and their corresponding habitat complexity metrics under multiple flow regimes. This approach bridges laboratory findings and real-scale applications, providing predictive insights into how boulder-induced hydrodynamic complexity governs habitat diversity in restoration design.

2. Objectives

The primary objective is to develop and validate a Computational Fluid Dynamics (CFD) model using controlled laboratory experiments to accurately reproduce observed flow behavior and quantify habitat-scale hydrodynamic complexity metrics (HHCMs). The model is used to evaluate how these HHCMs metrics vary across different boulder configurations and flow regimes. High-resolution geomorphic data obtained through Structure-from-Motion (SfM) photogrammetry are incorporated to generate detailed Digital Elevation Models (DEMs) of the channel bed. Using this framework, key hydrodynamic indicators including turbulent kinetic energy, Reynolds stresses, vorticity, energy gradients, and dissipation rates, are analyzed under varying hydraulic and geometric conditions. The study further seeks to establish relationships between flow regime and HHCMs metrics, improving understanding of how boulder-induced flow variability contributes to habitat diversity.

3. Methodology

This research integrates controlled laboratory flume experiments with CFD simulations to investigate boulder-induced flow dynamics and habitat-scale hydrodynamic complexity. Laboratory experiments were conducted in the Ecohydraulics Flume at Clarkson University, simulating a gravel-bed stream with a 0.5% bed slope under steady flow conditions. Four experimental scenarios (S_1–S_4) were designed to investigate the effects of varying boulder concentrations and flow rates on instream hydrodynamics (details of experimental scenarios are availabe in Golpira et al. (2022). The boulder concentration (λ) values were set at 0% (S_1), 2.4% (S_2), 5.4% (S_3), and 8.3% (S_4), representing progressive increases in boulder density within the test section. Each scenario was simulated under seven flow rates (50, 60, 75, 100, 125, 150, and 200 L/s) to capture a wide range of flow regimes from low to high . High-resolution Digital Elevation Models (DEMs) of the streambed morphology were generated using SfM photogrammetry to provide accurate geometric inputs for CFD modeling (Ziaur Rahman, 2023). The computational domain (Fig. 1) was developed to replicate the experimental setup, including the flume geometry, boulder arrangement, and inlet–outlet boundary conditions. The CFD model was developed using ANSYS Fluent solver and was calibrated and validated against Acoustic Doppler Velocimeter (ADV) measurements of velocity magnitude and turbulent kinetic energy (TKE) obtained from the laboratory experiments. Multiple turbulence closure models including the Standard k–ε (turbulent kinetic energy-dissipation rate), the k–ω (turbulent kineticenergy - specific dissipation rate), and the Reynolds Stress Model (RSM) were evaluated. A comprehensive sensitivity analysis was conducted to assess each model's ability to reproduce measured velocity magnitude and TKE across different flow regimes and boulder configurations. Model predictions were quantitatively compared with ADV measurements using statistical performance metrics including the coefficient of determination (R^2), root mean square error (RMSE), and mean bias error (BIAS). The analysis revealed that although the k–ε and k–ω models adequately predicted the velocity distributions, they exhibited limitations in accurately capturing turbulence anisotropy and localized wake structures downstream of the boulders. In particular, the k–ω model provided reasonable agreement with measured velocity magnitudes; however, both two-equation models showed deficiencies in resolving turbulent kinetic energy (TKE) in highly anisotropic regions. In contrast, the Reynolds Stress Model (RSM) demonstrated improved agreement with ADV measurements, especially in predicting TKE and complex flow features within zones of strong shear and recirculation. Based on this sensitivity assessment, the RSM turbulence model was selected for the final simulations.

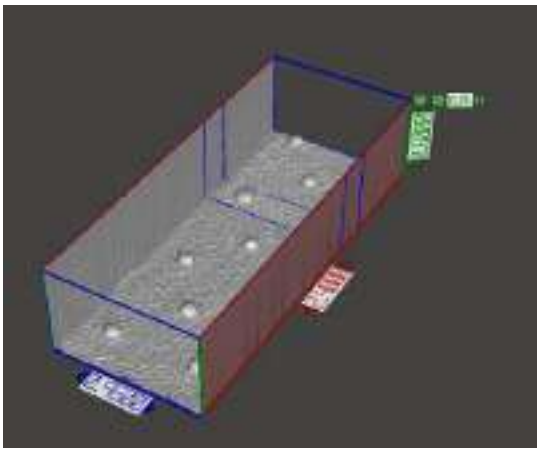

Fig. 1. Computational domain of the experimental flume with embedded boulders.

4. Habitat-scale Hydrodynamic Complexity Metrics

A key objective of this study is to quantify habitat-scale hydrodynamic complexity metrics (HHCMs) based on simulated mean and turbulent flow fields. A total eight hydraulic complexity metrics (M_1–M_8) were employed. Metrics M_1–M_4, which characterize spatial gradients and rotational components of kinetic energy, follow the formulations of Golpira et al. (2022). Metrics M_5–M_8, which describe turbulence-related properties, are based on Reggad et al. (2025). For example, the turbulent kinetic energy (M_5) (Eq.1) and energy dissipation rate (M_6) (Eq.2) are defined as:

$$M_5 = k_t = \frac{1}{2}\left(\overline{u'^2} + \overline{v'^2} + \overline{w'^2}\right) \quad (1)$$

$$M_6 = \varepsilon = \frac{2\pi}{u}\left[\frac{G_u(f) f^{\frac{5}{3}}}{A}\right]^{\frac{3}{2}} \quad (2)$$

Where, u', v', and w' are the velocity fluctuation of the streamwise, transverse and vertical components, $G_u(f)$is the power spectra of the streamwise velocity in the frequency (f) domain and f is the frequency in Hz, and the coefficient A is a constant equal to 0.56 (detials are availave in Reggad et al. (2025)).

5. Results and Discussions

This research is expected to identify a clear relationship between the dimensionless discharge parameter $Q^* = Q/\sqrt{gS_0R_v^3B^2}$ and the dimensionless habitat metrics across four experimental scenarios(S_1-S_4). Where Q is the discharge , g is the gravitational acceleration , S_0 is the bed slope, R_v is the volumetric hydraulic radius , and B is the channel width , H is the flow depth , and U_{reach} is the reach-averaged velocity. We expect that variations in discharge and structural complexity (boulder density) systematically influence the habitat metrics, which may increase or decrease depending on the metric definition and sensitivity. The findings are anticipated to establish a quantitative framework linking discharge scaling to habitat-scale hydraulic conditions, supporting the assessment and optimization of ecohydraulic stream restoration designs.

6. Conclusion

The expected results of this study include successful validation of a CFD model against laboratory measurements, confirming its ability to accurately reproduce mean and turbulent flow fields around instream boulders. The simulations are anticipated to reveal distinct spatial patterns of wake formation, recirculation zones, and high-shear regions that vary with flow regime and boulder geometry. Detailed distributions of habitat-scale hydrodynamic complexity metrics (HHCMs) such as turbulent kinetic energy, energy gradients, energy dissipation rates, Reynolds stresses, and vorticity are expected to demonstrate strong spatial variability and sensitivity to flow regime. The analyses will establish new relationships linking HHCMs with flow gegime and geometric parameters, providing predictive insight into how boulder placement enhances flow complexity and habitat diversity. Overall, the integration of CFD with high-resolution SfM-derived bathymetry is expected to advance ecohydraulic modeling capabilities and support the design of river restoration strategies that balance hydraulic efficiency with ecological functionality.

References

Brayshaw A (1984) Characteristics and origin of cluster bedforms in coarse-grained alluvial channels. Canadian Society of Petroleum Geologists, 10, 77-85.

Golpira A, Baki ABM, Ghamry H et al. (2022) An experimental study: effects of boulder placement on hydraulic metrics of instream habitat complexity. Scientific Reports. https://doi.org/https://doi.org/10.1038/s41598-022-17281-1

Katopodis C, Aadland L (2006) Effective dam removal and river channel restoration approaches. International Journal of River Basin Management, 4(3)

Liu M, Rajaratnam N, Zhu D (2003) Turbulence structure of hyraulic jumps of of low Froude numbers. J. Hydraul. Eng, 511–520.

Nepf H (2012). Flow and transport in regions with aquatic vegetation. Annual Review of Fluid Mechanics, 123-142.

Papanicolaou A, Dermisis D, Elhakeem M (2011) Investigating the role of clasts on the movement of sand in gravel bed rivers. J. Hydraul. Eng., 137.

Reggad N, Golpira A, Baki ABM, Ghamry H, Katopodis C (2025) Turbulent flow-based habitat complexity metrics around instream boulders in support of river restoration. Scientific Reports, 15.

Shamloo H, Rajaratnam N, Katopodis C (2001) Hydraulics of simple habitat structures. Journal of Hydraulic Research, 39 (4).

Van Zyll de Jong M, Cows IG (1997) An evaluation of instream habitat restoration techniques on salmonid population in a Newfoundland stream. Regulated Rivers-Research & Management 13(6), 603-614.

Ziaur Rahman M (2023) *Exploring Local Sediment Erosion and Deposition Patterns around Instream Boulders and their Corresponding Fish Spawning Habitat Suitability: An Experimental Investigation.* Master's Thesis, Clarkson Univeristy.

Book of Abstracts of the *16th International Symposium on Ecohydraulics*
Challenges and solutions in the time of global changes
August 16–20, 2026, Lausanne, Switzerland
ISSN: 2790-2420 | ISBN: 978-90-837233-9-6 | doi:[10.64697/iahr.proc.ise2026.abs]
© 2026 IAHR. CC BY-NC-ND 4.0

EFFECTS OF A HIGH-HEAD HYDROPOWER SYSTEM ON THE HYDROLOGY AND PHYSICAL ENVIONMENT IN A RIVER SYSTEM

Knut ALFREDSEN[1]

[1] Norwegian University of Science and Technology, Norway
email: knut.alfredsen@ntnu.no

ABSTRACT

Norway has several large high-head hydropower systems with multiple reservoirs and a network of brook intakes altering the natural flow regime and leading to a several changes in the physical environment in the river system affected by the regulation. Due to intake and release of water at many locations, such systems might have different flow regimes at different locations in the water course, and the impacted reaches might be many kilometers long. Here we have investigated the impacts of the regulation of the Lærdal river and evaluated the effects on the flow regime and other associated physical features like water temperature, river ice formation and river morphology after 50-years of regulation. The findings are discussed and related to other similar systems to look for patterns and typical regulation effects. Given plans for upgrades and changes in future operational strategies in Norwegian regulated rivers, understanding the scale and type of impact will be important for future mitigation measures.

Keywords: *Hydropower; hydrology; environmental impacts; bypass reaches; flood regimes*

1. Introduction

Impacts of hydropower regulation and other encroachments on flow regimes have been observed evaluated both on local and global scales (Grill et al. 2019; McManamay et al. 2022). Reduced flow, altered timing and rates of change are typical findings from studies of regulated rivers, and methods to evaluate and describe such changes are developed (e.g. Richter et al. 1996). The alteration of the hydrology of rivers lead to changes in the physical system, among others increased fragmentation of river system, sediment issues and temperature changes. The Norwegian system is dominated by high-head systems with relatively low production discharge and high head and large storage and water transfer systems (Alfredsen et al. 2021). The large transfer systems increase the impact area of the development, and the high storage system allows for significant alterations of the volume and timing of flow.

Here we will use a typical Norwegian hydropower development as a case to evaluate flow changes and how these influence the physical conditions in the river related to temperature, ice formation and sediments. The discussion also includes how other factors like climate change, land use changes influence the system and how such factors can be disentangled from the regulation impacts.

2. Materials and methods

2.1. Study site

The Lærdal river drains a 1182 km2 area of Filefjell and empties into the Sognefjord at Lærdalsøyri. The elevation difference is from 0 to 1917 m.a.s.l, so it is a steep catchment with large areas in the high mountains (median height is 1341 m.a.s.l. The annual average discharge is 32 m^3/s. The river system was regulated in 1974 through the Borgund power plant, and the Stuvane power plant was set in operation in 1986. The regulation consists of several reservoirs and brook intakes (Figure 1.

The Lærdal river is a national salmon river and once considered among Norways most prolific rivers for recreational angling.

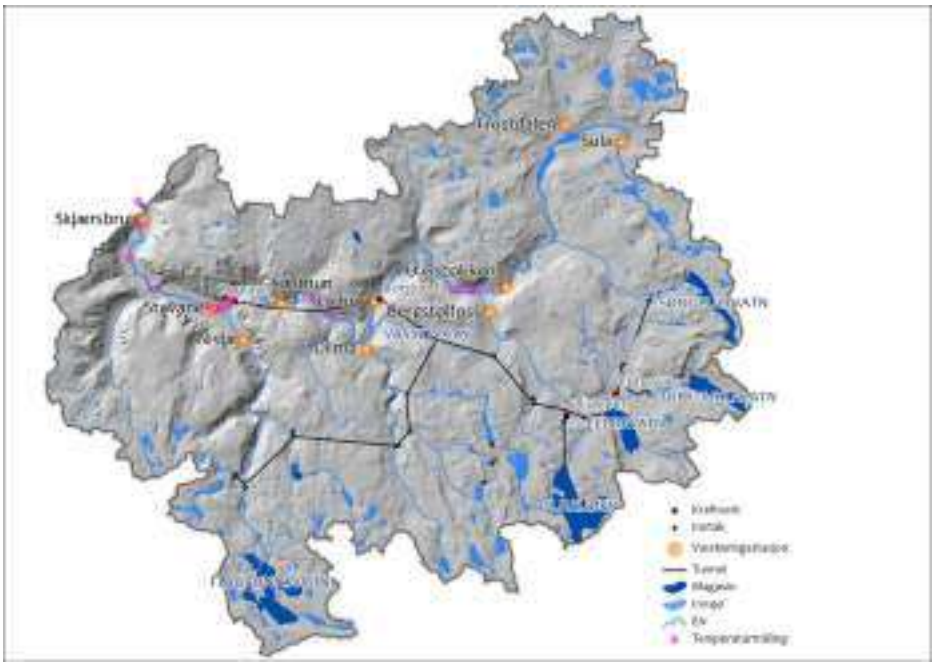

Figure 1 The Lærdal catchment and hydropower regulation.

2.2. Methods

Currently there are three discharge gauges in operation of which two have data from before the regulation. Several other abandoned stations exist, and these are also used to evaluate the regulation effects. Temperature data exists both from some long-term measurements and several short-term measurements. Good temperature data from before the regulation is scarce. Some information of winter conditions and some aerial imagery of the river before and after regulation is also available.

Time series analysis are used to evaluate the long term evaluation of flow and temperature, and we have used the IHA method (Richter et al. 1996) to describe key factors of the flow regime. A similar approach (Olden and Naiman 2010) is used to evaluate temperature. We have also used hydrological modelling to evaluate pre-regulation flow generation. We have evaluated the changes in the river morphology through analysis of aerial imagery.

3. Results and Discussion

The flow regime of the bypass reaches shows a typical bypass pattern before and after the regulation (Figure 2).

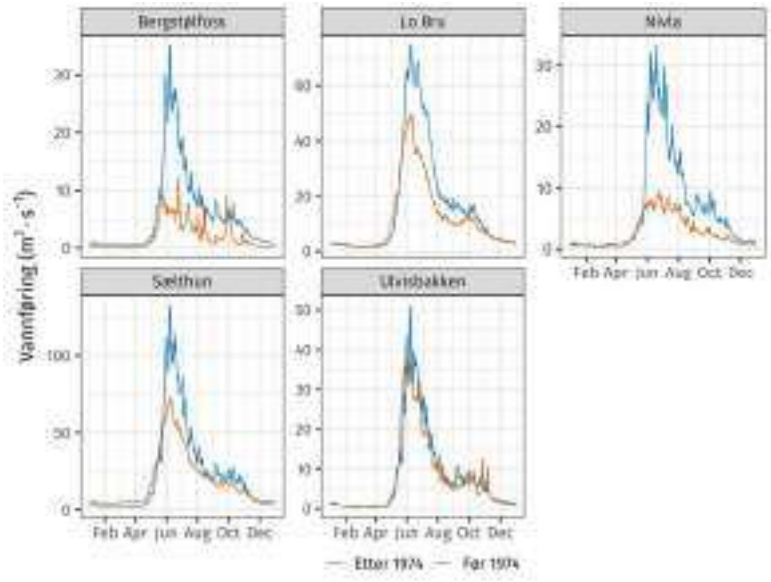

Figure 2 Flow reduction in transferred tributaries to the Lærdal river. The station Ulvisbakken is unregulated and shows the natural regime over the period analysed.

The flow downstream of the Stuvane power plant is shown in Figure 3. Pre regulation data is computed from the gauge Skjærsbrui downstream of Stuvane. We see a redistribution pattern of increased winter flow and reduced spring flood consistent with the operation of the hydropower plant.

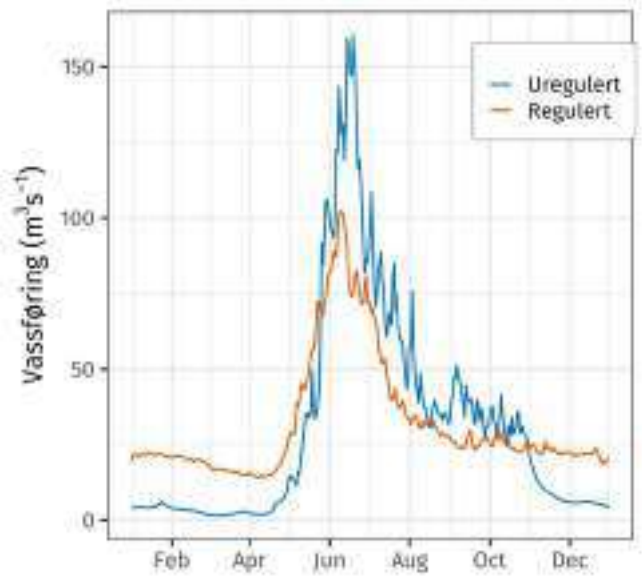

The results show the alteration of the flow patterns, further analysis show flood reductions due to reservoir storage, a result that is preferable for the local community and flood exposed infrastructure but also detrimental for sediment transport and maintenance of gravel bars. The ice cover once present is removed for a large part of the river and we see patterns of temperature changes for parts of the year.

References

Alfredsen, K., P.-A. Amundsen, L.Hahn, P. M. Harrison, I. P. Helland, E. G. Martins, W. M. Twardek and M. Power (2021). A synoptic history of the development, production and environmental oversight of hydropower in Brazil, Canada, and Norway. Hydrobiologia doi:10.1007/s10750-021-04709-4(0123456789().,-volV) (01234567 89().,-volV)

Grill, G., B. Lehner, M. Thieme, B. Geenen, D. Tickner, F. Antonelli, S. Babu, P. Borrelli, L. Cheng, H. Crochetiere, H. Ehalt Macedo, R. Filgueiras, M. Goichot, J. Higgins, Z. Hogan, B. Lip, M. E. McClain, J. Meng, M. Mulligan, C. Nilsson, J. D. Olden, J. J. Opperman, P. Petry, C. Reidy Liermann, L. Sáenz, S. Salinas-Rodríguez, P. Schelle, R. J. P. Schmitt, J. Snider, F. Tan, K. Tockner, P. H. Valdujo, A. van Soesbergen and C. Zarfl (2019). Mapping the world's free-flowing rivers. Nature **569**(7755): 215-221 doi:10.1038/s41586-019-1111-9

McManamay, R., R. George, R. Morrison and B. Ruddel (2022). Mapping hydrologic alteration and ecological consequences in stream reaches of the conterminous United States. Scientifc Data **9** doi:10.1038/s41597-022-01566-1

Olden, J. and R. Naiman (2010). Incorporating thermal regimes into environmental flows assessments: modifying dam operations to restore freshwater ecosystem integrity. Freshwater Biology **55**(1): 86-107

Richter, B., J. Baumgartner, J. Powell and D. Braun (1996). A Method for Assessing Hydrologic Alteration within Ecosystems. Conservation Biology **10**(4): 1163-1174

Book of Abstracts of the *16th International Symposium on Ecohydraulics*
Challenges and solutions in the time of global changes
August 16–20, 2026, Lausanne, Switzerland
ISSN: 2790-2420 | ISBN: 978-90-837233-9-6 | doi:[10.64697/iahr.proc.ise2026.abs]
© 2026 IAHR. CC BY-NC-ND 4.0

RIVER RESTORATION: THE ROLE OF HABITAT HETEROGENEITY AND FLOOD REFUGIA

Chantal Mariette HISCHIER[1,2], Nico BÄTZ[1], Cristina RACHELLY[3],
Paul DEMUTH[4], Volker WEITBRECHT[4], David Florian VETSCH[4], Christian DINKEL[1], Christine WEBER[1]

[1] Eawag, Swiss Federal Institute of Aquatic Science and Technology,
Department of Surface Waters – Research and Management, 6047 Kastanienbaum, Switzerland
chantal.hischier@eawag.ch, nico.baetz@eawag.ch, christian.dinkel@eawag.ch, christine.weber@eawag.ch
[2] Swiss Federal Institute of Technology (ETH) Zurich,
Department of Environmental Systems Science, 8092 Zurich, Switzerland
[3] IUB Engineering AG, 3000 Bern, Switzerland
cristina.rachelly@iub-ag.ch
[4] Swiss Federal Institute of Technology (ETH) Zurich,
Laboratory of Hydraulics, Hydrology and Glaciology (VAW), 8093 Zurich, Switzerland
demuth@vaw.baug.ethz.ch, weitbrecht@vaw.baug.ethz.ch, vetsch@vaw.baug.ethz.ch

ABSTRACT

Floods are the most frequent disturbances and expected to become more intense due to climate change. To investigate the effect of floods of varying intensity and river morphology on habitat heterogeneity and refugia availability for macrophytes and macroinvertebrates, we compared restored, slightly modified, and heavily modified reaches across ten Swiss rivers. Based on hydraulic field data and hydrodynamic numerical modelling of mean flow (Q_M) and six flood intensities (HQ_1–HQ_{100}), we showed that restored reaches offer higher habitat heterogeneity and refugia availability than modified reaches across most flow intensities. As flow intensity increased, both habitat heterogeneity and refugia availability declined – except in areas along riverbanks. Our results showed a strong positive correlation between habitat heterogeneity and refugia availability, encouraging river management to enhance river resilience by improving structural heterogeneity. Our insights provide guidance for conservation and restoration of habitat heterogeneity and flood refugia in the face of climate change with more intense and frequent floods expected.

Keywords: river management; floods; climate change; macrophytes; macroinvertebrates; hydrodynamic numerical modelling

1. The Role of Habitat Heterogeneity and Flood Refugia for River Resilience

Floods are a key feature of natural rivers and shape riverine ecosystems in contrasting ways (Humphries et al. 2024). While floods lead to mortality and displacement of riverine organisms, they also initiate key ecological processes such as dispersal of organisms or seeds and reshape habitat heterogeneity (Lake 2000). Habitat heterogeneity is defined as spatial variation of habitat conditions and promotes biodiversity by providing habitats that buffer extreme events such as floods (McCabe et al. 2025). Habitats that mitigate disturbance effects serve as refugia, which remain understudied and barely considered in restoration despite their crucial role for river resilience (Mathers et al. 2022). Furthermore, it is still unclear to which extent greater habitat heterogeneity translates into higher refugia availability at varying flow intensities and morphologies (Van Looy et al. 2019).

2. Study Design and Methods

2.1 Study design

In our study, we investigated how flow intensity and river morphology influence habitat heterogeneity and refugia availability in ten Swiss rivers (Fig. 1). In each river, three 100-m-long reaches with different morphologies (heavily modified, slightly modified, restored) were compared and investigated by drone surveys as well as topographic and hydraulic measurements. We used this observational data to create hydrodynamic numerical models for each reach. Based on simulated water depth, flow velocity and bed shear stress, we quantified habitat heterogeneity and refugia availability for macrophytes and macroinvertebrates at mean flow (Q_M) and six flood intensities with different return periods (HQ_1–HQ_{100}). We considered macroinvertebrates and macrophytes, as these two organism groups cover gradients in mobility (mobile, sessile) and relation to refugia (use, provision).

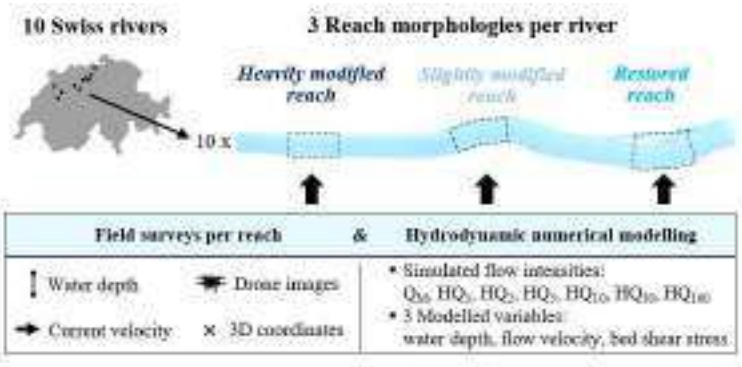

Fig. 1. *Study design. We investigated three reach morphologies (heavily modified, slightly modified, restored) in ten Swiss rivers, resulting in 30 surveyed reaches in total. All reaches were studied by field measurements and hydrodynamic numerical modelling.*

2.2 Field surveys and hydrodynamic numerical modelling

In all 30 investigated reaches, we recorded water depth, flow velocity and 3D point coordinates at 51 points. These measurement points were representative for the corresponding reach and included 21 Thalweg, 10 kink and 20 stratified-random points. In addition to these topographic and hydraulic measurements, we conducted drone surveys in every reach. All field surveys were completed between January and June 2024 at intermediate flow conditions. To simulate water depth, flow velocity and bed shear stress in every reach at mean flow (Q_M) and six flood intensities (HQ_1–HQ_{100}), we used our field measurements and drone images to create hydrodynamic numerical models of every reach. Based on simulated water depth, flow velocity and bed shear stress, we quantified habitat heterogeneity and flood refugia for macrophytes and macroinvertebrates. Habitat heterogeneity was quantified by the coefficient of variation (CV) of flow velocity and bed shear stress in the active channel per reach at mean flow and six flood intensities. Refugia availability was quantified as areas with flow velocity $\leq$ 0.8 m/s for macrophytes (Riis and Biggs 2003) and bed shear stress $\leq$ 10 N/m^2 for macroinvertebrates (Hauer et al. 2012) in the active channel of a reach relative to the wetted area in the active channel at six flood intensities.

3. Results and Discussion

3.1 Habitat heterogeneity and refugia availability

Restored reaches showed highest habitat heterogeneity in flow velocity and bed shear stress (Fig. 2a) for most flow intensities ($F = 8.99$, $P < 0.001$). Bank removal and other restoration measures are known to increase channel width and variability in flow velocity and depth in the river channel, leading to areas with, e.g., lower bed shear stress even at high flood intensities (Rachelly et al. 2021). We observed that restored reaches offered more such low-flow velocity and low-bed shear stress areas than modified reaches, especially along riverbanks (e.g., Langete river in Fig. 2b; Mathers et al. 2022). Habitat heterogeneity significantly decreased with increasing flow intensity (–45% in flow velocity CV, $F = 42.82$, $P < 0.001$; –43% in bed shear stress CV: $F = 24.60$, $P < 0.001$).

Refugia availability tended to be higher in restored compared to modified reaches. This trend was, however, not statistically significant – possibly due to deviating, reach-specific effects (macrophytes: $\chi 2 =$

12.98, P = 0.37; macroinvertebrates: $\chi 2 = 3.85$, P = 0.99). Flood refugia were available along riverbanks in restored and slightly modified reaches, providing areas with suitable conditions for macrophytes and macroinvertebrates even at high flow intensities (e.g., in Langete river in Fig. 2b). We thus see great potential to enhance river resilience by restoring riverbanks and floodplain areas – which are key transition zones between aquatic and terrestrial habitats (Mathers et al. 2022). Similar to habitat heterogeneity, also refugia availability was significantly reduced by increasing flow intensity from HQ_1 to HQ_{100} (–29 percentage points for macrophytes, $\chi 2 = 53.25$, P < 0.001; –17 percentage points for macroinvertebrates, $\chi 2 = 33.35$, P < 0.01).

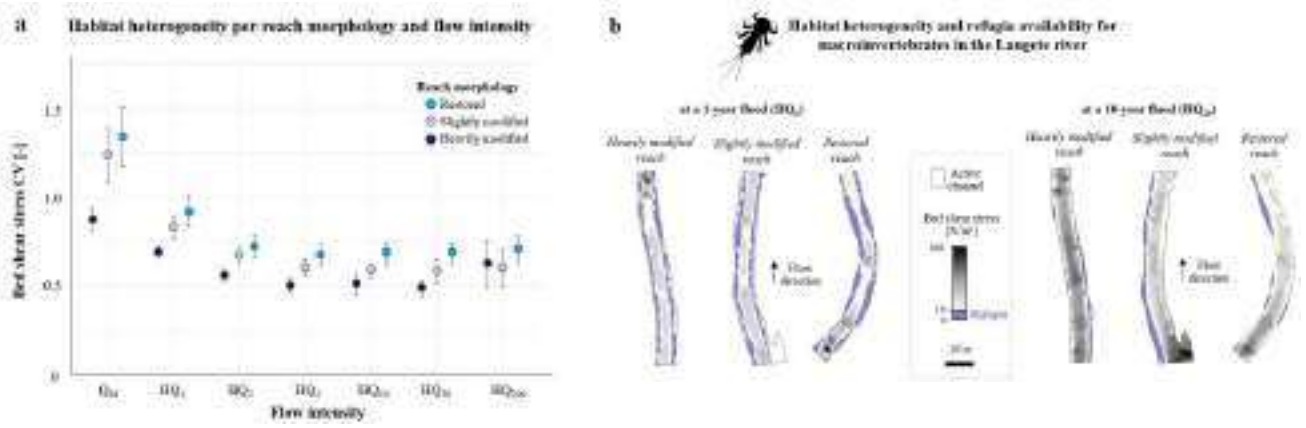

Fig. 2. *Habitat heterogeneity and refugia availability for macroinvertebrates across ten rivers and in the Langete river. (a) Bed shear stress coefficient of variation (CV) as a measure for habitat heterogeneity is shown across ten rivers per reach morphology at mean flow (Q_M) and six flood intensities (HQ_1–HQ_{100}). Circles represent the mean and whiskers the corresponding standard error. (b) Habitat heterogeneity in the Langete river is shown in grey and purple shades and macroinvertebrate refugia in purple during a 1-year flood (HQ_1; on the left) and during a 10-year flood (HQ_{10}; on the right) per reach morphology. Macroinvertebrate refugia were defined as areas with bed shear stress ≤ 10 N/m^2 relative to the wetted area in the active channel of a reach at a given flow intensity.*

3.2 Implications for river management

Habitat heterogeneity and refugia availability were positively correlated (macrophytes: Spearman's rank correlation coefficient $\rho = 0.73$, P < 0.001; macroinvertebrates: $\rho = 0.61$, P < 0.001). We found that variability in correlations increased with flow intensity and that correlations were particularly strong in restored reaches. Our results revealed the potential of restoration measures to increase habitat heterogeneity, leading to higher refugia availability and associated river resilience. We propose further studies, first, to define dynamic reference or target states for restoring habitat heterogeneity and refugia. Second, to investigate how much habitat heterogeneity and refugia are required to maintain river biodiversity and resilience (Scott et al. 2022). Third, to develop and implement multifunctional restoration measures, considering both ecological needs and flood safety for humans. Given the importance of refugia for river resilience and the expected increase in flood intensity due to climate change, refugia should be an integral part in future river restoration projects.

Acknowledgements

This study was funded by the Swiss Federal Office for the Environment (FOEN), the Swiss Federal Institute of Aquatic Science and Technology (Eawag), the Swiss Federal Institute for Forest, Snow and Landscape Research (WSL), the Platform of Hydraulic Constructions (PL-LCH) at EPF Lausanne, and the Laboratory of Hydraulics, Hydrology and Glaciology (VAW) at ETH Zurich. We are grateful to FOEN and the Cantons and municipalities of Aargau and Bern for field work permissions and river data. We thank Maïva Brunnberg and Tara Behnsen for assisting in the field, Christoph Vorburger, Andreas Scheidegger and Gaspar Dugac for statistical advice and Rosi Siber for GIS support.

References

Hauer, C., G. Unfer, W. Graf, P. Leitner, B. Zeiringer, and H. Habersack. 2012. Hydro-morphologically related variance in benthic drift and its importance for numerical habitat modelling. Hydrobiologia **683**:83-108.

Humphries, P., E. Wohl, A. A. Agostinho, R. K. Kopf, N. McCasker, P. Moyle, and J. Thorp. 2024. Flood ecology. Bioscience **74**:355-368.

Lake, P. S. 2000. Disturbance, patchiness, and diversity in streams. Journal of the North American Benthological Society **19**:573-592.

Mathers, K. L., C. T. Robinson, and C. Weber. 2022. Patchiness in flow refugia use by macroinvertebrates following an artific ial flood pulse. River Research and Applications **38**:696-707.

McCabe, C. L., C. D. Matthaei, and J. D. Tonkin. 2025. The ecological benefits of more room for rivers. Nature Water **3**:260-270.

Rachelly, C., K. L. Mathers, C. Weber, V. Weitbrecht, R. M. Boes, and D. F. Vetsch. 2021. How does sediment supply influence refugia availability in river widenings? Journal of Ecohydraulics **6**:1-19.

Riis, T., and B. J. Biggs. 2003. Hydrologic and hydraulic control of macrophyte establishment and performance in streams. Lim nology and Oceanography **48**:1488-1497.

Scott, D. N., S. Shahverdian, R. Flitcroft, and E. Wohl. 2022. Geomorphic heterogeneity as a framework for assessing river co rridor processes and characteristics. River Research and Applications **38**:1893-1901.

Van Looy, K., J. D. Tonkin, M. Floury, C. Leigh, J. Soininen, S. Larsen, J. Heino, N. L. Poff, M. Delong, S. C. Jahnig, T. Da try, N. Bonada, J. Rosebery, A. Jamoneau, S. J. Ormerod, K. J. Collier, and C. Wolter. 2019. The three Rs of river ecosystem resilience: resources, recruitment, and refugia. River Research and Applications **35**:107-120.

Book of Abstracts of the *16th International Symposium on Ecohydraulics*
Challenges and solutions in the time of global changes
August 16–20, 2026, Lausanne, Switzerland
ISSN: 2790-2420 | ISBN: 978-90-837233-9-6 | doi:[10.64697/iahr.proc.ise2026.abs]
© 2026 IAHR. CC BY-NC-ND 4.0

FLOW RESISTANCE CHARACTERISTICS AND FLOW STRUCTURE OF OPEN CHANNELS DUE TO DIFFERENCES IN VEGETATION ARRANGEMENT AND DENSITY

Takayuki TANAKA[1], Kanta SUGIURA[1]

[1] National Institute of Technology, Toyota College, Japan
email: tanaka-c@toyota-ct.ac.jp

ABSTRACT

Vegetation within river channels plays a significant role in enhancing environmental functions, such as improving water quality and sediment purification capacity and creating habitats for organisms. It also contributes greatly to river development that fosters high water accessibility by creating inviting waterside spaces. However, during floods, vegetation increases flow resistance, presenting a drawback. Therefore, establishing appropriate vegetation management techniques for each river and waterway is essential. This study experimentally investigates the effects of various configurations and differences in vegetation density on flow resistance characteristics and momentum transport characteristics in vegetation communities undergoing elastic deformation. As a result, we clarified the flow characteristics, secondary flow distribution characteristics, and momentum transport characteristics under each vegetation growth condition.

Keywords: *vegetation*; *open channel flow*; *resistance characteristics*; *momentum transport*

1. Introduction

Vegetation within river channels plays a significant role in enhancing environmental functions, such as improving water quality and sediment purification capacity, creating habitats for organisms, and contributing to the development of highly accessible riverside spaces that foster a sense of connection to water. On the other hand, since vegetation has disadvantages such as increasing flow resistance during floods, it is necessary to establish appropriate vegetation management techniques for each river and waterway. Therefore, elucidating the resistance characteristics and flow mechanisms of open channels with vegetation communities is highly useful in hydraulic engineering.

Due to the differing flow structures caused by the rigidity of vegetated open channels, various studies have been conducted on the distinction between rigid and flexible systems. Focusing on research using rigid simulated vegetation, an early example is the work by Raupach et al. (1981). They employed rigid cylindrical rods as simulated vegetation and investigated the flow mechanisms in streams where the entire riverbed was covered with simulated vegetation. Liu et al. (2008) conducted detailed experiments using rigid dowel arrays, characterizing velocity distributions and turbulence intensity inside and outside the canopy through point measurements, thereby elucidating flow structures within the vegetation. As an example of research on flexible vegetation, Kim et al. (2024) modeled partial vegetation patches using flexible bodies, demonstrating channel flow changes, recirculation behind the patches, and turbulence activation at the patch scale. This provides valuable insights for understanding spatial variations during full-scale installation.

Research has been conducted on open-channel flows with diverse vegetation communities, but studies examining resistance characteristics under varying vegetation density and arrangement conditions remain insufficient.

Therefore, this study experimentally investigates the flow resistance characteristics and flow mechanisms in open channels with vegetation communities arranged in a downstream sequence, when the density and arrangement of the vegetation zones are altered.

2. Experimental apparatus and conditions

The experiment was conducted using a circulating variable-gradient channel made of glass, measuring 4 m in length, 20 cm in width, and 20 cm in height. The vegetation zone model was created by aligning and attaching 6.10 nylon bristles (diameter 0.242 mm, bending modulus EI = 1.45 × 10^4 g·cm²) to a plastic plate, bent to follow the water flow, at a height of 5.5 cm. The vegetation model was placed from the upstream end of the channel over a range of 20 cm to 360 cm. The arrangement patterns are shown in Fig.1.

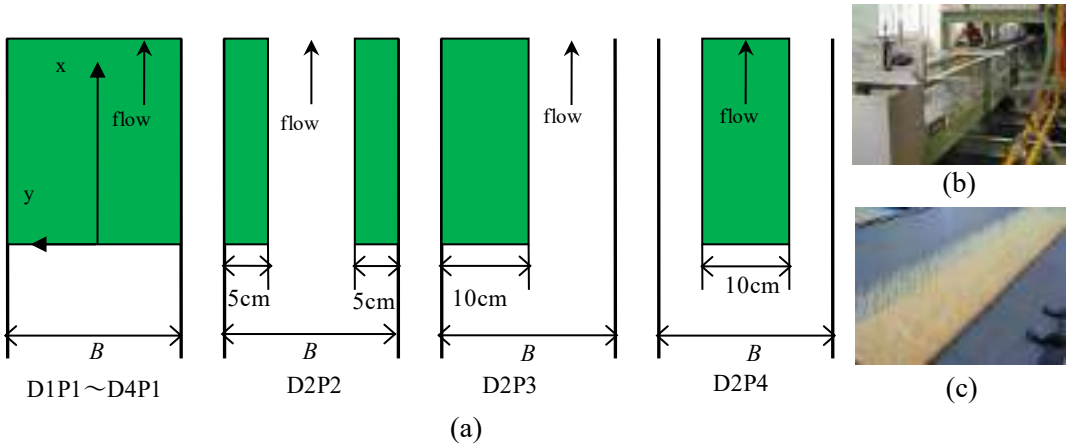

Fig. 1. Experimental Channel Overview; (a) Vegetation arrangement in experimental channels, (b) Photograph of the experimental Channel, (c) Model of simulated vegetation

P1 indicates full-channel vegetation placement, P2 indicates placement on both banks, P3 indicates placement on one bank, and P4 indicates placement in the channel center. Vegetation density was set using the number of plants per unit area λ, as shown in Table 1.

Table 1. Experimental conditions

Case	Number of vegetation per unit area λ (1/cm²)	Bed slope I 1/500	Bed slope I 1/1000	Vegetation height H_V (cm)	Vegetation diameter d (mm)	Simulated vegetation
		Flow Rate Q (l/s)				
D1P1	4.0	1.0～6.0	1.0～6.0	5.5	0.242	Nylon brewsuru
D2P1	2.0					
D3P1	1.0					
D4P1	0.5					
D2P1～D2P4	2.0					

The number of plants gradually decreased from D1 to D4. Additionally, the number of vegetation units from D2P1 to D2P4 when changing the configuration was standardized to D2. The coordinate system uses the center of the channel bottom at the leading edge of the vegetation zone as the origin, with the x-axis in the downstream direction, the y-axis in the cross-flow direction, and the z-axis in the vertical direction, forming a right-handed coordinate system. Furthermore, the respective flow velocity components are denoted as u, v, w, the mean values as U, V, W, and the fluctuating components as u', v', w'. As shown in Table 1, for six cases with bed slope I = 1/500 and 1/1,000, flow rates were varied incrementally from 1.0 to 6.0 l/s in 0.5 l/s steps, and water depth was measured using a point gauge. Additionally, as a supplementary measure, a weir at the downstream end of the channel was used to minimize the impact of the downstream end and measure the water depth. Here, since no significant differences in time-averaged water depth were observed across the cross-section, measurements were taken at the channel center, within the region where time-averaged water depth showed almost no variation in the downstream direction.

Point measurements of flow velocity were conducted to examine the flow mechanism. Flow velocity measurements were conducted using both I-type and L-type electromagnetic flow meters. The sampling frequency was set to 100 Hz for all cases, and the number of sampled data points was set to 4,096.

3. Flow resistance characteristics

In the configuration pattern, the flow rate was varied in 0.5 l/s increments from Q=1.0 l/s, and the water depth was measured. Fig. 2 shows the relationship between flow rate and water depth for each bed slope. Here, in

the clear state, the Reynolds number ranges from 4,400 to 26,000 at flow rates of Q = 1 l/s to 6 l/s, and all conditions exhibit turbulent flow.

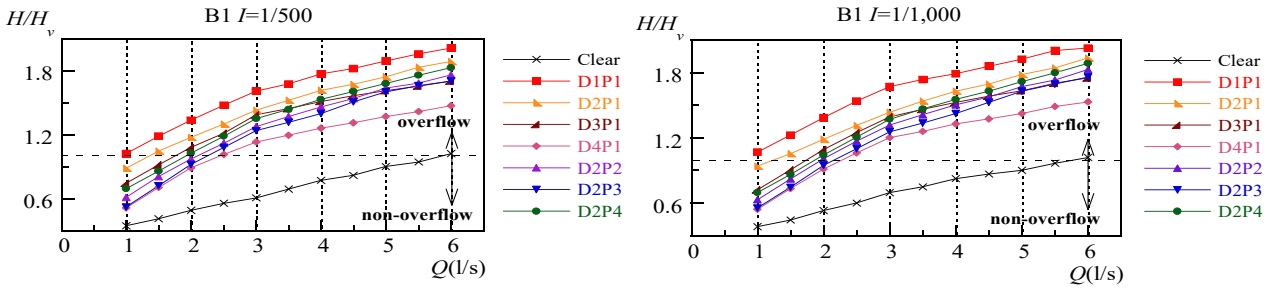

Fig. 2. Relationship between flow rate and water depth at each bed slope.

In D1P1, where vegetation is placed across the entire channel bed, the water depth is approximately twice that of the vegetation-free Clear condition at any flow rate. Furthermore, it was found that for D2P1 to D2P4, where the number of vegetation units was the same in both the flow direction and cross-flow direction, flow resistance increased in the following order: single-bank arrangement, double-bank arrangement, channel-canter arrangement, and full-area arrangement. In D3P1, it was confirmed that the relationship between flow resistance and vegetation width changes at Q=3.0 l/s, specifically when vegetation has a finite width narrower than the channel width. Furthermore, compared to configurations with vegetation of finite width, it was confirmed that reducing the overall density of the vegetation zone beyond a certain density resulted in lower flow resistance. These trends were similar for both channel gradients.

4. Fluid mechanism

4.1. Isoclines of the mainstream velocity and secondary flow vectors in the cross section

Fig. 3 shows the contour lines of the mainstream velocity U and the secondary flow vectors for D2P2 and D2P4 during overflow conditions at a flow rate Q = 6 l/s.

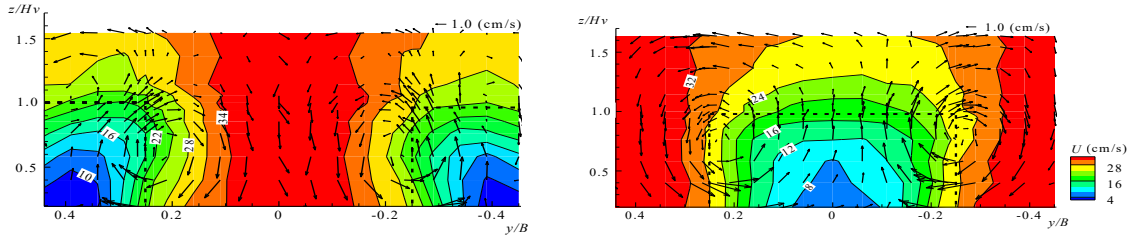

(a) D2P2 Q=6.0 l/s (b) D2P4 Q=6.0 l/s

Fig. 3. Relationship between flow rate and water depth at each bed slope.

Since the flow of D1P1 to D4P1 in the full-area configuration is theoretically considered to remain unchanged in the transverse direction, this study examines D2P2 and D2P4 when the configuration is altered. In all cases, within the vegetation zone, the mainstream velocity is suppressed compared to the periphery, and a tendency is observed where the mainstream velocity increases sharply as one moves toward the non-vegetation area.

Focusing on the secondary flow vectors, it became clear that upward flow occurs in vegetated areas and downward flow in non-vegetated areas, with circulation currents developing primarily near the vegetation zone boundary. Furthermore, D2P4 exhibits larger secondary flow vector values compared to D2P2. This likely suppresses the main flow velocity and increases flow resistance.

4.2. Momentum transport characteristics

The total momentum transport in the transverse and vertical directions is calculated using Eq. (1) and (2):

$$\overline{uv} = \overline{(U+u')(V+v')} = UV + \overline{u'v'} \quad (1)$$

$$\overline{uw} = \overline{(U+u')(W+w')} = UW + \overline{u'w'} \quad (2)$$

where UV, UW denotes momentum transport due to advection, while $\overline{u'v'}$, $\overline{u'w'}$ denotes momentum transport due to velocity fluctuations.

Fig. 4 shows the momentum transport at the vegetation zone boundaries for D2P2 and D2P4.

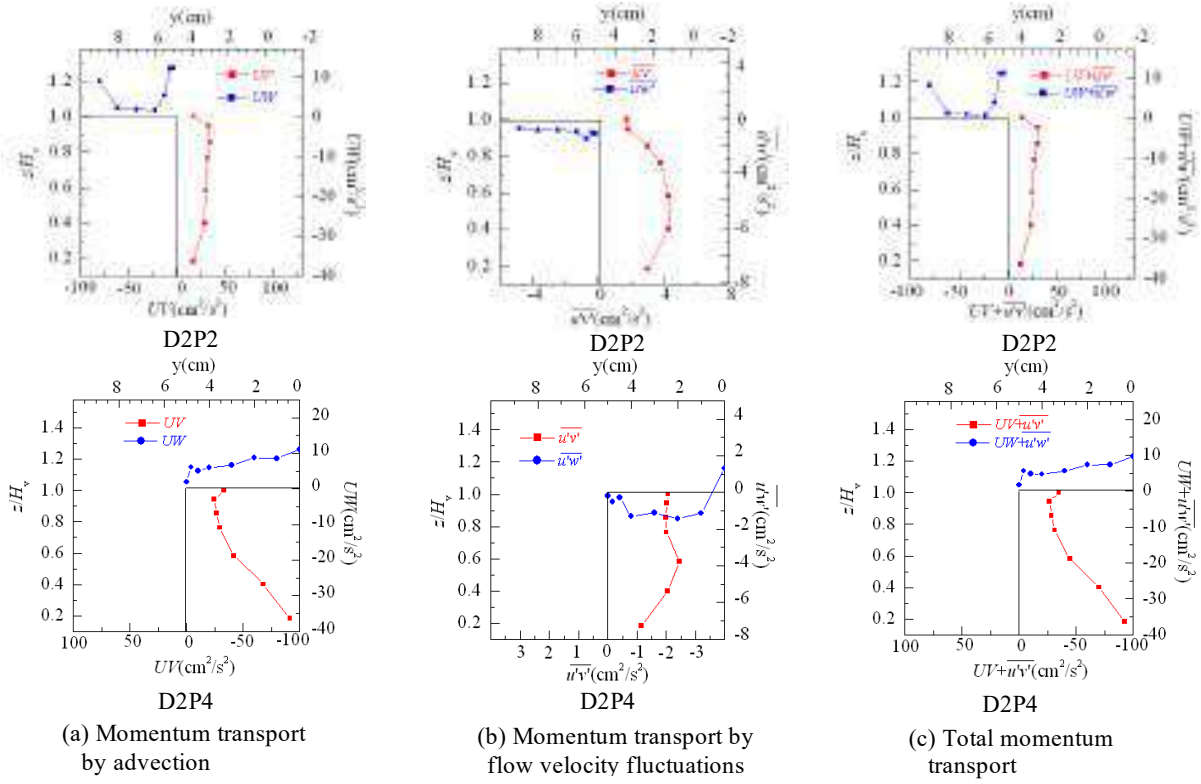

(a) Momentum transport by advection

(b) Momentum transport by flow velocity fluctuations

(c) Total momentum transport

Fig. 4. Distribution of momentum transport at vegetation zone boundaries.

Focusing on momentum transport due to advection in D2P2 and D2P4, the cross-sectional change values are dominant over the vertical change values in both cases. This indicates that in flows with vegetation under overflow conditions, momentum exchange in the cross-flow direction is more active than in the vertical direction. Furthermore, comparing these values reveals that the relationship between flow resistance characteristics and the magnitude of momentum transport due to advection is nearly identical.

In momentum transport due to flow velocity fluctuations, it was confirmed that in all cases, the cross-sectional variation values were dominant compared to the vertical variation values. Furthermore, comparing the momentum transport due to advection with that due to flow velocity fluctuations in each case reveals that the momentum transport due to advection is larger, indicating a greater influence of advection-driven momentum transport. Therefore, it became clear that in the experimental cases, momentum transport due to advection is more dominant than momentum transport due to flow velocity fluctuations as a factor in flow resistance characteristics.

Focusing on the total momentum transport, which is the sum of momentum transport due to advection and momentum transport due to velocity fluctuations, it can be observed that the total momentum transport exhibits a distribution pattern similar to that of momentum transport due to advection. Furthermore, focusing on the total momentum transport in the transverse direction, it was observed that D2P4, where the flow resistance characteristics were greatest, exhibited a larger total momentum transport compared to the other cases. This suggests that the relationship between resistance levels in the main channel and vegetation areas can be explained by their respective total momentum transport values.

5. Conclusions

This study clarified the flow resistance characteristics and flow mechanisms in open channels with vegetation communities arranged in a downstream sequence, when the density and arrangement of the vegetation zones were altered. The flow resistance characteristics suggest that the magnitude of resistance can be quantitatively evaluated based on the total momentum transport at the boundary between the main channel and the vegetated area.

References

D. Liu, P. Diplas, J. D. Fairbanks, C. C. Hodges (2008) An experimental study of flow through rigid vegetation, Journal of geophysical research:Earth Surface, Vol.113, Article ID F04015

Hyun Dong Kim, Xiao Yu, David Kaplan (2024) Steady Flow Over a Finite Patch of Submerged Flexible Vegetation, Water Resources Research, Vol.60, No.1, e2023WR035222

Raupach, M. R. and Thom, A. S. : Turbulence in and above plant canopies, Ann. Rev. Fluid Mech, Vol. 13, 97-129

Book of Abstracts of the *16th International Symposium on Ecohydraulics*
Challenges and solutions in the time of global changes
August 16–20, 2026, Lausanne, Switzerland
ISSN: 2790-2420 | ISBN: 978-90-837233-9-6 | doi:[10.64697/iahr.proc.ise2026.abs]
© 2026 IAHR. CC BY-NC-ND 4.0

FLOW DRAG PARAMETERISATION OF LEAKY BARRIERS FOR NATURAL FLOOD MANAGEMENT

Kate BRADBROOK[1], Elizabeth FOLLETT[2], Barry HANKIN[3]

[1,3]JBA Consulting, UK
email: kate.bradbrook@jbaconsulting.com
email: barry.hankin@jbaconsulting.com

[2] University of Liverpool
email: e.follett@liverpool.ac.uk

ABSTRACT

Natural Flood Management relies on working-with-nature measures including leaky barriers (log jams) and other measures to provide flood mitigation benefits. Guidance highlights a need for improved representation of such structures across flow magnitude and spatial scale. This study presents a depth average modelling approach that represents leaky barriers as porous regions with specified loss coefficients, avoiding the overhead and instability of bespoke rating curves and the coarse locality of raised Manning's n. A canopy-drag formulation is adapted to derive theoretical quadratic loss coefficients expressed in terms of measurable barrier properties. Key implementation issues are addressed, and derived coefficients are tested against laboratory flume experiments using two depth-averaged hydrodynamic models (TUFLOW, HECRAS 2D) and two 3D CFD codes (FLOW3D, OpenFOAM). The method is then applied at catchment scale using the two depth-averaged models and compared with Manning's uplift and stage–discharge approaches. The porous region quadratic loss method is demonstrated to be a flexible, computationally efficient alternative for catchment modelling, with guidance on parameter selection and caveats for high-flow regimes and model sensitivity.

Keywords: Natural flood management; leaky barriers; log jams; porosity modelling.

1. Overview

Natural Flood Management figures prominently in the priorities of both regulators (e.g. the UK Environment Agency) and investors (e.g. the World Bank). Leaky barriers (Fig. 1) are an established element of such solutions but the Environment Agency 2024 "Working with natural processes to reduce flood risk" Evidence Directory Update points to a need to "better understand how to improve leaky barrier representation within models, including at varying (flow) magnitudes".

The backwater rise upstream of a leaky barrier increases with number, size and packing density of the logs and the length of the barrier (Follett et al. 2020). Momentum loss within the barrier depends on the number of logs per bed area and scale of individual logs, consistent with the law for drag in canopies (Raupach 1994, Belcher et al. 2012, Finnigan 2000, Nepf 2012). Follett and Hankin (2022) identified ways to represent leaky barriers in 2D depth-averaged hydraulic models, through bespoke rating curves and raised reach-averaged Manning's n values, based on the leaky barrier characteristics and number of barriers per reach length. However, at a catchment scale, the rating curve approach can be time consuming and lead to model instability with a large number of structures. The raised Manning's approach, whilst shown to satisfactorily reproduce the storage effects of the barriers, cannot reproduce structure-scale flow dynamics.



Fig.1. Leaky barriers in Nant Drysiog, Bryn, Wales

In this paper we present an alternative approach using porous regions, an in-built option now available in many modelling packages, giving guidance on selection of loss coefficients to represent the physical restrictions and drag losses within the barrier. TUFLOW has long offered such functionality (the FLC layer) and HEC-RAS has recently (from version 6.6) introduced a similar porosity and flow drag layer option. The TUFLOW approach was originally designed for modelling bridges and fences in 2D and has the advantage of allowing several layers to be defined with different porosities. This could have significant advantages for modelling leaky barriers with a lower gap (Follet et al. 2021) as well as overtopping situations. HEC-RAS allows specification of a maximum height (thickness), allowing higher discharges to overtop the barrier. Nevertheless, these approaches in both platforms adjust a depth-averaged porosity rather than simulating true overflow or underflow and this impacts of this limitation are investigated through comparison with 3D CFD simulations.

In order to define theoretical loss coefficients for different types of leaky barrier, we expand on the approach of Follett et al. (2020) in adapting the canopy drag model. The performance of these values are tested in both 2D and 3D CFD models of flume experiments and compared against the data of Follett et al. (2020 and 2021) before being applied in 2D catchment models at Nethercote, UK.

2. Porosity modelling

Many CFD and hydrodynamic models incorporate options to modify the void fraction (porosity) of cells (or cell sides) and/or apply associated losses. There are commonly two types of loss: the Darcy-type viscous flow losses which are a linear function of velocity and applicable to dense porous media with minimal voids and slow flow, and the Forchheimer-type turbulent flow losses which are a quadratic function of velocity.

Following Follett et al (2020), the canopy drag model can be adapted to represent leaky barriers by assuming the momentum loss within the barrier is proportional to the number, size, and packing density of the logs and the barrier length. A quadratic drag law is therefore applicable for typical flow velocities observed in field settings (>1.6e-6 m/s for 0.3m log diameter, Tanino et al. 2005, Nepf 2012).

Careful examination of the exact implementation methods for porous losses within different models is required when deriving coefficients with respect to three main aspects:

- Whether cell volume/cell side width is adjusted with respect to a prescribed porosity and if the losses are defined using the associated "microscopic velocity" in the gaps between the solid, or the "macroscopic velocity" over the whole cell
- Whether constants such the additional factor of one half are included in the coefficients or the momentum equations
- Whether the losses are applied as a fixed total loss (e.g. for "thin" baffle-type elements on cell sides) or are cumulative over the number of cells within the porous media. In the latter case, the influence of cell size needs to be checked.

The implementation within two depth-averaged hydrodynamic models (HEC-RAS and TUFLOW) and two CFD models (FLOW3D and OPENFOAM) are presented and compared, and expressions for appropriate coefficients for leaky barriers are derived in terms of the number of logs per square metre of leaky barrier cross-section, the average log diameter and the solid volume occupied by the logs.

3. Validation of porosity methods at lab scale

In order to test implementation of the approaches described in the previous section, a range of leaky barrier experiments from Schalko et al. (2018) as analysed in Follett et al. (2020) are recreated using HEC-RAS 2D, TUFLOW, FLOW3D and OPENFOAM (e.g. Fig.2). The use of the CFD models enable limitations of the 2D depth-averaged approaches to be disaggregated from the use of the porous region quadratic loss method. The impact of various modelling options in terms of mesh size and thin (baffle) or thick (porous region) approaches are investigated in terms of accuracy and model stability.

The theoretical approach described by Follett et al. (2020) required adjustments above a critical discharge, where a region of falling water occurs downstream of the dam (e.g. Fig.2c). In previous translations to 2D modelling, a custom stage-discharge curve has been used to represent individual structures (Follett and Hankin, 2022). However, both the 3D and 2D models using a porous region reproduced this adequately (Fig.2d), allowing retention of fixed drag parameters across a wider range of flow rates.

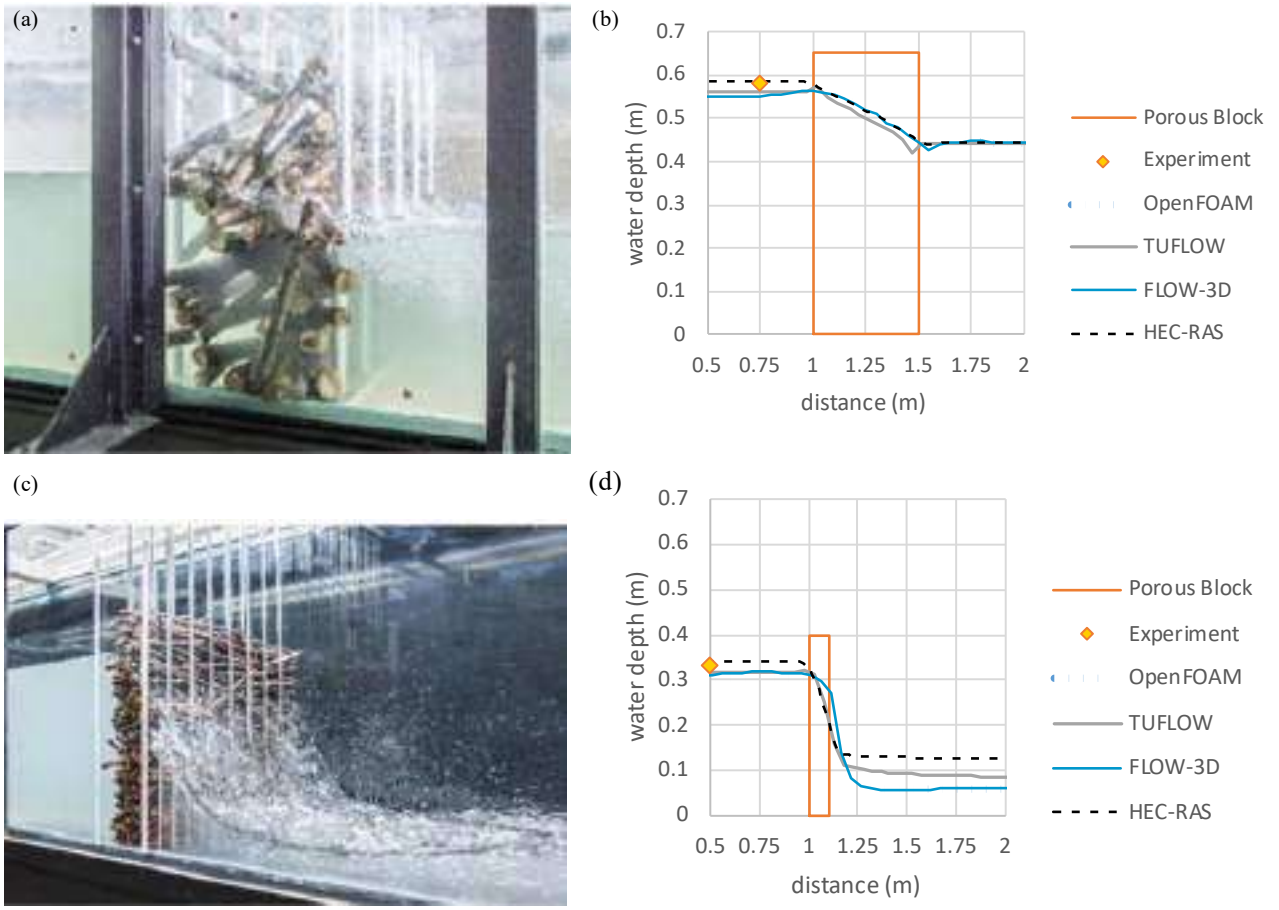

Fig.2 Examples of observed and predicted water level profiles for experiments by Schalko et al. (2018) as analysed in Follett et al. (2020): (a), (b) Experiment B26.5 with 0.065m diameter logs and open porosity 0.77 for a flow rate of 0.25m^3/s per unit width and downstream depth 0.443m (c), (d) Experiment A13.4 with 0.007m diameter sticks and open porosity 0.69 for a flow rate of 0.08m^3/s per unit width and downstream depth (after flow recovery) of 0.1m

4. Catchment scale porosity modelling

Using the understanding developed through the laboratory-scale modelling, this approach is applied using two depth-averaged models to the Nethercote catchment (Shipston-on-Stour, UK). There are 37 leaky barriers in this 7.4km^2 catchment and Champion et al (2024) presented results modelling these using HEC-RAS 2D through both a Manning's n uplift and individual stage-discharge curves for each barrier. We compare those results to the use of porous region quadratic loss methods in both a HEC-RAS 2D and TUFLOW model of this catchment for a range of flows from normal conditions to flood flows.

5. Conclusions

Whilst uncertainties will always exist in modelling the impact natural flood management elements at catchment scale, the porous region quadratic loss approach is shown to be a useful tool for modellers and guidance on parameter selection is provided.

Acknowledgements

JBA Labs for the funding to undertake this study. I. Schalko for permission to use data and photographs from her experiments.

References

Belcher, S, Harman, I, & Finnigan, J (2012) The wind in the willows: Flows in forest canopies in complex terrain, Annual Review of Fluid Mechanics, 44, 479–504, https://doi.org/10.1146/annurev-fluid-120710-101036

Finnigan, J (2000) Turbulence in plant canopies, Annual Review of Fluid Mechanics, 32, 519–571, https://doi.org/10.1146/annurev.fluid.32.1.519

Follett, E, Schalko, I, Nepf, H (2020) Momentum and energy predict the backwater rise generated by a large wood jam, Geophysical Research Letters 47, e2020GL089346 https://doi. org/10.1029/2020GL089346

Follett, E, Schalko, I, Nepf, H (2021) Logjams with a lower gap: backwater rise and flow distribution beneath and through logjam predicted by two-box momentum balance, Geophysical Research Letters 48, e2021GL094279 https://doi.org/10.1029/2021GL094279

Follett, E, and Hankin, B (2022) Investigation of effect of logjams series for varying channel and barrier physical properties using a sparse input data 1D network model, Environmental Modelling and Software, 158, 105543, https://doi.org/10.1016/j.envsoft.2022.105543

Nepf, H, (2012) Flow and transport in regions with aquatic vegetation, Annual Review of Fluid Mechanics, 44:123–42, https://doi.org/10.1146/annurev-fluid-120710-101048

Raupach, M (1994) Simplified expressions for vegetation roughness length and zero-plane displacement as functions of canopy height and area index, Boundary-Layer Meteorology, 71, 211–216, https://doi.org/10.1007/BF00709229

Schalko, I, Schmocker, L, Weitbrecht, V, & Boes, R (2018) Backwater rise due to large wood accumulations, Journal of Hydraulic Engineering, 144, 04018056, https://doi.org/10.1061/(ASCE)HY.1943-7900.0001501

Tanino Y, Nepf H, Kulis P (2005) Gravity currents in aquatic canopies, Water Resources Research, 41:W12402, https://doi.org/10.1029/2005WR004216

Book of Abstracts of the *16th International Symposium on Ecohydraulics*
Challenges and solutions in the time of global changes
August 16–20, 2026, Lausanne, Switzerland
ISSN: 2790-2420 | ISBN: 978-90-837233-9-6 | doi:[10.64697/iahr.proc.ise2026.abs]
© 2026 IAHR. CC BY-NC-ND 4.0

THREE DIMENSIONAL NUMERICAL SIMULATION OF TURBULENT FLOW WITH BRIDGE OVERTOPPING

Yongjun KWON[1], Hyung-Suk KIM[2]

[1] Kunsan National University, Republic of Korea
email: dydwns0507@kunsan.ac.kr

[2] Kunsan National University
email: hskim0824@kunsan.ac.kr

ABSTRACT

A 3D numerical model based on the RANS equations coupling with the density function method was developed to examine the turbulent flow with overtopping around a bridge under extreme hydrologic conditions. Numerical simulations revealed that, under overtopping conditions, the upstream velocity decreased due to the backwater effect, while the maximum flow velocity induced by overtopping reached approximately $U_{over,max}/U$ =2.0. As the upstream discharge increases, the water-level difference between the upstream and downstream sections becomes more pronounced, generating strong shear layers and extensive recirculation zones downstream of the bridge, along with notable free-surface oscillations. This study provides three-dimensional insights into bridge hydraulics under extreme flow conditions and delivers fundamental hydraulic data that can support future bridge design, evaluation, and maintenance for flood-safety enhancement.

Keywords: numerical model, Overtopping, Bridge, Turbulent flow.

1. Introduction

Recent climate change has led to an increase in both the frequency and intensity of extreme rainfall events, posing significant challenges to the stability of hydraulic infrastructures. According to the long-term climate change assessment conducted by the Korea Meteorological Administration, the frequency of heavy precipitation events has shown a persistent upward trend over the past century. Furthermore, the Intergovernmental Panel on Climate Change (IPCC) scenarios indicate that extreme climate indices will continue to rise through 2050, even under carbon-neutral conditions. These findings implies the need to re-evaluate the adequacy of current design standards applied to water resource infrastructures, including bridges, levees, and dams, during their design and maintenance phases.

Kara et al. (2014) proposed a numerical model that combines a Large Eddy Simulation (LES) framework with the Level Set Method (LSM) for free-surface tracking. Their model was applied to bridge overtopping flows and demonstrated high accuracy in predicting free-surface displacements occurring upstream and downstream of the bridge. Based on these results, they further analyzed the mean flow characteristics and turbulence structures around the bridge. Chua et al. (2018) employed an LES model to numerically reproduce the hydraulic model experiments conducted at the Georgia Institute of Technology for a bridge over the Towaliga River in the United States. Their study investigated the effects of bridge setback configurations and showed that the extent of recirculation zones and the characteristics of shear-layer vortices varied depending on the setback conditions, thereby clarifying the associated flow structures. Lazzarin et al. (2024) conducted a study on a bridge located along Po River. Utilizing a combination of the Volume of Fluid (VOF) method and Detached

Eddy Simulation (DES), they examined both free-surface and pressure-flow conditions. Their analysis provided detailed insights into the flow structures and shear-stress variations occurring around the bridge piers and deck. In recent years, South Korea has experienced rapid increases in extreme floods, resulting in pressure flow and overtopping around bridges. However, related research remains relatively limited. Therefore, this study employs a three-dimensional numerical modeling approach to simulate the flow characteristics associated with bridge overtopping under extreme hydrological conditions.

2. Results

Fig.1 presents the three-dimensional free-surface flow patterns under overtopping conditions, visualized using the density function obtained from the numerical simulation. As the upstream inflow traverses the bridge, portion of the discharge passes through the area between the channel bed and the underside of the deck, producing pressure flow. The remaining discharge overtops the deck, accompanied by an abrupt free-surface drawdown. Downstream of the bridge, the flow subsequently plunges, generating irregular wave patterns. Following the ensuing hydraulic jump, the free surface exhibits wave-like undulations that gradually decay and return to a free flow state. When the downstream water level remains constant and only the upstream discharge increases, the water level difference between the upstream and downstream of the bridge becomes larger. As a result, a jet-like flow occurs after the plunge, and more intense free-surface fluctuations are observed. The downstream waves also exhibit relatively larger amplitudes before gradually dissipating as they propagate. The three-dimensional numerical simulation effectively captures the overall flow structures that develop around the bridge under overtopping conditions

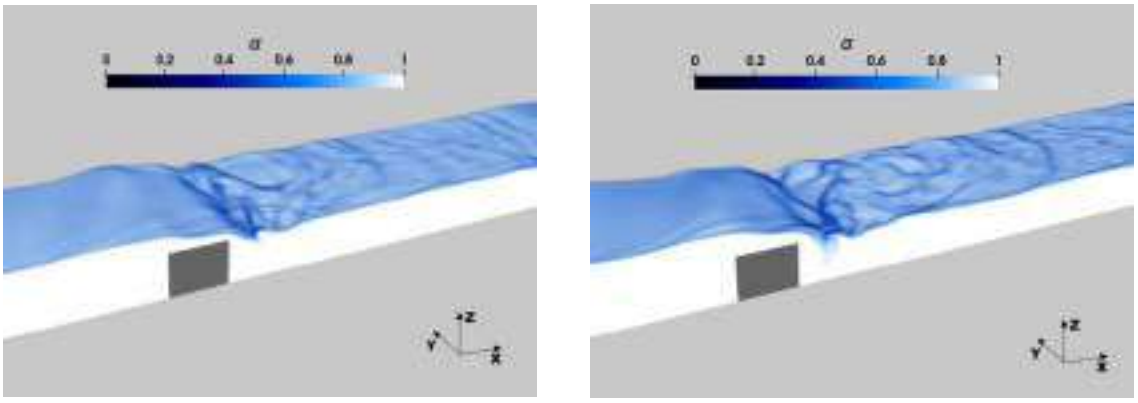

Fig. 1. Water surface around a bridge by the density function

3. Conclusion

Through the three-dimensional numerical simulations conducted in this study, the flow characteristics associated with bridge overtopping were identified. The mean velocity and turbulent kinetic energy around the bridge under extreme hydraulic conditions were examined. Future investigations encompassing a wider range of hydraulic conditions and bridge configurations are expected to enhance the quantitative reliability of hydraulic stability assessments.

Acknowledgements

This work was supported by Korea Environment Industry & Technology Institute (KEITI) through Research and Development on the Technology for Securing the Water Resources Stability in Response to Future Change, funded by Korea Ministry of Climate, Energy, Environment(MCEE)(2480000388).

References

Kara S, Mulahasan S, Stoesser T (2014) Flow dynamics through a submerged bridge opening with overtopping, Journal of Hydraulic Research, 53(2), 37-41.
Chua KV, Fraga B, Stoesser T, Hong SH, Sturm T (2018) Effect of bridge abutment length on turbulence structure and flow through the opening, Journal of Hydraulic Engineering, 145(6), 1-19.
Lazzarin T, Constantinescu G, Viero D P. (2024) Advanced hydrodynamic modelling of flow at a river bridge: Insights from 3D computational fluid dynamics, Procedia Structural Integrity, 62, 625-632.

Book of Abstracts of the *16th International Symposium on Ecohydraulics*
Challenges and solutions in the time of global changes
August 16–20, 2026, Lausanne, Switzerland
ISSN: 2790-2420 | ISBN: 978-90-837233-9-6 | doi:[10.64697/iahr.proc.ise2026.abs]
© 2026 IAHR. CC BY-NC-ND 4.0

IN-STREAM MESOHABITAT DELINEATION BASED ON HYDROACOUSTIC DATA AND HIERARCHICAL CLUSTERING

Kerstin SCHLOBIES[1], Erik VAN ROOIJEN[2], Davide VANZO[3], Eliisa S. LOTSARI[4]

[1,4] Water and Environmental Engineering, Department of Built Environment, Aalto University, Aalto, Finland
email: kerstin.schlobies@aalto.fi (for author 1)
email: eliisa.s.lotsari@aalto.fi (for author 4)
[2] Rijkswaterstaat Water, Verkeer en Leefomgeving, Afdeling Informatiemanagement leefomgeving en watermodellen (VWIL), Utrecht, The Netherlands
email: erik.van.rooijen@rws.nl (for author 2)
[3] Institute for Water and Environment, Karlsruhe Institute of Technology, Karlsruhe, Germany
email: davide.vanzo@kit.edu (for author 3)
[4] Department of History and Geography, Faculty of Social Sciences and Economics, University of Eastern Finland, Joensuu, Finland

ABSTRACT

Restoring rivers through dam removal can substantially alter fluvial mesohabitat composition, providing insights into how restored river reaches evolve. Our case study is the Nordic Hiitolanjoki River, the most important landlocked salmon river in Finland, where three dams were removed and replaced with restored rapids between 2021 and 2023. We collected thousands of hydroacoustic measurements using an Acoustic Doppler Current Profiler (ADCP) downstream of the removed dams before and after the dam removal under comparable discharge conditions. These datasets were used to delineate hydraulic units (HUs). To do so, we developed PatchBuilder, a Python-based tool that performs fast hierarchical clustering with a spatial contiguity constraint to delineate mesohabitat patches based on interpolated water depth and depth-averaged flow velocity from field data. In a further step, we applied deterministic classification to group the delineated HUs into overarching habitats of similar hydraulic characteristics. Our findings indicate a shift in the high-velocity core in two of the three studied reaches following dam removal and rapids restoration. The approach demonstrates the potential of hierarchical clustering for mesohabitat delineation to assess river restoration outcomes. Furthermore, this framework supports the assessment of habitat composition, thereby contributing to strategies aimed at mitigating habitat loss in aquatic ecosystems.

Keywords: habitat delineation; hydraulic units (HUs); dam removal; river restoration; hydroacoustics; ADCP

1. Introduction

Human activities, such as flow regulation for hydropower generation have substantially modified hydromorphological processes in rivers (Grill et al., 2019; Zarfl et al., 2015). Habitat homogenization, fragmentation and loss are leading, and persistent causes of species decline in freshwater systems (Reid et al., 2019; Ruhi et al., 2018; WWF, 2018). To not only slow down but reverse biodiversity loss, a process described as 'bending the curve', river restoration must be integrated with ambitious conservation strategies such as protecting and restoring habitats and emphasizing river connectivity (Tickner et al., 2020). Dam removal has emerged as an efficient restoration measure to enable longitudinal continuity and to reestablish natural sediment and flow regimes (Bellmore et al., 2019).

Here, our aim is to identify the impacts of dam removals and restoration actions on physical habitat composition downstream of three restoration sites in the lowland, meandering Hiitolanjoki River (Fig. 1). Therefore, we delineated spatially continuous, homogeneous hydraulic units (HUs) and assessed pre- and post-restoration mesoscale habitat changes under similar discharge conditions.

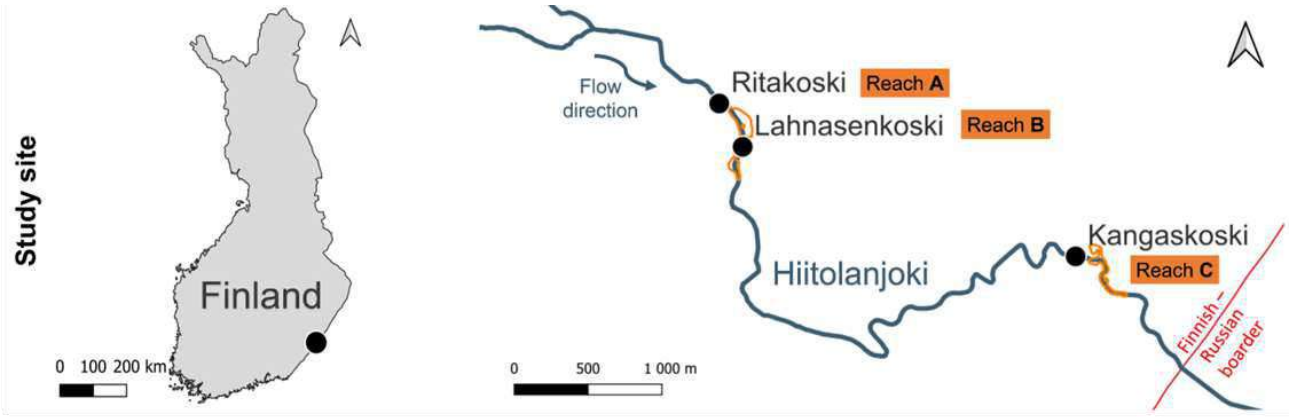

Fig. 1. The study reaches A, B and C and their locations at Hiitolanjoki River in Finland. Mesohabitats are delineated for the extents of Reach A, B and C downstream of their former dams at Ritakoski, Lahnasenkoski and Kangaskoski.

Hiitolanjoki River is characterized by an average discharge of 11 m³/s with peak floods caused by spring snowmelt (Schlobies et al., 2025). The discharge range during monitoring was 3.2 to 19.6 m³/s capturing low and high flow events. Hiitolanjoki River flows into Lake Ladoga in Russia and hosts Finland's last naturally reproducing population of landlocked salmon (*Salmo salar* m. *sebago*) (Ozerov et al., 2010). This critically endangered species has experienced substantial habitat loss due to longitudinal fragmentation and channel simplification. Between 2021 and 2023, three consecutive mid-sized dams which were originally constructed in the early 20th century were replaced by whitewater rapids to overcome a total vertical drop of 18 meters. The study area comprises three formerly regulated and longitudinally disconnected reaches of about 150-450 m length and 25-65 m width, hereafter referred to as Reach A (Ritakoski), Reach B (Lahnasenkoski), and Reach C (Kangaskoski). These reaches are located less than 5 km apart and lie downstream of their respective former dam sites (Fig. 1).

2. Methods

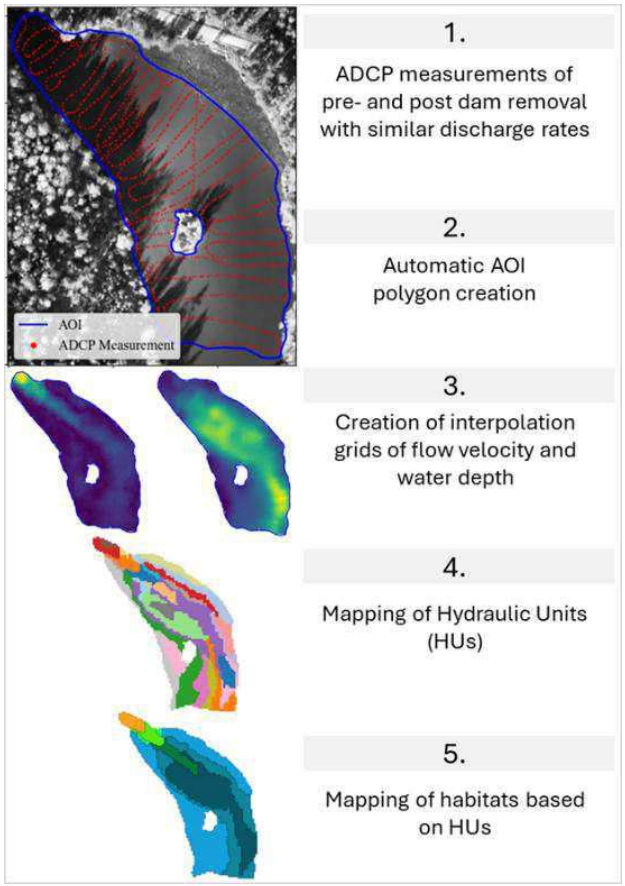

Fig. 2. Schematic representation of the mesohabitat delineation approach.

The hydraulic variables flow velocity and water depth were simultaneously collected with an Acoustic Doppler Current Profiler (ADCP) and are the basis for delineating HUs (Fig. 2, step 1). To account for the varying ADCP data sampling extents per pre- and post-restoration field campaign, we only included measurements within an Area of Interest (AOI) per study reach for the subsequent mesohabitat delineation to ensure sufficient overlap (Fig. 2, step 2). We applied inverse distance-weighted interpolation per pre- and post-restoration date based on the extent of a 2 × 2 m void grid of the AOI (Fig. 2, step 3). Hereby, we included spike-filtered ADCP measurements, which were cell-wise aggregated by their mean to counteract locally denser point measurement sampling. Flow velocity was calculated from the interpolated u and v vector components to preserve the vector properties of velocity and ensured accurate physical representation of the flow field. For the automatic delineation of in-stream habitat patches we made use of the principles of the BASEmeso, an agglomerative hierarchical clustering algorithm with an added spatial contiguity criterion (van Rooijen et al., 2021). Based on its fundamental spatial concepts of contiguous patch

homogeneity and patch boundary contrast, we created a new Python-based tool called PatchBuilder. This tool enables efficient geospatial patch delineation based on irregular mesh or rectangular grid-cell polygons and associated numeric variables and is applicable across a range of fields and use cases. Here, PatchBuilder groups the equally weighted, gridded and standardized input variables flow velocity and water depth in patches based on how similar these are to each other. It is a bottom-up clustering approach, where initially all patches are singletons, i.e. patches consist of a single grid cell containing water depth and flow velocity information. At each iteration, similar patches are merged until all grid cells are part of one bigger root patch, using a 4-neighbour rule. (Fig. 2, step 4). In a next step, we applied a deterministic, rule-based classification based on mean flow velocity and mean water depth. Patch-wise means were normalized to [0,1] to define a reach-specific, dimensionless feature space, which was subdivided into nine hydraulic habitat classes. The delineated patches were deterministically assigned to one of the nine classes to spatially group HUs of broadly similar water depth and flow velocity (Fig. 2, step 5).

3. Preliminary Results

Our findings indicate a shift in the high-velocity core of Reach B and C due to the dam removals and the restoration of the bypass channels. Pre-restoration peak flow velocities in Reach B and C occurred close to the turbine outlet while the respective hydropower plants were still operating. Post-restoration higher flow velocities occur adjacent to the restored rapids. In Reach A the most downstream part is affected by the subsequent restoration of the Lahnasenkoski rapids indicating higher flow conditions compared to pre-restoration. The delineated mesohabitats accurately represented the spatial patterns of flow velocity and water depth, reflecting homogeneous hydraulic conditions within clearly defined boundaries. Distinct hydraulic features, such as peak flow velocities near hydropower plant outlets, were effectively depicted. The hydraulic patches provide a spatially explicit representation of physical habitat composition and support field-based ecological surveys and habitat-oriented monitoring.

While this study enhances the understanding of hydraulic characteristics and habitat composition following multiple dam removals in a Nordic river, further research is essential to investigate the impact of the rapids as additional habitat and methods to evaluate changes in habitat structure and diversity.

Acknowledgements

Funding from MVTT-project ("Impacts of multiple dam removals on river channel hydro-morphodynamics and mesohabitat diversity", grant number: 48169) enabled the research work of Schlobies, and further fieldwork, data analysis and publishing. Funding from the Research Council of Finland (DefrostingRivers project, grant number: 338480) enabled the field measurements and salary of Lotsari. The work for this paper was also financially supported by Natural Resources Institute Finland (Luke: DamRem project number 41007-00178000 [2020-2023]), Department of Built Environment (Aalto University) and Department of Geographical and Historical Studies (University of Eastern Finland). The infrastructure was provided by University of Eastern Finland during the year 2021, via Lotsari's affiliation, and thereafter by Aalto University and HYDRO-RI-Platform project (grant number: 346167).

References

Bellmore JR, Pess GR, Duda JJ, O'Connor JE, East AE, Foley MM, Wilcox AC, Major JJ, Shafroth PB, Morley SA, Magirl CS, Anderson CW, Evans JE, Torgersen CE, Craig LS (2019) Conceptualizing ecological responses to dam removal: If you remove it, what's to come? BioScience, 69, 26–39

Grill G, Lehner B, Thieme M, Geenen B, Tickner D, Antonelli F, Babu S, Borrelli P, Cheng L, Crochetiere H, et al. (2019) Mapping the world's free-flowing rivers, Nature, 569, 215–221

Reid AJ, Carlson AK, Creed IF, Eliason EJ, Gell PA, Johnson PTJ, Kidd KA, MacCormack TJ, Olden JD, Ormerod SJ, Smol JP, Taylor WW, Tockner K, Vermaire JC, Dudgeon D, Cooke SJ (2019) Emerging threats and persistent conservation challenges for freshwater biodiversity, Biological Reviews, 94, 849–873

Ruhi A, Dong X, McDaniel CH, Batzer DP, Sabo JL (2018) Detrimental effects of a novel flow regime on the functional trajectory of an aquatic invertebrate metacommunity, Global Change Biology, 24, 3749–3765

Tickner D, Opperman JJ, Abell R, Acreman M, Arthington AH, Bunn SE, Cooke SJ, Dalton J, Darwall W, Edwards G, Harrison I, Hughes K, Jones T, Leclère D, Lynch AJ, Leonard P, McClain ME, Muruven D, Olden JD, Young L (2020) Bending the curve of global freshwater biodiversity loss: An emergency recovery plan, BioScience, 70, 330–342

van Rooijen E, Vanzo D, Vetsch DF, Boes RM, Siviglia A (2021) Enhancing an unsupervised clustering algorithm with a spatial contiguity constraint for river habitat analysis, Ecohydrology, 14, e2285

WWF (2018) Living Planet Report 2018: Aiming higher, WWF International, Gland, Switzerland, 148 pp.

Zarfl C, Lumsdon AE, Berlekamp J, Tydecks L, Tockner K (2015) A global boom in hydropower dam construction, Aquatic Sciences, 77, 161–170

Book of Abstracts of the *16th International Symposium on Ecohydraulics*
Challenges and solutions in the time of global changes
August 16–20, 2026, Lausanne, Switzerland
ISSN: 2790-2420 | ISBN: 978-90-837233-9-6 | doi:[10.64697/iahr.proc.ise2026.abs]
© 2026 IAHR. CC BY-NC-ND 4.0

SCALE RESOLVED NUMERICAL SIMULATIONS OF A NOVEL EDDY-BASED FISH GUIDANCE SYSTEM (EGS)

Eric LILLBERG[1], Mikaela LARSSON[1], David Florian VETSCH[2], Kamal Prasad PANDEY[2], Bjørn Winther SOLEMSLIE[3], Ismail ALBAYRAK[2], Armin PETER[4], Torbjørn FORSETH[3], Ole Gunnar DAHLHAUG[5], Robert M. BOES[2], Ana T. SILVA[3,1]

[1] Vattenfall Research and Development, Älvkarleby Laboratory, Älvkarleby, Sweden
[2] Laboratory of Hydraulics, Hydrology and Glaciology (VAW), ETH Zurich, Zurich, Switzerland
[3] Norwegian Institute for Nature Research (NINA), Trondheim, Norway
[4] FishConsulting GmbH, Olten, Switzerland
[5] Norwegian University of Science and Technology (NTNU), Trondheim, Norway

ABSTRACT

In the scope of the FishPath project, the behavioral response of Atlantic salmon smolts (*Salmo salar*) and European eels (*Anguilla Anguilla*) to different types of vortex generating obstacles is investigated. Tests of three different vortex generating obstacles, together with observations of resulting fish behavior, were performed in two different size laboratory flumes at ETH Zurich. In the small-scale flume tests, only two obstacles were present, and the turbulent flow field was measured using ADV. In the medium size flume tests, several more obstacles were used to form a continuous Eddy-based fish Guidance Systems (EGS). In an additional small-scale test performed in a flume at NTNU Trondheim, similar obstacles were also used together with PIV measurements to capture the details of wake formation close to the obstacle. The two small flume tests provide the hydraulic data used for verification and validation of a computational fluid dynamics (CFD) model, which is in turn used to evaluate the vorticity created by the different types of EGSs developed within the FishPath project. The CFD model is developed using the open-source computational physics tool OpenFOAM. The Navier-Stokes equations for incompressible, viscous flow are solved using a finite volume framework together with an improved delayed detached eddy (IDDES) turbulence model for closure. The turbulent flow fields and eddy structures for several EGS configurations and different approach flow velocities are evaluated. For some EGS configurations, the free surface is also included by a volume of fluid (VOF) approach. The simulated mean and time dependent flow quantities are compared to measurements and show very good agreement for cases both with and without the free surface.

Keywords: CFD; DES; OpenFOAM; Downstream fish migration; fish passage; behavioural guidance structure

1. Introduction

Hydropower plants (HPPs), weirs, and other river structures often block or delay fish migration (Silva, 2018). Downstream passage through turbines or spillways can cause injury or mortality, reducing global fish populations (Cox et al., 2023). Most fish passage solutions target upstream migration, while downstream solutions remain limited both in research and applications. Physical barriers like horizontal bar rack bypass systems (HBR-BSs) work at small HPPs (Calles et al., 2021; Maddahi et al., 2022; Meister et al., 2022; Kjaerås et al., 2023), but large-scale run-of-river plants lack comparable solutions. Mechanical-behavioral barriers, louvers, angled racks, and curved bar racks (CBRs), use wider spacing and hydraulic cues to guide fish (Beck et al., 2020; Albayrak et al., 2020; Kjærås et al., 2025). Fish-friendly turbines help but are limited by their low-head applications (Koukouvinis, 2023). High costs, head loss, clogging, and maintenance restrict these systems under varied conditions. Many species respond to turbulent eddies (Lupandin, 2005; Liao, 2007) offering potential for new guidance systems. The FishPath project explores salmon and eel reactions to eddies in turbulent flows to develop an eddy-based guidance system (EGS). Streamwise, transverse, and vertical eddy generators were tested in a flume, and the flow fields are simulated numerically using CFD models. Vertical and streamwise eddies triggered avoidance reaction in fish tests (Kamal, 2026), making them prime candidates

for EGS design. By using validated eddy-resolving CFD models, the details of the turbulent flows can be studied together with fish behavior to improve the EGS design for increased fish avoidance and improved guidance efficiency.

2. Methods

2.1. Hydraulic measurements and flume set-ups

Small flume tests were performed in a 13.5 m long, 0.5 m wide and 0.7 m deep recirculating open channel ethohydraulic flume at the Laboratory of Hydraulics, Hydrology and Glaciology (VAW) of ETH Zurich, c.f. fig 1 top. The test section comprises 2.5 m long observation area with a rigid top surface at z =0.475 m exactly at water surface and two obstacles placed at 15 degree angle and 0.69 m longitudinal spacing. One obstacle was placed at the wall of flume and second at the center of flume. Two different approach flow velocities were used, Uo = 0.3 m/s and Uo = 0.6 m/s. The time dependent flow field was measured using an ADV probeat 100 Hz recording frequency for 60 seconds.

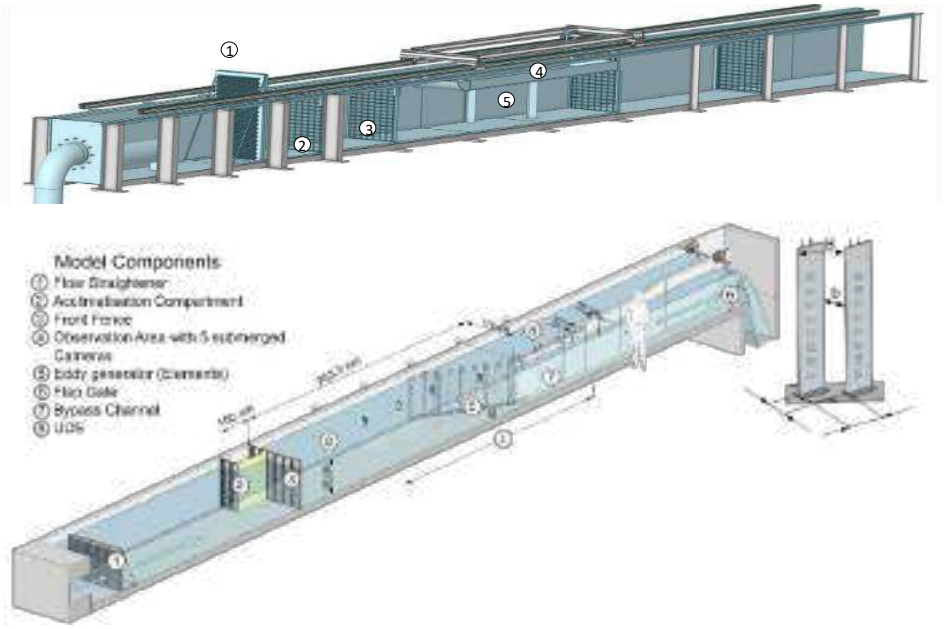

Fig. 1. Schematic 3D views of the small and medium scale ethohydraulic flumes installed at ETH Zurich used for fish tests and validation

The medium size flume tests at ETH Zurich were performed in a 30 m x 1.5 m x 1.2 m open channel ethohydraulic flume at the Laboratory of Hydraulics, Hydrology, and Glaciology (VAW), ETH Zurich, c.f. fig. 1 bottom. The EGS with streamwise eddy generators (elements) was installed along a 1.1 m wide section adjacent to a full depth bypass channel of 0.25 m width. The mean approach velocity was fixed at U_o= 0.6 m/s and water depth of 0.9 m and bypass velocity was adjusted to 0.72 m/s. Six configurations of the EGS were tested, combining two EGS angles to the flow direction $\theta = \theta 1$ and $\theta 2$, ($15° < \theta < 45°$ and $\theta 2 > \theta 1$), and three lateral spacings between consecutive elements in streamwise direction $b = S1$, $S2$, and $S3$ (100 mm < b < 200 mm and $S3 > S2 > S1$).

Particle Image Velocimetry (PIV) measurements were performed in a small size flume at NTNU Trondheim, with a 0.66 m by 1.2 m test section, c.f. fig 2. The PIV camera was mounted at the free surface looking down, giving detailed measurements of the near wake flow structures for the downstream obstacle at different depths. Here the flow approach velocity was U_o=0.6 m/s

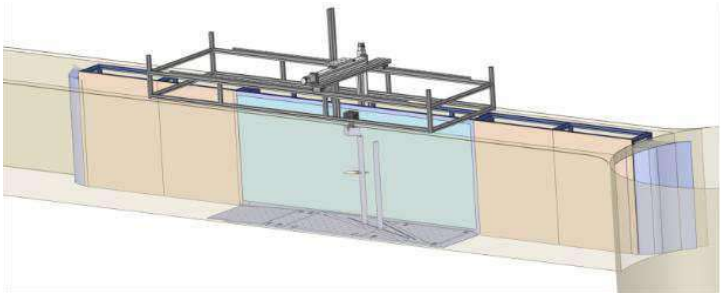

Fig. 2. A schematic 3D view of the small scale flume at NTNU Trondheim used for validation

2.2. Numerical model

The numerical model was developed using the open source computational physics tool OpenFOAM. The Navier-Stokes equations for incompressible, viscous flow are solved using a finite volume framework together with an improved delayed detached eddy simulation (IDDES) turbulence model for closure. The IDDES model uses a komegaSST turbulence model formulation in the near wall region, i.e. kOmegaSSTIDDES, which reduces the requirement on the wall-normal spatial resolution. For some EGS configurations, the free surface was also included by a volume of fluid (VOF) approach. The smallest mesh control volume (cell) size is chosen large enough for the small scale flume models, as to be able to use similar size for the medium flume model. Typically, the smallest volume mesh cell size is 0.005 m and the total cell count for the small scale flumes is 7.000.000, and for the medium size flume 25.000.000. The boundary layers are resolved on all walls with an average $y^+ < 55$ for all geometries and approach velocities. The mesh was automatically generated using the OpenFOAM native meshing tool snappyHexMesh.

3. Results and discussions

The simulated mean and time dependent flow quantities are compared to the ADV and PIV measurements. In figs 3-4, the mean velocity field and turbulent kinetic energy (TKE) for the small flume tests at ETH Zurich are shown respectively. The red circles indicate the points where the ADV measurements were made. The simulated flow quantities show very good agreement with the ADV measurements.

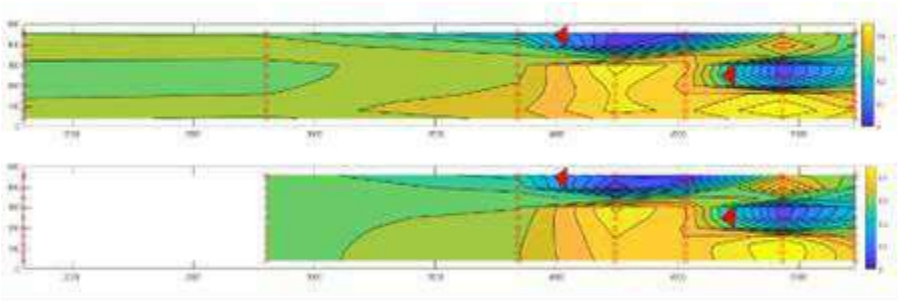

Fig. 3. Mean velocity ADV measurements in ETH small flume (top) and corresponding CFD results (bottom) for U_0=0.3 m/s

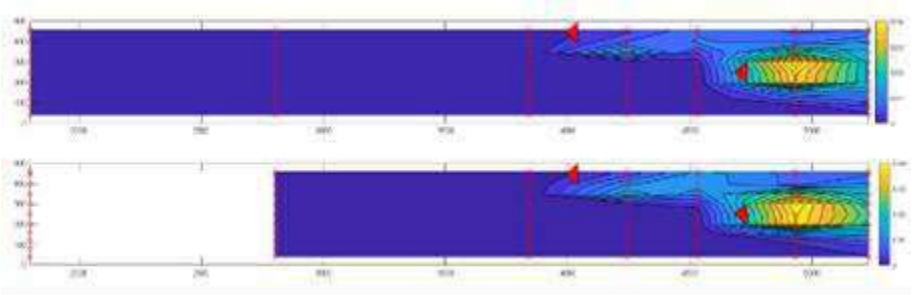

Fig. 4. Turbulent kinetic energy ADV measurements in ETH small flume (top) and corresponding CFD results (bottom) for U_0=0.3 m/s

In figure 5 a) and b), the three-dimensional flow field in the NTNU flume and the medium size flume at ETH Zurich are shown respectively, for an approach velocity of 0.6 m/s. The turbulence structures in the wakes of the obstacles are visualized using an iso-surface of the Q-Criterion, colored with velocity magnitude. In figure 5 a), the free surface is also included, visualized using an iso-surface of the volume fraction of water, α=0.5, colored with velocity magnitude.

In both figure 5a) and b), the coherent vortical structures created by the obstacles and the resulting complex flow patterns are clearly seen. In figure 5 a), the depression on the free surface over the obstacles and the downstream wave pattern is also visible. The simulated time dependent turbulent flow structures is then evaluated together with the fish behavior to further investigate the impact of the flow field on guiding efficiency.

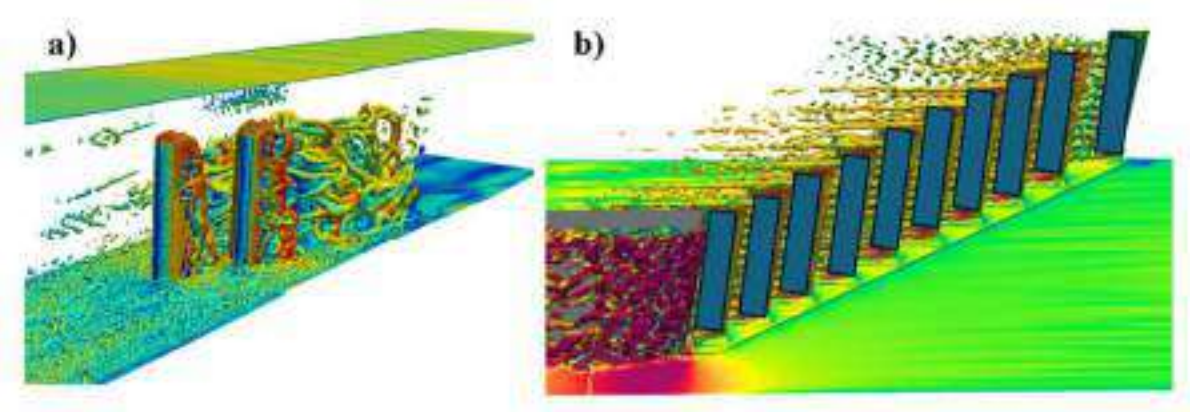

Fig. 5. a) Flow field in NTNU flume. Iso-surfaces of water volume fraction α=0.5 and Q=55 coloured with velocity magnitude for U_0=0.6 m/s. **b)** The EGS in the medium sized flume at ETH Zurich. Iso-surface of Q=15 coloured with velocity magnitude for U_0=0.6 m/s.

4. Conclusions and outlook

This study presents numerical simulations of the turbulent flow fields from different vortex generating obstacles and EGS configurations. The simulated results show very good agreement when compared to the measured data. The CFD model results are used for the detailed study of the vorticity and flow field generated by the different obstacles which directly impacts fish behavior. Measures of turbulent time and length scales are evaluated together with fish response and serves as a viable tool for improving the design of the EGS concept.

Acknowledgements

The authors gratefully acknowledge the Norwegian Research Council for supporting the FishPath Project through NINA

References

Pandey KP, Albayrak I, Peter A, Rorseth T, Lillberg E, Vetsch D, Larsson M, Boes RM, Silva AT, (2026) Development of a novel eddy-based fish guidance system (EGS) (PART-1) Book of Extended Abstracts, 16th International Symposium on Ecohydraulics, Lausanne, 16–21 August 2026.
Albayrak I, Boes RM, Kriewitz-Byun CR, Peter A, Tullis BP (2020) Fish guidance structures: hydraulic performance and fish guidance efficiencies. Journal of Ecohydraulics, 5(2), 113–131.
Beck C, Albayrak I, Meister J, Boes RM (2020) Hydraulic performance of fish guidance structures with curved bars – Part 1: head loss assessment. Journal of Hydraulic Research, 58(5), 807–818.
Beck C, Albayrak I, Meister J, Peter A, Selz OM, Leuch C, Vetsch DF, Boes RM (2020) Swimming behavior of downstream-moving fish at innovative curved-bar rack bypass systems for fish protection at water intakes. Water, 12(11), 3244.
Calles O, Elghagen J, Nyqvist D, Harbicht A, Nilsson PA (2021) Efficient and timely downstream passage solutions for European silver eels at hydropower dams. Ecological Engineering, 170, 106350.
Cox RX, Kingsford RT, Suthers I, Felder S (2023) Fish injury from movements across hydraulic structures: a review. Water, 15(10), 1888.
Kjærås H, Baktoft H, Silva AT, Gjelland KØ, Økland F, Forseth T, Szabo-Mészáros M, Calles O (2023) Three-dimensional migratory behaviour of European silver eels (Anguilla anguilla) approaching a hydropower plant. Journal of Fish Biology, 102(2), 465–478.
Kjærås H, Baktoft H, Silva AT, Gjelland KØ, Økland F, Maddahi M, Albayrak I, Lia L, Boes RM, Forseth T (2025) Full-scale performance evaluation of a partial-depth floating fish guidance bar rack. Ecological Engineering, 221, 107778.
Koukouvinis P, Anagnostopoulos J (2023) State of the art in designing fish-friendly turbines: concepts and performance indicators. Energies, 16(6), 2661.
Liao JC (2007) A review of fish swimming mechanics and behaviour in altered flows. Philosophical Transactions of the Royal Society B: Biological Sciences, 362(1487), 1973–1993.
Lupandin AI (2005) Effect of flow turbulence on swimming speed of fish. Biology Bulletin, 32(5), 461–466.
Maddahi M, Hagenbüchli R, Mendez R, Zaugg C, Boes RM, Albayrak I (2022) Field investigation of hydraulics and fish guidance efficiency of a horizontal bar rack-bypass system. Water, 14, 776.
Meister J, Selz OM, Beck C, Peter A, Albayrak I, Boes RM (2022) Protection and guidance of downstream-moving fish with horizontal bar rack bypass systems. Ecological Engineering, 178, 106584.
Silva AT, Lucas MC, Castro-Santos T, Katopodis C, Baumgartner LJ, Thiem JD, Aarestrup K, Pompeu PS, O'Brien GC, Braun DC, Burnett NJ, Zhu D, Fjeldstad HS, Forseth T, Rajaratnam N, Williams JG, Cooke SJ (2018) The future of fish passage science, engineering, and practice. Fish and Fisheries, 19(2), 340-362.
Silva AT, Aldven D, Muller S, Pandey KP, Lillberg E, Vetsch DF, Calles O, Forseth T, Albayrak I (2026) Large-scale performance evaluation of novel eddy-based fish guidance system (Part 2). Book of Extended Abstracts, 16th International Symposium on Ecohydraulics, Lausanne, 16–21 August 2026.

Book of Abstracts of the *16th International Symposium on Ecohydraulics*
Challenges and solutions in the time of global changes
August 16–20, 2026, Lausanne, Switzerland
ISSN: 2790-2420 | ISBN: 978-90-837233-9-6 | doi:[10.64697/iahr.proc.ise2026.abs]
© 2026 IAHR. CC BY-NC-ND 4.0

APPLYING TESLA VALVE PRINCIPLES TO OPEN-CHANNEL CONDITIONS FOR ECOHYDRAULIC BARRIERS

Inga KLEINEWIETFELD[1], Elena-Maria KLOPRIES[2]

[1,2]Institute of Hydraulic Engineering and Water Resources Management, RWTH Aachen University, Germany

email: kleinewietfeld@iww.rwth-aachen.de

email: klopries@iww.rwth-aachen.de

ABSTRACT

Diversion hydropower plants often create competing flow fields at the confluence of the tailrace channel and the bypass reach, causing upstream-migrating fish to follow the stronger tailrace current and miss the fishway entrance. To counteract this "dead-end effect," a physical–hydraulic barrier based on the directional flow properties of the Tesla valve is investigated. The concept aims to modify local hydraulics by generating turbulence to reduce the hydraulic attraction of the tailrace channel.

In this study, the original Tesla valve geometry was transferred to an open-channel environment, an application largely unexplored in existing research. Initial flume experiments show a distinct hydraulic response: Upstream backwater, accelerated flow and water level reduction over the structures, pronounced turbulence and recirculation downstream. These first results provide the hydraulic basis for designing the upcoming ecohydraulic experiments.

Keywords: Tesla valve; open-channel hydraulics; turbulent flow; fish guidance; ecohydraulics; diversion hydropower; physical model

1. Introduction

Maintaining a healthy aquatic biodiversity requires longitudinal connectivity in river systems. However, hydraulic structures such as weirs and hydropower plants continue to pose major obstacles for migratory fish (Larinier, 2001; Sheer and Steel, 2006). In the state of North Rhine-Westphalia in Germany alone, more than 450 hydropower installations are distributed along a river network exceeding 50,000 km. In particular at diversion hydropower plants, the discharge-dominant tailrace channel creates a challenging hydraulic situation: upstream-migrating fish tend to follow the strongest available flow (Adam and Lehmann, 2011; Schwevers and Adam, 2018) and are therefore frequently guided into the tailrace channel instead of locating a possible fishway entrance at the weir in the bypass channel. This "dead-end effect" increases predation pressure, hampers upstream migration and can lead to long-term deterioration of population dynamics and ecological status (Carvajal-Quintero et al., 2017; Mueller et al., 2011). Consequently, German water legislation requires hydropower operators to ensure upstream migratory continuity through effective protection measures, which in practice often include behavioral or physical fish-entry barriers (DWA, 2014; Schwevers and Adam, 2018).

Fish orientation is strongly influenced by velocity gradients and dominant discharge cues (Roth et al., 2025; Farzadkhoo et al., 2023). Turbulence characteristics such as turbulent kinetic energy (TKE), Reynolds shear stress and vortex scale significantly affect swimming stability and energetic expenditure (Odeh et al., 2002; Liao and Cotel, 2013; Lupandin, 2005). Experimental studies in vertical slot fishways demonstrate that many non-salmonid species preferentially select zones of lower TKE (typically < 0.02 m²/s²) and modify tail-beat kinematics under elevated turbulence levels (Farzadkhoo et al., 2023; Ouyang et al., 2025).

Critical swimming speed decreases when vortex scales approach fish body length (Lupandin, 2005), and excessive turbulence intensity reduces swimming performance (Hockley et al., 2014). Conversely, structured vortex shedding may be exploited energetically under specific conditions (Liao and Cotel, 2013), indicating that turbulence structure, rather than magnitude alone, determines biological response. This research aims to develop a physical–hydraulic barrier that exploits behavioral preferences of fish. By deliberately modifying flow fields at the confluence of the tailrace channel and the bypass channel, the inflow to the tailrace channel can be made unattractive, while strengthening the guiding flow toward the fishway in the bypass channel.

2. Concept of the Tesla Valve Barrier

2.1. Functional principle

The central element of the barrier is inspired by the Tesla valve. Originally patented by Nikola Tesla in 1920, the device achieves strong directional flow resistance without any moving parts, relying solely on its asymmetric internal geometry (Tesla, 1920). Under forward flow, water follows the main straight channel with limited turbulence generation. Under reverse flow, however, the fluid is diverted into lateral loops, producing repeated deflections, leading to colliding jets, recirculation zones, and intense vortical structures.

This geometry-induced flow division is the core mechanism of the resulting flow behavior. Reverse flow experiences substantially higher energy losses, expressed as increased pressure gradients, early onset of turbulence, and pronounced recirculation. Small variations in flow velocity or in the geometric deflection angle between the main channel and the lateral loops can significantly alter vortex formation and energy dissipation.

To date, Tesla valves have been applied mainly in microfluidics, thermal management systems, and safety devices, including passive check-valve functions, flow diodes, oscillating heat pipes, and micro-mixers. Numerous modified geometries exist, adapted to application-specific requirements (Purwidyantri and Briliant, 2023; Son and Hwang, 2024). In this research, however, the original patent geometry is deliberately chosen to allow a direct and unbiased transfer of Tesla's mechanism to open-channel conditions.

2.2. Transfer to open-channel hydraulics

Although the Tesla valve has been studied extensively under internal (pipe) flow conditions—where pressure-driven transport and confinement dominate—its behavior in open-channel environments remains largely unexplored. Only a few studies have attempted to apply Tesla-inspired geometries to open channels.

Keizer (2016) conducted large-scale flume experiments and showed that Tesla-like asymmetric flow paths can generate strong reverse-flow vortices, upstream backwater and localized energy dissipation even without conduit confinement. Depending on channel slope, the structures produced pond–stream–pond patterns or even hydraulic jumps, demonstrating that open-channel conditions fundamentally alter the flow processes compared to pipe flow.

More recently, Son and Hwang (2024) investigated bidirectional open-channel flows using a geometry based on the Tesla valve principle, involving asymmetric flow division and loop-induced separation, but not replicating Tesla's original design. Their adapted design produced circular flow regions, directional flow resistance and turbulence asymmetry; however, the hydraulic response differed significantly from that of internal flows due to the interplay of inertia, gravity and the free surface.

These findings indicate that applying the Tesla valve geometry to open-channel conditions opens a largely unexplored field for analyzing hydraulic processes and their ecohydraulic signatures. In this study, the reverse-flow mechanism is deliberately used in controlled laboratory experiments to investigate its turbulence generation, water level dynamics, and flow-steering effects.

3. Physical Model Investigations

3.1. Experimental setup

For the initial hydraulic investigations, the original Tesla valve geometry was transferred into a full-scale open-channel test section in the hydraulic laboratory at IWW. The test flume has a total length of approximately 17 m, a width of 0.30 m and a height of 0.32 m. The pump system allows a maximum discharge of 0.036 m^3/s. The valve geometry was integrated into the flume as shown in Fig. 1, and the number of Tesla valve components can be varied between one and eight to assess their influence on turbulence generation and flow steering.

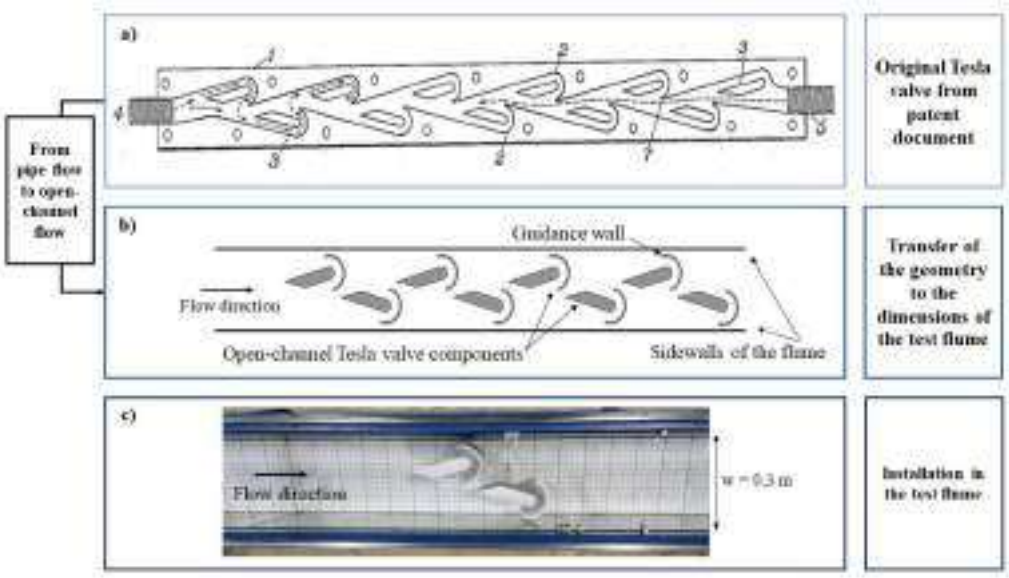

Fig. 1: Transfer of the original Tesla valve into the hydraulic laboratory setup: a) original Tesla valve geometry as documented in Nikola Tesla's patent (1920, U.S. Patent 1,329,559); b) CAD section of the adapted Tesla valve geometry scaled to the flume width; c) installation of two Tesla valve component sets in the IWW test flume (Photo: Kleinewietfeld, 2025).

3.2. Preliminary hydraulic observations

Initial measurements are shown in Fig 2. The hydraulic behavior was investigated for two different discharges, Q_1 and Q_2, with subcritical flow conditions. The water levels were examined for two sets of Tesla valve components, with and without a guidance wall, which strongly deflects the flow.

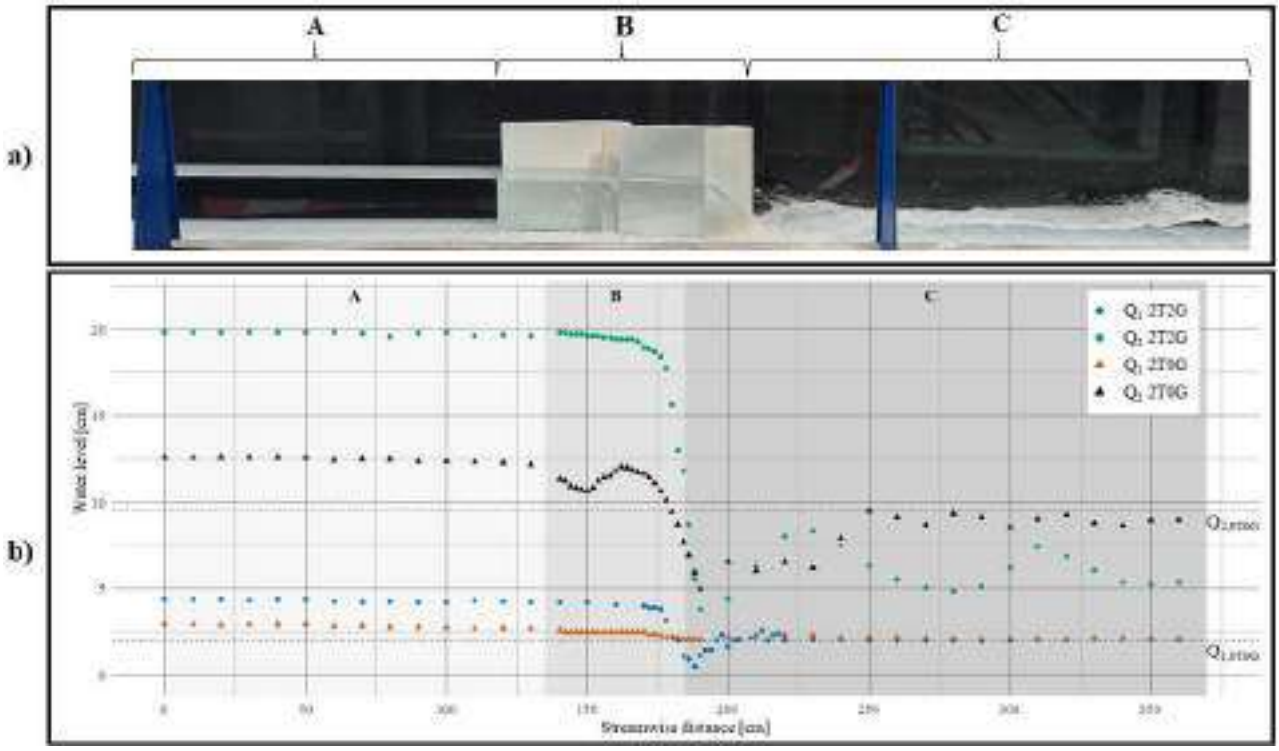

Fig. 2 a) Photograph of the experimental setup, showing the flow region upstream of the components (A), across the components (B), and downstream of the components (C) (Photo: Kleinewietfeld, 2025). Flow direction is from left to right. b) Measured water levels in streamwise direction in regions (A), (B), and (C). The measurements were taken in streamwise direction, 0.005 m from the right sidewall of the flume at two discharges, $Q_1 < Q_2$. Two setups were examined for each discharge, one with (2T2G) and one without (2T0G) deflection of the flow by the guidance wall. The dotted line shows the water level without structures (0T0G).

Upstream of the structures, a significant rise in the water level was measured for Q_2, which was further increased by the built-in guidance walls (Q_2 2T2G). The difference in water level between the 2T2G scenario and the one without structures (0T0G) is for Q_2 10,3 cm and for Q_1 2,5 cm.

This indicates a backwater effect due to the increased flow resistance (Fig. 2, area A). When the flow passes over the components (Fig. 2, area B), the water level drops noticeably. Particularly in the setups with guidance walls and at high discharge Q_2, a further drop in water levels can be observed at the beginning of region C. This leads to Δh_{AC} of 1.65 cm (Q_1 2T0G) to 16 cm (Q_2 2T2G). The associated acceleration of the flow leads to a significant increase in the local Froude number, resulting in a distinct hydraulic jump for the scenarios with guidance walls in region C (2T2G). Downstream of the components, pronounced turbulence and unsteady flow structures develop, consistent with the expected flow separation and recirculation induced by the Tesla valve geometry.

These initial measurements qualitatively confirm the anticipated hydraulic flow formation under free-surface conditions. In subsequent project stages, these phenomena will be quantified through detailed PIV and ADV measurements. In addition, the number and arrangement of the Tesla elements will be systematically varied to analyse their influence on turbulence generation and flow steering. Fish-relevant hydraulic parameters—such as turbulent kinetic energy, velocity gradients and turbulence intensity—will be extracted as preparatory data for future ecohydraulic experiments at the IWW laboratory. These experiments will involve representative species from different flow guilds, ranging from rheophilic (Salmo trutta fario, Barbus barbus) to indifferent and limnophilic taxa (Perca fluviatilis, Rutilus rutilus, Scardinius erythrophthalmus, Abramis brama), enabling the assessment of species-specific responses to modified hydraulic conditions. In future work, the resulting flow fields will be evaluated against established fish passage thresholds defined in DWA-M 509 (DWA, 2014), including maximum flow velocity, minimum guidance velocity and energy dissipation rates.

Acknowledgements

The Tesla4Fisch project is funded by the state of North Rhine-Westphalia using funds from the European Regional Development Fund (ERDF) and the Just Transition Fund (JTF) (ERDF/JTF Program NRW 2021-2027) as part of the GreenEconomy.IN.NRW innovation competition. The funding code is IN-EC-2-010a.

References

Adam B, Lehmann B (2011) Ethohydraulik: Grundlagen, Methoden und Erkenntnisse, Springer, Berlin Heidelberg.
Carvajal-Quintero JD, Escobar-Camacho D, Maldonado-Ocampo JA, et al (2017) Fish diversity loss in Neotropical freshwater ecosystems, Ecology and Evolution, 7, 7001–7011.
DWA (2014) DWA-M 509: Fischaufstiegsanlagen und fischpassierbare Bauwerke – Bemessung, Gestaltung, Qualitätssicherung, Deutsche Vereinigung für Wasserwirtschaft, Abwasser und Abfall e.V., Hennef, 140 pp.
Farzadkhoo M, Kingsford RT, Suthers IM, Felder S (2023) Flow hydrodynamics drive effective fish attraction behaviour into slotted fishway entrances, Australian Journal of Civil Engineering, 21, 782–796. DOI: 10.1007/s42241-023-0047-6.
Hockley FA, Wilson CAME, Brew A, Cable J (2014) Fish responses to flow velocity and turbulence in relation to size, sex and parasite load, Journal of the Royal Society Interface, 11, 20130814.
Keizer K (2016) Determination whether a large scale Tesla valve could be applicable as a fish passage, Additional Thesis, Delft University of Technology, Department of Civil Engineering, Delft, 39 pp.
Larinier M (2001) Dams, fish and fisheries: Opportunities, challenges and conflict resolution, FAO Fisheries Technical Paper No. 419, Food and Agriculture Organization of the United Nations, Rome, 45–90.
Liao JC, Cotel A (2013) Effects of turbulence on fish swimming in aquaculture, in: Palstra AP, Planas JV (eds) Swimming Physiology of Fish, Springer, Berlin Heidelberg, 109–127.
Lupandin AI (2005) Effect of flow turbulence on swimming speed of fish, Biology Bulletin, 32(5), 461–466.
Mueller M, Pander J, Geist J (2011) The ecological importance of tributaries and their management for fish migration, Journal of Applied Ichthyology, 27, 545–550.
Odeh M, Noreika JF, Haro A, Maynard A, Castro-Santos T, Cada GF (2002) Evaluation of the effects of turbulence on the behavior of migratory fish, U.S. Geological Survey, S.O. Conte Anadromous Fish Research Center, Turners Falls, MA, prepared for Bonneville Power Administration, Portland, OR, March 2002.
Ouyang J, Li S, Zeng L, Li Q, Yang X (2025) Fish swimming behavior and strategies under different hydrodynamic conditions in fishways with various vertical slot configurations, Fishes, 10, 415. DOI: 10.3390/fishes10080415.
Purwidyantri A, Prabowo BA (2023) Tesla valve microfluidics: The rise of forgotten technology, Chemosensors, 11, 256.
Roth MS, Wagner F, Roessger T, Kopecki I, Powalla D, Stamm J (2025) An experimental approach for the quantitative assessment of downstream swimming fish behavior, River Research & Applications, 41, 499–514. DOI: 10.1002/rra.4375.
Schwevers U, Adam B (2018) Sackgassenwirkung von Ausleitungskraftwerken für stromaufwärts wandernde Fische, Wasser und Abfall, 20, 67–71.
Sheer MB, Steel EA (2006) Lost watersheds: Barriers, aquatic habitat connectivity, and salmon persistence in the Willamette and Lower Columbia River Basins, Transactions of the American Fisheries Society, 135, 1654–1669.
Son S, Hwang JH (2024) Application of Tesla valve to bidirectional open-channel flows, KSCE Journal of Civil Engineering, 28, 1011–1025.
Tesla N (1920) Valvular conduit, U.S. Patent 1,329,559, filed Feb 21, 1916, issued Feb 3, 1920.

Book of Abstracts of the *16th International Symposium on Ecohydraulics*
Challenges and solutions in the time of global changes
August 16–20, 2026, Lausanne, Switzerland
ISSN: 2790-2420 | ISBN: 978-90-837233-9-6 | doi:[10.64697/iahr.proc.ise2026.abs]
© 2026 IAHR. CC BY-NC-ND 4.0

PREDICTING FISH HABITAT SUITABILITY USING HABITAT-SCALE HYDRODYNAMIC COMPLEXITY METRICS INTEGRATED INTO THE RIVER2D MODEL

Abul B.M. Baki[1*]; Hasan Zobeyer[2]; Md Aminul Islam Shagor[1]; Haitham Ghamry[3]; Christos Katopodis[4]; and Tom A. Langen[5]

[1]Department of Civil and Environmental Engineering, Clarkson University, Potsdam, NY, USA

[2]Department of Water Resource Engineering, Bangladesh University of Engineering & Technology, Dhaka, BANGLADESH

[3]Freshwater Institute, Fisheries and Oceans Canada, 501 University Cres, Winnipeg, MB, CANADA

[4]Katopodis Ecohydraulics Ltd., 122 Valence Avenue, Winnipeg, MB, CANADA

[5]Department of Biology, Clarkson University, Potsdam, NY, USA

*Corresponding author: Abul B.M. Baki; abaki@clarkson.edu

ABSTRACT

Nature-based instream habitat structures (IHSs) enhance hydraulic and ecological complexity, yet most suitability assessments rely on simplified hydraulics and hydrology alone. This study integrates the Habitat-scale Hydrodynamic Complexity Metrics (HHCMs) framework into a validated River2D physical-scale model derived from the Ecohydraulics Flume at Clarkson University for an instream boulder-dominated channel. Flow scenarios spanning low (SR < 1.0), medium (SR = 1.5, 2.5), and flood (SR = 3.5) submergence, and boulder densities ($\lambda = 0$–8.3%) were simulated. HHCMs were synthesized into a bounded Fish Suitability Index (FSI; 0–1) and spatially aggregated as Weighted Usable Area (WUA). Preliminary results indicate that the uniform bed (no-boulder) condition produced substantially lower weighted usable area (WUA), whereas the introduction of boulders have increased WUA by creating hydraulic refugia and wake zones. Among the tested configurations, moderate boulder densities showed the most favorable balance between habitat availability and flow connectivity. Results confirm that hydrodynamic refuge and layout, not density alone, govern reach-scale suitability, establishing HHCM-based FSI as a predictive ecohydraulics restoration design tool.

Keywords: Fish suitability index (FSI); habitat-scale hydrodynamic complexity metrics; instream boulders; River2D model; weighted usable area (WUA).

1. Introduction

The nature-based instream habitat structures (IHSs), such as boulders, wooden logs, and vegetation, have been commonly used to restore degraded streams by enhancing instream complexity and ecological value. These structures are designed to modify channel morphology, increase flow complexity, stabilize sediments, and enhance ecological connectivity, thereby mitigating habitat degradation. IHSs alter local hydraulic conditions by generating velocity gradients, turbulent kinetic energy (TKE), Reynolds shear stresses (RSS), and coherent structures (Monsalve et al., 2017). These hydrodynamic modifications create pools, riffles, eddies, and wakes, that provide shelters, foraging opportunities, and resting zones for fish and other aquatic organisms. Ecological responses to changes in riverine habitats are typically assessed by examining the relationship between river discharge and biological responses. However, aquatic organisms interact with the hydro- and morphodynamics of a river (e.g., velocity, turbulence, sediment transport) rather than just hydrology (i.e., river flows). Hydroelectric and other projects that regulate rivers produce hydrodynamics quite different from natural conditions both upstream and downstream of such structures,

affecting habitat suitability, fish migrations, and fish populations (Katopodis, 2022; Katopodis and Williams, 2012). Traditional approaches to habitat suitability, such as 1-D and 2-D models (e.g., PHABISM, River2D), often are limited to reach-scale flow characteristics or local variables (velocity, depth, substrate), frequently overlooking the complex flow patterns created by natural in-stream structures (Katopodis, 2022). To overcome these limitations, (Crowder and Diplas, 2002, 2006) introduced habitat complexity metrics (HCM) that quantify habitat complexity using mean flow characteristics. Metrics like M_1 and M_2 reflect energy gradients and the spatial change of kinetic energy, while M_3 and M_4 measure flow recirculation in the vertical and horizonal planes respectively, indicating eddy strength and flow complexity (Kozarek et al., 2010) (details can be found in Golpira et al., 2023). In addition to conventional HCM (M_1-M_4), (Reggad et al., 2025) suggested additional turbulence-related parameters as new metrics to account for habitat complexity due to flow turbulence. Metrics M_5 (TKE), M_6 (turbulent energy dissipation rate), M_7 (maximum integral eddy length scale), and M_8 (projected near-bed RSS). Metrics M_5 to M_8 are turbulence-related parameters that are expected to affect fish swimming and mobility (details can be found in Reggad et al., 2025). Hereafter, these habitat complexity metrics are collectively referred to as habitat-scale hydrodynamic complexity metrics (HHCMs) when applied at the channel or stream-reach scale. The recent ecohydraulics approach has therefore emphasized the use of habitat-scale hydrodynamic complexity metrics (HHCMs) to quantify spatial flow heterogeneity and their associated fish habitat suitability (Reggad et al., 2025). Building on this concept, the present study will develop the River2D model (Steffler and Blackburn, 2002) for physical scale flumes to integrate the HHCMs framework for a boulder-dominated open channel, then HHCMs will be computed from River2D outputs and synthesized into a fish suitability index (FSI) to justify the habitat suitability in a river system.

2. Objectives

This study aims to integrate habitat-scale hydrodynamic complexity into the River2D model for the predictive assessment of fish habitat suitability within nature-based restoration. The specific objectives are: (1) to develop a River2D model that incorporates the habitat-scale hydrodynamic complexity metrics (HHCMs) for physical-scale and boulder-dominated open-channel, and (2) to compute and synthesize HHCMs into a fish suitability index (FSI) for evaluating habitat conditions for different arrangements of boulders and flow scenarios.

3. Methodology

The Ecohydraulics Flume at Clarkson University (13.00 m long, 0.96 m wide, and 1.00 m high; Golpira et al., 2023; Reggad et al., 2025) was used to construct the physical-scale representation of a boulder-dominated open channel, which subsequently served as the computational domain for the River2D model. Simulations were conducted under a constant bed slope (S_0 = 0.50%) and fixed bed substrate size (d_{50} = 6.1 mm), following the experimentally surveyed bathymetry. Boulder density (λ) was systematically varied from 0 (no-boulder condition) up to 8.3%, equivalent to a maximum plan-view areal blockage of 8.3% (details in Golpira et al., 2023). Targeted flow scenarios represent four submergence ratios (SRs=H/D_h, where H is the depth of the water and D_h is the height of the Boulder): low flow (SR < 1.0), medium flow (SR = 1.5, 2.5), and flood flow (SR = 3.5). In this study, the River2D model was calibrated and validated against experimentally observed data for the no-boulder, 3.4%, 5.4%, and 8.3% boulder density configurations. A total of four HHCMs (M_1, M_2, M_4, and M_8) were evaluated, M_3 was not considered because it requires vertical (z-plane) velocity variations that cannot be resolved by the depth-averaged River2D model, while M_5–M_7 require turbulence fluctuation information that is not available from River2D outputs. To estimate the HHCMs, grid-scale calculations were performed using River2D outputs for several flow scenarios spanning low (SR < 1.0), medium (SR = 1.5, 2.5), and flood (SR = 3.5) submergence. The mean-flow metrics M_1, M_2 and M_4 were computed from spatial velocity gradients, $M_1 = U_{avg}\left|\frac{(U_2 - U_1)}{\Delta S}\right|$, where U_1 and U_2 are velocity magnitudes at points 1 and 2, $M_2 = \frac{2U_{avg}}{U_{min}^2}\left|\frac{(U_2 - U_1)}{\Delta S}\right|$, where U_{min} is the minimum velocity between the points 1 and 2, $M_4 = \frac{\sum\left|\frac{\Delta V}{\Delta x}\frac{\Delta U}{\Delta y}\right| \Delta x \cdot \Delta y}{\sum \Delta x \cdot \Delta y}$, where $\left|\frac{\Delta V}{\Delta x} - \frac{\Delta U}{\Delta y}\right|$, is the vorticity around z-axis at a point and (Δx·Δy) is the area

of the cell. The projected near-bed Reynolds shear stress metric (M_8) was estimated using the Boussinesq eddy-viscosity formulation implemented in River2D, expressed as $M_8 = \tau_{xy} = \nu_t \left(\frac{\Delta V}{\Delta x} + \frac{\Delta U}{\Delta y}\right)$, where ν_t is the eddy viscosity coefficient. This formulation represents the depth-averaged approximation of Reynolds shear stress based on the Boussinesq hypothesis, where the turbulent Reynolds stresses $-\rho u_i' u_j'$ are parameterized using the eddy viscosity and velocity gradients.

4. Discussion and Results

A quadratic polynomial relationship linking the dimensionless energy metric ($\frac{M_1 H}{U_{reach}^2}$) to the Atlantic salmon dimensionless resting time ($t^* = t_{rest}/\sqrt{L/g}$) (Katopodis and Gervais, 2012) following the relationship derived by Tusher et al. (2026), where g is the gravitational acceleration, t_{rest} is the fish resting time, and L is fish fork length.) was then applied (Fig. 1a) to derive the cell-scale FSI. FSI values were constrained to the physical bounds $0 \leq FSI \leq 1$, where 0 represents hydraulically unusable habitat and 1 denotes optimal resting conditions. Cells yielding FSI < 0.01 were treated as unsuitable and assigned FSI = 0. Values exceeding the theoretical upper bound (FSI > 1), arising from polynomial extrapolation, were truncated to FSI = 1.The weighted usable area (WUA) for each experimental scenario was calculated as shown in Eq. 1:

$$WUA = \frac{\sum_i^n FSI_i \times A_i}{\sum_i^n A_i} \quad (1)$$

where FSI_i is the fish suitability index at cell i and A_i is the cell area (0.02 m × 0.02 m). WUA is reported as a percentage of the total modeled domain for physical interpretation. The analysis focused on the central 1.44 m × 0.92 m section of the flume (7.80–9.22 m streamwise, 0.03–0.91 m cross-stream, Fig. 1b), capturing two full repetition cycles of the boulder pattern. Boulder-free buffer zones of 1.0 m were preserved upstream and downstream to minimize numerical boundary artifacts.

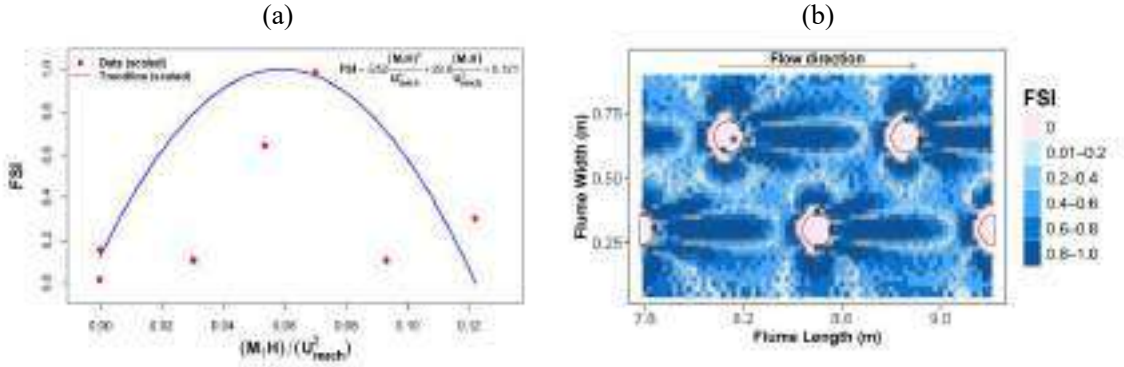

Fig. 1. (a) Quadratic relationship between FSI and dimensionless energy gradient ($\frac{M_1 H}{U_{reach}^2}$) derived from Tusher et al. (2026), (b) Distribution of FSI for resting time for the 3.4% boulder-density scenario for high flow (0.06 m³/s). Higher FSI values (dark blue) represent more hydraulically suitable zones, while FSI = 0 (light pink).

Preliminary results from the calibrated River2D model for different boulder-density scenarios indicate that the introduction of instream boulders significantly alters the hydraulic complexity and associated habitat suitability. Compared with the no-boulder condition, the presence of boulders generates wake zones and localized low-velocity refugia that can increase the weighted usable area (WUA). However, increasing boulder density does not certainly lead to a proportional increase in habitat suitability, as excessive structural complexity may also create higher energy gradients and local flow obstruction near boulder faces. These results suggest that an optimal balance between wake-zone formation and longitudinal passage connectivity is necessary to enhance reach-scale habitat conditions. The HHCM-based flow suitability

index (FSI) framework provides a useful approach to quantify these hydraulic–habitat interactions. Future analyses will further examine how different submergence ratios (SR) influence hydraulic complexity and habitat suitability under varying flow conditions.

5. Conclusion

The results indicate that the weighted usable area (WUA) reached 54.1% for the 3.4% boulder density under the low-flow condition, which is substantially higher than the no-boulder scenario, where WUA remained notably lower. Although increasing structural complexity through higher boulder densities is generally expected to enhance habitat suitability, this trend was not consistent across all habitat parameters. In the present analysis, the flow suitability index (FSI) was derived solely from the dimensionless resting time parameter t^*. Future analyses will incorporate additional behavioral indicators such as ground speed, passage efficiency, and passage time to develop a combined suitability scale for different flow scenarios and to better understand how hydraulic complexity influences overall fish movement and behavior.

References

Baki ABM, Golpira A, Rampinelli GC, Patrizio L, Zhu DZ (2019) Numerical modelling of nature-like fish passage using a 2D shallow water model, Proceedings of the CSCE Annual Conference: Growing with Youth – Croître avec les jeunes, Laval (Greater Montreal), Canada, June 12–15 2019

Baki ABM, Zhu DZ, Rajaratnam N (2014) Mean flow characteristics in a rock-ramp-type fish pass, Journal of Hydraulic Engineering, 140, 156–168

Crowder DW, Diplas P (2002) Vorticity and circulation: spatial metrics for evaluating flow complexity in stream habitats, Canadian Journal of Fisheries and Aquatic Sciences, 59, 633–645

Crowder DW, Diplas P (2006) Applying spatial hydraulic principles to quantify stream habitat, River Research and Applications, 22, 79–89

Golpira A, Baki ABM, Zhu DZ (2020) Higher-order velocity moments, turbulence scales and energy dissipation rate around a boulder in a rock-ramp fish passage, Sustainability, 12, 5385

Golpira A, Baki ABM, Ghamry H, Katopodis C, Withers J, Minkoff D (2022) An experimental study: effects of boulder placement on hydraulic metrics of instream habitat complexity, Scientific Reports, 12, 13156

Katopodis C, Williams JG (2012) The development of fish passage research in a historical context, Ecological Engineering, 48, 8–18

Katopodis C, Gervais R (2012) Ecohydraulic analysis of fish fatigue data, River Research and Applications, 28, 444–456

Katopodis C (2022) A perspective on e-flows at hydroelectric projects in Canada, Hydrobiologia, 849, 461–484

Kozarek JL, Hession WC, Dolloff CA, Diplas P (2010) Hydraulic complexity metrics for evaluating in-stream brook trout habitat, Journal of Hydraulic Engineering, 136, 1067–1076

Monsalve A, Yager EM, Schmeeckle MW (2017) Effects of bed forms and large protruding grains on near-bed flow hydraulics in low relative submergence conditions, Journal of Geophysical Research: Earth Surface, 122, 1845–1866

Reggad N, Golpira A, Baki ABM, Ghamry H, Katopodis C (2025) Turbulent flow-based habitat complexity metrics around instream boulders in support of river restoration, Scientific Reports, 15, 10650

Steffler P, Blackburn J (2002) River2D, Two dimensional depth averaged model of river hydrodynamics and fish habitat: Introduction to depth averaged modeling and user's manual, University of Alberta, Edmonton, Canada

Tusher MSH, Langen TA, Ghamry H, Katopodis C, Baki ABM (2026) Movement behavior of juvenile salmonids in boulder-dominated channels: Effects of boulder dispersion, flow rate, and species, Journal of Ecohydraulics, doi: 10.1080/24705357.2026.2646669

Book of Abstracts of the *16th International Symposium on Ecohydraulics*
Challenges and solutions in the time of global changes
August 16–20, 2026, Lausanne, Switzerland
ISSN: 2790-2420 | ISBN: 978-90-837233-9-6 | doi:[10.64697/iahr.proc.ise2026.abs]
© 2026 IAHR. CC BY-NC-ND 4.0

ENVIRONMENTAL AND HYDRAULIC EFFECTS OF PILOT RIVERBANK PROTECTION WORKS ON THE MANU RIVER: A DECADAL POST-PROJECT EVALUATION

Kazumitsu MURAOKA[1], Minako MATSUKAWA[2]

[1] JICA Expert, Bangladesh Water Development Board, Bangladesh
email: kazumitsu.muraoka@gmail.com

[2] JICA Expert, General Economics Division, Planning Commission, Bangladesh
email: minako.matsukawa1005@gmail.com

ABSTRACT

Riverbank erosion and the resulting degradation of the riverine environment and ecosystem constitute major challenges for water and land management. In this study, we introduce a novel concept for a riverbank protection structure with the potential to improve riverbank management in Bangladesh. A pilot implementation was carried out along the Manu River in Moulvibazar District in 2016, and its effects on both erosion control and environmental restoration were examined. The pilot facilities have functioned successfully, stabilizing the riverbank, creating a nature-friendly waterfront, and improving water access for residents. Based on field investigations conducted ten years after construction, this study reports changes in river morphology, the structural integrity of the embankment protection, and the status of vegetation recovery. Recommendations for riverbank management in Bangladesh are also presented.

Keywords: Bangladesh; bank protection; nature interactive recovery; vegetation, nature-based solutions

1. Introduction

Riverbank erosion is one of the most serious land management issues in Bangladesh (Bangladesh Water Development Board (2022)). The monsoon climate, with its distinct rainy and dry seasons, causes substantial fluctuations in river conditions that can eventually lead to large-scale erosion. Moreover, riverbank erosion often degrades the riverine environment and has become a factor that threatens people's livelihoods. Although various approaches exist for riverbank protection that ensures ecological diversity, Bangladesh's extremely challenging geographical conditions, particularly the scarcity of essential construction materials such as stone or gravel, have made it extremely difficult to develop riverbank protection structures that both preserve water environment diversity and provide effective flood control.

Matsuki (2013) proposed a continuous series of stone spur dikes along the Mekong River in Lao PDR, designed to utilize locally available materials and construction capacities. The implemented measures effectively interrupted the progression of riverbank erosion, facilitated sediment deposition through natural fluvial processes, and consequently achieved notable improvements in riparian environmental restoration. Hossain and Sakai (2008a, 2008b) investigated and analyzed river and flood control embankment based on field visits to embankment sites in Bangladesh and suggested a proper design and construction method of embankments to control and minimize the extent of flood hazards in the long run.

However, conventional engineering approaches are often difficult to implement due to limited availability of construction materials and resource constraints, prompting the exploration of alternative protection concepts that are both environmentally compatible and locally feasible. In response to these challenges, a novel riverbank protection concept was introduced and applied as a pilot construction along the Manu River in Moulvibazar District in 2016 and completed in 2017. The location map is presented in Fig. 1. The pilot installation aimed to stabilize the riverbank, promote nature-friendly waterfront development, and improve



Fig. 1. Manu River pilot study site in Moulvibazar.

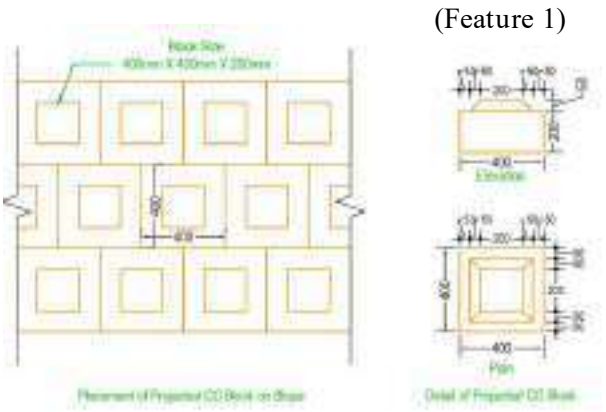

Fig. 3. CC blocks with projection.

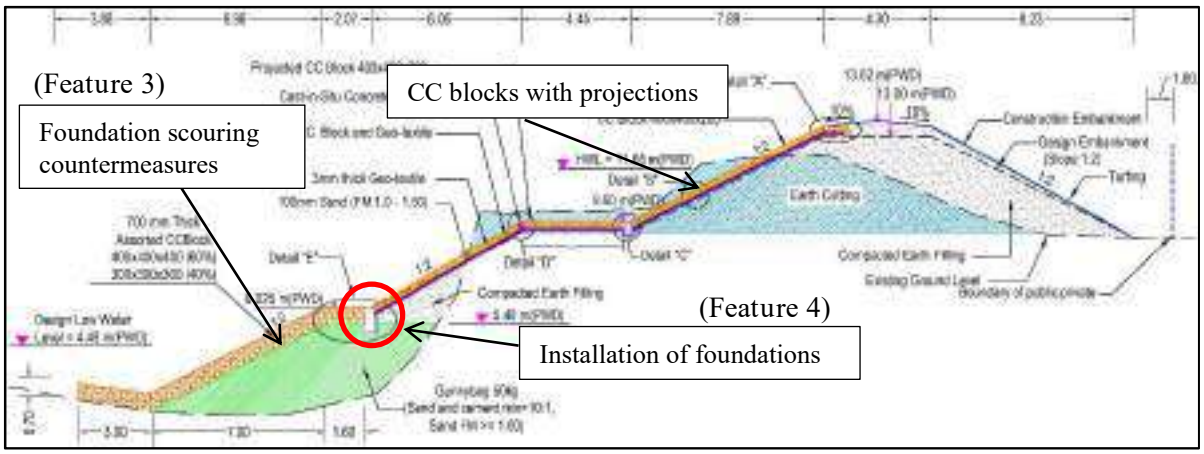

Fig. 2. Standard cross section of novel riverbank protection.

local water access by utilizing materials and construction practices appropriate for the region. Early observations indicated that the facilities contributed to both erosion control and environmental restoration. Nearly a decade after implementation, it has become essential to assess the long-term performance and morphological impacts of this pilot initiative. Therefore, this study examines changes in river morphology, evaluates the structural integrity of the embankment protection, and assesses vegetation recovery based on field investigations conducted ten years after construction. The study also recommends enhanced riverbank protection and management strategies for monsoon-prone regions.

2. Methodology

2.1. Improvement design of riverbank protection

The design of the pilot work incorporated the following four improvements, and the standard cross-section is shown in Fig. 2.

First, (Feature 1) introduces improved CC blocks with projections on their top surface (Fig. 3) for the protection of embankment slopes. These blocks, based on conventional designs used by the Bangladesh Water Development Board (BWDB), are engineered to decelerate near-surface flow velocity and limit the generation of secondary flows along the riverbank, thereby reducing local scouring and the risk of embankment damage.

Second, (Feature 2) focuses on the restoration of the original bank alignment. While conventional repairs often involve setting back the embankment landward due to budget constraints, resulting in irregular alignments that

intensify erosion, this project restores the original alignment to ensure enhanced long-term structural and hydraulic stability.

The stability of the system is further reinforced by (Feature 3), which involves specialized foundation work at the toe of the bank slope to support the slope covering.

Finally, (Feature 4) utilizes embankments of mortar-filled gunny bags instead of boulders and geotextile sheets under the low water level. This method is specifically designed to avoid the difficulties of soil compaction in water and to prevent the leakage of soil materials, ensuring the integrity of the underwater structure.

2.2. Monitoring method

To evaluate the current condition and effectiveness of the pilot work along the Manu River, two field investigations were conducted in October 2021 and January 2022. In addition, a further visual inspection was carried out in February 2025, following the record-breaking flood that occurred on 12 August 2024, in order to assess the embankment's performance under extreme hydrological conditions. These surveys aimed to document the present status of the riverbank, assess the structural and environmental performance of the protection work, and examine changes to the surrounding river environment. The survey activities included observations of the waterside environment and vegetation, river cross-sectional measurements, drone-based aerial photography, topographic surveying, and flow-velocity profiling using an Acoustic Doppler Current Profiler (ADCP), together with bathymetric surveying.

3. Results and discussions

3.1. Transition from Erosion to Sedimentation

Prior to the intervention, local scouring near the embankment toe contributed to riverbank failure. Following construction, the section presents a depositional trend, the local scouring has disappeared, and the embankment remains stable. These findings indicate that stability was achieved through the integrated performance of Features 1 to 4. Specifically, improved CC blocks decelerated near-surface flow and limited secondary flows, while restoring the original bank alignment ensured hydraulic consistency. Furthermore, specialized foundation work and mortar-filled gunny bags provided robust structural support and prevented soil leakage. This combination effectively mitigated damage risk and facilitated long-term stabilization.

3.2. Morphological changes of the river

Prior to the pilot work, the thalweg had shifted toward the right bank due to local scouring; however, by 2017, immediately after construction, sediment deposition along the revetment began to appear. In Fig. 4., the yellow dashed line represents the thalweg in 2013, the red line in 2017, and the white line in 2021. Within the pilot section, the thalweg clearly migrated toward the center of the river and has remained stable thereafter. Fig. 5. presents the contour map, which indicates that the river channel has become hydraulically stable following the pilot installation. Furthermore, Fig. 6. shows the flow-velocity distribution across the river. The velocity along the right bank has decreased, while higher velocities are observed toward the center (Point A). The ADCP survey results also confirm that the river channel has stabilized.



Fig. 4. Thalweg Shifting of the River.



Fig. 5. Contour Lines of the Survey Area.

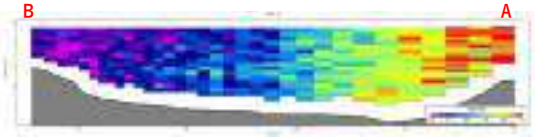

Fig. 6. Velocity Profiles of Cross Section (A-B).



Fig. 7. Photographs taken (a)before construction, (b)immediately after completion, and (c)ten years later.

3.3. Changes in the riverine environment

Before construction, the site was severely degraded due to extensive riverbank collapse, creating harsh conditions in which people could not safely approach the waterfront. However, immediately after the pilot installation, sediment deposition began, and a nature-interactive recovery of riparian vegetation gradually emerged. Comparative photographs are presented in Fig. 7. According to local residents, fish have taken refuge in the gaps between the concrete blocks, which were used as an alternative to dumped stones, contributing to a nature-interactive recovery of the waterside environment and the restoration of a favorable fishing habitat. However, it has also been pointed out that excessive sediment accumulation and vigorous vegetation growth are hindering embankment maintenance activities. Moving forward, management practices that balance environmental conservation with the upkeep of healthy river management facilities will be required.

3.4. Stability of the embankment under the highest recorded flood

In August 2024, heavy rainfall in eastern Bangladesh triggered widespread flooding, resulting in extensive embankment breaches and inundation across the region. The Manu River also recorded its highest-ever water level, exceeding the danger level by 91 cm, which caused severe damage in the surrounding areas. Nevertheless, the riverbank protection at the pilot site withstood the event without sustaining any damage and remained structurally sound. A visual inspection conducted in February 2025 further confirmed that no significant changes had occurred in river morphology or in the waterside vegetation and related environmental conditions.

4. Conclusion

A decade after completion, the pilot riverbank protection work demonstrated strong performance, remaining intact even during the record flood of 2024. Stabilization of the main channel contributed to steady sediment deposition and a gradual recovery of the riverine environment. Positive feedback from local residents also indicates improvements in both safety and the waterside ecosystem. The results suggest that this protection method, which relies on locally feasible materials and environmentally compatible features, is a practical and sustainable option for monsoon-prone regions. At the same time, future management will need to address issues such as excessive sedimentation and vigorous vegetation growth. Overall, the pilot project shows promising potential for wider application in riverbank management in Bangladesh.

Acknowledgements

The research reported in this paper is fully supported by the Grant Aid of the Project for Capacity Development of Management for Sustainable Water Related Infrastructure from the technical assistance project provided by the Government of Japan. The writers gratefully acknowledge this support. Any opinions, findings, and conclusions expressed in this paper are those of the authors and do not necessarily reflect the views of the sponsor. The authors wish to express heartfelt thanks and gratitude to our honorable Dr. Robin Kumar Biswas, Additional Chief Engineer of Bangladesh Water Development Board for his great cooperation, valuable suggestions and constant encouragement.

References

Bangladesh Water Development Board. (2022). BWDB Annual Report 2022/2023, Bangladesh Water Development Board.
Hossain M.Z. and Sakai T. (2008a). Severity of flood embankments in Bangladesh and its remedial approach, Agricultural Engine ering International: the CIGR E-journal, Manuscript LW 08 004, Vol.10, No.1, pp. 27-53.
Hossain M.Z. and Sakai T. (2008b). Performance and Maintenance of River Embankments in Bangladesh, Japanese Society of Irrigation, Drainage and Rural Engineering, pp. 608-609.
Matsuki H. (2013). Groyne to prevent riverbank erosion on Mekong River, Annuals of the River Engineering, Japan Society of Civil Engineers, 19, 123-128.
Japan International Cooperation Agency. (2017). Final and Main Report for The Project for Capacity Development of Management for Sustainable Water Related Infrastructure in the People's Republic of Bangladesh, September 2017, Japan International Cooperation Agency, 129 pp.

Book of Abstracts of the *16th International Symposium on Ecohydraulics*
Challenges and solutions in the time of global changes
August 16–20, 2026, Lausanne, Switzerland
ISSN: 2790-2420 | ISBN: 978-90-837233-9-6 | doi:[10.64697/iahr.proc.ise2026.abs]
© 2026 IAHR. CC BY-NC-ND 4.0

IMPROVING FISH RECEPTION CONDITIONS AT THE OUTLET OF DOWNSTREAM MIGRATION DEVICES AND SPILLWAYS USING FIELD MEASUREMENTS AND URANS-VOF MODELING

Antoine ECORCE[1,4], Dominique COURRET[2,4], Ludovic CHATELLIER[3,4], Laurent DAVID[3,4],

[1] CNRS, IMFT, University of Toulouse, Allée du Pr. Camille Soula, 31400 Toulouse, France
antoine.ecorce@imft.fr

[2] Office Français de la Biodiversité—DRAS, 2 Allée du Professeur Camille Soula, 31400 Toulouse, France
dominique.courret@ofb.gouv.fr

[3] CNRS, Institut PPRIME, University of Poitiers, ISAE-ENSMA, UPR 3346, 11 Boulevard Marie et Pierre Curie, 86073 Poitiers, cedex 9, France
laurent.david@univ-poitiers.fr, ludovic.chatellier@ensma.fr

[4] Pôle R&D Ecohydraulique OFB-IMFT-PPRIME

ABSTRACT

During their downstream migration, fish encounter obstacles such as waterfalls, spillways and downstream migration devices, and are forced to pass through them. However, the current criterion for ensuring the safe reception of fish is not entirely satisfactory as it overlooks jet characteristics. This study investigated the waterfall at the outlet of the Pébernat hydro-power plant's downstream migration device (Ariège River, France), where fish are forced to pass through a 3 m drop. The aim was to characterize the jet's hydrodynamics in the air and in the receiving pool, before and after the deepening work on the pool. The study combines in situ measurements of the pressure exerted by the jet on the pool's bottom with URANS-VOF 3D modelling. The model captures the order of magnitude of the high dynamic pressure values recorded on site. As the risk of damage to fish is likely to be related to the highest dynamic pressures, this modelling approach appears to be a promising tool for characterizing the jet's hydrodynamics in detail, both in the air and in the receiving pool. This is all the more interesting given that in situ measurements are difficult to carry out. A comparison of the situation before and after the deepening work, based on measurements and modelling results, reveals a significant improvement in fish reception conditions. The sharp decrease in maximum dynamic pressure at the bottom (from ~280 mbar to ~150 mbar) is consistent with the observed reduction in fish injury rates. These findings highlight the reliability of 3D modelling as a tool for refining criteria to ensure safe fish reception and for designing solutions.

Keywords: fish migration; water drops; impact pressure; OpenFOAM; URANS; VOF

1. Introduction

During their downstream migration, fish encounter obstacles such as waterfalls and must pass through them by way of spillways (weirs, overflow or underflow gates) or via downstream migration devices implemented to prevent them from being entrained in water intakes and injured by the turbines of hydroelectric power plants (HPPs). The criterion for ensuring safe reception in fish reception areas, currently used in France (Courret et al., 2008) and the USA (USFWS, 2019), was proposed by Odeh and Orvis (1998), who set a minimum water depth. To our knowledge, this is the only existing criterion. It requires a minimum water depth equal to a quarter of the fall height or at least one metre for falls lower than four metres. However, this criterion is not entirely satisfactory as it does not consider the characteristics of the jet, such as flow rate, jet thickness and aeration level.

At certain sites in France, the conditions for fish downstream of waterfalls are expected to be harmful. For example, this has been demonstrated at the outlet of the downstream migration device installed at the Pébernat

site on the Ariège River, where 9% of salmon smolts were injured (Bercovitz et al., 2022). Work has been carried out at this site to deepen the reception area, reducing the rate of injured smolts to less than 1% with only minor damage. The present study aims to characterise the hydrodynamics of the jet in air and in the receiving pool before and after the work by combining in situ measurements of the bottom pressure of the jet with URANS-VOF 3D modelling.

2. Methods

2.1 Site presentation

The study was conducted at the Pébernat HPP, which is operated by Electricité de France (EDF), on the Ariège River in southwestern France (43.133819 N, 1.600293 E) (see Tétard et al., 2023 for a detailed presentation of the site). The downstream migration device bypass consists of a 2 m wide flap gate with a flow rate of 2 m³/s and a 3 m drop to the receiving pool. The aperture angle of the flap gate is automatically adjusted to maintain the correct flow rate. Two topographies of the receiving pool bed are considered (Fig.1):

- the original flat bottom with a water depth of 0.43 meters (pre-work situation),

- and the deepened bottom with an inclined profile and water depth varying from 0.56 m to 1.18m (post-work situation).

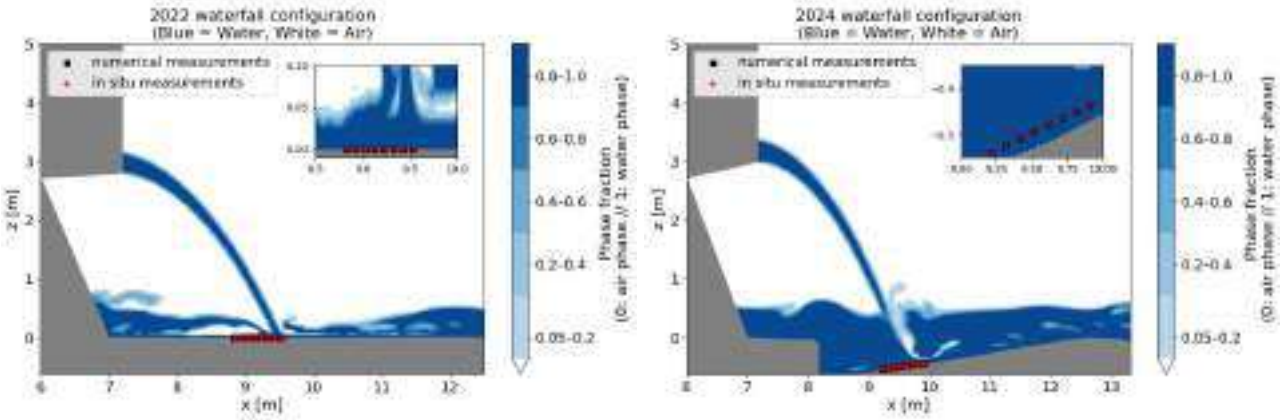

Fig. 1. Pre-work configuration in 2022 on the left and post-work configuration in 2024 on the right**.**

2.2 In situ measurements

The receiving pool bathymetry, water levels and probe positioning were surveyed using a Leica Flexline TS06 electronic tacheometer. The pressure exerted by the jet on the bottom was measured using a plate that was 1.05 m long, 0.30 m wide and fastened to the bottom. The plate had eight holes spaced 10 cm apart that formed a longitudinal line relative to the jet axis (see Fig. 1). Capillaries were then connected to these holes and to pressure sensors. The eight sensors were distributed as follows: three 250 mbar sensors, one 400 mbar sensor and four 1 bar sensors. Measurements were conducted at a 500Hz acquisition frequency for 130s.. These measurements were carried out in three successive stages. (I) Centering the plate laterally with respect to the jet width and longitudinally with respect to the jet impact (II) Acquiring reference pressure measurements in the pool at rest. (III) Acquiring pressure measurement with the established jet.

2.3 Construction of the numerical model

To reduce computational costs, the numerical model consists of two sub-models, named 'Upstream' and 'Downstream'. The Upstream sub-model represents the intake channel, the flap gate and the initial stage of the drop. The physical quantities (e.g. air/water phase distribution and velocity) established at the end of the flap gate are then injected as inlet conditions for the Downstream sub-model, which represents the drop impacting the reception area (see Fig. 1). The geometry was constructed to accurately represent the in situ situation using construction plans and topographical surveys. Numerical simulations were performed using the Unsteady Reynolds-Averaged Navier–Stokes (URANS) model with the open-source OpenFOAM software (version 2412). Each sub-model uses the Volume of Fluid (VOF) method with the k-ε turbulence model, as in a similar study by David et al. (2023) on the Las Rives site (Ariège River). The k-omega SST turbulence model was tested, showing non-significant changes. Pressures at the bottom are extracted at in-situ measurement points and recalculated in the model based on topography (Fig. 1). These pressures were recorded at an acquisition frequency of 500 Hz over a period of 150 seconds.

3. Results

The results presented focus on dynamic pressure (pdyn), which is obtained by subtracting hydrostatic pressure (ρgh) from measured total pressure (ptot). The variables used are: ρ (water density [kg/m³]), g (gravitational acceleration [m/s²]) and h (water column height [m]). The following box plots show the 5th and 95th percentiles (ends of vertical lines), the 25th and 75th percentiles (edges of boxes) and the median value (horizontal line inside boxes).

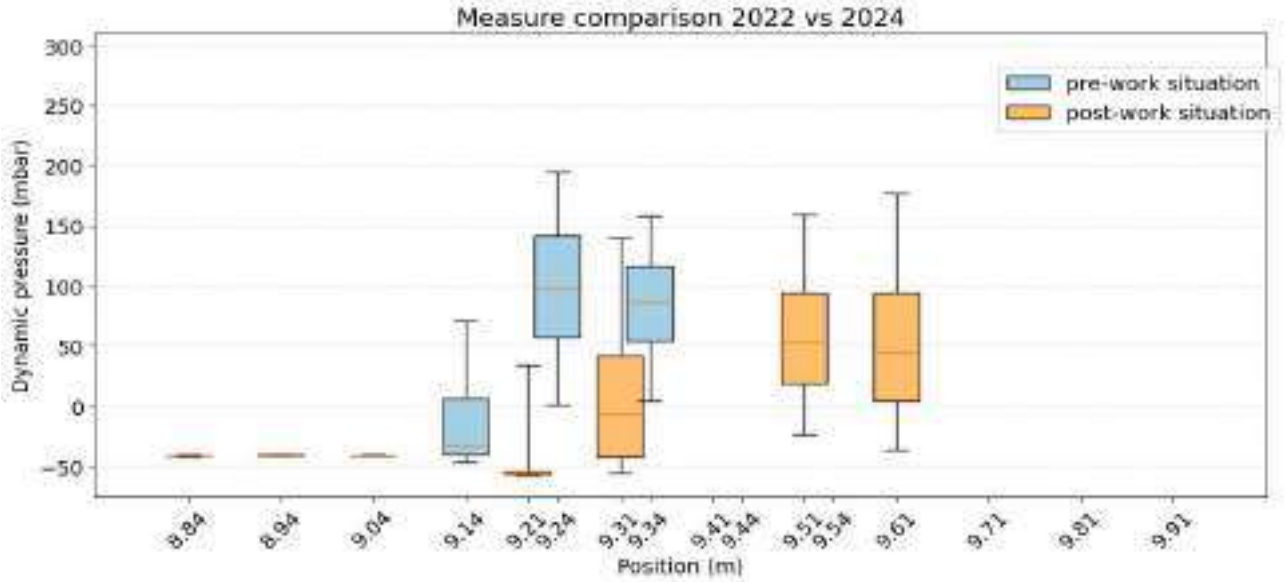

Fig. 2. Box plots of the measured dynamic pressure along the jet axis in the pre-work situation (2022) and the post-work situation (2024).

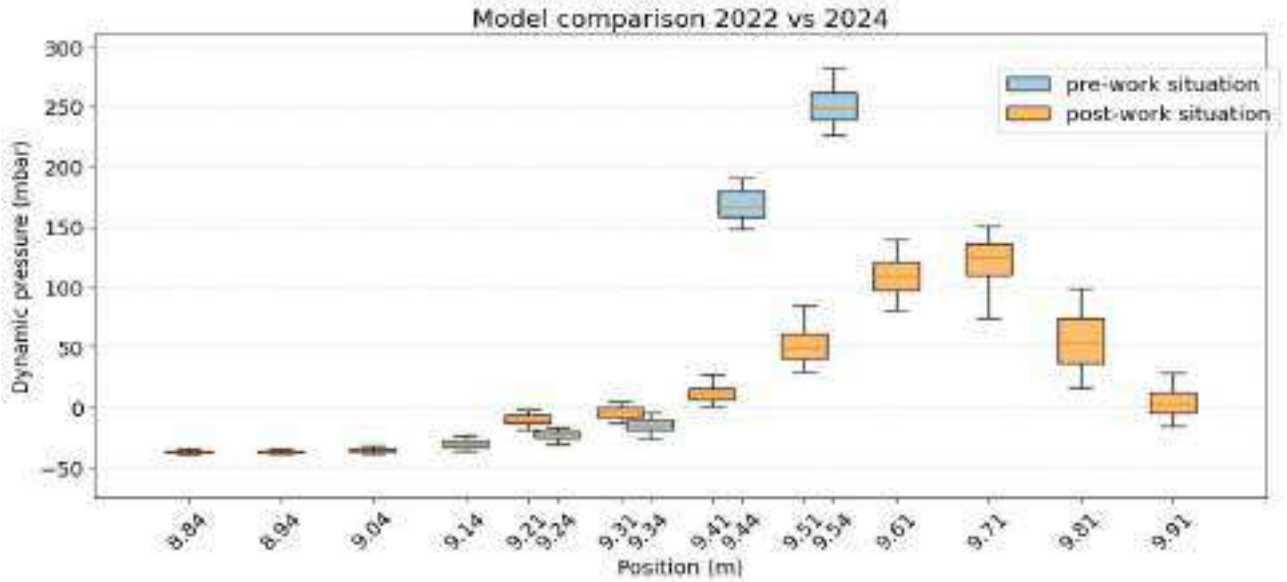

Fig. 3. Box plots of the dynamic pressure extracted from the numerical modelling along the jet axis in the pre-work situation (2022) and the post-work situation (2024).

3.1 Comparison of in situ measurement and numerical modelling results

In situ measurement and numerical modelling results on the dynamic pressure exerted by the jet on the bottom can be compared by looking at Figs. 2-3. The model reflects quite well the order of magnitude of the high values recorded on site, in particular in the post-work situation at x = 9.51 m and 9.61 m (100-150 mbar). The highest measured values appear a bit higher than the modelled ones. One explanation could be the use of the URANS model, which reduces the variability of model values compared to what is captured during direct measurement. In the pre-work situation, the highest pressures modelled at x = 9.54 m (250-280 mbar) cannot be compared to the measured ones, which are not available at this position. However, measured values obtained at x = 9.34 m and x = 9.24 m are much higher than modelled ones. One explanation could be that the modelled jet trajectory impacts further downstream than during the measurement. The low values of pressure are less well represented by the model. This may be explained by the way the data are measured in situ. On the

measurement plate, the holes are oriented vertically. Thus, when the jet oscillates, the flow can impact the holes tangentially. This physical phenomenon is not captured by the model because the pressures are extracted at specific points before the jet impacts any wall (bottom or measuring plate).

3.2 Comparison of pre-work and post-work results

Comparison of pre-work and post-work measured dynamic pressures cannot be fully drawn, as in the pre-work situation, only two sensors detect significant values and the peak of pressures may not be surveyed (Fig. 2). Nevertheless, measurement in the pre-work situation at x = 9.24 m and 9.34 m shows notably higher maximum, 75th percentile and median values, ranging from 100 to 200 mbar, than measurements in the post-work situation at x = 9.51 m and 9.61 m, ranging from 50 to 175 mbar. Modelled dynamic pressures can be compared in a more informative manner (Fig. 3). Firstly, the deepening of the bottom induced a shift further downstream of the jet impact on the bottom, as shown in Fig. 1. The pressure peak appears at x = 9.54 m in the pre-work situation and at x = 9.71 m in the post-work situation. Moreover, the jet impact zone appears more dispersed after the deepening, spreading over approximately 40 cm between x = 9.41 m and 9.81 m, compared to before, spreading over approximately 20 cm between x = 9.34 m and after 9.54 m. The maximum dynamic pressures reach 280 mbar at x = 9.54 m in the pre-work situation, which corresponds to the maximum theoretical value given the drop of about 3 m, meaning that the core of the jet impacts the bottom without being dissipated. In the post-work situation, maximum dynamic pressures are reduced to 150 mbar, meaning that the core of the jet no longer impacts the bottom.

4. Conclusion and perspectives

The comparison between field measurements and URANS-VOF 3D modeling results confirms that the model captures quite well the order of magnitude of the high dynamic pressure values recorded on site, as already shown by David et al. (2023). Considering that the risk of damage to fish is probably related to the highest dynamic pressures, this modeling approach appears to be a promising tool to characterize in detail the hydrodynamics of the jet in the air and in the receiving pool. It is all the more interesting given that in situ measurements are difficult to carry out. The comparison between the situations before and after the deepening work reveals, both in measurements and in modeling results, a significant improvement in fish-reception conditions, with a sharp decrease in maximum bottom dynamic pressure, consistent with the observed reduction in fish injury rates. This study is part of a broader research program aimed at better understanding the link between reception conditions (e.g., jet characteristics, water depth, pressure on the bottom) and fish survival rates, and ultimately at improving criteria to ensure a safe reception. The present findings highlight that 3D modeling is one of the reliable modeling tools to refine criteria and design solutions.

Acknowledgements

The authors are very grateful to EDF Hydraulique Aude-Ariege for their welcome on the hydroelectric scheme and their contributions to the study, and to all people too numerous to cite, involved in the tricky pressure measurement on site.

References

Bercovitz Y, Tissot L, Sagnes P, Courret D, Lebert F, Lagarrigue T, Mataix V, Dumond L (2022) Evaluation of fish injuries at the outlet of downstream passage devices: preliminary in situ and laboratory experiments with Sensor Fish, 39th world congress of IAHR, Granada – Spain, 19-24 June 2022.

Courret D, Larinier M (2008) Guide pour la conception de prises d'eau "ichtyocompatibles" pour les petites centrales hydroélectriques, Guide technique ADEME, pôle écohydraulique Onema-IMFT-Cemagref, 78 p.

David L, Devaux Y, Chatellier L, Courret D (2023) Numerical simulations of a waterfall in a downstream basin, 40th world congress of IAHR, Vienna – Austria, 21-25 August 2023.

Odeh M, Orvis C (1998) Downstream fish passage design considerations and developments at hydroelectric projects in the Northeast USA, In: Jungwirth M., Schmutz S. & Weiss S. (Eds), Fish Migration and Fish Bypasses, Fishing News Books, 267-280.

Tétard S, Courret D, Tissot L, Richard S, Lagarrigue T, Frey A, Mataix V, Mercier O, Tomanova S (2023) Evaluation of a fine-spaced angled rack with surface bypass in providing safe and timely downstream passage for salmon smolts and silver eels. Knowl. Manag. Aquat. Ecosyst., 424, 25.

USFWS (2019) Fish Passage Engineering Design Criteria. U.S. Fish and Wildlife Service, Northeast Region R5, Hadley, Massachusetts.

Book of Abstracts of the *16th International Symposium on Ecohydraulics*
Challenges and solutions in the time of global changes
August 16–20, 2026, Lausanne, Switzerland
ISSN: 2790-2420 | ISBN: 978-90-837233-9-6 | doi:[10.64697/iahr.proc.ise2026.abs]
© 2026 IAHR. CC BY-NC-ND 4.0

FIELD-SCALE FLOW CONDITIONS AROUND ENGINEERED LOGJAMS: INSIGHTS FROM LARGE-SCALE PIV

Felix BROß[1,2], Isabella SCHALKO[2]

[1] Institute of Fluid Dynamics, ETH Zurich, Switzerland
email: bross@ethz.ch

[2] Swiss Federal Research Institute WSL, Switzerland
email: isabella.schalko@wsl.ch

ABSTRACT

Engineered logjams (ELJs) are widely used in river restoration to increase flow heterogeneity, yet quantitative field measurements that document their effects at full scale remain scarce. In this study, we used drone-based Large-Scale Particle Image Velocimetry (LSPIV) to characterize the surface flow field around a selected ELJ in a restored reach of the Emme River (Switzerland). The analysis focused on how ELJ geometry and discharge influence flow patterns. The ELJ generated distinct hydraulic signatures, including accelerated jets in the gaps between ELJ elements and pronounced wakes with reduced velocities downstream. Maximum gap velocities reached more than twice the upstream reference velocity, whereas wake regions exhibited strong deceleration and recirculation zones. Across three measurement days with moderate discharge variation, wake length and structure remained consistent, suggesting that ELJ-induced low-velocity zones are relatively robust under baseflow conditions. In contrast, gap velocities increased at lower discharges due to enhanced relative contraction. These results provide rare field-based evidence of ELJ hydraulics at full scale and support ongoing efforts to evaluate and design nature-based restoration measures.

Keywords: engineered logjams; flow heterogeneity; Large-Scale PIV; nature-based solutions; wake dynamics

1. Introduction

Engineered logjams (ELJs) are increasingly used in river restoration (Roni et al., 2015, Wohl et al., 2019) to enhance local flow heterogeneity (Blanckaert et al., 2014, Müller et al., 2022) and create diverse hydraulic habitats (L'Hommedieu et al., 2020). While laboratory studies provide detailed insights under controlled boundary conditions (Schalko et al., 2023), quantitative field data at full scale remain limited (Blanckaert et al., 2014, Schnauder et al., 2021). Spatially resolved flow measurements are particularly scarce, even though flow structure governs scour, wake formation, and near-bed hydraulic gradients that are relevant for habitat suitability.

This study presents field observations from an ELJ installed in a restored reach of the Emme River (Switzerland). In this abstract, the focus was placed exclusively on the hydraulic response, aiming for a minimal but robust characterization suitable for practical design guidance. Flow fields were captured with drone-based Large-Scale Particle Image Velocimetry (LSPIV) under three discharge conditions representative of winter baseflow.

2. Methods

The monitored section is part of a 730 m restored reach of the Emme River (Canton Solothurn, Switzerland), where several ELJs were installed as partial-spanning structures. One site with an ELJ composed of a side and a center jam was selected for detailed hydraulic monitoring. Surface velocities in streamwise and lateral direction (u, v) were measured using drone-based LSPIV following established workflows: stabilization of airborne videos using ground control points, background subtraction, contrast enhancement, and multi-pass cross-correlation for velocity quantification. Velocities were normalized using a spatially averaged upstream reference velocity U. We compare (i) approach flow, (ii) jet development in gaps, and (iii) wake characteristics

downstream of the ELJ. Discharge varied moderately across the three surveys from January to March 2025 with Q_1 = 4.2 m³/s, Q_2 = 3.6 m³/s, and Q_3 = 2.5 m³/s, enabling assessment of flow sensitivity.

3. Results

The resulting flow field induced by the ELJ placement is qualitatively illustrated in Fig. 1. Upstream of the ELJ, flow remained largely uniform, with minor reductions near the banks. Pronounced flow acceleration occurred in the gaps between the side and center jam as well as between the center jam and the channel bank. Maximum normalized velocities ($u/U \approx 2.4$) occurred between the side and center jam, reflecting stronger effective blockage where the structure occupied a larger fraction of the channel width. The ELJ generated wakes with recirculation zones downstream of the side jam with u/U = -0.24 and the center jam with u/U = -0.16. The wake length amounted to 2 (side jam) and 4 (center jam) times the respective jam width, indicating the footprint of the ELJ to alter the local flow conditions. Wake length did not strongly depend on discharge, suggesting that velocity refugia downstream of ELJs remain stable across the measured low-flow conditions. Across the three measurement days, gap velocities increased as discharge decreased, reflecting relative contraction effects under shallower flow. In contrast, wake length and qualitative wake structure remained similar. Local morphology (e.g., sediment banks) exerted a comparable influence on the flow field as the discharge changed.

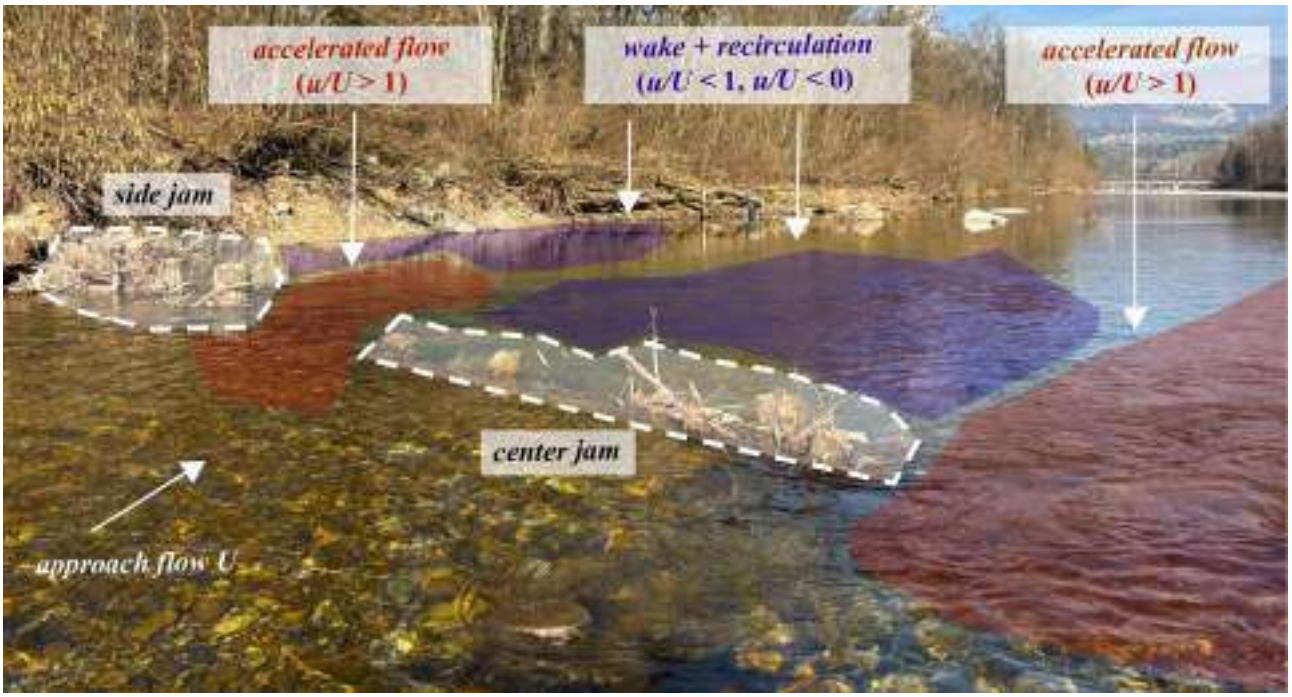

Fig. 1. Engineered logjam at the Emme River with highlighted jams (white) as well as regions of accelerated (red) and decelerated flow (blue) (photo: I. Schalko)

4. Conclusions and Outlook

This field study demonstrates that partial-spanning ELJs substantially enhance hydraulic heterogeneity by creating accelerated jet regions and persistent wake zones. Wake characteristics were surprisingly insensitive to discharge, highlighting their potential relevance as stable low-velocity habitat. These findings highlight the importance of considering partial-spanning ELJ geometry when designing nature-based solutions to achieve targeted flow heterogeneity. Future work will include vertical velocity measurements using Acoustic Doppler Velocimetry (ADV) and quantitative morphological surveys to link surface velocities to three-dimensional flow structures and to assess interactions between flow, deposition, and scour. These additional datasets will support refined design recommendations for ELJs in dynamic gravel-bed rivers.

Acknowledgements

The authors thank Clémence Dorthe for the support during the field experiments and data analysis. The authors are funded by the Swiss National Science Foundation (Nr. 209091).

References

Blanckaert K, Han R, Pilotto F, Pusch M (2014) Effects of large wood on morphology, flow and turbulence in a lowland river, in: River Flow 2014. CRC Press

L'Hommedieu W, Tullos D, Jones J (2020) Effects of an engineered log jam on spatial variability of the flow field across submergence depths. River Research and Applications, 36(3), 383-397
Müller S, Follett E, Ouro P, Wilson CAME (2022) Influence of channel-spanning engineered logjam structures on channel hydrodynamics. Water Resources Research, 58(12), e2022WR032111
Roni P, Beechie T, Pess G, Hanson K (2015) Wood placement in river restoration: fact, fiction, and future direction. Can. J. Fish. Aquat. Sci. 72, 466–478
Schalko I, Follett E, Nepf H (2023) Impact of Lateral Gap on Flow Distribution, Backwater Rise, and Turbulence Generated by a Logjam. Water Resources Research 59, e2023WR034689
Schnauder I, Anlanger C, Koll K. (2022) Wake flow patterns and turbulence around naturally deposited and installed trees in a gravel bed river. International Review of Hydrobiology, 107(1-2), 22-33
Wohl E, Kramer N, Ruiz-Villanueva V, Scott DN, Comiti F, Gurnell AM, Piegay H, Lininger KB, Jaeger KL, Walters DM, Fausch KD (2019) The Natural Wood Regime in Rivers. BioScience 69, 259–273

Book of Abstracts of the *16th International Symposium on Ecohydraulics*
Challenges and solutions in the time of global changes
August 16–20, 2026, Lausanne, Switzerland
ISSN: 2790-2420 | ISBN: 978-90-837233-9-6 | doi:[10.64697/iahr.proc.ise2026.abs]
© 2026 IAHR. CC BY-NC-ND 4.0

QUANTIFYING LATERAL BEDLOAD TRANSPORT FROM BATHYMETRIC SCANS: EXPERIMENTS WITH A YAWED SUBMERGED VANE ARRAY

Mirko MUSA[1], Chien-Yung TSENG[2], Jiyong LEE[3], Michele GUALA[4]

[1] Laboratory of Sustainable River Engineering, Energy and Morphodynamics (STREEM), School of Architecture, Civil and Environmental Engineering, EPFL, Switzerland
email: mirko.musa@epfl.ch

[2] Department of Civil and Environmental Engineering, Colorado State University, Fort Collins, CO, USA
email: CY.Tseng@colostate.edu

[3] Environmental Sciences Division, Oak Ridge National Laboratory, Oak Ridge, TN, USA.
email: leej6@ornl.gov

[4] St. Anthony Falls Laboratory, Department of Civil, Environmental, and Geo-Engineering, University of Minnesota, Minneapolis, MN, USA
email: mguala@umn.edu

ABSTRACT

This study investigates how a yawed array of porous submerged vanes can redirect bedload laterally in a large quasi-field-scale open channel under live-bed conditions. To measure this redirection, we introduce a new methodology that merges Lagrangian bedform tracking, Eulerian remapping of transport fields, and a mass-conservative control-volume analysis. This approach enables the quantitative estimation of lateral bedload transport directly from bathymetric data. Experiments with and without the vane array reveal that the structures generate coherent lateral steering of migrating bedforms and produce a marked cross-channel modulation of streamwise sediment transport. The induced lateral transport reaches 9–18% of the domain-averaged streamwise rate, and its peak occurs near the third vane row. The methodology also identifies the streamwise location where laterally steered sediment converges, providing critical guidance for sediment-bypass system design.

Keywords: submerged vanes; sediment training; fluid-sediment-structure interaction; lateral bedload; bedforms; bathymetry scan.

1. Introduction

Managing sediment transport is central to river engineering and stream restoration practices. In the context of ecohydraulics, sediment regulation influences channel morphology, habitat heterogeneity, and long-term geomorphic resilience. Among the various sediment-management approaches, submerged vanes—such as those proposed by Odgaard and Wang (1991)—are short structures installed on the riverbed to modify local flow structures and shear stresses in order to redirect sediment laterally. Recent research has shown that porous vanes can achieve these effects while minimizing local scour (Lee et al., 2022). When vanes are yawed relative to the mean flow, they generate a cross-flow drag that can steer bedforms and sediment transport. In this study, porous vanes were selected not to perform a direct comparison with the more conventional solid-vane configuration, but rather to investigate a distinct class of flow obstruction that is both relevant from an engineering standpoint and representative of submerged vegetation and other nature-based sediment-control solutions. Porous elements may therefore serve both as alternative sediment-management structures and as idealized surrogates for vegetation in studies of river morphodynamics (Follett and Nepf, 2012; van Dijk et al., 2013; Schalko et al., 2019; Redolfi et al., 2021; Ismail et al., 2021).

A key limitation in existing research is the absence of quantitative methods to evaluate lateral sediment fluxes and thus the performance of these porous vanes—especially under live-bed conditions dominated by migrating bedforms. The recent study by Tseng et al. (2024) addresses this gap by conducting 36 hours of continuous experiments in a large flume with a uniform sediment distribution, employing high-resolution laser bathymetry to monitor the spatiotemporal evolution of dunes. By integrating a Eulerian averaging framework with mass-conservation-based control volumes, a new methodology is developed to quantify the lateral bedload transport generated by vane arrays. Building upon the work of Tseng et al. (2024), this extended abstract demonstrates the newly developed approach for quantifying lateral sediment transport and explores its broader applicability within sediment-transport research, particularly in the contexts of river restoration and ecohydraulics.

2. Methodology

2.1. Experimental Set-up

The experiments were carried out in the Main Channel at the St. Anthony Falls Laboratory, a 2.75 m-wide, 85 m-long facility containing a 0.4 m-thick layer of nearly uniform quartz sand (d_{50} = 0.42 mm). Two runs were performed under identical hydraulic and sediment transport conditions, one serving as a baseline (no structures) and the other employing a vane array positioned along the right half of the channel. The array consisted of sixteen porous vanes, each 0.18 m wide and 0.06 m tall above the bed, yawed at 45° with respect to the flow and arranged in three rows with streamwise and spanwise spacing of 1.08 m and 0.36 m, respectively (Figure 1). Experiments were performed in lived bed conditions (i.e., with active sediment transport) with tridimensional dunes migrating in the channel (see top panel in Figure 1). Bed morphology was monitored for 36 hours using a laser line-scanner mounted on a traversing carriage producing repeat bathymetry over a 12 m-long and 0.5 m-wide domain with a temporal resolution of 376 s. These data resolved the full spectrum of coexisting bedforms and captured their migration over several dune turnover cycles. Downstream bedload flux was independently recorded using five weighing pans spanning the channel width. Further details on the experimental setup and control conditions can be found in Tseng et al. (2024).

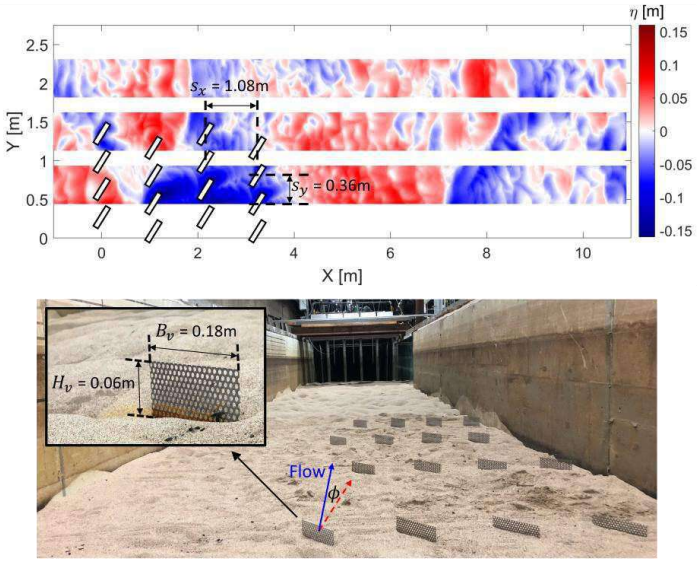

Figure 1: Experimental set-up. The top panel shows the top view of the array (white elements) and the three laser-scanned regions; the blue-red colors refer to the detrended bed elevation η.

2.2. Lagrangian Quantification of Streamwise Bedload Transport Using Bedform Tracking

The evolving bed morphology was analyzed using the bedform tracking algorithm developed by (Lee et al., 2021) which analyzes sign changes in longitudinal bed-slope gradients of 1D longitudinal bed elevation profiles from the scan. For each detected bedform, its length λ_b, height h_b, and migration velocity u_b were extracted from successive scans. The contribution of each bedform to the streamwise bedload transport rate was then calculated using the classical expression

$$q_{b,x} = \frac{1}{2}(1-p)\,u_b h_b$$

with porosity $p = 0.3$. These quantities describe sediment transport in a Lagrangian framework tied to individual migrating bedforms.

2.3. Eulerian Mapping of Bedload Transport

Because bedforms continuously enter and exit any fixed spatial region, a purely Lagrangian description cannot provide a spatially complete flux field. To address this limitation, we introduce a Eulerian-average grid-mapping algorithm that assigns bedform properties to all grid cells intersected by their length λ_b, thereby converting discrete, Lagrangian-tracked bedform characteristics into spatially continuous 2D (X–Y) fields. At each time instant, all bedforms overlapping a grid cell contribute to the Eulerian-averaged migration velocity, height, and bedload transport rate,

$$\{U_b, H_b, q_{s,x}\}(X,Y,t) = \mathbb{E}\{u_b, h_b, q_{b,x}\}_t$$

where $\mathbb{E}\{\cdot\}_t$ denotes the Eulerian-averaging operator. The resulting instantaneous fields are subsequently time-averaged to obtain converged Eulerian quantities, $\bar{Q}(X,Y) = \langle Q(X,Y,t)\rangle$, yielding an average Eulerian field of $\bar{U}_b, \bar{H}_b$, and $\bar{q}_{s,x}$, over the 36-h measurement period. A convergence analysis showed that the selected 0.5 m × 0.04 m Eulerian-average window captured a sufficient number of bedforms per grid to ensure both statistical robustness and adequate spatial resolution inside and outside the vane array.

2.4. Quantification of Lateral Bedload Transport

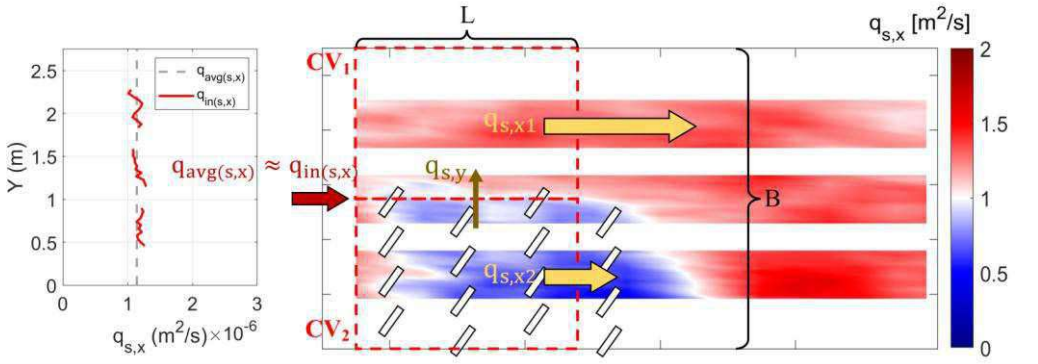

Figure 2: A schematic of the control volume approach to quantify the lateral bedload sediment transport rate. The left panel shows a uniform volumetric sediment influx profile, $q_{in_{s,x}}$, at the beginning of CV1 and CV2 ($X \approx -0.5$ m). The underlying colormap represent the represents the Eulerian-averaged streamwise bedload transport rate, $q_{s,x}$, for the vane experiment.

To quantify the vane array's effectiveness in redirecting sediment, we applied a control-volume (CV) mass-conservation framework to estimate lateral bedload transport (Figure 2). Two control volumes (CV1 and CV2) were defined to partition the channel into the unobstructed and vane-array regions, extending from $X = -0.5$m to a downstream boundary $X = L$. The streamwise bedload influx at the upstream boundary was nearly uniform across the channel, enabling the assumption

$$q_{\text{in},s,x} \approx q_{\text{avg},s,x}$$

where $q_{\text{avg},s,x}$is the domain-averaged streamwise transport rate. Applying sediment mass conservation to the upper (CV1) and lower (CV2) halves of the channel yields

$$CV_1: \frac{B}{2} q_{\text{avg},s,x} + L q_{s,y} = \frac{B}{2} q_{s,x1}$$
$$CV_2: \frac{B}{2} q_{\text{avg},s,x} = \frac{B}{2} q_{s,x2} + L q_{s,y}$$

where $q_{s,x1}$and $q_{s,x2}$are the width-averaged outflows from the two control volumes. Subtraction gives the lateral bedload transport rate

$$q_{s,y} = \frac{B}{4L} (q_{s,x1} - q_{s,x2}) C_M$$

with C_M accounting for unscanned gaps between laser domains and ensuring global mass balance. A second implementation using moving 1.5 m control volumes provided a spatially resolved description of the lateral transport within and downstream of the array.

3. Results

The bathymetric data show a clear reorientation of bedforms downstream of yawed vanes. Chevron-shaped scour patterns and crestlines tilted toward the unobstructed side confirm that the cross-stream component of vane-induced drag alters bedform trajectories. These patterns remain coherent across the three vane rows, although their intensity varies with wake interactions.

Eulerian maps reveal a substantial reduction in bedform migration velocity and height within the vane array, leading to a marked depression in streamwise sediment flux (colormap in Figure 3). On the unobstructed side, accelerated flow induces elevated sediment transport. Downstream of the array, bedform properties gradually recover to baseline conditions, consistent with independent weighing-pan measurements.

The cumulative control-volume analysis shows that the vane array produces a net positive lateral flux toward the unobstructed side for $0 < X < 5$ m, with a maximum near $X \approx 2.5$ m, corresponding to the third vane row (**Error! Reference source not found.**). The peak lateral flux reaches approximately

$$q_{s,y} \approx (1-2) \times 10^{-7}\ m^2/s$$

equivalent to 9–18% of the domain-averaged streamwise flux $q_{\mathrm{avg},x} = 1.14 \times 10^{-6}\ m^s/s$. Local moving-CV estimates confirm this trend and additionally show a small reversal of lateral flux near the downstream end of the array, likely reflecting a rebalancing of spanwise shear stress and weak morphodynamic oscillations.

4. Conclusions

This study demonstrates experimentally that yawed porous vanes can impose significant lateral steering of bedload under live-bed dunes migration. The newly developed methodology—combining Lagrangian bedform tracking, Eulerian grid remapping and a control-volume mass-balance approach—successfully quantifies lateral sediment flux using only bathymetric scans. The vane array redirects up to 18% of the total sediment flux laterally, with maximum transport occurring near the third vane row and vanishing roughly one array length downstream.

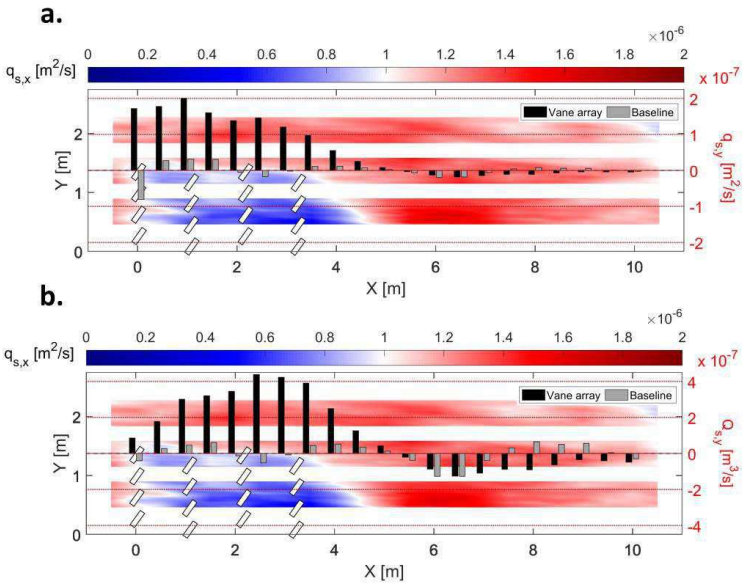

Figure 3: The computed lateral bedload transport across the evolving control-volume geometry is shown for both the baseline and vane-array scenarios. The color contour illustrates the streamwise bedload transport rate, $q_{s,x}$ [m^2/s]. The red vertical axis on the right corresponds to the overlaid bar chart, which reports: (a) the mean lateral bedload transport rate per unit length, $q_{s,y}$ [m^2/s]; and (b) the total volumetric lateral bedload transport flux, $Q_{s,y}=q_{s,x} \cdot L$ [m^3/s], for both the vane-array (black bars) and baseline (gray bars) cases.

Beyond documenting the effect of this specific vane array, the methodology establishes a generalizable framework for quantifying two-dimensional bedload transport fields in rivers and laboratory channels. It offers a useful tool for evaluating sediment-steering structures and optimizing the placement of sediment collectors or bypass inlets in river-reservoir systems. Future work will investigate the direct eco-geomorphological coupling between the flow and porous elements. Natural features like large woody debris (LWD) or aquatic vegetation act as porous structures, modulating the bleeding flow analogously to porous vanes. This interaction alters sediment dynamics and may facilitate the development of ecologically beneficial scour and deposition patterns characteristic of natural, heterogeneous riverine environments.

References

Follett, E.M., Nepf, H.M., 2012. Sediment patterns near a model patch of reedy emergent vegetation. Geomorphology 179, 141–151. https://doi.org/10.1016/j.geomorph.2012.08.006

Ismail, H., Xu, Y., Liu, X., 2021. Flow and Scour around Idealized Porous Engineered Log Jam Structures. Journal of Hydraulic Engineering 147, 04020089. https://doi.org/10.1061/(ASCE)HY.1943-7900.0001833

Lee, J., Marr, J., Guala, M., 2022. On Sediment Mass Flux Directionality Induced by Yawed Permeable Vanes under Near-Critical Mobility Conditions. Journal of Hydraulic Engineering 148, 1–17. https://doi.org/10.1061/(asce)hy.1943-7900.0002006

Lee, J., Musa, M., Guala, M., 2021. Scale-Dependent Bedform Migration and Deformation in the Physical and Spectral Domains. Journal of Geophysical Research: Earth Surface 126. https://doi.org/10.1029/2020JF005811

Odgaard, A.J., Wang, Y., 1991. Sediment Management with Submerged Vanes. II: Applications. Journal of Hydraulic Engineering 117, 284–302. https://doi.org/10.1061/(ASCE)0733-9429(1991)117:3(284)

Redolfi, M., Musa, M., Guala, M., 2021. On steady alternate bars forced by a localized asymmetric drag distribution in erodible channels. Journal of Fluid Mechanics 916, A13. https://doi.org/10.1017/jfm.2021.122

Schalko, I., Lageder, C., Schmocker, L., Weitbrecht, V., Boes, R.M., 2019. Laboratory Flume Experiments on the Formation of Spanwise Large Wood Accumulations: Part II—Effect on local scour. Water Resources Research 55, 4871–4885. https://doi.org/10.1029/2019WR024789

Tseng, C.-Y., Lee, J., Guala, M., Musa, M., 2024. Experimental Tests of Lateral Bedload Transport Induced by a Yawed Submerged Vane Array in Open-Channel Flows. Journal of Hydraulic Engineering 150, 04024045. https://doi.org/10.1061/JHEND8.HYENG-14076

van Dijk, W.M., Teske, R., van de Lageweg, W.I., Kleinhans, M.G., 2013. Effects of vegetation distribution on experimental river channel dynamics. Water Resources Research 49, 7558–7574. https://doi.org/10.1002/2013WR013574

Book of Abstracts of the *16th International Symposium on Ecohydraulics*
Challenges and solutions in the time of global changes
August 16–20, 2026, Lausanne, Switzerland
ISSN: 2790-2420 | ISBN: 978-90-837233-9-6 | doi:[10.64697/iahr.proc.ise2026.abs]
© 2026 IAHR. CC BY-NC-ND 4.0

INSIGHTS INTO THE SETTLING AND INTERACTION BEHAVIOUR OF SPHERICAL MICROPLASTICS

Mohammadmehdi Ramezani[1], Siamak Seyfi[1], Camillo De Castro[1], Shooka Karimpour[1]

[1] Department of Civil Engineering, Lassonde School of Engineering, York University, Toronto, ON, Canada

email: ramzani@yorku.ca
email: seyfi@yorku.ca
email: camillo@yorku.ca
email: Shooka.Karimpour@lassonde.yorku.ca

ABSTRACT

Microplastics are increasingly recognized as persistent contaminants in freshwater environments, yet the physical mechanisms governing their transport, including settling and interaction behaviour, remain poorly understood. This study investigates the settling dynamics and particle–particle interactions of spherical microplastics using a combined numerical and experimental approach. High-resolution large eddy simulations solving the incompressible Navier–Stokes equations coupled with six-degree-of-freedom particle motion are performed, and the resulting particle motions are compared with and validated against in-house particle tracking velocimetry (PTV) experiments. Particle Reynolds numbers are varied numerically through changes in particle density and experimentally through controlled changes in fluid viscosity and density using water–glycerin mixtures. The results indicate that wake-induced interactions play an important role during settling, while the developed numerical–experimental framework provides a basis for systematically exploring interaction regimes and informing improved representations of microplastic transport in ecohydraulic systems.

Keywords: *Microplastics; Wake dynamics; Computational Fluid Dynamics; Particle-particle interaction*

1. Introduction

Microplastics (MPs), defined as plastic particles with sizes smaller than 5 mm, have drawn increasing attention as an emerging contaminant in freshwater environments, including rivers, streams, and floodplains (D'Avignon et al. 2022). The concern over microplastic pollution is typically attributed to their long-lasting and ubiquitous presence in these environments and to the significant threats they pose to flora and fauna, as well as to human health through different pathways, including their role as vectors for pathogens and chemical contaminants and their transfer through aquatic food chains (Gola et al. 2021). This challenge is fundamentally an ecohydraulic problem, as the physical processes governing particle motion and settling directly determine the exposure levels and biological uptake of contaminants by aquatic organisms within their habitats.

Although the occurrence and sources of microplastics are well-documented, the physical mechanisms governing their transport, retention, and resuspension within aquatic systems have received relatively little attention. In this context, to address this gap, several studies have focused on the settling and rising behaviour of microplastics, including their size-, shape-, and density-dependent dynamics, aiming at understanding the underlying physical processes and developing kinematic and dynamic models capable of predicting microplastic pathways and sinks in water bodies (Waldschläger and Schüttrumpf 2019; Shamskhany and Karimpour 2022). However, field observations indicate that these predictive models often fail to fully capture the complexity of microplastic behaviour in the environment.

One of the reasons for these failures can be attributed to the limited knowledge and capability of existing models when microplastic particles interact with each other or with other particles and natural materials present in aquatic environments, leading to complex behaviours that are not captured by current modelling approaches.

Motivated by this gap in the field, this work sheds new light on this issue by investigating particle–particle interactions of spherical microplastics in a quiescent environment using numerical simulations, which are validated and compared with in-house particle tracking velocimetry (PTV) experiments. A particular emphasis is placed on situations in which a particle becomes entrapped in the wake of another particle, leading to altered relative motion and settling behaviour, while the drafting, kissing, and tumbling (DKT) (Fortes et al. 1987) concepts are also briefly addressed where relevant.

2. Methodology

This study investigates particle–particle interactions of spherical microplastics in a quiescent environment using a combined numerical and experimental approach. In the absence of imposed bulk flow, the particle dynamics are governed by gravity, buoyancy, and hydrodynamic interactions arising from particle-induced wakes. Here, we restrict the analysis to dilute particle conditions to isolate pairwise interaction mechanisms. In order to resolve the bidirectional (two-way) solid particle motion in an ambient fluid, we adopt an overset mesh technique, in which a moving body-fitted grid surrounding each particle overlaps with a stationary background grid, and flow variables are transferred between the grids through interpolation. Numerical simulations resolve the incompressible Navier–Stokes and continuity equations for the fluid phase, coupled with 6-degree-of-freedom rigid-body equations of motion for spherical particles, as expressed below (Wang et al. 2023; Ramezani and Karimpour 2025):

$$\nabla . \boldsymbol{u} = 0 \tag{1}$$

$$\frac{\partial \rho \boldsymbol{u}}{\partial t} + \nabla \cdot (\rho \boldsymbol{u}\boldsymbol{u}) = \nabla \cdot (\mu \nabla \boldsymbol{u}) - (\boldsymbol{g} \cdot \boldsymbol{x}) \nabla \rho - \nabla p_d \tag{2}$$

where $\boldsymbol{u}$ is the velocity vector, ρ is fluid density, μ is dynamic viscosity, $\boldsymbol{g}$ is gravitational acceleration, $\boldsymbol{x}$ is the position vector, and p_d is the dynamic pressure. The interface between fluid phases is captured using the volume of fluid (VOF) method, as follows:

$$\frac{\partial \alpha}{\partial t} + \nabla \cdot \boldsymbol{u}\alpha + \nabla \cdot \boldsymbol{u_c}\alpha(1-\alpha) = 0 \tag{3}$$

Here, α is the volume fraction of water, and $\boldsymbol{u_c}$ is artificial compression velocity introduced to sharpen the phase interface, defined as follows:

$$\boldsymbol{u_c} = C_\alpha |\boldsymbol{u}| \frac{\nabla \alpha}{|\nabla \alpha|} \tag{4}$$

where $C_\alpha = 1$ is constant, representing the compression length. The density of the mixture is also calculated as given by:

$$\rho = \rho_w \alpha + \rho_a (1-\alpha) \tag{5}$$

where the subscripts w and a denote water and air phases. For turbulence modeling, a Large Eddy Simulation (LES) approach is used, in which the large, energy-containing flow structures are explicitly resolved, while the effects of unresolved subgrid-scale motions are modeled using a *k*-equation for the subgrid-scale turbulent kinetic energy. The motion of microplastic particles is tracked using a six-degree-of-freedom (6-DOF) formulation, in which the translational and rotational motions are governed by Newton's second law and the angular momentum balance. The translational acceleration of the particle, denoted by a_f, is given by (Chen et al. 2019):

$$\boldsymbol{a}_f = \frac{\boldsymbol{F}_f}{m_f} \tag{6}$$

while the angular acceleration, $\boldsymbol{\theta}_f$, is computed as:

$$\boldsymbol{\theta}_f = \boldsymbol{I}_f^{-1} \cdot \boldsymbol{M}_f \tag{7}$$

Here, m_f and $\boldsymbol{I}_f$ are the particle mass and moment of inertia, respectively. The total force acting on the particle is expressed as:

$$\boldsymbol{F}_f = \iint_S (p\,\boldsymbol{I} + \boldsymbol{\tau}) \cdot d\boldsymbol{S} + \boldsymbol{F}_{constraint} + m_f\,\boldsymbol{g} \tag{8}$$

and the corresponding torque is given by:

$$\boldsymbol{M}_f = \iint_S \boldsymbol{r}_{CS} \times (p\,\boldsymbol{I} + \boldsymbol{\tau}) \cdot d\boldsymbol{S} + \boldsymbol{r}_{CM} \times \boldsymbol{F}_{constraint} + \boldsymbol{r}_{CG} \times m_f\,\boldsymbol{g} \tag{9}$$

The translational and rotational equations of motion are integrated in time using the Newmark time-integration scheme, providing a stable and second-order accurate update of particle velocities and positions during fluid–particle interactions. In these expressions, $\boldsymbol{\tau}$ denotes the viscous stress tensor, $\boldsymbol{F}_{constraint}$ represents constraint forces arising from particle–particle interactions, and $\boldsymbol{r}_{CS}$, $\boldsymbol{r}_{CM}$, and $\boldsymbol{r}_{CG}$ are position vectors from the particle center to the surface, center of mass, and center of gravity, respectively.

The numerical experiments were designed to replicate the in-house PTV experiments while avoiding unnecessary numerical expense. A rectangular container was considered, with 90% of its height filled with water. The width and depth of the container were selected such that wall effects on particle settling behaviour were negligible. The initial position of the microplastic particles was set sufficiently below the water surface to avoid free-surface effects and to ensure that particle motion was governed by fluid–particle and particle–particle interactions. The grid resolution was selected such that at least 80% of the turbulent kinetic energy was resolved, ensuring that the dominant flow dynamics and particle-induced wake structures were accurately captured and that relevant interaction mechanisms were not missed.

3. Results

Different scenarios corresponding to varying particle Reynolds numbers, Re_p, were considered. In the numerical simulations, water was used as the ambient fluid, and variations in Re_p were achieved by changing the particle density relative to the fluid. In contrast, the PTV experiments were performed using three water–glycerin mixtures: pure water (G0), 25% glycerin by volume (G25), and 50% glycerin by volume (G50). In the experimental cases, variations in Re_p arose from changes in the fluid viscosity and density associated with the different glycerin concentrations. Together, these conditions resulted in particle Reynolds numbers spanning a transitional regime relevant to particle settling. It is noted that, across all PTV experimental cases, particles reached their terminal settling velocity before entering the measurement field of view (FOV), and their subsequent vertical motion was tracked throughout the FOV.

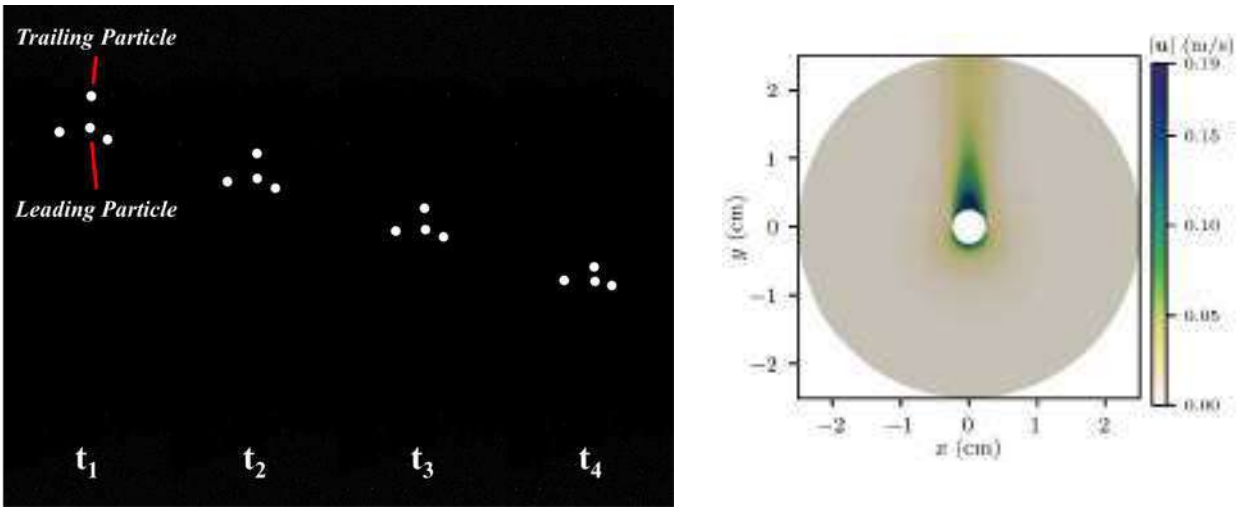

(a) (b)

Fig. 1. (a) Temporal evolution of four spherical particles settling across four distinct time instances (time step Δt = 0.1 s), where the leading particle and trailing particle undergo the drafting process and (b) Wake structure around a settling spherical microplastic particle in a numerical simulation.

In multiple-particle releases, interaction events were frequently observed as particles approached one another during settling. To systematically analyze these interactions, particles were examined in pairs and labelled as *leading* and *trailing* based on their instantaneous vertical positions. A consistent feature of interacting pairs is the acceleration of the trailing particle as it approaches the leading particle from above. This acceleration occurs as the trailing particle enters the wake region of the leading particle, resulting in a reduction of the effective drag. As the interaction progresses, the trailing particle may eventually reach the leading particle. This sequence corresponds to the classical drafting–kissing–tumbling framework. However, the present results indicate that the drafting phase itself exhibits a wide range of interaction modes that are not captured by simplified or idealized descriptions. In particular, the onset and evolution of drafting varied substantially across cases, even under nominally identical fluid conditions. Although classical DKT models assume a relatively uniform acceleration once the trailing particle enters the wake, the results show that drafting may initiate over a range of vertical and lateral separation distances, with different acceleration histories. These variations depict the sensitivity of the drafting process to the instantaneous wake structure of the leading particle and to the influence of other neighbouring particles present within the settling field. Figure 1 illustrates a representative particle pair undergoing the drafting phase.

Figure 1(a) shows the temporal evolution of two interacting particles at successive time steps settling within a four-particle system, highlighting the acceleration of the trailing particle relative to the leading particle. Figure 1(b) shows the wake structure around a settling spherical microplastic particle obtained from numerical simulations, illustrating the formation of a particle-induced wake in a quiescent fluid. The findings of these numerical simulations are used to examine the hydrodynamic mechanisms governing particle–particle interactions during the drafting phase. By resolving the flow field around interacting particles, the simulations enable direct assessment of wake structure, interaction initiation, and interaction mode under controlled conditions. This numerical framework provides a systematic basis for investigating the parameters influencing drafting behaviour and for interpreting the range of interaction modes observed during multiple-particle settling. The identified interaction mechanisms are fundamental to the transport and retention of microplastics in freshwater systems. Understanding these physical processes is essential for predicting the spatial distribution and accumulation patterns of plastic contaminants within aquatic habitats.

References

Chen H, Qian L, Ma Z, et al (2019) Application of an overset mesh based numerical wave tank for modelling realistic free-surface hydrodynamic problems. Ocean Eng 176:97–117. https://doi.org/10.1016/j.oceaneng.2019.02.001

D'Avignon G, Gregory-Eaves I, Ricciardi A (2022) Microplastics in lakes and rivers: an issue of emerging significance to limnology. Environ Rev 30:228–244. https://doi.org/10.1139/er-2021-0048

Fortes AF, Joseph DD, Lundgren TS (1987) Nonlinear mechanics of fluidization of beds of spherical particles. J Fluid Mech 177 :467–483. https://doi.org/10.1017/S0022112087001046

Gola D, Kumar Tyagi P, Arya A, et al (2021) The impact of microplastics on marine environment: A review. Environ Nanotechnology, Monit Manag 16:100552. https://doi.org/10.1016/j.enmm.2021.100552

Ramezani M, Karimpour S (2025) Turbulence and Self-Similarity in Classical Hydraulic Jumps. In: Azimi A., Robinson C (eds) Proceedings of the Canadian Society for Civil Engineering Annual Conference. Springer, Cham, Niagara Falls, ON, Canada, pp 159–173

Shamskhany A, Karimpour S (2022) Entrainment and vertical mixing of aquatic microplastics in turbulent flow: The coupled role of particle size and density. Mar Pollut Bull 184:114160. https://doi.org/10.1016/j.marpolbul.2022.114160

Waldschläger K, Schüttrumpf H (2019) Effects of Particle Properties on the Settling and Rise Velocities of Microplastics in Freshwater under Laboratory Conditions. Environ Sci Technol 53:1958–1966. https://doi.org/10.1021/acs.est.8b06794

Wang K, Ma X, Bai W, et al (2023) Two-dimensional numerical simulation of water entry of a cylinder into waves using OpenFOAM. Ocean Eng 269:113516. https://doi.org/10.1016/j.oceaneng.2022.113516

Session A2

Organism-flow interactions: movement, transport, and sensing

Book of Abstracts of the *16th International Symposium on Ecohydraulics*
Challenges and solutions in the time of global changes
August 16–20, 2026, Lausanne, Switzerland
ISSN: 2790-2420 | ISBN: 978-90-837233-9-6 | doi:[10.64697/iahr.proc.ise2026.abs]
© 2026 IAHR. CC BY-NC-ND 4.0

FISH PATHWAYS IN BOULDER-DOMINATED NATURE-LIKE FISHWAYS: LINKING SPATIAL VARIABILITY AND ENERGY EXPENDITURE

Md Aminul Islam Shagor[1]; Md. Sajjad Hossain Tusher[2]; Tom A. Langen[3]; Haitham Ghamry[4], Christos Katopodis[5], Abul B.M. Baki[1*]

[1]Department of Civil and Environmental Engineering, Clarkson University, Potsdam, NY, USA

[2]H&H Dept, GFT Infrastructure, Inc., Houston, Texas, USA

[3]Department of Biology, Clarkson University, Potsdam, NY, USA

[4]Freshwater Institute, Fisheries and Oceans Canada, 501 University Cres, Winnipeg, MB, CANADA

[5]Katopodis Ecohydraulics Ltd., 122 Valence Avenue, Winnipeg, MB, CANADA

*Corresponding author: Abul B.M. Baki; abaki@clarkson.edu

ABSTRACT

Hydraulic complexity strongly influences fish movement and energy use, making it a key factor in the design of nature-like fishways. This study examines the fish migratory pathways and associated energy consumption of juvenile Atlantic salmon (*Salmo salar*) and Rainbow trout (*Oncorhynchus mykiss*) across ten nature-like fishways, including rock-ramp (random and regular) and rock-weir (I-shape, and V-shape) under low (0.06 m^3/s) and high(0.07 m^3/s)-flow conditions. Fish trajectories captured by synchronized cameras were analyzed to quantify explored area (EA), Fish trajectory Path Length (FTPL), and spatial probability $P_H(x,y)$ using 1.0 cm kernel density estimation. Preliminary findings show that denser boulder patterns ($\lambda = 5.4$ %) promote greater spatial exploration (EA = 1.5 %) and longer pathways (FTPL = 3.6 m), indicating higher energy demand but improved passage connectivity. Ongoing analyses will integrate drag-based propulsive energy consumption of summing fish to assess hydrodynamic efficiency and identify energetically optimal migratory routes. The results will support the development of effective fish passage facilities for hydraulically and behaviorally efficient nature-like fishways.

Keywords: Explored area; fish passage; Instream boulder placement; movement ecology; salmonids; spatial variability; fish trajectory path length.

1. Introduction

Nature-like fishways are increasingly used to restore longitudinal connectivity in rivers by mimicking the hydraulic conditions of natural streams (Katopodis and Williams 2012; Katopodis et al. 2001). Instream boulders are commonly employed to generate hydraulic heterogeneity, creating velocity refugia and flow corridors that aid upstream passage of fish. The arrangement, density, and geometry of these boulders strongly influence local hydraulics and, consequently, fish behavior and passage success (Baki et al., 2012; Katopodis and Gervais, 2016; Katopodis et al. 2001). Previous studies have often inferred effective pathways from hydraulic fields (Haro et al., 2008; Katopodis and Williams 2012; Richer et al., 2020), but direct behavioral evidence remains limited. Understanding how fish interact with spatial variability, whether through exploration, resting, or efficient passage can provide deeper insights into the functional design of nature-like fishways. Juvenile salmonids, such as Atlantic salmon (*Salmo salar*) and rainbow trout (*Oncorhynchus mykiss*), are particularly suitable model species due to their ecological importance and sensitivity to hydraulic conditions. In this study, we directly quantify effective fish pathways using detailed trajectory data from flume experiments with ten boulder arrangements (Rock -Ramp including regular and randomly placed boulders and Rock-weir including I-shape and V-shape weirs) under two

flow conditions. This behavioral evidence complements hydraulic analyses and supports the optimization of fishway design for multiple species and flow regimes.

2. Objectives

This study aims to investigate the effective fish migration pathways of juvenile Atlantic salmon and rainbow trout combining fish movement data and hydraulic results in various nature-like fishways under low- and high-flow conditions. The specific objectives are: (1) Identify the migrating fish pathways using video-tracking and (2) Explore the fish energy expenditure for optimum swimming pathways.

3. Methodology

Experiments were conducted in the Ecohydraulics flume at Clarkson University (16 m × 0.96 m × 0.60 m), a recirculating system supplied by an underground tank and pump with a constant bed slope of 0.005. The bed was lined with fixed gravel (D_{50} = 6.1 mm) to simulate a natural streambed, consistent with previous studies on low-gradient gravel-bed channels. Flow depth was maintained at 0.20 m using the downstream tailgate, with flow rates of 0.06 m³/s and 0.07 m³/s representing low- and high-flow conditions, respectively. The Atlantic salmon (n = 26) had a mean fork length of 12.42 ± 1.02 cm and mean mass of 42.50 ± 9.35 g, while the rainbow trout (n = 18) had a mean fork length of 12.22 ± 1.60 cm and mean mass of 45.20 ± 8.25 g. Further details on fish sourcing, holding conditions, and experimental configurations are provided in this paper (details are in Tusher et al. (2026)). A control volume (CV) of 1.68 m × 0.96 m, located 4.65 m downstream of the fish release point, was designated for detailed behavioral analysis. Ten boulder arrangements were tested, including a bare channel (S1), three rock-ramp configurations (λ = 3.4%, 5.4%, 8.3%), three randomized rock ramp boulder layouts, and three rock-weir patterns (V-upstream, V-downstream, I-shape). The present analysis focuses on the bare channel and three rock-ramp densities (S1, S2, S3). Fish trajectories were recorded using three top-mounted GoPro Hero 12 cameras, each covering 0.54 m × 0.96 m segments to span the 1.68 m × 0.96 m CV area. Additional underwater cameras verified resting behavior and cross-validated top-view tracking. Cameras operated at 120 fps, 1/480 s shutter speed, and 1080p linear resolution to minimize distortion and ensure positional accuracy. Fish trajectories were extracted from the recorded videos using Tracker v6.3.3 (Open Source Physics), which allows frame-by-frame determination of fish coordinates and movement parameters such as velocity and acceleration. A similar video-tracking approach using Tracker has been applied in eco-hydraulic fish swimming studies (Zhang et al., 2025).

4. Data Analysis

Fish trajectories extracted from video tracking were processed in R v4.3.1. Horizontal positions (x, y) were used to calculate three behavioral metrics (Mozzi et al., 2024a): explored area (EA), trajectory length (TL), and spatial use probability ($P_H(x,y)$). EA was defined as the fraction of the control volume (CV; 1.62 × 0.96 m = 1.55 m²) visited by each fish. The CV was discretized into a 1 cm × 1 cm grid (15,552 cells) (Mozzi et al., 2024b), and each trajectory was mapped to the occupied cells. The number of unique cells visited was normalized by the total number of cells, yielding a relative EA per fish. Pattern-level EA values were calculated as the mean across all fish within each treatment. FTPL was computed as the cumulative two-dimensional path length of each fish within the CV, obtained by summing Euclidean distances between successive time-ordered positions. FTPL thus reflects the energetic effort required to traverse the CV. Group averages were then used for comparison among treatments. Spatial use probability ($P_H(x,y)$) was derived using kernel density estimation (KDE; bin width = 1.0 cm) (Mozzi et al., 2024a; Vokoun, 2003). The resulting heatmaps describe the likelihood of fish occurrence at specific (x, y) locations and were normalized by total detections to enable treatment comparisons. Reflection at arena boundaries was applied in high-flow conditions (notably S3H) to reduce edge bias in density estimation. Future analyses will couple EA, FTPL, and $P_H(x,y)$ with drag-based propulsive energy metrics to assess hydrodynamic efficiency and identify energetically optimal routes.

5. Results and Discussions

Preliminary results from rock-ramp fishways indicate clear effects of boulder density and flow, as well as channel boundaries, on fish movements (Fig.1). Under low-flow conditions, Atlantic salmon in the bare channel (S1L) displayed limited exploration (EA = 0.6%), shorter trajectory lengths (FTPL = 1.7 m), and movements near the channel boundary, suggesting direct upstream passage with minimal lateral movement. In contrast, higher-density rock-ramp patterns (S3L, λ = 5.4%) promoted greater exploration (EA = 1.1%), longer trajectories (FTPL = 2.0 m), and use of channel boundaries, as fish interacted more with flow heterogeneity created by boulders.

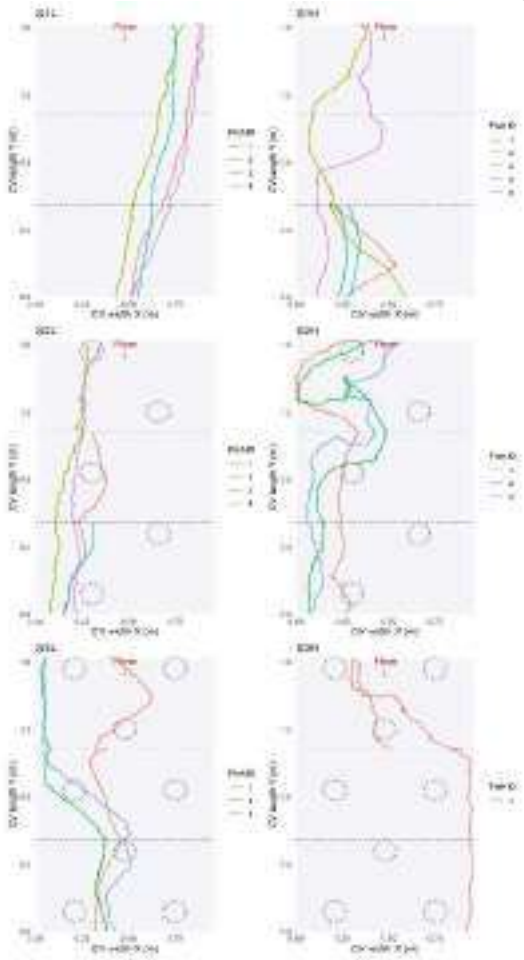

Fig. 1. : Fish Pathway for pattern S1(No boulder), S2(3.4% Boulder Density), S3 (5.4% Boulder Density) High and Low flow.

At high flow, these contrasts became more pronounced: S1H remained low in exploration (EA =0.6%, TL = 1.2 m), while S3H elicited extensive exploration (EA = 1.5%), long trajectories (FTPL = 3.6 m), and use of channel boundaries, reflecting both increased search for energetically favorable microhabitats and higher movement effort. Probability density maps $P_{H(x,y)}$ (Fig.2) showed that fish consistently utilized corridors adjacent to boulders under high flow, confirming their role in providing velocity refuges. These trends align with prior work where instream boulders were shown to create hydraulic patches that guide or delay fish. Importantly, our findings suggest a trade-off: denser boulder fields enhance habitat exploration but increase energetic demand, while sparse or no-boulder conditions enable more direct but less exploratory passage, at least in hydraulic conditions that are suitable for upstream passage. While these results are based on three rock-ramp patterns and a single species (Atlantic salmon) where not all the fish trajectories are shown, future analyses will expand to all ten nature-like fishways (including No boulders, Rock-Ramp, V and I-shaped weirs) and to two species (Atlantic salmon and rainbow trout) for both identifying fish pathways and exploring fish energy expenditure along the pathways. The findings will enable us to evaluate species-specific strategies, compare ramp versus weir designs, and ultimately propose a framework of effective pathways based on both spatial (EA, FTPL, $P_{H(x,y)}$) and energetic metrics. We expect that rainbow trout, for example, will exhibit broader spatial coverage at low flow, while Atlantic salmon will sustain longer movement distances at higher flow, consistent with interspecific behavioral strategies. The next phase of our study is to analyze the results and observations from random and boulder-weirs scenarios.

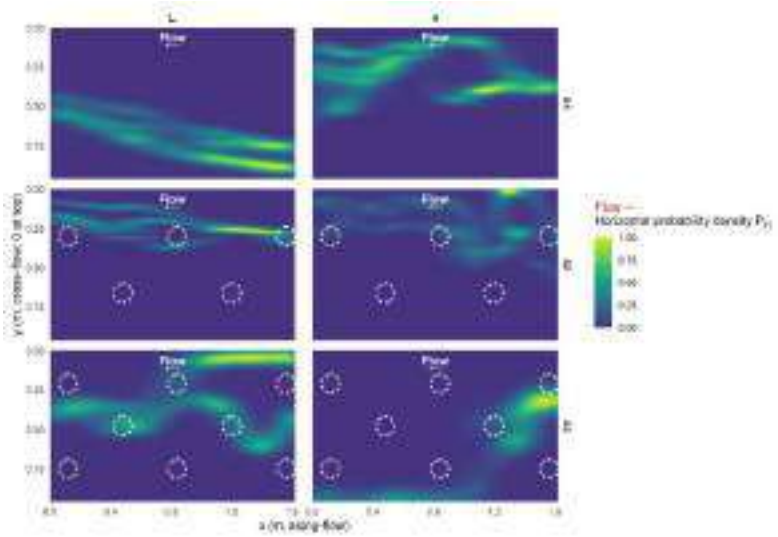

Fig.2. Probability density maps $P_H(x,y)$ pattern S1, S2, S3 (High (H) and Low flow (L)).

6. Conclusion

This study demonstrates that direct fish trajectory analysis provides a powerful framework for identifying effective pathways in nature-like fishways. Early results suggest that while denser boulder arrangements enhance spatial use, they may impose greater energetic costs. By integrating EA, FTPL, spatial probability maps $P_H(x,y)$, and energy expenditure, we aim to produce a comprehensive assessment of fish passage efficiency across multiple boulder arrangements. The outcome will guide evidence-based optimization of fishway design for different salmonid species and flow regimes.

References

Baki AB, Zhu DZ, Courtice G, Rajaratnam N (2012) Exploring the potential fish pathways in an experimental rocky ramp type nature-like fishpass, 9th International Symposium on Ecohydraulics 2012, September 17–21, Vienna, Austria

Haro A, Franklin A, Castro-Santos T, Noreika J (2008) Design and Evaluation of Nature-Like Fishways for Passage of Northeastern Diadromous Fishes Final Report, S.O. Conte Anadromous Fish Research Laboratory (CAFRL), U.S.G.S, 31 p

Katopodis C, Gervais R (2016) Fish swimming performance database and analyses, DFO Can Sci Advis Sec Res Doc 2016/002, vi + 5 50 p

Katopodis C, Williams JG (2012) The development of fish passage research in a historical context, Ecological Engineering, 48, 8–18, doi: 10.1016/j.ecoleng.2011.07.004

Katopodis C, Kells JA, Acharya M (2001) Nature-like and conventional fishways: alternative concepts, Canadian Water Resources Journal, 26(2), 211–232

Mozzi G, Nyqvist D, Ashraf MU, Comoglio C, Domenici P, Schumann S, Manes C (2024) The interplay of group size and flow velocity modulates fish exploratory behaviour, Sci Rep, 14, 13186, https://doi.org/10.1038/s41598-024-63975-z

Richer EE, Fetherman ER, Krone EA, Wright FB, Kondratieff MC (2020) Multispecies Fish Passage Evaluation at a Rock-Ramp Fishway in a Colorado Transition Zone Stream, North Am J Fish Manag, 40, 1510–1522, https://doi.org/10.1002/nafm.10516

Vokoun JC (2003) Kernel Density Estimates of Linear Home Ranges for Stream Fishes: Advantages and Data Requirements, North Am J Fish Manag, 23, 1020–1029, https://doi.org/10.1577/M02-141

Zhang W, Nie R, Liu X, Wang L (2025) Eco-hydraulic characteristics of rock weirs for fish habitat restoration, Physics of Fluids, 37(11), 115102, https://doi.org/10.1063/5.0301619

Tusher MSH, Langen TA, Ghamry H, Katopodis C, Baki ABM (2026) Movement behavior of juvenile salmonids in boulder-dominated channels: Effects of boulder dispersion, flow rate, and species, Journal of Ecohydraulics, doi: 10.1080/24705357.2026.2646669

Book of Abstracts of the *16th International Symposium on Ecohydraulics*
Challenges and solutions in the time of global changes
August 16–20, 2026, Lausanne, Switzerland
ISSN: 2790-2420 | ISBN: 978-90-837233-9-6 | doi:[10.64697/iahr.proc.ise2026.abs]
© 2026 IAHR. CC BY-NC-ND 4.0

THE PATCH-SCALE MATTERS: HABITAT-SPECIFIC RESPONSE OF MACROINVERTEBRATE DRIFT TO FLOW PULSES

Nathalie FRIESE [1 †], Kate L. MATHERS [1 2], Christine WEBER [1], Diego TONOLLA [3], Nico BÄTZ [1]

1: Eawag, Swiss Federal Institute of Aquatic Science and Technology, Surface Waters – Research and Management, Switzerland
email: Christine.Weber@eawag.ch
email: Nico.Baetz@eawag.ch
2:Loughborough University, Geography and Environment, Loughborough, UK
email: K.Mathers@lboro.ac.uk
3: ZHAW, Zurich University of Applied Sciences, Institute of Natural Resource Sciences, Wädenswil, Switzerland
email: Diego.Tonolla@zhaw.ch

†: In memory of our late colleague Nathalie Friese, whose dedication to riverine macroinvertebrate ecology continues to inspire our work. Her passion for conservation and freshwater research lives on through this study.

ABSTRACT

Flow pulses generated by on-demand hydropower (i.e. hydropeaking) strongly affect riverine benthic communities by causing macroinvertebrate drift. Because benthic community composition is inherently patchy, macroinvertebrate drift responses are therefore also likely to be habitat specific. We investigated how patch-scale hydraulic processes mediate macroinvertebrate drift during short-term flow pulses using an *in-situ* portable flume. The flume allowed simulation of rapid flow pulses on 45 patches characterized by either slow (< 0.5 m s^{-1}) or fast (> 0.5 m s^{-1}) current velocity within a pre-alpine river reach supporting an unimpacted macroinvertebrate community. This *in-situ* approach bridges the gap between controlled laboratory flumes and observational studies in regulated rivers. In patches with slow current, drift intensity was primarily influenced by absolute current velocity (V40) and current velocity rise rate (V40rate), whereas in patches with fast current, the relative change in current velocity (V40%) was more influential. Moreover, V40% significantly shaped drift composition in slow-current habitats. These results demonstrate that flow-pulse-induced drift arises from patch-scale hydraulic stress rather than being uniform across the reach. Incorporating such habitat-specific processes into ecohydraulic models can improve the assessment of drift risk, identify vulnerable areas, and guide targeted mitigation strategies to reduce flow pulse induced hydraulic stress in sensitive habitats.

Keywords: Hydropeaking; Macroinvertebrates; Habitat response; Patch-scale hydraulics; Habitat modelling; River managemen.

1. Introduction

Benthic macroinvertebrate communities in rivers exhibit strong spatial patchiness, reflecting diverse hydraulic and morphological conditions that shape the habitat mosaic (Beisel et al. 2000; Stanford et al. 2005). These communities are generally adapted to natural flow pulses, such as floods, and to the hydraulic stress they impose on individual habitat patches. For instance, some species use drift to disperse or recolonize after disturbance, while others persist in interstitial refugia during high flows.

Despite their resilience to natural flow pulses, macroinvertebrates are sensitive to long-term anthropogenic flow alteration. Hydropeaking, caused by on-demand hydropower production, generates rapid, daily recurring flow pulses that differ fundamentally from natural floods in both frequency and recovery time (Hayes et al. 2025). With each event, the associated involuntary (“catastrophic”) drift depletes local communities and impedes recolonization, resulting in a long-term decline in biomass and richness (Naman et al. 2016). Although

hydropeaking acts at the reach scale, the resulting hydraulic stress varies among patches within the habitat mosaic (Bätz et al. 2025). Given that benthic community composition is inherently patchy, macroinvertebrate drift responses are also likely to be habitat specific.

Understanding patch-scale responses is therefore critical for developing management strategies that account for the spatial heterogeneity within the habitat mosaic. However, most existing studies have focused either on controlled laboratory flumes, which simplify natural communities, or on already regulated rivers, where long-term alteration obscures immediate drift responses due to changes in the community composition. To bridge this gap, we conducted *in-situ* flume experiments in a natural, unregulated river to simulate hydropeaking-like flow pulses under real field conditions. Each patch was treated as a distinct ecological unit defined by its hydraulic characteristics. We hypothesized that drift responses would differ between habitat types, reflecting habitat-specific variations in benthic density, richness, and hydraulic sensitivity.

2. Methods

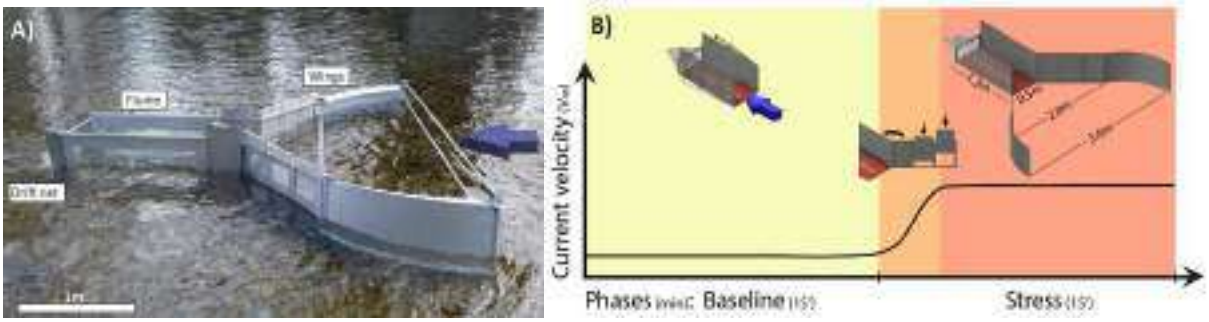

Fig. 1. A) Portable flume used for in-situ experiments, showing its three main components: the flume body, consisting of two Plexiglas side walls forming the core experimental area; wings, mounted at a 45° angle to the upstream end to increase current velocity; and a drift net attached downstream to collect drifting macroinvertebrates. **B)** Schematic representation of the two experimental phases. During the baseline phase (15 min), the flume with folded wings was placed on the riverbed to measure base drift. The stress phase began with a short (3 min) up-ramping period as the wings were unfolded and attached, followed by a 13 min period at steady high current velocity. The arrow in both panels indicates flow direction. All figures adapted from Friese et al. (2025).

2.1. Study design

Experiments were conducted in the Emme River, a pre-alpine river in central Switzerland characterized by a near-natural flow and sediment regime. Using a portable field flume (Fig. 1A) adapted from Gibbins et al. (2007), we simulated short-term flow pulses across 45 patches (0.5 × 1.2 m) representing two habitat types: slow-current (< 0.5 m s^{-1}) and fast-current (> 0.5 m s^{-1}). Each patch was exposed to two hydraulic phases (Fig. 1B):

- Baseline phase (15 min): unaltered near-natural hydraulic conditions;
- Stress phase (15 min): increased current velocity, mimicking hydraulic stress during a flow pulse.

Macroinvertebrate drift was collected using drift nets positioned at the exit of the portable flume. In the laboratory, macroinvertebrates were counted and identified to the lowest possible level.

Previous studies indicate that macroinvertebrates respond rapidly to abrupt hydraulic increases, with drift peaks occurring within 5–10 minutes after the onset of a flow pulse (e.g., Bruno et al., 2010). The 15-minute stress phase therefore captures the expected peak drift response associated with rapid hydraulic perturbation.

2.2. Data treatment

Hydraulic variables derived for each phase included, mean current velocity at 40% of the water depth (V40), the rate of current velocity increase (V40rate), and relative change in current velocity (V40%). Differences in water depth between baseline and stress phases were negligible and within measurement uncertainty, and were therefore not considered in the analysis. Macroinvertebrate drift intensity (individuals/min·m^2), defined as the number of individual drifting divided by phase duration and the wetted cross-sectional area of the drift net, was detrended to remove non-hydraulic variability (e.g., temperature, turbidity, conductivity). Mann–Whitney U tests assessed differences in drift intensity between habitat types.

Quantile regressions were applied to evaluate drift responses to hydraulic stress. Unlike standard regressions, this approach estimates relationships across different parts of the response distribution, capturing both typical (i.e. 0.5 quantile) and extreme (i.e. 0.1, 0.9 quantiles) drift reactions. Models were constrained through the origin, as drift cannot occur when current velocity is zero, and a power function was fitted to account for nonlinear relationships.

3. Results

3.1. Habitat-specific responses

Across 45 experiments, 4´885 individuals from 34 taxa were recorded, dominated by Simuliidae (41 %), Chironomidae (21 %), Baetidae (11 %), Heptageniidae (11 %), Nemouridae (6 %), and *Leuctra* sp. (5 %). Baseline current velocity differed clearly between habitat types (slow-current: 0.44 ± 0.04 m/s; fast-current: 0.60 ± 0.05 m/s; mean ± SD). Although both habitat types showed comparable drift intensity during the baseline phase (Fig. 2A), patches with slow current exhibited a significantly stronger increase in drift intensity (+358 %) than those with fast current (+281 %; Mann–Whitney U = −2.96, p = 0.003).

3.2. Hydraulic variables driving drift

Quantile regression revealed that, in patches with slow-current, drift intensity reacted stronger to current velocity (V40) and rate of current velocity increase (V40rate) than in patches with fast-current (Fig.2B-D). Conversely, in patches with fast-current, relative change in current velocity (V40%) had a stronger influence on drift intensity. For patches with slow current, V40% was also found to influence drift assemblage.

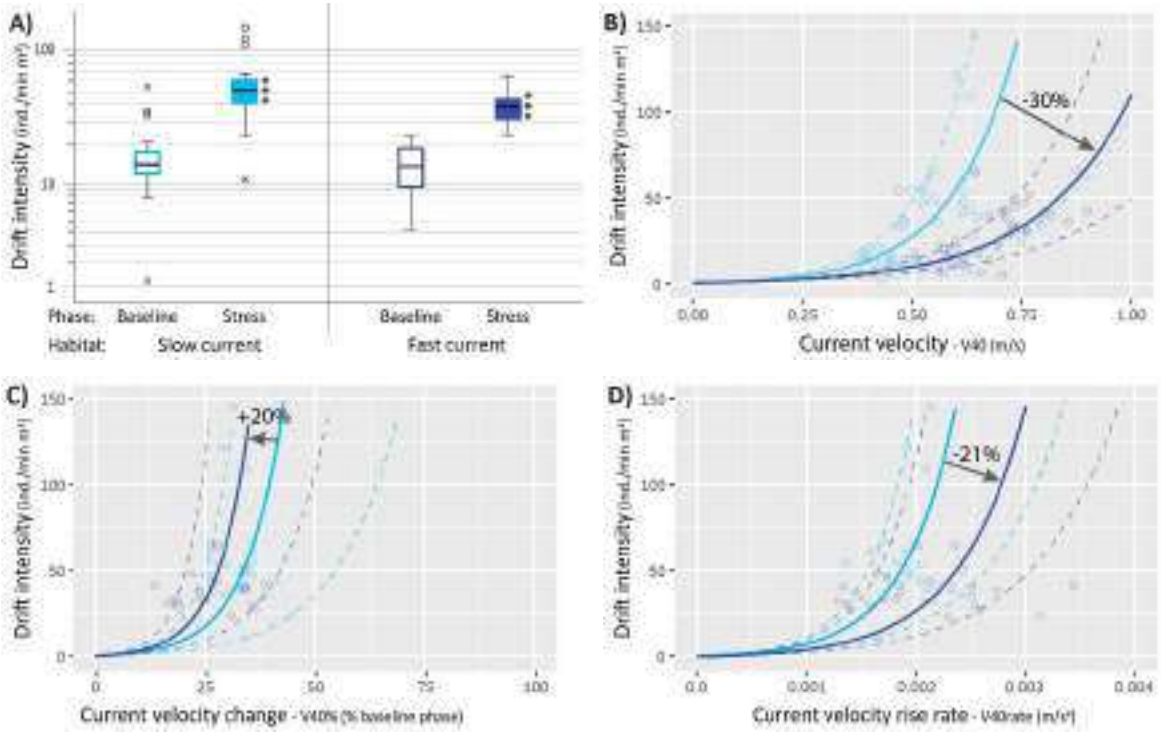

Fig. 2. A) Drift intensity during the baseline and stress phases for patches with slow and fast current. Note that the Y-axis is logarithmic. **B–D)** Quantile regressions between drift intensity and the three hydraulic variables, differentiated by patch habitat type (light blue = slow-current; dark blue = fast-current habitats). The percentages indicate the difference between patches with fast current relative to those with slow current across the 0.5-quantile regression. Positive values indicate a stronger effect in fast-current patches, whereas negative values indicate a stronger effect in slow-current patches. All figures adapted from Friese et al. (2025)

4. Discussion

Our results demonstrate that flow pulse induced drift is not spatially uniform but emerges from interactions between hydraulic stress and patch scale characteristics of the instream habitat and macroinvertebrate community.

In patches with slow-current, drift intensity was primarily driven by absolute current velocity (V40), while in patches with fast-current, drift intensity correlated most strongly with percentage change in current velocity (V40%). For patches with slow current, V40% was also found to be influential on the drift assemblage. As presented in more detail in Friese et al. (2025) benthic assemblage differed significantly between the two habitat types which likely interacts with the changing hydraulic conditions to mediate macroinvertebrate drift.

These findings suggest that hydropeaking mitigation should better account for processes operating at the patch scale, and thus for the spatial heterogeneity in hydraulic conditions, benthic assemblages, and their interactions. Hydropeaking mitigation measures could limit current velocity (V40) during peak flow and current velocity rise rate (V40rate) in habitat with slow-current and reducing the relative change in current velocity (V40%) in patches with fast-current.

5. Conclusions

This study demonstrates that the effects of flow pulses (e.g. hydropeaking) on macroinvertebrate drift are mediated by patch-scale hydraulic stress rather than being uniform across the reach. Habitat type and community composition within the habitat mosaic determine local drift responses, with patches with slow-current responding primarily to absolute current velocity and patches with fast-current to the relative change in current velocity. Integrating these patch-scale differences into ecohydraulic models will enable managers to better assess drift risk, identify vulnerable areas within a reach, and design more spatially targeted mitigation measures.

Acknowledgements

We thank Franziska Fechner, Karen Isabella Deniz, Lucie Sprecher, Marta Antonelli, and Christian Dinkel for their support during fieldwork and laboratory analyses, and Jonas Steiner for the graphical representation of the portable flume (Fig. 1). We are also grateful to Lorenzo Gorla and Tabea Dalbert for their valuable discussions on earlier drafts. Financial support was provided by the Swiss Federal Office for the Environment (FOEN).

References

Bätz N, Judes C, Vanzo D, Lamouroux N, Capra H, Baumgartner J, Berger B, Weber C. 2025. Patch-scale habitat dynamics: three metrics to assess ecological impacts of frequent hydropeaking. Journal of Ecohydraulics. 10(1):79-106.

Beisel JN, Usseglio-Polatera P, Moreteau JC. 2000. The spatial heterogeneity of a river bottom: a key factor determining macroinvertebrate communities. Hydrobiologia. 422(0):163-171.

Bruno MC, Maiolini B, Carolli M, Silveri L (2010). Short time-scale impacts of hydropeaking on benthic invertebrates in an Alpine stream (Trentino, Italy). Limnologica - Ecology and Management of Inland Waters, 40**,** 281-290.

Friese N, Mathers KL, Weber C, Tonolla D, Bätz N. 2025. Habitat-Specific Response of Macroinvertebrate Drift to Flow Pulses: Implications for Hydropeaking Management. Freshwater Biology. 70(10):e70103.

Gibbins C, Vericat D, Batalla RJ. 2007. When is stream invertebrate drift catastrophic? The role of hydraulics and sediment transport in initiating drift during flood events. Freshwater Biology. 52(12):2369-2384.

Hayes DS, Bätz N, Tonolla D, Merl K, Auer S, Gorla L, Weber C, Naudascher R, Silva LGM, Schmutz S et al. 2025. Why hydropeaking frequency matters: effects of recurring stranding on fish. Journal of Ecohydraulics.1-17.

Naman SM, Rosenfeld JS, Richardson JS. 2016. Causes and consequences of invertebrate drift in running waters: from individuals to populations and trophic fluxes. Canadian Journal of Fisheries and Aquatic Sciences. 73(8):1292-1305.

Stanford JA, Lorang MS, Hauer FR. 2005. The shifting habitat mosaic of river ecosystems. SIL Proceedings, 1922-2010. 29(1):123-136.

Book of Abstracts of the *16th International Symposium on Ecohydraulics*
Challenges and solutions in the time of global changes
August 16–20, 2026, Lausanne, Switzerland
ISSN: 2790-2420 | ISBN: 978-90-837233-9-6 | doi:[10.64697/iahr.proc.ise2026.abs]
© 2026 IAHR. CC BY-NC-ND 4.0

IMPACT OF ANTHROPIZED RIVER HYDRODYNAMIC CONDITIONS ON SILVER EEL MIGRATION SPEEDS

Utashi D. CIRAANE[1], Damien SONNY[2], Gaia FALGAS[3], Pierre ARCHAMBEAU[1], Benjamin DEWALS[1], Michel PIROTTON[1], Sébastien ERPICUM[1]

[1] UR-UEE, Laboratory of Hydraulics in Environmental and Civil Engineering (HECE), University of Liège, Belgium
email: d.ciraane@uliege.be
[2] PROFISH, Belgium
[3] École nationale supérieure de l'énergie, l'eau et l'environnement, France

ABSTRACT

Important peaks in river discharge promote the seaward migrations of European silver eels (Anguilla Anguilla). However, such metrics are not easily transferable across rivers or on different river sections due to morphological differences in river cross-sections. Nonetheless, the flow velocity is a robust and replicable metric across rivers and a main component of the discharge. This study examined the relationship between the migration speed of fourteen silver eels and the mean flow velocity computed using a one-dimensional hydrodynamic model. The results revealed a strong correlation between both variables (Pearson $r = 0.92$| Spearman $\rho = 0.91$, $p < 0.01$). They also suggested that above a mean flow velocity of 0.4 BL/s ~ 0.4 m/s, the downstream migration was quasi-linearly correlated to the mean flow velocity, while it was slower than mean flow velocity below this threshold. These findings suggest that migrating eels favor high flow velocities, typically occurring during important annual peaks in river discharges. Thus, the flow velocity may serve as a more robust, reliable, and transferable metric for designing and implementing sustainable strategies and solutions for rapid and safe seaward migrations of silver eels in anthropized rivers.

Keywords: Fish migration, Flow velocity, Meuse River, Numerical modelling, Fish tracking

1. Introduction

The understanding of river hydrodynamics in the seaward migration of European silver eels (Anguilla anguilla) requires further refinement. The consensus is that eels are commonly observed migrating downstream during or after major discharge peaks (pulses) (Vøllestad et al., 1986; Teichert et al., 2020). Beyond some thresholds, strong discharge pulses (positive followed by negative gradient) promote seaward movements. Such behavior has been noticed across various eel-inhabited rivers (Cullen & McCarthy, 2003; Bultel et al., 2014; Teichert et al., 2020). However, reported discharge thresholds vary spatially due to differences in river morphologies. Identical discharges, even normalised, may result in distinct hydrodynamic conditions depending on river slope, cross-section, and substrate (Lamouroux et al., 2002; Snelder et al., 2011). This highlights the difficulty of applying discharge thresholds across rivers. Discharge peaks may thus mask a more consistent, location-independent parameter linked to flow variation and eel migration speed. Previous research have recommended examining water depth and flow velocity to better understand the variability in silver eel catches near obstacles (Frost, 1950; Deelder, 1984).

Flow velocities needs further investigations (Deelder, 1984). A given discharge flowing through a river section fills a specific cross-sectional area and produces a mean flow velocity. The cross-sectional area varies with the water depth. However, in large anthropized rivers used for navigation, depth variations are controlled and often negligible and discharge variations translate almost exclusively into mean flow velocity variations. This makes the mean flow velocity a more transferable and consistent metric across anthropized river sections and water bodies. Nonetheless, the influence of the mean flow velocity on the seaward migration speeds of European eels remains understudied (Deelder, 1984). Hence, this study aimed to assess the influence of the mean flow

velocity on 14 seaward migrating silver eels using numerically computed hydrodynamic conditions of the lower Meuse River in Belgium.

2. Methods

The case study lies along the lower Meuse River in Wallonia, Belgium. It spans 44.3 km, from Huy upstream to Hermalle-sous-Argenteau downstream as shown in **Figure 1**. Key hydraulic infrastructures include: a navigation canal (the Albert canal) and three movable dams (Ampsin, Ivoz-Ramet, and Monsin). The canal links the city of Liège to the port of Antwerp near the North Sea. The three dams regulate upstream water levels, ensuring year-round navigability. Each dam, except Monsin, possesses navigation locks and all dams are equipped with run-of-river hydropower plants. At each dam, fish passages are frequently monitored and improved (Renardy et al., 2021; Life4Fish, 2023; Sonny, 2025). The fish data used in this study were collected in the framework of the Walloneel project (Sonny, 2025). The project aimed to improve the understanding of eel migration dynamics and success from and through the Walloon Meuse River. A total of 339 silver eels were captured. Of these, 95 (28%) were tagged with acoustic and passive telemetry devices and monitored over three years (2021–2023). Detection rates reached 74.7% (n = 71), with 84.5% (n = 60) migrating downstream. Fourteen eels (23.3%) crossed the whole 44.3 km of the study area. The 14 trajectories were used by this study to explore the influence of recorded and simulated hydrodynamic conditions of the Meuse River on silver eel migration speeds.

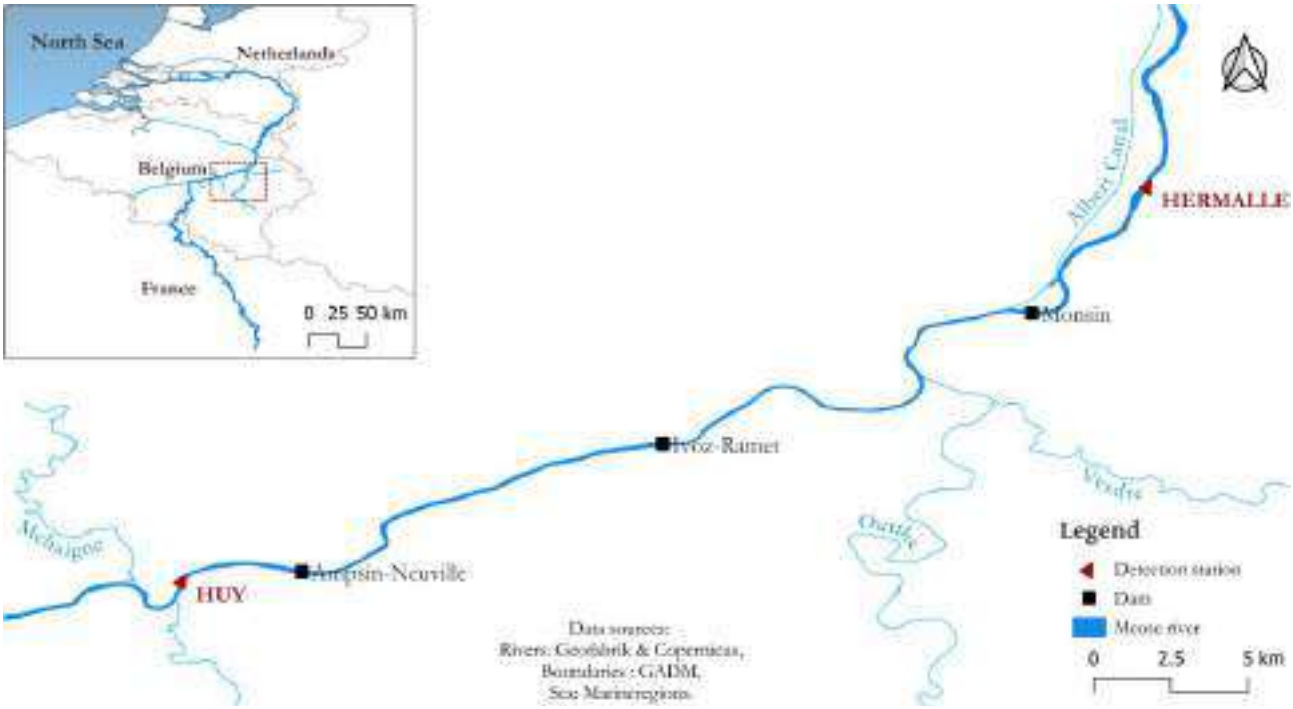

Figure 1: 44.3 Km of the Meuse River investigated hydrodynamically

The Meuse River hydrodynamic conditions were computed with a one-dimensional (1D) model. The model was built using the computational fluid dynamics software WOLF (Archambeau et al., 2024). WOLF solvers have been validated through various scientific and industrial projects (Ciraane et al., 2025). Model inputs included bathymetry, flow infiltrations, friction coefficients, boundary and initial conditions. For this study, river cross sections were extracted from sonar bathymetric data with a one-meter resolution. The distance between two successive cross sections was 100 m. Hydrographs from 11 hydrometric stations located in the watershed were used to infiltrate water in the model (SPW, 2024). The friction coefficient was obtained from (Ciraane et al., 2025) who calibrated a 1D hydrodynamic model for Atlantic salmon smolts in the region. The mean water levels recorded near dams were used as downstream boundary conditions since limited. Steady state solutions were precomputed as initial conditions for first time steps. The model cover the temporal extents of the field surveys (2021, 2022, and 2023). Fish trajectories were used to extract the mean flow velocities investigated in the analyses.

The impact of hydrodynamic conditions on silver eel migration speed was investigated with the discharge and the mean flow velocity. On one hand, the discharges reported on the Meuse river hydrograph were analysed to validate the pulse (peak) effect reported in the literature (Vøllestad et al., 1986; Teichert et al., 2020). The

validation consisted in comparing recorded eel detections at the inlet and outlet of the case study with concomitant discharge fluctuations and intensities. On the other hand, the mean flow velocity was investigated as a more transferable metric across rivers. Three methods were developed to compute the mean flow velocity between upstream and downstream eel detections. The first, the mean method, averaged all simulated velocities over space and time. The second, the forward method, tracked a water particle released at the time of the upstream detection until it reached the downstream station. The third, the backward method, reconstructed from the downstream to the upstream station, the velocity of a water particle arriving at the downstream station simultaneously with the eel. Correlation analyses compared mean flow velocities from each method with recorded migration speeds. The combination of the three methods into one dataset was also statistically tested using Pearson and Spearman correlations. Polynomial models were also fitted to explore relationships between silver eel migration speeds and mean flow velocities.

3. Results

3.1. River discharge

Silver eels migrated downstream during high river discharges. At both detection stations, 96.42% (n = 27) of detections occurred simultaneously with a peak in river discharge as shown in **Figure 2**. Only one silver eel (3290) was first detected away from a strong pulse. This detection occurred in summer when the river discharges were typically low. However, all final detections occurred when discharge exceeded 334 m³/s, indicating systematic migration during high flows for both positive and negative flow gradients. Fast migrations were also linked to high river discharges at first detection. When discharges exceeded 260 m³/s, eels crossed the 44.3 km of the case study under 21 hours. In contrast, 28.6% (n = 4) took 7 to 272 days when discharge was below 181 m³/s. The fastest eels (71.4%| n = 10) were detected between late November and mid-March, the season of high river discharges in the Meuse River.

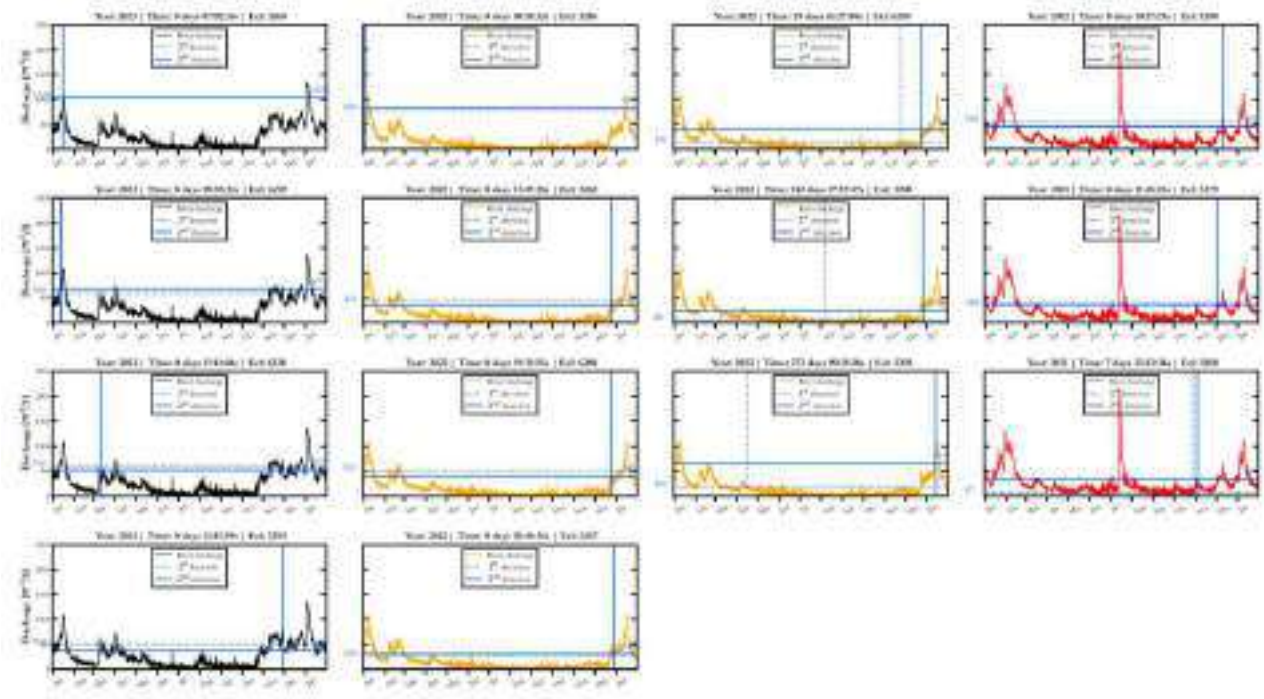

Figure 2: Concomitant plots of annual Meuse River hydrographs at the hydrometric station of Amay and corresponding individual silver eel detections at Huy (upstream) and Hermalle (downstream).

3.2. Flow velocity

The migration speeds of silver eels were strongly correlated with the mean flow velocities. All three computation methods of the mean flow velocity (mean, forward, and backward) yielded strong correlations with the migration speeds as shown in **Figure 3**. The strongest correlations were found with the mean method (Pearson $r = 0.97$| Spearman $\rho = 0.96$, $p < 0.01$) and the forward method ($r = 0.97$| $\rho = 0.95$, $p < 0.01$). The backward method suggested lower but still important correlation ($r = 0.85$| $\rho = 0.82$, $p < 0.01$). The combined dataset also confirmed the strong correlation ($r = 0.92$| $\rho = 0.91$, $p < 0.01$) as shown in **Figure 3**. Besides, the graph and the fitted model on the combined dataset suggested that above a mean flow velocity of 0.4~0.5 BL/s (0.4~0.5 m/s), all three computation methods yielded similar results, and the linear correlation was the

strongest. The graph also revealed that silver eels were generally faster than the mean flow velocity, indicating active swimming or preference for high-velocity zones in the flow. These findings support the use of flow velocity as a more robust and transferable metric in migratory studies.

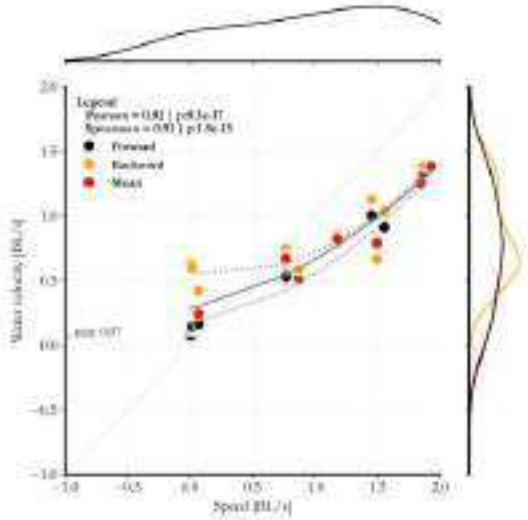

Figure 3: High correlation between silver eel migration speeds and mean flow velocities

4. Conclusions

The migrations speeds of silver eels are highly correlated with the mean flow velocities. The hydrodynamic investigation of the Meuse River has revealed strong correlations between both variables for 14 seaward migrating silver eels. Even though the causation effect was not investigated, all silver eels were potentially swimming when the mean flow velocities were above 0.4~0.5 BL/s | 0.4~0.5 m/s. Nevertheless, the study's results confirm literature observations of silver eel migration speeds during peaks in river discharge but suggest that seawards migrations are related to high flow velocities which in large anthropized rivers are only available during the rare important peaks in the river discharge. These findings pave the way for more exploration of the flow velocity in the implementation of sustainable solutions for safer, faster, and better downstream migration of silver eels in anthropized rivers.

References

Archambeau, P., Erpicum, S., Dewals, B., & Pirotton, M. (2024). *WOLF software*. https://wolf.hece.uliege.be/

Bultel, E., Lasne, E., Acou, A., Guillaudeau, J., Bertier, C., & Feunteun, E. (2014). Migration behaviour of silver eels (*Anguilla anguilla*) in a large estuary of Western Europe inferred from acoustic telemetry. *Estuarine, Coastal and Shelf Science*, *137*, 23–31. https://doi.org/10.1016/j.ecss.2013.11.023

Ciraane, U. D., Sonny, D., Lerquet, M., Archambeau, P., Dewals, B., Pirotton, M., Sacré, P., Benitez, J.-P., Ovidio, M., & Erpicum, S. (2025). Impact of anthropized river hydrodynamic conditions on the downstream migration of Atlantic salmon smolts. *Science of The Total Environment*, *982*, 179556. https://doi.org/10.1016/j.scitotenv.2025.179556

Cullen, P., & McCarthy, T. K. (2003). Hydrometric and Meteorological Factors Affecting the Seaward Migration of Silver eels (Anguilla anguilla, L.) in the Lower River Shannon. *Environmental Biology of Fishes*, *67*(4), 349–357. https://doi.org/10.1023/A:1025878830457

Deelder, C. L. (1984). *Synopsis of biological data on the eel Anguilla anguilla (Linnaeus, 1758)* (p. 73). FOOD AND AGRICULTURE ORGANIZATION OF THE UNITED NATIONS. https://www.fao.org/3/a-ap945e.pdf

Frost, W. E. (1950). The Eel Fisheries of the River Bann, Northern Ireland, and Observations on the Age of the Silver Eels. *Journal Du Conseil*, *16*(3), 358–383. https://doi.org/10.1093/icesjms/16.3.358

Lamouroux, N., Poff, N. L., & Angermeier, P. L. (2002). Intercontinental Convergence of Stream Fish Community Traits Along Geomorphic and Hydraulic Gradients. *Ecology*, *83*(7), 1792–1807. https://doi.org/10.1890/0012-9658(2002)083%255B1792:ICOSFC%255D2.0.CO;2

Life4Fish. (2023). *Life4Fish*. https://www.life4fish.be/en

Renardy, S., Takriet, A., Benitez, J.-P., Dierckx, A., Baeyens, R., Coeck, J., Pauwels, I. S., Mouton, A., Archambeau, P., Dewals, B., Pirotton, M., Erpicum, S., & Ovidio, M. (2021). Trying to choose the less bad route: Individual migratory behaviour of Atlantic salmon smolts (Salmo salar L.) approaching a bifurcation between a hydropower station and a navigation canal. *Ecological Engineering*, *169*, 106304. https://doi.org/10.1016/j.ecoleng.2021.106304

Snelder, T., Booker, D., & Lamouroux, N. (2011). A Method to Assess and Define Environmental Flow Rules for Large Jurisdictional Regions. *JAWRA Journal of the American Water Resources Association*, *47*(4), 828–840. https://doi.org/10.1111/j.1752-1688.2011.00556.x

Sonny, D. (2025). *Downstream migration success of silver eels at the basin scale in the Belgian River Meuse* (WALLONEEL). PROFISH.

SPW, S. P. de W. (2024). *L'hydrométrie en Wallonie*. L'hydrométrie en Wallonie. https://hydrometrie.wallonie.be/home.html

Teichert, N., Tétard, S., Trancart, T., Feunteun, E., Acou, A., & de Oliveira, E. (2020). Resolving the trade-off between silver eel escapement and hydropower generation with simple decision rules for turbine shutdown. *Journal of Environmental Management*, *261*, 110212. https://doi.org/10.1016/j.jenvman.2020.110212

Vøllestad, L. A., Jonsson, B., Hvidsten, N. A., Næsje, T. F., Haraldstad, Ø., & Ruud-Hansen, J. (1986). Environmental Factors Regulating the Seaward Migration of European Silver Eels (Anguilla anguilla). *Canadian Journal of Fisheries and Aquatic Sciences*, *43*(10), 1909–1916. https://doi.org/10.1139/f86-236

Book of Abstracts of the *16th International Symposium on Ecohydraulics*
Challenges and solutions in the time of global changes
August 16–20, 2026, Lausanne, Switzerland
ISSN: 2790-2420 | ISBN: 978-90-837233-9-6 | doi:[10.64697/iahr.proc.ise2026.abs]
© 2026 IAHR. CC BY-NC-ND 4.0

WIND-POWERED AERATION SYSTEM FOR EFFECTIVE CYANOBACTERIA CONTROL IN RESERVOIRS

Şebnem ELÇI[1], Oğuz HAZAR[1], İnci Tüney Kızılkaya[2]

[1] Izmir Institute of Technology, Department of Civil Engineering, Izmir, Urla, 35430, Türkiye
sebnemelci@iyte.edu.tr
oguzhazar@iyte.edu.tr
[2] Ege University, Faculty of Science, Department of Hydrobiology, Türkiye
inci.tuney@ege.edu.tr

ABSTRACT

Thermal stratification, a natural phenomenon in warmer seasons due to rising air temperatures, negatively impacts water quality by fostering excessive cyanobacterial growth. This study explores the use of a wind-powered aeration system to eliminate thermal stratification and its effects on cyanobacteria distribution under laboratory conditions. These turbines harness wind energy to draw air into the water column, avoiding the need for electrical conversion. Various geometric configurations of Savonius rotors were tested for destratification efficiency, with the 4S(45) rotor achieving a 95.6% destratification efficiency. This rotor was also used to investigate the effect of artificial destratification on cyanobacteria populations. Results show that artificial aeration and mixing relocate cyanobacteria from optimal growth areas, causing them to settle at the bottom.

Keywords: *Savonius wind turbine; thermal stratification; artificial destratification; Cyanobacteria*

1. INTRODUCTION

Thermal stratification harms water quality by preventing dissolved oxygen from rising, leading to anoxic conditions and releasing oxidized materials like ammonia, sulfur, iron, manganese, and phosphorus, which stimulate cyanobacteria growth (Elçi, 2008; Foley et al., 2012; Vural et al., 2021; Sondergaard et al., 2002). Cyanobacteria consume nutrients, reduce water transparency, inhibit plant growth, alter biodiversity, and produce toxins such as microcystin. The WHO limits these toxins in drinking water to 1 µg/L, with a fatal dose for animals at >106 cells/mL (Bullerjahn & Post, 2014; Tomitani et al., 2006; WHO, 1998).

Artificial mixing with air diffusers reduces thermal stratification and disrupts cyanobacteria buoyancy, causing them to sink due to insufficient light and nutrients (Gibbs & Howard-Williams, 2018; Patterson & Imberger, 1989; Visser et al., 2016). This increases DO concentrations and decreases levels of dissolved phosphorus, nitrogen, iron, and manganese (Ma et al., 2015). Hypolimnetic oxygenation supports habitats for cold-water fish species (Beutel & Horne, 1999). Wind-powered oxygenation systems prevent fish winterkill in lakes (Schierholz et al., 1976) and improve water quality by increasing oxygen levels and inactivating phosphorus, with efficiency linked to wind speed (Osuch & Podsiadłowski, 2012).

In this study, the destratification efficiency using air diffusers powered by wind-driven Savonius rotors and the effect of aeration on the cyanobacteria population were investigated. The air pumps are directly powered by the rotors, eliminating the need for electricity and costly infrastructure.

2. METHODS

2.1. Experimental Setup

The experimental setup (Fig. 1.) includes a Savonius-type wind turbine, fans, a water tank, air diffusers, and interconnected heating and cooling systems. The wind-powered aeration system, designed to mitigate thermal stratification, employs a multi-stage Savonius-type wind turbine that directly drives a diaphragm pump via a belt–pulley mechanism. By harnessing wind energy, the system delivers 17.6 L/h of air to a diffuser positioned

at the bottom of the tank, promoting vertical mixing within the water column. To ensure accurate sampling for cyanobacteria cell count without disturbance and precise sampling, a specialized apparatus was designed. This apparatus includes a stationary frame indicating water depth and a movable slide with an intake hose for specifying sampling depth. The slide is secured at the desired sampling point with clamps. A syringe attached to the hose gathers the sample, which is then transferred to test tubes. To avoid cross-contamination, air is introduced through a check valve, expelling the remaining water back into the tank. Details about the experimental setup can be found in (Elci et al., 2023; Hazar et al., 2024).

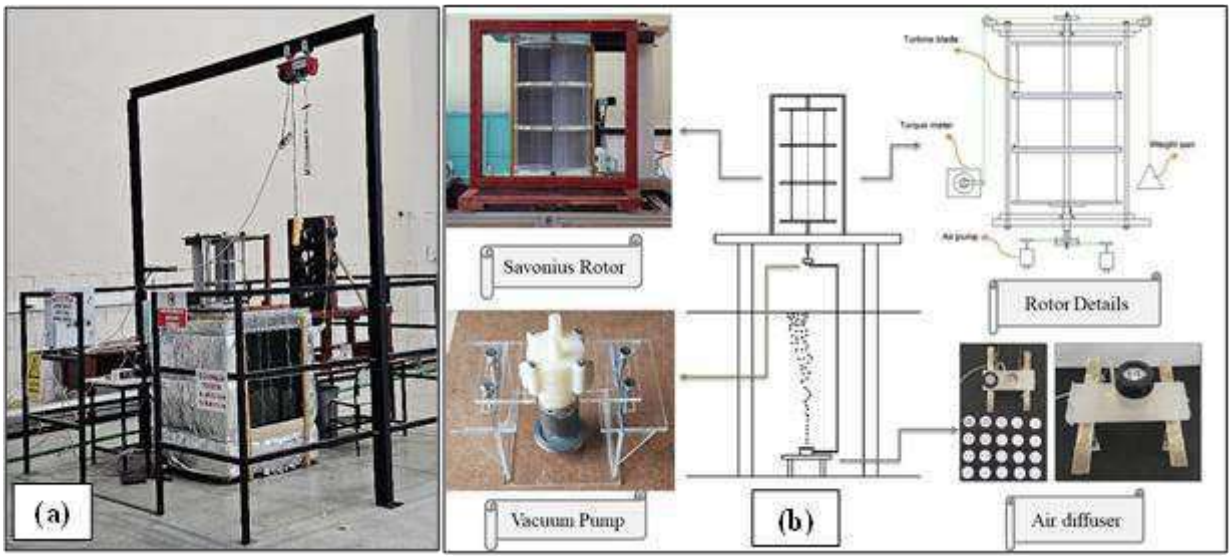

Fig. 1. (a) View of experimental setup, (b) Components of the wind power aeration system.

2.2. Methodology

Two distinct Savonius rotor classes were developed: a three-stage rotor with blades that can be aligned or set with a 60° phase shift, and a four-stage rotor with blades that can be fully aligned or separated by 90° or 45° between stages (Table 1). Thermal stratification in the water tank is created using a top heater and bottom cooling systems, as detailed in Hazar and Elçi (2024). Each rotor was tested for destratification efficiency, and the best-performing rotor was also used to investigate the aeration process's effect on the cyanobacteria population.

Table 1. Attributes of Savonius turbine

Rotor Type	Total Rotor Height (m)	Stage Height (m)	Rotor Width (m)	Aspect Ratio	Number of Stages	Blade Diameter (m)
Three-stage with 0° phase shift, 3S(0)	0.5	0.5	0.3	1.67	1	0.16
Three-stage with 60° phase shift, 3S(60)	0.5	0.17	0.3	1.67	3	0.16
Four-stage with 0° phase shift, 4S(0)	0.5	0.5	0.3	1.67	1	0.16
Four-stage with 90° phase shift, 4S(90)	0.5	0.25	0.3	1.67	2	0.16
Four-stage with 45° phase shift, 4S(45)	0.5	0.13	0.3	1.67	4	0.16

Destratification efficiency (η), as defined by Asaeda & Imberger (1993) and given in Eq. (1), was calculated to compare the efficiency of using one, two, or three diffusers.

$$\eta = \frac{\Delta PE}{\rho_{-} g Q_0 H_A \ln\left(1+\frac{H}{H_A}\right)\Delta t} \quad (1)$$

Where ρ- is the reference density, H_A is the atmospheric pressure, and Q_0 is the air flow rate at the free surface, g is the gravitational acceleration, H is the water depth, and Δt is the mixing time. To calculate ΔPE, initial potential energy is subtracted from the final mixed and homogenous water body as shown in Eq. (2).

$$\Delta PE = \int_0^h \rho_m \, g \, A(z) z dz_{-} \int_0^h \rho(z) \, g \, A(z) z dz \quad (2)$$

Where ρm is the density of the mixed water, ρ(z) is the density of water at z height, g is the gravitational acceleration, A(z) is the area of the surface of the water column at height z, and z- is the reference height.

Microcystis aeruginosa was gathered from the UTEX Algae Culture Collection for use in this study and the purchased cyanobacteria were supplied in a 3N Bold medium. The organisms were monitored, and their volumes were progressively increased with each inoculation. This process continued until the target cyanobacteria cell concentration of 1x10-6 cells/mL was reached. Before inoculating the test tank with cyanobacteria, the water sample was analyzed to ensure it was suitable for cyanobacteria survival. Upon evaluation, the water was deemed fit for the study. After adding cyanobacterial biomass to the water tank, the thermal stratification process was initiated. Once stratification was established, samples were taken from different depths and cell counts were performed using a microscope to determine cyanobacteria concentration. Following the aeration process and the elimination of thermal stratification, samples were taken from the same depths and the cyanobacteria concentration was determined again through microscopic counts.

3. RESULTS AND DISCUSSION

The highest destratification efficiency of 95.6% was achieved using a 4S(45) rotor with a single air diffuser, providing an air discharge rate of 17.6 l/hr. The same rotor was used to observe the effect of the artificial destratification on the cyanobacteria population. Aeration substantially altered both the physical structure of the water column and the vertical distribution of cyanobacteria. Under stratified conditions, the temperature profile exhibited a strong gradient, with warm surface waters (~25 °C at 90 cm) overlying cooler bottom layers (~12–13 °C at 10 cm) (Fig. 2., t=0 min). After 28 minutes of aeration, this gradient was largely eliminated, and the water column became nearly isothermal, confirming the breakdown of stratification and effective vertical mixing (Fig.2.).

Cyanobacterial cell counts reflected these physical changes. Before aeration, populations were unevenly distributed, with higher concentrations in the mid-depths (30–50 cm) and relatively lower counts at the surface (90 cm) and near the bottom (20 cm) (Fig. 3.). This pattern indicates that stratified conditions supported cyanobacterial accumulation at intermediate depths, where light and nutrient conditions were most favorable. After aeration, cell counts became more homogeneous across depths. Mid-depth abundances declined, while surface counts at 90 cm increased substantially, indicating upward redistribution of cells. Populations at 20 cm (near-bottom) and 70 cm remained relatively stable, suggesting that mixing primarily shifted biomass from mid-layers toward the surface. Overall, aeration reduced vertical heterogeneity in cyanobacterial populations by breaking down stratification and redistributing cells. By shifting biomass from mid-depth accumulations toward the surface and promoting more uniform profiles, aeration may reduce the risk of localized bloom intensification. Additionally, this redistribution increases exposure of cyanobacteria to less favorable conditions (e.g., higher turbulence and variable light availability at the surface), potentially contributing to bloom control.

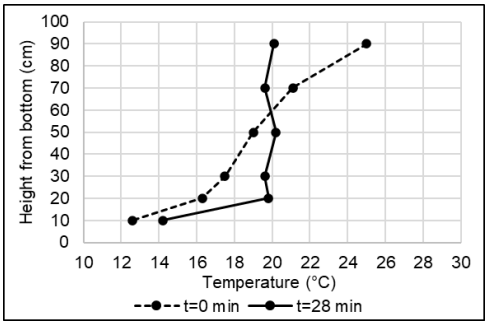

Fig. 2. Comparison of temperature variation before and after the destratification of the water column

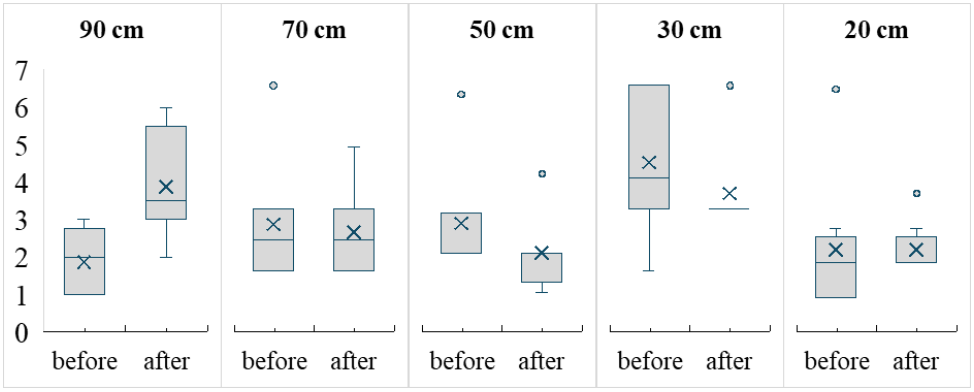

Fig. 3. Microcystis aeruginosa cellcounts along the water column before and after mixing

4. CONCLUSION

The study yielded the following conclusions:

Savonius rotors with varying physical structures were integrated with different numbers of pumps/air diffusers and tested for destratification efficiency. The results indicated that the rotor configured with four layers and a 45-degree phase shift between each layer achieved the best destratification efficiency at 95.6%.

The effect of artificial mixing through aeration on hydrodynamics and cyanobacterial biomass was investigated. The findings showed that in thermal stratification conditions, cyanobacteria concentrated in the middle layers and near the surface, where light and temperature were favorable for their growth. After aeration and artificial mixing, the population in these areas decreased, with some cyanobacteria settling to the bottom. Consequently, aeration with artificial mixing was observed to be a significant method for controlling cyanobacteria populations.

Acknowledgements

This research was supported by a grant from The Scientific and Technological Research Council of Turkey (TUBITAK) under Project No: 122M849.

References

Asaeda T, Imberger J (1993) Structure of bubble plumes in linearly stratified environments, Journal of Fluid Mechanics, 249, 35–57.

Beutel MW, Horne AJ (1999) A review of the effects of hypolimnetic oxygenation on lake and reservoir water quality, Lake and Reservoir Management, 15(4), 285–297. https://doi. org/10.1080/07438149909354124.

Bullerjahn GS, Post AF (2014) Physiology and molecular biology of aquatic cyanobacteria, Frontiers in Microbiology, 5:359. doi:10.3389/fmicb.201 4.00359

Elçi S, Hazar O, Bahadıroğlu N, Karakaya D, Bor A (2023) Destratification of thermally stratified water columns by air diffusers, Journal of Hydro-environment Research, 46, 44-59. https://doi.org/10.1016/j.jher.2022.12.001.

Elçi Ş (2008) Effects of thermal stratification and mixing on reservoir water quality, Limnology, 9, 135–142. https://doi.org/10.1007/s10201-008-0240-x.

Foley B, Jones ID, Maberly SC, Rippey B (2012) Long-term changes in oxygen depletion in a small temperate lake: Effects of climate change and eutrophication, Freshwater Biology, 57(2), 278–289. doi:10.1111/j.1365-2427.2011.02662.x

Gibbs MM, Howard-Williams C (2018) Physical processes for in-lake restoration: destratification and mixing. In: Hamilton, D., Collier, K., Quinn, J., Howard- Williams, C. (Eds.), Lake Restoration Handbook. Springer, Cham, pp. 165–205.

Hazar O, Elçi S (2024) Mitigating thermal stratification inlakes/reservoirs through wind-powered air diffusers, Water Environment Research, 96(9), e11127. https://doi.org/10.1002/wer.11127

Ma WX, Huang TL, Li X (2015) Study of the application of the water-lifting aerators to improve the water quality of a stratified, eutrophicated reservoir, Ecological Engineering, 83, 281–290. https://doi.org/10.1016/j.ecoleng.2015.06.022.

Osuch E, Podsiadłowski S (2012) Efficiency of Pulverizing Aeration on Lake Panieńskie, Limnological Review, 12(3), 139-145.

Patterson JC, Imberger J (1989) Simulation of bubble plume destratification systems in reservoirs, Aquatic Sciences, 51(1), 3–18. .

Schierholz PM, Somervell Jr WL, Babcock W, Hartel R, Timbre K (1976) Wind-powered aeration for remote locations: Final report, March 15, 1975–August 31. Web. doi:10.2172/7089104.

Sondergaard M, Wolter KD, Ripl E (2002) Chemical treatment of water and sediments with special references to lakes, In M. R. Perrow & A. J. Davy (Eds.), Handbook of Ecological Restoration. Cambridge University Press, 184-205.

Tomitani A, Knoll AH, Cavanaugh CM, Ohno T (2006) The evolutionary diversification of cyanobacteria: molecular phylogenetic and paleontological perspectives, Proceedings of the National Academy of Sciences, 103, 5442–5447. doi: 10.1073/pnas.0600999103

Visser PM, Ibelings BW, Bormans M, Huisman J (2016) Artificial mixing to control cyanobacterial blooms: a review, Aquatic Ecology, 50, 423–441. .

Vural AB, Elçi Ş, Ökten HE (2021) An experimental study on release mechanism of iron and manganese from sediments to the water column in reservoirs, Environmental Research and Technology, 4(3), 190-198. https://doi.org/10.35208/ert.833975

WHO, 1998. Cyanobacterial toxins: Microcystin-LR in Drinking Water. In Guidelines for drinking-water quality, 2nd edition Addendum to Vol. 2. Health criteria and other supporting information. Geneva, Switzerland.
Earth System Sciences, 19, 4041-4053 (in the case of a journal article)

Book of Abstracts of the *16th International Symposium on Ecohydraulics*
Challenges and solutions in the time of global changes
August 16–20, 2026, Lausanne, Switzerland
ISSN: 2790-2420 | ISBN: 978-90-837233-9-6 | doi:[10.64697/iahr.proc.ise2026.abs]
© 2026 IAHR. CC BY-NC-ND 4.0

A WOOD-SHAPED SENSOR FOR LARGE WOOD MOTION DETECTION

Jiangtao YANG, Frank SEIDEL, Mário J. FRANCA

Institute for Water and Environment, Karlsruhe Institute of Technology, Karlsruhe, Germany
Email : jiangtao.yang@kit.edu

ABSTRACT

When transported in rivers, large wood elements interact among themselves and with flow, sediments, riverbed and riverbanks, leading to its physical debarking. This debarking process in rivers is mainly dominated by the motion and impact of the large wood, but the relationship between these is still unclear. Here, we introduce an Inertial Measurement Unit (IMU) based motion sensor, enclosed in a 3D wood-shaped casing, to monitor the motion and impact of large wood during fluvial transport. The motion sensor enables us to monitor accelerations and motion direction through a gyroscope, along three axes in a Cartesian Coordinate system. The 3D printed casing is made with controlled geometry, inertia and density to represent the motion of large wood during fluvial transport. Two tests, including a pendulum test, and a rotation test, were conducted to investigate the accuracy the accelerometer and gyroscope signals. Results show that the sensor can well capture the accelerometer and gyroscope in the pendulum and rotation tests. Additionally, preliminary results of the sensor when transported in a flume flow will be presented. Future work will focus on monitoring complex motion in flume and field experiments, interpreting wood movement using IMU signals, and ultimately linking motion characteristics to physical debarking processes during fluvial transport.

Keywords: Large wood; Wood motion; Wood degradation; Wood-shaped sensor; Wood budget.

1. Introduction

Large wood, that is, wood elements with size > 1 m in length and 0.1 m in diameter, is of great significance in river dynamics, local environment and fluvial ecosystems (Keller and Swanson, 1979; Naiman et al., 2002). After being introduced into rivers by avalanches, bank retreatment, flooding events, wildfire, etc, large wood interacts with river flow, sediments, river channel, and also the other wood logs during the fluvial transport, leading to its physical degradation (Piégay et al., 2005; Wohl, 2011; Merten et al., 2013). This physical degradation, characterized by physical processes such as abrasion, breakage and weathering, can be divided into the following two procedures: the debarking process and the debranching process. The debarking of large wood primarily occurs through abrasion and collision during transport, leading to the detachment of bark from large trunks and fragmented branches (Yang et al., 2025). In contrast, debranching results from the rotation of large woods and collisions with the riverbed, with the extent of this process closely tied to the wood's structural properties that can be characterized by the complexity of the branch such as Horton-Strahler branch order (Hortobágyi et al., 2024). These two processes not only contribute to the mass loss of the large wood itself, further changing its motion and accumulation characteristics; but also influence the local habitat by providing nutrients to fishes and micro-organisms, and the stability of wood-related structures in rivers (Gurnell et al., 2002; Ruiz-Villanueva et al., 2016; Wohl, 2019). However, the physical degradation and its influence to the environment and ecology of local river system are seldom considered in previous research.

Our previous research investigated the wood debarking process based on a series of laboratory experiments. Results showed that the debarking process of large wood during fluvial transport can be divided into the following two processes: wood expansion and wood abrasion. Moreover, three debarking patterns, including expansion dominated, expansion-abrasion and abrasion dominated patterns, are identified under varying motion from floating dominated regime to rolling-sliding-floating regime and to rolling-sliding regime (Yang et al., 2025, under review). These three debarking patterns correspond to the three motion regimes of large wood during fluvial transport, namely the congested, un/semi-congested and hyper-congested regimes (Ruiz-

Villanueva et al., 2019). To better understand the three debarking patterns, it is therefore of great significance to analyze the motion and impact of large wood during fluvial transport, to establish the relationship between wood debarking and wood motion.

Current methods for large wood detection can be summarized into the following three categories: the tagging methods, the video-based monitoring and machine learning techniques, and the Inertial Measurement Unit (IMU) based techniques (MacVicar et al., 2009; Spreitzer et al., 2019; Aarnink et al., 2025). The tagging method uses tags such as Radio-Frequency Identification (RFID) that are attached on the objects, and radio waves are used to automatically identify and track objects. The video-based monitoring and machine learning techniques, in the other way, requires identification of the objects for tracking analysis. These two methods have been applied in field monitoring of large wood during fluvial transport, however, they failed to capture the detailed motion behavior, in particular, the rotation of large wood during fluvial transport. The IMU based motion senor, which tracks the objects by recording the accelerometer and gyroscope along three axes, has been successfully applied to monitor the motion and impact of large wood during fluvial transport in both laboratory and field scales. However, how to interpret the IMU signals to explain the motion is still unclear. Additionally, this is the first attempt to explain the debarking phenomenon using the motion characteristics captured by the IMU based motion sensor combined with laboratory degradation experiments using a rotating apparatus.

A wood-shaped sensor based on the IMU-based motion sensor and the 3D printing technology was designed to monitor the motion and impact of large wood during fluvial transport. We aim to solve the following two questions: (1) how to understand the motion of large wood using the accelerometer and gyroscope signals from the wood-shaped motion sensor? And (2) is it possible to explain the debarking phenomenon of large wood during fluvial transport by its motion characteristics? To solve these questions, a series of preliminary tests including a pendulum test and a rotation test were conducted to test the accuracy of the sensor. Flume and field experiments will be carried out to analyze the motion and impact of large wood, further contributing to the interpretation of wood debarking using the motion characteristics during fluvial transport.

2. Wood-shaped motion sensor

Figure 1 shows the printed wood-shaped sensor. A 3D printer (Formlabs Form 4) was used to print the wood-shaped surface. Printing material with relatively high strength (Tough 2000 Resin) was used, to avoid wear and change in shape during monitoring the motion of wood in rivers. The printed wood-shaped sensor is hollow inside (Figure 1e), with a height of 0.18 m, a diameter of 0.12 m and a density of 0.58 g/m^3. The density of the wood-shaped sensor is set to be similar to that of dry wood samples from river environment, so as to ensure that the senor can well represent large wood in rivers. a IMU sensor (MetaMotion S), which is able to monitor the accelerometer and gyroscope in all three dimensions (nine degree of freedom), was put in a water proof box and then was installed in the center of the wood-shaped sensor. Details of the sensor's parameter are listed in Table 1.

Table 1. Details of the wood-shaped sensor

Parameter			Specification
Height			0.18 m
Diameter			0.12 m
Density			0.58 g/m^3
Printing material	Type		Tough 2000 Resin
	Tensile strength		40.4 MPa
	Tensile modulus		1800 MPa
	Hardness		76 D
	Density		1.09 g/cc
IMU sensor	Type		Metamotion S
	Accelerometer	Range	± 16 g
		Resolution	16 bit
		Sample rate	0.001 Hz – 800 Hz
	Gyroscope	Range	± 2000°/s
		Resolution	16 bit
		Sample rate	0.001 Hz – 800 Hz
	Magnetometer	Range	±1300μT (x,y-axis), ±2500μT (z-axis)
		Resolution	0.3μT
		Sample rate	0.001 Hz – 25 Hz



Fig. 1. The wood debarking experiment and wood-shaped motion sensor: (a) the wood debarking experiment; (b) wood sample before the debarking; (c) wood sample after the debarking; (d) the printed sensor with same size of the wood sample in the debarking experiment; (e) the sensor box; (f) the lower part and the upper part of the wood-shaped sensor and (f) the internal structure and axes of the sensor.

3. Tests and results

Two preliminary tests were conducted to investigate the performance of the wood-shaped sensor, including a pendulum test for analyzing the accuracy of the accelerometer, a rotation test for investigating the accuracy of gyroscope.



Fig. 2. Preliminary tests: (a) the pendulum test; (b) the rotation test.

In the pendulum test, the sensor was put inside a cubic printed box and was suspended using a 50 cm steel wire. A board marked with angles from 0° to 45° relative to the *Z*-axis was placed behind the setup to visually track the sensor's position during the experiment (Figure 2a). At the start of the test, the sensor was pulled to an angle of 45° from the Z-axis and then released to oscillate freely. Throughout the entire motion, the acceleration in all three directions was recorded (Figure 3). Because the sensor was not perfectly aligned perpendicular to the Z-axis, the measured accelerations along the three axes exhibited a cyclic increase and decrease. As the oscillation gradually damped, the peak acceleration values also diminished until, at the end of the experiment, the accelerations along each axis equaled the corresponding gravitational components in their respective directions. Moreover, the accelerations from both theory and the sensor at angles of 5° - 35°, with an interval of 5°, were calculated and compared. The monitored accelerations are in good agreement with those from calculation, as shown in Table 2.

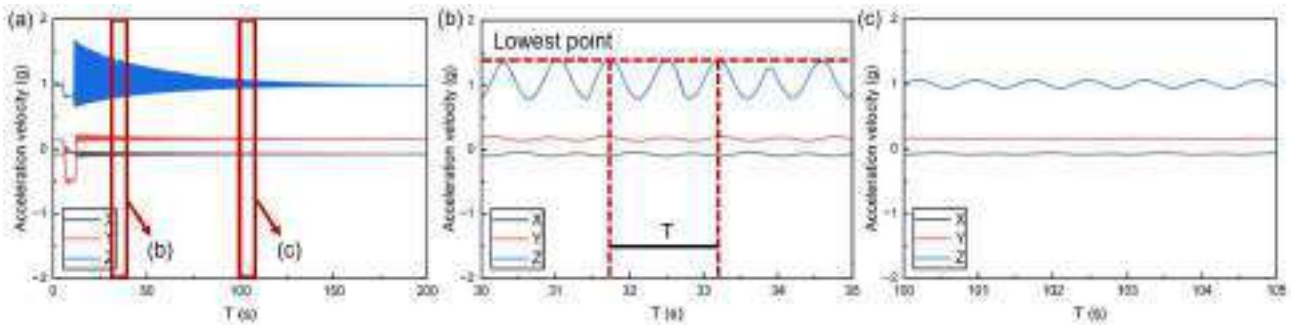

Fig. 3. Pendulum test: (a) Variation of acceleration velocity in X, Y and Z directions during the whole experiment; (b) t = 30 – 35 s (c) t = 100 – 105 s.

Table 2. The accuracy of the IMU sensor regarding accelerometer and gyroscope signals

Test	Result							
Pendulum test	Angle (°)	5	10	15	20	25	30	35
	Measured (g)	0.999	1.019	1.056	1.107	1.170	1.294	1.375
	Calculated (g)	1.008	1.030	1.068	1.121	1.187	1.268	1.362
	Error (%)	0.89	1.07	1.12	1.25	1.43	2.05	0.95
Rotation test (*X*-axis)	Measured (rad/min)	92.52	118.27	143.89	177.80	203.47	237.40	117.72
	Setting (rad/min)	92	118	144	178	203	237	118
	Error (%)	0.57	0.23	0.08	0.11	0.23	0.17	0.24

For the rotation test, a rotation machine, in which the rotational speed can be directly set and read, was used (Figure 2b). After fixing the sensor on the machine, the rotational speed of the machine was set to gradually increase and then decrease with a series of constant intervals. The sensor was then used to record the rotational speed from different dimensions during the whole experiments. The recorded rotational speed of each constant interval from the sensor was then compared with that obtained from the machine (Figure 4 and Table 2). Results show that the sensor can well capture the characteristics of rotation motion, further contributing to the detection of motion and impact of large wood during fluvial transport.

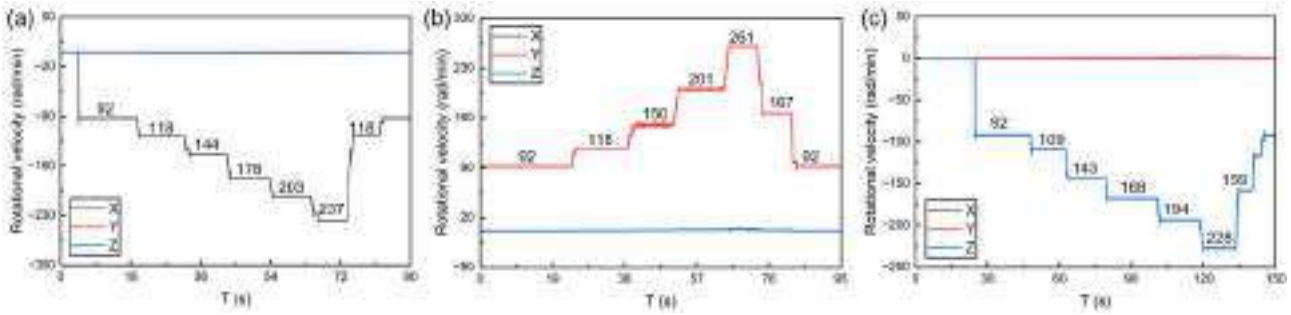

Fig. 4. Rotation tests along three dimensions: (a) X as rotational axis; (b) Y as rotational axis and (c) Z as rotational axis.

4. Conclusions and perspectives

In this extended abstract, we introduce a wood-shaped sensor to monitor the motion and impact of large wood during fluvial transport. An IMU based motion sensor was used to monitor both the accelerometer and gyroscope along three dimensions, while 3D printing was used to generate a wood-shaped surface, to characterize the motion and impact of large wood during fluvial transport. Preliminary tests including a pendulum test and a rotation test were then used to analyse the accuracy of the sensor. Results from these two tests show that the sensor can well capture the acceleration and rotation during the experiment. However, further experiments including flume and field experiments need to be done to test the sensor, so as to apply the sensor in monitoring the motion and impact of large wood during fluvial transport. Additionally, how to interpret the complex motion behaviour of large wood during fluvial transport and how to link the motion to large wood debarking during fluvial transport needs to be investigated.

References

Aarnink, J., Fornari, A., Rouge, F., Ceriotti, G., & Ruiz-Villanueva, V. (2025). Tracking floating wood during a flood: New insights from drone surveys and machine learning. Journal of Geophysical Research: Earth Surface, 130(11), e2024JF008193.

Keller, E. A., & Swanson, F. J. (1979). Effects of large organic material on channel form and fluvial processes. Earth Surface Processes, 4 (4), 361–380.

Gurnell, A. M., Piégay, H., Swanson, F. J., & Gregory, S. V. (2002). Large wood and fluvial processes. Freshwater biology, 47(4), 601-619.

Hortobágyi, B., Milan, D., Bourgeau, F., & Piégay, H. (2024). How quickly does wood fragment in rivers? Methodological challenges, preliminary findings, and perspectives. Earth Surface Processes and Landforms, 49(10), 3073-3092.

MacVicar, B. J., Piégay, H., Henderson, A., Comiti, F., Oberlin, C., & Pecorari, E. (2009). Quantifying the temporal dynamics of wood in large rivers: field trials of wood surveying, dating, tracking, and monitoring techniques. Earth Surface Processes and Landforms, 34(15), 2031-2046.

Merten, E. C., Vaz, P. G., Decker-Fritz, J. A., Finlay, J. C., & Stefan, H. G. (2013). Relative importance of breakage and decay as processes depleting large wood from streams. Geomorphology, 190, 40-47.

Naiman, R. J., Balian, E. V., Bartz, K. K., Bilby, R. E., & Latterell, J. J. (2002). Dead wood dynamics in stream ecosystems. In Proceedings of the symposium on the ecology and management of dead wood in western forests (pp. 23-48). US Department of Agriculture, Forest Service, Pacific Southwest Research Station.

Piégay, H., Gregory, K. J., Bondarev, V., Chin, A., Dahlstrom, N., Elosegi, A., ... & Zawiejska, J. (2005). Public perception as a barrier to introducing wood in rivers for restoration purposes. Environmental Management, 36(5), 665-674.

Ruiz-Villanueva, V., Piégay, H., Gurnell, A. M., Marston, R. A., & Stoffel, M. (2016). Recent advances quantifying the large wood dynamics in river basins: New methods and remaining challenges. Reviews of Geophysics, 54(3), 611-652.

Ruiz-Villanueva, V., Mazzorana, B., Bladé, E., Bürkli, L., Iribarren-Anacona, P., Mao, L., ... & Wohl, E. (2019). Characterization of wood-laden flows in rivers. Earth Surface Processes and Landforms, 44(9), 1694-1709.

Spreitzer, G., Gibson, J., Tang, M., Tunnicliffe, J., & Friedrich, H. (2019). SmartWood: Laboratory experiments for assessing the effectiveness of smart sensors for monitoring large wood movement behaviour. Catena, 182, 104145.

Wohl, E. (2011). Threshold-induced complex behavior of wood in mountain streams. Geology, 39(6), 587-590.

Wohl, E., Kramer, N., Ruiz-Villanueva, V., Scott, D. N., Comiti, F., Gurnell, A. M., ... & Fausch, K. D. (2019). The natural wood regime in rivers. BioScience, 69(4), 259-273.

Yang, J., Seidel, F., and Franca, M. J.: Experimental insights into the abrasion of large wood in rivers, EGU General Assembly 2025, Vienna, Austria, 27 Apr–2 May 2025, EGU25-6721.

Book of Abstracts of the *16th International Symposium on Ecohydraulics*
Challenges and solutions in the time of global changes
August 16–20, 2026, Lausanne, Switzerland
ISSN: 2790-2420 | ISBN: 978-90-837233-9-6 | doi:[10.64697/iahr.proc.ise2026.abs]
© 2026 IAHR. CC BY-NC-ND 4.0

THE EFFECT OF DIFFERENT FLOW PULSE ON THE BIOMASS PERIPHYTON IN AN EXPERIMENT FLUME

Longfei SUN[1,2], Leixiang WU[1,2], Wei HUANG[1,*]

[1] State Key Laboratory of Water Cycle and Water Security, China Institute of Water Resources and Hydropower Research, Beijing 100038, China

[2] Department of Water Ecology and Environment, China Institute of Water Resources and Hydropower Research, Beijing 100038, China
email: huangwei@iwhr.com

ABSTRACT

This study investigates the response relationships of periphyton to hydrological disturbances under environmental baseflow and multiple pulse conditions, analyzing the correlation between periphyton and multiple pulses. Pulses of 15-minute duration at a flow velocity of 1.00 m/s were applied, observing the scour characteristics and recovery processes of pre-cultured periphyton communities subjected to 1-4 pulse treatments. The results show significant differences in the resistance of different periphyton taxa to hydrodynamic flushing. Furthermore, under the flow velocity of 1.00 m/s, 80% of the biomass was effectively reduced within 15 minutes, inhibiting algal proliferation. Multiple pulse disturbances continuously reduced biomass, increased the diversity of primary producers, changed the growth pattern of attached organisms, playing a key role in regulating periphyton and contributing to the stability of river ecosystems.

Keywords: Periphyton; Pulse disturbance; Hydraulic shear; Biomass scour; Community recovery

1. Introduction

In rivers regulated by human activities, natural hydrological regimes, particularly flood pulses, are often attenuated, leading to reduced flow velocities and hydrological homogenization in downstream reaches. Under such altered hydrodynamic conditions and with sufficient nutrients, abnormal proliferation of periphyton readily occurs, triggering a series of aquatic ecological and environmental problems. Traditional chemical and physical algae control methods suffer from drawbacks such as high cost and significant side effects. Utilizing restorative hydrological processes for ecological regulation is considered a more sustainable management approach.

Eco-hydraulics, serving as a bridge between hydrodynamics and ecology, focuses on understanding how hydrodynamic conditions influence the life cycle, behavior, distribution, and community structure of aquatic organisms. By precisely controlling pulse frequency, this study systematically analyzes the regulatory pathways of hydrodynamic disturbance regimes on the structure and functional succession of periphyton communities, providing a theoretical basis for ecological operation.

2. Materials and Methods

2.1. Experimental System and Hydrodynamic Control

The experiment was conducted in a specially designed flume system (length 4.0 m, width 0.3 m, depth 0.5 m). The flume bottom was paved with standard marble tiles (7.0 cm × 9.0 cm) serving as homogeneous substrates for periphyton colonization. A variable frequency drive controlled the rotational speed of a centrifugal pump, combined with a precision regulating valve, to generate a stable and uniform turbulent flow field in the experimental section. Prior to the experiment, a portable Doppler velocimeter (LS300-a) was used to perform multi-point calibration of the flow velocity across the flume cross-section, ensuring that the near-bed velocity at the substrate surface remained stable at the target value of 1.00 m/s (±0.02 m/s) during pulse phases. This velocity was selected based on preliminary experiments, aiming to generate a hydraulic shear stress sufficient to effectively scour most of the periphyton biofilm without eroding the substrate itself.

2.2. Periphyton Community Pre-cultivation and Pulse Experiment Design

Clean marble substrates were placed in a natural river for a four-week pre-cultivation period to allow the formation of mature, stable, and high-biomass periphyton communities on their surfaces, simulating scenarios of excessive algal growth under natural conditions.

A single-factor (pulse frequency) completely randomized design was employed. The cultivated substrates were randomly divided into four groups (1, 2, 3, 4), with three replicates per group. The pre-cultivated mature periphyton communities were randomly assigned to four treatments: Group #1 received 4 consecutive pulses (one per week), Group #2 received 3 pulses, Group #3 received 2 pulses, and Group #4 received only 1 pulse. Each pulse lasted 15 minutes, simulating short-term flood release events. After the pulses, all substrates were transferred back to cultivation flumes with a base flow velocity (0.1 m/s) for a 6-7 day recovery period to observe community dynamics and succession processes. Figure 1 illustrates the experimental setup.



Figure 1 Multiple pulse experimental device flushing inclined plate

3. Results and Analysis

3.1. Efficiency and Cumulative Effects of Hydrodynamic Scour

A single pulse event demonstrated the powerful role of hydraulic shear stress in the instantaneous removal of biomass. The average instantaneous scour rate of the first pulse was as high as (80.26 ± 6.41)%, proving that the hydrodynamic force generated at 1.00 m/s was sufficient to overcome the attachment strength of most algal individuals, causing them to detach from the substrate.

However, the core finding of eco-hydraulics lies in revealing the cumulative effect of pulse frequency. As the number of pulses increased, biomass was continuously and significantly suppressed (ANOVA, $p < 0.01$). As shown in Figure 1, the final biomass of Substrate 1 (experiencing four pulses) was suppressed to 1.7% of the initial value, a level significantly lower than that of Substrate 4 experiencing only a single pulse ($p < 0.001$). This indicates that although the scour rate of a single pulse is high, maintaining a long-term low biomass state relies on multiple, intermittent hydrodynamic disturbances.

3.2. Shift in Patterns of Community Recovery Dynamics

The most critical eco-hydraulic finding of the experiment is the fundamental impact of pulse frequency on community recovery patterns.

After a single pulse (Group #4), the community exhibited strong resilience, with biomass rebounding rapidly within one week, and the recovery curve fitting an exponential growth model. This suggests that after a single disturbance, the system quickly returns to its pre-disturbance ecological state, driven by the remaining "propagule bank" and favorable living conditions. In contrast, multiple pulses (Groups #1, #2) fundamentally altered the recovery trajectory. Biomass growth shifted to a slow linear pattern ($y = a + kt$). This transition from exponential to linear growth is a strong ecological signal, indicating that multiple hydrodynamic disturbances have profoundly changed the internal feedback mechanisms of the system, possibly due to the repeated removal of highly competitive, fast-growing species, or a functional restructuring of the community.

4. Discussion

The experiment confirmed that at a flow velocity of 1.00 m/s, a single 15-minute pulse can instantaneously remove approximately 80% of periphyton biomass, while four consecutive pulses can sustained low-level stability of biomass (reduced to 1.7%). The study revealed that multiple hydrological pulses, through the

coupled mechanism of "physical scour" and "ecological selection," alter the recovery dynamics of periphyton communities, achieving a transition from physical removal to ecological regulation.And the research results provide a solid eco-hydraulic theoretical foundation and specific parameter references for implementing "pulse-style" ecological flow management through hydraulic engineering operations.

Boundary layer theory analysis indicates that the shear stress ($\tau \approx 2.4$ Pa) generated by the 1.00 m/s flow velocity exceeds the critical detachment threshold for most diatoms. A combined management mode of "baseflow - pulse sequence" is recommended for ecological operation. By optimizing pulse frequency ($\geqslant 3$ times/month) rather than simply increasing flow velocity, ecologically oriented control of periphyton communities can be achieved. This regulation strategy provides a new perspective for river ecological restoration.

Acknowledgements

This work was supported by the National Natural Science Foundation of China [grant number U2443218] and the IWHR Research & Development Support Program [grant number WE0145B052021]..

References

Growns I, Growns J E. Ecological effects of flow regulation on macroinvertebrate and periphytic diatom assemblages in the Hawkesbury–Nepean River, Australia [J]. Regulated Rivers-research & Management, 2001, 17: 275-93.
Collier K J. Effects of flow regulation and sediment flushing on instream habitat and benthic invertebrates in a New Zealand river influenced by a volcanic eruption [J]. River Research and Applications, 2002, 18(3).
Lessard J, Hicks D M, Snelder T H, et al. Dam Design can Impede Adaptive Management of Environmental Flows: A Case Study from the Opuha Dam, New Zealand [J]. ENVIRONMENTAL MANAGEMENT, 2013, 51(2): 459-73.
Horner R R, Welch E B, Seeley M R, et al. Responses of periphyton to changes in current velocity, suspended sediment and phosphorus concentration [J]. Freshwater Biology, 1990, 24(2).
King S A. Hydrodynamic control of filamentous macroalgae in a sub-tropical spring-fed river in Florida, USA [J]. Hydrobiologia, 2014, 734(1).
Clausen B, Biggs B. Relationships between benthic biota and hydrological indices in New Zealand streams [J]. Freshwater Biolo gy, 1997, 38(2).
Fovet O, Belaud G, Litrico X, et al. A Model for Fixed Algae Management in Open Channels Using Flushing Flows [J]. River Research and Applications, 2012, 28(7): 960-72.
Davie A W, Mitrovic S M. Benthic algal biomass and assemblage changes following environmental flow releases and unregulated tributary flows downstream of a major storage [J]. Marine and Freshwater Research, 2014, 65: 1059-71.
Hart D, Biggs B, Nikora V, et al. Flow effects on periphyton patches and their ecological consequences in a New Zealand river [J]. Freshwater Biology, 2013, 58: 1588.
Bunn S E, Arthington A H. Basic Principles and Ecological Consequences of Altered Flow Regimes for Aquatic Biodiversity [J]. Environmental Management, 2002, 30(4): 492-507.

Book of Abstracts of the *16th International Symposium on Ecohydraulics*
Challenges and solutions in the time of global changes
August 16–20, 2026, Lausanne, Switzerland
ISSN: 2790-2420 | ISBN: 978-90-837233-9-6 | doi:[10.64697/iahr.proc.ise2026.abs]
© 2026 IAHR. CC BY-NC-ND 4.0

HYDRODYNAMIC CUES AND MOVEMENT BEHAVIOUR OF SEA LAMPREY: INSIGHTS FOR CONTROL AND CONSERVATION

Daniel P. Zielinski[1]

[1] Great Lakes Fishery Commission, USA
email: dzielinski@glfc.org

ABSTRACT

Water flow is a dominant environmental feature that provides critical sensory cues for fish, influencing both decision-making and swimming performance. Sea lamprey (*Petromyzon marinus*), a species of conservation concern in its native region and a target for invasive species control in the Laurentian Great Lakes, exhibit movement behaviours mediated by hydrodynamic signals such as flow direction, velocity magnitude, turbulence, and recent experience. Recent studies using acoustic telemetry and computational fluid dynamics reveal sea lamprey respond to multiple hydraulic cues, with behaviours shaped by context-specific factors like energy conservation and predator avoidance. Understanding these responses offers valuable insights for improving invasive species control strategies and informing conservation efforts.

Keywords: Sea lamprey; migration; hydrodynamics, turbulence; invasive species management

1. Introduction

Water flow (i.e., hydrodynamics) is a predominant feature in the aquatic environment that provides sensory input, in the form of flow direction, magnitude, and rate of change (e.g., velocity gradients, water acceleration) used by fish to inform decision making. At sufficient intensities, flows can also directly influence fish swimming performance and movements. Bulk flow direction provides cues on flow direction while flow perturbations (i.e., turbulence) can be indicative of fine details of the space surrounding fish including conspecifics, select habitat types, or potential dangers. The spatial and temporal scale of turbulence can also have varying effects on fish swimming performance, potentially influencing energy expenditure or destabilizing movements. Fish possess a mechanosensory lateral line and inner ear to detect whole body accelerations and local flow conditions at the body surface. Manipulation of water flow has been widely used to alter fish movement at instream barriers (e.g., dams and hydropower stations) by directing fish towards fishways or other low-mortality passage routes (Romine et al. 2016). Both field and laboratory studies of the effect of water flow on fish behavior have yielded key insights into habitat preferences (Lacey and Millar 2004; Olden et al. 2014) and descriptions of swimming kinematics (Chagnaud et al. 2008; Liao et al. 2003). Therefore, flow remains one of the most effective and promising avenues for manipulating the movement and distribution of fishes.

Sea lamprey, Petromyzon marinus, are a unique model species to study hydrodynamic mediated movement due to several key factors: (1) they have a primitive biology; (2) they are of conservation concern in their native range in the Atlantic Ocean; and (3) they are highly invasive in the Laurentian Great Lakes, and target of a multi-million-dollar invasive species control program (Seifkes , 2017). While sea lamprey lack canal neuromasts (e.g., associated with detection of velocity gradients), they do possess superficial neuromasts which are associated with detecting prevailing (i.e., bulk) velocities. Ayali et al. (2009) posited that interaction between movement and superficial neuromasts has an important role in regulating swimming and responses to turbulence. Greater understanding of the behaviors that influence sea lamprey movements during upstream migration could yield management solutions. Here, new insights into the response of sea lamprey to hydraulics cues – sourced from research conducted in support of control efforts in the Laurentian Great Lakes – is systematically reviewed. Lessons learned from this research have potential to benefit both future control and conservation efforts.

2. Flow-driven behavior and rheotaxis

Kerr et al. (2025) analyzed movement for acoustically tagged sea lamprey through a large open-river setting with fine scale hydraulics simulated using a computational fluid dynamics model to test if sea lamprey respond hydrodynamic features similarly to other migratory fish species. The study found sea lamprey movements were influenced by multiple hydraulic cues, including flow direction, (i.e., rheotaxis), velocity magnitude, turbulence, and prior experiences. The models that incorporated all these behaviors vastly outperformed simpler models that only assumed fish responses to bulk flow direction. These findings suggest that sea lamprey rely on more nuanced information from flow fields; however, aspects of the response (i.e., turbulence metrics) were not clear. Models including turbulent kinetic energy (i.e., magnitude of velocity fluctuations) or spatial velocity gradient (i.e., precursor to turbulence) performed similarly, confounding which feature sea lamprey are responding to. This complexity underscores the importance of further research into fish responses to turbulence.

Overall, the set of responses to hydrodynamic features for sea lamprey was very similar to observations for other migratory fish species (Zielinski et al., 2024), many of which possess both superficial and canal neuromasts. While metrics such as flow magnitude, direction, and turbulence are common in fish movement models, the integration of prior experience remains relatively rare despite its potential to improve predictive accuracy. As observed in Kerr et al. (2025), turbulence metrics are particularly challenging to interpret, as their influence may depend more on measurement limitations than on true sensory stimuli. Moreover, contextual preferences complicate modeling efforts: turbulence levels that appear benign in calm flows may elicit entirely different responses in chaotic environments, and species-specific differences further limit the applicability of universal thresholds.

3. Thalweg tracking and energy efficiency

Griffen et al. (2005) found acoustically tracked sea lamprey often tracked the thalweg—the deepest part of the channel—during upstream migration in a smaller river compared to the study site of Kerr et el., (2025). This behavior is hypothesized to be mediated by flow field characteristics and hydrostatic pressure. While following the thalweg typically results in less direct and potentially longer migration paths, it offers a significant energetic advantage because streamwise velocities are generally lower in these regions, reducing swimming effort. Tracking the thalweg may also be a result of predator avoidance. Combined with Kerr et al., (2025), these studies highlight differing migration behaviors that are context specific (i.e., energy conservation and predator avoidance in shallow river with defined thalweg versus movement paths integrating multiple hydraulic factors in a deeper, open-river setting).

4. Hydraulic influence on barrier passage

Hydraulic conditions also play a critical role in determining whether sea lamprey can successfully pass migration barriers. In the Laurentian Great Lakes, sea lamprey control barriers are designed to maintain a a 45-cm vertical differential between the barrier crest and tailwater elevation and feature an 18-cm overhanging lip (Zielinski et al., 2019). Using scaled physical modeling, Reynolds et al. (2025) found sea lamprey passage success and failure at inundated barriers (i.e., no longer maintaining the 45-cm differential) was correlated with time- and horizontally averaged streamwise velocity, energy dissipation rate, and vertical eddy length scale. For example, barriers with tailwater regions exhibiting rotational flow regimes—such as horizontal rollers associated with plunging flows—were linked to higher passage rates compared to barriers dominated by streaming flows.

5. Turbulence as an attractant or deterrent

Finally, Zielinski et al. (2020) observed sea lamprey attraction to a turbulence plume in a small, shallow river. The turbulence plume was generated using an underwater venturi-style pump (Flow Velocity Enhancement System, Whooshh Innovations Inc, Seattle, WA, USA). Using ADCP measurements and computational fluid dynamics modelling, the plume was characterized by an increase in turbulent kinetic energy and turbulence intensity, with negligible change in time-averaged streamwise velocity. Sea lamprey were observed, using lighted tags, to shift their lateral position in the river closer to the turbulence plume compared to baseline conditions. In contrast, Lewandowski et al. (2021) found upstream passage probability of sea lamprey decreased far more rapidly than a co-occurring native fish, *Catotomus commersonii,* as turbulence increased in a modified fishway. These studies highlight turbulence as an important environmental context within flowing water, but the response to variable intensities of turbulence is not expected to be universal. Beyond

certain thresholds, turbulence may impair swimming stability and increase energy expenditure, transforming an initially favorable cue into a detrimental condition.

6. Conclusion

Overall, these recent studies highlight that sea lamprey rely on an integrated suite of hydraulic cues including velocity vectors (i.e., magnitude, direction), turbulence, and prior experience to guide movement decisions. While the suite of hydraulic cues is similar to other fish, sea lamprey responses to each specific cue is clearly species and context specific. In smaller rivers with clear thalweg structure, sea lamprey appear to optimize energy expenditure and minimize predation risk by following deeper, lower-velocity paths. In larger, more complex systems, movement patterns are shaped by overlapping stimuli where turbulence, velocity magnitude and direction, and past exposure interact to determine route selection. These differences suggest sea lamprey migratory behaviors weigh the energetic and ecological tradeoffs embedded in the hydrodynamic environment. Notably, their remains some uncertainty about the exact nature of response to specific turbulence cues, and as such is, it is still an area of active research. The primitive nature of the sea lamprey mechanosensory lateral line also suggests that these responses may be conserved or at least incorporated into the responses of fishes with move evolved lateral line systems (i.e., those that possess canal neuromasts).

Sea lamprey interactions with barriers and consistent turbulence cues demonstrate that hydraulic features, naturally occurring or engineered, can strongly influence passage success, attraction, or avoidance. These insights have implications for both sea lamprey control and conservation efforts. For control programs in the Laurentian Great Lakes, enhancing barrier effectiveness may require modifications that promote streaming flow conditions and increased overall turbulence levels when barriers become inundated. Engineered turbulence plumes could also serve to guide sea lamprey toward traps or non-passable structures. Conversely, conservation efforts may benefit from using these same principles to facilitate movement. Barriers or fishways that promote rotational flow regimes with generally low overall turbulence may help reduce sea lamprey blockage.

References

Ayali A, Gelman S, Tytell ED, Cohen AH (2009) Lateral-line activity during undulatory body motions suggests a feedback link in closed-loop control of sea lamprey swimming, Canadian Journal of Zoology, 87(8), pp.671-683.

Chagnaud BP, Brucker C, Hofmann MH, Bleckman H (2008) Measuring flow velocity and flow direction by spatial and temporal analysis of flow fluctuations, The Journal of Neuroscience, 28(17):4479-4487.

Griffen KR, Holbrook CM, Zielinski DP, Cahill CL, Wagner MW (2025) Not all who meander are lost: migrating sea lamprey follow river thalwegs to facilitate safe and efficient passage upstream, Journal of Experimental Biology, 228(4), pJEB249539.

Kerr JR, Zielinski DP, Goodwin RA, Holbrook RA, McLaughlin RL (2025) Upriver migrating sea lamprey exhibit similar responses to hydrodynamic features as other up and downriver-moving species. Frontiers in Freshwater Science, 3, p.1528481.

Lacey RWJ, Millar RG (2004) Reach scale hydraulic assessment of instream salmonid habitat restoration, Journal of the American Water Resources Association, 40(6):1631-1644.

Lewandoski S, Hrodey P, Miehls S, Piszczek P, Zielinski DP (2021) Behavioral responses of sea lamprey (*Petromyzon marinus*) and white sucker (*Catostomus commersonii*) to turbulent flow during fishway passage attempts, Canadian Journal of Fisheries and Aquatic Sciences. DOI:10.1139/cjfas-2020-0223.

Liao JC, Beal DN, Lauder GV, Triantafyllou MS (2003) Fish exploiting vortices decrease muscle activity, Science, 302(5650):1566-1569.

Olden JD, Konrad CP, Melis TS, Kennard MJ, Freeman MC, Mims MC, Bray EN, Gido KB, Hemphill NP, Lytle DA, McMullen LE (2014). Are large-scale flow experiments informing the science and management of freshwater ecosystems?, Frontiers in Ecology and the Environment, 12(3):176-185.

Reynolds K, Hondzo M, Voller V, Zielinski DP (2024). Hydraulic characteristics of effective sea lamprey barriers, Journal of Great Lakes Research, p.102489. https://doi.org/10.1016/j.jglr.2024.102489.

Romine JG, Perry RW, Pope AC, Stumpner P, Liedtke TL, Kumagai KK, Reeves RL (2016) Evaluation of a floating fish guidance structure at a hydrodynamically complex river junction in the Sacramento–San Joaquin River Delta, California, USA, Marine and Freshwater Research, 68(5):878-888.

Siefkes MJ (2017) Use of physiological knowledge to control the invasive sea lamprey (Petromyzon marinus) in the Laurentian Great Lakes, Conservation Physiology, 5(1), p.cox031.

Zielinski DP, Kerr J, Baerum KM, Simmons OM, Silva AT, Goodwin RA (2024) Advancements in riverine fish movement modeling: bridging environmental complexity and fish behavior, Reviews in Fisheries Science and Aquaculture, 1-16, doi:10.1080/23308249.2024.2374964.

Zielinski DP, McLaughlin RL, Castro-Santos T, Paudel B, Hrodey P, Muir A (2019) Alternative sea lamprey barrier technologies: history as a control tool, Reviews in Fisheries Science and Aquaculture, 27(4), 438-457.

Zielinski DP, Miehls S, Burns G, Coutant C (2020). Adult sea lamprey respond to induced turbulence in a low current system, Journal of Ecohydraulics, DOI: 10.1080/24705357.2020.1775504.

Book of Abstracts of the *16th International Symposium on Ecohydraulics*
Challenges and solutions in the time of global changes
August 16–20, 2026, Lausanne, Switzerland
ISSN: 2790-2420 | ISBN: 978-90-837233-9-6 | doi:[10.64697/iahr.proc.ise2026.abs]
© 2026 IAHR. CC BY-NC-ND 4.0

HYDRODYNAMIC THRESHOLDS FOR RESUSPENSION OF DRIFTING FISH EGGS IN BOTTOM VORTEX STRUCTURES

Yiheng GAO, Rui HAN*, Hongyi YANG, Miaoran FU

State Key Laboratory of Water Cycle and Water Security, China Institute of Water Resources and Hydropower Research, Beijing 100038, China
email: gaoyiheng@edu.iwhr.com

email:hanrui_first@163.com
email:yanghongyi@edu.iwhr.com
email: fumiaoran@edu.iwhr.com

ABSTRACT

Hydropower development alters river hydraulic characteristics, adversely affecting the transport of drifting fish eggs. There is an urgent need to clarify the critical hydrodynamic conditions and thresholds for drifting fish egg resuspension. Studying the transport mechanism of drifting fish eggs in bottom vortex structures can supplement existing knowledge on hydrodynamic transport conditions and thresholds. This experiment quantified the critical flow field characteristics that initiate egg motion by capturing egg transport trajectories and local flow field distributions, analysed the transport mechanism of eggs on riverbeds, and established a critical threshold formula for the resuspension of drifting fish eggs in bottom vortices during transport. Based on the energy conservation theorem, we tracked changes in egg kinetic and potential energy to establish critical thresholds for egg transport. This provides a reference for quantitatively assessing the impact of river hydrodynamic conditions on the transport and resuspension of drifting fish eggs.

Keywords: Drifting fish eggs; Critical thresholds; Vortex structures; Resuspension

1. Introduction

The construction and operation of hydraulic projects convert the natural value of river ecosystems into utilizable economic value, but inevitably disrupt river connectivity (Grill et al., 2019), alter river hydrological and thermal regimes (Shang et al., 2022), sediment regimes, and river morphology (Wang et al., 2023). These changes seriously threaten the reproduction and population survival of fish species that produce drifting eggs (Granzotti et al., 2018; Yao et al., 2025; Orsi et al., 2014; Zhang et al., 2025). Existing research indicates that drifting fish eggs require certain flow velocities to maintain their drifting incubation (Kocovsky et al., 2012), while turbulence is also an important parameter for keeping eggs suspended (Kolar et al., 2007). However, most current studies focus on hydraulic characteristics in the surface water layer, lacking research on thresholds for eggs that settle to the river bottom but continue to drift with flow. Therefore, this study systematically investigates the movement characteristics of drifting fish eggs through laboratory experiments, considering turbulent effects, to clarify the multi-factor threshold conditions controlling egg resuspension on riverbeds.

2. Materials and methods

Following our previous work (Zhu et al., 2025), the experimental setup consisted of a hydrodynamic-microtopography simulation flume system, using artificial dunes to create bottom vortices, and recording velocity fields through Particle Image Velocimetry (PIV). The experiment employed agar model eggs with diameters of 5mm and 6mm, whose physical characteristics resemble naturally drifting fish eggs in the upper Yangtze River.

Under low-flow conditions, after the flow reached a stable state, 100 artificial eggs were released at the bed surface with zero initial velocity. The flow rate was gradually increased until 50% to 99% of the eggs were

transported out of the observation area within a 20-second time span, at which point the egg resuspension threshold was considered reached. Flow fields and egg movement trajectories were recorded.

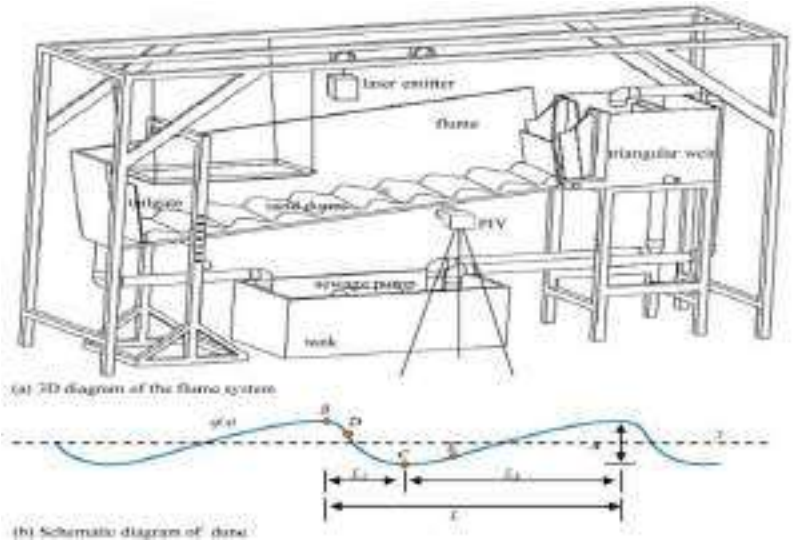

Fig.1.Schematic of the Experimental Flume Design and Flow Monitoring System

To establish a quantitative threshold for egg resuspension, we used dimensional analysis combined with the energy conservation theorem to develop a comprehensive threshold formula considering hydrodynamic characteristics and egg properties:

$$Ec = \frac{UFd}{Ws\omega m} \tag{1}$$

In the formula, Ec is a dimensionless parameter that characterizes the ratio of flow-induced forces to the egg's resistance to motion, U represents the local flow velocity, vorticity ω (s^{-1}), and flow drag force Fd, while based on the density ρ and diameter d of the egg, its settling velocity Ws and particle mass m (kg) are calculated.

After obtaining the critical hydrodynamic conditions for fish egg resuspension, binary search is used to explore the critical threshold. Binary search is an efficient algorithm for finding a specific element in an ordered array by repeatedly halving the search interval(Yan et al., 2020). Starting with the middle element, it compares the target value to the midpoint. If the target is smaller, it continues searching in the left half; if larger, in the right half. This process repeats until the target is found or the interval is empty, achieving O(log n) time complexity(Yang et al., 2023).

3. Results and discussion

Through flume experiments, we systematically observed the initiation process of drifting fish eggs under different working conditions (slope, dune size, egg diameter). The experiment successfully captured the complete process of eggs progressing from "trapped by dunes" to "Resuspension" and finally to "drifting away from dunes."



Trapping Entrainment Resuspension

Fig.2. Schematic diagram of the fish egg resuspension process.

Superimposing egg movement trajectories with bottom flow field characteristics (velocity, vorticity, streamlines) in the flume, as shown in Fig. 3, revealed that high vorticity zones (vorticity > 1.5 s^{-1}) are concentrated in shear bands between mainstream and low-velocity zones, lee sides of dunes, and wake zones behind obstacles. These areas correspond to centers of intense vortex generation and energy dissipation in the flow field. The movement of drifting fish eggs on dune beds showed significant periodic characteristics.

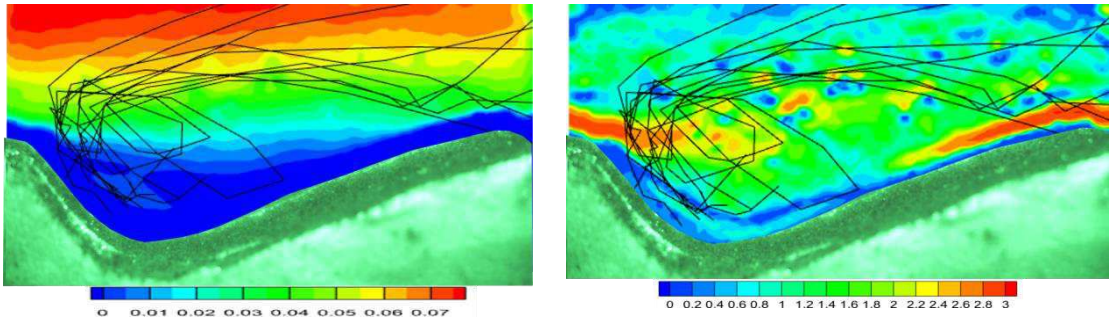

Flow Velocity Field Contour Plot (b) Flow Vorticity Field Contour Plot

Fig.3. Composite Plot of Flow Field and Fish Egg Trajectories

Using the threshold formula (Equation 1), we correlated the initiation state of fish eggs with their energy state (kinetic and potential energy) in the flow field, defining total energy greater than zero as the physical criterion for effective initiation. Through statistical analysis of experimental data, we established a quantitative relationship model between threshold and initiation probability, and used the binary search to determine the dimensionless critical threshold parameter of 0.00177 for achieving 80% initiation probability.

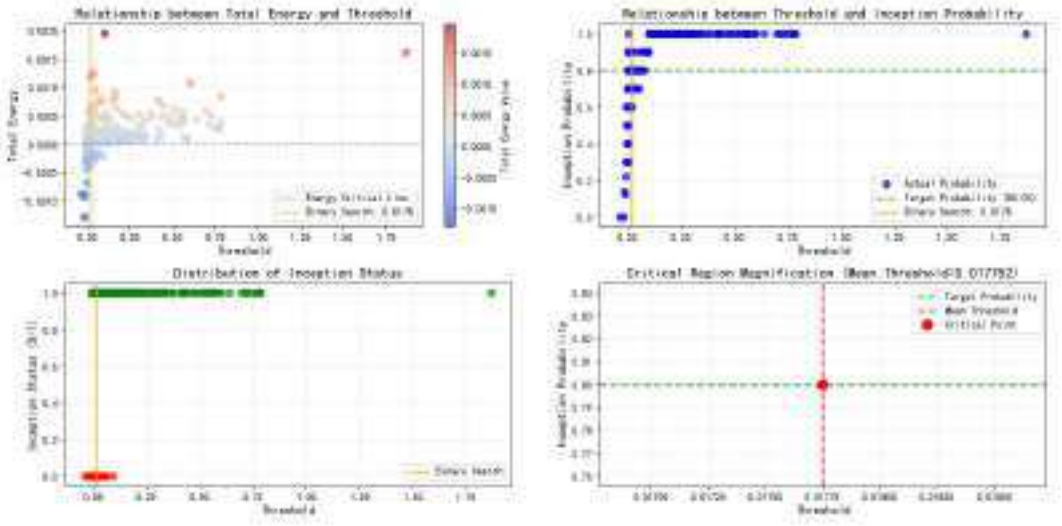

Fig.4. Quantitative Relationship Model between Critical Threshold and Inception Probability

4. Conclusions

This study systematically investigated the resuspension and transport mechanisms of drifting fish eggs over dune-shaped bedforms under controlled laboratory conditions. The main conclusions are as follows:

(1) Critical hydrodynamic thresholds for egg resuspension were identified, with near-bed velocity ≈ 0.05 m/s and vorticity > 1.5 s^{-1};

(2) The complete resuspension process was revealed, showing how bottom vortex structures control egg movement trajectories;

(3) An energy-based critical threshold model was established, with a dimensionless critical parameter of 0.00177 for 80% initiation probability;

(4) The mechanistic framework supports quantitative assessment of hydropower impacts on fish egg transport and informs ecological flow management strategies.

Acknowledgements

This work was supported by the National Key Research and Development Program of China (2022YFC3203903) and the National Natural Science Foundation of China (52179083).

References

Grill G ,Lehner B ,Thieme M , et al.Author Correction: Mapping the world's free-flowing rivers.[J].Nature,2019,572(7768):E9.
Shang W X, Peng S M, Wang Y, et al. Analysis of the ecological impact of the Xiaolangdi Reservoir on the lower Yellow River [J]. Water Resources Protection, 2022, 38(1): 160-166+175.
Wang K, Xiao Y, Mao J Q, et al. Study on the spawning period of typical fish in the lower reaches of Jinsha River under the influence of water temperature change [J]. Journal of Hohai University (Natural Sciences), 2023, 51(2): 50-55.

Granzotti R V, Miranda L E, Agostinho A A, et al. Downstream impacts of dams: shifts in benthic invertivorous fish assemblage s [J]. Aquatic Sciences, 2018, 80: 1-14.
YAO R, ZHUGE Y, YU X, et al. Study on response of water temperature characteristics in reservoir-river systems to climate change [J]. Water Resources and Hydropower Engineering, 2025, 56(5): 59-70.
Orsi M, Britton J. Long-term changes in the fish assemblage of a neotropical hydroelectric reservoir [J]. Journal of fish bio logy, 2014, 84(6): 1964-1970.
ZHANG Qifan, JING Pingfei, LI Xiaonan, et al. Study on the coordinating strategy of the Three Gorges Reservoir for ecological operation to promote spawning of the four major Chinese carps and comprehensive utilization demand[J]. Water Resources and Hydropower Engineering,2025, 56(9): 15- 29.
Kocovsky P M, Chapman D C, McKenna J E, Thermaland hydrologic suitability of Lake Erie and its major tribu-taries for spawning of Asian carps[J]. Journal of GreatLakes Research, 2012, 38(1):159-166.
KOLAR C S, CHAPMAN D C, COURTENAY W R Jr, et al. Bigheaded Carps: A Biological Synopsis and Environmental Risk Assessment [M]. Bethesda, Md: American Fisheries Society, 2007: 226.
ZHU L, LI W, CHEN D, et al. Experimental study on the response mechanisms of drift egg transport and adhesive egg hatching to reservoir impoundment in the lower Jinsha River [J]. Animals, 2025, 15(17): 2488. DOI: 10.3390/ani15172488.
YAN X L, YANG G L, WANG L. EKF-SLAM algorithm based on bisection method [J]. Navigation, Positioning and Timing, 2020, 7(3): 77-83. DOI: 10.19306/j.cnki.2095-8110.2020.03.011.
YANG S J, WU C F, YE H L, et al. Application of the bisection method in upper mantle temperature simulation [J]. Journal of G eology, 2023, 47(2): 182-187.

Book of Abstracts of the *16th International Symposium on Ecohydraulics*
Challenges and solutions in the time of global changes
August 16–20, 2026, Lausanne, Switzerland
ISSN: 2790-2420 | ISBN: 978-90-837233-9-6 | doi:[10.64697/iahr.proc.ise2026.abs]
© 2026 IAHR. CC BY-NC-ND 4.0

A PREDICTIVE MODEL FOR ASSESSING FISH LARVAL DRIFT UNDER VARIABLE HYDROLOGICAL CONDITIONS

Wiktoria CUDNA[1], Piotr PARASIEWICZ[1]

[1] National Inland Fisheries Research Institute, Poland

email: w.cudna@infish.com.pl

ABSTRACT

This study develops a predictive model for the spatial distribution of fish larval drift in the Vistula River, identifying the primary hydrological drivers of this critical ecological process. Research was conducted using nocturnal sampling during the peak drift season (April–July) near the ENEA Połaniec Power Plant, integrated with hydrodynamic modeling to interpolate depth and flow velocity. Larval density data were transformed into a binary presence/absence indicator based on a lower-quartile threshold of 0.044 larvae/m³. A logistic regression model was calibrated using AIC-based stepwise selection to determine the influence of environmental variables. The results identify water depth, flow velocity, and local morphological heterogeneity (depth variability) as significant predictors. The model achieved a success rate of 0.70 and an Area Under the ROC Curve (AUC) of 0.68, demonstrating its utility as a diagnostic tool for assessing hydrotechnical impacts on riverine larval niches.

Keywords: fish larval drift, spatial modeling, Vistula River, hydrodynamics, logistic regression, habitat suitability

1. Introduction

Fish larval drift is a fundamental mechanism for dispersal and recruitment in riverine ecosystems, representing an integral part of the colonization cycle. This process exhibits a distinct diel periodicity, reaching its maximum intensity during nocturnal hours when a significant majority of individuals move under the cover of darkness. While traditionally viewed as passive transport, contemporary studies suggest that drift is an active dispersal process triggered by decreasing light intensity, serving as an adaptive behavioral response to minimize exposure to visual predators. Despite its importance, the physical variables governing larval spatial distribution in large, complex systems remain poorly defined. The objective of this study was to develop a predictive larval niche model based on logistic regression and hydrodynamic cues, such as depth, flow velocity, and local morphological variability, on the Vistula River near the ENEA Połaniec Power Plant. These findings provide a technical basis for evaluating the impacts of hydrotechnical infrastructure on fish dispersal routes, thereby supporting effective environmental resource management.

2. Methods

2.1. Study site and sampling

The study focused on two sections of the Vistula River in the vicinity of the ENEA Połaniec Power Plant, selected to represent diverse morphological conditions. Field sampling was conducted between April and July 2024. To capture peak larval movement, all samples were collected between 20:00 and 04:00.

2.2. Data acquisition and hydrodynamics

Bathymetry and flow velocity measurements were obtained through field surveys. These empirical data were processed through a hydrodynamic model to interpolate depth and velocity values across the study reaches, ensuring that each biological sampling station was associated with precise physical parameters.

2.3. Variable preparation and modeling logic

Larval density was calculated as larvae per cubic meter (larvae/m³). To ensure model stability given the high stochasticity of catch data, density was transformed into a binary response variable (presence/absence). The presence threshold was set at the lower quartile (0.044 larvae/m³). The primary predictor variables were:

- Depth (m) and flow velocity (m s^{-1}): direct values extracted from the hydrodynamic model;
- Depth variability (Δd) calculated as the "Range" statistic using a 3x3 neighborhood Focal Statistic in ArcGIS Pro:

$$\Delta d = d_{max} - d_{min} \quad (1)$$

where d = depth.

This variable serves as an ecohydrological proxy for spatial heterogeneity and riverbed morphology, identifying areas of rapid depth change

- range share [%] depth variability (x): calculated as

$$x = \frac{\Delta d}{d} * 100 \quad (2)$$

where d = absolute depth.

This metric represents local acceleration and pressure gradients.

Variables such as "distance from the bank" and "velocity changes" were also tested but were found to be statistically insignificant and were excluded from the final model.

2.4. Software and statistical specification

Statistical analysis was performed in R with statistical package from SimStream 8.0 and spatial processing in ArcGIS Pro. The probability of larval occurrence was defined by the logistic regression equation:

$$p = \frac{1}{(1 + e^{-z})} \quad (3)$$

p = probability of presence/high abundance = constant, $z = b_1 \times x_1 + b_2 \times x_2 + \ldots\ldots + b_n \times x_n + a$, $x_{1..n}$ = significant physical variables, $b_{1..n}$ = regression coefficients (obtained from statistical package), a = constatnt.

Variable selection followed a stepwise approach based on the Akaike Information Criterion (AIC). To maintain all parameters identified by the AIC as informative for the model's predictive structure, the significance threshold for inclusion was set to p = 1.0.

3. Results and discussion

3.1. Statistical performance

The model calibration produced a robust predictive signal for a complex riverine environment. While the metrics reflect the stochastic nature of large-river larval dispersal, they represent a "good" fit for management applications (Table 1).

Table 1. Performance metrics and statistical thresholds for the fish larval drift predictive model.

Success Rate	0.70
Area Under the ROC Curve (AUC)	0.68
Probability Cutoff Value	0.38

3.2. Regression coefficients

The coefficients for the significant physical variables are detailed below (Table 2). Note that positive coefficients indicate an increased probability of larval presence, while negative values indicate a decrease.

Table 2. Model coefficients for environmental drivers of fish larval presence in the Vistula River.

Variable	Coefficient
Depth (m)	0.013
Flow velocity (m/s)	-0.011
Depth variability (Δd)	-0.03
Normalized depth variability (x_{norm})	0.07

3.3. Interpretative discussion

The significance of depth variability (Δd) and its range share (x) suggests that larval drift is not merely passive transport, but an active dispersal process heavily influenced by hydrodynamic cues. These variables serve as

proxies for pressure gradients and local flow accelerations that aquatic organisms integrate across multiple timescales to navigate heterogeneous river environments (Goodwin et al., 2023; Goodwin et al., 2014). The negative coefficient for flow velocity and the positive coefficient for normalized depth variability align with theories of strain-driven behavior and the modulation of flow-field experience (Goodwin et al., 2023). In this context, larvae may actively seek specific hydraulic signatures or occupy near-shore niches to minimize predation risk, which is further supported by the nocturnal peak in activity captured in our sampling window between 20:00 and 04:00 (Magoulick and Graham, 2025). Predictive map (Fig. 1) captured distinct spatial gradients that generally align with empirical observations of non-random larval distribution in large rivers. While the AUC of 0.68 reflects the turbulent and non-linear nature of the Vistula, it demonstrates that the model successfully captures the fundamental environmental drivers of the larval niche.

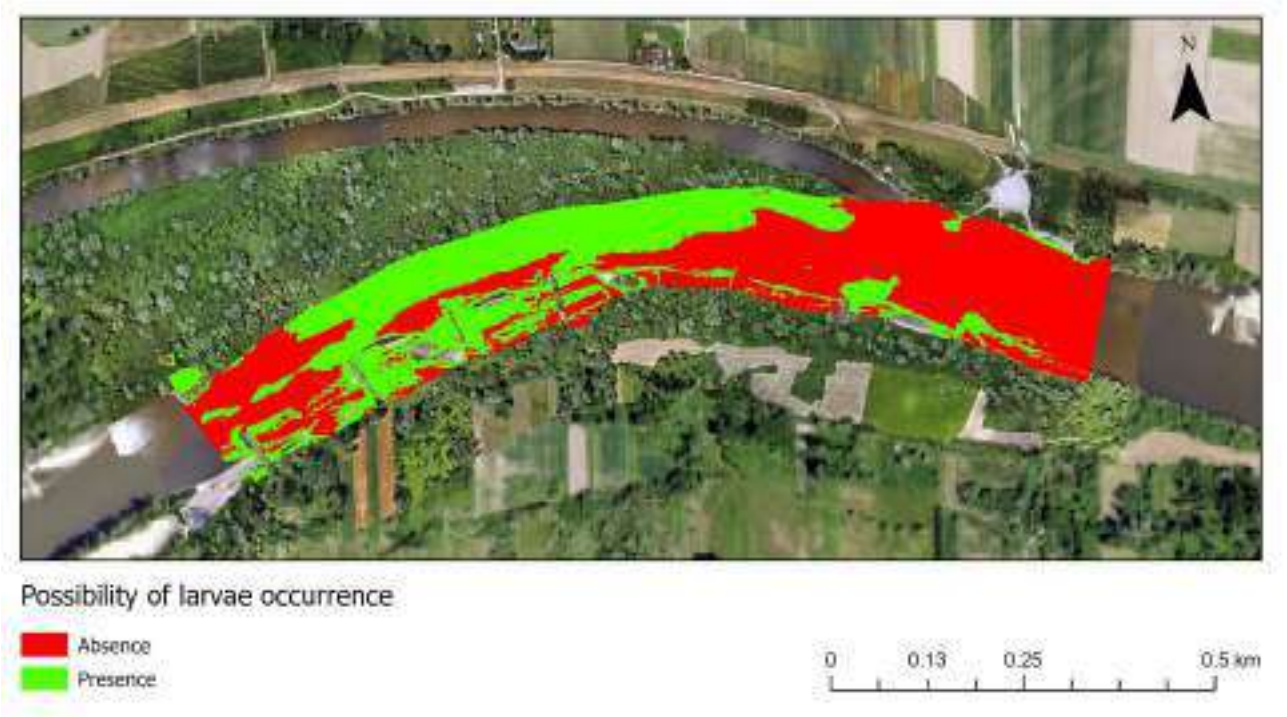

Fig. 1. Map of one of the site with distribution of fish larval drift in Vistula River, modelled for a flow rate of Q = 100 m³/s. Possibility of larvae occurrence was assessed using a two-level scale: 0 – absence, 2 – presence. Orthomosaic – acquired by drone, by Katarzyna Suska. Basemap: Orthophotomap geoportal.gov.pl

4. Conclusion

The developed model successfully identifies depth, flow velocity, and morphological heterogeneity as the primary determinants of the fish larval niche in the Vistula River near the ENEA Połaniec Power Plant. By incorporating spatial derivatives of depth and acknowledging the active nature of drift triggered by decreasing light intensity, this tool provides practical value for forecasting the ecological consequences of hydrotechnical modifications. To enhance the model's universality and predictive power, subsequent research must focus on multi-river validation and the integration of larger datasets.

Acknowledgements

The authors would like to express their gratitude to the ENEA Połaniec Power Plant for providing access and funding that enabled the completion of this research, as well as to the National Inland Fisheries Research Institute (statutory work Z-018).**References**

Goodwin RA, Lai YG, Taflin DE, Smith DL, McQuirk J, Trang R and Reeves R (2023) Predicting near-term, out-of-sample fish passage, guidance, and movement across diverse river environments by cognitively relating momentary behavioral decisions to multiscale memories of past hydrodynamic experiences. Front. Ecol. Evol. 11:703946.

Goodwin, R. A., Politano, M., Garvin, J. W., Nestler, J. M., Hay, D., Anderson, J. J., Weber, L. J., Dimperio, E., Smith, D. L., & Timko, M. (2014). Fish navigation of large dams emerges from their modulation of flow field experience. *Proceedings of the National Academy of Sciences of the United States of America*, *111*(14), 5277–5282.

Magoulick, D. D., & Graham, C. L. (2025). Relationships between larval fish drift, time of day and discharge in an Ozark stream. Journal of Freshwater Ecology, 40(1).

Rushing Rivers Institute. 2014. SimStream: A MesoHABSIM Simulation Software. Available online: https://rushingrivers.org/ (accessed on 25 November 2025)

Zitek A, Schmutz S, Ploner A. (2004). Fish drift in a Danube sidearm-system: II. Seasonal and diurnal patterns. J Fish Biol. 65(5):1339–1357.

Book of Abstracts of the *16th International Symposium on Ecohydraulics*
Challenges and solutions in the time of global changes
August 16–20, 2026, Lausanne, Switzerland
ISSN: 2790-2420 | ISBN: 978-90-837233-9-6 | doi:[10.64697/iahr.proc.ise2026.abs]
© 2026 IAHR. CC BY-NC-ND 4.0

SEASONAL, NOCTURNAL AND SPATIAL DYNAMICS OF ICHTHYOPLANKTON DRIFT NEAR THE POŁANIEC POWER PLANT, VISTULA RIVER, POLAND

Wojciech PREKURAT, Piotr PARASIEWICZ

National Inland Fisheries Research Institute, Poland
email: w.prekurat@infish.com.pl

ABSTRACT

This study analyzed the drift of early developmental stages of fish (ichthyoplankton) in the vicinity of the Połaniec Power Plant, one of the largest installations of this type in Poland, using an open cooling system. Samples were collected at night in bi-weekly cycles from May to July 2024 using conical plankton nets in cross-sections located upstream and downstream of the power plant's infrastructure, as well as in the cooling water intake channel and the heated water discharge channel. A total of 4,026 larvae were collected from 18,990 m³ of filtered water. Drift exhibited strong seasonal growth, peaking in early July, and showed a pronounced nocturnal pattern with maximum activity around midnight. Spatial variability was high, with the highest concentrations along the riverbanks and downstream of the power plant. Entrainment losses were estimated at 7.6 million larvae, representing 6.75% of the parallel drifting population. The results indicate that while entrainment is measurable, local larval production in the downstream reach may partially compensate for the losses.

Keywords: Ichthyoplankton; Fish larvae; Drift dynamics; Power plant impact; Fish mortality; Vistula River; Once-through cooling system

1. Introduction

Large lowland rivers such as Vistula are dynamic ecosystems whose fish communities depend on successful transport and survival of drifting early life stages. Ichthyoplankton drift is a major component of recruitment for many rheophilic and eurytopic species (Pavlov, 1994; Humphries & Lake, 2000; Reichard et al., 2002; Sonny et al., 2006; Reichard & Jurajda, 2007; Lechner et al., 2016; Cooke et al., 2022). At the same time, rivers are often modified by hydrotechnical infrastructure, including power plants using once-through cooling systems. These systems may entrain larvae and alter hydraulic and thermal regimes (Barnthouse, 2013; Janáč &Reichard, 2016; Mikołajczyk et al., 2020; Bănăduc et al., 2024). The Połaniec Power Plant (Połaniec TPP) is one of the largest thermal power plants in Poland, withdrawing up to 66 $m^3 s^{-1}$ from the Vistula River. Despite several local studies (Mikołajczyk et al., 2022; Nowak et al., 2025), comprehensive analysis integrating seasonal, diel and spatial drift patterns in the full river cross-section has not yet been carried out. This study aimed to quantify seasonal, diel and spatial patterns of ichthyoplankton drift in the vicinity of the power plant and to estimate entrainment-related losses. The results can serve as a basis for developing recommendations aimed at protecting river biodiversity and minimizing the impact of the energy industry on the aquatic ecosystem through potential technological modifications.

2. Materials and Methods

2.1. Study area

The study was conducted on the Vistula River near the (Połaniec TPP), located in southeastern Poland. The power plant, with a gross installed capacity of 1,674 MW, operates an open cooling system. Water is drawn directly from the Vistula River through two short technical channels on the left bank and, after cooling,

discharged back into the river through an approximately 2.4 km long discharge channel. To ensure stable water intake, especially during low water levels, a flexible rubber weir was installed in September 2019. The average river flow in this area is 264 $m^3 s^{-1}$. The upstream profile (U) served as reference, while the downstream profile (D) represented river sections affected by the weir. The intake channel (CC) and the warm-water discharge channel (WC) were also monitored.

2.2. Sampling procedure

Ichthyoplankton sampling covered 12 sampling nights in 6 two-week campaigns from 6 May to 17 July 2024. Measurements were performed at night (20:00–04:00 CEST). Samples were collected using conical plankton nets (length 2 m, inlet area 0.15 m^2). Two mesh sizes were used: 1000 µm for the U, D, and WC profiles, and both 500 µm and 1000 µm for the CC channel. The nets were immersed perpendicular to the flow direction, just below the water surface. The net exposure time was typically 15 minutes.

2.3. Data analysis

Larval concentrations were standardised to individuals per 100 m^3. Cross-sectional larval density D was estimated as a weighted mean across sampling points: for riverine profiles (U, D) and the warm channel (WC), weights were proportional to local density at each point (reflecting observed larval preference for near-bank zones); for the intake channel (CC), an arithmetic mean was applied, assuming uniform lateral distribution. The total number of larvae drifting in the profile at night was calculated as:

$$N = D * Q * T$$

where D - larvae density for the entire river cross-section [pcs/m^3], Q - average flow in the profile on a given night [$m^3 s^{-1}$], T - duration of the night drift, set to a constant value of 8.5 h (30600 s) [s].

The total number of larvae in the season was calculated by summing the measured N values and linearly interpolating the N values during periods without measurements (taking the arithmetic mean of N from adjacent measurement nights and multiplying it by the interval length). Daily drift was assumed to be negligible. Final results were rounded to the nearest million. To calculate losses, the proportion of larvae in the CC channel relative to the river population was calculated. Linear interpolation between bi-weekly sampling nights is considered appropriate given the gradual, unimodal seasonal progression of drift density observed (Fig. 1); the smooth increase and decline in larval abundances across the monitoring period suggests that inter-sampling variability is low relative to the seasonal trend, supporting the validity of this approach. Larval flux is expected to occur predominantly in nocturnal pulses rather than as a continuous process, consistent with the strong diel signal recorded (Fig. 2); daytime drift was therefore treated as negligible in seasonal total estimates.

3. Results

3.1. Seasonal dynamics

The first fish larvae were detected in the samples in early May. Their numbers gradually increased, reaching a seasonal peak in the first half of July, after which they began to decline. See Fig. 1.

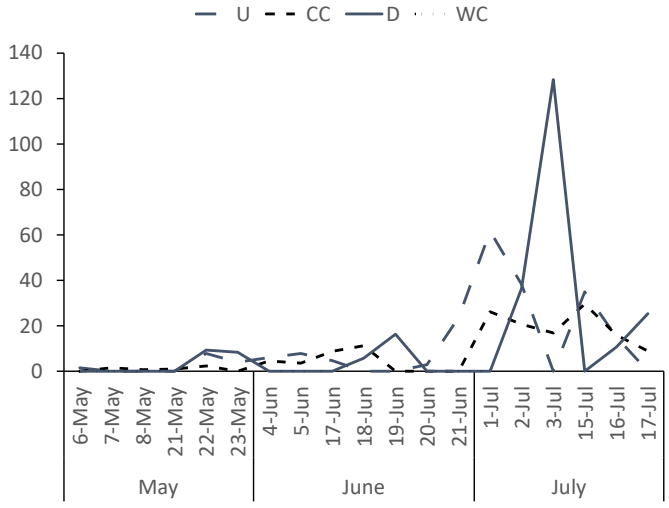

Fig. 1. Seasonal dynamics of larval drift in individual profiles [mean density 100^{-3}].

3.2. Nocturnal dynamics

Drift activity showed a distinct nocturnal pattern, with highest concentrations between 23:30 and 00:30. Considerably lower abundances were observed during early evening and pre-dawn hours. See Fig. 2. This pattern is consistent with light-avoidance behavior widely reported for drifting fish larvae (Reichard et al., 2002; Oesmann, 2003;), and corresponds to the documented nocturnal drift of most larval fish species in the Vistula (Mikołajczyk et al., 2020, 2022; Nowak et al., 2025), with daytime drift considered negligible. The strong nocturnal peak also implies that larval flux occurs in discrete nightly pulses rather than as a continuous process, which should be taken into account when interpreting entrainment estimates derived from daytime or continuous monitoring approaches.

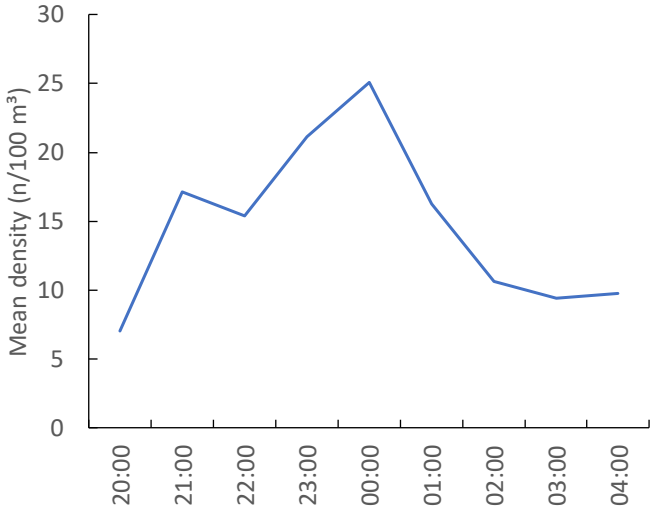

Fig. 2. Nocturnal drift activity.

3.3. Spatial patterns

The highest maximum densities were recorded in profile D. In profiles U and D, the highest larval densities were found near the right bank. Furthermore, significantly higher densities of drifting larvae were found in the littoral zones compared to the main stream. See Fig. 3.

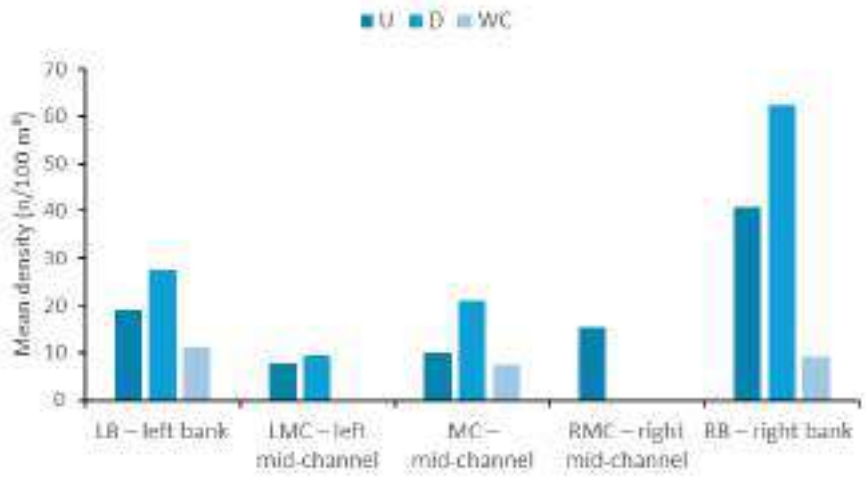

Fig. 3. Comparison of the average larvae density from three points in the profiles of the Vistula River (U and D) and the warm channel (WC).

3.4. Entrainment estimates

Season-long entrainment losses were estimated at 7.6 million larvae, corresponding to 6.75% of the drifting population. The total estimated ichthyoplankton population during the monitoring period for each profile is summarized in the Table 1.

Table 1. Entrainment estimates [mln]

Profile	Estimated Population
U* (Upstream)	112
CC* (Cold Channel)	7,6

% Entrained Larvae	6.75 %
D** (Downstream)	149
WC** (Warm Channel)	6,5

*71 nights, **56 nights

4. Conclusions

The results of the study highlight the complex interaction between river hydrodynamics and ichthyoplankton drift, leading to the following key conclusions:

- Spatial and temporal dynamics: ichthyoplankton drift exhibited strong seasonal and nocturnal dynamics, with a peak in July corresponding to the spawning periods of the main Vistula fish species. The drift showed a strong spatial pattern, with marked differences in larval abundance between sampling profiles and cross-sectional positions. Larval densities in the downstream profile D were notably higher than in the upstream reference profile U (149 vs. 112 million larvae estimated over the season; Table 1). This difference may reflect the availability of favourable spawning and rearing habitats in the downstream reach.
- Role of shoreline zones: shoreline zones played a key role as major drift corridors, exhibiting significantly higher larval concentrations compared to the main current. This is evidenced by the cross-sectional sampling in profiles U and D, where bank-side measurement points consistently recorded the highest larval densities (Fig. 3).
- Impact of the cooling system: Entrainment by the cooling system caused measurable losses (approx. 7.6 million larvae over the study period). However, these losses were limited relative to the total riverine population (approx. 6.75%) and did not translate into a significant reduction in overall abundance, suggesting no major negative impact on future recruitment to the adult fish stock.
- Compensatory mechanisms the observed losses appear to be partially compensated by local larval production in the warm discharge channel (WC), estimated at approximately 6.5 million larvae over the study period. Larval abundance in the downstream profile (D) exceeded that in the upstream reference (U) by approximately 33%, suggesting additional local recruitment in the downstream reach.

References

Bănăduc, D., Curtean-Bănăduc, A., Barinova, S., Lozano, V. L., Afanasyev, S., Leite, T., Branco, P., Gomez Isaza, D. F., Geist, J., Tegos, A., Simić, S. B., Olosutean, H., & Cianfanglione, K. (2024). Multi-Interacting Natural and Anthropogenic Stressors on Freshwater Ecosystems: Their Current Status and Future Prospects for 21st Century. Water, 16(11), 1483 pp.

Barnthouse, L. W. (2013). Impacts of entrainment and impingement on fish populations: A review of the scientific evidence. Environmental Science & Policy, 31, 149-156

Cooke, S. J., Lennox, R. J., & Thorstad, E. B. (2022). The Movement Ecology of Fishes. Journal of Fish Biology, 101(5), 1078–1114

Humphries, P., & Lake, P. S. (2000). Fish larvae and the ecology of stream start: a review, synthesis and perspectives. Fresh water Biology, 44(3), 367-382

Janáč, M., & Reichard, M. (2016). Use of Drift Nets to Infer Fish Transport and Migration Strategies in Inland Aquatic Ecosys tems. In P. Morais & F. Daverat (Eds.), An introduction to fish migration (pp. 197–213). CRC Press. https://doi.org/10.1201/b21321-14

Lechner, A., Keckeis, H., & Humphries, P. (2016). Patterns and processes in the drift of early developmental stages of fish in rivers: a review. Reviews in Fish Biology and Fisheries, 26, 471-489

Mikołajczyk T, Nowak M, Skowronek D, Mikołajczyk Ł, Wawręty R (2020) Wpływ elektrowni termicznych na ichtiofaunę. TNZ-PNWI, Kraków-Oświęcim-Bystra

Mikołajczyk, T., Nowak, M., Skowronek, D., Mikołajczyk, Ł., & Wawręty, R. (2022). Szacunkowe straty w ichtiofaunie Wisły oraz Narwi spowodowane zasysaniem larw ryb i wczesnych form narybkowych do systemów chłodzących Elektrowni Połaniec, Kozienice i Ostrołęka B. TNZ, Oświęcim

Nowak, M., Skowronek, D., Janik-Superson, K., Mikołajczyk, Ł., Wawręty, R., Mikołajczyk, T., Krawczyk, D., & Jeziorski, S. (2025). Entrainment of fish larvae into Połaniec Power Plant: another considerable threat for the ichthyofauna of the Vistula River (Poland). Biologia, 615-628

Oesmann, S. (2003). Vertical, lateral and diurnal drift patterns of fish larvae in a large lowland river, the Elbe. Journal o f Applied Ichthyology. 19. 284 - 293. 10.1046/j.1439-0426.2003.00503.x

Pavlov, D. S. (1994). The downstream migration of young fishes in rivers: mechanisms and distribution. Folia Zoologica, 43(3), 193-208

Reichard, M., Jurajda, P., & Ondračková, M. (2002). The effect of light intensity on the drift of young-of-the-year cyprinid fishes. Folia Zoologica, 51(3), 219-226

Book of Abstracts of the *16th International Symposium on Ecohydraulics*
Challenges and solutions in the time of global changes
August 16–20, 2026, Lausanne, Switzerland
ISSN: 2790-2420 | ISBN: 978-90-837233-9-6 | doi:[10.64697/iahr.proc.ise2026.abs]
© 2026 IAHR. CC BY-NC-ND 4.0

USING FIELD AND FLUME STUDIES PAIRED WITH HYDRODYNAMIC MODELING TO INFORM A FRESHWATER MUSSEL REINTRODUCTION

Megan DINICOLA[1], Belize LANE[2]

[1,2] Utah State University Department of Civil and Environmental Engineering, United States of America
email: A02315573@usu.edu

email: belize.lane@usu.edu

ABSTRACT

Species reintroductions are an important conservation tool but require both conscious release planning as well as adequate monitoring to ensure success. A widely imperiled aquatic fauna, freshwater mussels, are a sessile benthic animal that have complicated life histories and require stable sediments to provide structure to their environment. While reintroductions of mussels are becoming more common, there is still a lack of knowledge of what the suitable physical habitat thresholds are for the size of mussels typically used in reintroductions. Here, we use a combination of field and flume studies paired with a hydrodynamic model to inform the first mussel reintroduction in Texas, USA. Shear stress-based mussel mobility thresholds and physical habitat types guided the selection of suitable reintroduction locations. The local river authority had previously selected reintroduction sites based on site visits and local knowledge, which partially matched the model results, showing the validity of using modeling analysis paired with physical testing can provide increased success for reintroduction projects.

Keywords: freshwater mussels; reintroductions; subadult; mobilization

1. Background/Motivation

Freshwater mussels (Bivalvia: Unionidae) are sessile benthic fauna that have complicated life histories and require stable sediments to provide structure to their environment (Haag, 2012). Although they are important ecosystem engineers and an indicator fauna, mussels are highly imperiled across the globe (Haag, 2012). As a restoration technique to combat these decreasing populations, reintroductions are becoming a more popular way to bolster current populations and renew populations in reaches where mussels have previously been extirpated (Carey et al., 2015). While most studies to date have focused on adult mussels (e.g. Randklev et al., 2019; Roberts et al., 2022; Vaessen et al., 2024), reintroductions are often carried out using subadult mussels (Montesanto et al., 2023). Subadult mussels are defined as the age class where mussels are living at or near the bed surface but are not yet at reproducing age, typically between 20 and 40mm in length (Haag, 2012).

In order to maximize reintroduction success, this study used paired field and flume experiments to quantify shear stress-based mobilization thresholds and identify stable areas within the channel to reintroduce native subadult freshwater mussels. These methods were used to support a reintroduction effort in the Mission Reach of the San Antonio River, Texas, USA, which was the subject of one of the largest urban river restorations in the world.

2. Methods

2.1. Study Site

The Mission Reach of the San Antonio River is an 8-km reach in south central Texas, USA. The reach sits just downstream from downtown San Antonio and experiences an extremely flashy, rain-dominated hydrograph. The Mission Reach was the subject of one of the largest urban river restoration projects in the world that was completed in 2013 (Lombardi, 2014). A key component of the restoration was the addition of approximately 30 channel spanning engineered low-head barriers that create varying habitat types and have a canoe chute that bisects the upstream sill to allow fish passage and downstream recreational boat traffic. In the time since the restoration, native fish, insects and plants have recolonized the main stem of the reach but the mussels that

were extirpated decades ago have not repopulated the reach. The local river authority (SARA) is planning to reintroduce native mussels to build a self-sustaining population.

2.2. Framework development

Suitable physical habitat characteristics for reintroducing subadult mussels were selected using a spatial modeling framework based on subadult shear stress-based mussel mobility thresholds, habitat types, hydrologic analysis and a HEC RAS 2D model (Figure 1).

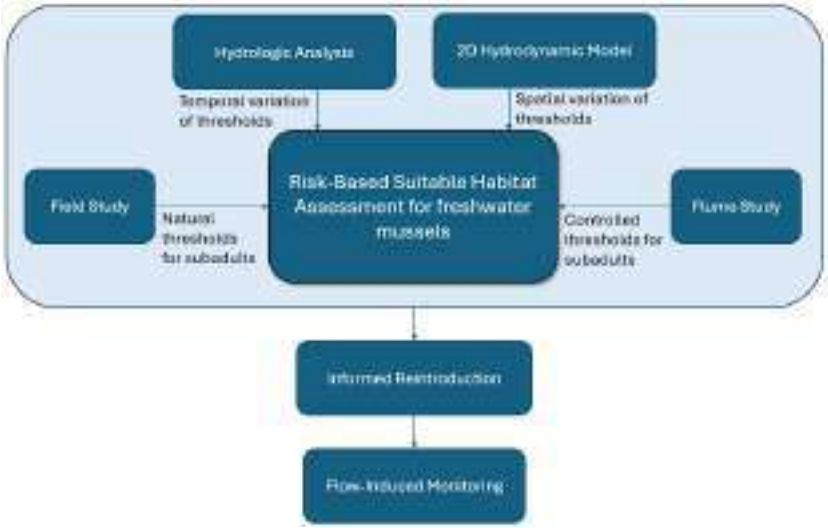

Figure 1. A framework for the study that combines field, flume and hydrodynamic modelling studies to inform subadult freshwater mussel placement for reintroduction efforts and then assess these placement locations for suitability using post reintroduction monitoring.

Subadult mussel mobility thresholds were developed using a flume study looking at mussel mobility for a range of mussel sizes and sediment types (DiNicola et al., in revision). These thresholds were generalized through the creation of a new equation for the mussel mobility index (T_m) that compares the shear stress felt by subadult mussels (τ_m) to the critical shear stress of the surrounding sediments (τ_c):

$$T_m = \frac{\tau_m}{\tau_c} \tag{1}$$

τ_m is a function of shear velocity and water density [$\rho(U^2_{*\mathrm{m}})$], with shear velocity being defined as:

$$U_{*\mathrm{m}} = \frac{U}{5.75 log_{10}\left(\frac{12d}{b_d m_l}\right)} \tag{2}$$

Where U - average velocity [cm/s], d - water depth [cm], m_l - total length of the target mussel [cm], b_d - burial depth fraction (DiNicola et al., in revision). The critical shear stress equation used follows Allen and Vaughn (2010):

$$\tau_c = \theta_c g D(\rho_s - \rho) \tag{3}$$

Where θ_c – Shield's parameter, g - acceleration due to gravity [cm/s^3], D - characteristic grain size [cm], ρ_s - density of sediment. For this study, Shield's parameter was taken as 0.045 for all reaches and D was set as the average D_{84} for the entire study area, as a prior study in the Mission Reach showed no significant difference in D_{84} between stable and mobile portions of the bed (DiNicola et al., 2025). This flume study showed subadult mussels were stable in all tested sediment types up to a T_m value of 0.35, after which mobilization began to occur across all size classes (DiNicola et al., in revision).

A 2D HEC-RAS model was developed for the entire Mission Reach to identify simulated stable locations over a range of flows ecologically relevant to the growth of subadult mussels. The model was developed using cross sectional surveys completed in 2022 and calibrated and validated using depth and velocity measurements taken during ecological assessments conducted by SARA, as well as photos taken during floods. The model was run at a series of flows, ranging from baseflow (~1.4 m^3/s) to a 2-year recurrence flow (516 m^3/s). The two-year recurrence interval was selected because significant growth in subadult mussels is expected over this period, increasing their ability to withstand larger flow events (Haag, 2012).

The resulting velocity and depth HEC RAS output rasters (Figure 2c-d) were used to analyze suitable subadult mussel habitat using the following steps. Using Eq. (1), the mussel mobility index (T_m) was calculated across the reach for each flow step and the maximum T_m value for each cell was extracted from across the range of flows to understand the highest threat to mussel stability (Figure 2a). This maximized T_m raster was then adjusted by habitat types delineated using methods outlined in DiNicola et al (2025; Figure 2b). DiNicola et al (2025) showed areas within the Back of Bar and Boulder Field habitat types have increased influence on subadult mussel stability and may not be well accounted for in a HEC RAS model. Next, the adjusted raster was reduced to only include the low flow wetted area of the channel, as mussels can only survive long term in perpetually wetted areas (Strayer, 2008). Finally, the T_m raster was classified into patches where the T_m threshold was less than 0.35 (DiNicola et al., in revision) and were larger than 25m^2, or the minimum area needed to be considered a possible reintroduction area (Figure 2a).

3. Results

Initial results show high levels of suitable mussel habitat for reintroduction in areas of low mussel mobility index and within habitat types that are related to increased stability. Additional expected results include a comparison of different selected sites for reintroduction potential and the verification of two reintroduction sites based on an initial cohort of live subadult mussels reintroduced in the Mission Reach in fall of 2024.

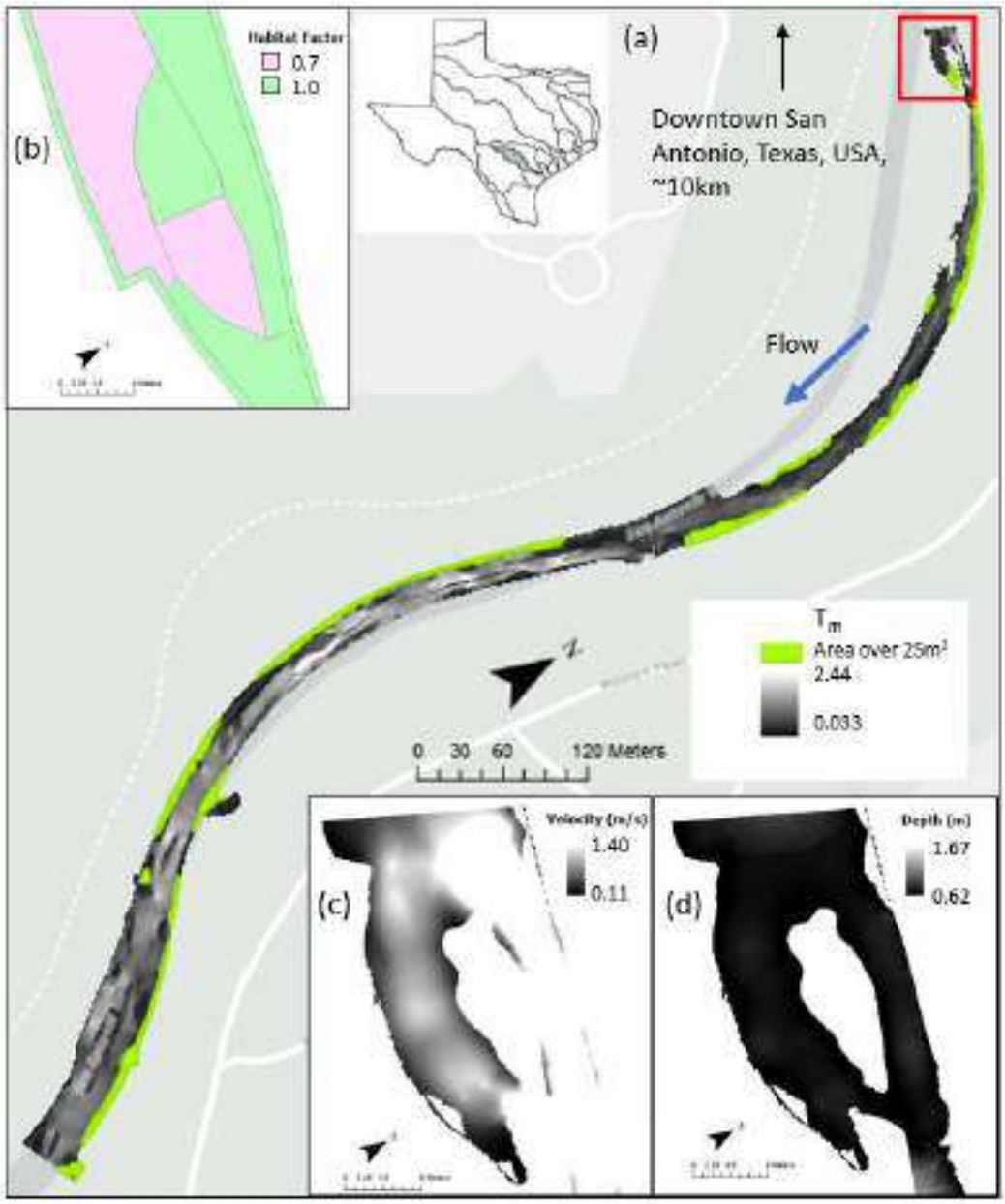

Figure 2. A maximized T_m raster with suitable habitat patches highlighted (a) for a potential reintroduction site in the Mission Reach of the San Antonio River, Texas, USA based on input layers of habitat types (b) and HECRAS 2D model outputs (c, d).

4. Discussion

Freshwater mussel reintroductions are an important restoration activity that supports biodiversity goals. In this study we introduce a series of methods to assess suitable physical habitat for reintroductions. Previous studies have characterized the habitat that adult mussels currently occupy (e.g. Randklev et al., 2019; Roberts et al., 2022; Vaessen et al., 2024) but with this study we attempt to predict suitable habitat for subadult mussels using bed stability and geomorphic features.

We expect these results to provide managers with general guidance on high stability habitat conditions for the reintroduction of subadult mussels. While DiNicola et al. (2025) provides some recommendations based on field studies with 3D printed mussels, this study pairs the conclusions from their field study with a flume study to further characterize habitats beyond those directly in study areas. The methods and analysis presented here provide a repeatable method for assessing large river reaches with a hydraulic model and simple assessments of grain size and habitat types. This model is unique as it targets subadult mussel habitat suitability specifically through the use of the T_m parameter and attempts to fill a gap in current reintroduction practices.

In conclusion, this study uses mobilization thresholds set through flume and field studies to assess suitable subadult mussel habitat for reintroduction across a large, restored river reach. These methods could be used to help managers highlight important data collection and modeling efforts that will provide the highest likelihood of success for future freshwater mussel reintroduction projects.

Acknowledgements

The authors would like to thank Austin Davis, Mitch Magruder and Shaun Donovan at the San Antonio River Authority for providing site access and vital local knowledge. We would also like to thank The Meadows Cetner for Water and the Environment Biological Monitoring Team for their assistance in field data collection.

References

Allen DC, Vaughn CC (2010) Complex hydraulic and substrate variables limit freshwater mussel species richness and abundance, J. N. Am. Benthol. Soc., 29(2):383–394.
Carey CS, Jones JW, Butler RS, Hallerman EM (2015) Restoring the endangered oyster mussel (Epioblasma capsaeformis) to the upper Clinch River, Virginia: an evaluation of population restoration techniques: Freshwater mussel population restoration techniques. Restor. Ecol. 23(4), 447–454.
DiNicola M, Riggins C, Schultz S, Phillips C, Lane B (2025) Assessing suitable habitat for freshwater mussel reintroductions using 3D-printed subadult replicates, Scientific Reports, 15:33119.
DiNicola M, Riggins CL, Garoutte C, Crookston B, Lane B (in revision) Using 3D printed replicates to assess subadult freshwater mussel mobilization thresholds in a flume, Journal of Ecohydraulics.
Haag, WR (2012) North American Freshwater Mussels: Natural History, Ecology, and Conservation, Cambridge University Press.
Lombardi A (2014) Ecosystem under restoration: A sustainable future for the cultural landscape of San Antonio River, Texas. *WIT Trans. Ecol. Environ.* 191, 1139–1151.
Montesanto F, Ohlman LM, Pegg MA (2023) Survival and growth assessment after reintroduction of the pocketbook mussel, Lampsilis cardium Rafinesque, 1820 among three streams in Nebraska (USA), Aquatic Conserv: Mar Freshw Ecosyst, 33:535–548.
Randklev CR, Hart MA, Khan JM, Tsakiris ET, Robertson CR (2019) Hydraulic requirements of freshwater mussels (Unionidae) and a conceptual framework for how they respond to high flows, Ecosphere
Roberts MO, Jacobson RB, Erwin SO (2022) Hydraulics of freshwater mussel habitat in select reaches of the Big River, Missouri, USGS and US Fish and Wildlife, 2022-5002.
Strayer D (2008) Freshwater Mussel Ecology: A Multifactor Approach to Distribution and Abundance, University of California Press.
Vaessen Q, Houbrechts G, Campenhout JV, Hambuckers A (2014) Which enviornmental factors influence the distribution patterns of an endangered freshwater mussel (Unio crassus)? Geomorphology, 454:109180.

Book of Abstracts of the *16th International Symposium on Ecohydraulics*
Challenges and solutions in the time of global changes
August 16–20, 2026, Lausanne, Switzerland
ISSN: 2790-2420 | ISBN: 978-90-837233-9-6 | doi:[10.64697/iahr.proc.ise2026.abs]
© 2026 IAHR. CC BY-NC-ND 4.0

PREFERENTIAL PATHS OF GRASS CARP LARVAE SWIMMING THROUGH PATCHES OF FLOATING VEGETATION: INSIGHTS FROM LABORATORY EXPERIMENTS

Rafael O. TINOCO[1], Vindhyawasini PRASAD[2]

[1] University of Illinois Urbana Champaign
email: tinoco@illinois.edu

[2] Louisiana State University
email: vindhy@lsu.edu

ABSTRACT

Grass carp (*Ctenopharyngodon idella*) is one of four invasive carp species in North America (grass carp, black carp, silver carp, and bighead carp). Once they establish in a water body, they outcompete endemic species and can permanently change the local ecosystem. Efforts to mitigate their spread have had various levels of success. While most strategies focused on removal of adult specimens, recent studies have focused on understanding the transport of early life stages on streams, identifying their response to turbulent conditions (Tinoco et al. 2022) and potential flow-based capture strategies (Prasad et al. 2024, 2025). We conducted a series of laboratory experiments with live grass carp larvae to identify potential preferential pathways and capture areas through a channel with a patch of floating vegetation. We tested different submergence ratios of a dense patch of flexible vegetation over a range of subcritical turbulent flows. Particle image velocimetry was used to characterize the velocity field through and below the patch. The study revealed a clear active response of grass carp larvae to vegetation-generated turbulence and coherent flow structures. Comparing the flow turbulence statistics to the spatial distribution of larvae, we identified that larvae not only looked for areas of low velocity, but rather avoided regions of high shear, and stayed away from areas where turbulent eddies matched the size of larvae. The results provide useful guidelines for the design of monitoring, capturing, and management strategies of fish larvae in vegetated streams.

Keywords: *Grass carp; Invasive fish*; *Turbulence; Floating vegetation.*

1. Methods

Experiments were conducted in an Odell-Kovasznay type recirculating flume at the Ecohydraulics and Ecomorphodynamics Laboratory at the University of Illinois Urbana Champaign. The flume (Fig.1a) is 0.15 m wide, with a straight test section 2 m long, and maximum water depth of 0.6 m. A 1 m long patch was made with flexible plants, $h = 7$ cm long. To ensure an inflection point in the velocity profile, volumetric frontal area of the patch was set as $a = 10\ m^{-1}$, such that the parameter $ah = 0.7$. Two water depths were tested, $H = 0.20\ m$ and $0.30\ m$. A continuous-wave laser with a cylindrical lens and a 5 MP high-speed camera were used for the particle image velocimetry (PIV) setup (Fig.1b) to characterize the velocity field. Depth-averaged velocities for the tests covered a range of $U = 5.1 - 12.2\ cm/s$. Live larvae ~72 hours post-hatching were released upstream of the patch and allow to recirculate for several minutes before collecting images. Sixty seconds-long videos with 1920 x 1080 pixels resolution and time-lapses with 4000 x 6000 pixels image resolution were captured for each test. To assess active response of larvae to the flow conditions, experiments were repeated with euthanized larvae and compared with the patterns identified from live larvae.

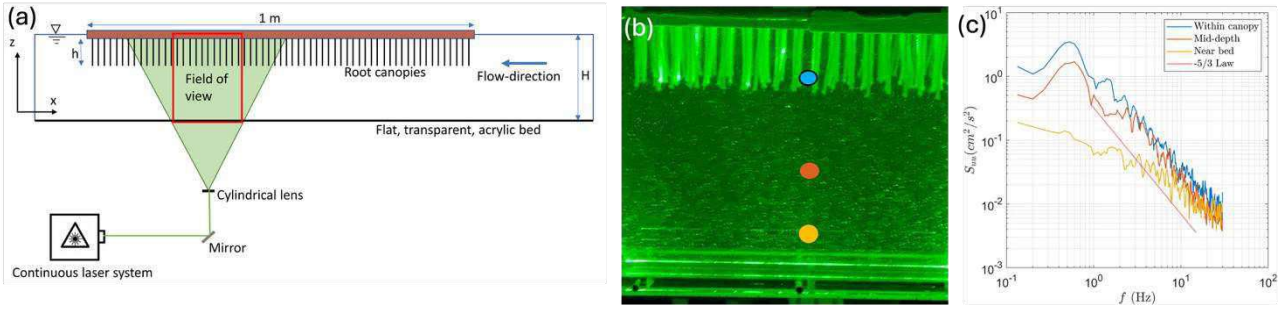

Fig. 1. *(a) Side-view sketch of the experimental setup indicating field of view and location of PIV test section. (b Side view of the vegetation patch and 3-reference locations: within the patch (blue), mid depth (orange), and near-bed (yellow). (c) Velocity spectra showing identifiable turbulence timescales at 3 relevant locations.*

2. Results and Discussion

Velocity data showed four distinguishable regions: high speed flow near the bed, low-speed flow within the patch, a mixing layer at the interface, and a recirculation region at the downstream end of the patch. Analysis of velocity spectra (Fig.1c) showed distinct time scales associated to these layers, with smaller-scale stem-scale turbulence within the patch, and canopy-scale turbulence below it. The collected video and time-lapses identified distinct behavior from the grass carp larvae (as shown in Fig.2): (1) Rather than seeking the regions of lower velocity as shelter, larvae moved away from the patch and away from the shear layer region, seemingly preferring to swim through regions of higher velocity. (2) Larvae avoided areas where turbulent eddies length scales were close to larvae size, preferring areas with eddies much larger that their size. (3) Larvae accumulated at the recirculation zone at the downstream end of the patch. (4) Tests with dead larvae didn't show the same patterns described in (1), (2) and (3), proving that the observed accumulation and avoidance corresponded to an active response rather than just passive transport by the flow.

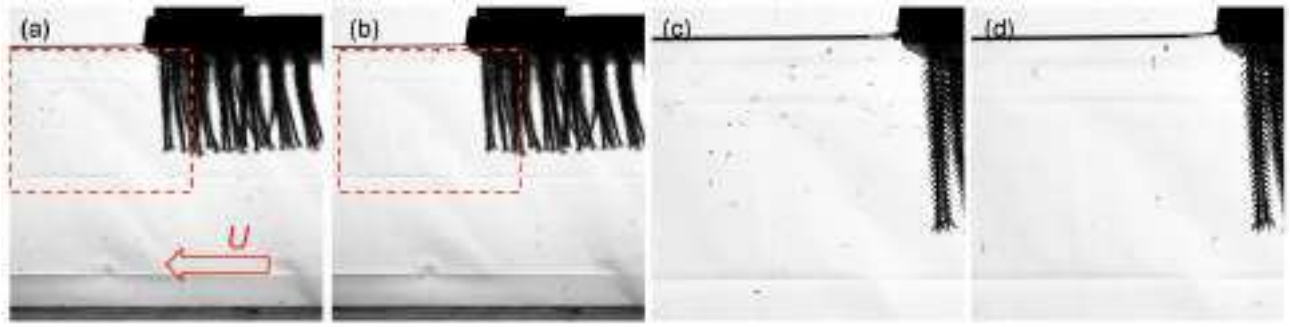

Fig. 2. Test with live (a) and dead (b) larvae. Notice the accumulation of live larvae at the downstream end of the patch (flow right to left) and preference to pass close to the bed instead of through the plants. Zoomed-in views of the downstream regions marked in a,b are shown in c,d, respectively. Dead larvae (b) do not accumulate on the wake, and a large percentage travel and are captured within the plants.

Consistent results across two water depths and three velocities confirm the active response of grass carp larvae to the flow patterns generated by a dense patch of floating vegetation. Such patterns can be used to better inform sampling and monitoring strategies of invasive fish in affected rivers.

Acknowledgements

Research was funded by the cooperative agreement G21AC10372 for CESU-affiliated partner with U.S. Geological Survey – Great Rivers Cooperative Ecosystem Studies Unit. All handling methods used in this study were in accordance with protocols approved by the Institutional Animal Care and Use Committee within the guidelines of the University of Illinois at Urbana-Champaign. Any use of trade, firm, or product names is for descriptive purposes only and does not imply endorsement by the U.S. Government.

References

Prasad, V., Suski, C.D., Jackson, P.R., George, A., Chapman, D., Fischer, J.R. and Tinoco, R.O. (2024). Limiting downstream dispersal of invasive carp egg surrogates using a laboratory-scale oblique bubble screen. Journal of Ecohydraulics, TJOE (2332994).

Prasad V., Andrade Ramos J.M., Suski C.D., Jackson P.R., George A.E., Chapman D., Fischer J.R., Stahlschmidt B.H., Tinoco R.O. (2025). Efficacy of oblique bubble screen deterrents on redirecting live eggs and larvae of grass carp", Water Resources Research, WRCR70586.

Tinoco, R. O., Prada, A. F., George, A. E., Stahlschmidt, B. H., Jackson, P. R., & Chapman, D. C. (2022). Identifying turbulence features hindering swimming capabilities of grass carp larvae (*Ctenopharyngodon idella*) through submerged vegetation. Journal of Ecohydraulics, 7(1), 4-16.

Book of Abstracts of the *16th International Symposium on Ecohydraulics*
Challenges and solutions in the time of global changes
August 16–20, 2026, Lausanne, Switzerland
ISSN: 2790-2420 | ISBN: 978-90-837233-9-6 | doi:[10.64697/iahr.proc.ise2026.abs]
© 2026 IAHR. CC BY-NC-ND 4.0

PATHWAYS: AN ALGORITHM FOR MODELING MULTIPLE SWIMMING PATHS BETWEEN HABITATS AND THEIR ENERGETIC COSTS IN A 2D FLOW FIELD

Patrick HOLZAPFEL[1], Daniel WILDT[2], Lisa SCHMALFUSS[1], Gregory PASTERNACK[3], Christoph HAUER[1]

[1] CD-Laboratory for Sediment Research and Management, Institute of Hydraulic Engineering and River Research, Department of Landscape, Water and Infrastructure, BOKU University, Austria
patrick.holzapfel@boku.ac.at

[2] AFRY Austria GmbH, Austria
daniel.wildt@afry.com

[3] University of California Davis, USA
gpast@ucdavis.edu

ABSTRACT

Fluvial ecosystems form dynamic mosaics of interconnected habitat patches. The spatial arrangement and temporal variability of these patches influence fish life cycles. For salmonid larvae, access to post-emergence rearing habitats is constrained not primarily by distance but by the energetic cost of moving through flowing water. We present *Pathways*, a Python algorithm quantifies microhabitat connectivity by identifying energetically feasible movement routes across two-dimensional, depth-averaged hydrodynamic fields and summarizing accessibility through an energy-based connectivity metric. Habitat patches are delineated using Habitat Suitability Modeling to identify source and target functional units. The algorithm computes multiple candidate paths across the flow field and evaluates their feasibility using species- and size-specific fatigue relationships across different implemented swimming modes, retaining only those routes consistent with sustained swimming capacity. For each feasible route, *Pathways* calculates the time-integrated swimming power required to traverse local velocity fields, treating this value as the energetic cost of movement. Connectivity from a source to one or multiple targets is summarized using the Habitat Connectivity Index (HCI), which weighting target Weighted Usable Area (WUA) by the median energetic cost across feasible routes and scales this value by a Probability of Discoverability term representing the likelihood that a fish can successfully locate and reach the target under its movement and energetic constraints. Pathways outputs feasible pathways, path-specific energetic costs, and patch-level connectivity metrics, and operates directly on depth-averaged hydrodynamic grids. We applied the framework to grayling larvae in a riffle–pool reach of the Gail River (Austria) to address three questions: (i) How does discharge during emergence influence access to rearing habitats? (ii) How much do individual spawning locations differ in connectivity, and how does discharge modulate these differences? Results demonstrate strong discharge sensitivity and distinct variation in modeled connectivity among spawning sites, with mean HCI values declining from 69.8 m^2 mJ^{-1} at low flow to 3.4 m^2 mJ^{-1} at mean high flow. These findings indicate that increasing discharge substantially reduces accessible habitat by elevating movement costs and constraining the spatial extent of reachable habitat.

Keywords: habitat connectivity; larval dispersal; path energy cost; grayling; river hydraulics

1. Introduction

For riverine fish, successful completion of the life cycle depends not only on habitat availability but also on functional connectivity between spawning, nursery, and rearing habitats (Bisson et al., 1982; Schiemer & Spindler, 1989). In salmonids, the spatial relationship between spawning grounds and post-emergence habitats is particularly critical, as larvae must rapidly access low-velocity, shallow nursery areas suited to their limited swimming capacity.

Traditional habitat connectivity metrics, largely adapted from terrestrial landscape ecology, emphasize Euclidean or hydrographic distance between patches. However, in riverine systems, accessibility is governed less by distance than by hydraulic resistance and the energetic cost of movement through flowing water. For larval fish, swimming can represent a major component of metabolic expenditure, and excessive energy loss during dispersal may reduce growth, survival, and recruitment success. Connectivity in rivers therefore requires an energetically explicit framework.

This study introduces an energy-based habitat connectivity concept for salmonid larvae. Connectivity is quantified using (i) the energetic swimming cost required to reach target habitats, (ii) the Weighted Usable Area to represent habitat quality, (iii) the median cost across multiple feasible pathways rather than a single least-cost path, and (iv) a Probability of Discoverability reflecting movement potential and energetic constraints across different modeled swimming modes. These components are integrated into a Python-based ecohydraulic algorithm that identifies multiple energetically feasible routes across hydrodynamic flow fields and computes patch-level connectivity metrics. The framework was applied to grayling larvae to evaluate how discharge influences access to rearing habitats, and how connectivity varies among spawning locations.

2. Methods

In this study, the Habitat Connectivity Index (HCIj,i) for a given starting location j (e.g., a spawning site) is calculated by dividing the Weighted Usable Area (WUAj,i) of each target patch i (e.g., rearing habitat; Bovee & Cochnauer, 1977) by the median energetic cost of all modeled paths leading to that patch (Wj,i). This value is further adjusted by a Probability of Discoverability term (PDj,i) as described in Holzapfel et al., 2026a.

$$HCI_{tot,j} = \sum_{i=1}^{n} \frac{WUA_{j,i}}{\widetilde{W_{j,i}}} * P_{D_{j,i}} \quad (1)$$

Accordingly, we developed an algorithm to find multiple candidate routes between start and target locations within a hydrodynamic field and to compute the energetic cost ($W_{j,i}$) for traversing each route. Available paths for fish movement between habitats within the model domain are evaluated based on the energetic cost of locomotion, which depends on swimming mode. The Pathways algorithm implements the distinct swimming modes described by Pavlov et al. (2008) and Zens et al. (2017) (

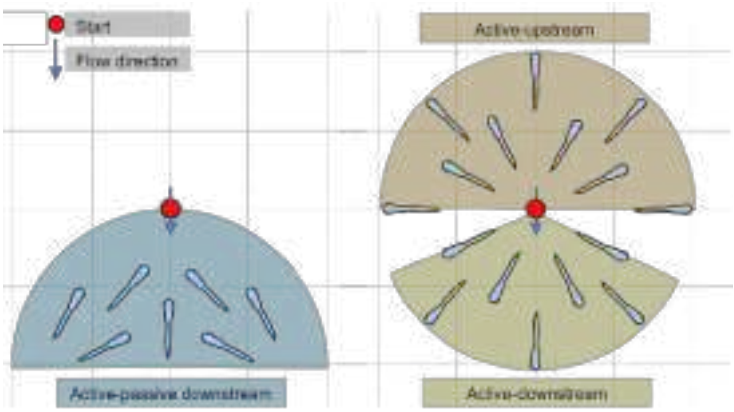

Fig 1. Swimming modes implemented in the Pathways algorithm (modified after Holzapfel et. al., 2026a)

) to compute mode-specific energy expenditure and identify feasible routes, using species- and size-dependent fatigue curves to parameterize swimming endurance (Katopodis & Gervais 2016).

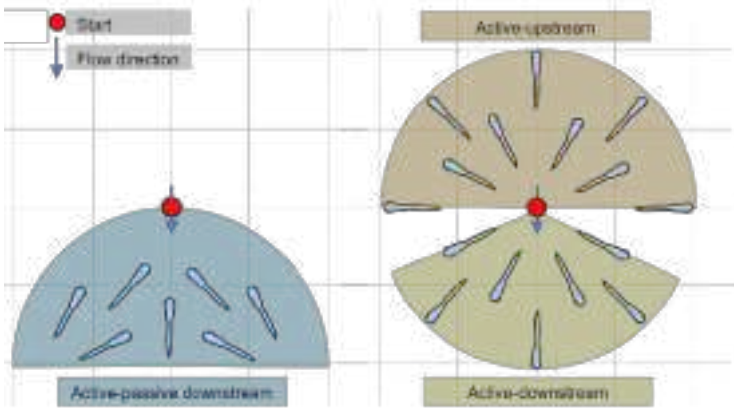

Fig 1. Swimming modes implemented in the Pathways algorithm (modified after Holzapfel et. al., 2026a)

This energy is calculated as the time integral of the power P needed to swim at a relative velocity Ur through a fluid velocity field u (McElroy et al., 2012). The Python implementation is publicly available on Zenodo (doi.org/10.5281/zenodo.15488580; Holzapfel et al., 2026b). We employed the depth-averaged 2D model HydroAS (Nujic, 1998) to compute hydraulic variables under steady-state conditions on a 0.5 m Cartesian grid, enabling assessment of discharge scenarios (n=5) statistically relevant to post-emergence dispersal in the Austrian Gail River. Seven spawning patches were analyzed with respect to their connectivity to early rearing habitats. A conceptual flowchart illustrating the design and application of the Pathways algorithm is shown in Fig 2.

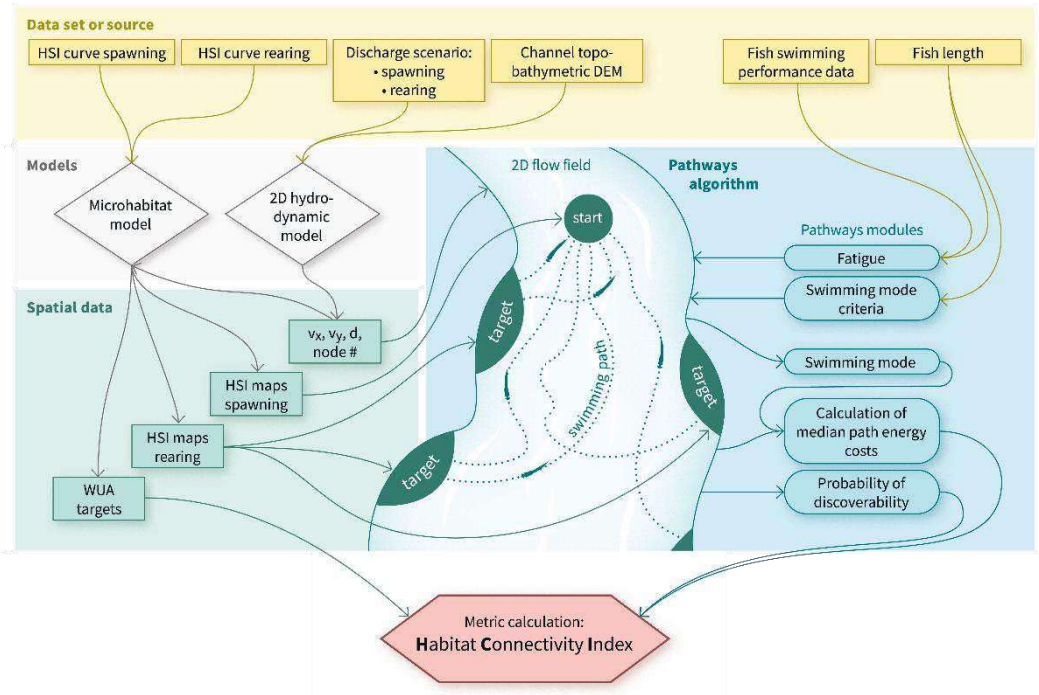

Fig 2. Conceptual flowchart illustrating the design and application of the Pathways algorithm, developed as a tool for calculating an energy-based Habitat Connectivity Index (Holzapfel et.al., 2026a)

3. Results

Figure 4a shows patch-specific HCI_{tot} as a function of discharge together with reach-scale rearing WUA. P4 has the lowest modelled connectivity, peaking at 3.7 m^2mJ^{-1}at low flow conditions (Q_L=49.7 m^3s^{-1}) and declining thereafter. P6 and P7 are high at Q_L (98.4 and 82.5 m^2mJ^{-1}) and remain comparatively stable across the modeled range. In contrast, P5 reaches 127.9 m^2mJ^{-1} at Q_L but drops to 14.2 at mean flow conditions (Q_M=74.4 m^3s^{-1}) and to zero for $Q>Q_M$ indicating strong discharge sensitivity. P3 is consistently low at Q_L and Q_M (45.2 and 10.9 $m^2\ mJ^{-1}$) because accessible rearing habitat is located primarily upstream. Elevated energetic costs down-weight these links, yielding $HCI_{tot} < 0.2$ m^2mJ^{-1} beyond Q_M. P1 shows the highest values at Q_M and Q_1 (Q=111.3 m^3s^{-1}), while P2 tracks the reach-wide average and remains nonzero at Q_{MH}. Across all spawning patches, the mean modeled HCI_{tot} declines with increasing discharge and is well described by a

power-law fit. In contrast, the among-patch variability, quantified by the coefficient of variation (*CV*), increases approximately linearly with discharge. Correspondingly, *CV* is high at Q_{MH} (Q=187.0 m^3s-1, CV=1.14) and highest at Q_2 (Q=149.5 m^3s^{-1}, CV=1.30), whereas it is lower at Q_L (Q=49.7 m^3s^{-1}, CV=0.53) and reaches its minimum at Q_M (Q=74.4 m^3s^{-1}, CV=0.47), indicating the most uniform patch performance at this flow (Fig 3b).

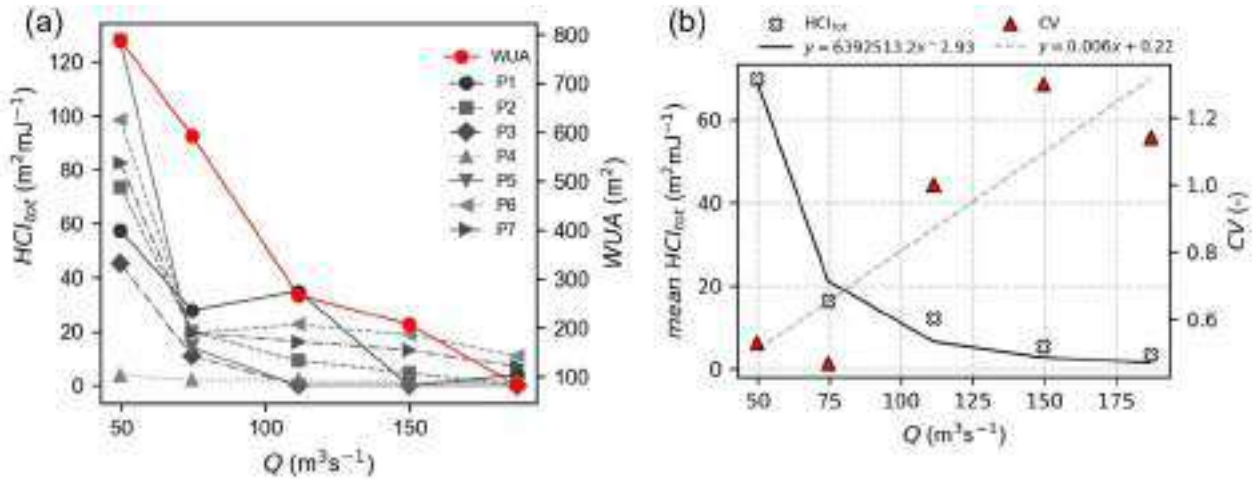

Fig 3. (a) Patch-wise HCI_{tot} values and total WUA across the domain as function of discharge; (b) mean HCI_{tot} values and coefficient of variance (*CV*) computed across all spawning patches as function of discharge (modified after Holzapfel et. al., 2026a).

4. Conclusions

We present a biologically grounded habitat connectivity metric coupled with the *Pathways* algorithm that integrates multiple energetic path costs, swimming modes, and length-dependent fatigue, and expresses connectivity as *WUA* (m^2) accessible at median path energy cost, quantified as *HCItot* ($m^2\,mJ^{-1}$). Applied to the Austrian Gail River, the framework shows that connectivity between grayling (*Thymallus thymallus*) spawning and rearing patches is highly sensitive to discharge during emergence and to the spatial configuration of spawning patches, with variability increasing as discharge rises. The approach supports transparent cost-benefit analyses to prioritize restoration actions, such as gravel augmentation or nesting-site placement, and is adaptable across life stages, species, and ecological scenarios. Together, these advances provide a transferable tool to diagnose and enhance functional connectivity in rivers and to inform conservation and management.

References

Bisson PA (1982) A system of naming habitat types in small streams. with examples of habitat utilization by salmonids during low streamflow. In Acquisition and utilization of aquatic habitat inventory information, Am. Fish. Soc., West. Div., Symp. Proc., 1982.

Holzapfel P, Wildt D, Schmalfuss L, Pasternack G, Hauer C (2026a) Quantifying connectivity between functional fish habitats: A novel energy-based approach assessing multiple pathways, Ecological Modelling, 515, 111515, https://doi.org/10.1016/j.ecolmodel.2026.111515.

Holzapfel P, Wildt D, Schmalfuss, L (2026b) Pathways: An Algorithm for Modeling Multiple Swimming Paths between Habitats and Their Energetic Costs in a 2D Flow Field. Zenodo. https://doi.org/10.5281/zenodo.15488580

Katopodis C, Gervais R (2016) Fish swimming performance database and analyses. Canadian Science Advisory Secretariat.

McElroy B, DeLonay A, Jacobson R (2012) Optimum swimming pathways of fish spawning migrations in rivers. Ecology 93.1, pp. 29–34. doi: 10.1890/11-1082.1.

Pavlov DS, Mikheev VN, Lupandin, AI, Skorobogatov MA (2008) Ecological and behavioural influences on juvenile fish migrations in regulated rivers: a review of experimental and field studies. Hydrobiologia, 609, 125-138.

Schiemer F, Spindler T (1989) Endangered fish species of the Danube river in Austria. - Regulated Rivers: Research and Management 4.

Zens B, Glas M, Tritthart M, Habersack H, Keckeis H (2017) Movement patterns and rheoreaction of larvae of a fluvial specialist (nase, Chondrostoma nasus): The role of active versus passive components of behaviour in dispersal. Canadian Journal of Fisheries and Aquatic Sciences, 75(2), 193–200. https://doi.org/10.1139/cjfas-2016-0276

Session A3

Ecomorphodynamics: linking flow, sediment and biota, instabilities, and patterns' formation

Book of Abstracts of the *16th International Symposium on Ecohydraulics*
Challenges and solutions in the time of global changes
August 16–20, 2026, Lausanne, Switzerland
ISSN: 2790-2420 | ISBN: 978-90-837233-9-6 | doi:[10.64697/iahr.proc.ise2026.abs]
© 2026 IAHR. CC BY-NC-ND 4.0

FROM STOCKPILE EROSION TO CHANNEL ADJUSTMENT: INVESTIGATING THE HYDRO-MORPHOLOGICAL IMPACTS OF SEDIMENT REPLENISHMENT VIA NUMERICAL SIMULATION

Jiaqi LIN[1], Sameh A. KANTOUSH[2], Tetsuya SUMI[2]

[1]China Institute of Water Resources and Hydropower Research, Beijing, 100038, China
email: linjiaqi19950205@126.com

[2]Disaster Prevention Research Institute (DPRI), Kyoto University, Kyoto, 611-0011, Japan.
email: kantoush.samehahmed.2n@kyoto-u.ac.jp
email: sumi.tetsuya.2s@kyoto-u.ac.jp

ABSTRACT

Sediment replenishment (SR) is a widely adopted river management strategy globally, yet its long-term implementation in Japan exhibits distinct characteristics that warrant deeper investigation into its geomorphological impacts. This study examines the erosion of SR stockpiles and their downstream effects in the Naka River using field analysis and a two-dimensional depth-averaged hydromorphodynamic numerical model (Telemac-2D). We evaluated the influence of flushing flow (magnitude and frequency) and stockpile configuration (location and geometry) using key metrics such as transport ratio (TR) and the Hydro-Geomorphological Index of Diversity (HMID). Results show that higher-magnitude flushing flows are less effective in promoting stockpile erosion; instead, an optimal discharge of about 40% of the bankfull flow, applied with typical duration and frequency, achieves the optimal erosion effectiveness. Introducing a second flood pulse or using a double-stockpile SR arrangement enhanced erosion as well, increasing TR by 1.5% and 3%, respectively. Regarding the downstream impacts, the additional sediment supply from SR site stimulated the formation of riffles and bars, elevating HMID values locally. These findings offer important insights for predicting SR erosion and associated hydro-morphological changes in the Naka River, while providing practical guidance for designing effective sediment replenishment in similar fluvial systems worldwide.

Keywords: *Sediment replenishment, Numerical simulation, Stockpile erosion, Hydro-morphological Impacts, Telemac-2D*

1. Introduction

SR, as a common mitigation approach for river restoration, has already been implemented around the world (Brousse et al., 2019; Gaeuman, 2014; SA Kantoush & Sumi, 2011; Stahly et al., 2019). During the implementation of SR, the erosion process of the SR stockpile and the downstream geomorphological changes are the essential patterns that affects whether the projects are successfully conducted or not (Sameh Kantoush, Sumi, & Kubota, 2010).

Numerous numerical and experimental models have been developed to analyze sediment replenishment (SR) erosion and downstream geomorphic responses (Cajot et al., 2012; Chardon et al., 2021; Hiroshi & Parker, 2012; Schleiss et al., 2016). While two-dimensional (2D) models are widely used for their efficacy in simulating flow and sediment transport, key challenges persist. Specifically, the complex relationships among flushing flow, SR erosion, and downstream hydo-morpho-ecological impacts have not been thoroughly examined. Furthermore, the influence of SR characteristics, such as placement locations, sizes of placed stockpiles remains inadequately studied in project-based contexts.

To address these gaps, this study establishes a two-dimensional model to simulate geomorphological changes induced by SR implementation in the Naka River. Using this model, we evaluate the impacts of different SR characteristics—including flushing flow magnitude, replenishment location, and sizes of placed stockpiles—

on the erosion process and downstream responses. The effectiveness is assessed using key indicators such as transport ratios (TR), and Hydro-Geomorphological Index of Diversity (HMID) (Gostner et al., 2012).

2. Materials and methods

The Naka River in Japan, located in Tokushima Prefecture, was selected as the study area for our SR simulation research. The construction of replenishment sites was implemented downstream of the Nagayasuguchi dam as a stockpile on the right side of the bank with a volume of approximately 200,000 m^3. During flood seasons, the flushing flow released from the upstream dam erodes the stockpile and transports the sediment downstream (**Error! Reference source not found.**, Left). The study reach is the 13km meandering channel downstream of the SR site.

Regarding the numerical simulation, we established a 2D numerical model based on the triangle finite element method in Telemac-2D. The mesh size is 20m for the flood plain, 10m for the active channel, and 4m for the SR site (**Error! Reference source not found.**, Right). The 2017 DEM data measured by Green Lidar (including the underwater part) was utilized to interpolate the topographical value of the study domain.

Moreover, the bank erosion mode is crucial for simulating erosion in replenished material. In Telemac, this mode is called 'Maxslope', developed by El Kadi Abderrezzak et al. (2016). It uses the angle of repose (φ) to govern failure: at each time step, the slope of each element is compared to φ; if steeper, the element is rotated around its axis until the slope equals φ.

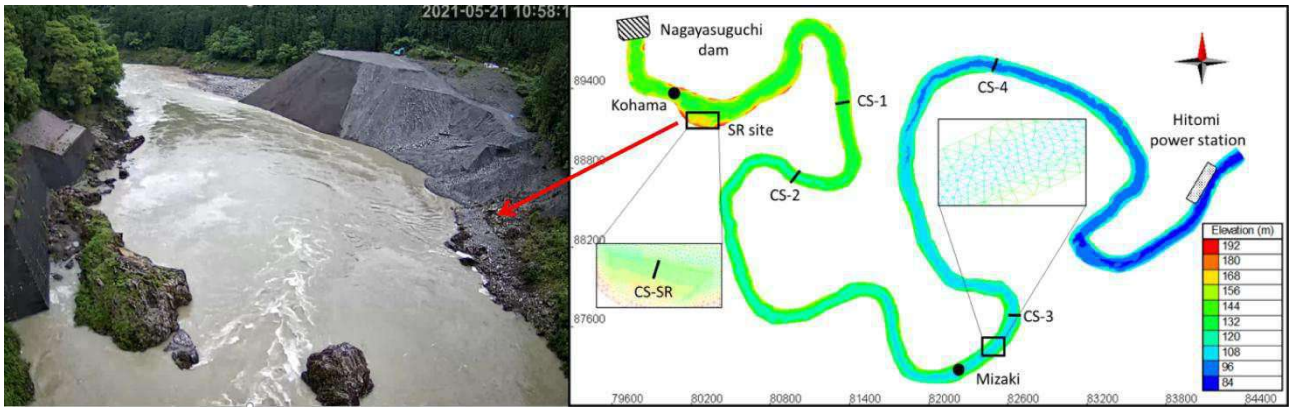

Fig. 1 Left figure: the SR stockpile downstream of the Nagayasuguchi dam; Right figure: the geometric mesh for numerical simulation (CS means the measured cross sections).

The assessment of simulated hydro-morpho-ecological changes is based on three indicators. Among them, the Transport Ratio (TR) serves as a measure of the efficiency of sediment redistribution (SR) and is defined as follows:

$$\mathrm{TR} = \frac{\text{Transported volume } (\mathrm{m}^3)}{\text{Accumulated placed volume } (\mathrm{m}^3)} * 100 \quad (1)$$

where the transported volume is the total volume of sediment that is eroded and transported to the downstream reach, and the accumulated volume is the total volume of sediment placed at the SR site.

The Hydro-Geomorphological Index of Diversity (HMID) is a simple indicator to access the diversity and quality of the habitat structures (Gostner et al., 2012):

$$\mathrm{HMID}_{\mathrm{Site}} = \left(1 + \frac{\sigma_v}{\mu_v}\right)^2 \cdot \left(1 + \frac{\sigma_d}{\mu_d}\right)^2 \quad (2)$$

Where σ_v, σ_d and μ_v,μ_d are the standard deviation and mean value of flow velocity and water depth within the investigated reach.

To investigate the impact of flushing magnitude and frequency on SR erosion, we designed single and double flood scenarios (

Fig. 2 (a) and (b)). The double-flushing pulses was designed based on different flushing durations by maintaining the same increasing water volume and replenishing sediment sizes. Subsequently, two new SR strategies were developed: SC-SR1, which reduces height, increases length, and shifts position mid-channel; and SC-SR2, which incorporates additional stockpiles (

Fig. 2 (c)).

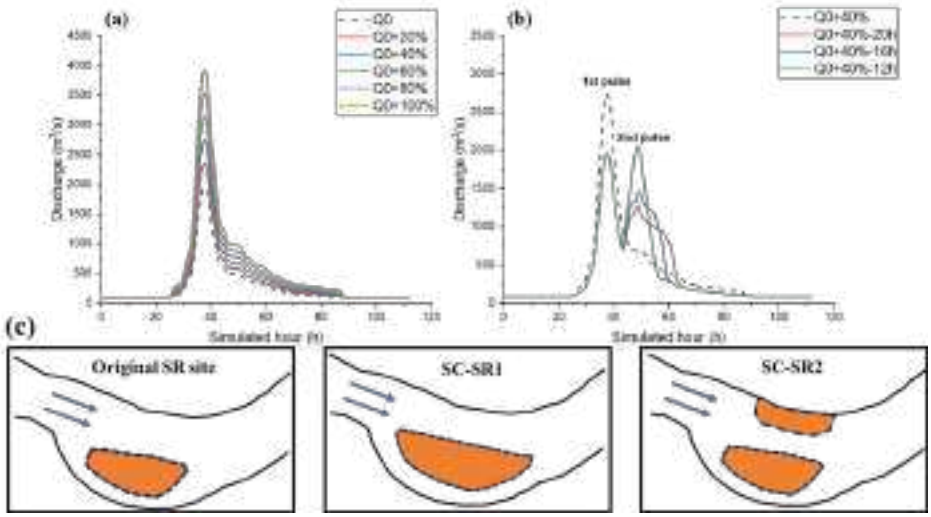

Fig. 2 Designed hydrographs and SR sites for the simulated scenarios. (a) Hydrographs for single flood cases; (b) hydrographs for two flood cases; (c) plan view of the replenishment stockpile for new arrangements.

3. Results and discussion

Considering the SR stockpile erosion, for single flood case, a higher magnitude of flushing flow cannot efficiently promote the erosion of SR sediment since the increase in TR is only approximately 2% if the flushing magnitude is increased by 100%. Q0+40% is the optimal value of flushing flow where the increasing rate of TR reaches the maximum (**Fig. 3** (a)). Moreover, introducing an additional flood pulse with optimal duration (16h for this case) can efficiently facilitate SR erosion, and the eroded volume and TR are enhanced by approximately 1.5% compared with those in the case of a single flood pulse (**Fig. 3** (b)). Owing to the new arrangement of SR site, Constructing an additional stockpile (SC-SR2) can narrow the channel to increase the flow velocity and submerged ratio and promote the SR sediment transportation (more sediment eroded for SC-SR2 in **Fig. 3** (c)).

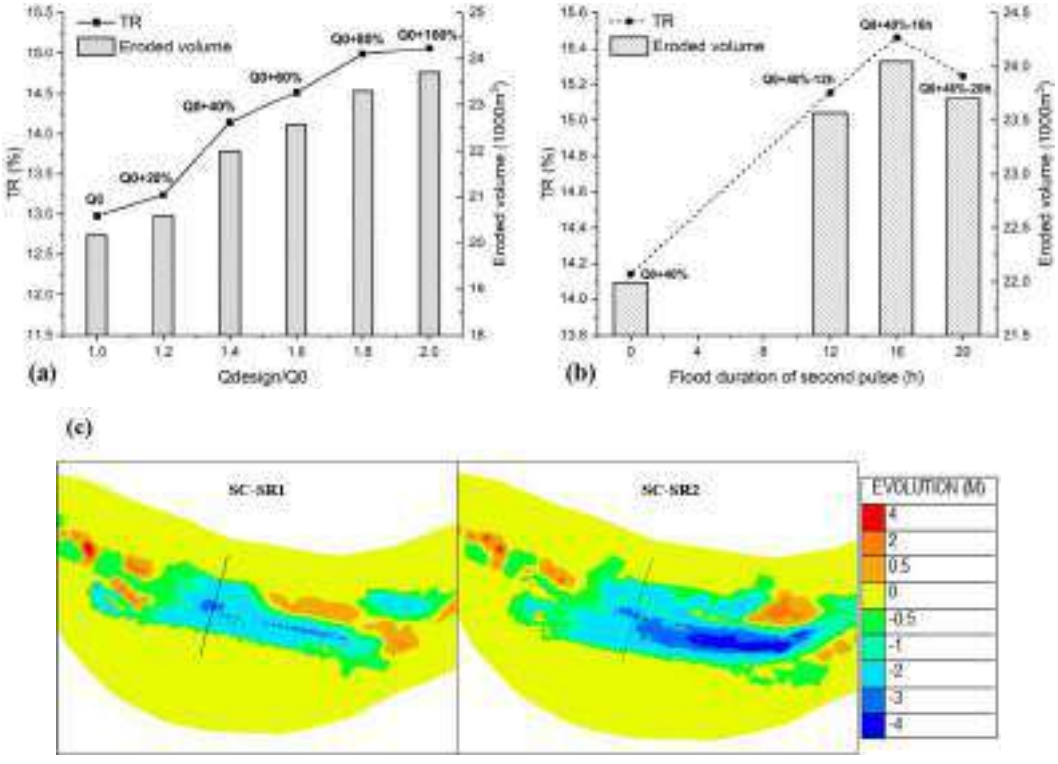

Fig. 3 (a) The variation of TR value and eroded volume at the SR site with the increase of single flood magnitude. (b) TR and eroded volume at the SR site between a single flood pulse and two flood pulses. (c) The sediment erosion and deposition at the SR site for new SR arrangement scenarios.

The downstream response was assessed based on the variation of HMID value (**Table 1**). The double-flood pulse (SC-SR2) resulted in greater sediment deposition along the reach compared to the single-flood event, with the most pronounced impact on HMID (average enhance 8.91%). The bed evolution results indicate that significant sediment deposition occurred in SC-SR2, particularly along the convex bank of the meandering channel. This process facilitated the formation of multiple point bars, which subsequently altered the local flow regime, leading to higher HMID values. These newly formed point bars contribute to ecological restoration in the SR by providing critical habitats and enhancing hydrologic and geomorphic stability.

Table 1 The results of HMID for scenarios of different flood pules and SR arrangement. The variation is calculated based on the initial condition (before SR).

Distance from SR site (km)	Before SR	Q0		Q0+40%-16h		SC-SR1		SC-SR2	
	Value	Value	Variation	Value	Variation	Value	Variation	Value	Variation
0~1	9.929	10.052	1.22%	10.42	4.71%	9.622	-3.19%	10.68	7.03%
1~2	11.191	11.892	5.89%	12.452	10.13%	11.597	3.50%	11.78	5.00%
2~3	9.976	11.06	9.80%	10.946	8.86%	11.595	13.96%	11.518	13.39%
3~4	9.46	9.971	5.12%	9.928	4.71%	9.827	3.73%	9.877	4.22%
4~5	11.324	12.3	7.93%	12.402	8.69%	12.358	8.37%	12.363	8.40%
5~6	11.32	11.512	1.67%	11.369	0.43%	11.305	-0.13%	11.335	0.13%
6~7	7.835	9.312	15.86%	9.687	19.12%	9.608	18.45%	9.616	18.52%
7~8	10.835	12.287	11.82%	12.303	11.93%	12.495	13.29%	12.497	13.30%
8~9	8.55	9.218	7.25%	9.658	11.47%	9.687	11.74%	9.685	11.72%
9~10	9.105	9.125	0.22%	9.238	1.44%	9.26	1.67%	9.269	1.77%
10~11	9.346	10.708	12.72%	10.865	13.98%	10.895	14.22%	10.882	14.12%
11~12	15.467	18.578	16.75%	18.417	16.02%	18.177	14.91%	18.201	15.02%
12~13	10.746	11.418	5.89%	10.707	-0.36%	11.098	3.17%	11.106	3.24%
Average	10.391	11.341	7.86%	11.415	8.55%	11.348	7.98%	11.447	8.91%

4. Conclusion

This study employed a two-dimensional numerical model to simulate sediment replenishment (SR) stockpile erosion and its downstream geomorphological impacts in the Naka River, Japan. Numerical experiments reveal that contrary to expectations, higher-magnitude flushing flows are less effective than a moderate discharge of approximately 40% bankfull flow. Erosion and sediment transport were further enhanced by either a second flood pulse or a double-stockpile configuration. The resulting sediment pulse stimulated the formation of bars and riffles near the site, increasing habitat diversity as measured by the HMID. Notably, the double-stockpile arrangement combined with double floods was identified as the most effective strategy for both maximizing stockpile erosion and optimizing downstream habitat heterogeneity.

References

[1]Brousse, G., et al. (2019). Channel response to sediment replenishment in a large gravel-bed river: The case of the Saint-Sauveur dam in the Buëch River (Southern Alps, France). *River Research and Applications, 36*(6), 880-893.

[2]Cajot, S., et al. (2012). *Reservoir sediment management using replenishment: a numerical study of Nunome Dam.* International Symposium on Dams for a changing world-80th Annual Meeting and 24th Congress of CIGB-ICOLD.

[3]Chardon, V., et al. (2021). Efficiency and sustainability of gravel augmentation to restore large regulated rivers: Insights from three experiments on the Rhine River (France/Germany). *Geomorphology, 380*, 107639.

[4]El Kadi Abderrezzak, K., et al. (2016). Modelling river bank erosion using a 2D depth-averaged numerical model of flow and non-cohesive, non-uniform sediment transport. *Advances in Water Resources, 93*, 75-88.

[5]Gaeuman, D. (2014). *Analyses to support gravel augmentation recommendations for the Trinity River, California*.

[6]Gostner, W., et al. (2012). The hydro-morphological index of diversity: a tool for describing habitat heterogeneity in river engineering projects. *Hydrobiologia, 712*(1), 43-60.

[7]Hiroshi, M., & Parker, G. (2012). Numerical simulation of low-flow channel evolution due to sediment augmentation. *International Journal of Sediment Research, 27*(3), 351-361.

[8]Kantoush, S., & Sumi, T. (2011). *Sediment replenishing measures for revitalization of Japanese rivers below dams.* Paper presented at the Proceedings of the 34th World Congress of the International Association for Hydro-Environment Research and Engineering: 33rd Hydrology and Water Resources Symposium and 10th Conference on Hydraulics in Water Engineering.
[9]Kantoush, S., Sumi, T., & Kubota, A. (2010). Geomorphic response of rivers below dams by sediment replenishment technique. *River Flow 2010*, 1155-1164.
[10]Schleiss, A. J., et al. (2016). Reservoir sedimentation. *Journal of Hydraulic Research, 54*(6), 595-614.
[11]Stahly, S., et al. (2019). Sediment replenishment combined with an artificial flood improves river habitats downstream of a dam. *Sci Rep, 9*(1), 5176.

Book of Abstracts of the *16th International Symposium on Ecohydraulics*
Challenges and solutions in the time of global changes
August 16–20, 2026, Lausanne, Switzerland
ISSN: 2790-2420 | ISBN: 978-90-837233-9-6 | doi:[10.64697/iahr.proc.ise2026.abs]
© 2026 IAHR. CC BY-NC-ND 4.0

GENERATING SYNTHETIC TERRAIN MODELS FROM SPARSE HISTORIC DATASETS FOR ECOHYDRAULIC ASSESSMENT

Jared STIEVE[1], Belize LANE[2], Anzy LEE[3]

[1] Civil and Environmental Engineering, Utah State University, Logan, Utah, USA
email: jared.stieve@usu.edu

[2,3] Civil and Environmental Engineering, Utah State University, Logan, Utah, USA
email: belize.lane@usu.edu
email: anzy.lee@usu.edu

ABSTRACT

A challenge in assessing long-term channel change and the impact to aquatic habitat is having sufficient channel morphology to quantify habitat conditions at a relevant scale and resolution. Current ecohydraulic approaches (e.g. 2D aquatic habitat modeling) require high-resolution digital elevation models (DEMs) as input into 2D hydraulic models. This allows us to accurately characterize microhabitat conditions for a range of species and life stages. Unfortunately, many historic, long-term channel morphology monitoring protocols rely on channel thalweg and cross-section surveys which are too coarse to use simple interpolation schemes to create DEMs. New geometric channel modeling techniques can potentially reverse engineer high-resolution terrains using these sparse datasets. In this presentation, we will show how we leverage channel thalweg and cross-section data with aerial imagery to reverse engineer synthetic terrains for a highly dynamic river in California. This will then allow us to characterize changes in aquatic habitat using 2D hydraulic models as the channel morphology evolved following episodic, extreme inputs of sediment following anthropogenic disturbances.

Keywords: DEM, synthetic river channels, channel variability functions, disturbances, River Builder, reverse-engineer, ecohydraulics, historic aerial imagery

1. Introduction

How rivers change and recover from large disturbances, how these altered processes impact aquatic ecosystems and what drives these changes remain poorly understood, especially at longer time scales (> 10 years). A challenge often found is having sufficient data though time to quantify these changes (Fields et al., 2025). Modern surveying techniques and remote sensing have opened opportunities to collect this type of data but often do not allow us to look back at historic change (Carbonneau et al., 2012; Conner & Tonina, 2014; Tonina et al., 2020). Historic surveys of river change have often relied on thalweg and cross-section measurements (Madej, 1999; Madej & Ozaki, 1996). Although these provide high accuracy data, they are often too coarse to use modern ecohydraulic assessment techniques such as 2D hydraulic modeling. Aerial imagery has also been used to assess river change in planform, but historic aerial imagery often does not allow accurate bed morphology information to be obtained (O'Connor et al., 2003). New techniques in river geometric modeling (Lee et al., 2023) potentially allow the reverse engineering of historic river terrains based on key geomorphic variability features. Here we present a methodology to reverse-engineer historic river terrains in Redwood Creek, CA using these thalweg and sparse cross-section surveys supplemented with aerial imagery. This methodology results in high-resolution terrains which can be input into 2D hydraulic models to understand habitat changes through time, as multi-decadal sparse channel morphology surveys have been performed in the watershed.

2. Methods

2.1 Study site

Redwood Creek, which is a 720 km^2 coastal winter rain-dominated watershed in Northwestern California. The watershed historically was an old growth Redwood and Douglass fir forest, with few areas of oak savanna and open grasslands. Starting in the early-1950s, large scale logging occurred in the watershed, with 80 percent of the watershed being logged by 1992. Large floods in 1964, 1972, and 1975 triggered widespread landslides, substantially increasing sediment supplied to the stream (Warrick et al., 2013) which resulted in large channel morphology changes in the form of bed aggradation and bank erosion and increases in sediment supply (Madej, 1999; Madej et al., 2009; Madej & Ozaki, 1996) . Redwood Creek is also an important ecosystem for multiple salmonid species, including Coho and Chinook salmon. Salmon populations in the region have been historically suppressed due to a host of factors, including degraded freshwater habitat. Salmon bury eggs in gravel within rivers, and the typical period of egg incubation is October to March. During this period salmon eggs are susceptible to large flow events which can scour the bed. If scour reaches eggs, water will wash away eggs. If these events are frequent and spatially widespread, impacts on populations may be felt. Summer rearing habitat can also be a bottleneck for populations as area and size of pools impact how many juvenile salmon can survive these low-flow conditions (Mossop & Bradford, 2006).

2.2 Thalweg and width series

The United Stage Geological Survey (USGS) with Redwood National Park (RNP) performed channel thalweg elevation and cross-section elevation surveys within Redwood Creek, CA (Madej et al., 2018). These surveys were performed from 1977 to 2006. Three reaches were selected for the thalweg survey, with each reach having 2-5 cross-sections surveyed within them spaced approximately 0.5 to 3 km (Figure 1A). Additionally, aerial imagery from GoogleEarth is available at different points in time near the channel survey dates (Figure 1A). Using aerial imagery, we manually digitized the wetted extents of the channel during summer, which corresponds to a low-flow condition. We also manually digitized the active channel, areas without large vegetation, which approximates the bankfull channel. For the active channel, we created station lines every 3 m along the active channel and clipped these to the active channel extents. For the low flow channel, we created station lines every 1 m along the low flow channel centerline and clipped to the low flow channel extents. Then for each active channel station line, we joined the nearest low flow channel width to the closest active channel width. This resulted in a series of active and low flow channel widths every 3 m located at the same location.

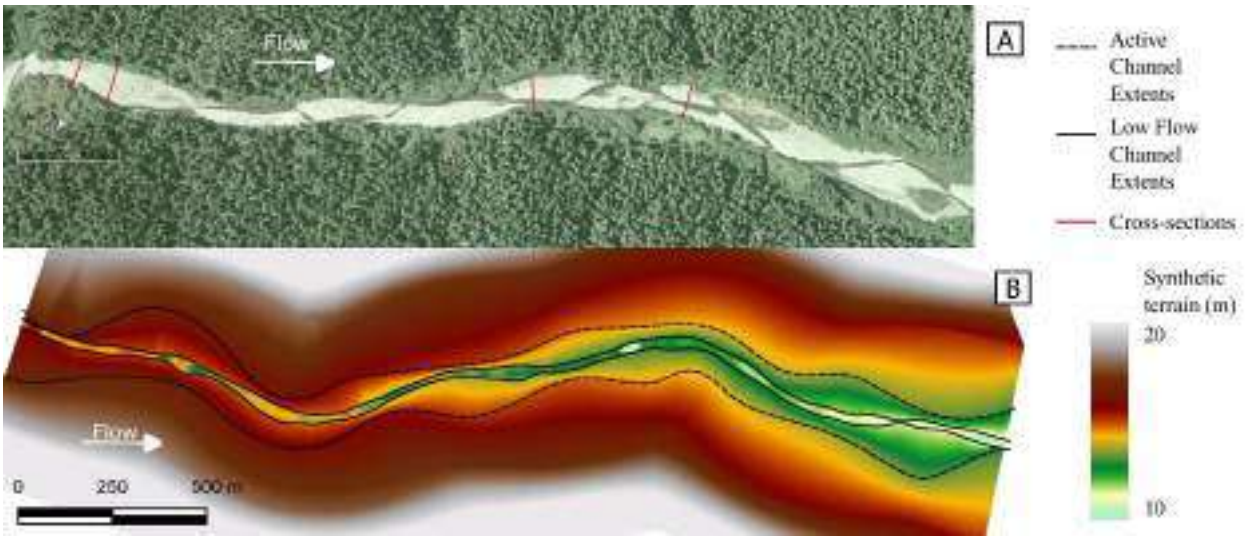

Figure 1: Historic aerial imagery (A) and synthetic terrain with channel extents (B) for Redwood Creek, CA.

2.3 Synthetic terrain generation

We used RiverBuilder (1.3.0), an open-source software which creates synthetic river channels from geomorphic variability functions and reach-average channel attributes (Pasternack & Zhang, 2021). The width and thalweg series are used to create geomorphic variability functions by fast Fourier transform of the series. This process decomposes the signal into a combination of sinusoidal functions which describe how the width or thalweg elevation varies. Additional reach-average channel attributes needed include channel slope, channel length, and minimum width and depths. These were found through channel thalweg and cross-section surveys, in addition to the aerial imagery analysis. These channel parameters, along with geomorphic variability functions, are the inputs used for RiverBuilder, and used to develop synthetic river channels from sparse data to mimic the real river channels.

2.4 Ecohydraulic assessment

For the ecohydraulic assessment of salmon habitat, we plan to assess two critical life-stages for salmon populations: egg incubation and summer rearing. For both cases 2D hydraulic models will be developed using HEC-RAS 2D (U.S. Army Corps of Engineers Hydrologic Engineering Center, 2024). For egg incubation we will assess probability of scour for various flow events. For summer rearing habitat we will look at size and distribution of pools, important summer habitats along with using bioenergetic models to better assess the conditions within individual pools.

3. Preliminary results

Using width and thalweg series, we were able to reverse engineer synthetic terrains that mimic real terrains (**Error! Reference source not found.**; Figure 2). Between the synthetic and measured thalweg series, the mean error was 0.41 m, the mean absolute error was 0.51 m, and standard deviation of error was 0.59 m.

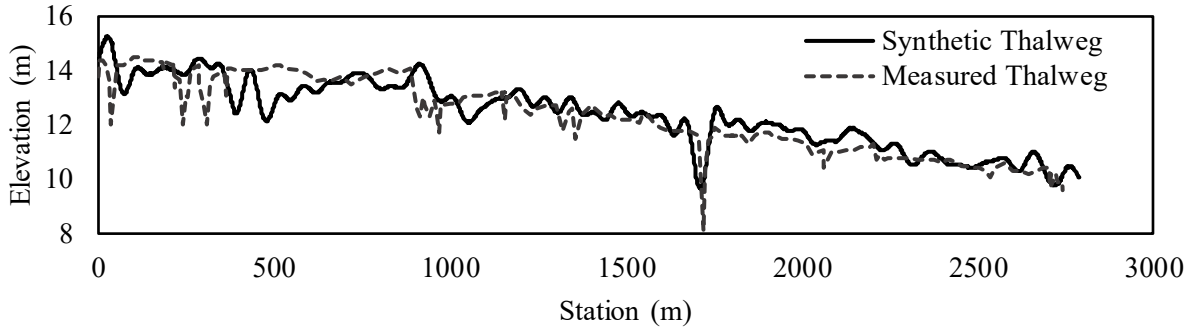

Figure 2: Comparison of measured and synthetic thalweg elevations for Redwood Creek, CA.

4. Future directions

The generation of synthetic terrains from sparse datasets and aerial imagery will allow us to use modern ecohydraulic assessment tools to track aquatic habitat changes over historic periods of disturbance and recovery. In this system, we are interested in tracking how probability of bed scour shifts as bedforms develop and grain size distributions shift post-disturbance. To accomplish this, we will develop 2D hydraulic models and then use the shield stress to predict bed mobility (Czuba et al., 2018; May et al., 2009). We will also use 2D hydraulic models to assess summer rearing habitat. In low-flow conditions, pools become important habitats for juvenile salmonids. Redwood Creek saw large changes in available pool habitat following disturbances (Madej, 1999). Although pools can be identified through thalweg profiles, using 2D hydraulic models allows us to assess the interplay of depth and velocity on habitat within pools and quantify the number of fish that can be supported (Carmichael et al., 2020). These also allow us to run different low flow scenarios and build relationships with how pool habitat quality varies with discharge which can be used to set environmental flows.

5. Conclusions

This paper provides and tests a method for generating synthetic river terrains from sparse field data and aerial imagery. These terrains can be used to look back at historic river channels, which provides opportunities to study how rivers have changed due to various types of disturbances such as wildfire, logging or urbanization. Understanding how these events impact aquatic habitat can better protect and restore critical habitats from future disturbances. Additionally, these methods can be used to efficiently monitor rivers in the future. By limiting the number of in-channel measurements that need to be taken to accurately describe the channel, monitoring costs can be lowered.

References

Carbonneau, P., Fonstad, M. A., Marcus, W. A., & Dugdale, S. J. (2012). Making riverscapes real. *Geomorphology, Geospatial Technologies and Geomorphological Mapping Proceedings of the 41st Annual Binghamton Geomorphology Symposium*, *137*(1), 74–86. https://doi.org/10.1016/j.geomorph.2010.09.030

Carmichael, R. A., Tonina, D., Keeley, E. R., Benjankar, R. M., & See, K. E. (2020). Some like it slow: A bioenergetic evaluation of habitat quality for juvenile Chinook salmon in the Lemhi River, Idaho. *Canadian Journal of Fisheries and Aquatic Sciences*, *77*(7), 1221–1232. https://doi.org/10.1139/cjfas-2019-0136

Conner, J. T., & Tonina, D. (2014). Effect of cross-section interpolated bathymetry on 2D hydrodynamic model results in a large river. *Earth Surface Processes and Landforms*, *39*(4), 463–475. https://doi.org/10.1002/esp.3458

Czuba, C. R., Czuba, J. A., Magirl, C. S., Gendaszek, A. S., & Konrad, C. P. (2018). Effect of river confinement on depth and spatial extent of bed disturbance affecting salmon redds. *Journal of Ecohydraulics*, *3*(1), 4–17. https://doi.org/10.1080/24705357.2018.1457986

Fields, J. F., Renshaw, C. E., Dethier, E. N., & Magilligan, F. J. (2025). The longer arc of channel recovery post-dam removal. *Geomorphology*, *468*, 109442. https://doi.org/10.1016/j.geomorph.2024.109442

Lee, A., Lane, B., & Pasternack, G. B. (2023). Identifying key channel variability functions controlling ecohydraulic conditions using synthetic channel archetypes. *Ecohydrology*, *16*(4), e2533. https://doi.org/10.1002/eco.2533

Madej, M. A. (1999). Temporal and spatial variability in thalweg profiles of a gravel-bed river. *Earth Surface Processes and Landforms*, *24*(12), 1153–1169. https://doi.org/10.1002/(SICI)1096-9837(199911)24:12%253C1153::AID-ESP41%253E3.0.CO;2-8

Madej, M. A., & Ozaki, V. (1996). Channel Response to Sediment Wave Propagation and Movement, Redwood Creek, California, Usa. *Earth Surface Processes and Landforms*, *21*(10), 911–927. https://doi.org/10.1002/(SICI)1096-9837(199610)21:10%253C911::AID-ESP621%253E3.0.CO;2-1

Madej, M. A., Ozaki, V., Truesdell, R., Falvo, C. I., Enns, K. D., Bell, T. M., Everette, A. L., & Faundeen, J. L. (2018). *River Channel Survey Data, Redwood Creek, California, 1953-2013* [Dataset]. U.S. Geological Survey. https://doi.org/10.5066/P9G0N0TN

Madej, M. A., Sutherland, D. G., Lisle, T. E., & Pryor, B. (2009). Channel responses to varying sediment input: A flume experiment modeled after Redwood Creek, California. *Geomorphology*, *103*(4), 507–519. https://doi.org/10.1016/j.geomorph.2008.07.017

May, C. L., Pryor, B., Lisle, T. E., & Lang, M. (2009). Coupling hydrodynamic modeling and empirical measures of bed mobility to predict the risk of scour and fill of salmon redds in a large regulated river. *Water Resources Research*, *45*(5). https://doi.org/10.1029/2007WR006498

Mossop, B., & Bradford, M. J. (2006). Using thalweg profiling to assess and monitor juvenile salmon (Oncorhynchus spp.) habitat in small streams. *Canadian Journal of Fisheries and Aquatic Sciences*, *63*(7), 1515–1525. https://doi.org/10.1139/f06-060

O'Connor, J. E., Jones, M. A., & Haluska, T. L. (2003). Flood plain and channel dynamics of the Quinault and Queets Rivers, Washington, USA. *Geomorphology, Interactions between Wood and Channel Forms and Processes*, *51*(1), 31–59. https://doi.org/10.1016/S0169-555X(02)00324-0

Pasternack, G. B., & Zhang, M. (2021). River builder user's manual for version 1.2. 0. *University of California, Davis, CA*.

Tonina, D., McKean, J. A., Benjankar, R. M., Yager, E., Carmichael, R. A., Chen, Q., Carpenter, A., Kelsey, L. G., & Edmondson, M. R. (2020). Evaluating the performance of topobathymetric LiDAR to support multi-dimensional flow modelling in a gravel-bed mountain stream. *Earth Surface Processes and Landforms*, *45*(12), 2850–2868. https://doi.org/10.1002/esp.4934

U.S. Army Corps of Engineers Hydrologic Engineering Center. (2024). *HEC-RAS River Analysis System* (Version 6.6) [Computer software]. https://www.hec.usace.army.mil/software/hec-ras/

Warrick, J. A., Madej, M. A., Goñi, M. A., & Wheatcroft, R. A. (2013). Trends in the suspended-sediment yields of coastal rivers of northern California, 1955–2010. *Journal of Hydrology*, *489*, 108–123. https://doi.org/10.1016/j.jhydrol.2013.02.041

Book of Abstracts of the *16th International Symposium on Ecohydraulics*
Challenges and solutions in the time of global changes
August 16–20, 2026, Lausanne, Switzerland
ISSN: 2790-2420 | ISBN: 978-90-837233-9-6 | doi:[10.64697/iahr.proc.ise2026.abs]
© 2026 IAHR. CC BY-NC-ND 4.0

CURRENT RIVERBED CONDITIONS FOR BENTHIC INVERTEBRATES AND POTENTIAL EFFECTS OF SEDIMENT REPLENISHMENT IN THE UJI RIVER, JAPAN

Sohei KOBAYASHI[1], Boyuan CAI[2], Sameh KANTOUSH[1]

[1] Disaster Prevention Research Institute, Kyoto University
email: kobayashi.sohei.7a@kyoto-u.ac.jp
email: kantoush.samehahmed.2n@kyoto-u.ac.jp

[2] Faculty of Engineering, Kyoto University
email: cai.boyuan.73v@st.kyoto-u.ac.jp

ABSTRACT

Channel incision and riverbed armoring caused by sediment deficit can lead to serious environmental issues, including outbreaks of certain organisms and the loss of species diversity in rivers. The changes in cross-sectional shape, flood-flow characteristics, and riverbed stability for benthic invertebrates, as well as the current spatial distribution of these organisms, were examined in the Uji River, Kyoto, Japan. Although the upstream dam was constructed about 60 years ago, channel incision and riverbed armoring have still been progressing over the past 20 years, as indicated by changes in cross sections, bed grain size, the Shields parameter, and water level. Benthic communities were dominated by net-spinning caddisflies, sessile clams, and less-mobile snails, all of which prefer stable bed conditions. Caddisflies were more abundant in riffles, whereas clams and snails were more abundant in runs and pools within sites, and all groups were more abundant at sites with higher bed stability. Sediment replenishment with appropriate grain size and volume can improve riverbed conditions and reduce caddisfly abundance to an appropriate level by enhancing the riverbed mobility and disturbance necessary for maintaining species diversity.

Keywords: channel incision, bed stability, armouring, sediment replenishment, Shield's parameter, benthic invertebrates, caddisflies

1. Introduction

Sediment shortage and channel degradation caused by upstream dam construction and downstream sand mining have led to various issues in rivers. In the Uji River, Kyoto, Japan, the riverbed became armored (with increased grain size) after the construction of the Amagase Dam in 1964, which led to bed stabilization and resulted in a high production of caddisflies that emerge from the river and annoy riverside residents and tourists (Kobayashi and Takemon, 2014; Kobayashi et al., 2017, Fig. 1). Sediment replenishment is one of the measures that can improve the condition of the armored riverbed by enhancing sediment mobility and disturbance to caddisflies in the river (Kantoush and Sumi, 2011; Auel et al., 2017).

In this study, we analyzed river cross-sections and flow discharge data and conducted field surveys to obtain data on the spatial distribution of caddisflies. Our objectives were to (1) understand historical changes in flow, channel morphology, and bed stability in the Uji River, (2) examine relationships among hydraulic conditions, riverbed properties, bed stability, and caddisfly abundance, and (3) evaluate the sediment replenishment required to effectively regulate caddisfly abundance in the Uji River.

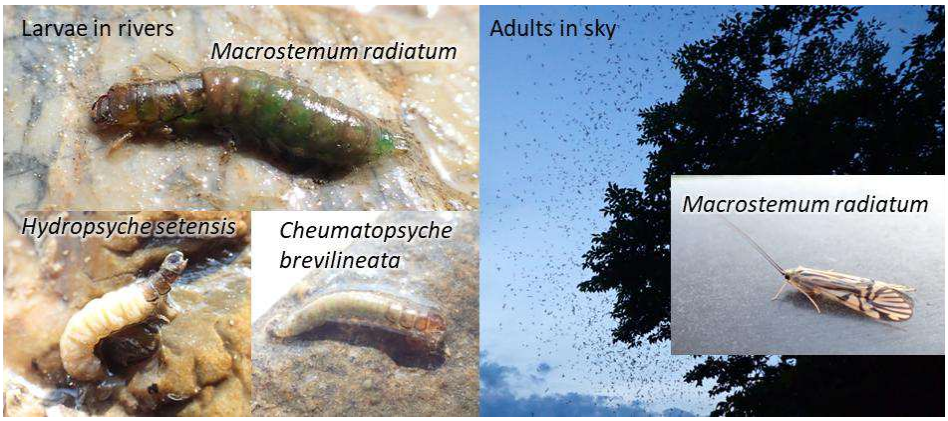

Fig. 1. Larvae and adults of caddisflies in the Uji River

2. Study Site and Methods

The Uji River, a 16–17 km-long reach, flows from the Amagase Dam to the confluence point where it joins other tributaries to form the Yodo River downstream. Because of the water storage and regulation by Lake Biwa upstream, the flow of the Uji River is relatively stable, with a base flow of 50–100 m³/s and flood flows of 200–1000 m³/s.

Data on daily discharge at the Uji Gauge Station (upstream boundary) and daily water level at the Uji-Sansen Station (downstream boundary) during 2002–2023, as well as river cross-sections of the Uji River (37.2–53.2 k.p., 200-m intervals) from 2000 to 2022, were obtained from the Yodogawa River Office. Bed grain size (d_{60}) for different years was determined from figures in past reports of the river office using Plot Digitizer. HEC-RAS was used to calculate potential one-dimensional (1-D) flow conditions, including shear stress, during large floods (500, and 1000 m³/s).

Field surveys were conducted at three sites near major bridges (Uji, Keiji, and Ingen), where gravel bars and pool–riffle structures were well developed, in mid-October 2024, when the flow was low and stable. At each site, three typical river habitats (i.e., riffle, run, and pool) were defined. At each of ten sampling locations (four from riffles, four from runs, and two from pools), water depth and flow velocities at different depths (surface, mid-depth, and bottom) were measured. After taking five photographs of the riverbed for grain-size analysis, invertebrates within a 900 cm² quadrat were collected by washing stones inside the quadrat with a D-frame net (0.5 mm mesh) placing on the downstream side.

ImageJ was used for image analysis to obtain randomly selected 125 particles from the bed images. Invertebrates including caddisflies were sorted and classified into different taxa (mainly genus or species) using books of keys for species identification and numbers are counted for each taxon.

3. Results

3.1. Discharge, channel shape and hydraulics

During 2002–2023, the flow discharge at the upstream gauge station showed a weak tendency toward increasing maximum and high (95-day) flows, and decreasing baseflow (185-day) and low (245-day) discharge. A decline in minimum water level was also observed at the downstream station.

Progress of channel incision was evident in the cross sections of all three sites; the lowest bed level gradually decreased, and the channel became narrower over the years. Riverbed grain size (D_{60}) at the three sites increased over the years.

Potential flow characteristics during floods calculated using HEC-RAS suggested that, for a given discharge, the flow became deeper, narrower, faster, and associated with greater shear stress over the years. However, as the riverbed grain size increased with time, the dimensionless Shields parameter decreased (lower than the critical shear stress, Fig. 2), indicating an increase in bed stability.

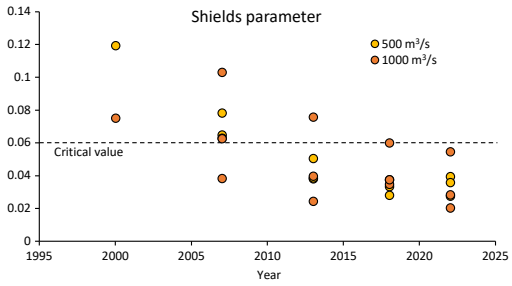

Fig. 2. Changes in Shield's parameter in the last 20 years at the middle site

3.2. Spatial distribution of caddisflies

Typically, flow velocity was higher in riffles and lower in pools, while water depth was greater in pools and runs and shallower in riffles at each site, with no obvious differences among sites. Riverbed grain size tended to be larger in riffles than in pools and was greater at the upstream site (Uji) than at the downstream site (Ingen). Because of the difference in grain size, Shields parameter, index of bed mobility calculated based on the grain size and potential shear stress during floods was higher at the downstream site than at the upstream site.

The benthic communities were dominated by three net-spinning caddisfly species (*Macrostemum radiatum*, *Hydropsyche setensis*, and *Cheumatopsyche brevilineata*), sessile type clam (*Limnoperna fortunei*) and less-mobile snail (*Semisulcospira*). The three caddisflies were more abundant in riffles than in runs and pools, especially *H. setensis*, across sites, and were more numerous at the upstream site than at the downstream sites (Fig. 3). The clam and snail were more abundant in runs and pools than in riffles, while they were more abundant at the upstream site than downstream sites. Significant correlations between physical parameters and caddisfly abundance were evident: abundance was positively correlated with flow velocity and grain size within sites, but negatively correlated with Shields parameter among sites. The clam and snail were also abundant and more in runs and pools than in riffles, while they also negatively correlated with Shields parameter among sites.

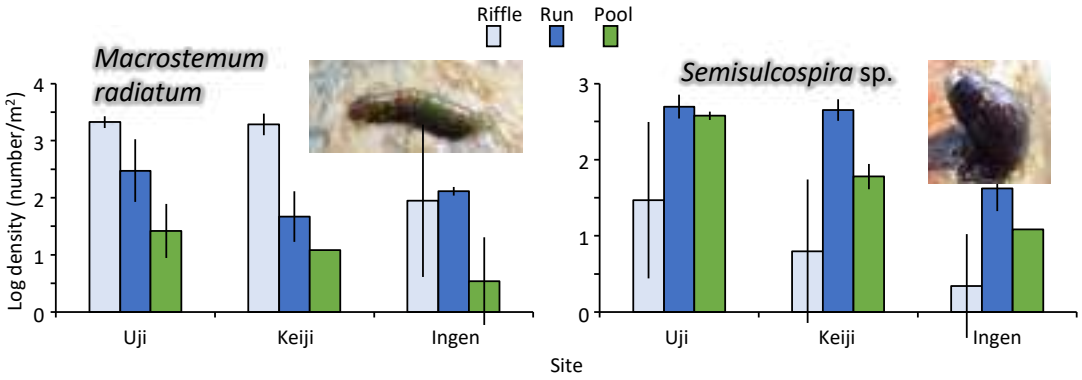

Fig. 3. Abundance (mean ± SD) of major benthic invertebrates in different habitats at the three sites of Uji River

4. Discussion

4.1. Channel degradation in Uji River

Riverbed degradation has been progressing continuously even after 2000, and the bed material has become coarser and more stable (Fig. 2). Due to sediment shortage after the construction of the Amagase Dam in 1964, erosion is still the dominant process, which washes away finer particles and exposes the clay layer beneath the sediment. In addition, the water level at annual minimum flow and the cross-sectional shape suggest that the flow in the Uji River has become narrower and deeper due to channel incision that originated downstream in the Yodo River.

4.2. Control of caddisflies by sediment replenishment

The benthic communities of the Uji River were dominated by net-spinning caddisflies, clams, and snails, all of which are adapted to stable bed environments (Kobayashi et al., 2010; 2013). As expected, caddisfly

abundance was correlated with bed stability (i.e., negatively correlated with the Shields parameter). Therefore, to reduce bed stability and the abundance of caddisflies, sediment replenishment with an appropriate quantity and grain size is recommended. A variety of particle sizes, including sand, gravel, and small cobbles, is required to create a desirable bed composition for the ecosystem, while excessive silt and sand may fill and clog riverbed interstices and also may be beneficial to caddisflies as nesting materials.

The Yodogawa River Office plans to conduct sediment replenishment in the future. They estimated that the bed grain size at the Uji site would decrease from 9 cm to 6–7.5 cm by adding 15,000 m³ (mainly of sand and gravel) per year, and to 3 cm by adding 50,000 m³ per year. In the latter case, the Shields parameter is close to 0.06, which is sufficient for promoting sediment mobility, bed disturbance, and reduction of caddisfly abundance.

Acknowledgements

We thank the employees of the Yodogawa River Office for providing data for the analysis and supporting our field survey.

References

Bullen KE, Bolt BA (1985) An Introduction to the Theory of Seismology, Cambridge, 400 pp. (in the case of a book)
Mrokowska MM, Rowiński PM, Kalinowska MB (2015) A methodological approach of estimating resistance to flow under unsteady flow conditions, Hydrology and Earth System Sciences, 19, 4041-4053 (in the case of a journal article)
Auel C, Kobayashi S, Takemon Y, Sumi T (2017) Effects of sediment bypass tunnels on grain size distribution and benthic habitats in regulated rivers. International Journal of River Basin Management, 15(4), 433-444.
Kantoush SA, Sumi T (2011) Sediment replenishing measures for revitalization of Japanese rivers below dams. In Proceedings of the 34th World Congress of the International Association for Hydro-Environment Research and Engineering: 33rd Hydrology and Water Resources Symposium and 10th Conference on Hydraulics in Water Engineering (pp. 2838-2846). Barton, ACT: Engineers Australia.
Kobayashi S, Akamatsu F, Nakanishi S, Yajima Y, Miwa J, Amano K (2013) Benthic invertebrate communities of Japanese rivers revealed from national environmental census: spatial distributions of total biomass and major taxa. Japanese Journal of Limnology, 74, 129–152 (In Japanese with English Abstract).
Kobayashi S, Nakanishi S, Oshima Y, Amano K (2010) Physical characteristics and macroinvertebrate biomass of riffles in the Toyo River, Aichi Prefecture. Japanese Journal of Limnology, 71, 147–164 (In Japanese with English Abstract).
Kobayashi S, Nozaki T, Takemon Y (2017) Caddisfly community of the Seta-Uji, the outlet river of the Lake Biwa, Japanese Journal of Ecology, 67, 13–29 (In Japanese with English Abstract).
Kobayashi S, Takemon Y (2014) Changes in hydrology, water quality, and caddisfly biomass for the past half-ccentury in the Uji River. Disaster Prevention Research Institute Annuals, 57B, 561–569 (In Japanese with English Abstract).

Book of Abstracts of the *16th International Symposium on Ecohydraulics*
Challenges and solutions in the time of global changes
August 16–20, 2026, Lausanne, Switzerland
ISSN: 2790-2420 | ISBN: 978-90-837233-9-6 | doi:[10.64697/iahr.proc.ise2026.abs]
© 2026 IAHR. CC BY-NC-ND 4.0

ANALYSES OF RIPARIAN VEGETATION ESTABLISHMENT DUE TO FLOW REGIME CHANGES FOCUSED ON VEGETATION RECRUITMENT AND FLOOD RISK – A CASE OF THE UPPER-MIDDLE NAKDONG-GANG RIVER IN KOREA

Hyoseop WOO[1], Chang Rae JANG[2], Sung-uk CHOI[3]

[1] Visiting Professor, Department of Civil and Environmental Engineering, Yonsei University, Seoul, Korea

email: hswoo0603@gmail.com

[2] Professor, Korea National University of Transportation, Chungju, Korea

Email: cljang@cjnua.c.kr

[3] Professor, Department of Civil and Environmental Engineering, Yonsei University, Seoul, Korea

Email: schoi@yonsei.ac.kr

ABSTRACT

This study presents a representative case of the "from white river to green river" phenomenon, describing riparian forestation in a 1.8 km reach of the upper–middle Nakdong-gang River, Korea. Following the construction of the Andong Dam in 1976 and the Imha Dam in 1991, the reach experienced substantial alterations in flow regime and sediment transport. These changes enabled the colonization of vegetation on formerly unvegetated sandbars between 1991 and 1994, resulting in the establishment of willow-dominated riparian forests by 2024. To mitigate the perceived flood risk associated with forested floodplains, river managers have periodically cleared woody vegetation, most recently in 2024, without conducting prior scientific evaluations. Numerical hydraulic modeling conducted in this study shows that the complete removal of woody and herbaceous vegetation can lower the flood stage by 0.65 m under the 100-year design flood. These findings underscore the importance of vegetation management strategies being based on scientific assessments rather than arbitrary clearance practices.

Keywords: flood risk; flow regime; numerical analyses; riparian vegetation; willow patches

1. Introduction

This study examines a representative case of the "from white river to green river" phenomenon (Woo, 2010), normally known as riparian forestation, focusing on a forested reach approximately 1.8 km long along the Nakdong-gang River, located in the middle to upper reach of the river. Significant alterations in flow regime and sediment transport occurred in this reach following the construction of the Andong Dam at a main river reach in 1976 and, more markedly, the Imha Dam at a tributary in 1991. As a result, extensive sandbars that once characterized this alluvial river have been colonized, established, and successively developed into riparian woodlands dominated by willow species aged approximately 20 years. Because simultaneous spillway releases from the two upstream dams can induce floodplain inundation and increase flood risk in the area, the area has been subject to periodic vegetation clearing as part of flood management practices. The most recent clearing was carried out in 2024. However, such interventions have been implemented without scientific justification or standardized management criteria.

Tree cutting and removal in riparian zones have become increasingly common in river management practices (Benifei et al., 2015; Giovannini et al., 2025). However, such interventions typically produce two contrasting outcomes—a reduction in flood risk on one hand and ecological degradation on the other—thereby

necessitating a comprehensive scientific assessment of their respective benefits and drawbacks. The authors conducted a study in 2024 to investigate the scientific validity of this management practice (Woo et al., 2025, I & II). In this study, we focused on flood risk and riparian vegetation, highlighting some of the original work that aligns with the ISE presentation.

2. Study area and analyses of aerial photos

The study area encompasses approximately 1.8 km of the right-bank forested reach of the Nakdong-gang River (See B areas in Fig. 1), which fronts Byeongsan-seowon, located in the southeast of South Korea. The upper left photo in Fig. 1 presents an aerial photograph of the study reach taken in 1971, before the upstream two dams were completed. It shows that most of the sandbars exhibited no visible signs of vegetation colonization at that time. Only bar A appears to have been partially converted into cultivated land.

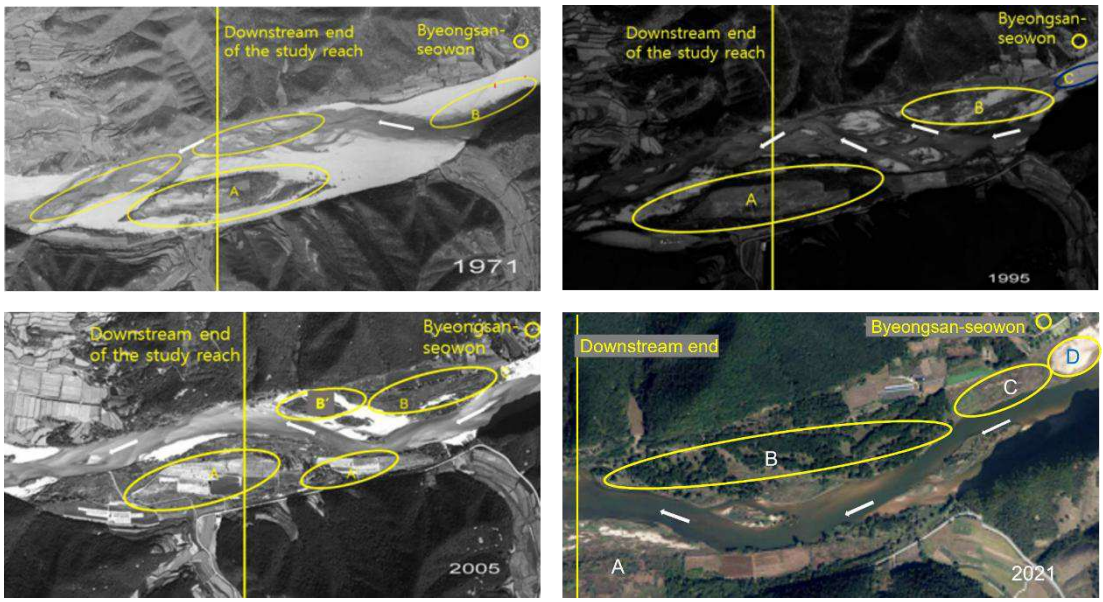

The upper right photo of Fig. 1, taken in 1995, three years after completion of the upstream Imha Dam (the second dam after Andong dam, the first dam), shows the irregular pattern of vegetation establishment on the right-bank bar B. With the onset of impoundment in late 1991, annual natural floods in the Nakdong-gang River downstream of the two dams effectively ceased, producing dramatic changes in both discharge and sediment regimes. Consequently, the reduction in bed shear stress during intermittent floods likely allowed vegetation to colonize and establish on the sandbars. The downstream portion of the bar B exhibits a typical braided-channel morphology. Lastly, the central open space and surrounding vegetation on the left-bank bar A were the result of agricultural activity.

The lower left photo of Fig. 1, taken ten years later in 2005, shows that most parts of the right-bank bar B became forested, except for several white areas. These white areas correspond to zones of relatively low bed elevation where infrequent floods are channeled during high water. Vegetation in the study area consists primarily of willow species (Salix spp.) among woody plants, and reed (*Phragmites communis*) and cogon grass (*Imperata cylindrica var. koenigii*) among herbaceous species.

Finally, the lower right photo of Fig. 1, taken sixteen years later in 2021, reveals that herbaceous vegetation had colonized even those bare sand surfaces that were visible in white in 2005. The whitish, no-vegetation bar C and the white bar D in this image appear to have been periodically cleared for landscape management purposes around Byeongsan-seowon, a historical monument.

3. Vegetation recruitment and establishment

Fig. 2 illustrates yearly changes in surface cover within the study reach (Bar B) across 1988, 1995, and 2022, showing the areal distribution of water surface, sandbar, herbaceous vegetation, and woody vegetation. As shown in this figure, the sandbars in the study reach consisted entirely of bare sand (median grain size: 1.7 mm) up to 1988, with virtually no vegetation present. After 1988, and particularly following the completion of the Imha Dam in 1991, the water surface area decreased, while the exposed sandbar area expanded, allowing vegetation to establish and increase in coverage. As shown in Fig. 3, woody vegetation, dominated by willow species (Salix spp.), expanded from 0 ha before 1988 to 10.2 ha in 2022, accounting for 56% of the total river

area and 60% of the total sandbar area. Similarly, herbaceous vegetation, primarily reeds (Phragmites australis), increased from 0 ha in 1988 to 6.7 ha in 2022, representing 37% of the total river area and 39% of the total sandbar area.

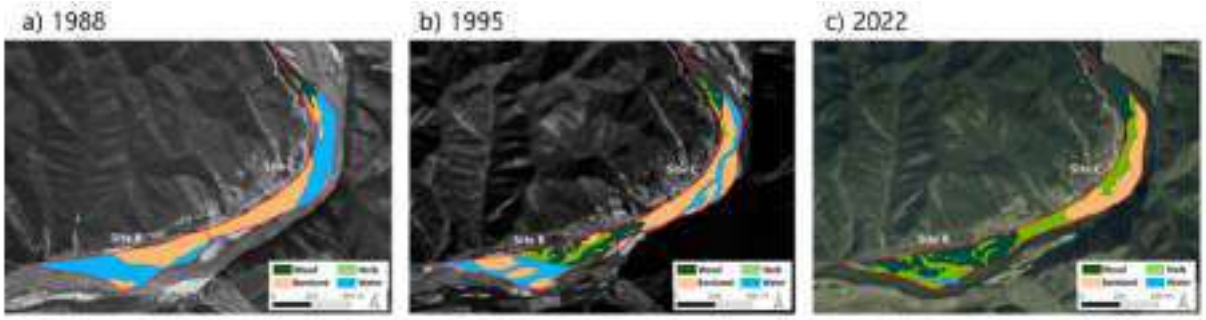

4. Numerical analyses

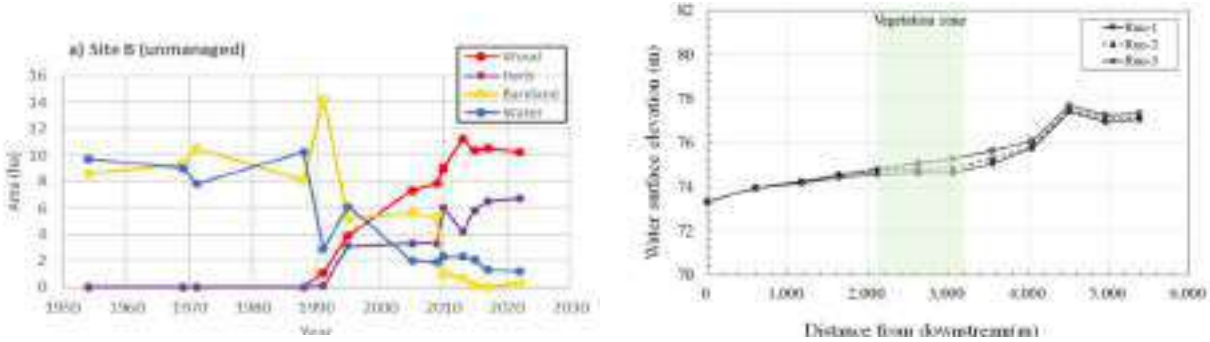

4.1 Groundcover conditions for simulation

In this study, a numerical simulation was conducted to investigate how the presence of woody vegetation patches in Bar B, located in the lower right corner of Fig. 1, affects flood-flow characteristics in the surrounding channel. The two-dimensional numerical model, Nays2D, incorporated in the iRIC platform (Shimizu et al., 2020), was applied to the study area, which includes the bar B, the cultivated bar A, and the managed bars C and D in Fig.1. The simulation conditions were established as follows:

- Run-1 (Green river condition): woody vegetation distributed on the floodplain with herbaceous plants on the ground surface, corresponding to the recent condition of Bar B (Fig. 5 left);
- Run-2: Woody vegetation removed by river-management activities, leaving only herbaceous vegetation on the floodplain (representing the post-2024 condition) (Fig. 5, right); and
- Run-3 (White river condition): no woody or herbaceous vegetation on the floodplain is assumed, representing the pre-1990s condition before dam regulation significantly affected flow regime

The design flood discharge applied to the model was 7,000 m³/s, corresponding to the 100-year return period for this reach. In the simulation, the base Manning's roughness coefficient for the channel bed was uniformly set to 0.026. As shown in Fig. 5 (left and right), a higher roughness value of 0.035 was assigned to areas covered by herbaceous vegetation on the sandbars. To account for the additional flow resistance induced by woody vegetation, as shown in Fig. 5 (left), only tree stems were considered, and vegetation (tree) density, representing canopy permeability, was set to 0.86 stems/m, as estimated from field surveys. The drag coefficient was assumed to be 1.0.

4.2 Results

Fig. 4 presents the longitudinal variation in water surface elevation for each vegetation condition. Although the water level showed little lateral variation within an individual cross-section, the plotted values represent the cross-sectionally averaged elevations. The 2-D numerical model, Nays2D, was verified with the result of the 1-D model, HEC-RAS, which has been widely used in Korea for both steady and unsteady hydraulic routing. This verification process can minimize the uncertainty of the 2-D model used for this study.

In Run-1, which includes woody vegetation stands, the water surface begins to rise from approximately 1,400 m, just upstream of the vegetated zone, and continues to increase up to 3,055 m, where the vegetation zone

ends. The elevation further increases upstream, reaching the maximum water level around 4,500 m, primarily due to topographic influences (a narrow, sharply curved). Under Run-2, where woody vegetation was removed but herbaceous vegetation remained on the floodplain, the water surface shows a similar longitudinal trend to that of Run-1. In contrast, under Run-3, which represents the non-vegetated (white river) condition, the water surface remains nearly constant between 2,100 m and 3,055 m, but begins to rise upstream of 3,055 m, again reaching its maximum elevation near 4,500 m.

The continued rise in water surface upstream of 3,055 m in Runs 1 and 2 can be attributed to increased flow resistance caused by woody and herbaceous vegetation. This elevated water level is further amplified by local topographic effects, such as sharp channel bends and narrowed channel width, which together sustain the higher water surface elevation.



5. Conclusions

The study area experienced vegetation colonization and establishment between 1991 and 1994, culminating in the development of a riparian forest dominated by willow species by 2024. When woody vegetation stands are present on the floodplain, the trees act as hydraulic obstructions, concentrating flow within the main channel. This concentration increases flow velocity and shear stress, potentially compromising channel stability and increasing flood risk.

Complete removal of woody and herbaceous vegetation from the study reach was estimated to reduce the flood stage by approximately 0.65 m under the 100-year design flood. This reduction is comparable to the 0.8 m difference observed during flood events in Italy's Magra River. Although the present study did not explicitly evaluate the ecological consequences of vegetation removal, the persistence of an herbaceous layer is expected to mitigate potential adverse impacts, suggesting that overall ecological degradation may remain limited.

If river managers aim to mitigate flood risk through vegetation management, such interventions should be informed by scientific analysis, as demonstrated in this study, rather than arbitrary clearance practices. This recommendation is further supported by the consideration that vegetation removal in upstream reaches can accelerate flood wave propagation and increase downstream flood peaks.

Acknowledgements

The authors greatly appreciate the financial support from the Ministry of Environment and Korea Environmental Industry & Technology Institute's R&D project 'Technology Development for Securing Water Resource Stability in Response to Future Changes (RS-2024-00335281).'

References

Benifei R, Solari L, Vargas-Luna A., Geering G, van Oorschot M. (2015). Effect of vegetation on floods: The case of the River Magra, E-proceedings of the 36th IAHR World Congress, Hague, The Netherlands.

Giovannini MRM, Lama GFC, Scopetani L, Francalanci S, Signorile A, Saracino R, Preti F. (2025). Evaluating the impacts of riparian plants on flood hazard within vegetated rivers. Journal of Flood Risk Management, 18.

Shimizu Y, et al. (2020). Advances in computational morphodynamics using the International River Interface Cooperative(iRIC) software. Earth Surface Processes and Landforms.

Woo, Hyoseop. (2010). Trend in ecological river engineering in Korea. Journal of Hydro-environment Research. 4. 269-278.

Woo H, Jang, C-R, Cho K-H, Kim W, Kim D. (2025). Analyses of riparian vegetation establishment due to flow and sediment regime changes - A case of the Byeongsan-seowon reach of the upper-middle Nakdong-gang River (I&II). Ecology and Resilient Infrastructure, 12(1) and 12(2). (in Korean)

Book of Abstracts of the *16th International Symposium on Ecohydraulics*
Challenges and solutions in the time of global changes
August 16–20, 2026, Lausanne, Switzerland
ISSN: 2790-2420 | ISBN: 978-90-837233-9-6 | doi:[10.64697/iahr.proc.ise2026.abs]
© 2026 IAHR. CC BY-NC-ND 4.0

INUNDATION DYNAMICS AND CHANNEL NETWORK CHANGES IN RESPONSE TO FLOODS IN AN ALPINE BRAIDED RIVER

Mahmoud Omer Mahmoud AWADALLAH[1], Davide VANZO[2], David Florian VETSCH[3], Robert Michael BOES[4], Francesco CAPONI[5]

[1] Laboratory of Hydraulics, Hydrology and Glaciology (VAW), ETH Zurich, Switzerland
email: awadallah@vaw.baug.ethz.ch

[2] Institute of Water and Environment, Karlsruhe Institute of Technology (KIT), Karlsruhe, Germany
email: davide.vanzo@kit.edu

[3,4,5] Laboratory of Hydraulics, Hydrology and Glaciology (VAW), ETH Zurich, Switzerland
email: vetsch@vaw.baug.ethz.ch
email: boes@vaw.baug.ethz.ch
email: caponi@vaw.baug.ethz.ch

ABSTRACT

Braided river reaches in Alpine regions are often subject to (near) natural flood events that actively reshape their morphology. These changes can reconfigure channel networks and, in turn, directly influence key biogeomorphic characteristics, such as hydraulic variables, inundation frequency, and residence time, which are relevant to several aquatic and riparian species. Although some studies have examined how these characteristics vary with discharge-dependent surface-water connectivity, applications to highly variable, evolving channel networks remain scarce. Using 2-D hydrodynamic modelling and morphological analysis of an Alpine, braided reach in Switzerland, we link changes in riverbed topography and channel networks to inundation frequencies across three topographic surveys (Jan-20, Mar-23, and Feb-25). Our results show that although the overall riverbed morphology returned back in Feb-25 to be as incised as in Jan-20, the surface water connectivity did not. In Feb-25, the channel network transitioned to a single-thread-dominated network, with the threshold discharge required to activate secondary channels rising from about 2 m^3/s to 25 m^3/s, compared to ~8 m^3/s in Jan-20. When comparing the inundation frequency in two contrasting flow regimes (hydropeaking-dominated and flood-dominated), this resulted in a decrease of about 50% of floodplain areas infrequently inundated (maximum total duration of 4 days per month) and an overall decrease in total wetted areas. This change may have a direct impact on the spatial distribution of fluvial habitats and their persistence over time. This evaluation framework can support a more holistic ecological assessment, a step towards promoting resilient riverine environments.

Keywords: channel-network; surface-water; connectivity; hydropeaking regime; 2D hydrodynamic modelling

1. Introduction

Alpine braided river reaches are known to be subjected to morphological disturbances that can actively change their templates and channel-network structures (Tockner et al., 2003). These channel networks facilitate the connectivity of surface water, which plays an important role in maintaining key biogeomorphic characteristics at these reaches (Czuba et al., 2019). While the influence of surface-water connectivity on residence time and flood-water retention has been studied in lowland river reaches where the channel network remains relatively stable over decadal timescales (Czuba et al., 2019; Tull et al., 2023), similar studies in rivers subject to regular changes in network structure are scarce. The variability of the channel network and its activation thresholds with discharge can result in different ecological performances for those reaches (Ashmore & Sauks, 2006). In regulated rivers, this is especially important as discharge may change by an order of magnitude within short

time, such as during hydropeaking events, affecting inundation dynamics, with excessive inundation-duration that can negatively affect riparian vegetation establishment (Jiang et al., 2023). This study focuses on the quantification of channel-network variability with discharge in an active braided-plain reach in response to flood events and on its influence on inundation-duration variability across two monthly flow series characterized by: (1) a hydropeaking flow regime and (2) a flood-impacted flow regime. This is evaluated using morphological analysis of the reach topography and 2-D hydrodynamic modelling.

2. Data and method

We used three topographical scans, in the form of digital elevation models (DEM), for a braid-plain near Cabbiolo in the Moesa River, Switzerland (Fig. 1(a)). The flood events occurring at the reach significantly changed the braid-plain morphology in between the topographical surveys. The reach is subjected to hydropeaking regime with a maximum peaking discharge of 14 m^3/s that typically operates twice per day. Outside the power production hours, the reach is subjected to residual flows ranging from 2 to 6 m^3/s that varies seasonally (Antonetti et al., 2023). To quantify planform changes, we computed the relative elevation of the braid-plain with respect to the main channel elevation for each topographical scan, typically presented in a cumulative frequency distribution of the relative elevations (Fig. 1(b)).

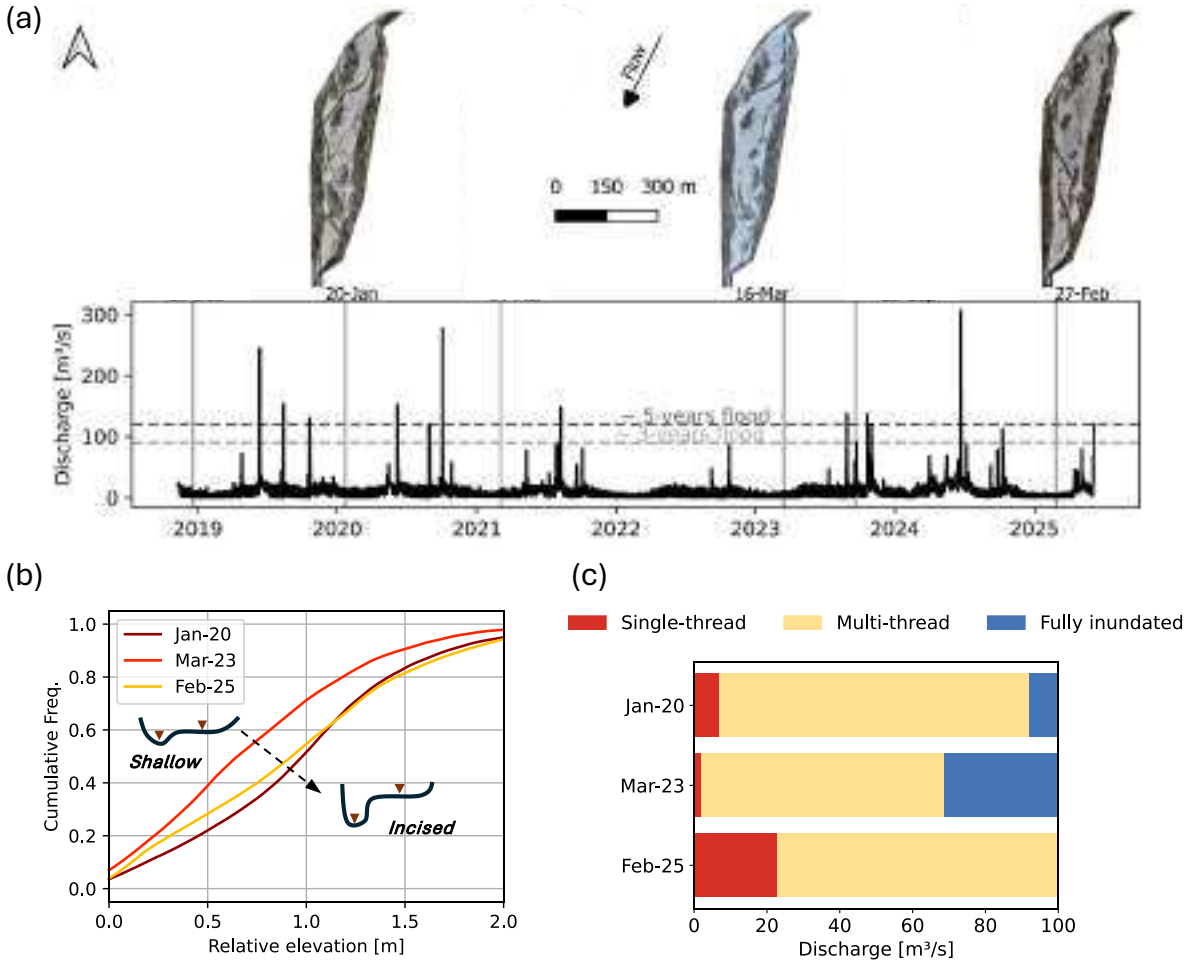

Fig. 1. (a) The three morphologies (Jan-20, Mar-23, and Feb-25) of the Moesa braid-plain with discharge time series subjected to the reach. (b) Relative elevation of the braid-plain from the main channel elevation for the three morphologies. (c) Discharge thresholds for the three morphological regime activation (i.e., single-thread, multi-thread, and fully inundated).

We used the 2-D hydrodynamic freeware BASEMENT v4.0.2 (Vetsch et al., 2023) that solves the 2-D shallow water equations with a finite volume method on unstructured computational meshes (Vanzo et al., 2021). Computational meshes were generated using the QGIS plugin BASEmesh v2 (Vanzo et al., 2021) with a maximum cell size of 1 m^2 with an average size of 0.65 m^2, resulting in a total of ~ 180,000 cells. We used the calibrated roughness coefficients from a previous study done at the same reach (van Rooijen et al., 2022). The models were then used to simulate a range of flow discharges from 1 to 100 m^3/s with a step of 1 m^3/s. To identify the discharges at which the morphology transitions from single-thread to multi-thread and from multi-thread to fully inundated, we used the approach of Czuba et al. (2019). This proposes that morphology transitions from a single-thread to multi-thread at a discharge where the maximum island area are reached (i.e.,

all the main secondary channels area connected), while it transitions from multi-thread to fully inundated at a discharge where the maximum islands' count peaked (all the possible secondary channels area activated, and higher discharges inundate only islands' tops). We then compared the discharge thresholds obtained with different morphologies (Fig. 1(c)).

We tested how inundation frequency varies among morphologies during months relevant for successful riparian vegetation germination. To focus on the effect of morphology, we used a 10-minutes discharge time series for May and August of the year 2019 to all morphologies (Fig. 2(a)). In May 2019, discharges were residual-flow and hydropeaking-dominated, with a maximum of ~20 m^3/s, while August 2019 discharges additionally featured flood events. To align with the simulated discharge scenarios, the discharge time series was rounded to the nearest integers, and monthly occurrence counts were computed. For each computational cell, we identified the smallest discharge required for inundation and replaced that discharge with its monthly occurrence count, converted to duration (1 occurrence = 10 minutes of inundation) (Fig. 2(b)). The sum of the cell's area was normalized by the overall reach area (95847 m^2)

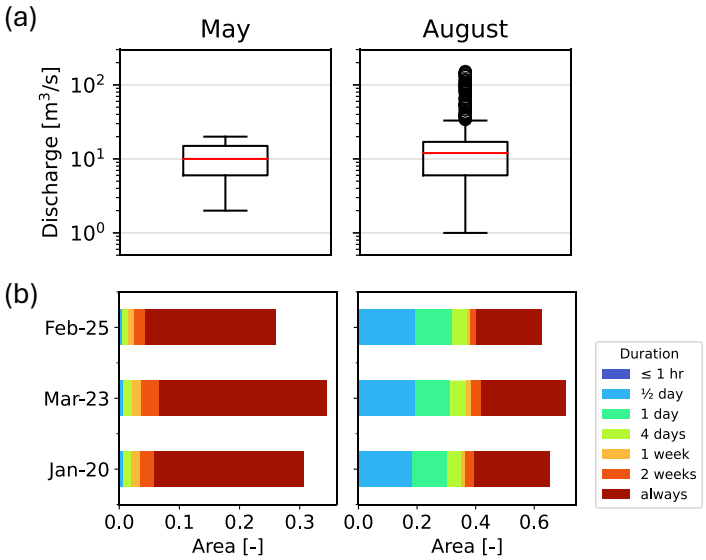

Fig. 2. (a) Boxplot of the 10-minutes time series of the discharges in May and August 2019. (b) Inundation duration for each morphology in those months.

3. Results and discussion

The relative elevation distribution shows that the Mar-23 topography has more areas of the braid-plain at smaller relative elevations to the main channel (i.e., shallower) compared to the Jan-20 and Feb-25 topographies (Fig. 1(b)). The Jan-20 and Feb-25 topographies have similar relative elevation distributions, with the Jan-20 topography being slightly more incised. This suggests that, in terms of relative elevation, the braid-plain shows a tendency toward dynamic equilibrium: after being significantly shallower in Mar-23, Feb-25 returned to levels similar to Jan-20 (van Rooijen et al., 2022). Interestingly, this dynamic equilibrium is not observed in the discharge thresholds that transition the morphology from single- to multi-thread (Fig. 1(c)). The results show that the Mar-23 morphology exhibited the lowest thresholds for transitioning from single- to multi-thread (~2 m^3/s) followed by Jan-20 (~8 m^3/s). For Feb-25, however, this threshold rose to ~25 m^3/s, which exceeds the maximum discharge in a hydropeaking regime (Fig. 2(a)). Likewise, the discharge transitioning the morphology from multi-thread to fully inundated was lowest for Mar-23 (~70 m^3/s), followed by Jan-20 (~90 m^3/s), whereas for Feb-25 the threshold was >100 m^3/s (outside the simulated range). Although the Feb-25 morphology was slightly shallower than Jan-20, this did not translate into a smaller discharge threshold for transitioning to multi-thread. This indicates that the transition to multi-thread may also be controlled by spatial morphological characteristics (e.g., fluvial deposits) that block major secondary channels from being activated (see the left side of the upstream braid-plain in Feb-25; Fig. 1(a))

The monthly inundation-duration for the different morphologies shows different trends depending on the hydrologic regime (Fig. 2). In the May 2019 discharge series, which was dominated by residual-hydropeaking regime (Fig. 2(a)), more than 80% of the inundated area was continuously wet ("always" class; Fig. 2(b)). The area inundated for a maximum duration of 4 days per month (i.e., infrequently inundated) in Jan-20 and Mar-23 was nearly that in the Feb-25 scenario. Because the Feb-25 morphology remained single-thread even at the month's highest discharge, the discharge variation inundated only marginal areas along the main channel

shores, whereas in the other two morphologies, secondary channels were already activated within the hydropeaking operation. In the August series, the regime included multiple flood events that are able to activate most of the braid-plain's secondary channels across morphologies (Fig. 2(b)), resulting in similar inundation-duration areas.

This study demonstrates the key role of channel network structure and its connectivity in shaping the inundation duration dynamics, which may influence hydraulic characteristics that are relevant to mobile aquatic species (Rachelly et al., 2021). It may also impact potential locations for seed deposits and water retention time relevant to particulate and solute transport. Our study highlights that in dynamically changing river reaches, surface-water connectivity can change drastically, with a direct influence on relevant biogeomorphic processes. This evaluation framework can inform restoration practices, guiding towards more effective conservation measures.

Acknowledgements

This study was conducted as part of the interdisciplinary research program "Hydraulic Engineering and Ecology," currently in its fifth project phase, "Resilient Rivers: Refugia – Connectivity – Stepping Stones", co-funded by the Swiss Federal Office for the Environment (FOEN).

References

Antonetti, M., Hoppler, L., Tonolla, D., Vanzo, D., Schmid, M., & Doering, M. (2023). Integrating two-dimensional water temperature simulations into a fish habitat model to improve hydro- and thermopeaking impact assessment. River Research and Applications, 39(3), 501–521.

Ashmore, P., & Sauks, E. (2006). Prediction of discharge from water surface width in a braided river with implications for at-a-station hydraulic geometry. Water Resources Research, 42(3).

Czuba, J. A., David, S. R., Edmonds, D. A., & Ward, A. S. (2019). Dynamics of Surface-Water Connectivity in a Low-Gradient Meandering River Floodplain. Water Resources Research, 55(3), 1849–1870.

Jiang, W., Pan, H., Yang, N., & Xiao, H. (2023). Dam inundation duration as a dominant constraint on riparian vegetation recovery. Science of The Total Environment, 904, 166427.

Rachelly, C., Mathers, K. L., Weber, C., Weitbrecht, V., Boes, R. M., & Vetsch, D. F. (2021). How does sediment supply influence refugia availability in river widenings? Journal of Ecohydraulics, 6(2), 121–138.

Tockner, K., Ward, J. V, Arscott, D. B., Edwards, P. J., Kollmann, J., Gurnell, A. M., Petts, G. E., & Maiolini, B. (2003). The Tagliamento River: A model ecosystem of European importance. Aquatic Sciences, 65(3), 239–253.

Tull, N., Moodie, A. J., & Passalacqua, P. (2023). River-floodplain connectivity and residence times controlled by topographic bluffs along a backwater transition. Frontiers in Water, 5.

van Rooijen, E., Siviglia, A., Vetsch, D. F., Boes, R. M., & Vanzo, D. (2022). Quantifying fluvial habitat changes due to multiple subsequent floods in a braided alpine reach. Journal of Ecohydraulics, 9(1), 1–21.

Vanzo, D., Peter, S., Vonwiller, L., Bürgler, M., Weberndorfer, M., Siviglia, A., Conde, D., & Vetsch, D. F. (2021). BASEMENT v3: A modular freeware for river process modelling over multiple computational backends. Environmental Modelling and Software, 143, 105102.

Vetsch, D., Siviglia, A., Bacigaluppi, P., Bürgler, M., Caponi, F., Conde, D., Gerke, E., Halso, M., Kammerer, S., Koch, A., Peter, S., Vanzo, D., Vonwiller, L., & Weberndorfer, M. (2023). System Manuals of BASEMENT, Version 4.0.0. Laboratory of Hydraulics, Glaciology and Hydrology (VAW). ETH Zurich.

Book of Abstracts of the *16th International Symposium on Ecohydraulics*
Challenges and solutions in the time of global changes
August 16–20, 2026, Lausanne, Switzerland
ISSN: 2790-2420 | ISBN: 978-90-837233-9-6 | doi:[10.64697/iahr.proc.ise2026.abs]
© 2026 IAHR. CC BY-NC-ND 4.0

MODELLING THE ROLE OF HYDROPEAKING ON VEGETATION ESTABLISHMENT DYNAMICS ON GRAVEL BARS

Francesco CAPONI[1], David F. VETSCH[1], Davide VANZO[2]

[1]Laboratory of Hydraulics, Hydrology, and Glaciology (VAW), ETH Zurich, Zürich, Switzerland
email: caponi@vaw.baug.ethz.ch
email: vetsch@vaw.baug.ethz.ch

[2] Institute of Water and Environment, Karlsruhe Institute of Technology (KIT), Karlsruhe, Germany
email: davide.vanzo@kit.edu

ABSTRACT

The flow regime is a critical driver of riparian vegetation dynamics along river corridors. Plants rely on the natural alternation of benign and disturbance-driven periods to develop and maintain their ecological functions. However, hydropeaking - the rapid sub-daily variation of flow discharge- has been increasingly recognized to affect vegetation growth by interrupting inundation-free periods. Despite this increasing evidence, the effect of hydropeaking on early vegetation establishment remains largely unexplored. Here, we disentangle this effect by applying a recruitment model based on the concept of the window of opportunity (WoO) on a 12-km long reach along the Alpine Rhine River, Switzerland, which experiences daily hydropeaking and showed vegetation recruitment dynamics on alternate gravel bars. To estimate area for potential recruitment, we setup and run a 2D hydrodynamics model and used it to derive spatially distributed water level time series in the period 1996-2022 based on measured discharges. We then created an alternative hydrological scenario, which differs only in the hydropeaking signal, and we compared the associated successful recruitment area to the estimated ones. We found that hydropeaking affects the vegetation extend on bars when floods coincided with the growing season. In contrast, the effect of hydropeaking tends to vanish in years when floods occurred after the growing season. The model results indicate that successful recruitment events depend on vegetation stress resistance, indicating that fast-growing vegetation may also profit from early floods. Our study advances our understanding of complex disturbance-dependent systems in hydropower-impacted systems and may prove a quantitative foundation for the design of e-flows and hydropower operation.

Keywords: hydropeaking; vegetation; recruitment model; river bars; Alpine Rhine

1. Introduction

Hydroelectric energy production has multiple benefits for today's society but may also pose significant impairment to river ecosystems. In hydroelectric-impacted rivers, the flow regime is usually influenced by water abstractions in upper catchment areas, and abrupt water releases in the downstream section of the main river reach from turbine switching on and off for energy production. Rapid fluctuations in daily and sub daily water levels caused by turbine operation, that is, hydropeaking, are increasingly evidenced to influence the life and habitat of aquatic organisms, fish and riparian vegetation (Sacheri et al. 2025, Tonolla et al. 2023, Liu et al. 2022). As hydropower is the most abundant source of sustainable energy in alpine and mountain areas, quantifying the multiple impacts of hydropeaking to limit the degradation of fluvial habitat is crucial for sustainable river management (Hayes et al. 2023; Venus et al. 2025).

Riparian vegetation and water level fluctuations are closely interconnected at various temporal and spatial scales (Friedman et al. 2022). Recruitment events are primarily controlled by yearly floods that inundate bar surfaces providing seed and vegetation material for plant growth. The success of such events depends on the subsequent inundation frequency, often occurring at shorter time scales. Hydropeaking significantly decreases

inundation-free periods to only few hours or days, triggering various physiological responses in plants, from anisotropic root growth, reduction of above-ground plant biomass (Gorla et al. 2015), and germination (Bejerano et al. 2020).

Recruitment models for vegetation have been widely used to investigate the impact of hydrological forcing on ecosystem dynamics. WoO-based models assume that vegetation requires uninterrupted disturbance-free periods for germination and early growth, until they can stand certain amounts of stress due to subsequent inundations (Balke et al. 2014). Recent applications showed that they could help understanding the impact of flow regulations on vegetation dynamics in gravel bars and provide a quantitative basis for management practices (Caponi et al. 2019, Serlet et al. 2024). However, the influence of hydropeaking on recruitment remains limited.

In this study we aim to shed light on the role of hydropeaking on vegetation recruitment in a regulated gravel bed river. We apply a WoO model along 15 km reach of the Alpine Rhine River characterized by alternating bars in two hydrological scenarios, with and without hydropeaking. We then compared the potential area for recruitment over 27 years in the two scenarios and relate it to hydrological variables.

2. Data and Methods

2.1. Study reach and data analysis

The study reach is located along the Alpine Rhine River in Switzerland between Landquart and the Ill confluence. The river morphology is characterized by alternating bars (Adami et al. 2016) composed of bare gravel (d_{50} = 60 mm), which are partially vegetated (Caponi et al. 2019). The river is channelized with a trapezoidal cross-section shape 80 m wide and with an average slope of 2.9 m/km. Of the 24 bars comprised in the reach, we focus our analysis on 12 steady gravel bars, where an increase in vegetation cover was observed between 1996 and 2017 and that show limited morphological changes (Caponi et al. 2019).

We used 15-minutes averaged discharge data measured at the Bangs gauging station (Voralberg, Austria) from 1996 to 2022. The station is located before the Inn confluence at km 61.98 and about 5 km downstream of the study reach, with no major tributaries in between. To create an alternative hydrological scenario without hydropeaking, we performed a threshold analysis based on the approach proposed by Zolezzi et al. 2011, which enabled us to dissect the original time series into baseflow, flood peaks, and hydropeaking. We then created a new time series of discharges only using floods and the base flow. To reconstruct the time series of the water levels for a specified hydrological scenario, we set up a 2D hydrodynamics model (BASEMENT, Vanzo et al. 2021) and simulated stepwise discharge values as upstream boundary conditions ranging from 10 to 2010 m^3/s with steps of 50 m^3/s kept constant for about 22 hours to ensure steady state in the computational domain.

2.2. Vegetation establishment model

To estimate vegetation establishment success, we used the WoO model developed in Caponi et al. 2019 and extended it to account for spatially variable water levels. The model searches for any inundation event within the growing season, i.e. dispersal event, (April to September) and calculates the consecutive inundation period after dewatering within the calendar year. The disturbance is then compared with the vegetation resistance, which increases following logistic growth. This assumes that vegetation resistance remains very low at the beginning and then sharply increases up to a maximum value (set to 60 days) depending on the growth rate, σ. A dispersal event is then classified as successful if the resistance remains greater than the disturbance until the end of the year. The corresponding area suitable for recruitment (A_{veg}) is then used for comparison.

3. Results and Discussion

Figure 1 shows the area for vegetation recruitment A_{veg} in the two hydrological scenarios over the years. Recruitment varies according to year, ranging from 0 (in 1999, 2008, 2020) to 82.4 % in 2009 for the scenario without hydropeaking. Simulations show that recruitment area is generally larger without hydropeaking, with the maximum difference between the scenarios about 3 times in 2003. We could identify two periods of three years, in which the recruitment area was the lowest (below 12% of the total area available), between 1998 and 2000 and between 2011 and 2013. When looking at the maximum discharge recorded after the growing seasons, the four highest discharges measured in 1999, 2002, 2008, and 2020 resulted in a vegetation area suitable for recruitment lower than 3%. Although some variability cannot be explained solely by floods occurring late in the season, our results strongly suggest that hydropeaking effects tend to be suppressed when the disturbance regime is high. In fact, floods occurring outside the growing season cannot trigger new recruitment events and thus act only as disturbance.

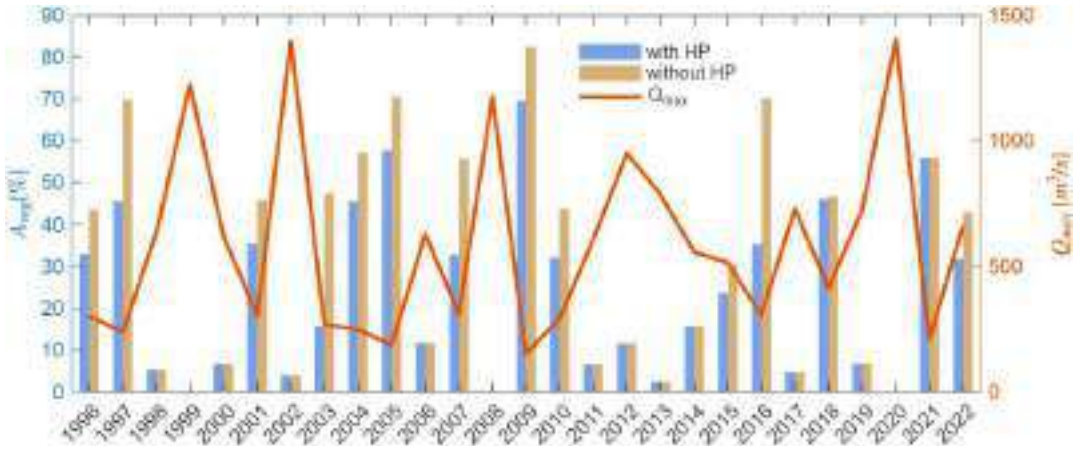

Fig. 1. Vegetation recruitment area (A_{veg}) normalized by the total available bar surface area per year in the two hydrological scenarios (with and without hydropeaking). The solid line refers to the maximum discharge recorded every year after the growing season (September-December).

This also means that in winter-dry years, the flood timing during the growing season is crucial to allow vegetation to have enough disturbance-free period and successfully establish. As suggested by Balke and Nilsson, 2019, a shift in the flood timing with respect to the start (and end) of the growing season might have large impact on time ecological processes. Our results also suggest that flow regime modification impact strongly depends on the way plants cope with stress derived from long inundation periods (encapsulated in the parameter σ in our model), their recovery time, and psychological adaptation (Bejerano et al. 2020). Also, sediment transport associated with flooding can have an important role in determining the success of the recruitment process. Although this aspect is not specifically accounted for in this analysis, previous results suggest that on steady bars riverbed changes are limited and uprooting solely by flow drag unlikely already for small plants (Caponi et al. 2019, Adami et al. 2016). Overall, our study provides modelling evidence that hydropeaking may have a strong influence on vegetation dynamics and that its effect varies depending on the flood timing.

Acknowledgements

The authors would like to acknowledge Pascal Wild for his contributions to this work through his master thesis project at ETH Zurich.

References

Shacheri, F., Czuba, J. A., & Perkins, M. A. (2025). Isolating the compounding effects of dam hydropeaking and climate change on freshwater mussel recruitment. *Science of The Total Environment*, *977*, 179390. https://doi.org/10.1016/j.scitotenv.2025.179390

Tonolla, D., Dossi, F., Kastenhofer, O., Doering, M., Hauer, C., Graf, W., & Schülting, L. (2023). Effects of hydropeaking on drift, stranding and community composition of macroinvertebrates: A field experimental approach in three regulated Swiss rivers. *River Research and Applications*, *39*(3), 427–443. https://doi.org/https://doi.org/10.1002/rra.4019

Liu, X., & Xu, Q. (2022). Hydropeaking impacts on riverine plants downstream from the world's largest hydropower dam, the Three Gorges Dam. *Science of The Total Environment*, *845*, 157137. https://doi.org/10.1016/J.SCITOTENV.2022.157137

Friedman, J. M., Eurich, A. M., Auble, G. T., Scott, M. L., Shafroth, P. B., & Gibson, P. P. (2022). Response of riparian vegetation to short- and long-term hydrologic variation. *Ecological Applications*, *32*(8). https://doi.org/10.1002/eap.2689

Bejarano, M. D., Sordo-Ward, Á., Alonso, C., Jansson, R., & Nilsson, C. (2020). Hydropeaking affects germination and establishment of riverbank vegetation. *Ecological Applications*, *0*(0), 1–16. https://doi.org/10.1002/eap.2076

Gorla, L., Signarbieux, C., Turberg, P., Buttler, A., & Perona, P. (2015). Effects of hydropeaking waves' offsets on growth performances of juvenile Salix species. *Ecological Engineering*, *77*, 297–306. https://doi.org/10.1016/j.ecoleng.2015.01.019

Balke, T., Herman, P. M. J., & Bouma, T. J. (2014). Critical transitions in disturbance-driven ecosystems: identifying Windows of Opportunity for recovery. *Journal of Ecology*, *102*(3), 700–708. https://doi.org/10.1111/1365-2745.12241

Serlet, A., Gurnell, A., & Zolezzi, G. (2024). Modelling flow regulation effects on vegetation recruitment and survival on alternate bars in channelized rivers. *River Research and Applications*, *40*(6), 1067–1086. https://doi.org/10.1002/rra.4278

Caponi, F., Koch, A., Bertoldi, W., Vetsch, D. F., & Siviglia, A. (2019). When Does Vegetation Establish on Gravel Bars? Observations and Modeling in the Alpine Rhine River. *Frontiers in Environmental Science*, *7*. https://doi.org/10.3389/fenvs.2019.00124

Adami, L., Bertoldi, W., & Zolezzi, G. (2016). Multidecadal dynamics of alternate bars in the Alpine Rhine River. *Water Resources Research*, *52*(11), 8938–8955. https://doi.org/10.1002/2015WR018228

Zolezzi, G., Siviglia, A., Toffolon, M., & Maiolini, B. (2011). Thermopeaking in alpine streams: Event characterization and time scales. *Ecohydrology*, *4*(4), 564–576. https://doi.org/10.1002/eco.132

Vanzo, D., Peter, S., Vonwiller, L., Bürgler, M., Weberndorfer, M., Siviglia, A., Conde, D., & Vetsch, D. F. (2021). basement v3: A modular freeware for river process modelling over multiple computational backends. *Environmental Modelling & Software*, *143*, 105102. https://doi.org/10.1016/j.envsoft.2021.105102

Balke, T., & Nilsson, C. (2019). Increasing Synchrony of Annual River-Flood Peaks and Growing Season in Europe. *Geophysical Research Letters*, *46*(17–18), 10446–10453. https://doi.org/10.1029/2019GL084612

Hayes, D. S., Bruno, M. C., Alp, M., Boavida, I., Batalla, R. J., Bejarano, M. D., Noack, M., Vanzo, D., Casas-Mulet, R., Vericat, D., Carolli, M., Tonolla, D., Halleraker, J. H., Gosselin, M. P., Chiogna, G., Zolezzi, G., & Venus, T. E. (2023). 100 key questions to guide hydropeaking research and policy. Renewable and Sustainable Energy Reviews, 187, 113729. https://doi.org/10.1016/J.RSER.2023.113729

Venus, T. E., Ola, O., Alp, M., Bätz, N., Bejarano, M. D., Boavida, I., Bruno, M. C., Casas-Mulet, R., Carolli, M., Chiogna, G., Gosselin, M. P., Halleraker, J. H., Noack, M., Tonolla, D., Vanzo, D., & Hayes, D. S. (2025). The power of hydropeaking: Trade-offs between flexible hydropower and river ecosystem services in Europe. Ecological Economics, 233, 108583. https://doi.org/10.1016/J.ECOLECON.2025.108583

Book of Abstracts of the *16th International Symposium on Ecohydraulics*
Challenges and solutions in the time of global changes
August 16–20, 2026, Lausanne, Switzerland
ISSN: 2790-2420 | ISBN: 978-90-837233-9-6 | doi:[10.64697/iahr.proc.ise2026.abs]
© 2026 IAHR. CC BY-NC-ND 4.0

LANDSCAPE METRICS AS INDICATORS FOR HABITAT COMPLEXITY IN RESTORED RIVER REACHES

Paul DEMUTH[1], Volker WEITBRECHT[1], Chantal M. HISCHIER[2,3], Christine WEBER[2], Robert M. BOES[1], David F. VETSCH[1]

[1]Laboratory of Hydraulics, Hydrology, and Glaciology (VAW) ETH Zurich, Switzerland
demuth@vaw.baug.ethz.ch, weitbrecht@vaw.baug.ethz.ch, boes@vaw.baug.ethz.ch, vetsch@vaw.baug.ethz.ch
[2]Swiss Federal Institute of Aquatic Science and Technology, Department of Surface Waters – Research and Management, Eawag, Kastanienbaum, Switzerland
[3]Department of Environmental Systems Science, ETH Zurich, Switzerland
chantal.hischier@eawag.ch, christine.weber@eawag.ch

ABSTRACT

River restoration aims to re-establish geomorphic and ecological processes in degraded channels, for instance by channel widening in gravel-bed rivers. This study investigates how two different initiation measures (initial widening and initial side channel) affect morphological development and habitat complexity over time. Laboratory flume experiments combined with 2D hydrodynamic simulations provide detailed hydraulic data. Habitat complexity is quantified using two landscape metrics - Edge Density and Shannon's Diversity Index. Results show that the initial widening setup gradually increases habitat complexity as channel migration progresses, while the side channel configuration generates and maintains high complexity from the very beginning. The study demonstrates that landscape metrics are a valuable tool for evaluating restoration outcomes and linking morphological dynamics to habitat complexity.

Keywords: reach-scale river restoration, gravel-bed rivers, Edge Density, Shannon's Diversity Index

1. Introduction

Rivers are dynamic systems, in which the interaction of water, sediment, vegetation and channel morphology shapes a wide range of aquatic and riparian habitats – sustaining ecological diversity and resilience. However, over recent centuries, human interventions, such as land use change, infrastructure, and flow regulation, have profoundly altered discharge regimes, sediment supply, morphology and riparian vegetation. The resulting degradation of most natural rivers has contributed to a global decline in freshwater biodiversity and a loss of ecosystem functions.

To re-establish ecosystem functions and geomorphic processes, river restoration has become a central component of sustainable water management. Self-formed widened reaches have proven effective in enhancing morphodynamic development in degraded gravel-bed rivers. The success of such measures depends on several factors, including sediment supply, slope, and length of the wider reach (Rachelly 2021). Consequently, various initiation measures can be implemented to trigger or increase channel complexity and dynamics. To ensure that such restoration efforts achieve their intended ecological outcomes, systematic monitoring is essential. Monitoring enables the evaluation of project success, supports adaptive management, and facilitates long-term learning across different catchments (Hoffmann et al. 2022).

Landscape metrics describe measurable aspects of landscape composition and configuration. They provide a quantitative framework for evaluating changes in habitat complexity and spatial patterns, to investigate whether spatial patterns become more heterogeneous or homogeneous (Turner & Gardner 2015). Traditionally used in terrestrial landscape ecology, we apply them as indicators of habitat complexity and patchiness to fluvial ecosystems.

In this study, we compared two different initiation measures and the resulting physical habitat development over time, using two different landscape metrics. Experiments in a laboratory flume were performed, and 2D hydrodynamic numerical simulations provided detailed information on hydraulic parameters to evaluate the relationship between morphological development and physical habitat complexity.

2. Methodology

Laboratory experiments were conducted in a 31.6 m long and 4 m wide flume with an initial bed slope of 0.003. As a reference, the Emme River (47°09'48.3"N, 7°33'04.4"E), a typical pre-Alpine gravel-bed river, was selected to establish a reasonable relation between hydrological, sedimentological, and geometrical values. Scaling between prototype and model followed Froude similarity with a scale factor of $\lambda = 35$. Within the flume, a trapezoidal main channel $b_0 = 0.79$ m wide was built, including a one-sided widened section positioned along the central part of the channel, reaching a maximum width of $b_{max} = 3.22$ m (Fig. 1a). The mobile bed and the sediment supplied corresponded to a well-graded gravel-bed river with a mean grainsize diameter $d_m = 1.48$ mm and a geometric standard deviation of $\sigma_g = 2.49$.

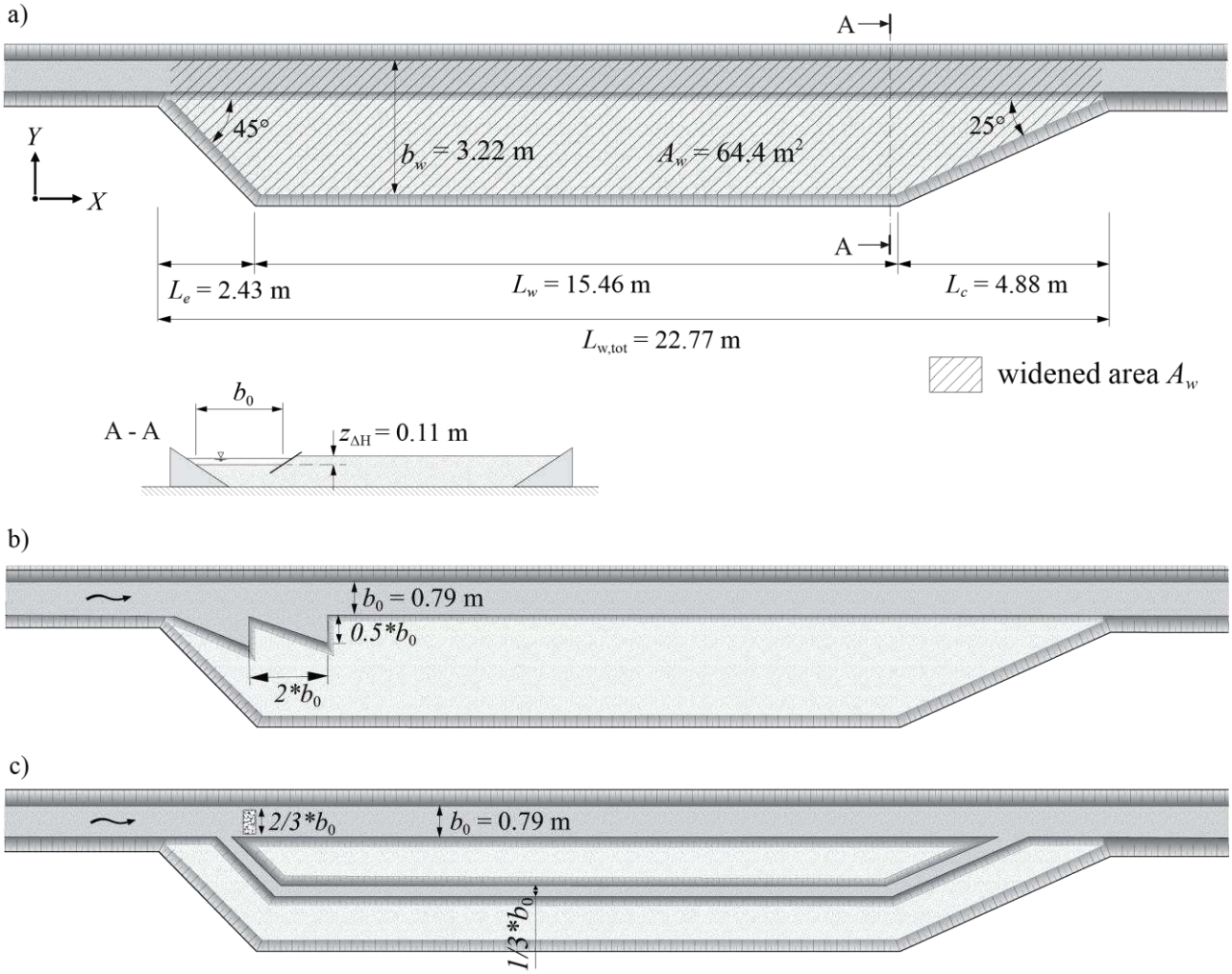

Fig. 1. (a) Planform geometry and cross-section of the experimental flume. Planform of (b) initial widening and (c) initial side channel configuration.

Starting from a straight channel, two initiation measures were implemented (Fig. 1b, c) – initial widening (series IW) and long side channel (series SC). For the initial widening, the floodplain was lowered to the mean bed elevation in two consecutive triangular zones at the beginning of the wider area. The planform dimension of one initial triangle had a length of $2*b_0$ and a width of $0.5*b_0$ following the initiation measures tested by Rachelly (2021). Further, a long trapezoidal side channel in the main channel was excavated to mean bed elevation with a fixed central island.

Morphological evolution was measured using high-resolution laser scanning between consecutive intervals. Each interval included two hydrographs of bed-forming discharges and represent approximately 5 years in

nature. The laser scans served as input for 2D hydrodynamic numerical simulations with BASEMENT, version 4 (Vetsch et al. 2023), which provided three hydraulic variables - water depth h, flow velocity v, and bed shear stress τ for the simulated bed-forming discharge. The hydraulic variables were divided into 3 to 5 ecologically relevant categories ($h_1 \leq 0.45$ m, $0.45 < h_2 \leq 0.75$ m, $0.75 < h_3 \leq 1.15$ m, $1.15 < h_4 \leq 1.5$ m, $h_5 > 1.5$ m; $v_1 \leq 0.1$ m/s, $0.1 < v_2 \leq 0.4$ m/s, $0.4 < v_3 \leq 1.0$ m/s, $1.0 < v_4 \leq 2.0$ m/s, $v_5 > 2.0$ m/s; $\tau_1 \leq 10$ N/m^2, $10 < \tau_2 \leq 20$ N/m^2, $\tau_3 > 20$ N/m^2).

For each of these categories two landscape metrics, i.e. Edge Density (ED) and Shannon's Diversity Index (SHDI) were calculated to assess habitat complexity (Turner & Gardner 2015). ED quantifies the total length of boundaries between classes per unit area, representing spatial fragmentation and patchiness. Higher ED implies more interfaces and potential ecological niches. SHDI combines richness and evenness to describe overall diversity. High SHDI values (>1) indicate a complex and evenly distributed mosaic of habitat types, whereas low values (<1) reflect a simplified and homogeneous reach.

3. Results and Discussion

3.1. Initiation measures

Pictures of the resulting topography for both initiation measures are shown in Fig. 2. With the initial widening, the channel eroded steadily and evenly across the wider area, a process described as primary erosion by Requena (2008). Over time, a dominant bar formed on the left, fixed side of the channel. This influenced the main flow direction, pushing it towards the floodplain and eventually leading to channel migration. The fixed embankment on the right restricted further channel migration. The initial widening only slightly accelerated the morphological adjustment, leaving the final topography similar to the experiment without initiation measures (Demuth et al 2025).

In contrast, the river rapidly adjusted in the experiments with the side channel. The middle island eroded substantially during the early stage of the experiments, while its downstream part persisted until the end of the experimental series. The wider area remained dynamic throughout the experiments, with continuous bar shifting and sediment relocation.

It should be noted that both initiation measures were tested under conditions of high sediment supply. This is crucial for the development of a morphodynamic active river reaches, as channel responses would likely differ substantially when sediment supply is reduced.

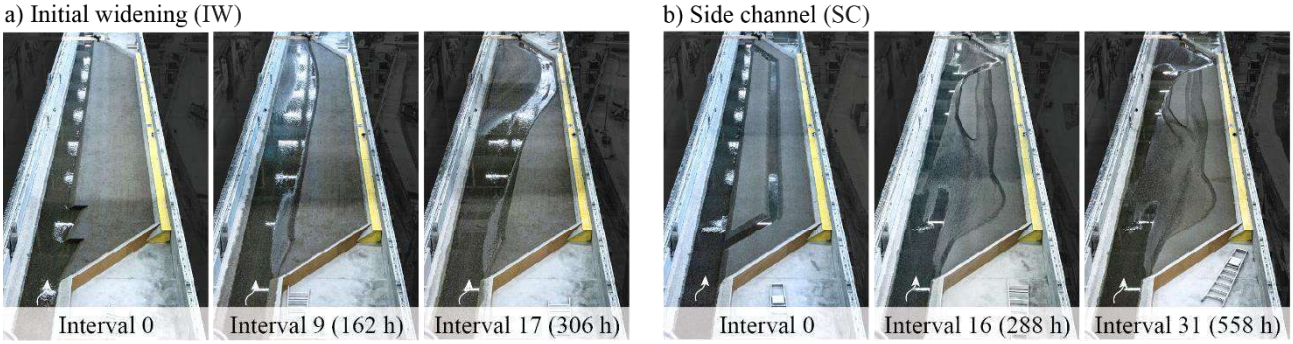

Fig. 2. Temporal evolution of (a) the initial widening (IW) and (b) the side channel configuration (SC). The photographs show a discharge of 1 l/s (low discharge) for visualisation purposes.

3.2. Habitat complexity

To assess habitat complexity over time, SHDI and ED were derived based on water depth h, flow velocity v, and bed shear stress τ after consecutive intervals from numerical simulations (Fig. 3). In series IW, both metrics were initially low at the starting point of the widening process but increased gradually over time as channel migration enhanced dynamics and habitat complexity. Conversely, in series SC, both SHDI and ED were high from the beginning and remained relatively stable, indicating that the initial side channel configuration established a diverse and spatially complex habitat structure that persisted throughout the experiments. Both initiation measures lead to similar habitat complexity over time, while visually the SC approach seemed to be more diverse.

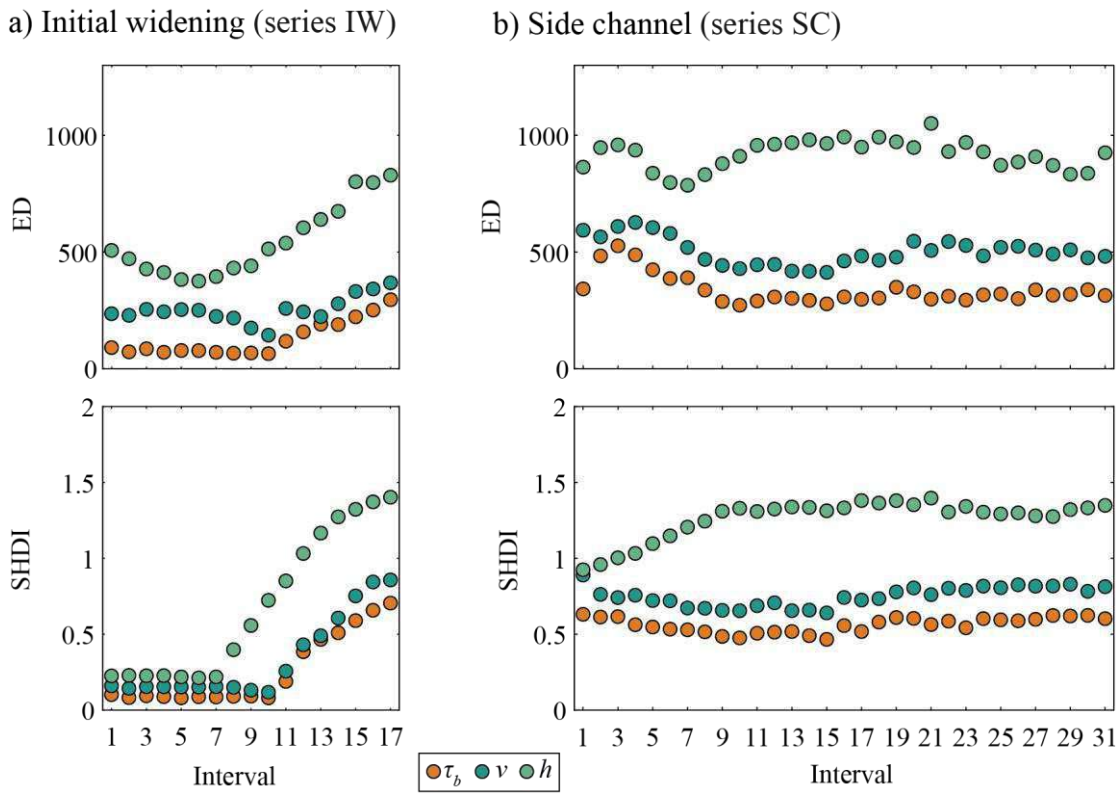

Fig. 3. Temporal evolution of the landscape metrics Edge Density (ED) and Shannon's Diversity Index (SHDI) for (a) the initial widening and (b) the side channel configuration for water depth h, flow velocity v, and bed shear stress τ for numerically simulated bed-forming discharge.

4. Conclusion and outlook

This study demonstrates that different initiation measures can distinctly influence morphological development and habitat complexity in widened river reaches. The initial widening (series IW) promotes gradual habitat complexity as morphological adjustments followed over time. In contrast, the side-channel configuration (series SC) immediately generates and sustains habitat complexity.

Further studies are needed to test a broader set of landscape metrics and their ability to capture different aspects of spatio-temporal habitat complexity. Integrating an appropriate number of ecosystem-relevant landscape metrics in future monitoring might allow a more comparable quantification of restoration success across projects and rivers.

Acknowledgements

This study is part of the research project "Resilient Rivers: Refugia – Connectivity – Stepping stones" of the Swiss national transdisciplinary research program "Hydraulic Engineering and Ecology". The first author is financially supported by the Swiss Federal Office for the Environment (FOEN), contract number 21.0202.PJ / CC00D6EEF.

References

Demuth P, Vetsch DF, Boes RM, Weitbrecht V (2025) Effect of bank height on morphodynamics in a one-sided widened gravel-bed river. Earth Surface Processes and Landforms (accepted).

Hoffmann S, Weber C, Mitchell C (2022) Principles for leading, learning, and synthesizing in inter- and transdisciplinary research. BioScience 72: 963–977.

Rachelly C (2021) Sediment Supply Control on River Widening Morphodynamics and Refugia Availability. In: Boes, R.M. (Eds.) VAW-Mitteilungen, Vol. 265. Laboratory of Hydraulics, Hydrology and Glaciology (VAW), ETH Zurich, Switzerland.

Requena P (2008) Seitenerosion in kiesführenden Flüssen, Prozessverständnis und quantitative Beschreibung (Lateral erosion in gravel-bed rivers, process and quantitative description). In: Minor, H.-E. (Eds.) VAW-Mitteilungen, Vol. 210, Laboratory of Hydraulics, Hydrology and Glaciology (VAW), ETH Zurich, Switzerland (in German).

Turner MG, Gardner RH (2015). Landscape metrics. In Landscape ecology in theory and practice: Pattern and process (pp. 97-142). New York, NY: Springer New York.

Vetsch DF, Frei S, Halso MC, Schierjott JC, Bürgler M, Vanzo D (2023) Basement V4 - A Multipurpose Modelling Environment for Simulation of Flood Hazards and River Morphodynamics Across Scales. In: SimHydro, 125-138. Singapore: Springer Nature Singapore.

Book of Abstracts of the *16th International Symposium on Ecohydraulics*
Challenges and solutions in the time of global changes
August 16–20, 2026, Lausanne, Switzerland
ISSN: 2790-2420 | ISBN: 978-90-837233-9-6 | doi:[10.64697/iahr.proc.ise2026.abs]
© 2026 IAHR. CC BY-NC-ND 4.0

DISCHARGE-DEPENDENT BRAIDED RIVER NETWORKS: PROPERTIES AND IMPLICATIONS FOR DISPERSION PROCESSES

Margherita VENDRUSCOLO[1], Carlo CAMPOREALE[1], Luca RIDOLFI[1]

[1] Department of Environment, Land and Infrastructure Engineering (DIATI), Politecnico di Torino, Corso Duca degli Abruzzi, 24, 10129 Torino, ITALY

email: margherita.vendruscolo@polito.it
email: carlo.camporeale@polito.it
email: luca.ridolfi@polito.it

ABSTRACT

Braided rivers are fascinating systems, which have been extensively studied for their morphodynamics, yet their network structure remains under-explored. We apply a graph-based approach to examine how varying flow conditions can impact braided networks' topological structure and hydraulic properties distribution. We then assess how the structural features of the river influence dispersion capacity during substance transport.

Keywords: Braided rivers; Substance transport; Dispersion; Network analysis.

1. Introduction

Braided rivers belong to a complex class of river morphology, characterized by multiple heterogeneous channels which intersect and bifurcate. Due to their network-like pattern they are particularly suitable for modeling through graphs (Connor-Streich et al., 2018). We employ a graph-based approach to answer how the network structure depends on flow conditions and how this affects dispersion in transport processes in braided rivers. Since braided networks act as natural mixer on chemicals, seeds, or pollutants, this process can critically impact ecological conditions and biogeochemical functioning.

As an example, we consider a braided reach of the Borbera Stream, in Northern Italy.

2. Methodology

2.1 Data: Borbera Stream Networks

As case study we selected a reach of the Borbera Stream, located between Cabella Ligure and Albera Ligure in Piedmont Region (Italy). The reach is approximately 3km long and 200m wide and exhibits a naturally braided riverbed, in the absence of tributaries or anthropic structures. The mass-median-diameter is approximately d_{50}=2cm. Borbera Stream's flow rate regime is characterized by a strong variability throughout the year, with a maximum yearly discharge of 45m^3/s. For this reach, a DTM with 1m resolution was available.

Graphs of the Borbera reach were obtained from fixed-bed hydraulic simulations of 9 different flow conditions performed in GeoHECRAS. Flow conditions were selected from a range of discharges, associated with very different return times values, in order to give a significant description of the possible river flow conditions. From the resulting floodmaps graphs were extracted through an ArcPy procedure which assigns nodes and edges. Afterwards, processing in MATLAB allowed to associate to each edge a single value of the hydraulic properties (i.e., water discharge, velocity, width…), by averaging over different cross-sections.

2.2 Mathematical Model

The mathematical model used to describe the dispersion process in a braided network is the one introduced in our recent paper (Vendruscolo et al., 2025), which follows the steps of the seminal paper by Rodríguez-Iturbe et al. (1979), adapted to the case of graphs. The model components are mean edges travel times - i.e., the time spent in each edge by the substance - and bifurcation probabilities - i.e., how the substance is split at river bifurcations. These parameters are combined with the network topology to analytically compute the river's response to the injection of a time-dependent substance distribution at the inlet. The resulting equation for the substance distribution at the outlet reads as in Eq. (1):

$$\boldsymbol{u(t)} = \int_0^t \left[\mathbf{A}e^{\mathbf{A}(t-\tau)}\right]_{in,out} \boldsymbol{i_0(\tau)}\, d\tau. \qquad (1)$$

Here $u(t)$ represents the unique time-dependent discharge distribution of substance, computed at the network outlet; $i_0(t)$ is the input temporal distribution of substance; finally, $\mathbf{A}$ is a matrix which contains network structure, edges travel times and bifurcation probabilities.

3. Findings

3.1 Network properties

We analyze the networks obtained in 9 water flow conditions and derive the statistical distributions of both topological and hydraulic properties. Some network examples for low, medium and high flow conditions are shown in Fig. 1. Topological properties are summarized in Table 1. It can be observed that the overall network complexity peaks at intermediate-flow scenarios, while being lower for low and high flow conditions. This is associated with the activation of new channels as the water flow increases, followed by channel merging for even higher flow values. In addition to this, we show the statistical distributions of different hydraulic variables (channels length, velocity, discharge…) and discuss the relationship between their mean values and tails with the discharge conditions.



Fig. 1. Examples of the extracted network topologies for 3 cases, respectively in low, medium and high flow conditions.

Table 1. Networks' topological properties: number of edges, nodes, bifurcations and braiding index (computed as the average number of active channels per cross section). Each case ID corresponds to a different network configuration

case ID	Q_w [m³/s]	N. edges	N. nodes	N. biforc	B.I.
S001	1.5	98	70	30	2
S010	11.1	228	159	70	3
S020	20.1	300	211	93	4
S030	29.1	419	291	134	4.33
S045	45	568	321	148	5.1
S060	60	701	477	224	5.63
S100	113.5	393	269	125	5.4
S190	193.06	271	184	88	3.7
S262	262.8	236	161	76	3.78

3.2 Network-induced dispersion

Using the model described in Section 2.2, we simulate in all networks the transport of a conservative substance, which we suppose to be injected at the inlets as a square temporal distribution. After transport, the substance reaches the network outlets with different temporal distributions in each case, as displayed in Fig. 2. The curves represent the time-dependent substance discharge computed at the network's outlets. We show that mean value and standard deviation are higher for cases where the total water discharge is lower. This can be substantially ascribed to the fact that the substance's travel is slower, therefore the edges travel times take higher values. Subsequently, *ad hoc* tests are performed, with the aim of highlighting the impact of network topology on substance temporal distribution, while minimizing the impact of travel times.

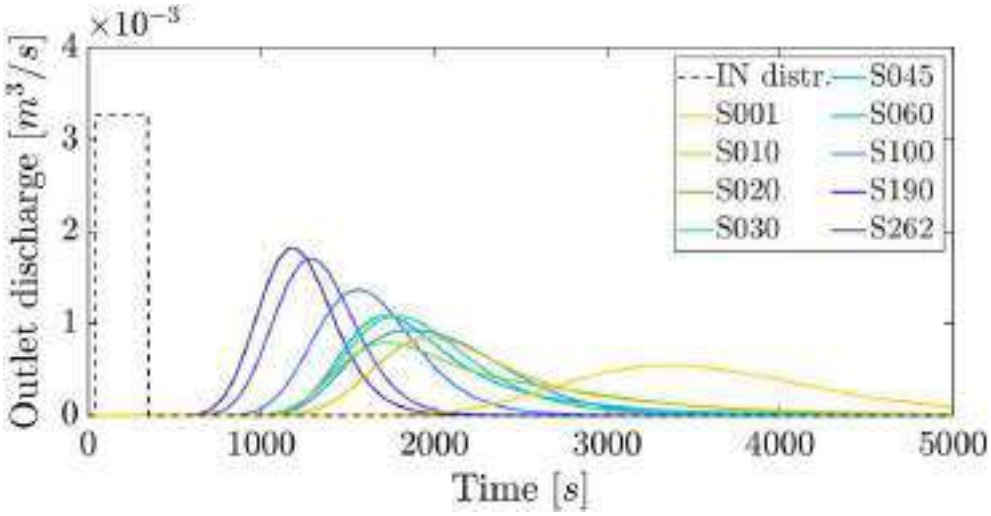

Fig. 2. Substance discharge at the networks' outlet for all cases.

4. Discussion

In this Section we elaborate on the results and provide detailed information regarding the impact of topology on dispersion and the sensitivity of the model to errors in the computation of bifurcation parameters. Furthermore, we illustrate how this approach proves to be a reliable tool for primary assessment of a river's dispersive capacity, with potential applications on the transport of solutes, sediments and macro-invertebrates.

5. Conclusion

In this study, we have extracted braided-river networks across a range of flow conditions. Quantifying their topological and hydraulic properties, we have shown that network complexity peaks at intermediate discharges. The application of the dispersion model to the same networks has demonstrated that travel times strongly control dispersion, while network topology provides an additional, measurable influence on transport outcomes. Ultimately, the dispersion capacity of the river is associated with the total water flow at the time of computing. Therefore, as for the discharge values, we can attribute a probability distribution to the river network's dispersion capacity. Together, these findings offer a new framework for linking flow dynamics, network structure, and transport processes. This is strictly linked to the ecological conditions of the river system, if we consider, for example, the dispersion of pollutants in a braided network.

References

Connor-Streich G, Henshaw AJ, Brasington J, Bertoldi W, Harvey GL. Let's get connected: A new graph theory-based approach and toolbox for understanding braided river morphodynamics. WIREs Water. 2018; 5:e1296.

Rodríguez-Iturbe, I., & Valdés, J. B. (1979). The geomorphologic structure of hydrologic response. Water Resources Research, 15 (6), 1409-1420.

Vendruscolo, M., Salerno, L., Camporeale, C., & Ridolfi, L. (2025, May). Network-driven dispersion in transport phenomena. Phys. Rev. E, 111, 054313.

Book of Abstracts of the *16th International Symposium on Ecohydraulics*
Challenges and solutions in the time of global changes
August 16–20, 2026, Lausanne, Switzerland
ISSN: 2790-2420 | ISBN: 978-90-837233-9-6 | doi:[10.64697/iahr.proc.ise2026.abs]
© 2026 IAHR. CC BY-NC-ND 4.0

NUMERICAL MODELLING OF BIOMORPHODYNAMICS: A COMPARISON OF EXISTING CLOSURES FOR BEDLOAD TRANSPORT IN VEGETATED FLOWS

Antonia DALLMEIER[1], Francesco CAPONI[2], Davide VANZO[3], Hannah SCHWEDHELM[1], Rebekka KOPMANN[4], Nils RÜTHER[1]

[1] Chair of Hydraulic Engineering, Technical University of Munich (TUM), Germany
email: antonia.dallmeier@tum.de

[2] Laboratory of Hydraulics, Hydrology and Glaciology, Federal Institute of Technology Zurich (ETH), Switzerland

[3] Institute for Water and Environment, Karlsruhe Institute of Technology (KIT), Germany

[4] Department of Hydraulic Engineering, Federal Waterways Engineering and Research Institute (BAW), Karlsruhe, Germany

ABSTRACT

Vegetation significantly influences hydraulic and morphodynamic processes in rivers, yet accurately capturing these interactions in numerical models remains challenging. This study compares different formulations for adjusting vegetation drag and sediment transport in vegetated flows, implemented within the openTELEMAC modelling framework and evaluated using a simplified two-dimensional setup. The resulting morphological responses are interpreted in the context of trends reported in the literature. The analysis reveals substantial differences between the tested approaches and underscores the importance of selecting appropriate process representations when modelling biomorphodynamic behaviour. These findings provide a foundation for future model improvements and validation using laboratory experiments and field observations.

Keywords: Shear stress partitioning, vegetation drag, sediment transport, morphodynamics, numerical modelling, openTELEMAC.

1. Introduction

Morphodynamic processes play a key role in shaping riverine ecosystems (Bertoldi et al., 2011; Gurnell, 2014). In the presence of vegetation, these processes are further modified as vegetation increases hydraulic resistance and redistributes shear stress between the bed and vegetation elements (Raupach, 1992; Le Bouteiller and Venditti, 2015). To predict morphological evolution and assess ecosystem quality, two-dimensional (2D) numerical simulations based on the shallow-water equations offer a powerful tool. However, their reliability depends on accurately representing relevant physical processes, which becomes particularly challenging when accounting for vegetation effects on sediment transport. Although several approaches have been proposed in recent years to improve predictions of bedload transport in vegetated flows (e.g., Armanini and Cavedon, 2019; Yang and Nepf, 2019; Wang et al., 2024), no comparative study has yet applied 2D numerical modelling to evaluate their applicability. Integrating vegetation effects on both hydraulics and sediment dynamics is therefore essential for achieving robust morphodynamic predictions (Vargas-Luna et al., 2015; D'Ippolito et al., 2023).

This study investigates the impact of various vegetation drag formulations and sediment transport adjustment methods on simulated bedload transport in vegetated flows, using the numerical software openTELEMAC. A simplified numerical test case was designed, combining two vegetation drag models with two approaches for calculating sediment transport under vegetated conditions, resulting in four model configurations. This analysis evaluates the interaction between hydraulic resistance and morphodynamic response and assesses the robustness of these two parameterizations (hydraulic and morphodynamic) in predicting deposition patterns consistent with trends reported in the literature.

2. Methods

2.1. Vegetation drag models

In this study, vegetation-induced hydraulic resistance is represented using the approaches of Baptist et al. (2007) (BAPT) and Stone and Shen (2002) (STEN). These methods are well-suited for the examined conditions because they explicitly distinguish between emergent and submerged rigid vegetation. This aligns with the simplified test case used in this study, in which vegetation is idealized as rigid cylinders, an assumption supported by laboratory data on sediment transport in rigid vegetated flows (Kothyari et al., 2009; Vargas-Luna et al., 2015; D'Ippolito et al., 2023). In openTELEMAC, both approaches are implemented as additional friction forces superimposed on the bottom friction.

2.2. Sediment transport adjustment methods

The influence of vegetation on bedload transport is represented using two methods:

- The Einstein and Banks (1950) partitioning method (EB), which calculates the effective bed shear stress based on the Keulegan resistance law.
- The Armanini and Cavedon (2019) approach, later modified by Bonilla-Porras et al. (2021) for submerged vegetation (BP), which adjusts the Shields parameter and dimensionless transport rate based on vegetation properties.

2.3. Numerical setup

A simplified two-dimensional test case, which resembles a modification of the laboratory experiments by Armanini and Cavedon (2019), was simulated using openTELEMAC v8p4 (Fig. 1). The mesh represents a 15 m long and 0.5 m wide straight channel with an element size of 0.05 m. The central 4 m section contains vegetation, whereas the upstream and downstream sections are without any vegetation. The flow direction is from left to right (Fig. 1). Each simulation started from a morphodynamic equilibrium (initial slope $S_0 = 0.2\ \%$) obtained under unvegetated conditions applying a constant flow rate of $Q_w = 0.02\ m^3/s$, a constant sediment transport rate of $Q_s = 0.003757\ kg/s$ and a constant water depth at the outlet of $h_w = 0.102\ m$ (see Fig. 1, left side). A total of eight simulations were performed by combining the two vegetation drag models and two sediment adjustment methods under both emergent ($h_p > h_w$) and submerged ($h_p = 0.10\ m$) conditions. Each simulation ran until steady-state conditions were achieved, defined here as when the discharge and bedload transport rate exiting the domain were equal to the amount entering the domain, and therefore no bed-level changes occurred. Model results were evaluated based on the final bottom elevation.

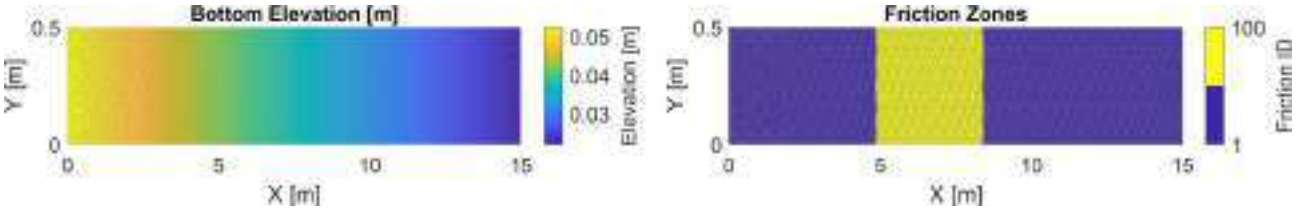

Fig. 1. Bottom elevation and friction zones in 2D plan view of the simplified numerical test case.

3. Results and Discussion

Figure 2 presents the final bottom and free surface elevations along the longitudinal centreline of the channel for the emergent (left) and submerged (right) vegetation cases. The bottom and free surface profiles of the initial morphodynamic equilibrium conditions are shown in grey for reference.

Across both flow conditions, the BP sediment adjustment method produced unexpected erosion patterns that contradict typical observations reported in the literature (e.g., Kothyari et al., 2009; Le Bouteiller and Venditti, 2015; Caponi and Siviglia, 2018; D'Ippolito et al., 2023), where sediment deposition is generally expected within densely vegetated zones. This contrasting behaviour indicates that the BP method implemented in openTELEMAC requires further investigation to clarify its underlying mechanisms. In contrast, the EB shear-stress partitioning approach yielded results that align more closely with expected trends reported in literature.

The choice of vegetation drag model also affected the morphological response, though to a lesser extent than the choice of sediment adjustment method. Because the BP formulation uses the total shear stress to compute the adjusted Shields parameter, thereby directly incorporating vegetation drag (Bonilla-Porras et al., 2021; Dallmeier et al., 2025), its sensitivity to the drag representation is particularly strong. Differences between

drag models become especially pronounced under emergent conditions, where vegetation exerts substantial hydraulic resistance.

Overall, the simulations revealed distinct sensitivities: vegetation drag formulations primarily influenced the flow field and near-bed velocities, whereas sediment adjustment approaches controlled the magnitude and spatial distribution of bedload transport. In addition to the choice of formulation for hydrodynamic and morphodynamic modelling, the vegetation submergence ratio was identified as a key parameter governing the morphodynamic response.

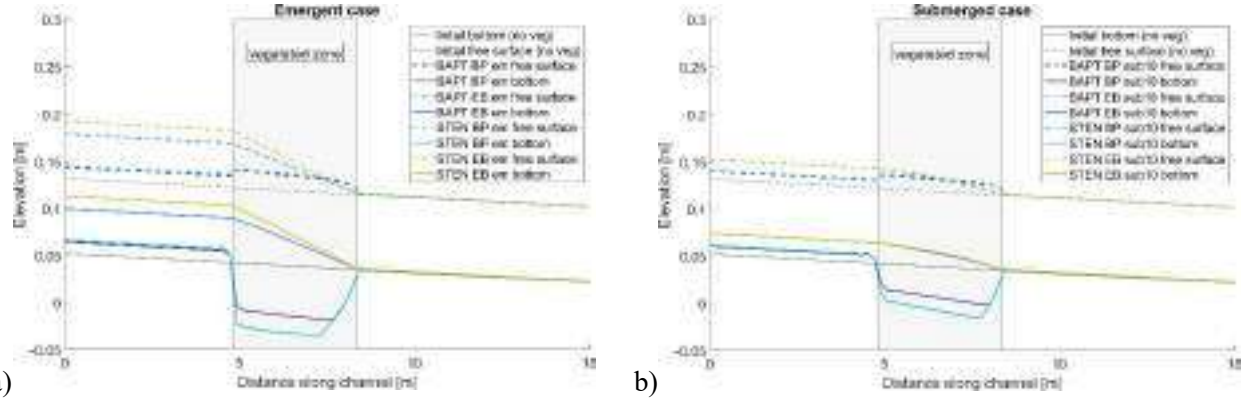

a) b)

Fig. 2. Final bottom and free surface elevations of the simulations a) in emergent conditions and b) in submerged conditions.

4. Conclusion

This study provides a systematic comparison of vegetation drag formulations and sediment transport adjustment methods in openTELEMAC, applied to a simplified test case. The results demonstrated that the formulation choice strongly influenced the predicted riverbed patterns. Additionally, the Shields-adjustment approach by Bonilla-Porras et al. (2021) yielded erosion trends that are contrary to commonly observed deposition patterns within densely vegetated zones. This contrasting behaviour highlights the need for careful selection and evaluation of process representations when modelling morphodynamics in vegetated flows.

The analysis helps identify suitable modelling strategies for vegetated flows. Future work will extend this evaluation to more complex geometries and include validation against laboratory and field datasets to further establish the applicability of these modelling approaches in ecohydraulic research.

References

Armanini A, Cavedon, V (2019) Bed-load through emergent vegetation. Advances in Water Resources, 129, 250–259. doi:10.1016/j.advwatres.2019.05.021.

Baptist MJ, Babovic V, Rodríguez Uthurburu J, Keijzer M, Uittenbogaard RE, Mynett A, Verwey A (2007) On inducing equations for vegetation resistance. Journal of Hydraulic Research, 45, 435–450. doi:10.1080/00221686.2007.9521778.

Bertoldi W, Gurnell AM, Drake NA (2011) The topographic signature of vegetation development along a braided river: Results of a combined analysis of airborne lidar, color air photographs, and ground measurements. Water Resources Research, 47, 1-13. https://doi.org/10.1029/2010WR010319.

Bonilla-Porras JA, Armanini A, Crosato A (2021) Extended Einstein's parameters to include vegetation in existing bedload predictors. Advances in Water Resources, 152, 103928. doi:10.1016/j.advwatres.2021.103928.

Caponi F, Siviglia A (2018) Numerical Modelling of Plant Root Controls on Gravel Bed River Morphodynamics. Geophys ical Research Letters, 45, 9013–9023. https://doi.org/10.1029/2018GL078696.

D'Ippolito A, Calomino F, Dey S, Gaudio R, Penna N (2023) Bedload transport through emergent vegetation: Current status and its future prospect. Environmental Fluid Mechanics, 23, 711–733. https://doi.org/10.1007/s10652-023-09918-0.

Dallmeier A, Kopmann R, Casas Mulet R, Schwedhelm H, Folke F, Rüther N (2025) A Novel Biomorphodynamic Model to Enhance Bedload Transport Modelling in Emergent and Submerged Rigid Vegetation. Water, 17, 23, 3336. https://doi.org/10.3390/w17233336.

Einstein HA, Banks RB (1950) Fluid resistance of composite roughness, Eos Transactions American Geophysical Union (AGU), 31(4), 603–610.

Gurnell A (2014) Plants as river system engineers. Earth Surface Processes and Landforms, 39, 4–25. https://doi.org/10.1002/esp.3397.

Kothyari UC, Hashimoto H, Hayashi K (2009) Effect of tall vegetation on sediment transport by channel flows. Journal of Hydraulic Research, 47, 700–710. https://doi.org/10.3826/jhr.2009.3317.

Le Bouteiller C, Venditti JG (2015) Sediment transport and shear stress partitioning in a vegetated flow, Water Resources Research, 51, 2901–2922. doi:10.1002/2014WR015825.

Raupach M (1992) Drag and drag partition on rough surfaces, Boundary-Layer Meteorology, 60(4), 375–395. doi:10.1007/BF00155203.

Stone BM, Shen HT (2002) Hydraulic Resistance of Flow in Channels with Cylindrical Roughness, Journal of Hydraulic Engineering, 128, 500–506. doi:10.1061/(ASCE)0733-9429(2002)128:5(500).

Vargas-Luna A, Crosato A, Uijttewaal WS (2015) Effects of vegetation on flow and sediment transport: Comparative analyses and validation of predicting models. Earth Surface Processes and Landforms, 40, 157–176. https://doi.org/10.1002/esp.3633.

Wang X, Gualtieri C, Huai W, Liu H, Yu S (2024) An improved formula for bed-load rate in open channel flows with emergent vegetation, Physics of Fluids, 36, 013309 (2024). doi: 10.1063/5.0185667.
Yang QJ, Nepf HM (2019) Impact of vegetation on bed load transport rate and bedform characteristics. Water Resources Research, 55, 6109–6124. https://doi.org/10.1029/2018WR024404.

Book of Abstracts of the *16th International Symposium on Ecohydraulics*
Challenges and solutions in the time of global changes
August 16–20, 2026, Lausanne, Switzerland
ISSN: 2790-2420 | ISBN: 978-90-837233-9-6 | doi:[10.64697/iahr.proc.ise2026.abs]
© 2026 IAHR. CC BY-NC-ND 4.0

PARTIALLY VEGETATED MEANDERING FLUME: PRELIMINARY RESULTS ON FLOW VELOCITY DISTRIBUTION IN THE BEND APEX AREA

Donatella TERMINI[1,2]

[1] Department of Engineering, University of Palermo (Italy)
email: donatella.termini@unipa.it

[2] NBFC, National Biodiversity Future Center, Palermo, Italy

ABSTRACT

Understanding flow characteristics and dispersion processes in partially vegetated rivers is especially important with respect to the identification of the water quality and the ecosystem conditions. This paper focuses on highly curved channels and examines how the presence of square patches of flexible submerged vegetation on the bed affects flow patterns. The analysis is conducted with the aid of data collected in a large amplitude meandering flume constructed at the Department of Engineering – University of Palermo (Italy). In particular, the analysis examines the apex area of the flume to investigate the effect of a patchily-vegetated bed on the mean streamwise flow velocity distribution and on the mixing-layer formation in both vertical and horizontal planes.

Keywords: Rivers, hydrodynamics, flexible vegetation, heterogeneity, shear layer.

1. Introduction

Flows over submerged vegetation patches in rivers are common in nature. Understanding flow characteristics and turbulent structure in the presence of vegetation is especially important with respect to environmental processes as sediment transport and mixing of transported quantities. On one hand vegetation modifies flow and sediment transport, influencing bed morphology and river's evolution; on the other hand vegetation influences the distribution of nutrients and oxygen and water quality conditions. The alteration of hydrological conditions in fluvial systems determines continuous changes in river morphology and in riparian or riverbed vegetation. Consequently, the spatial distribution of vegetation might change in time and in space depending on the combination of many factors which might affect the settling, and growth of the vegetated elements. A large number of studies have analysed flow around finite patches of emergent vegetation both in the laboratory and in the field (among others Zong and Nepf 2012, Ortiz et al. 2013, Devi et al., 2019). Few works have been conducted over flexible vegetated patches (see as an example Devi and Kumar, 2016). All these studies highlighted that the heterogeneous distribution of vegetation on the bed determines abrupt variations in bed roughness. According to White and Nepf (2007), this could result in the development of shear-induced vortices, in the horizontal and vertical planes, which in turn could determine secondary cross-circulations affecting the mass and momentum exchange processes. Identifying flow circulation between vegetated and non-vegetated areas is extremely important for investigating many ecological and morphodynamic processes. In fact, while the faster flow in non-vegetated areas could carry sediment and nutrient loads, in vegetated areas sediment retention could occur.

However, the impact of patchy vegetation—particularly flexible and submerged types—on riverine hydrodynamics remains poorly characterized, as the three-dimensional nature of the flow makes systematic investigation challenging. Furthermore, most studies on vegetated flows have been conducted in straight channels, overlooking the effects of centrifugal forces occurring in curved channel reaches.

This study investigates the effect of submerged flexible-vegetation patches on flow patterns at the bend apex area of a large-amplitude meandering flume. As literature shows (e.g., Dietrich and Smith, 1983; Termini and Piraino, 2012), in high-curvature bends the non-linear feedback between vertical profiles of stream-wise velocity and cross-circulation is significant and hydrodynamic processes are more complex than those developing either in straight or in moderate-curvature bends. The analysis is conducted by the aid of data collected in a laboratory meandering flume with bed covered by squared patches of flexible vegetation.

2. Experimental data

The laboratory flume, constructed at Department of Engineering - University of Palermo – Italy, follows the sine-generated curve with deflection angle at the inflection section equal to θo=110°. The length of the channel axis is approximately 28 m and the walls are of transparent 3 mm thick plexiglass, approximately 0.67 m high; the channel's width is constant and equal to 0.50 m. To exclude the effects due to the bed deformation, the bed was rigid with a uniform slope equal to 0.2% along the channel axis. The bed was covered with square islands (patches) of flexible vegetation (artificial) characterized by flexural properties comparable to those of *Festuca arundinacea*, a species of monocotyledonous angiosperms belonging to the Poaceae family (or Gramineae). The square vegetated patches were arranged as two aligned islands in the transverse direction, with a percentage of coverage of 10% (see Figure 1). In this work, analysis concerns the streamwise flow velocity data measured, by using a DOP 2000 - by Signal Processing s.a., in the area around the apex section of the central bend during an experimental run conducted with flow discharge Q = 0.124 m^3/s.

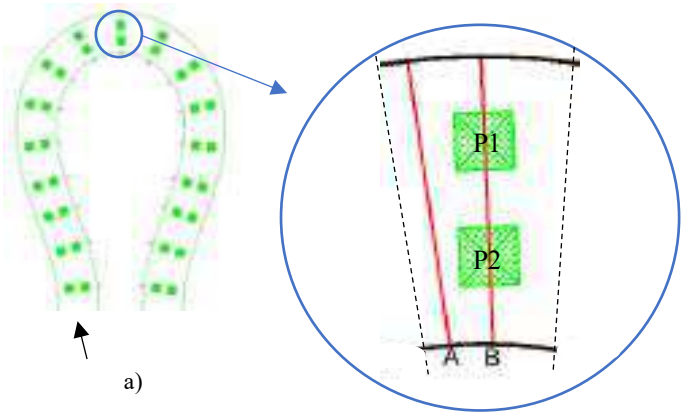

Figure 1. a) Schematic view of the central meander wave with flexible vegetated patches and investigated area; b) sections considered for the analysis

3. Results

To investigate how vegetated patches influence flow characteristics, we processed the measured data to determine the streamwise flow velocity distributions inside and around vegetated patches P1 and P2 (Figure 1).

Due to the heterogeneity of the bed roughness, the analysis has been operated considering that the time-averaged approach must be supplemented by the spatial averaged one (Smith and McLean 1977; Nikora et al. 2001). The spatial average has been applied to three time-averaged streamwise velocity profiles spaced 3 mm apart. These velocity profiles show a typical S-shape assuming low negative/positive values inside the vegetated layer; as one moves from the bed towards the free surface the velocity increases in value and the profile changes the concavity with a formation of an inflection point. Because of the presence of the inflection point these profiles can be interpreted by the hyperbolic tangent function, written as follows (Ghisalberti and Nepf, 2002; Carollo et al., 2008):

$$u = \overline{u} + \frac{\Delta u}{2} tanh\left(\frac{z-\bar{z}}{2\theta}\right) \quad (1)$$

with:

$$\theta = \int_{-\infty}^{+\infty} \left[\frac{1}{4} - \left(\frac{u-\overline{u}}{\Delta u}\right)^2\right] dz \quad (2)$$

where u_1 and u_2 are respectively lowest and highest values of flow velocity, $\bar{u} = (u_1 + u_2)/2$, $\bar{z}$ is the distance from the bed where $u=\bar{u}$ and $\Delta u=u_2-u_1$, θ is the momentum thickness which is related to the Kelvin-Helmholtz instability (Ghisalberti and Nepf, 2002).

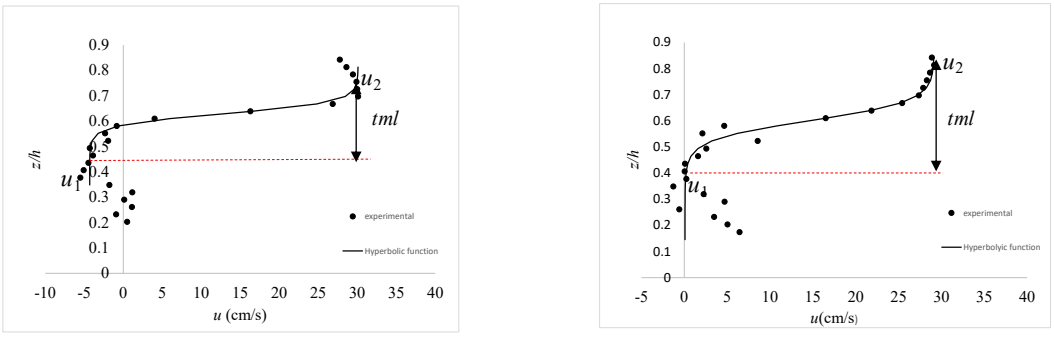

Figure 2. Vertical velocity profiles and hyperpobolic function: a) vegetated patch P1; b) vegetated patch P2

Thus, the velocity profile can be approximated by a three layers' scheme, characterized by two layers of constant velocity (i.e., u_1 and u_2) and an intermediate mixing-layer layer. The mixing-layer thickness in the vertical direction can be defined as $tml=z_2-z_1$, i.e. as the distance between the first positions where $u=u_1$ and $u=u_2$ occur, as shown in Figure 2. The thickness of the mixing-layer identifies the vertical spatial extent of the shear layer due to the presence of vegetation.

Thus, inside the vegetated area a shear layer develops in the vertical plane, indicating the formation of large-scale eddies, which produce a motion of fluid towards the bed and the free surface through the whole flow depth (Carollo et al., 2008), playing a crucial role in mass and momentum exchange between the vegetated layer and the flow above. In the vegetated patch P1, which is closer to the outer bank, the thickness of the mixing-layer is lower than that obtained inside the vegetated patch P2, which is closer to the inner bank. The lower thickness of the mixing layer occurring in vegetated patch P1 could be related to the outer bank effect in agreement with what previously obtained in the same channel without vegetation on the bed (Termini, 2015).

The influence of vegetated patches on the streamwise velocity distribution has been also investigated in the horizontal plane. To this aim, the horizontal streamwise velocity profiles at the top of the vegetation layer have been analysed in various sections within the examined area. In this work the sections A and B of Figure 1, respectively upstream of the vegetated patches and crossing the vegetated patches, have been considered (Figure 3). For simplicity, the analysis in section B is based on velocity measurements taken within the central area affected by the vegetated patches.

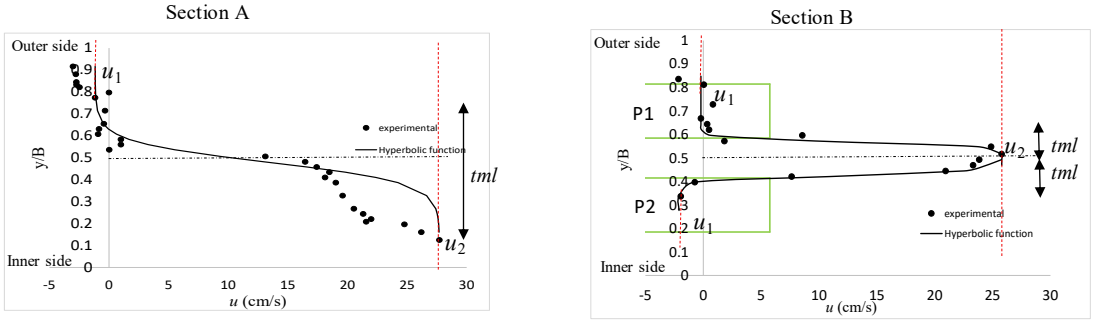

Figure 3. Horizontal streamwise velocity profiles and hyperpobolic function

Figure 3 illustrates that in section A, i.e. within the non-vegetated area upstream of the considered vegetated patches, the horizontal streamwise velocity profile exhibits a distinct gradient, with higher values close to the inner bank and lower values close to the outer bank. Consequently, an inflection point is observed around the channel centerline, indicating the development of a mixing layer in the central region, whose thickness was around $3Lv$ (Lv=length of patch's edge). This highlights that the presence of the vegetated patches also affects

the velocity distribution in the non-vegetated areas. In section B, which crosses the center of the patches P1 and P2, a clear velocity gradient is observed: the streamwise velocity increases in value passing from each vegetated patch towards the center of the channel, i.e. from the vegetated area towards the central non-vegetated area. The velocity profile extending from each patch toward the channel's center shows a changing concavity with the formation of an inflection point.
Analogously to the analysis in vertical direction, the hyperbolic function has been applied to the lateral direction by employing Equations (1)-(2) with the substitution of the variable z (distance from the bed) for the variable y (distance from the examined patch's center). The thickness of the mixing-layer has been estimated as $tml=y_2-y_1$, where with y_2 and y_1 are the distances from the considered patch's center of the first positions with $u=u_1$ and $u=u_2$, respectively. The mixing-layer thickness was similar for both patches, with a mean value of approximately $0.84Lv$. From this analysis (Figure 3) it is clear that a lateral shear layer develops close to the lateral edge of each vegetated patch, indicating the formation of vortices which are responsible for momentum exchange in the central area of the channel.

4. Conclusion

This study analyses the effect of square patches of flexible and submerged vegetation on flow characteristics, with the aid of experimental data collected in a high-amplitude sine-generated laboratory flume, at the Department of Engineering of the University of Palermo. In particular, the analysis concerns the streamwise velocity profiles along two sections, respectively located inside the vegetated patches (i.e., along the apex section of the flume) and in the non-vegetated area upstream of them.
Results show that inside the vegetated patches the vertical streamwise velocity profile shows a typical S-shape with a formation of a shear layer, indicating the evolution of large-scale eddies responsible to mass and momentum exchange between the vegetated layer and the flow above. The thickness of the mixing-layer sligthly reduces passing from the inner bank to the outer bank. A lateral shear layer also develops on the horizontal plane close to the lateral edge of each vegetated patch, highlighting the formation of vortices responsible for the momentum exchange in the central area of the channel. This could influence transport and mixing of sediment and substances, exerting an important role on ecosystem functioning in bends.

Acknowledgements

This work has been supported by Project "WETland ecosystem restoration through WISE strategic adaptation across borders - WETWISE", Cod. C1-2.3-69, CUP B73C25000190002, in the ambit of program INTERREG VI – A Italia Malta 2021-2027.

References

Carollo, F.G., Ferro, V. & Termini, D. 2008. Flow velocity profile and turbulence characteristics in a vegetated straight flume" International Congress Riverflow 2008. ISBN978-605-60136-1 4.
Devi T.B., Kumar B. 2016. Flow characteristics in an alluvial channel covered partially with submerged vegetation. Ecol. Eng. 94, 478–492.
Devi TB, Sharma A, Kumar B (2019) Flow characteristics in a partly vegetated channel with emergent vegetation and seepage. Ecohydroly & Hydrobiology 19(1):93–108. https:// doi. org/ 10. 1016/j. ecohyd.2018. 07. 006
Dietrich, W.E., Smith, D. (1983). Influence of the Point Bar on Flow Through Curved Channels, Water Resources Research, 19(5): 1173-1192.
Ghisalberti M., Nepf H.M. (2002). Mixing layer and coherent structures in vegetated acquatic flows. Journal of Geophysical Research, 107 (2), 3-1–3-11.
Nikora, V., Goring, D., McEvan, I. & Griffiths, G. (2001). Spatially Averaged Open-Channel Flow over Rough Bed. *Journal of Hydraulic Engineering*.Vol. 127: Issue 2.
Ortiz S. , Breidenbach J., Kändler G. (2013). Early detection of bark beetle green attack using TerraSAR-X and RapidEye data. Remote Sens., 5 , pp. 1912-1931
Smith, J.D. & McLean, S.R. (1977). Spatially averaged flow over a wavy surface. *Oceans and Atmopheres*. Vol 82: Issue 12.
Termini D. (2015). Flexible Vegetation Behavior And Effects On Flow Conveyance: Experimental Observations". 2015. International Journal of River Basin Management. 13(4), 401-411. doi:10.1080/15715124.2015.1012519.
Termini, D., Piraino, M., (2011). Experimental analysis of cross-sectional flow motion in a large amplitude meandering bend. Earth Surface Processes and Landforms 36(2), 244-256.
Termini, D. (2015). Momentum transport and bed shear stress distribution in a meandering bend: experimental analysis in a laboratory flume. Advances in Water Resources. Vol. 128, 128-141
White B., Nepf H. 2007. Shear instability and coherent structures in shallow flow adjacent to a porous layer. Journal of Fluid Mechanics, 593:1-32. DOI: 10.1017/S0022112007008415
Zong L., Nepf H. 2012. Vortex development behind a finite porous obstruction in a channel. J. Fluid Mech., 691, 368–391.

Book of Abstracts of the *16th International Symposium on Ecohydraulics*
Challenges and solutions in the time of global changes
August 16–20, 2026, Lausanne, Switzerland
ISSN: 2790-2420 | ISBN: 978-90-837233-9-6 | doi:[10.64697/iahr.proc.ise2026.abs]
© 2026 IAHR. CC BY-NC-ND 4.0

FLOODPLAIN VEGETATION CONTROLS ON IN-CHANNEL HABITAT AVAILABILITY AND REFUGE IN A MEANDERING MORPHOLOGY

Davide VANZO[1], Nicolas R.A. PAVA[1], Andrew W. TRANMER[2], Daniel C. WHITE[3]

[1] Institute for Water and Environment, Karlsruhe Institute of Technology, Germany
email: davide.vanzo@kit.edu; nicolas.pava@student.kit.edu

[2]Center for Ecohydraulics Research, Department of Civil and Environmental Engineering, University of Idaho, USA
email: andyt@uidaho.edu
[3]Department of Civil and Environmental Engineering, Colorado State University, USA
email: danny.white@colostate.edu

ABSTRACT

Habitat availability and hydraulic refuge are essential for juvenile fish to ensure future breeding populations, yet the influence of floodplain vegetation on habitats and refuge across flow conditions is not well understood. Using mobile-bed flume experiments and two-dimensional habitat modeling, we assess how floodplain vegetation density affects in-channel hydro-morphological characteristics. Habitat metrics show strong, non-linear differences among vegetation scenarios, particularly at intermediate discharges (3–30 m^3/s). These explorative results highlight the broader influence of floodplain vegetation on channel hydraulic heterogeneity and underscore the need for further work across species and metrics to support more effective river management.

Keywords: floodplain vegetation, channel morphology, aquatic habitat, refuge, hydrodynamics, modelling.

1. Introduction

In-channel hydraulic refuge is essential for juvenile salmonids across a range of flow conditions, from large floods when high velocities severely limit in-channel refuge, to very low flows, when depths may become insufficient to support suitable habitat (Benjankar et al., 2025; Tonolla et al., 2021). Although floodplain inundation typically moderates main-channel velocities during high flows (e.g. McKean and Tonina, 2013), recent flume experiments demonstrate that dense floodplain vegetation can substantially restrict channel-floodplain exchange, increasing in-channel velocities (White et al., 2023, 2025) and potentially reducing habitat suitability. Those same experiments show that vegetation density also influences bed morphology, producing different pool-riffle structures that further govern low-flow habitat availability. However, the distribution and persistence of habitat refuge across the full range of hydrologic conditions remains poorly understood, particularly regarding the extent to which vegetation-mediated hydraulics and morphology govern in-channel habitat.

Gravel-bed rivers with lateral floodplain connectivity typically offer diverse hydraulic environments for aquatic organisms across a range of flow conditions, the sustained suitability of which is driven by a complex interplay of flow, sediment, and wood regimes (Caamano et al., 2012; Wohl et al., 2015, 2019). Foundational habitat-suitability work (e.g., Raleigh et al., 1984) shows that juvenile and adult salmonids prefer a range of velocity, depth, and substrate that balance opportunities for foraging, predator avoidance, and refuge from high flows. Other research emphasizes that hydraulic heterogeneity, riffle-pool sequences, large wood, and secondary flow features increase available habitat by creating mosaics of velocity and depth conditions (Benjankar et al., 2025; Beechie et al., 2023).

Despite the obvious ecological importance of refuge across flows, the link between floodplain vegetation and the availability of hydraulic refuge remains poorly studied. Much of the literature on vegetation in river corridors has focused on the role of riparian plants in bank stabilization, sediment trapping, and roughness

generation (e.g. Aberle & Järvelä, 2013; Baptist et al., 2007; Benjankar et al., 2011; Tranmer et al., 2024). For example, rigid-stem vegetation has been shown to reduce mean flow velocities and increase localized turbulence and residence time in vegetated patches (Yager & Schmeeckle, 2013; Lightbody et al., 2019). However, most of these insights come from patch-scale or simplified channel experiments, and it remains unclear how vegetation effects translate to reach-scale, compound-channel settings where lateral floodplain flows interact with meander-driven secondary currents. This gap limits our ability to assess how vegetation-mediated turbulence, flow partitioning, and morphology influence the formation and persistence of hydraulic refuge across both high- and low-flow conditions.

This study investigates how vegetation-driven channel morphology affects in-channel juvenile salmonid habitat in gravel-bed rivers. Using scaled, mobile-bed flume experiments (from White et al. 2023, 2025) and two-dimensional hydraulic and habitat modeling, we evaluate how different combinations of flow and floodplain vegetation density produce distinct depth- and velocity-based habitat suitability for juvenile brown trout. Specifically, we 1) quantify how vegetation density on the floodplain limits in-channel hydraulic refuge during high flows by increasing in-channel velocities and 2) determine how vegetation-mediated morphological differences shape low-flow rearing habitat, with the expectation that denser vegetated floodplains generate greater physical heterogeneity and improved low-flow habitat.

2. Methods

2.1. Experimental Inputs and Numerical Model Setup

We used measured topography and flow conditions derived from seven flume runs presented in White et al. (2025), which represent a compound meandering gravel-bed channel with bare (VO), low- (V1), and high-density (V2) floodplain vegetation conditions. In-channel self-formed morphologies are generated via three morphogenic flow conditions, namely bankfull (BF), low overbank (DR01), and high overbank (DR02) (see Table 1). These experiments were conducted at a geometric scale of 20, simulating a 20-m wide channel with a 30° crossing angle meandering planform. Each flume run (see White et al. 2025) produced high-resolution measurements of water surface elevation, flow depth, and velocity, across the channel and floodplain.

We developed a two-dimensional hydrodynamic model in BASEMENT v.4 (Vetsch et al. 2024), solving the depth-averaged shallow-water equations using the flume topography generated from Structure-from-Motion point clouds as hydraulic model terrain. Separate Strickler roughness coefficient (k_s) values were calibrated for the floodplain and the channel. Model inflows were scaled up to prototype discharges using Froude similarity, matching the seven flume-tested flow conditions. To calibrate the model, we minimized deviation between simulated and observed water surface elevations, using the root mean square error by iteratively adjusting the roughness coefficient. We validated the model by comparing modeled and measured velocities across the floodplain and in the channel.

2.2. Habitat Suitability Assessment

Hydraulic model outputs (depth and depth-averaged velocity) were post-processed to quantify habitat suitability for juvenile brown trout (*Salmo trutta*). Species-specific depth and velocity preference curves were applied to each computational cell following standard ecohydraulic formulations, yielding a composite habitat suitability index ($HSI = \sqrt{SI_d SI_v}$, with SI_d and SI_v suitability indexes for depth and velocity). For each modeled discharge, we computed Weighted Usable Area (*WUA*), and the Overall Suitability Index (*OSI=WUA/Atot,* with *Atot* total wetted area). Habitat metrics were extracted for all seven flow scenarios to assess how hydraulic refuge and usable habitat respond to discharge under given floodplain density, but varying equilibrium topographies produced by different vegetation treatments. Comparisons among runs focused on discharge-dependent trends in *WUA* and *OSI*, emphasizing the sensitivity of low-flow habitat availability to vegetation-driven morphological differences.

3. Results

Results reveal a non-trivial relationship between floodplain characteristics, specifically vegetation density, the resulting self-formed in-channel morphologies, and the resulting habitat suitability for juvenile brown trout. Figure 1 illustrates this by showing the spatial distribution of the *HSI* at a discharge of $Q = 10\ m^3/s$ across four morphological scenarios. Under low overbank formative discharges (panels a and b), suitable habitats are largely confined to pool areas (e.g. red areas), and their extent increases with higher floodplain vegetation density (compare a with b). In contrast, scenarios with high overbank formative discharges (panels c and d) exhibit an overall increase in suitability relative to panels and b. However, the influence of vegetation density reverses: higher vegetation density leads to lower in-channel suitability (d compared to c).

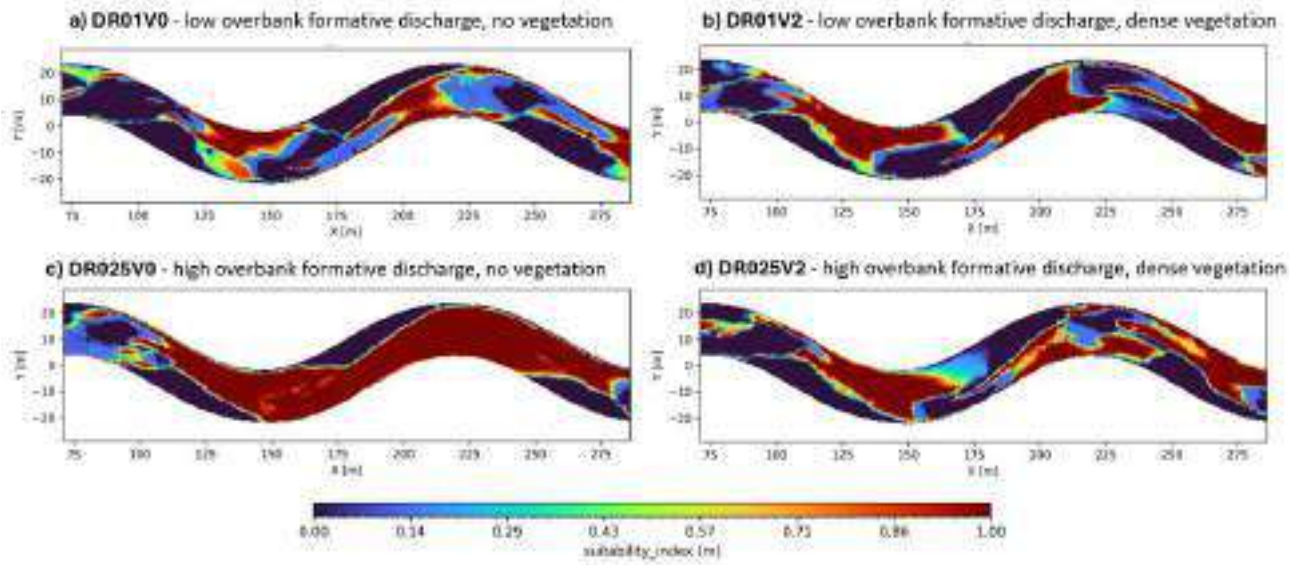

Fig. 1. Spatial distribution of the Habitat Suitability Index (*HSI*) at discharge Q=10m³/s in four different simulated scenarios. Top panels refer to channel morphologies generated by low overbank formative discharge (Q=143m³/s) with no (a) and dense (b) floodplain vegetation. Bottom panels: channel morphologies generated by high overbank formative discharge (Q=304m³/s) with no (c) and dense (d) vegetation.

Figure 2 presents the Overall Suitability Index (OSI) across a discharge range from 1 to 50 m³/s for all seven investigated scenarios. As expected, each scenario exhibits the well-established pattern in the discharge–habitat relationship: habitat availability increases with discharge, reaches an optimum, and subsequently declines as flows become too high. However, the discharge at which maximum OSI occurs varies substantially across scenarios, underscoring the strong influence of floodplain vegetation and its interaction with channel morphology. These differences further highlight the non-linear and highly scenario-dependent feedback between vegetation density, emergent geomorphic features, and the resulting in-channel habitat conditions. Together, these results point to a complex interplay in which small changes in floodplain characteristics can shift the discharge threshold associated with optimal habitat availability.

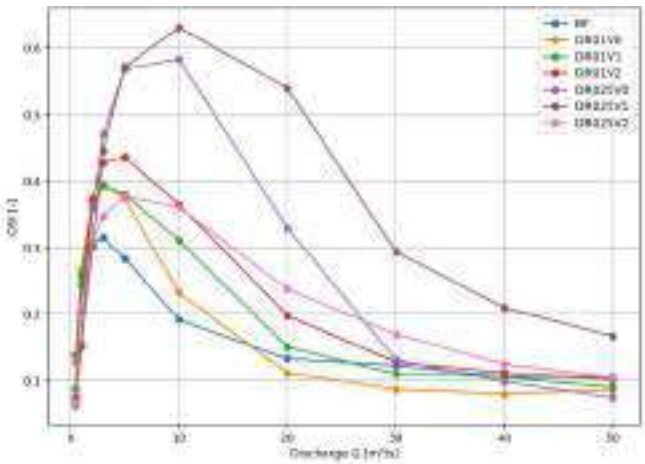

Fig. 2. Overall Suitability Index (*OSI*) across a discharge range from 1 to 50 m³/s for all the seven investigated scenarios.

4. Discussion

Our results highlight a clear and previously underappreciated link between floodplain vegetation density and the physical heterogeneity of the channel that ultimately shapes native aquatic habitat across a range of flow conditions. This connection emerges through the action of high, overbank discharges that interact with riparian vegetation, modifying flow resistance, mediating sediment transport, and driving distinct patterns of bed morphology. The resulting equilibrium bathymetries provide deeper and hydraulically more diverse channel conditions during low-flow periods, offering improved habitat suitability for juvenile salmonids. This demonstrates that floodplain vegetation exerts a far broader influence on channel hydraulics and habitat dynamics than typically assumed. Habitat metrics further articulate how vegetation-driven hydro-

morphodynamic changes translate into ecologically meaningful differences in juvenile trout refuge, as illustrated in Figure 2. The largest divergences among scenarios occur for discharges between roughly 3 and 30 m^3/s, a range where floodplain–channel feedbacks strongly modulate the availability of suitable habitat. At higher flows (>50 m^3/s), but still below the bankfull conditions, differences between scenarios diminish markedly, and overall habitat suitability remains low. This suggests that off channel habitats in the form of secondary channels, backwater areas, and floodplain depressions may be critical to support hydraulic refuge during high flow conditions (e.g., Benjankar et al., 2025).

Overall, these findings are still explorative, but they clearly indicate that floodplain vegetation density plays an important role in shaping channel hydraulics and habitat suitability. In the next phase, we will extend the analysis to additional species and adopt other ecologically relevant metrics to test the robustness of these patterns. More broadly, our results highlight that processes occurring on the floodplain—such as vegetation establishment, density, and persistence—have direct implications for in-channel morphology and habitat conditions. Understanding and quantifying these linkages is essential for designing more efficient and sustainable river management strategies, particularly under changing hydrologic regimes and increasing environmental pressures.

References

Aberle, J., & Järvelä, J. (2013). Flow resistance of emergent rigid and flexible floodplain vegetation. *Journal of Hydraulic Research*, *51*(1), 33–45. https://doi.org/10.1080/00221686.2012.754795

Baptist, M. J., Babovic, V., Uthurburu, J. R., Keijzer, M., Uittenbogaard, R. E., Mynett, A., & Verwey, A. (2007). On inducing equations for vegetation resistance. *Journal of Hydraulic Research*, *45*(4), 435–450. https://doi.org/10.1080/00221686.2007.9521778

Beechie, T. J., Fogel, C., Nicol, C., Jorgensen, J., Timpane-Padgham, B., & Kiffney, P. (2023). How does habitat restoration influence resilience of salmon populations to climate change? *Ecosphere*, *14*(2), e4402.

Benjankar, R., Egger, G., Jorde, K., Goodwin, P., & Glenn, N. F. (2011). Dynamic floodplain vegetation model development for the Kootenai River, USA. *Journal of Environmental Management*, *92*(12), 3058–3070. https://doi.org/10.1016/j.jenvman.2011.07.017

Benjankar, R., Tonina, D., Tranmer, A. W., Paudel, S., & Shrestha, A. (2025). The importance of floodplain width on hydraulic variability and aquatic-riparian habitat in semi-confined, regulated river systems. *Ecological Engineering*, *216*, 107637.

Bovee, K. D. (1986). *Development and evaluation of habitat suitability criteria for use in the instream flow incremental methodology* (Vol. 86). National Ecology Center, Division of Wildlife and Contaminant Research, Fish ….

Caamaño, D., Goodwin, P., & Buffington, J. M. (2012). Flow structure through pool-riffle sequences and a conceptual model for their sustainability in gravel-bed rivers. *River research and applications*, *28*(3), 377-389.

McKean, J., & Tonina, D. (2013). Bed stability in unconfined gravel bed mountain streams: With implications for salmon spawning viability in future climates. *Journal of Geophysical Research: Earth Surface*, *118*(3), 1227-1240.

Lightbody, A. F., Kui, L., Stella, J. C., Skorko, K. W., Bywater-Reyes, S., & Wilcox, A. C. (2019). Riparian vegetation and sediment supply regulate the morphodynamic response of an experimental stream to floods. *Frontiers in Environmental Science*, *7*, 40.

Raleigh, R. F., Zuckerman, L. D., & Nelson, P. C. (1984). *Habitat suitability index models and instream flow suitability curves: brown trout*. Western Energy and Land Use Team, Division of Biological Services, Research ….

Tonolla, D., Geilhausen, M., & Doering, M. (2021). Seven decades of hydrogeomorphological changes in a near-natural (Sense River) and a hydropower-regulated (Sarine River) pre-Alpine river floodplain in Western Switzerland. *Earth Surface Processes and Landforms*, *46*(1), 252–266. https://doi.org/10.1002/esp.5017

Tranmer, A. W., Ji, U., Ahn, M., Jung, S. H., & Yager, E. M. (2024). Characterizing erosion and deposition in and around riparian vegetation patches: Complex flow hydraulics, sediment supply, and morphodynamic feedbacks. *Water Resources Research*, *60*(2), e2023WR034859.

Vetsch, D. F., Frei, S., Halso, M. C., Schierjott, J. C., Bürgler, M., & Vanzo, D. (2024). Basement v4, a multipurpose modelling environment for simulation of flood hazards and river morphodynamics across scales. In P. Gourbesville & G. Caignaert (Eds.), Advances in hydroinformatics—simhydro 2023 volume 1 (pp. 125–138). doi:https://doi.org/10.1007/978-981-97-4072-7_8

White, D. C., Morrison, R. R., & Nelson, P. A. (2023). Experimental Observations of Floodplain Vegetation, Bedforms, and Sediment Transport Interactions in a Meandering Channel. *Journal of Geophysical Research: Earth Surface*, *128*(9), e2023JF007136. https://doi.org/10.1029/2023JF007136

White, D. C., Morrison, R. R., & Nelson, P. A. (2025). Floodplain Vegetation Density Effects on Meandering Channel Flow Patterns and Channel-Floodplain Hydraulic Exchange. *Journal of Geophysical Research: Earth Surface*, *130*(7), e2024JF008038. https://doi.org/10.1029/2024JF008038

Wohl, E., Bledsoe, B. P., Jacobson, R. B., Poff, N. L., Rathburn, S. L., Walters, D. M., & Wilcox, A. C. (2015). The Natural Sediment Regime in Rivers: Broadening the Foundation for Ecosystem Management. *BioScience*, *65*(4), 358–371. https://doi.org/10.1093/biosci/biv002

Wohl, E., Kramer, N., Ruiz-Villanueva, V., Scott, D. N., Comiti, F., Gurnell, A. M., et al. (2019). The natural wood regime in rivers. *BioScience*, *69*(4), 259–273.

Yager, E. M., & Schmeeckle, M. W. (2013). The influence of vegetation on turbulence and bed load transport. *Journal of Geophysical Research: Earth Surface*, *118*(3), 1585-1601.

Book of Abstracts of the *16th International Symposium on Ecohydraulics*
Challenges and solutions in the time of global changes
August 16–20, 2026, Lausanne, Switzerland
ISSN: 2790-2420 | ISBN: 978-90-837233-9-6 | doi:[10.64697/iahr.proc.ise2026.abs]
© 2026 IAHR. CC BY-NC-ND 4.0

A MULTI-STAGE DISCHARGE FRAMEWORK FOR DIAGNOSING SEDIMENT TRANSPORT REGIMES AND BED DISTURBANCE IN DAM-INFLUENCED RIVER REACHES USING FIXED-BED 2D HYDRODYNAMIC MODELLING

Morihiro HARADA[1]

[1] Center for Environmental and Societal Sustainability, Gifu University, Japan
email: harada.morihiro.i3@f.gifu-u.ac.jp

ABSTRACT

This study presents a reach-scale diagnostic framework for evaluating sediment transport regimes and bed disturbance in dam-influenced rivers by integrating long-term discharge records with fixed-bed two-dimensional (2D) hydrodynamic simulations. A multi-stage discharge system was constructed by discretizing 15 years of hourly discharge data into 28 representative flow stages based on cumulative frequency, and each stage was simulated using ALB/LP-derived high-resolution topography. The results show that sediment-transport activation and morphological response differ markedly among river reaches, with high flows producing large sediment fluxes but limited bed deformation in some sections, reflecting low bed-change efficiency. In contrast, moderate flows trigger pronounced bed disturbance in geomorphically sensitive reaches, particularly those with compound channels or strong planform confinement. The framework also identifies the discharge ranges that effectively drive habitat-forming bed renewal, distinguishing them from flows that merely convey sediment. Because these assessments can be derived from fixed-bed simulations with modest computational cost, the method provides a practical and physically interpretable tool for supporting dam-release planning, sediment management, and geomorphic river rehabilitation.

Keywords: *sediment regime; multi-stage discharge; fixed-bed 2D model; bed disturbance efficiency*

1. Introduction

Sediment transport regimes and bed disturbance are fundamental drivers of geomorphic and ecological functioning in river systems, particularly in gravel-bed rivers. Recent ecohydrological perspectives emphasize that these processes are governed jointly by the natural flow regime (Poff et al., 1997) and the natural sediment regime (Wohl et al., 2015). In dam-regulated rivers, however, these regimes are often decoupled, altering disturbance dynamics and diminishing geomorphic processes that sustain channel morphology and habitat renewal.

The Kizugawa River, a major sandy tributary of the Yodo River system in western Japan, has been widely studied as a representative gravel-sandy river ecosystem. Previous studies have shown that channel morphology, sediment supply, and river engineering practices strongly influence aquatic and riparian habitats, while progressive bed degradation and reduced inundation frequency of backwaters have led to the loss of habitats supporting diverse fish and macroinvertebrate communities (Nagatani et al., 2017). Ecological engineering studies using traditional bamboo gabions have demonstrated their potential to enhance habitat heterogeneity and provide microhabitats for aquatic organisms (Nagatani et al., 2017), while hierarchical frameworks linking sediment supply, bar–floodplain morphology, and habitat types have been proposed for gravel-sandy rivers in Japan.

Despite these advances, practical tools for diagnosing how different discharge levels contribute to sediment transport and bed disturbance across river reaches remain limited. To address this gap, this study develops a simplified yet physically interpretable framework integrating multi-year hydrographs, high-resolution ALB/LP topography, and fixed-bed two-dimensional hydrodynamic simulations to characterize discharge-

dependent sediment transport and bed disturbance. The approach is applied to the Kizu River in the Yodo River system, Japan, using a 27-km study corridor from 1 to 27 kp, subdivided into an upstream reach (18–27 kp) and a downstream reach (1–17 kp), as shown in Fig. 1.

2. Methods

2.1. Construction of multi-stage discharge system

Hourly discharge data observed at the Inooka Water Level Observatory on the Kizu River from 2009 to 2023 were used to construct the multi-stage discharge system. The long-term hydrograph was discretized into 28 representative flow stages based on the cumulative frequency distribution (Fig. 2): nine stages at 10% intervals for 0–90% cumulative frequency, nine stages at 1% intervals for 90–99%, and ten stages at 0.1% intervals for 99–100%. This approach preserves key characteristics of the flow regime while enabling efficient, stage-based assessment of sediment transport and bed disturbance.

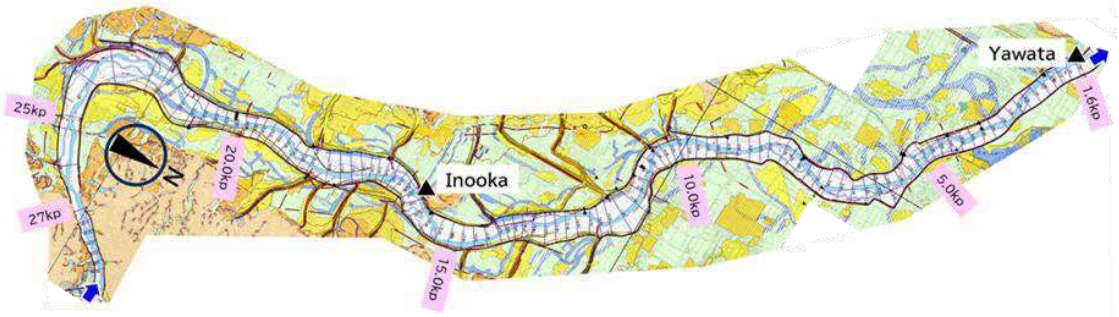

Fig. 1. Plan view of the study corridor along the Kizu River, showing the upstream and downstream reaches and the location of the Inooka Water Level Observatory. The 27-km corridor extends from 27 kp (upstream, left) to 1.6 kp near Yawata (downstream, right). The Inooka Observatory is located near the center of the study area and provides the discharge records used for constructing the multi-stage flow system.

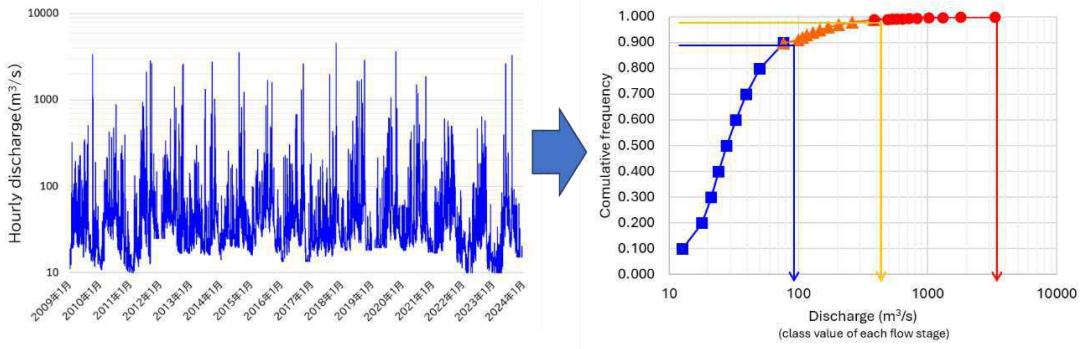

Fig. 2. Construction of the 28-stage discharge system based on the cumulative frequency of hourly flow data at the Inooka Water Level Observatory.

2.2. Hydrodynamic model

Hydrodynamic simulations for all discharge stages were performed using the depth-averaged, horizontal 2D solver Nays2DH implemented in the iRIC platform. High-resolution ALB (2022) and LP (2019) point-cloud datasets were used to construct detailed computational grids for each river reach, representing mountainous, valley-floor, and alluvial-fan sections. Roughness coefficients and grain-size distributions (d_{50}–d_{84}) were assigned based on field observations. The model computed water depth, velocity, and shear-stress components (τ_x, τ_y), from which dimensionless shear stress and unit-width sediment transport rates were derived using Ashida–Michiue bedload functions.

2.3. Computation of sediment-transport and bed-disturbance indicators

For each of the 28 discharge stages, spatial sediment-related metrics were calculated from the hydrodynamic model outputs. Water-covered cells, sediment-active cells, and erosion or deposition cells were identified based on thresholds of flow depth, sediment transport rate, and bed-change indicators. Total sediment flux (Q_B) was obtained by integrating unit-width sediment transport rates over the computational domain. Bed-disturbance intensity was quantified using the sediment mass-balance term ΔQ_B, representing local divergence of sediment flux. From these variables, three diagnostic indicators were defined: (i) sediment-transport

efficiency (Q_{Bx} / Q_w), expressing the proportion of flow discharge contributing to sediment transport; (ii) bed-change contribution rate (ΔQ_b / Q_{Bx}), indicating how much of the transported sediment leads to actual morphological adjustment; and (iii) bed-change efficiency (ΔQ_b / Q_w), representing the expected magnitude of bed disturbance per unit discharge. These indicators allow systematic comparison of sediment-transport potential and disturbance sensitivity across reaches and discharge stages.

3. Results

3.1. Sediment-transport activation and bed disturbance across representative flow stages

The three representative flow stages reveal clear contrasts in sediment-process activation across sections A–Y (Fig. 3). Under the normal-flow stage (Q = 27 m³/s), sediment-transport and bed-change grids remain highly localized. In the high-flow stage (Q = 383 m³/s), sediment-transport activation becomes widespread, while erosion and deposition occur intermittently across many sections. The rare peak-flow stage (Q = 3323 m³/s) produces substantial increases in water-covered, sediment-transport, and erosion/deposition grids, yet morphological response remains heterogenous. Fig. 3 illustrates these patterns for one representative section of the study corridor. By comparing sediment-transport activation with actual aggradation and degradation, the method identifies the discharge ranges that meaningfully contribute to habitat-forming bed renewal, distinguishing them from flows that merely convey sediment downstream.

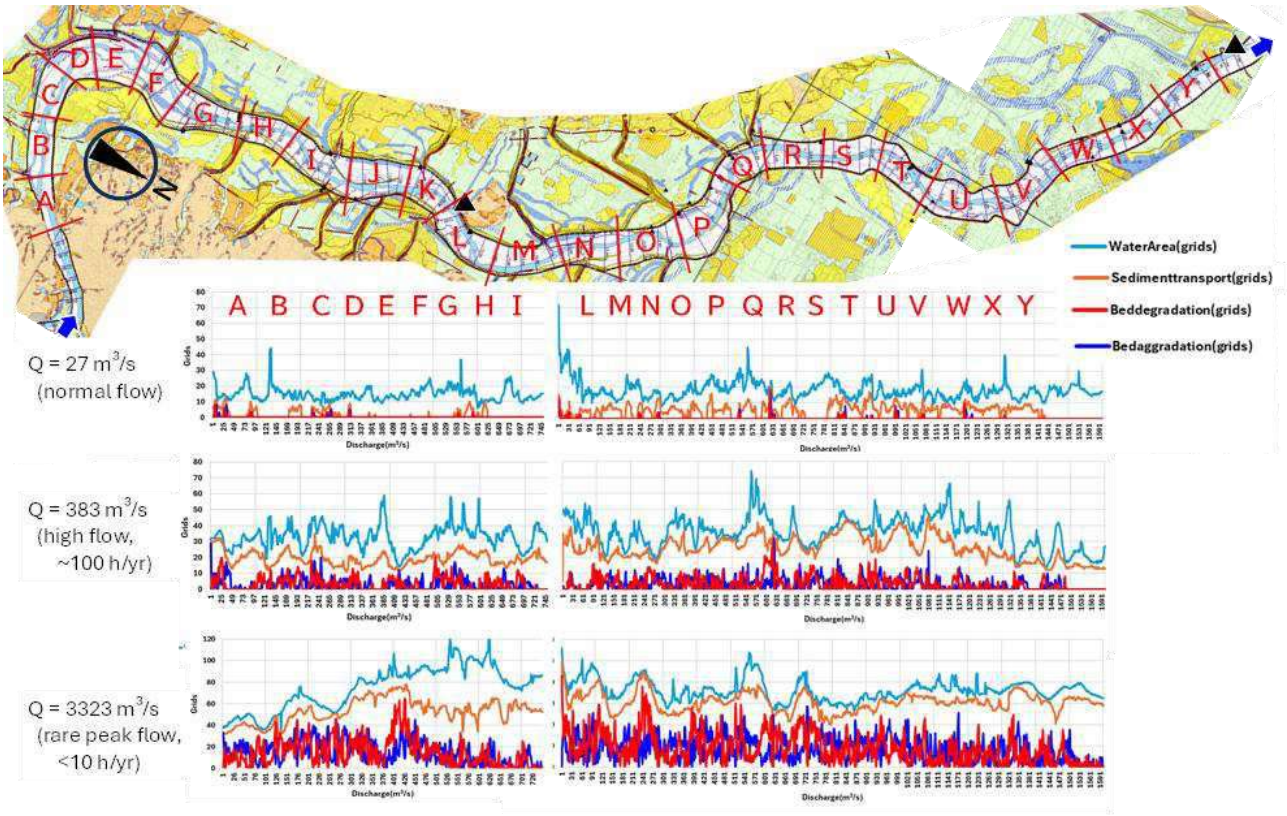

Fig. 3. Cross-sectional variation in sediment-related indicators along the study corridor under representative flow stages.

3.2. Flow-dependent efficiency metrics for sediment transport and morphological disturbance

The behavior of sediment-related processes with increasing discharge is first illustrated in Fig. 4(a), which shows the variation in water-covered width, sediment-transport width, and the number of aggradation/degradation grids for one representative reach among those shown in Fig. 3. As discharge increases, both the water-surface width and the width over which sediment transport occurs expand steadily; however, noticeable bed-level change emerges only at discharges around 300 m³/s, indicating that substantial morphological adjustment is confined to a limited range of intermediate-to-high flows.

Building on these patterns, the efficiency metrics in Fig. 4(b–c) further clarify how sediment mobility translates into geomorphic change. Sediment-transport efficiency (Q_{bx}/Q_w) increases sharply with discharge, reflecting the strong expansion of sediment-transport width at higher flows. In contrast, the bed-change contribution rate

($\Delta Q_b/Q_{bx}$) decreases with increasing discharge, showing that an increasingly smaller fraction of the mobilized sediment contributes to actual bed deformation. The bed-change efficiency ($\Delta Q_b/Q_w$) exhibits a peaked response, rising only within a limited intermediate discharge range before declining at both lower and higher flows. This pattern highlights the specific flow stages that are most effective for bed renewal.

Together, these metrics distinguish flow stages that meaningfully reshape the channel from those that merely transport sediment. These flow stages correspond to the discharge ranges most likely to drive geomorphic disturbance and associated habitat renewal in gravel–sand river systems. Importantly, these insights are obtained from fixed-bed 2D simulations, which require far less computational effort than full morphodynamic modelling while still capturing the essential flow-dependent characteristics of channel response.

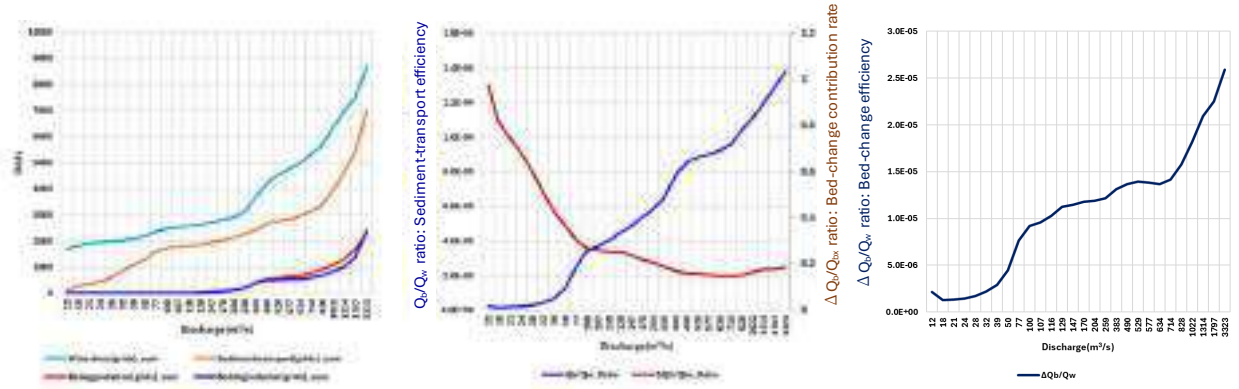

(a) (b) (c)

Fig. 4. Flow-dependent sediment-process activation and efficiency metrics for one representative section. (a) Water-covered, sediment-transport, and aggradation/degradation grids. (b) Sediment-transport efficiency (Q_{bx}/Q_w) and bed-change contribution rate ($\Delta Q_b/Q_{bx}$). (c) Bed-change efficiency ($\Delta Q_b/Q_w$)

3.3. Implications for dam operation and sediment-management planning

The proposed multi-stage diagnostic framework provides practical insights for dam operation and sediment-management planning. By identifying discharge thresholds that activate sediment transport or induce bed disturbance, the method supports the design of environmental flows aimed at promoting habitat renewal. The framework also highlights reaches where sediment mobility is high but morphological response is limited ("disturbance-starved" reaches), indicating locations where sediment replenishment or targeted flow releases may be required. Because the analysis is based on computationally efficient fixed-bed simulations, the approach can serve as a rapid screening tool for evaluating alternative flow-management and sediment-management scenarios.

4. Conclusions

This study presents a practical and generalizable framework for diagnosing sediment regimes using multi-stage discharge simulations. By integrating long-term flow variability with high-definition terrain and fixed-bed hydrodynamics, the method reveals reach-specific disturbance sensitivity and sediment transport efficiency. The approach can assist dam operation, sediment management, and ecohydraulic rehabilitation planning.

Acknowledgements

This study received support from the Japan Society for the Promotion of Science (JSPS) KAKENHI (Grant Numbers 25H00757 and 23K28277) and from the Water Environment Center (WEC), Japan, whose assistance is gratefully acknowledged.

References

Nagatani N, Ueno K, Takebayashi H, Sumi T, Takemon Y, Kato Y, Okazaki S (2017) Restoration of physical habitat diversity in river channels using traditional bamboo gabion works. *Journal of Japan Society of Civil Engineers,* Ser. B1 (Hydraulic Engineering), 73, I_1195–I_1200.

Poff NL, Allan JD, Bain MB, Karr JR, Prestegaard KL, Richter BD, Sparks RE, Stromberg JC (1997) The natural flow regime. *BioScience*, 47, 769–784.

Wohl E, Bledsoe BP, Jacobson RB, Poff NL, Rathburn SL, Walters DM, Wilcox AC (2015) The natural sediment regime in rivers: broadening the foundation for ecosystem management. *BioScience*, 65, 358–371.

Book of Abstracts of the *16th International Symposium on Ecohydraulics*
Challenges and solutions in the time of global changes
August 16–20, 2026, Lausanne, Switzerland
ISSN: 2790-2420 | ISBN: 978-90-837233-9-6 | doi:[10.64697/iahr.proc.ise2026.abs]
© 2026 IAHR. CC BY-NC-ND 4.0

HYDROLOGY DRIVEN WETLANDS MORPHOLOGY AND ITS ROLE IN THE WATER-CARBON BUDGET

Filippo MIELE[1,2], Benjamin KARGERE[1] , Meret AEPPLI[2], Sara BONETTI[1]

[1] Laboratory of Catchment Hydrology and Geomorphology, EPFL WALLIS-VALAIS, CH
email: filippo.miele@epfl.ch
email: benjamin.kargere@epfl.ch
email: sara.bonetti@epfl.ch
[2] Soil Biogeochemistry laboratory, EPFL WALLIS-VALAIS, CH
email: meret.aeppli@epfl.ch

ABSTRACT

Keywords: *wetland morphology; wetland carbon fluxes; wetlands hydrology*

Introduction

Wetlands are among the most productive and ecologically vital ecosystems on the planet, playing a critical role in carbon (C) and water cycling (Griscom et al., 2017; Tiemyer et al., 2021). Their ability to store large amounts of soil organic carbon (SOC) is mainly due to the slow degradation of organic material under water-logged, oxygen-limited conditions. However, uncontrolled drainage of wetlands, largely caused by human intervention, leads to rapid decomposition of organic matter, with subsequent increase of carbon dioxide (CO_2) emissions to the atmosphere. As a consequence, wet zones may convert from CO_2 sinks into CO_2 sources.

Restoring degraded wetlands is a worldwide environmental priority, not only for biodiversity conservation but also for climate mitigation through carbon sequestration. Despite the general relevance of wetland restoration projects, forecasting their beneficial effects is often challenged by the complexity of coupled water-soil-vegetation dynamics that regulate soil respiration rate and shape micro-scale morphology and vegetation features over short and long timescales. As a result, a significant number of studies have reported two major reasons for failure of restoration works: either pioneer vegetation was not restored into its original status (Kreyling et al., 2021) or net positive CO_2 emissions from the wetland to the atmosphere were observed despite increased water table levels (Vàzquez-Lule et al., 2021), meaning that the water supply alone may not suffice to guarantee C source-to-sink transitions.

Several C budget models have been proposed to describe water and C cycles at the wetland ecosystem scale (Mack et al., 2023). These models track the (negative) gross primary productivity (*GPP*) coming from carbon fixation through photosynthetic pathways and the (positive) ecosystem respiration, which is further partitioned between autotrophic (R_a) and heterotrophic (R_h) metabolic rates. These rates are known to be modulated by water availability (generally encoded in water table depth, *WTD*) and surface temperature ($T_{a\text{-}w}$). Empirical relationships used to relate metabolic rates and hydrological and climatic factors have been proposed and calibrated at the wetland scale (Oikawa et al., 2024). While these ecosystem-scale models accurately replicate time series of net CO_2 emissions at specific sites, their reliance on empirical laws limits their transferability to other locations. In addition, they fall short in explaining how heterogeneities in wetland features (e.g., in soil, morphology, vegetation) interact to shape overall C fluxes, as they are formulated by averaging relevant spatially distributed quantities. Lastly, such models predict long-term trends in C budget for stationary conditions, but their applicability is limited in wetlands experiencing abrupt changes, such as drying or rewetting events.

Landscape evolution models have been proposed and successfully applied to predict evolving surface morphologies of diverse environments (Bonetti et al., 2020; Zhou et al., 2024). Such models describe 2D spatially explicit surface dynamics of flow-mediated sediment transport, deposition, and erosion. Due to the nonlinearity of the underlying dynamics, surface instabilities are triggered, and surface roughness arises from deterministic equations. In the context of tidal wetlands, such models predict emerging patterns of branching riverine structures that can be even enhanced or inhibited in the presence of vegetation (Weerman et al., 2010; Visjel et al., 2023). Here, we aim to link micro-morphological patterns of wetland surfaces to their atmospheric carbon exchange. By exploiting a spatially explicit model that simulates long-term wetland morphodynamics, we forecast water, sediment, and vegetation spatial distribution to assess spatially explicit water-carbon cycling rates. Results show that explicitly considering such spatial effects might explain transitions from C-source to C-sink at the ecosystem scale. Results are further supported by comparison with satellite images and eddy covariance measurements in selected wetland sites.

1. Methods

The morphology of wetlands exhibits characteristic spatial features highly shaped by the type and frequency of water inputs. Recent numerical tools successfully describe the spatial patterns that water flow creates when interacting with sparsely vegetated sediment surfaces (Zhou et al., 2023). In these models, a sparsely vegetated sediment layer gets flooded, eroded, and transported according to the dominant hydrodynamic forces. Sediment erosion rates decrease for higher vegetation density due to higher friction and increased soil resistance. This slower motion further enhances vegetation growth. Thus, the presence of a few sparse patches of vegetated sediment dunes induces local flow redistribution with the consequent formation of deeper unvegetated channels where both flow and erosion rates are higher. We briefly introduce the governing equations in the following.

1.1. *The wetting algorithm*

The water height h – [m] is governed by the mass balance equation:

$$\frac{\partial h}{\partial t} = H_{in} - \nabla\,[q \cdot h] + P - Ih - E_{\Gamma_s} h \tag{1}$$

where q – [m/s] is the depth-average shallow water speed, H_{in} – [m/s] the water input, P – [m/s] the precipitation rate , I – [m/s] the infiltration rate, and $E_{\Gamma s}$ – [m/s] the surface evapotranspiration rate. Both infiltration and evapotranspiration are affected by the vegetation density (B – [1/m^{-2}]), through the following empirical form of $I \sim \frac{B+f}{B+1}$, where f is the infiltration contrast between bare soil and vegetated soil, while $E_{\Gamma_s} = \frac{N_H}{1+BK^{-1}}$, where N_H is the surface evapotranspiration rate and K – [1/m^{-2}] the vegetation carrying capacity (Getzin et al., 2016). We remark that, in this formulation, non-zero values for the water height h are imposed everywhere. The depth-averaged shallow water flow speed q obeys the following equation:

$$\frac{\partial q}{\partial t} = -g \cdot \nabla(h + S) + q \cdot \nabla q - \frac{\tau}{\rho g} + \nabla \cdot (Dq \nabla q) \tag{2}$$

where S – [m] is the sediment height, D_q – [m^2/s] the water diffusivity, and $\frac{\tau}{\rho} = \frac{g}{h^{\frac{1}{3}}} n^2 q^2$, n being the Manning coefficient. The sediment elevation S follows a standard continuity equation with a source term proportional to h and a sink term proportional to the erosion rate (Vijsel et al., 2023), which reads:

$$\frac{\partial S}{\partial t} = S_0 \frac{h - H_c}{Q_s - (h - H_c)} - E_s \left(1 - \frac{p_E B}{K}\right) \frac{\tau}{\rho} S - \nabla \cdot (D_S \nabla S), \tag{3}$$

Where E_S – [s/m$^{2[OBJ]}$], is the maximum sediment erodibility in the absence of vegetation, and the term $\left(1 - \frac{p_E B}{K}\right) \frac{\tau_{[OBJ]}}{\rho}$ accounts for the local shear stress, damped by the presence of the vegetation. p_E is the fraction of erodibility when vegetation is at carrying capacity. Sedimentation rate is, here, proportional to an effective water film layer $h_E = h\text{-}H_c$, with H_c=1mm, and its rate decreases with Q_s – [m], the water layer at which sediment input is halved. Similarly to sedimentation, the continuity equation for vegetation is balanced by the growth rate expressed by a logistic growth dynamic, which also depends on the local effective water film h_E, and a negative term due to vegetation erodibility. Therefore, its dynamics can be written as:

$$\frac{\partial B}{\partial t} = rB\left(1 - \frac{B}{K}\right)\frac{h_E}{Q_B - h_E} - E_B\frac{\tau}{\rho}B - \nabla \cdot (D_B \nabla B), \quad (4)$$

where r – [1/s] is the maximum growth rate, Q_B – [m] the water thickness at which vegetation growth is halved, E_B – [s/m^2] the maximum vegetation erodibility, and D_B – [m^2/s] the colonization rate expressed as an effective diffusivity coefficient. It is important to note that groundwater flow dynamics are neglected, as they minimally impact surface morphology: the subsurface is assumed to be constantly saturated, and subsurface flow effects are assumed to be negligible compared to surface dynamics. While this assumption holds for the long-term morphology evolution, this dramatically limits its applicability for short-term water-C dynamics, where vegetation's capture and release rates are strongly affected by seasonal belowground and aboveground fluctuations of WTD. Thus, a further equation for the "root-zone water," W – [m], is included here to relax the constraint of an imposed non-zero water table height and to allow spatially distributed values of negative water table depth,

$$\frac{\partial W}{\partial t} = Ih - E_{\Gamma_W}W + D_W\nabla^2 W, \quad (5)$$

where E_{Γ_W} – [1/s] is the storage evapotranspiration rate and D_W – [m^2/s] is the soil water diffusivity. The water table depth is, thus, equal to max(h, S - (WTL + W)), where WTL is the groundwater table level obtained as the steady state solution of the Boussinesq equation as derived in Cobb et al. (2024) and shown in Fig. 1a. The spatial distributions of vegetation density, sediment, and water table depth are inputs for the C sequestration (GPP) and release (R_a+R_h) rates, shown in Fig. 1b. Specifically, these rates are evaluated at each pixel (i) in the domain from the local WTD and the spatially averaged $T_{a\text{-}w}$ (see Oikawa et al., 2024 for details). The net ecosystem exchange is computed as $NEE = \sum_i -GPP_i + (R_a + R_h)_i$.

2. Results

In Fig. 1c, an initial homogenous sediment surface evolves, after 50 years, to a heterogeneous surface, where the channel widths and intensity of branching are shaped by the sediment diffusivity. This example is indicative of the time scale separation between the long-term morphological evolution and the short-term periods at which emissions are usually monitored (typically a few years). We thus assume that no significant changes in the morphology occur when we compute the spatially distributed NEE rates over periods of a few years. To highlight the impact of morphology driven C-emissions, we compare results from two distinct tidal wetlands that show different microtopographic features and contrast them with the recorded cumulative NEE emissions, measured through eddy-covariance flux measurements. In Fig. 1d, satellite images (Google Earth Pro v 7.3) of two restored US tidal wetlands show coarser and finer river ramification for Point-aux-Chenes (US-LA1, LA) and Plum Island Sound (US-Plm, MA), respectively. The spatial explicit model for sediment elevation qualitatively predicts these different morphologies for two different values of the sediment dispersion coefficient (Fig. 1d). In agreement with Vijsel et al., higher sediment diffusivity reduces the level of branching. Despite US-LA1 being subjected to an average lower tidal input (0.5 m) in comparison to US-Plm (1.2 m), its reduced elevation enhances sediment dispersion. In Fig. 1e, recorded cumulative NEE values show two opposite trends: US-LA1 acts as a C-source while US-Plm is a C-sink. Modeled NEE evaluated over the two steady states water-sediment-vegetation configurations shows good agreement with observations. The model suggests that the water supply rate itself does not guarantee optimal water-logged conditions for C-sink behavior. This is the case for a highly branched configuration (see US-Plm), in which the spatial water redistribution mitigates seasonal temperature fluctuations, and a larger portion of the wetland surface lies in optimal C-sink conditions. As a consequence, homogeneous landscapes might more strongly deviate from optimal conditions due to a greater sensitivity to water table fluctuations. This interpretation is further validated by comparisons between measured and modeled cumulative NEE trends for two other highly branched restored wetlands, US-Rush Ranch and US-Eden Landing, shown in Fig. 1e (see Oikawa et al., 2024 for flux-tower data and GPS coordinates).

3. Conclusions

Water-logged conditions are generally associated with C-sinks, especially in tidal wetlands, regardless of the water supply rate. Water not only shapes surface morphology via erosional and depositional processes but also drives local plant carbon fluxes and soil respiration rates. Although spatially averaged measurements of water table depth provide a general indication of the ecosystem's water stress, they do not capture the small-scale

heterogeneity of saturation conditions in complex wetland landscapes. By accounting for spatially explicit patterns of water, sediment, and vegetation in tidal wetlands, we showed that highly branched landscapes are more resilient for C-sequestration due to diversification of surface water and temperature conditions.

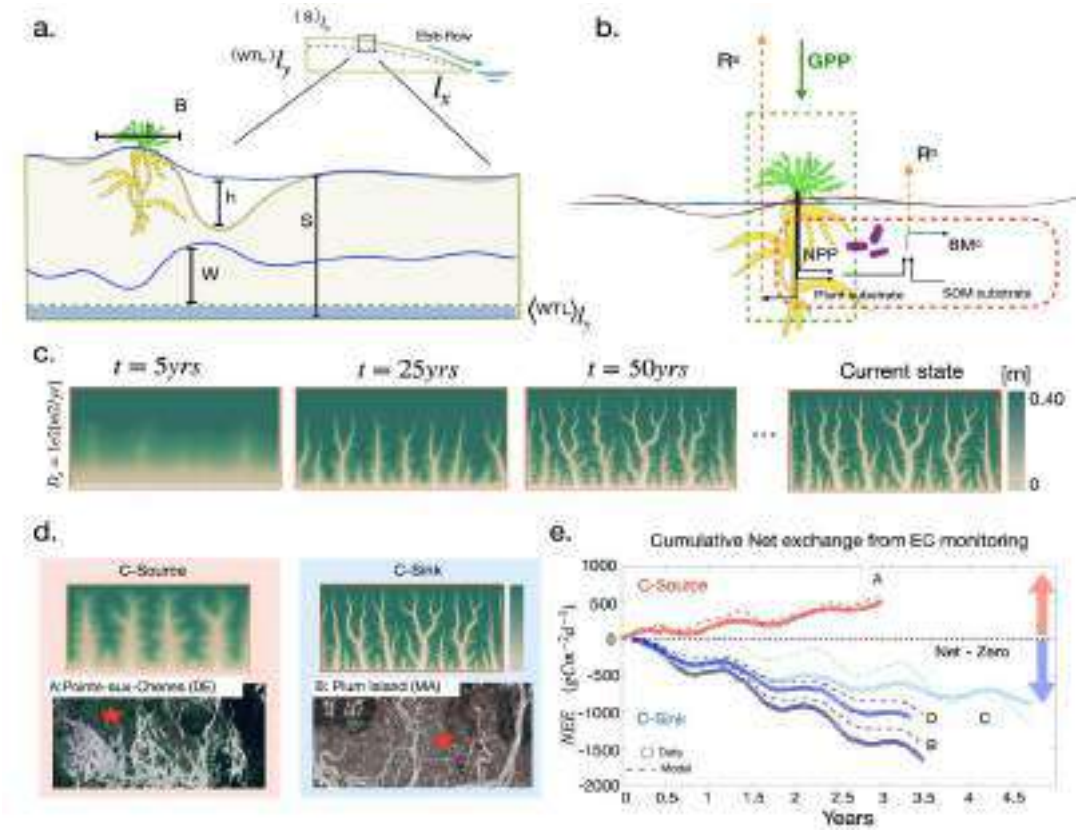

Fig.1. a) Relevant quantities modeled by the wetting algorithm. In the inset, the approximated water table level (WTL) from the steady-state solution of Boussinesq equation. b) Schematic view of the major carbon input (GPP) and output (R_a and R_h) rates for the biogeochemical model. c) Time sequence of the sediment elevation obtained by the adapted spatially explicit landscape evolution model. The model simulates the evolution of the elevation profile over a 500x200 m² domain, with reflecting boundary conditions at the top, left, and right sides, and open flow at the bottom, where branches coalesce. d) Left: comparison between simulated morphology and satellite images of two sites: Pointe-Aux-Chenes Brackish Marsh (LA), and US-Plum Island Sound (MA). Right: comparison between modeled and simulated cumulative NEE (C and D refer to US-Rush Ranch and US-Eden Landing sites, respectively; data obtained from AmeriFlux and Oikawa et al., 2024).

Acknowledgements

This work is supported by "Enterprise for Society Center" (E4S, Project title: Carbon removal in wetland restoration).

References

Bonetti S, Hooshyr M, Camporeale C, Porporato A, Channelization cascade in landscape evolution, (2020), Proc Natl.Acad.Sci U.S.A. 117 **(3)** 1375-1382

Cobb, A.R., Dommain, R., Yeap, K. et al. (2024), A unified explanation for the morphology of raised peatlands. Nature **625**, 79–84.

Getzin S, Yizhaq H, Bell B, Erickson TE, Postle A, Katra I, Tzuk O, Zelnik YR, Wiegand K, Wiegand T, Meron E, (2016), Discovery of fairy circles in Australia supports self-organization theory, Proc. Natl. Acad. Sci., **113(13)** 3551-3556

Griscom BW et al., (2017) Natural climate solutions, Proc. Natl. Acad. Sci. **114(44)** 11645-11650

Kreyling J., Tanneberger F, Jansen F. et al. (2021), Rewetting does not return drained fen peatlands to their old selves. Nat Commun **12**,

Mack SK, Lane RR, Deng J, Morris JT, Bauer JJ, (2023), Wetland carbon models: Applications for wetland carbon commercialization, Ecological Modelling, Vol. **476**, 110228

Oikawa PY et al., (2024), A new coupled biogeochemical modeling approach provides accurate predictions on methane and carbon dioxide fluxes across diverse tidal wetlands, Journ.Geophys.Research. Biogeosciences, Vol **119,** e2023JG007943

Tiemeyer B, Albiac Borraz E., Augustin J, Bechtold M, Beetz S, Beyer C, Drösler M, Ebli M, Eickenscheidt T, Fiedler S, Förster C, Freibauer A, Giebels M, Glatzel S, Heinichen J, Hoffmann M, Höper H, Jurasinski G, Leiber-Sauheitl K, Peichl-Brak M, Roßkopf N, Sommer M, and Zeitz J, (2016), High emissions of greenhouse gases from grasslands on peat and other organic soils. Glob Change Biol, **22**: 4134-4149

Vàzquez-Lule A, Vargar R, (2021), Biophysical drivers of net ecosystem and methane exchange across phenological phases in tidal salt marsh, Agric. And For. Meteorology, Vol **300**, 108309

Vijsel RC., Belzen J, Bouma T.J. et al. (2023), Vegetation controls on channel network complexity in coastal wetlands. Nat Commun **14**, 7158.

Weerman J.E.,Van de Koppel J., Eppinga M.B., Montserrat F., Liu Q.X., Herman P.M.J., (2010), Spatial Self-Organization on Intertidal Mudflats through Biophysical Stress Divergence, The American Naturalist, Jul;176(1):E15-32

Zhou, Z., Wei, Y., Geng, L. et al. , (2024), Cross-shore parallel tidal channel systems formed by alongshore currents. Nat Commun **15**

Book of Abstracts of the *16th International Symposium on Ecohydraulics*
Challenges and solutions in the time of global changes
August 16–20, 2026, Lausanne, Switzerland
ISSN: 2790-2420 | ISBN: 978-90-837233-9-6 | doi:[10.64697/iahr.proc.ise2026.abs]
© 2026 IAHR. CC BY-NC-ND 4.0

RIVER FLOW VARIABILITY AS A CATALYST FOR VEGETATION GROWTH AND CARBON PUMPING

Luca SALERNO[1], Matteo BERTAGNI[1], Carlo CAMPOREALE[1]

[1] Politecnico di Torino, Turin, Italy
email: luca.salerno@polito.it

ABSTRACT

Rivers reshape their floodplains through coupled hydrological, sedimentological, and biological processes that drive riverine landscape evolution and global carbon fluxes (Drake et al., 2018). Riparian zones are highly sensitive to flow variability, which supplies vegetation with moisture, nutrients, and seeds through flooding and sediment deposition, but can also uproot it during extreme events.

Together with photosynthetic carbon fixation by riparian vegetation, this recruitment, transport, and burial of biomass forms a two-step ecomorphodynamic carbon pumping (ECP) mechanism (Salerno et al., 2024) that moves carbon from the atmosphere to long-term reservoirs such as river sedimentary deposits and the ocean. The first step, ecomorphodynamic carbon export, recruits large-wood biomass through flood-induced uprooting, which may be retained or transported to the ocean; the second, enhanced net primary production, fixes carbon via vegetation encroachment on newly exposed riparian areas. The two steps generate compensating outgoing and incoming carbon fluxes.

To assess how vegetation reworking under flow fluctuations controls riverine carbon pumping, we develop a stochastic framework coupling river morphodynamics, flow variability, and vegetation growth and uprooting. Applied to sand-bed and gravel-bed rivers through generalized hydraulic-geometry scaling, it enables a comparative analysis of ECP across contrasting fluvial environments.

Keywords: carbon cycle; rivers; stochastic processes; riparian vegetation; morphodynamics

1. Materials and Methods

We develop a dimensionless hydrogeomorphological framework for the catalytic effect of intermittent flooding on carbon sequestration via riparian vegetation dynamics. The transect comprises (i) a rectangular active channel of longitudinal slope S, whose bed may host alternate bars, and (ii) an adjacent planar floodplain with lateral slope S_L.

1.1. Scaling

To scale the dimensional quantities, we use the bankfull condition (Fig. 1) (Parker et al., 2007), represented by the discharge Q_{bf}^*, water depth h_{bf}^*, and width B_{bf}^*, to provide dimensionless quantities $q = Q^*/Q_{bf}^*$, $h_0 = h_0^*/h_{bf}^*$, $y = 2y^*/B_{bf}^*$, $\beta = B_{bf}^*/(2h_{bf}^*)$, $d_s = D_{50}^*/h_{bf}^*$, $\theta = h_{bf}^* S/(D_{50}^* R)$, where D_{50}^* is the mean size diameter of sediments and $R \approx 1.65$ is their relative density for silicate sediments. We adopt generalized field-data-based hydro-geomorphological scaling (Calvani, et al, 2025) valid for single-thread sand-bed and gravel-bed rivers. The Einstein-like bankfull dimensionless parameter $\tilde{q} = Q_{bf}/\left(g\, D_{50}^{*3}\right)^{-0.5}$ is related to the aspect ratio, longitudinal channel slope, relative roughness and Shields parameter through power laws $\beta = 0.082\, \tilde{q}^{0.181} D_{84}^{-0.051} Rp^{0.26} \theta_c^{-0.09}$, $S = 1.01\, \tilde{q}^{-0.378} D_{84}^{0.107} Rp^{0.12} \theta_c^{1.19}$, $\theta = 2.45\, (D_{84})^{0.90} \theta c$, $d_s = 0.97\, \tilde{q}^{-0.378} D_{84}^{0.107} Rp^{0.12} \theta_c^{-0.189}$,where Rp is particle Reynolds number, D_{84} is the dimensionless grain diameter (D_{84}=D_{84}^*/D_{50}^*). In natural rivers, $\tilde{q}$ ranges from 10^4 to 10^8. We adopt a dimensionless time $t = t^*/t_{veg}^*$, where t_{veg}^* is a typical timescale for vegetation growth.

1.2. Hydrological regime

To represent the stochasticity of river flows, the dimensionless river discharge $q(t)$ is described via a compound Poisson process $dq/dt = -q/\tau + \xi$, wherein the river discharge undergoes rapid flood events (represented by the white shot noise ξ(t)) as a result of rainfalls, followed by exponential decays (Laio et al., 2001). This process is defined by three parameters: an average μ_q , a standard deviation σ_q (or coefficient of variation $c_q = \sigma_q/\mu_q$, and an integral timescale τ. The resulting probability distribution function for q is gamma-distributed with $\delta = 1/c_q^2$. The advantage of the compound Poisson process is the availability of

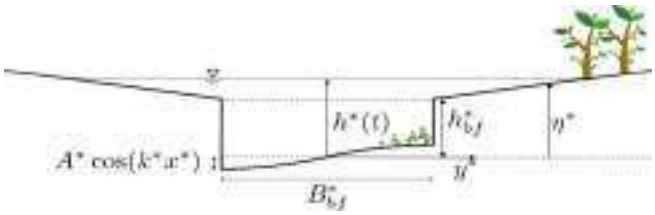

Fig. 1. *Riparian transect composed by an in-channel and out-channel components.*

closed form solutions for the temporal statistics, including the up-crossing and down-crossing times.

1.3. Hydromorphological relationships

In the quasi-trapezoidal geometry, the relationship between dimensionless discharge q and uniform water stage h_0 is: $q = h_0^{5/3}$ for $h_0 < 1$ (in-channel flow), and $q = h_0^{5/3} + (2^{\frac{5}{3}})/(\beta S_L)(h_0 - 1)^{8/3}$ for $h_0 > 1$ (overbank flow). We investigate the interactions between fluvial dynamics and riparian vegetation (Camporeale et al., 2013) considering the active channel separately from the floodplain. For the floodplain, the distribution p_{h0} is approximated to an exponential function, where $\hat{h} = h_0 - 1$ is the excess water stage with respect to overflow, with mean $\langle \hat{h} \rangle$. For the active channel, the morphology is dominated by the presence of free alternate bars, which emerge as finite-amplitude instabilities when the aspect ratio β exceeds a critical threshold. We model bar geometric features with a nonlinear framework that determines both wavelength and amplitude in closed-forms (Bertagni and Camporeale, 2018). Free alternate bars are represented as $\eta = A\, cos(kx)\, sin\left(\frac{\pi y}{2}\right)$, where k is the longitudinal wavenumber and A is the bar height.

1.4. Stochastic vegetation dynamics

The vegetation colonizing the bars within the active channel and the riparian zone in the floodplain differ, each characterized by distinct maximum biomass density (carrying capacity) K_{ac}^* and K_{fp}^*, and characteristic growth times T_{ac}^* and T_{fp}^*. Vegetation density is expressed in dimensionless form $\rho(t)$ by normalizing biomass with respect to carrying capacity. The temporal dynamics are modeled as a dichotomous stochastic process alternating between growth and decay phases (Ridolfi et al., 2011):

$$d\rho/dt = \begin{cases} \rho(1-\rho), & h < \eta \ (growth) \\ -\alpha\zeta(h)\rho, & h \geq \eta \ (decay) \end{cases} \quad (1)$$

where α is a species-dependent parameter linking water disturbance to biomass uprooting, and $\zeta(h)$ modulates the effect of hydraulic stress.

In the active channel, hydrological forcing causes alternation of emerged periods (mean time τ_g) during which vegetation can establish and grow, and submergence phases (mean time τ_d) during which physiological stress, biomass decay, and organic matter export occur. In the floodplain, vegetation decays are governed by episodic high-flow events that exceed channel capacity and periodically inundate the floodplain, producing hydrodynamic forces strong enough to cause uprooting. Therefore, vegetation dynamics in the floodplain correspond to the limit case $\tau_d \to 0$, simplifying to:

$$d\rho/dt = \rho(1-\rho) - \alpha\rho\sum(h_i - \eta)\delta(t - t_i), \quad (2)$$

where the sum refers to a censored white shot noise where only flow pulses exceeding critical hydraulic conditions for uprooting contribute to vegetation disturbance. The mean value of biomass density valid for both cases is:

$$\mu_\rho(x,y) = 1 - \alpha G/\tau_g, \quad (3)$$

where $G = \tau_d\langle\zeta\rangle$ for the active channel and $G = \langle\hat{h}\rangle$ for the floodplain.

2. Catalytic Index

Intermittent floods drive a catalytic behavior: biomass losses followed by regrowth accelerate the turnover between carbon fixation and export. We quantify it by comparing the biomass exported by fluvial disturbances with the maximum attainable under undisturbed conditions over the vegetation lifespan T_{life} .

2.1. Ecomorphodynamic carbon export

According to our vegetation model, biomass decays exponentially during submergence at a rate proportional to the mean exceedance stage $\langle\zeta\rangle$, leading to a biomass loss for each disturbance event:

$$\Delta\rho = \rho\left(1 - e^{-\alpha\langle\zeta\rangle\Delta t_i}\right). \tag{4}$$

Since decay events are exponentially distributed with mean duration τ_d, the average biomass drop per event is:

$$\langle\Delta\rho\rangle = \mu_\rho\,[\alpha\tau_d\langle\zeta\rangle/(1 + \alpha\tau_d\langle\zeta\rangle)] \tag{5}$$

2.2. Local and global index

The catalytic index (per unit area) is defined as the product of the average biomass drop per event and the rescaled event frequency nλ, where n is the ratio between T_{life} and a characteristic timescale for logistic growth, and $\lambda = \tau_g^{-1}$ is the number of events per unit time. The general expression for the local catalytic index per unit area is:

$$I(\boldsymbol{x}) = (n/\tau_g) \times [\alpha G/(1+\alpha G)] \times [1 - \alpha G/\tau_g]. \tag{6}$$

Values of I > 1 mean that hydrological disturbances enhance carbon removal, acting as a catalyst for biomass turnover and long-term storage; I < 1 indicates lower carbon fixation than the undisturbed case.

The global index is evaluated over a fluvial unit spanning one bar wavelength longitudinally and extending laterally to where mean biomass density reaches 98% of carrying capacity. Let r_A denote the ratio between areas of active channel and floodplain; r_K and r_T are analogous ratios for carrying capacities and characteristic vegetation timescales. The overall area-averaged catalytic index is:

$$I_{tot} = [\gamma\bar{\mathrm{I}}_{ac} + \bar{\mathrm{I}}_{fp}]/[\gamma n_{ac}^{-1} v_c + n_{fp}^{-1}], \tag{7}$$

where $\gamma = r_K\, r_A/r_T$, the overline refers to spatial average over the morphological unit, and v_c denotes the percentage cover ratio of vegetated area under undisturbed conditions. Flow stochasticity is essential for bar colonization; under constant-flow conditions, only very low discharges are compatible with vegetation development over bars.

3. Results

Our results show that the riparian zone contains areas where periodic uprooting drives net primary production above that of an undisturbed forest, yielding I > 1 and substantial ecomorphodynamic carbon pumping. For both river types, mean biomass density and the catalytic index along the floodplain depend clearly on model parameters: river size ($\tilde{q}$), sensitivity to uprooting (α), mean discharge ($\boldsymbol{\mu_q}$), flow variability ($\boldsymbol{\sigma_q}$), and vegetation lifespan.

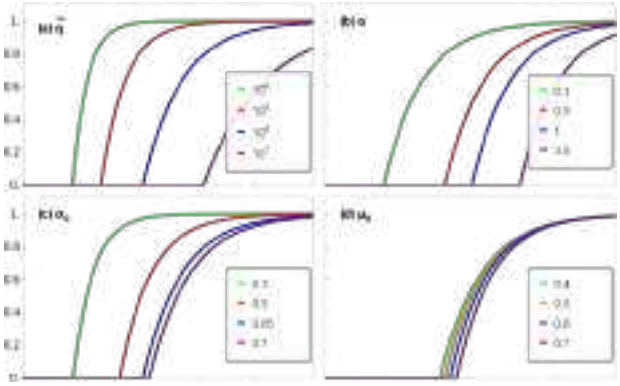

Fig. 2. *Mean biomass density along the floodplain for different model parameters; each panel varies one parameter while the others are fixed at benchmark values.*

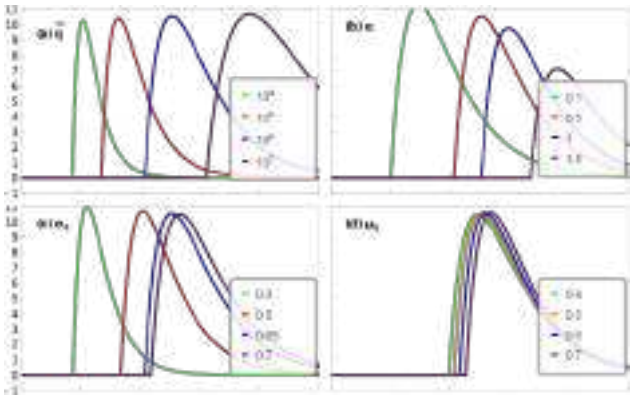

Fig. 3. *Local catalytic index along the floodplain; panel layout as in Fig. 2.*

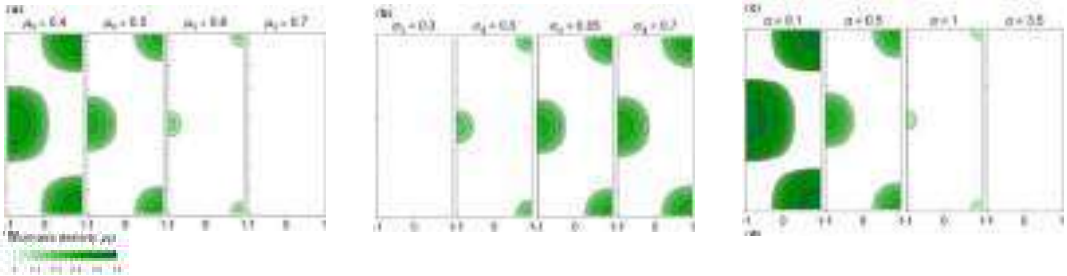

Fig. 4. *Mean biomass density along the alternate bars of a gravel-bed river (R_p = 3.85×10⁴) for different model parameters.*

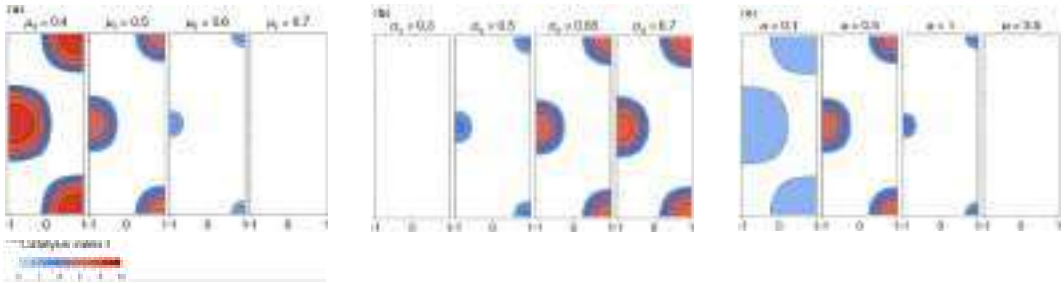

Fig. 5. *Local catalytic index along the alternate bars of a gravel-bed river (R_p = 3.85×10⁴).*

The global catalytic index as a function of mean discharge shows that moderate discharges maximize the catalytic effect, while very high or very low flows reduce it. Similarly, flow variability (σ_q) exhibits an optimal range for maximizing carbon pumping efficiency. The model demonstrates that highly regulated rivers—even in the presence of alternate bar systems—cannot sustain vegetation, as flow stochasticity is essential for bar colonization. The catalytic index provides a consistent quantification of the net increase in carbon export and turnover induced by hydrological variability across the entire fluvial corridor, demonstrating that river flow variability acts as a catalyst for vegetation dynamics and carbon sequestration in riparian zones. The sand-bed case ($\tilde{q} \approx 10^{10}$, $R_p \approx 4$) yields qualitatively similar spatial patterns of biomass and catalytic index, again peaking at intermediate flow variability; for conciseness only the gravel-bed maps are shown (Figs. 4–5), while the floodplain analysis (Figs. 2–3) applies to both bed types.

References

Bertagni MB, Camporeale C (2018) Finite amplitude of free alternate bars with suspended load, Water Resources Research, 54, 9 759-9773.

Camporeale C, Perucca E, Ridolfi L, Gurnell A (2013) Modeling the interactions between river morphodynamics and riparian vegetation, Reviews of Geophysics, 51, 379-414.

Calvani, G., Ruiz-Villanueva, V., Schwarz, M., & Perona, P. (2025). Towards unified scaling relationships for gravel-bed and sand-bed rivers. *Geomorphology*, 109972.

Drake TW, Raymond PA, Spencer RGM (2018) Terrestrial carbon inputs to inland waters: A current synthesis of estimates and uncertainty, Limnology and Oceanography Letters, 3(3), 132-142.

Laio F, Porporato A, Ridolfi L, Rodriguez-Iturbe I (2001) Plants in water-controlled ecosystems: active role in hydrologic processes and response to water stress: II. Probabilistic soil moisture dynamics, Advances in Water Resources, 24(7), 707-723

Parker G, Wilcock PR, Paola C, Dietrich WE, Pitlick J (2007) Physical basis for quasi-universal relations describing bankfull hydraulic geometry of single-thread gravel bed rivers, Journal of Geophysical Research: Earth Surface, 112(F4).

Ridolfi L, D'Odorico P, Laio F (2011) Noise-induced phenomena in the environmental sciences, Cambridge University Press

Salerno L, Giulio Tonolo F, Camporeale C (2024): A global dataset of carbon pumping by the world's largest tropical rivers, Scientific Data, 11(1), 647

Book of Abstracts of the *16th International Symposium on Ecohydraulics*
Challenges and solutions in the time of global changes
August 16–20, 2026, Lausanne, Switzerland
ISSN: 2790-2420 | ISBN: 978-90-837233-9-6 | doi:[10.64697/iahr.proc.ise2026.abs]
© 2026 IAHR. CC BY-NC-ND 4.0

DEVELOPMENT PATTERNS OF MANGROVES IN ARTIFICIAL COASTAL ZONES AND THEIR IMPACTS ON INVERTEBRATE POPULATIONS

Bangjie Sun[1,3*]

Zhaoyin Wang[1,2]

Mengzhen Xu[2]

Sabrina Yanan Jiang[1,3*]

Yi Zhou[1,3*]

[1]National Observation and Research Station of Coastal Ecological Environments in Macao, Macao Environmental Research Institute, Faculty of Innovation Engineering, Macau University of Science and Technology, Macao SAR 999078, China[2]Department of Hydraulic and Hydroelectric Engineering, Tsinghua University, Beijing 100084

[3]Macau University of Science and Technology Zhuhai MUST Science and Technology Research Institute, Zhuhai, Guangdong Province, 519031, P. R. China

E-mail addresses:

[1]First author: 3240009083@student.must.edu.mo (B.Sun)

zywang@tsinghua.edu.cn (Z. Wang)

mzxu@tsinghua.edu.cn (M. Xu)

3240008942@student.must.edu.mo (Y. Zhou)

[*]Corresponding author: ynjiang@must.edu.mo (S.Y. Jiang)

ABSTRACT

This study investigates the development patterns of mangroves in artificial coastal zones and their impact on invertebrate communities and populations. Samples of mangroves and invertebrates were collected and identified from five typical areas in Macau, while eDNA was used to assess species communities. The study found that mangrove development depends on the formation and growth of a mud layer; only a mud layer exceeding 30 cm in thickness can support the development of dense, lush mangroves reaching several meters in height. The minimum mud layer thickness required for the development of *Acanthus ilicifolius* stands is 5 cm, while that for *Kandelia obovata* stands is at least 10 cm. Mangrove forests promote the development of invertebrate communities. The number of invertebrate species, individual density, and biomass all increase with the age of the mangrove forest. In mangrove forests of *Avicennia marina*, the dominant invertebrate groups are turbellarians and *Uca*, while under *Aegiceras corniculatum* forests, the dominant species is the *Parasesarma*. Compared to natural sandy and rocky shores, the number and density of invertebrate species significantly decreased after artificial land creation and reclamation which altered the coastal zone. Following sedimentation of silt and clay and formation of a mud layers, mangrove forest developed and invertebrate species gradually increased. After more than two decades, the species richness of invertebrates in the artificial mangrove forests has reached pre-human disturbance levels, but the species composition is significantly different.

Keywords:

Ecohydraulics; Artificial coastal zone; Mangrove development; Sediment dynamics; Benthic invertebrates; Macau

1.Introduction

Due to economic development and urbanization in estuarine deltas and coastal regions, land resources are becoming increasingly scarce. Coastal reclamation has been implemented to expand land space in these areas. Both the rate and efficiency of artificial land formation, defined as the land area produced per unit volume of sediment, are considerably higher than those of natural land accretion. Most artificial lands along estuaries and coasts are fringed with hardened shorelines. The conversion of muddy and sandy coasts into hardened structures exerts survival pressure on invertebrates, forcing many individuals to disperse to other habitats.

Macau adopts artificial sediment accretion to reconstruct muddy coasts combined with mangrove afforestation. This practice not only alleviates the adverse effects of land reclamation on coastal invertebrate populations, but also markedly improves ecological conditions and promotes species diversity.

In this study, we selected artificially restored mangrove shorelines in Macau with different construction periods and environmental backgrounds. Through field sampling, species identification and eDNA analysis, we investigated the impacts of artificial land creation and mangrove plantation on coastal benthic invertebrate communities.



Fig. 1 Distribution of 10 sampling sites in three study areas in Macau

2.Study Area

The study zone is located in the western part of Macao. Three typical coastal areas were selected, representing three types of artificial coasts with different ages of mangrove forest.

3. Results

(1) Mangrove height/biomass increased with mud thickness; growth accelerated when mud layer exceeded 40 cm.The figure shows the relationships between mangrove height, aboveground biomass of mangroves, and thickness of mad layer. The mangrove species are *Aegiceras corniculatum*, *Kandelia obovata*, and *Avicennia marina*. As the thickness is less than 40 cm, mangrove biomass increases with the mangrove age slowly. Above 40 cm, the aboveground biomass of mangroves rises sharply.

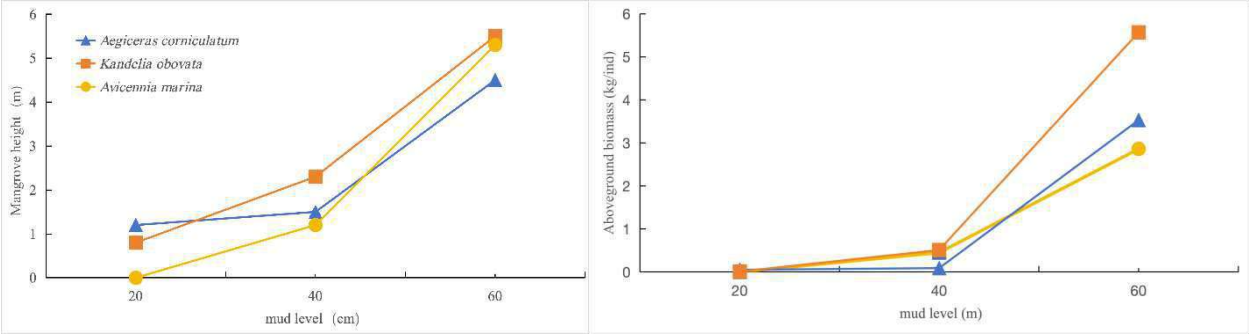

Fig. 2 Relationship between plant height of different mangrove species and mud thickness（Left figure）and Relationship between aboveground biomass of different mangrove species and fluid mud thickness（Right figure）

(2) When using eDNA to assess the density of invertebrate species, the detected biological signal Count value can reflect the total individual density of organisms. Figure 3 presents the Count values measured in mangroves of different ages. The Count value rises rapidly as mangrove stand age increases. Mangrove growth substantially promotes the development of invertebrate populations and the increase of individual density.

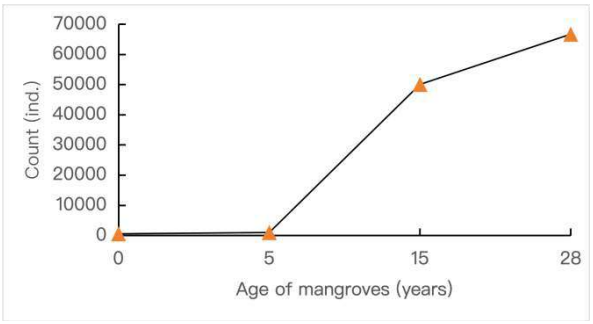

Figure 3 Relationship between the count of biological signals detected by eDNA and mangrove stand age

(3)Species diversity and community complexity increased with mangrove stand age. The dominant taxa shifted from basic benthic groups to mangrove-specific epifaunal groups as the forests matured. The community structure also became more sophisticated: Insecta and Demospongiae emerged as new dominant groups in 25-year mangrove stands. The number of dominant classes increased from two (Polychaeta and Gastropoda) in 5-year mangroves to five, resulting in a more diverse and stable community.

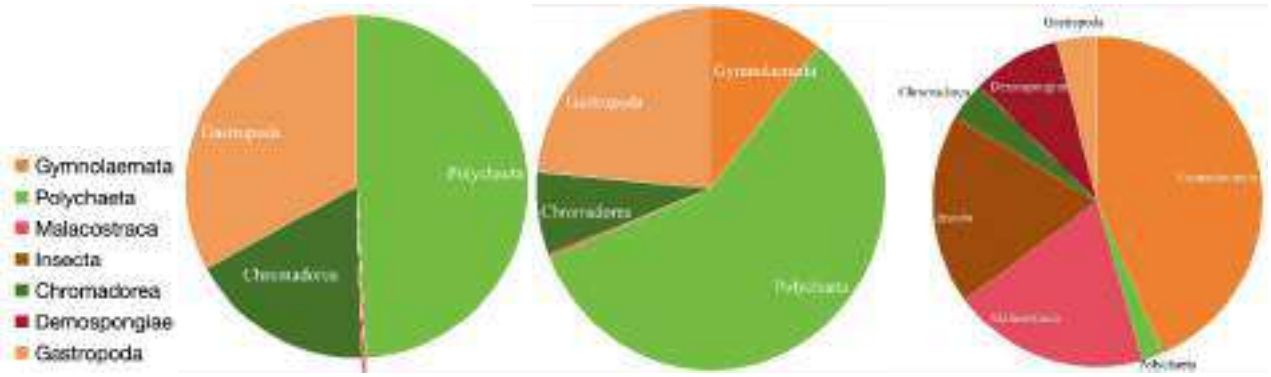

Figure. 4 Pie charts showing the invertebrate species composition in mangrove forests of different ages. (Left: 5-year mangroves; Middle: 15-year mangroves; Right: 28-year mangroves)

(4) The development of invertebrates biodiversity with age of mangrove foresgts. The species richness of inverttebrates reduced sharply after the natural coast changed into naked artificial coast. After plantation of mangroves the number of invertebrates increased and increased further with mangrove age. In the 28 years mangrove forest the species number of macrobenthic invertebrates exceeds that of the natural coastal zone.

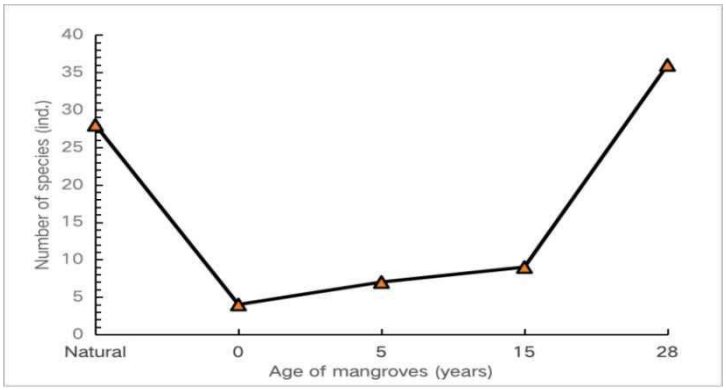

Figure 5 Changes in Species Number in Mangroves of Different Ages

4. Conclusions

Land creation in Macao has impaired the aquatic ecology of the coastal areas. The invertebrate communities have experienced a sharp decline in biodiversity following conversion to artificial coastal zones. The construction of tidal barriers and submerged breakwaters has promoted the deposition of fine sediments, and artificially planted mangroves have gradually restored the ecosystem. The development of mangroves is highly dependent on the formation and accumulation of a mud layer, which in turn facilitate the development of invertebrate communities.

The species richness, individual density and biomass of invertebrates all increase with the age of mangrove forests. Invertebrate diversity in 28-year mangrove forests far exceeds that in natural coastal zones. The dominant invertebrate species in mangroves are fiddler crabs, Corophium spp., sesarmid crabs, etc., which is distinctly different from natural coastal zones where barnacles and gastropods are the dominant taxa.

Acknowledgements

This work is supported by The Science and Technology Development Fund (FDCT), Macao SAR (no. 0017/2024/RIA1) and (no. 0001/2024/NRP).

References

[1] Alongi, D.M. (2014). Carbon cycling and storage in mangrove forests, Annual Review of Marine Science, 6, 195-219.
[2] Lee, S.K., Tan, W.H., & Havanond, S. (1996). Regeneration and colonization of mangrove on clay-filled reclaimed land in Singapore, Hydrobiologia, 319, 23-35.
[3] Zhao, L., Chen, D., Tan, H., Wang, Y., Qiao, Y., & Xing, Y. (2025). The response of mangrove degradation to mineral composition, Frontiers in Marine Science, 12, 1626088.
[4] Yu L Y, Lin S H, Jiao X Y, et al. (2019) Ecological problems and protection countermeasures of mangrove wetlands in the Guangdong-Hong Kong-Macao Greater Bay Area, Acta Scientiarum Naturalium Universitatis Pekinensis, 55(4), 782-790
[5] Thomsen P F, Willerslev E. (2015) Environmental DNA—an emerging tool in conservation for monitoring past and present biodiversity, Biological Reviews, 90(1), 266-279
[6] Ruppert K M, Kline R J, Rahman M S. (2019) Environmental DNA literature review: a new era in molecular ecology, Fisheries Research, 211, 105-115
[7] Quince C, Lanzén A, Curtis T P, et al. (2017) Accurate determination of microbial diversity from 16S rRNA amplicon sequencing, Nature Methods, 14(2), 162-165
[8] Deiner K, Fronhofer E A, Machler E, et al. (2017) Environmental DNA metabarcoding: transforming how we survey animal and plant communities, Molecular Ecology, 26(21), 5872-5895
[9] Taberlet P, Coissac E, Pompanon F, et al. (2012) Towards next-generation biodiversity assessment using DNA metabarcoding, Molecular Ecology, 21(8), 2045-2050
[10] Chen G C, Ye Y, Lu C Y. (2007) Variations of macrobenthic community during Kandelia candel mangrove restoration in Jiulong River Estuary, Ecological Engineering, 31(3), 215-224
[11] Chen G G, Wang W Q, Gu X, et al. (2021) Effects of mangrove plant community turnover on macrobenthic community structure in Zhangjiang Estuary, Acta Ecologica Sinica, 41(11), 4310-4317
[12] Wang W Q, Chen G C, Gu X, et al. (2023) Large-scale changes in macrobenthic biodiversity driven by mangrove afforestation, Journal of Applied Ecology, 60(10), 2066-2078
[13] Kristensen E, Bouillon S, Dittmar T, et al. (2008) Organic carbon dynamics in mangrove ecosystems: a review, Aquatic Botany, 89(2), 201-219
[14] Administration for Market Regulation of Guangdong Province of the People's Republic of China (2025) Technical guidelines for investigation and accounting of coastal blue carbon sink capacity Part 2: Mangrove, DB44/T 2607.2—2025, Guangzhou: Guangdong Science and Technology Press

Session A4

Ecohydraulics Across Space and Time: from habitats to catchments, instants to decades, and individuals to communities

Book of Abstracts of the *16th International Symposium on Ecohydraulics*
Challenges and solutions in the time of global changes
August 16–20, 2026, Lausanne, Switzerland
ISSN: 2790-2420 | ISBN: 978-90-837233-9-6 | doi:[10.64697/iahr.proc.ise2026.abs]
© 2026 IAHR. CC BY-NC-ND 4.0

FROM CROSS-SECTION AVERAGES TO IMMERSIVE, AGENT-BASED COMPUTATIONAL ECOHYDRAULICS

Sebastian SCHWINDT[1], Benjamin KEMMLER[1], Federica SCOLARI[1], Gregory B. Pasternack[2]

[1] Institute for Modelling Hydraulic and Environmental Systems (IWS), University of Stuttgart, Pfaffenwaldring 61, D-70569 Stuttgart, Germany
email: sebastian.schwindt@iws.uni-stuttgart.de, st160747@stud.uni-stuttgart.de, federica.scolari@iws.uni-stuttgart.de

[2] Department of Land, Air and Water Resources, University of California at Davis, One Shields Avenue, Davis, CA 95616-8626, USA
email: gpast@ucdavis.edu

ABSTRACT

Ecohydraulic simulation has progressed from 1D weighted usable area calculations following Bovee and Stalnaker, in which reach-averaged hydraulics are mapped to species- and lifestage-specific suitability curves, to 2D depth and velocity fields that compute per-pixel habitat suitability indices, resolving spatial heterogeneity and connectivity. Yet many passage problems demand 3D because fish respond to vertical shear, turbulence intensity, and coherent structures. 3D models can clarify possible swimming routes, delay zones, and sensory thresholds tied to pressure and vorticity. In particular, agent-based methods couple Eulerian hydraulics with Lagrangian agents to predict movement decisions. However, widespread adoption still needs more calibration data, behavioral rules transferable across flows and species, and validation against trajectories and survival. Ultimately, we showcase parcel-based solvers integrated with Unreal Engine to render high-resolution flows, enabling exploration of aquatic environments from the perspective of fish and testing of virtual interventions before field deployment.

Keywords: numerical simulations; WUA; HSI; habitat suitability; FLIP; Unreal Engine; Niagara Fluids.

1. Introduction

Restoring rivers and sustaining fish populations rely on defensible assessments of habitat to guide physical rehabilitation, for instance, by setting environmental flows (eflows) that balance ecological needs with hydropower operations (Acreman et al., 2014). To provide such guidance, ecohydraulic assessment methods translate hydraulics into biologically meaningful metrics. This contribution to the ecohydraulics conference walks through the evolution of computational ecohydraulic assessment methods with reference to numerical simulation tools over the past decades. We review 1D-approaches following guidelines from the U.S. Fish and Wildlife Service from a period when only the HEC-RAS predecessor HEC-2 was available. By the 2000s, 2D simulations had become a standard tool in computational hydraulics. 1D habitat-assessment equations were then still used to evaluate habitat suitability indices (HSIs) for each pixel in flow-velocity and water-depth maps, with some caveats regarding confusion between indices and probabilities. Today, unsteady and high-resolution 3D simulations are gaining ground and enable far more insight into physically available swimming routes for fish and other aquatic species, with emphasis on sensitivities to vertical shear, turbulence, and coherent structures. Building on that, we summarize agent-based methods as a mechanism to couple hydraulics with rule-based movement. Finally, we outline a forward path using fluid-parcel solvers integrated with realtime video engines to immersively explore rivers from the perspective of a fish.

2. Ecohydraulic modeling review

Developed in the 1970s to fill a gap in tools linking hydraulics with fish populations and aquatic communities, the instream flow incremental methodology (IFIM) comprises procedures for designing and negotiating

instream flows, centered on PHABSIM (Bovee, 1985) and later expanded for water-supply scenario evaluation (Stalnaker et al., 1995). In PHABSIM, weighted usable area (WUA) at discharge Q is computed by mapping cross-section-averaged velocity, water depth, and substrate from a 1D model for each transect segment of planform area into unitless suitabilities, combining them via a product or geometric mean, multiplying by the planform area to yield usable area for the segment, and summing reach-wide. Because spatial resolution derives from hydraulic modeling choices rather than ecological representativeness, and because the method assumes conditional independence and accurate preference curves, the biological meaning of WUA for habitat assessment remains contested (Railsback, 2016).

2D simulations yield spatially explicit rasters of velocity and depth, enabling per-pixel mapping to suitabilities and combination as a composite HSI (cHSI) via the product or, more commonly, the geometric mean, optionally including substrate and cover (Tuhtan et al., 2021). A cHSI raster preserves heterogeneity, connectivity, and patch structure that 1D approaches obscure, but usable habitat should be derived by thresholding cHSI rather than multiplying it by pixel area, because cHSI is not a probability and usable area is not an expectation. Operationally, pixels with cHSI $\geq$ $cHSI_{crit}$ are classified as usable and their areas summed, with typical $cHSI_{crit}$ values $\approx$0.4-0.75 (Schwindt et al., 2020). Coupled with velocity vectors, this thresholding supports assessments of physically available swimming routes, important for hydro-peaking evaluations (Larrieu et al., 2021). As an alternative to deterministic curves, fuzzy-logic systems translate rule sets into indices and can manage many rules needed for different species and their lifestages, though they smear information and uncertainty (Noack et al., 2013). Ultimately, deterministic and fuzzy-logic processing of 2D outputs indicate potential physical habitat suitability; neither guarantees that habitat is functionally used.

1D and 2D models miss the vertical structure that affects how fish approach, locate, and use passage routes. At intakes, spillways, weirs, and especially fishways, flows exhibit non-negligible vertical motions that steer fish. The intensity and dominant eddy size relative to body length, and their timescales, determine whether fish detect guidance cues, exploit refuges, or are fatigued and delayed. Unsteady 3D simulations can reproduce these guidance cues and map where eddies and shear layers intersect likely swim routes. Yet most 3D models use Reynolds-averaged Navier-Stokes equations, which smooth turbulent structures. Also, 3D flow fields are largely unexplored in habitat assessments and pure hydraulics still omit behavior and individual preferences.

Complementing physical simulations, the Eulerian-Lagrangian agent method (ELAM) represents a pathway toward combining information about the hydraulic environment with fish as Lagrangian agents to accommodate preferential swimming routes and ultimately integrate behavioral preference. ELAM couples a fixed-frame (Eulerian) hydrodynamic model with mobile, rule-based virtual fish to predict trajectories in complex flows. The Eulerian component supplies 2D or 3D fields of hydraulic quantities, potentially including flow acceleration. Those fields are sampled by each fish agent within a perceptual neighborhood. The Lagrangian component updates position from a chosen swim speed and orientation at discrete timesteps, while the agent layer encodes behavior-attraction to favorable cues (e.g., low-turbulence), avoidance of adverse stimuli, and stochastic exploration (Goodwin et al., 2006, 2014).

Eulerian solvers advance velocity and pressure on a fixed mesh. Fluid-implicit particle (FLIP) methods combine Eulerian pressure solves with Lagrangian parcels to move mass and momentum and enable agent-flow interactions: fluid parcel velocities are transferred to the mesh, a Poisson solve projects the mesh field to divergence-free form, and updated mesh velocities are mapped back to parcels (Brackbill & Ruppel, 1986). Parcel-based algorithms parallelize well on GPUs and support agent coupling. The commercial Unreal Engine's Niagara Fluids plugin provides a near-realtime FLIP solver whose 3D fields can host fish agents with specified maximum/burst swimming to test against local currents (Schwindt et al., submitted). This approach provides immersive, mechanistic insight, but lacks a turbulence model. Still, it has great potential to integrate with ELAM, accounting for behavioral drivers in addition to physical route analysis.

3. Methods and Materials

A conceptual vertical-slot fishway (VSF) served us to highlight the different insights gained from video game-engine and Eulerian 3D simulations compared to cross-section averaging (1D) and depth averaging (2D). The VSF was designed to overcome an elevation difference of 1.78 m across 13 pools (see sketch in Fig. 1). The design should allow for juvenile river trout (*Salmo trutta fario*) passage during at least 300 days per year according to German standards (DWA, 2014). 1D criteria were key according to the design standards and agreements with fisheries, requiring a maximum flow velocity of 1.2 m/s (instantaneously up to 1.8 m/s in the slots). Because these VSF design standards are based on steady 1D cross-section averaging, they are frequently debated (BAW, 2020). For the VSF considered here, meeting the design standards was merely a necessary

requirement, and our focus was on the insights gained through 2D and 3D simulations, in addition to immersive insights through FLIP simulations in Unreal Engine.

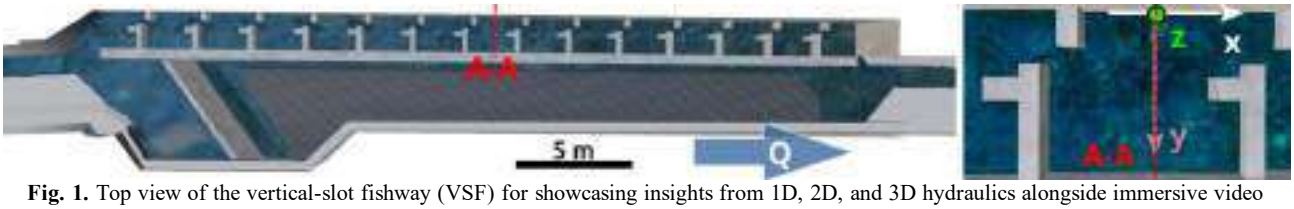

Fig. 1. Top view of the vertical-slot fishway (VSF) for showcasing insights from 1D, 2D, and 3D hydraulics alongside immersive video game-engine simulations. Transect A-A was used for cross-model comparisons between 3D OpenFOAM and FLIP in Unreal Engine.

The numerical models were established with OpenFOAM and a FLIP workflow in Niagara Fluids in Unreal Engine. Calibration and validation of both models were accomplished with measurements from physical flume experiments (Schwindt et al., submitted). The focus in this study was on flow patterns for two steady discharges, namely Q_{30} = 0.06 m³/s and Q_{mean} = 0.135 m³/s, and on differences between indicator (HSI)- and map-based habitat assessments when compared with immersive FLIP simulations.

4. Results & discussion

Regarding 1D-criteria, minimum water depth and maximum flow velocity requirements were respected for all flow scenarios across the 13 pools. However, these design criteria were fulfilled only after multiple iterative adaptations of the VSF, notably raising the bottom elevation of the pools by 0.01 m, improving the inlet design, and changing the bed substrate to coarse gravel (higher roughness).

The 2D outputs were transformed into cHSI for fish passage using binary thresholds: all depths $h < 0.2$ m were set to non-suitable (0) and $h \geq 0.2$ m to suitable (1); likewise, depth-averaged horizontal velocities $U > 1.2$ m/s were set to non-suitable (0) and $U \leq 1.2$ m/s to suitable (1), consistent with the passage criteria (see Methods). The U map is shown in Fig. 2a. For cHSI calculation, we used the geometric mean, which in this binary case reduced to the expression "*if((h>=0.2) & (U<=1.2), 1, 0)*". The resulting cHSI map is shown in Fig. 2b for Q_{mean} (0.135 m³/s). Usable habitat area was not relevant here because the VSF was not intended to provide dwelling or other habitat types beyond enabling fish to pass an otherwise insurmountable obstacle. Accordingly, critical locations were the slots, where cHSI should not be 0. Thus, the zoom on the pool upstream of transect A-A (Fig. 2c) provides relevant additional insights into velocity patterns compared with a 1D simulation. Notably, in the slot and the pool, high lateral heterogeneity is evident, indicating potential passage routes through the slots and resting areas in the pools.



Fig. 2. Depth-averaged flow velocity (a, c) and *cHSI* map (b) for the VSF at the mean annual discharge (Q_{mean} = 0.135 m³/s); panel (c) shows a close-up of depth-averaged flow velocity upstream of transect A-A (cf. Fig. 1).

OpenFOAM and Unreal Engine simulations enabled further insights into the 3D flow-velocity field that was especially important in the VSF. In particular, at transect A-A the 3D flow-velocity field was characterized by a high-velocity jet in the center of the pools, where the highest velocities occurred deeper in the water column than expected from textbook open-channel profiles (peak typically just below the free surface, ~0.1 to 0.3 depth), with considerably lower velocity right at solid boundaries. This low-velocity shelter near the solid boundaries and the smaller-scale patterns also apply to velocity profiles in the slots, indicating that potentially difficult-to-pass, high-velocity sections identified in 1D or 2D space might still host some routes for fish passage closer to solid boundaries or the free surface (albeit with higher injury risk).

The FLIP simulation underestimated water depth by ~25% due to particle clumping and the absence of a turbulence model in Niagara Fluids. Despite this technical shortcoming, the game-engine integration opens the door for immersive simulations, as depicted in Fig. 3, showing a juvenile river trout at different positions in the VSF under the Q_{30} and Q_{mean} scenarios, in addition to a 100-year flood event (1.0 m³/s). The stamina bar (bottom left) indicates the available energetic resources; it decreases when the fish swims against local flow faster than 1.2 m/s and recovers when the fish is dwelling in slower water. When the fish encountered currents stronger than 1.8 m/s, it was repelled (by model design).



Fig. 4. Swimming through the VSF with a fish agent in Unreal Engine: in the slow-flow zone of a pool at Q_{30} (a); preparing to pass a slot at Q_{mean} (b); and drifting downstream through the fully flooded VSF during a flood event (c).

The fish agent can be controlled by anyone interested (see data availability statements). But the human operator perspective also highlights a key challenge: humans steer the fish the way humans would swim, not like a fish. This challenge can be addressed by encoding species-specific decision rules for the fish character in Unreal Engine (e.g., via AI behavior trees and Blueprints/C++), which will require collaboration between experts in numerical simulations, game-engine programming, and biologists to inform meaningful rule sets.

5. Conclusions

1D WUA following Bovee and Stalnaker remains useful for screening and flow-habitat tradeoffs, but it does not resolve patch structure or passage routes. 2D modeling adds spatially explicit hydraulics and supports per-pixel suitability and defensible thresholding to delineate usable habitat, yet it still collapses vertical velocity structure. Contemporary restoration and passage questions hinge on inherently 3D flow dynamics, so unsteady 3D simulations are required when route selection, delay, fatigue risk, or injury are at issue. To this end, ELAM provides a behavioral link from hydraulic stimuli to movement and emergent outcomes, but it demands transferability tests and rigorous validation against observed swimming routes and survival. On the horizon, FLIP solvers coupled to realtime video game engines enable interactive, high-resolution flow fields that can be explored from the fish perspective, accelerating hypothesis testing and design iteration. We expect integrated pipelines in which 3D hydraulics, ELAM, and immersive visualization converge to produce defensible, decision-grade predictions for restoration, hydropower, and eflows.

Data and code availability

Post-processing codes with documentation are available at https://doi.org/10.5281/zenodo.16795740; the Unreal Engine project, including executables for running the simulation in gameplay-mode, is available https://doi.org/10.5281/zenodo.16943371; a video of the fish swimming through the VSF at different discharges is available at https://doi.org/10.5281/zenodo.17064148.

Acknowledgements

Benjamin Kemmler was funded by the German Research Foundation DFG (SCHW 2027/2-1, AOBJ: 448833641); Federica Scolari was funded by DFG (WI 2920/11-1, AOBJ: 691847).

References

Acreman M, Arthington AH, Colloff MJ, et al (2014) Environmental flows for natural, hybrid, and novel riverine ecosystems in a changing world. Frontiers in Ecology and the Environment 12:466–473.
BAW - Bundesanstalt für Wasserbau (2020) Hydraulik von Fischaufstiegsanlagen in Schlitzpassbauweise, Karlsruhe, 64 pp.
Bovee KD (1985) Evaluation of the Effects of Hydropeaking on Aquatic Macroinvertebrates using PHABSIM. In: Proceedings of the Symposium on Small Hydropower and Fisheries. American Fisheries Society, Bethesda, MD, USA, 236–241
Brackbill JU, Ruppel HM (1986) FLIP: A method for adaptively zoned, particle-in-cell calculations of fluid flows in two dimensions. Journal of Computational Physics 65:314–343.
DWA -Deutsche Vereinigung für Wasserwirtschaft, Abwasser und Abfall e.V. (2014) Merkblatt DWA-M 509. Fischaufstiegsanlagen und fischpassierbare Bauwerke [Technical bulletin for fishways]. Hennef, Germany, 334 pp.
Goodwin RA, Nestler JM, Anderson JJ, Weber LJ, Loucks DP (2006) Forecasting 3-D fish movement behavior using a Eulerian–Lagrangian–agent method (ELAM). Ecological Modelling 192:197–223.
Goodwin RA, Politano M, Garvin JW, Nestler JM, Hay D, Anderson J, Weber JL, Dimperio E et al. (2014) Fish navigation of large dams emerges from their modulation of flow field experience. Proceedings of the National Academy of Sciences 111:5277–5282.
Larrieu KG, Pasternack GB, Schwindt S (2021) Automated analysis of lateral river connectivity and fish stranding risks-Part 1: Review, theory and algorithm. Ecohydrology 14:e2268.
Noack M, Schneider M, Wieprecht S (2013) The Habitat Modelling System CASiMiR: A Multivariate Fuzzy Approach and its Applications. In: Ecohydraulics: An Integrated Approach. Wiley-Blackwell, Stuttgart, Germany, 75–91
Railsback SF (2016) Why It Is Time to Put PHABSIM Out to Pasture. Fisheries 41:720–725.
Schwindt S, Larrieu K, Pasternack GB, Rabone G (2020) River Architect. SoftwareX 11:100438
Schwindt S, Kemmler B, Scolari F, Larrieu K, Pasternack G (submitted) Fluid-implicit particle solvers in a video gaming engine provide new perspectives in hydraulic engineering, 46 pp.
Stalnaker C, Lamb BL, Henriksen J, Bovee KD, Bartholow J (1995) The Instream Flow Incremental Methodology - A Primer for IFIM. National Biological Service, U.S. Department of the Interior, Washington, D.C., USA, 47 pp.
Tuhtan JA, Noack M, Wieprecht S (2012) Estimating stranding risk due to hydropeaking for juvenile European grayling considering river morphology. KSCE Journal of Civil Engineering 16:197–206

Book of Abstracts of the *16th International Symposium on Ecohydraulics*
Challenges and solutions in the time of global changes
August 16–20, 2026, Lausanne, Switzerland
ISSN: 2790-2420 | ISBN: 978-90-837233-9-6 | doi:[10.64697/iahr.proc.ise2026.abs]
© 2026 IAHR. CC BY-NC-ND 4.0

EXTENDING ECO-HYDRAULICS INTO ECO-EVO-HYDRAULICS BY INTEGRATING FISH EVOLUTION INTO WATER RESOURCE MANAGEMENT

Xiatong CAI[1,2], Colin D. RENNIE[1], Simon BLANCHET[3], Daniel I. BOLNICK[4], Federico C.F. CALBOLI[5], Io S. DEFLEM[6], Bart HELLEMANS[7], Andrew P. HENDRY[8], Joke DE MEESTER[9,10], Abdolmajid MOHAMMADIAN[1], Filip A.M. VOLCKAERT[7], Patrick WILLEMS[9], Joost A.M. RAEYMAEKERS[2]

[1] Department of Civil Engineering, University of Ottawa, Canada
[2] Faculty of Biosciences and Aquaculture, Nord University, Norway
[3] Centre National de la Recherche Scientifique (CNRS), France
[4] Department of Ecology and Evolutionary Biology, University of Connecticut, USA
[5] Natural Resources Institute Finland, Finland
[6] Research Institute for Nature and Forest (INBO), Belgium
[7] Laboratory of Biodiversity and Evolutionary Genomics, KU Leuven, Belgium
[8] Department of Biology, Redpath Museum, McGill University, Canada
[9] Hydraulics and Geotechnics Section, KU Leuven, Belgium
[10] Flanders Hydraulics Research, Department of Mobility and Public Works, Flemish Government, Belgium

email: xiatong.c@uottawa.ca (for author 1)
email: colin.rennie@uottawa.ca (for author 2)
email: simon.blanchet@lilo.org (for author 3)
email: daniel.bolnick@uconn.edu (for author 4)
email: federico.calboli@luke.fi (for author 5)
email: io.deflem@inbo.be (for author 6)
email: bart.hellemans@kuleuven.be (for author 7)
email: andrew.hendry@mcgill.ca (for author 8)
email: joke.demeester@mow.vlaanderen.be (for author 9)
email: amohamma@uottawa.ca (for author 10)
email: filip.volckaert@kuleuven.be (for author 11)
email: patrick.willems@kuleuven.be (for author 12)
email: joost.raeymaekers@nord.no (for author 13)

ABSTRACT

Eco-hydraulics is primarily based on a concept to restore or regulate river habitat to a semi-natural state, such as through adaptive management on fish passages and habitat suitability (environmental flow and water quality). However, little attention has been given to the evolutionary changes of fish and how these evolutionary changes interact with river management. Recent studies show that rapid evolution can be observed in fish populations in response to river regulation, and this evolutionary response is also expected to feed back on zoogeomorphic engineering processes. Under the exacerbated stress of climate change, river regulation and human activities, understanding the interaction between fish evolution and eco-hydraulics in the river system becomes necessary. In this study, we highlight examples of fish evolutionary response to human regulation in river discharge and flow variance, as well as the potential feedback to river morphology, with the aim of raising awareness of piscine evolutionary dynamics in eco-hydraulics and extending eco-hydraulics into eco-evo-hydraulics.

Keywords: fish conservation; eco-hydraulics; eco-hydrology; zoogeomorphology; hydro-evolutionary feedback; eco-evo-hydraulics

1. Background

Eco-hydraulics is primarily based on a concept to restore or regulate river habitat to a semi-natural state, such as through adaptive management on fish passages and habitat suitability (environmental flow and water quality) (Katopodis & Aadland, 2006; Poff & Matthews, 2013). Although adaptive management adjusts regulation strategies through monitoring fish abundance (Katopodis, 2022), this ecological indicator is insufficient to support long-term conservation objectives under ongoing environmental change (Hoban *et al.*, 2020). The reason is that fish are found to rapidly evolve in order to adapt to different water environments (Hendry & Kinnison, 1999; Dermond, Sperlich & Brodersen, 2019; Jensen *et al.*, 2022; Cai *et al.*, 2025 [preprint]; Stanislawek *et al.*, 2025), and those traits, such as body size, that are under selection may directly influence how river systems should be regulated (Katopodis & Gervais, 2016). Thus, river regulation should consider this dynamic evolutionary process and also should protect the fish's adaptive potential to the ongoing environmental change (Thompson *et al.*, 2023). Besides, fish evolution is also expected to alter the zoogeomorphic engineering process in which fish physically modify their environment (Des Roches *et al.*, 2017; Butler *et al.*, 2018; Rice *et al.*, 2019). Thus, ignoring evolutionary dynamics may result in systematic bias in long-term hydrological and hydraulic modelling.

Three decades after the emergence of eco-hydraulics, we propose extending this field into eco-evo-hydraulics by explicitly incorporating eco-evolutionary dynamics into eco-hydraulics in review). Here, we present examples illustrating how river management can induce evolutionary responses in fish populations, and how these evolutionary responses can, in turn, feed back into zoogeomorphic engineering processes. Together, these examples highlight the need to bridge eco-hydraulics with evolutionary biology and to advance this emerging field at their interface.

2. Flow regulation selects for smaller fish body size and may affect fishway passage

Fishways are waterway structures on/around artificial or natural barriers to facilitate fish movement in order to restore river connectivity and support fish to complete their life cycle (Katopodis, 1992; Katopodis & Williams, 2012). Fish body length is associated with fish swimming ability and thus is an important factor in fishway design (Katopodis & Gervais, 2016). When body size is smaller than a threshold, fish face a challenge to pass the fishway. Recent studies found that due to reduced discharge from river regulation, large salmonid fish cannot access small streams for spawning because of low water levels (Carlson, Quinn & Hendry, 2011; Jensen *et al.*, 2022). Atlantic salmon (*Salmo salar*) in the River Eira, western Norway, adapted to reduced water flow caused by hydropower development by decreasing their body mass to approximately one-third of their original (Jensen *et al.*, 2022). Selective pressures imposed by fishways and reduced discharge can narrow the range of viable body-size phenotypes. This phenotypic filtering reduces the pool of individuals capable of completing migration and may constrain the maintenance of genetic diversity within local populations. In extreme cases, when the minimum body size required to pass a fishway exceeds the maximum body size able to access natal spawning habitats, migration becomes impossible, and no individuals can successfully complete the life cycle, posing a severe risk to local salmon populations.

3. Flow regimes interact with other environmental stressors to shape adaptive potential

The natural flow regime in eco-hydraulics focuses on aligning discharge timing with biological processes and maintaining habitat availability and heterogeneity across flow conditions (Poff *et al.*, 1997). However, it remains rarely discussed whether human-regulated flow regimes induce evolutionary responses in fish, which traits are under selection, and how these altered flow regimes affect fish adaptation to ongoing environmental change. A recent study found an association between flow variance and genetic allele frequency of three-spined stickleback (*Gasterosteus aculeatus*) in the Demer basin in Belgium (Cai *et al.*, 2025 [preprint]). Identified genes are associated with the function of fish morphological development and sensory systems. Fish morphology and behaviour are also subject to selection under both global warming and fishway passage (Podgorniak *et al.*, 2016; Abram *et al.*, 2017). When these selective pressures act on overlapping functional traits, they may constrain or redirect adaptive responses to ongoing climate change. However, the long-term evolutionary consequences of altered flow regimes, particularly their interaction with other environmental stressors in freshwater systems, remain largely unclear and require further investigation.

4. Fish evolution feedback to zoogeomorphic engineering processes

Many fish species physically interact with river morphology in ways that influence sediment size distribution, stability, mobility, transport, and spatial organization (Rice, 2021). For example, salmonids mobilize

substantial volumes of sediment during spawning through the construction of nests (redds) (Hassan *et al.*, 2008). The maximum grain size that can be mobilized is constrained by fish body size (Riebe *et al.*, 2014), thereby linking sediment dynamics to fish phenotypic traits. Consequently, evolutionary changes in fish populations driven by river regulation may feed back into zoogeomorphic engineering processes.

Similarly, other species such as barbel (*Barbus barbus*) disturb and reorganize bed sediments during foraging (Pledger, Rice & Millett, 2014). Therefore, altered flow regimes that modify fish behaviour may not only affect migration success (e.g., passage through fishways (Podgorniak *et al.*, 2016)), but also influence sediment dynamics and associated ecosystem processes.

5. Summary

In this extended abstract, we highlight how human regulation of river systems can drive evolutionary responses in fish populations, and how these evolutionary changes may, in turn, influence the design criteria of fish passage structures, river regulation strategies, and conservation planning (Figure 1). We further emphasize that evolutionary shifts induced by river regulation can feed back into zoogeomorphic engineering processes, thereby altering river morphology and sediment dynamics. Together, these interactions support the need to extend the field of eco-hydraulics toward eco-evo-hydraulics. This new niche aims to inform more robust conservation strategies and improve long-term predictions of river hydraulics and bed morphology.

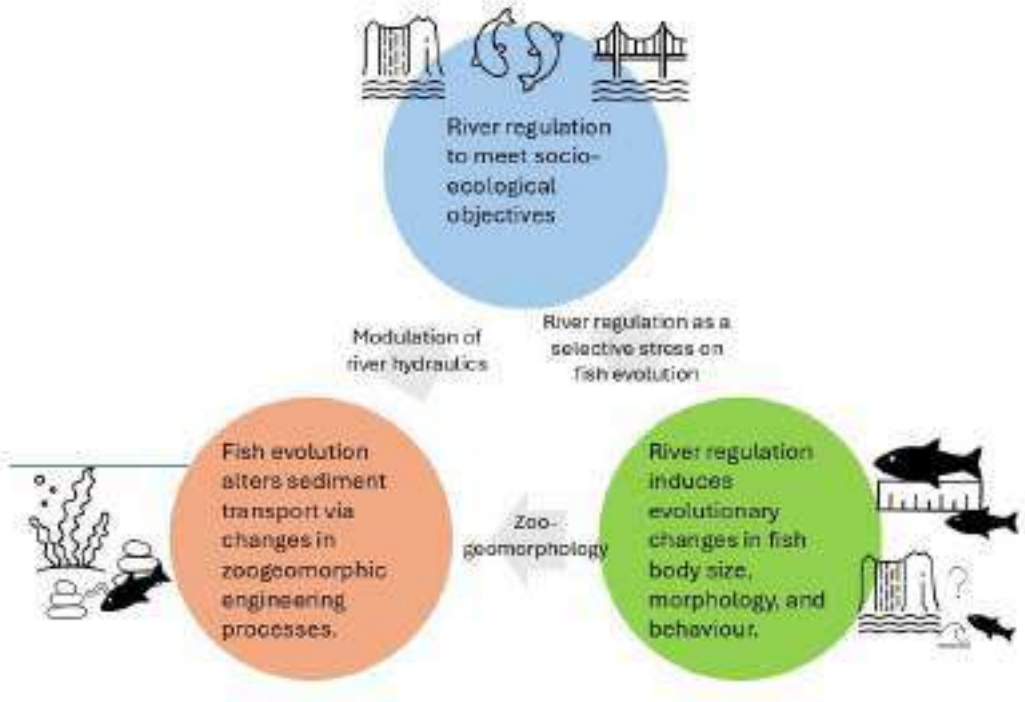

Fig. 1 Conceptual framework integrating river regulation, fish evolution, and zoogeomorphic engineering processes within eco-evo-hydraulics.

Acknowledgements

Research was funded in part by the Natural Sciences and Engineering Research Council (Canada) Discovery Grants to Rennie and Mohammadian.

References

Abram P.K., Boivin G., Moiroux J. & Brodeur J. (2017). Behavioural effects of temperature on ectothermic animals: unifying thermal physiology and behavioural plasticity. *Biological Reviews* **92**, 1859–1876. https://doi.org/10.1111/brv.12312

Butler D.R., Anzah F., Goff P.D. & Villa J. (2018). Zoogeomorphology and resilience theory. *Geomorphology* **305**, 154–162. https://doi.org/10.1016/j.geomorph.2017.08.036

Cai X., Deflem I., Rennie C.D., De Meester J., Willems P., Hendry A.P., *et al.* (2025). Fish show genetic evolutionary responses to river regulation. *bioRxiv*, 2025.08.01.668107. https://doi.org/10.1101/2025.08.01.668107

Cai X., Rennie C.D., Hendry A.P., Blanchet S., Bolnick D.I., Willems P., *et al.* (in review). Hydro-evolutionary feedbacks: integrating evolution into hydraulics and hydrology for fish conservation. *Water Resources Research*

Carlson S.M., Quinn T.P. & Hendry A.P. (2011). Eco-evolutionary dynamics in Pacific salmon. *Heredity* **106**, 438–447. https://doi.org/10.1038/hdy.2010.163

Dermond P., Sperlich N. & Brodersen J. (2019). Heritable morphological differentiation in salmonids from two distinct stream types. *Journal of Fish Biology* **95**, 1215–1222. https://doi.org/10.1111/jfb.14121

Des Roches S., Post D.M., Turley N.E., Bailey J.K., Hendry A.P., Kinnison M.T., *et al.* (2017). The ecological importance of intraspecific variation. *Nature Ecology & Evolution* **2**, 57–64. https://doi.org/10.1038/s41559-017-0402-5

Hassan M.A., Gottesfeld A.S., Montgomery D.R., Tunnicliffe J.F., Clarke G.K.C., Wynn G., *et al.* (2008). Salmon-driven bed load transport and bed morphology in mountain streams. *Geophysical Research Letters* **35**, 2007GL032997. https://doi.org/10.1029/2007GL032997

Hendry A.P. & Kinnison M.T. (1999). Perspective: the pace of modern life: measuring rates of contemporary microevolution. *Evolution* **53**, 1637–1653. https://doi.org/https://doi.org/10.2307/2640428

Hoban S., Bruford M., D'Urban Jackson J., Lopes-Fernandes M., Heuertz M., Hohenlohe P.A., *et al.* (2020). Genetic diversity targets and indicators in the CBD post-2020 Global Biodiversity Framework must be improved. *Biological Conservation* **248**, 108654. https://doi.org/10.1016/j.biocon.2020.108654

Jensen A.J., Hagen I.J., Czorlich Y., Bolstad G.H., Bremset G., Finstad B., *et al.* (2022). Large-effect loci mediate rapid adaptation of salmon body size after river regulation. *Proceedings of the National Academy of Sciences* **119**, e2207634119. https://doi.org/10.1073/pnas.2207634119

Katopodis C. (2022). A perspective on e-flows at hydroelectric projects in Canada. *Hydrobiologia* **849**, 461–484. https://doi.org/10.1007/s10750-020-04381-0

Katopodis C. (1992). *Introduction to fishway design.* Freshwater Institute Central and Arctic Region Department of Fisheries and Oceans, Winnipeg, Manitoba, Canada.

Katopodis C. & Aadland L.P. (2006). Effective dam removal and river channel restoration approaches. *International Journal of River Basin Management* **4**, 153–168. https://doi.org/10.1080/15715124.2006.9635285

Katopodis C. & Gervais R. (2016). *Fish swimming performance database and analyses*. DFO Can. Sci. Advis. Sec. Res. Doc., Ottawa, Canada.

Katopodis C. & Williams J.G. (2012). The development of fish passage research in a historical context. *Ecological Engineering* **48**, 8–18. https://doi.org/10.1016/j.ecoleng.2011.07.004

Pledger A.G., Rice S.P. & Millett J. (2014). Reduced bed material stability and increased bedload transport caused by foragin g fish: a flume study with juvenile Barbel (*Barbus* barbus). *Earth Surface Processes and Landforms* **39**, 1500–1513. https://doi.org/10.1002/esp.3592

Podgorniak T., Blanchet S., De Oliveira E., Daverat F. & Pierron F. (2016). To boldly climb: behavioural and cognitive differences in migrating European glass eels. *Royal Society Open Science* **3**, 150665. https://doi.org/10.1098/rsos.150665

Poff N.L., Allan J.D., Bain M.B., Karr J.R., Prestegaard K.L., Richter B.D., *et al.* (1997). The natural flow regime. *BioScience* **47**, 769–784. https://doi.org/10.2307/1313099

Poff N.L. & Matthews J.H. (2013). Environmental flows in the Anthropocence: past progress and future prospects. *Current Opinion in Environmental Sustainability* **5**, 667–675. https://doi.org/10.1016/j.cosust.2013.11.006

Rice S., Pledger A., Toone J. & Mathers K. (2019). Zoogeomorphological behaviours in fish and the potential impact of benthic feeding on bed material mobility in fluvial landscapes. *Earth Surface Processes and Landforms* **44**, 54–66. https://doi.org/10.1002/esp.4541

Rice S.P. (2021). Why so skeptical? The role of animals in fluvial geomorphology. *WIREs Water* **8**, e1549. https://doi.org/10.1002/wat2.1549

Riebe C.S., Sklar L.S., Overstreet B.T. & Wooster J.K. (2014). Optimal reproduction in salmon spawning substrates linked to grain size and fish length. *Water Resources Research* **50**, 898–918. https://doi.org/10.1002/2013WR014231

Stanislawek M., Richard M., Raffard A., Fargeot L., Lefort M., Poesy C., *et al.* (2025). Global warming and genomic diversity loss alter the biomass and the size distribution of experimental fish populations. *Global Change Biology* **31**, e70611. https://doi.org/10.1111/gcb.70611

Thompson L.M., Thurman L.L., Cook C.N., Beever E.A., Sgrò C.M., Battles A., *et al.* (2023). Connecting research and practice to enhance the evolutionary potential of species under climate change. *Conservation Science and Practice* **5**. https://doi.org/10.1111/csp2.12855

Book of Abstracts of the *16th International Symposium on Ecohydraulics*
Challenges and solutions in the time of global changes
August 16–20, 2026, Lausanne, Switzerland
ISSN: 2790-2420 | ISBN: 978-90-837233-9-6 | doi:[10.64697/iahr.proc.ise2026.abs]
© 2026 IAHR. CC BY-NC-ND 4.0

WAKE TURBULENCE AT LOW SUBMERGENCE: INTEGRAL LENGTH SCALES AND LINKS TO FISH BODY SIZE

Dan NILSSON[1], Anders ANDERSSON[1], Sofia LARSSON[1], Robin ANDERSSON[1], Mats BILLSTEIN[1,2]

[1] Department of Engineering Sciences and Mathematics, Luleå University of Technology, Luleå, Sweden
email: dan.nilsson@ltu.se
email: anders.andersson@ltu.se
email: sofia.larsson@ltu.se
email: robin.andersson@ltu.se

[2] Vattenfall Research and Development, Älvkarleby Laboratory, Älvkarleby, Sweden
email: mats.billstein@vattenfall.com

ABSTRACT

4D-PTV quantified energy-containing eddies in the wake of a cubic obstacle at two relative submergences via the integral length scale L. Expressing eddy size as $\chi = L/L_f$ connects these hydraulic scales to fish body length and habitat relevance. Linking wake turbulence to fish-scale interactions, this study provides a quantitative ecohydraulic scaling and demonstrates that increased submergence produces larger energy-containing eddies, suggesting greater biomechanical suitability for larger-bodied fish.

Keywords: *Relative submergence; Turbulence; Experiments; Boulder; Fish habitat*

1. Introduction

Ecologically important zones occur in shallow reaches of rivers and small streams where water depth is comparable to the largest bedforms. These reaches host complex hydraulics and provide critical habitat for aquatic fauna. Flow depth varies seasonally and under different hydropower operational regimes, leading to changes in relative submergence RS = h/D of bed structures (where h is the local flow depth and D is the characteristic size of the structure, e.g., boulder diameter). Bed structures modulate the turbulent field, and effects on fish swimming and performance depend on the size of energy-containing eddies relative to body length (Tritico & Cotel, 2010). Eddy size is quantified through the integral length scale L, a characteristic size of energy-containing motions, estimated from the spatial autocorrelation of velocity fluctuations. L is then compared with fish length L_f using $\chi = L/L_f$. The effect of RS on L and χ is then evaluated to connect channel hydraulics to fish-relevant scales.

2. Method

Volumetric Particle Tracking Velocimetry (4D-PTV) experiments were conducted in a laboratory flume to quantify the unsteady wake flow at RS = 1.25 and 2.0 (U_{avg} = 0.3 m/s), following the procedure outlined by

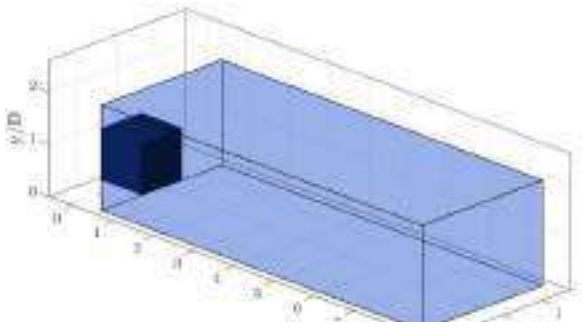

Fig. 1. Measurement region downstream of the cube.

Nilsson et al. (2025). The boulder was modeled as a sharp-edged cube (edge length D = 37.5 mm), and the measurement volume is shown in Fig. 1.

Integral length scales were derived from the autocorrelation functions of the fluctuating velocity components evaluated along multiple lines. The longitudinal autocorrelation function of the streamwise velocity fluctuations (separation along x) is

$$R_{uu}(r) = \frac{\langle u'(x,t)u'(x+r,t)\rangle_{x,t}}{\langle u'^2\rangle_{x,t}}, \quad (1)$$

where, r denotes the streamwise spatial separation (lag) between two samples, $u'(x,t) = u(x,t) - \bar{u}(x)$ with $\bar{u}(x) = \langle u(x,t)\rangle_t$. $\langle\cdot\rangle_{x,t}$ denotes averaging along the streamwise line and over time.

The integral length scale is obtained from the raw correlation by integrating from r = 0 to the first stable zero crossing (r_0):

$$L_{11} = \int_0^{r_0} R_{uu}(r)dr\,. \quad (2)$$

3. Results and Discussion

Figure 2 shows the streamwise spatial autocorrelation $R_{uu}(r/D)$ along the centerline (y/D = 0.5, z/D = 0) in the cube wake for RS = 1.25 and RS = 2. Integrating the raw correlation from r = 0 to the first stable zero crossing r_0 yields L_{11}/D = 0.373 (RS = 1.25) and 0.405 (RS = 2.0). This corresponds to L_{11} of 14.0 and 15.2 mm, i.e., an 8.6% increase in streamwise energy-containing eddy size at the higher submergence.

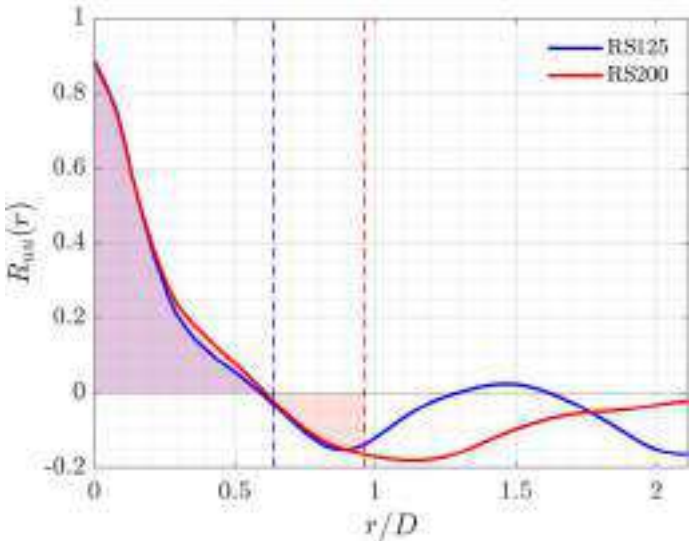

Fig. 2. Spatial autocorrelation $R_{uu}(r/D)$, dashed lines mark r_0, shaded area indicates the integral used for L_{11}.

Scaled to river-like conditions, L_{11}/D = 0.37-0.41 implies eddies of ~ 0.2 m in the wake of a 0.5 m cubical obstacle (using L_{11} as a proxy for energy-containing eddy size). Expressed as $\chi = L_{11}/L_f$, this corresponds to $\chi \approx 0.5$ for a 40 cm fish, $\chi \approx 1$ for a 20 cm fish, and $\chi \approx 2$ for a 10 cm fish, i.e., eddies below, at, and above body length, respectively. Consistent with laboratory observations (Tritico & Cotel, 2010), when $\chi \ll 1$ eddies are generally not destabilizing, station-holding is little affected. When $\chi \approx 1$, eddies are body-scale, and station-holding becomes challenging due to increased posture corrections, and when $\chi > 1$, eddies exceed body length, which tends to disrupt station-holding and increase energy expenditure. Notably, higher submergence (RS = 2.0) increases L_{11}/D by 8.6%, which proportionally increases $\chi = L_{11}/L_f$, implying slightly longer, more coherent disturbances. The increased magnitude of the integral length scale suggests an extended spatial coverage of energy-containing structures for the higher RS, indicating different biomechanical interactions between fish and wake structures. The study highlights ecologically relevant alterations in wake structure associated with varying submergence levels.

Acknowledgements

The research presented here was carried out as a part of the Swedish Centre for Sustainable Hydropower - SVC. svc.energiforsk.se

References

Nilsson, D.A., Andersson, A.G., Larsson, I.A.S., Andersson, R., Billstein, M. (2025). 3D-PTV investigation of flow dynamics around simplified stones at low submergence: Implications for instream habitat. *Water*.

Tritco, H.M. and Cotel, A.J. (2010). The effects of turbulent eddies on the stability and critical swimming speed of creek chub (Semotilus atromaculatus). THE JOURNAL OF EXPERIMENTAL BIOLOGY.

Book of Abstracts of the *16th International Symposium on Ecohydraulics*
Challenges and solutions in the time of global changes
August 16–20, 2026, Lausanne, Switzerland
ISSN: 2790-2420 | ISBN: 978-90-837233-9-6 | doi:[10.64697/iahr.proc.ise2026.abs]
© 2026 IAHR. CC BY-NC-ND 4.0

A TOOLBOX FOR ASSESSING PATCH-SCALE HABITAT DYNAMICS FOR MACROINVERTEBRATES IN FLOW-ALTERED RIVERS

Aude LECRIVAIN[1,2], Giovanni De CESARE [2], Christine WEBER[1], Nico BÄTZ[1]

1: Eawag, Swiss Federal Institute of Aquatic Science and Technology, Surface Waters – Research and Management, Switzerland

email: Aude.Lecrivain@eawag.ch
email: Christine.Weber@eawag.ch
email: Nico.Baetz@eawag.ch

2: EPFL, École Polytechnique Fédérale de Lausanne, Platform of Hydraulic Constructions (PL-LCH), Switzerland

email: Giovanni.DeCesare@epfl.ch

ABSTRACT

Understanding how flow variability and morphological change affect aquatic habitats is central to managing riverine ecosystems. Macroinvertebrates, are highly sensitive to changes in flow regime and river morphology, requiring a spatially and temporally resolved assessments that reflect ecologically meaningfull habitat conditions. To address this need, we present a modular Python-based toolbox developed to quantify macroinvertebrate-relevant habitat dynamics at the patch scale – defined here as a geographically fixed area (~0.25 m²) that reflects the scale at which macroinvertebrate larvae interact with and respond to their environment. The toolbox integrates high-resolution 2D hydrodynamic models (0.5 m spatial, 10 min temporal resolution), a generalized habitat classification, and ecologically derived criteria to generate a habitat time-series. From this, four patch-scale metrics are derived: habitat probability, habitat shifts, drift risk, and desiccation risk. Together, these metrics capture habitat dynamics, persistence and exposure to stress, key drivers of macroinvertebrate spatial distribution within a reach. While broadly applicable across taxa, flow regimes, and river morphologies, we demonstrate the toolbox's functionality using an alpine river affected by hydropeaking (i.e., sub-daily flow fluctuations caused by on-demand hydropower production). The toolbox identifies ecological hotspots, reveals trade-offs linked to structural complexity, and visualizes cumulative stressors exposure across time and space. By making patch-scale habitat dynamics both visible and quantifiable, the toolbox bridges the gap between process-based hydrodynamic modelling and ecological risk assessment. It offers a transferable, open-source approach that supports more spatially targeted river management, adaptive flow designs, and stratified long-term monitoring approaches in regulated river systems.

Keywords: Habitat assessment; Macroinvertebrates; Hydropeaking; Hydrodynamic modelling; Flow alteration; River restoration.

1. Introduction

In natural river systems, flow variability creates a shifting mosaic of habitats (Stanford et al., 2005), to which aquatic organisms have adapted to over millennia with life strategies and traits (Poff and Ward, 1990). Flow pulses, particularly during floods, can induce localized hydraulic stress (e.g., increased current velocity and shear stress) within individual habitat patches. However, patch-scale responses can differ markedly: some patches serve as low-stress refugia, while others show intense hydraulic disturbance (Weber et al., 2013). The composition and diversity of macroinvertebrate communities is strongly shaped by this spatio-temporal heterogeneity (Béjar et al., 2020).

Despite such adaptations to natural disturbances, macroinvertebrates remain highly vulnerable to anthropogenic changes to flow and morphology (Haase et al., 2023), including hydropower regulation (Grill et al. 2019), climate-driven changes to the flow regime, and river simplification (Hischier et al., 2026). These pressures collectively

alter habitat dynamics, their diversity and spatio-temporal arrangement, with long-term repercussions on macroinvertebrate biodiversity and abundance (Ruhi et al., 2018; Haase et al., 2023).

Current assessment tools often lack the ability to quantify how human alterations affect habitat dynamics at ecologically meaningful spatio-temporal scales (Bätz et al., 2023; 2025). To address this gap, we present a toolbox that quantifies patch-scale habitat dynamics and assesses the spatial distribution, persistence and risk exposure of macroinvertebrate-relevant habitats. We demonstrate its applicability through a case study under hydropeaking conditions, i.e. sub-daily flow fluctuations due to on-demand hydropower production.

2. Methods

The toolbox is a modular, Python-based code developed to quantify habitat dynamics for macrozoobenthos at the patch scale. Following the approach proposed by Bätz et al. (2025), it integrates flow time-series, 2D hydrodynamic model outputs, and ecological knowledge to compute spatio-temporal metrics for the assessment of habitat dynamics (Fig. 1). Here, we define a patch as a fixed geographical area of approximately 0.25 m², representing the spatial and temporal scale at which macroinvertebrate larvae perceive and respond to their environment (Béjar et al., 2020; Bätz et al., 2023).

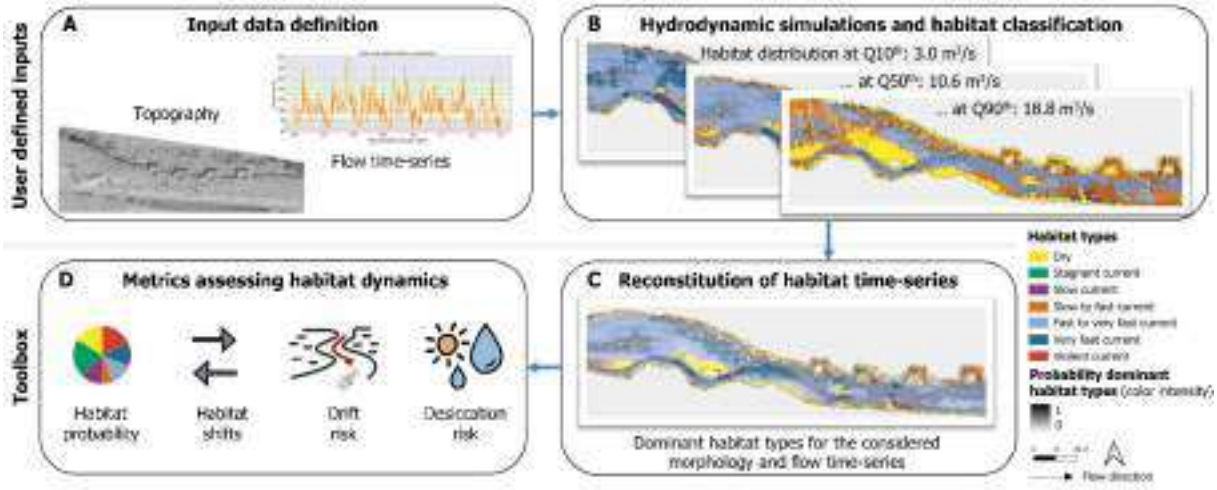

Fig. 1. Overview of the methodological workflow and required inputs for the toolbox (modified after Lecrivain et al., *Submitted*): **A)** User defined input data, including representative flow time-series and high resolution river morphologies; **B)** Hydrodynamic simulations for representative discrete flows and classification of macroinvertebrate-relevant habitat types; **C)** Generation of a habitat time-series by combining classified habitat maps with the flow time-series; **D)** Computation of spatially and temporally explicit patch-scale metrics describing macroinvertebrate habitat dynamics.

The toolbox requires a flow time-series (here at 10 min resolution) and high-resolution hydrodynamic simulations (0.5 m spatial resolution). For the demonstrative case study, steady-state simulations were performed for 13 flows ranging from the 1st to the 99th percentile of a typical weekly hydropeaking time-series, using BASEMENT v4.0. These simulations were calibrated and validated with field measurements of water depth and current velocity. Hydraulic outputs were classified into habitat types relevant to macroinvertebrates, following the generic scheme proposed by Tonolla (2023). Combining the spatial distribution of habitats across the flows with the temporal variability of the flow time-series, produced a continuous habitat time-series. This habitat time-series forms the basis for four patch-scale macroinvertebrate metrics, each of which capturing a distinct facet of habitat dynamics (details in Lecrivain et al., *Submitted*):

- Habitat probability: quantifies the likelihood of a given patch exhibiting specific habitat conditions over time, revealing dominant and less dominant habitat types.
- Habitat shifts: measures the number of shifts between different suitable habitat types within a patch, indicating habitat stability and persistence.
- Drift risk: assesses patch exposure to current velocity thresholds that are known to trigger passive drift, particularly in patches with lentic habitat conditions.
- Desiccation risk: evaluates the maximum continuous duration that each patch remains dry among all drying events, with special relevance for egg desiccation.

While the toolbox is broadly applicable, its functionality is demonstrated here through a hydropeaked alpine river reach, illustrating its ability to detect ecological vulnerabilities for macroinvertebrates at the patch scale.

3. Results and Discussion

Applied to an alpine river reach, the toolbox reproduced realistic patterns of habitat variability (Fig. 2). Under hydropeaking, the frequent flow pulses markedly increased habitat dynamics, reducing patch persistence and overall habitat stability. The four metrics captured distinct but complementary aspects these dynamics.

Structurally simple section of the reach (marked with "low complexity" in Fig. 2.), showed low habitat probability, frequent daily habitat shifts between suitable habitat types and consistently high drift risk, as current velocity thresholds were regularly exceeded. In contrast, morphologically more complex areas of the reach (e.g. lateral shelters, boulders and groynes) showed higher habitat probabilities, mosly fewer daily habitat shifts, and reduced drift and dessication risk. This suggests that adding structural complexity to chanalized rivers throuhg instream measures can mitigate, but not fully offset, the impacts of hydropeaking-induced hydraulic stress.

However, higher structural complexity also increased desiccation risk more elevated gently sloping areas (e.g. on bars), where hydropeaking led to prolonged drying of shallow patches. This spatial pattern reveals a trade-off: structural complexity can help buffering some hydraulic stresses but may amplify desscication risk, particularly where local topography promotes rapid dewatering.

Overall, these findings underscore the need for habitat-specific management and restoration strategies that priamary address the hydropeaking regime itself rather than relying exclusively on instream measures.

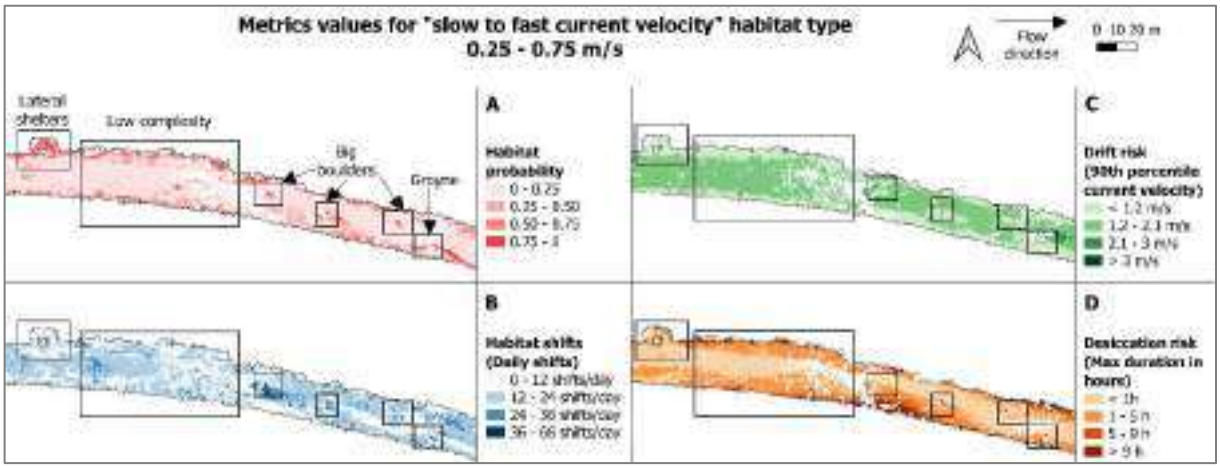

Fig. 2: Example outputs of the four metrics (modified after Lecrivain et al., *Submitted*). Black boxes highlight distinct structural features (see also topography in Fig. 1A). Only patches that exhibit habitat type "slow to fast current velocity" at least once in the habitat time-series are represented (see also flow time-series in Fig. 1A). **A)** Habitat probability: cumulative proportion of time that the habitat type occurs within a patch; **B)** Daily shifts: number of shifts between suitable habitat types within a patch; **C)** Drift risk: 90th percentile of current velocity experienced by a patch; **D)** Desiccation risk: longest uninterrupted dry period experienced by a patch.

4. Conclusions

The results demonstrate that the toolbox offers a powerful and sensitive tool for assessing patch-scale habitat dynamics for macroinvertebrates. It integrates hydrological forcing, geomorphic context and ecological criteria to reveal how structural complexity can both buffer and amplify ecological stress. Compared to existing ecohydraulic approaches, the toolbox provides spatially explicit, process-based assessment that integrates multiple stress dimensions (i.e. hydraulic, temporal, and geomorphic) within a single tool.

The four metrics capture distinct but complementary aspects of patch-scale habitat dynamics: habitat probability and daily shifts characterize habitat persistence and stability, while drift and desiccation risk capture hydraulic and drying stress, respectively. Together, they enable a more effective implementation of process-based river management. By clarifying drives of habitat dynamics and supporting ecological resilience, the toolbox enhances our ability to assess and manage complex river systems.

Beyond the presented case study, the toolbox offers a transferable approach for evaluating habitat dynamics across taxa, flow regimes, and restoration contexts, supporting a more spatially targeted river management and more stratified (i.e. distinguishing patches with lower vs higher persistence) long-term monitoring approaches in regulated river systems.

Acknowledgements

Special thanks are extended to Lorenzo Gorla (Swiss Federal Office for the Environment), Francesco Polli (Canton Ticino), Graziano Sangalli (Azienda Elettrica Ticinese), Alfred Wittwer (Swiss Federal Railways), and Renato Gaggini (Ecocontrol) for their support throughout the study. We also gratefully acknowledge Azin Amini (EPFL) and James Runnalls (Eawag) for their valuable input on hydrodynamic modelling, as well as Christian Dinkel (Eawag) for his assistance during fieldwork.

References

Bätz N, Judes C, Vanzo D, Lamouroux N, Capra H, Baumgartner J, Berger B, Weber C. 2025. Patch-scale habitat dynamics: three metrics to assess ecological impacts of frequent hydropeaking. Journal of Ecohydraulics. 10(1):79-106.

Bätz N, Judes C, Weber C. 2023. Nervous habitat patches: The effect of hydropeaking on habitat dynamics. River Research and Applications. 39(3):349-363.

Béjar M, Gibbins C, Vericat D, Batalla RJ. 2020. Influence of habitat heterogeneity and bed surface complexity on benthic invertebrate diversity in a gravel-bed river. River Research and Applications. 36(3):465-479.

Grill G, Lehner B, Thieme M, Geenen B, Tickner D, Antonelli F, Babu S, Borrelli P, Cheng L, Crochetiere H et al. 2019. Mapping the world's free-flowing rivers. Nature. 569(7755):215-221.

Haase P, Bowler DE, Baker NJ, Bonada N, Domisch S, Garcia Marquez JR, Heino J, Hering D, Jahnig SC, Schmidt-Kloiber A et al. 2023. The recovery of European freshwater biodiversity has come to a halt. Nature. 620(7974):582-588.

Hischier CM, Bätz N, Rachelly C, Demuth P, Weitbrecht V, Vetsch DF, Dinkel C, Dinkel C. 2026. From habitat heterogeneity to flood refugia: linking flow intensity and morphology to inform river management. Science of the Total Environment., 1018, 181484.

Lecrivain A, de Cesare G, Weber C, Bätz N. *Submitted*. Macroinvertebrate habitat dynamics under frequent hydropower-induced discharge fluctuations: Patch-scale metrics to quantify effects of hydropeaking and morphological complexity. Environmental Management.

Poff NL, Ward JV. 1990. Physical habitat template of lotic systems: Recovery in the context of historical pattern of spatiotemporal heterogeneity. Environmental Management. 14(5):629-645.

Ruhi A, Dong X, McDaniel CH, Batzer DP, Sabo JL. 2018. Detrimental effects of a novel flow regime on the functional trajectory of an aquatic invertebrate metacommunity. Global Change Biology. 24(8):3749-3765.

Stanford JA, Lorang MS, Hauer FR. 2005. The shifting habitat mosaic of river ecosystems. SIL Proceedings, 1922-2010. 29(1):123-136.

Tonolla DE. 2023. Erarbeitung und Beurteilung von Schwall-Sunk Massnahmen – Neue Erkenntnisse aus Forschung und Praxis [Development and assessment of hydropeaking measures – new findings from research and practice]. Report commissioned by the Swiss Federal Office for the Environment (FOEN).

Weber C, Nilsson C, Lind L, Alfredsen KT, Polvi L. 2013. Winter disturbances and riverine fish in temperate and cold regions. BioScience. 63(3):199-210.

Book of Abstracts of the *16th International Symposium on Ecohydraulics*
Challenges and solutions in the time of global changes
August 16–20, 2026, Lausanne, Switzerland
ISSN: 2790-2420 | ISBN: 978-90-837233-9-6 | doi:[10.64697/iahr.proc.ise2026.abs]
© 2026 IAHR. CC BY-NC-ND 4.0

MODELLING FISH HABITAT CHANGES DUE TO THE PRESENCE OF LARGE WOOD IN RIVERS

Marcos SANZ-RAMOS[1], Virginia RUIZ-VILLANUEVA[2], Ernest BLADÉ[1]

[1] Polytechnic University of Catalonia (UPC Barcelona-Tech) - International Center of Numerical Methods in Engineering (CIMNE), Flumen Research Institute, Barcelona, Spain
email: marcos.sanz-ramos@upc.edu
email: ernest.blade@upc.edu

[2] University of Bern, Institute of Geography, Bern, Switzerland
email: virginia.ruiz@unibe.ch

ABSTRACT

Large wood (LW) naturally occurs in rivers and plays an important role in shaping their form, flow, and ecosystems. It helps create and maintain fish habitats by changing how water moves and where it flows. Recent studies have used computer models to better understand how LW moves and interacts with water, including how logs float, collide, and settle. These interactions can change water depth, velocity, and energy, which in turn affect the weighted usable area (WUA) — a measure of how suitable different parts of a river are for fish and other aquatic life. Using numerical tools such as the Iber model, a first study about how LW affects habitat conditions is presented, especially during periods of low flow that are critical for defining ecological water needs. The results show that considering LW is essential for a more complete understanding of river habitats and that more research is needed to fully grasp its influence on river ecosystems.

Keywords: Numerical modelling; eco-hydraulic, large wood transport, Iber.

1. Introduction

Large wood (LW) plays a fundamental role in fluvial systems, influencing channel morphology, hydraulic patterns, and ecological processes (Braudrick and Grant, 2000; Gurnell and Bertoldi, 2022; Pinto et al., 2019; Scamardo and Wohl, 2024; Wohl, 2024). Its transport, deposition, and interaction with flow are critical components in river dynamics and habitat formation (Verdonschot and Verdonschot, 2023). In recent years, numerical modelling has become an essential tool for understanding and predicting large wood transport processes (Ruiz-Villanueva, 2024), offering insights into both the physical and ecological implications of wood mobility in riverine environments.

Accurate simulation of LW dynamics requires coupling hydrodynamic models with representations of wood movement, including buoyancy, drag, collision, and entrainment mechanisms (Panici, 2021; Persi et al., 2017; Ruiz-Villanueva et al., 2014b). These interactions can substantially alter local hydraulics, modifying flow velocity, depth distributions, and shear stress fields. Such hydraulic changes, in turn, have a direct impact on the weighted usable area (WUA) — a key metric in eco-hydraulic assessments used to quantify habitat suitability for aquatic organisms under varying flow conditions (Bovee, 1982).

This communication aims to integrate LW transport modelling with eco-hydraulic analysis for a better evaluation of how wood-related flow alterations influence fish habitat availability and suitability. To that end, several simulations were carried out using a numerical model that couples a Eulerian approach for hydrodynamics —and eco-hydraulics— with a Lagrangian approach for simulating large wood transport processes. The numerical results exemplify how important is the consideration of LW in river hydrodynamics, especially for low discharges, which are related to the calculation of the WUA.

2. Materials and methods

2.1. Numerical simulation tool: Iber

Iber (Bladé et al., 2014; Sanz-Ramos et al., 2025) is a freely distributed numerical (www.iberaula.com) tool that solves the two-dimensional depth-averaged shallow water equations (2D-SWE). Widely used for hydraulic studies (e.g., flood hazard and risk mapping), Iber also incorporates several calculation modules to compute morphodynamics and sediment transport processes (Bladé et al., 2019; Dehghan-Souraki et al., 2024), pollutant transport (Cea et al., 2016), large wood dynamics (Ruiz-Villanueva et al., 2014a), hydrological (Cea and Bladé, 2015) and soil erosion modelling (Costabile et al., 2024), urban drainage systems (Aranda et al., 2023; Sañudo et al., 2020), and eco-hydraulics (Sanz-Ramos et al., 2019, 2023).

The present study combines the large wood transport and the eco-hydraulic modules, which are fully coupled with the hydrodynamics, aiming to assess the potential effect of LW on the river in eco-hydraulic studies. To that end, the Instream Flow Incremental Methodology (Bovee, 1982) was applied in different scenarios considering a randomly distributed amount of LW in the computational domain. The LW were computed as cylindrical elements ranging from 0.1 to 0.5 m in diameter, 0.5 to 3 m in length, 500 to 1100 kg/m^3 of density, and 0 to 2π orientation.

2.2. Test cases

Three case studies were simulated, all of them considering both LW transport and eco-hydraulics by applying suitability curves for *Salmo trutta* (Martinez-Capel, 2011; Raleigh et al., 1986), *Luciobarbus bocagei* (Martínez Capel et al., 1999), *Pseudochondrostoma polylepis* (Martínez Capel et al., 1999) and *Squalius pyrenaicus* (Martínez Capel et al., 1999). The habitat criterion used was the multiplication of elemental suitability to obtain the WUA. One hundred LW were initially deposited within the domain.

First, a straight channel with constant slope (0.1%) and trapezoidal section (top width of 9 m and base width of 3 m) was discretized in a structured mesh of squared elements of 0.5 m side size. The inlet discharge varied from 0.1 to 2.5 with steps of 0.1 m^3/s; while the outlet condition was set as a supercritical regime. One hundred LW were initially deposited in the domain.

The second case study was a meandering channel with a curved section (diameter of 8 m) and an average slope of 1.4 %. This channel geometry aims to replicate the inundation of floodplains when the discharge is increased. As inlet conditions, steady flow conditions were simulated, ranging from 0.05 to 1.25 m^3/s with a step size of 0.05 m^3/s. The computational domain was discretized by triangular elements of 0.25 m.

Finally, a 3 km-length stream of the Eume River (Spain) was simulated, based on the IFIM, varying the discharge according to the experimental campaigns (0.620 m^3/s), Hydrological Plan of Galicia-Costa basin (1.567 and 3.350 m^3/s), previous studies of the hydrological plan (0.149, 0.328, 0.829, 1.141, 1.515, and 2.176 m^3/s), the average discharge of the river (11.770 m^3/s), and two additional to cover other ranges (0.560 and 1.200 m^3/s). An unstructured mesh of 3 m side-size was used to discretize the topographical data (IGN, 2022), while more than 2000 LW were initially placed within the 2/3 downstream part of the domain as elements that might modify the hydrodynamics (the first third upstream part is a rock layer without vegetation).

3. Results and discussion

The effect of the presence of LW in the evaluation of the potential fish habitat was assessed comparing the WUA (in m^2/m^2). Fig. 1a compares the results of WUA in the straight channel being, in general, greater for the three species and stadium evaluated. In general, presence of LW in the channel notably increased the suitability area for all stadiums (e.g., *Barbus bocagei* fry or Chondrostoma polylepis fry was increased more than twice). For low discharges, the presence of LW increased the WUA in more than 100% (e.g., all stadiums of *Chondrostoma polylepis* and *Barbus bocagei*). Although the geometry and discharges are not suitable for adults, LW changes the hydrodynamics, generating high depths and velocities, which favor the WUA of adults. By contrast, a reduction in WUA was obtained for *Squalius cephalus* (juvenile and fry stadiums) when the discharge increased. In such cases, the geometry of the channel and the presence of LW locally modified the hydrodynamics nearby the logs, increasing the flow velocity. Despite that, the WUA in these cases was above 0.45 m^2/m^2.

The curved channel (Fig. 1b) also presents a general increase in the WUA when LW is considered. The WUA was modified, especially for high discharges, because some flood-prone areas were inundated and the flow interacted with the deposited LW (e.g., *Salmo trutta* juvenile and adult for discharges between 0.6 and 1.25 m^3/s). Increments above 30% in WUA were observed for in different species and stadiums. In fact, LW were

mobilized and, thus, changed the hydrodynamics and the assessment of the WUA, highlighting that the evaluation of fish habitat suitability is a dynamic process (Sanz-Ramos et al., 2023).

The results of THE Eume River show a slight alteration in the WUA when LW is considered (Fig. 1c). Since the LW were randomly distributed over the computational domain, which covers a greater area than the flood area for the maximum discharge, several logs were located in the floodplains but never being flooded. Despite no significant changes in the curve pattern are visible, increments of 1-10% in WUA were obtained for the different species and stadiums analyzed, highlighting the positive effect of LW in terms of fish habitat availability and suitability

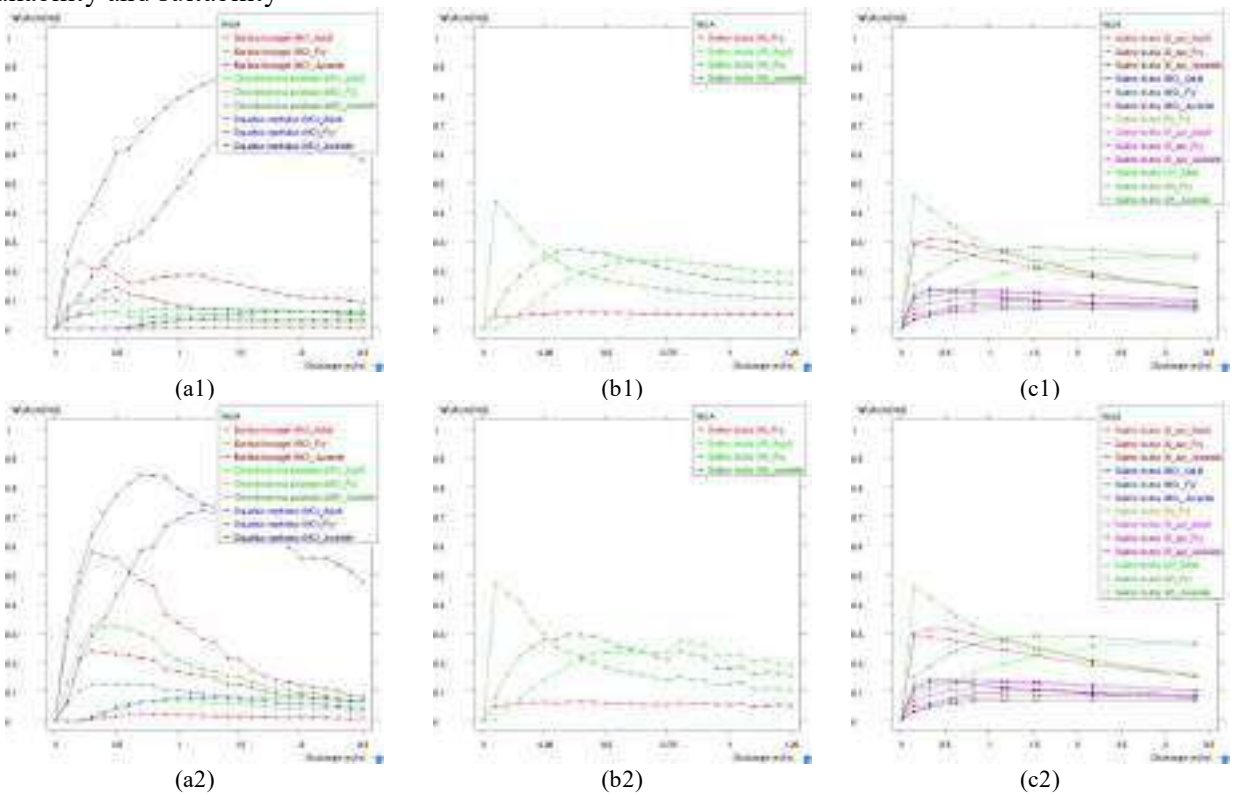

(a1) (b1) (c1)

(a2) (b2) (c2)

Fig. 1. (a) Straight channel: comparison between WUA without LW (a1) and with LW (a2). (b) Curved channel: comparison between WUA without LW (b1) and with LW (b2). (c) Eume River: comparison between WUA without LW (c1) and with LW (c2).

Apart from the uncertainty and simplifications to obtain the suitability curves (Boudreault et al., 2022; Palau et al., 2016), the performance of the numerical tool is consistent with the species and stadium analyzed. Low water depths and velocities provided higher WUA for fry and juvenile stadiums; while high depths and velocities promoted higher WUA for adults. Additionally, LW transport occurred during the simulation, especially for mid-high discharges, favoring the fluvial ecosystem (Ruiz-Villanueva and Consoli, 2025; Wohl et al., 2024).

The utilization of the "stepped discharge" inlet condition notably reduced the computational time and the model build-up process (Sanz-Ramos et al., 2019). Despite that, currently only the hydrodynamic and habitat modules are coupled and parallelized for GPU computing (Sanz-Ramos et al., 2023). The parallelization of the LW module of Iber will notably reduce the computational time, allowing more detailed studies even simulating entire rivers.

4. Conclusions

The presence of large wood (LW) in rivers represents an essential element for fish habitat generation and preservation. The results of coupling numerical modelling of large wood presence/transport and eco-hydraulic evaluation using Iber provided useful information to understand the role of LW in a more holistic approach for fish habitat assessment. This assessment particularly relevant for small discharges, such as those related to eco-hydraulic purposes (e.g., defining ecological discharges). In-depth research is necessary to gain a comprehensive understanding of the impact of the LW fluvial ecosystem.

References

Aranda, J. Á., Sánchez-Juny, M., Sanz-Ramos, M. and Beneyto, C.: Design of Drainage Downspouts Systems over a Road Embankment, Water, 15(20), 3529, doi:10.3390/w15203529, 2023.
Bladé, E., Cea, L., Corestein, G., Escolano, E., Puertas, J., Vázquez-Cendón, E., Dolz, J. and Coll, A.: Iber: herramienta de simulación numérica del flujo en ríos, Rev. Int. Métodos Numéricos para Cálculo y Diseño en Ing., 30(1), 1–10, doi:10.1016/j.rimni.2012.07.004, 2014.
Bladé, E., Sánchez-Juny, M., Arbat, M. and Dolz, J.: Computational Modeling of Fine Sediment Relocation Within a Dam Reservoir by Means of Artificial Flood Generation in a Reservoir Cascade, Water Resour. Res., 55(4), 3156–3170, doi:10.1029/2018WR024434, 2019.
Boudreault, J., Bergeron, N. E., St-Hilaire, A. and Chebana, F.: A new look at habitat suitability curves through functional data analysis, Ecol. Modell., 467, 109905, doi:10.1016/j.ecolmodel.2022.109905, 2022.
Bovee, K. D.: A guide to stream habitat analysis using the Instream Flow Incremental Methodology, Instream Flow Information, FWS/OBS–82/26. Fort Collins, Color., 12, 248, 1982.
Braudrick, C. A. and Grant, G. E.: When do logs move in rivers?, Water Resour. Res., 36(2), 571–583, doi:10.1029/1999WR900290, 2000.
Cea, L. and Bladé, E.: A simple and efficient unstructured finite volume scheme for solving the shallow water equations in overland flow applications, Water Resour. Res., 51(7), 5464–5486, doi:10.1002/2014WR016547, 2015.
Cea, L., Bermúdez, M., Puertas, J., Bladé, E., Corestein, G., Escolano, E., Conde, A., Bockelmann-Evans, B. and Ahmadian, R.: IberWQ: new simulation tool for 2D water quality modelling in rivers and shallow estuaries, J. Hydroinformatics, 18(5), 816–830, doi:10.2166/hydro.2016.235, 2016.
Costabile, P., Cea, L., Barbaro, G., Costanzo, C., Llena, M. and Vericat, D.: Evaluation of 2D hydrodynamic-based rainfall/runoff modelling for soil erosion assessment at a seasonal scale, J. Hydrol., 130778, doi:10.1016/j.jhydrol.2024.130778, 2024.
Dehghan-Souraki, D., López-Gómez, D., Bladé-Castellet, E., Larese, A. and Sanz-Ramos, M.: Optimizing sediment transport models by using the Monte Carlo simulation and deep neural network (DNN): A case study of the Riba-Roja reservoir, Environ. Model. Softw., 175, 105979, doi:10.1016/j.envsoft.2024.105979, 2024.
Gurnell, A. M. and Bertoldi, W.: Wood in Fluvial Systems, in Treatise on Geomorphology, pp. 320–352, Elsevier., 2022.
IGN: Digital Elevation Models, Cent. Descargas [online] Available from: http://centrodedescargas.cnig.es/CentroDescargas/ (Accessed 26 April 2022), 2022.
Martinez-Capel, F.: Modelos de Idoneidad de Microhábitat para el estudio del Régimen Ecológico de Caudales, , 1 [online] Available from: http://hdl.handle.net/10251/13641, 2011.
Martínez Capel, F., García De Jalón Lastra, D., Martínez-Capel, F. and García de Jalón, D.: Desarrollo de curvas de preferencia de microhábitat para Leuciscus pyrenaicus y Barbus bocagei por buceo en el río Jarama (Cuenca del Tajo), Limnetica, 17(1), 71–84, 1999.
Palau, A., Alcázar, J., Rocaspana, R., Aparicio, E. and Mariño, F.: Misusing physical habitat assessment techniques for environmental flows calculations, in Proceedings of 11th International Symposium on Ecohydraulics. Melbourne (Australia)., 2016.
Panici, D.: An Experimental and Numerical Approach to Modeling Large Wood Displacement in Rivers, Water Resour. Res., 57(7), doi:10.1029/2021WR029860, 2021.
Persi, E., Petaccia, G. and Sibilla, S.: Large wood transport modelling by a coupled Eulerian–Lagrangian approach, Nat. Hazards, doi:10.1007/s11069-017-2891-6, 2017.
Pinto, C., Ing, R., Browning, B., Delboni, V., Wilson, H., Martyn, D. and Harvey, G. L.: Hydromorphological, hydraulic and ecological effects of restored wood: findings and reflections from an academic partnership approach, Water Environ. J., 0(2018), wej.12457, doi:10.1111/wej.12457, 2019.
Raleigh, R. F., Zuckerman, L. D. and Nelson, P. C.: Habitat suitability index models and instream flow suitability curves: brown trout, revised. [online] Available from: https://usace.contentdm.oclc.org/digital/collection/p16021coll3/id/354, 1986.
Ruiz-Villanueva, V.: Numerical modelling of wood transport processes in mountain rivers and torrents: a review, in Fachtagung Wildbäche 2024: Modellierung von Wildbachprozessen, pp. 33–40, Swiss Federal Institute for Forest, Snow and Landscape Research, WSL., 2024.
Ruiz-Villanueva, V., Bladé Castellet, E., Díez-Herrero, A., Bodoque, J. M. and Sánchez-Juny, M.: Two-dimensional modelling of large wood transport during flash floods, Earth Surf. Process. Landforms, 39(4), 438–449, doi:10.1002/esp.3456, 2014a.
Ruiz-Villanueva, V., Bladé, E., Sánchez-Juny, M., Marti-Cardona, B., Díez-Herrero, A. and Bodoque, J. M.: Two-dimensional numerical modeling of wood transport, J. Hydroinformatics, 16(5), 1077, doi:10.2166/hydro.2014.026, 2014b.
Ruiz-Villanueva, V. and Consoli, G.: Instream Large Wood Enhances the Benefits of e-Floods in Regulated Mountain Rivers, River Res. Appl., 41(8), 1643–1657, doi:10.1002/rra.70009, 2025.
Sañudo, E., Cea, L. and Puertas, J.: Modelling Pluvial Flooding in Urban Areas Coupling the Models Iber and SWMM, Water (Switzerland), 12(9), 2647, doi:https://doi.org/10.3390/w12092647, 2020.
Sanz-Ramos, M., Bladé, E., Palau, A., Vericatl, D. and Ramos-Fuertes, A.: IberHABITAT: assessment of Physical Habitat Suitability and Weighted Usable Area for fishes. Application in the Eume River, Ribagua, 6(2), 158–167, doi:10.1080/23863781.2019.1664273, 2019.
Sanz-Ramos, M., López-Gómez, D., Bladé, E. and Dehghan-Souraki, D.: A CUDA Fortran GPU-parallelised hydrodynamic tool for high-resolution and long-term eco-hydraulic modelling, Environ. Model. Softw., 161(ii), 105628, doi:10.1016/j.envsoft.2023.105628, 2023.
Sanz-Ramos, M., Sañudo, E., López-Gómez, D., García-Feal, O., Bladé, E. and Cea, L.: Evolución de la modelización numérica bidimensional del flujo en lámina libre a través del software Iber, Ing. del Agua, 29(2), 114–131, doi:10.4995/ia.2025.23259, 2025.
Scamardo, J. E. and Wohl, E.: Recognizing the ephemeral stream floodplain: Identification and importance of flood zones in drylands, Earth Surf. Process. Landforms, 49(1), 210–235, doi:10.1002/esp.5754, 2024.
Verdonschot, P. F. M. and Verdonschot, R. C. M.: Ecological Functions and Management of Large Wood in Fluvial Systems, Curr. For. Reports, 10(1), 39–55, doi:10.1007/s40725-023-00209-x, 2023.
Wohl, E.: Ecosystem Benefits of Large Dead Wood in Freshwater Environments, Oxford Research Encyclopedia of Environmental Science. Edited by Hank Shugart et al. ISBN: 978-0-199-38941-4. Oxford University Press, article id. 907., 2024.
Wohl, E., Uno, H., Dunn, S. B., Kemper, J. T., Marshall, A., Means-Brous, M., Scamardo, J. E. and Triantafillou, S. P.: Why wood should move in rivers, River Res. Appl., 40(6), 976–987, doi:10.1002/rra.4114, 2024.

Book of Abstracts of the *16th International Symposium on Ecohydraulics*
Challenges and solutions in the time of global changes
August 16–20, 2026, Lausanne, Switzerland
ISSN: 2790-2420 | ISBN: 978-90-837233-9-6 | doi:[10.64697/iahr.proc.ise2026.abs]
© 2026 IAHR. CC BY-NC-ND 4.0

NEW TOOLS AND DATABASES FOR RIVER MESOHABITAT MODELING

Paolo VEZZA[1], Giovanni NEGRO[2], David FARÒ[3], Beatrice PINNA[4], Simone FORTE[5], Guido ZOLEZZI[6]

[1] Department of Environment, Land and Infrastructure Engineering (DIATI), Politecnico di Torino, Italy – INGENIO, Universitat Politècnica de València, Spain
email: paolo.vezza@polito.it, paovez@upvnet.upv.es

[2,4,5] Department of Environment, Land and Infrastructure Engineering (DIATI), Politecnico di Torino, Italy
emails: giovanni.negro@polito.it, beatrice.pinna@polito.it, simone.forte@polito.it

[3] Leibniz Institute of Freshwater Ecology and Inland Fisheries (IGB), Berlin, Germany
email: david.faro@igb-berlin.de

[6] Department of Department of Civil, Environmental and Mechanical Engineering (DICAM), University of Trento, Italy
email: guido.zolezzi@unitn.it

ABSTRACT

Recent advances in river habitat modeling have led to the development of a new suite of tools designed to enhance mesohabitat characterization and ecological assessment in both temporary and perennial rivers. In this work, we present the latest developments including new tools and databases. (1) A dedicated module for non-perennial rivers and streams (NPRs) has been developed in the framework of the MesoHABSIM methodology and it is now available to represent hydrological intermittency and habitat dynamics. For mesohabitat delineation, (2) a novel unsupervised classification algorithm (namely "*mesounit*") automates the delineation of hydro-morphological units (HMU) from high-resolution hydrodynamic simulations. The toolkit also incorporates (3) mesohabitat suitability models for more than 40 freshwater species and a comprehensive habitat model for the entire macroinvertebrate community, facilitating multi-species ecological predictions. Complementing these modeling tools, (4) a curated database currently compiles more than 400 applications in Italy, providing a valuable resource for calibration, validation, and comparative analysis. Together, these innovations represent a major step forward in the standardization, automation, and ecological realism of river mesohabitat modeling.

Keywords: *Temporary rivers*, *Large-scale simulations*, *Databases*, *Mesohabitat*, *SimStream-Web*.

1. Recent advances in mesohabitat modelling

Quantifying habitat availability for aquatic fauna is fundamental to understanding how hydrological and morphological alterations affect river ecosystems over space and time. Over the past decades, the use of the so called 'meso-scale' has become more and more popular in river habitat modelling, linking physical processes with ecological responses, and focusing on the spatial domain of geomorphic units (or hydro-morphological units, HMU) that structure riverine habitats. In this study, we present recent advances in river mesohabitat modeling, including: (1) a new module of the MesoHABitat SImulation Model (MesoHABSIM) for non-perennial rivers and streams (NPRs); (2) an unsupervised classification algorithm (*mesounit*) for the automatic delineation of mesohabitats; (3) a new set of mesohabitat suitability models for 40 European freshwater species and the entire macroinvertebrate community; and (4) a large database of mesohabitat modelling applications in Italy supporting comparative analyses, model validation and methodological standardization at large spatial scales.

Despite the widespread application of habitat models in perennial rivers, NPRs remain underrepresented due to their complex hydrological intermittency. Due to the scale of analysis, traditional micro-scale habitat suitability models fail to capture habitat dynamics during non-flowing phases, when river channels fragment

into isolated ponds or become dry after flow cessation. Negro et al. (2019) and Acuña et al. (2020) presented the first application of mesohabitat modeling to NPRs and have demonstrated that this approach effectively describes habitat evolution during non-flowing phases. To facilitate habitat modeling for NPRs, the new MesoHABSIM has been developed and it is freely available to all users through the *SimStream-Web* service (https://mesohabsim.isprambiente.it/app/home/), at the web page of the Italian National Institute for Environmental Protection and Research (ISPRA).

Two-dimensional (2D) hydrodynamic modeling is suited for habitat analyses in medium and large rivers to simulate spatial patterns of flow and hydraulic variables. However, mesohabitat delineation in large rivers often involves subjective interpretation, limiting reproducibility and scalability across river types. To address these challenges, a new unsupervised classification algorithm has been developed to automatically delineate mesohabitats from high-resolution hydrodynamic simulations. This algorithm (namely *mesounit* and revised from Farò et al., 2022) standardizes habitat mapping, reduces operator bias, and enables objective, repeatable identification of mesohabitats across diverse morphologies and hydrological conditions.

Recent developments in mesohabitat suitability modeling have also improved ecological realism for a broad range of aquatic species. Species-specific models have been created for more than 40 European freshwater taxa, including fish, crustaceans, and river mussels, covering different life stages, while a comprehensive community-level model for macroinvertebrates employs trait-based indices such as the Flow-T index to predict ecological responses to flow alteration. These models enhance predictive capacity, support multi-species assessments, and improve transferability across river systems (Virbkas et al., 2021, Negro et al., 2021, Costarrosa et al. 2024, Pinna et al. 2024).

Finally, river mesohabitat modeling now benefits from a large, curated database that compiles more than 400 MesoHABSIM applications conducted across the Italian territory. This dataset provides a valuable resource for comparative analysis, benchmarking, and methodological standardization. By integrating diverse hydromorphological and ecological datasets, the database supports the testing of new tools, improves model reliability, and promotes the consistent application of mesohabitat modeling in different river types.

2. Results and discussion

The integration of the new *SimStream-Web* module and the *mesounit* algorithm represents a major advancement in river mesohabitat modeling by extending its applicability to both non-perennial (NPRs) and large river systems. The new *SimStream-Web* module extends the MesoHABSIM framework to NPRs by producing the habitat–flow–time rating curves (Fig. 1).

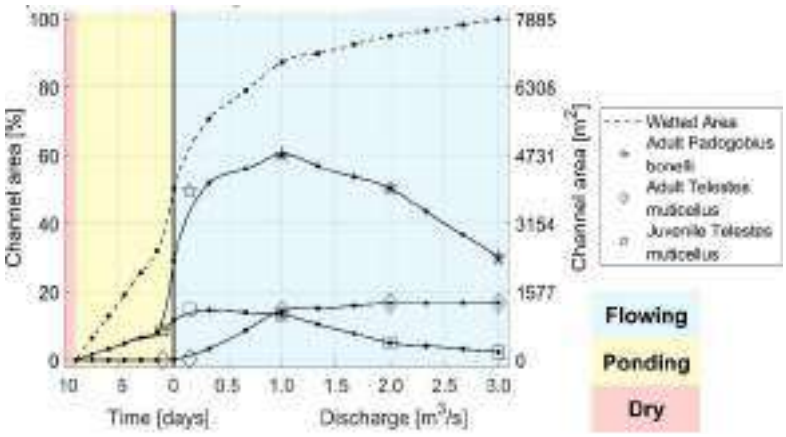

Fig. 1. The habitat-flow-time rating curves for the surveyed sub-reach computed using SimStream-Web. The evolution of total wetted area (%) and available habitat (%) for adult (square dot) and juvenile (diamond dot) *Telestes muticellus*, and adult *Padogobius bonelli* (star dot) per discharge and time. The flowing condition is highlighted in blue, the ponding condition, estimated to persist for 9 days in this example, in yellow, and the dry condition in red.

The new module allows a continuous representation of habitat dynamics after flow cessation, including transitions between flowing, ponding, and dry conditions. This temporal dimension is essential for NPRs, where hydrological intermittency drives rapid changes in habitat connectivity and aquatic community structure. The definition of these curves enables the construction of habitat time series for target species, offering a novel approach to describe habitat persistence and availability during non-flowing phases. This provides crucial insights for defining environmental flows and supporting adaptive management in temporary river systems. (Acuña et al., 2020, Negro et al. 2019).

The *mesounit* algorithm (revised from Farò et al., 2022) complements the development of river mesohabitat models by proposing an objective and reproducible delineation of mesohabitats. *Mesounit* is based on an unsupervised Simple Linear Iterative Clustering (SLIC) and aggregates fine-scale hydraulic data into homogeneous regions, defined using spatial homogeneity and heterogeneity metrics (Fig. 2). An optimal mesohabitat mosaic is chosen by minimizing a Global Score, eliminating operator bias and enhancing comparability across sites. The ability to automatically segment river channels into ecologically meaningful mesohabitats represents an important step toward the standardization of mesohabitat mapping, particularly in large or non-wadable rivers where field-based delineation is limited. This innovation facilitates the integration of physical modeling and large-scale ecological assessment, supporting more robust evaluations of habitat heterogeneity and its role in sustaining aquatic biodiversity.

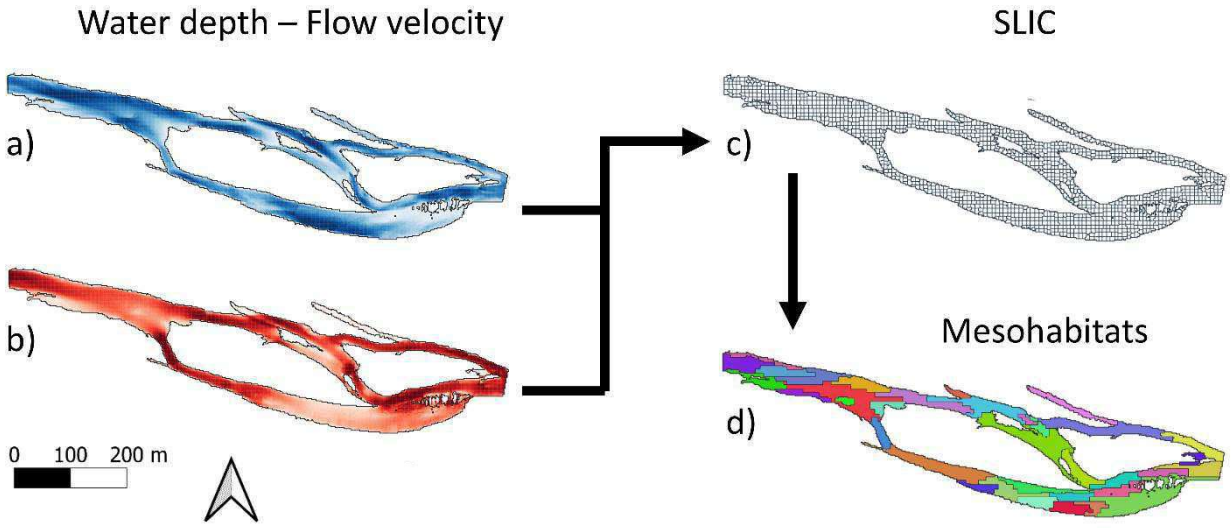

Fig. 2. Examples of segmentation steps based on the Piave River reach. (a/b) outputs of hydraulics modelling (water depth and flow velocity) (c) application of the SLIC algorithm (d) Example of optimal segmentation in mesohabitats.

Equally important are the advances in ecological modeling, which greatly expand the capacity of mesohabitat approaches to capture species-environment relationships at multiple biological and spatial scales. In this work, we present a new suite of mesohabitat suitability models developed for more than 40 European freshwater species, encompassing multiple life stages of fish, crustaceans, and river mussels. These species-specific models integrate empirical field data and hydromorphological predictors to describe habitat preferences at large spatial scales, with higher ecological realism, accounting for life-history traits and ontogenetic habitat shifts. By incorporating both physical (e.g., flow velocity, depth, substrate, gradient, habitat connectivity) and biological (e.g., cover use, flow affinity) descriptors, they enable the evaluation of flow alterations and habitat modification impacts on individual species and functional guilds.

A trait-based model for the entire macroinvertebrate community has been developed by Pinna et al. (2024). The model is based on the Flow-T index, which links biological traits to hydraulic and hydrological gradients. This approach moves beyond species-level prediction, allowing a process-oriented understanding of community responses to flow regulation and morphological change. Such integration of trait-based and species-specific modeling frameworks strengthens the ecological interpretability of mesohabitat simulations and facilitates their application to environmental flow design and biodiversity conservation planning.

Finally, the integration of more than 400 MesoHABSIM applications into a national-scale database provides an unprecedented foundation for model calibration, validation, and benchmarking (Fig. 3). This large dataset encompasses a wide diversity of hydromorphological contexts, river typologies, and biogeographic regions, ranging from Alpine mountain streams to lowland Mediterranean rivers, and includes both perennial and non-perennial systems. Such diversity allows for robust inter-site comparisons, cross-validation of habitat–flow relationships, and the identification of common ecological patterns at the national scale.

Beyond its immediate scientific value, the database serves as a key resource for developing standardized data collection and modeling protocols and for evaluating the transferability of habitat models under different climatic, morphological, and ecological conditions.

The integration of hydrodynamic, geomorphic, and biological datasets also opens new opportunities for meta-analyses, machine learning applications, and the development of predictive tools to assess ecological responses to flow alterations or restoration measures. Furthermore, this extensive repository promotes reproducibility and data sharing among users and within the scientific community, facilitating collaborative research and capacity building across institutions.

Collectively, these developments consolidate a coherent, automated, and scalable framework capable of supporting both fundamental research and applied river management across diverse hydrosystems, strengthening the role of mesohabitat modeling in ecological assessment, environmental flow design, and evidence-based decision-making.

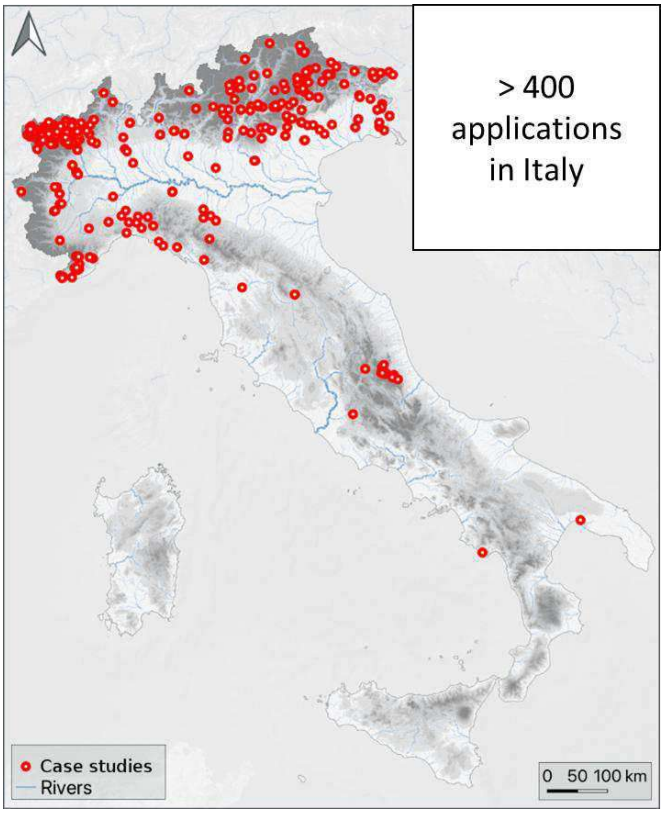

Fig. 3. Mesohabitat modelling applications in Italian rivers. Currently the database includes more than 400 applications.

References

Acuña V, Jorda-Capdevila, D, Vezza P, De Girolamo AM, McClain ME, Stubbington R, Pastor AV, Lamouroux N, Munné A, Datry T (2020) Accounting for flow intermittency in environmental flows design, Journal of Applied Ecology, 57(4), 742-753.

Costarrosa A, Jorda-Capdevila D, Porcar A, López-Doval JC, Pou-Rovira Q, Herrero A, Negro G, Colucci R Pinna B, Vezza P (2022) Suitability Models at Mesohabitat Scale of Native Freshwater Fish and Mussels for Their Application in Environmental Flows Assessment in the NE of the Iberian Peninsula. In Biology and Life Sciences Forum (Vol. 13, No. 1, p. 138). Mdpi.

Farò D, Baumgartner K, Vezza P, Zolezzi G (2022) A novel unsupervised method for assessing mesoscale river habitat structure and suitability from 2D hydraulic models in gravel-bed rivers, Ecohydrology, 15(7). 2

Forte S, Negro G, Pinna B., Spairani M, Candiotto A, Fenoglio S, Laini A, Pizzul E, Vezza P. Mesohabitat Suitability Criteria for Italian Freshwater Species. Ecological modelling and software. Under review.

Negro G, Vezza, P, Jorda-Capdevila, D, Bardina M., Garcia Burgos E, Sola Ortega C, Munné A (2019) Actas del III Congreso Ibérico de Restauración Fluvial. In Centro Ibérico de Restauración Fluvial (Ed.), Meso-scale habitat modeling in temporary rivers: the Gaià river case study. Centro Ibérico de Restauración Fluvial. (pp. 178–186).

Negro G, Fenoglio S, Quaranta E, Comoglio C, Garzia I, Vezza P (2021) Habitat Preferences of Italian Freshwater Fish: A Systematic Review of Data Availability for Applications of the MesoHABSIM Model. Frontiers in Environmental Science, 9: 634-737

Pinna B, Laini A, Negro G, Burgazzi G, Viaroli P, Vezza P (2024). Physical habitat modeling for river macroinvertebrate communities. Journal of Environmental Management, 358, 120919.

Virbickas T, Vezza P, Kriaučiūnienė J, Akstinas V, Šarauskienė D, Steponėnas A (2020) Impacts of low-head hydropower plants on cyprinid-dominated fish assemblages in Lithuanian rivers, Scientific Reports, 10(1), 21687.

Book of Abstracts of the *16th International Symposium on Ecohydraulics*
Challenges and solutions in the time of global changes
August 16–20, 2026, Lausanne, Switzerland
ISSN: 2790-2420 | ISBN: 978-90-837233-9-6 | doi:[10.64697/iahr.proc.ise2026.abs]
© 2026 IAHR. CC BY-NC-ND 4.0

REFINING THE FLOW-T MESOSCALE MODEL FOR RIVER MACROINVERTEBRATE COMMUNITIES

Beatrice PINNA[1], Alex LAINI[2], Gemma BURGAZZI[2], Simone GUARESCHI[3], Paolo VEZZA[1]

[1] Department of Environment, Land and Infrastructure Engineering (DIATI), Polytechnic of Turin, Turin, Italy
[2] Department of Life Sciences and Systems Biology (DBIOS), University of Turin, Turin, Italy
[3] Biodiversity and Conservation Area, Rey Juan Carlos University (URJC), Madrid, Spain
email: beatrice.pinna@polito.it

ABSTRACT

The Flow-T model, the first mesoscale habitat model developed for river macroinvertebrate communities, was refined and tested across multiple hydromorphological contexts in Northern Italy. The study aimed to evaluate its transferability and predictive accuracy in different river typologies, including braided, meandering, cascade, step-pool, and straight channel morphologies. New datasets collected in 2023-2024 from nineteen river and stream reaches were integrated with previous dataset (2019–2020), resulting in an expanded model calibrated and validated using a Random Forest (RF) approach. The refined model selected the 12 descriptors among classes of water surface gradient, flow velocity, substrate composition, water depth, and longitudinal connectivity, and achieved higher accuracy in both cross-validation ($R^2 = 0.79$) and pure validation ($R^2 = 0.68$). The demonstrated transferability and predictive power of the re-trained model confirm the extension of the MesoHABSIM methodology to a new ecological target.

Keywords

Macroinvertebrate communities; Random Forest; Mesoscale habitat modeling; Ecological flows

1. Introduction

Macroinvertebrate communities are universally recognized as key indicators of ecological status, playing a crucial role in river ecosystems, yet they are rarely targeted in habitat models. Among other models, MesoHABSIM (MesoHABitat Simulation Model, Parasiewicz et al., 2007), has been primarily used for fish species, with limited applications for macroinvertebrates (Vezza et al., 2016). Burgazzi et al. (2021) demonstrated that the mesohabitat scale has potential to represent the distribution of macroinvertebrate communities and supports its application in macroinvertebrate habitat modeling. To characterize the community response to hydromorphological variation, several indices have been developed in the last years. Among them, the Flow-T index (Laini et al., 2022) is effective describing the assemblage of taxa in different types of mesohabitats. The first version of the Flow-T-based model was successfully calibrated and validated in three braided rivers within the Po River Basin (Pinna et al., 2024), but its generalizability to other river morphologies remained uncertain. This study refines and extends the Flow-T model across a gradient of morphological contexts, aiming to improve its predictive performance and transferability to diverse river types.

2. Materials and Methods

The study was conducted across nineteen rivers and streams in Northern Italy, encompassing three main geomorphic and climatic contexts: continental multi-thread (e.g., Trebbia River), continental single-thread (e.g., Sangone River), and alpine single-thread channels (e.g., Savara Stream). Data was collected during the 2023 and 2024 summer low-flow periods. Hydromorphological descriptions were performed using i) Uncrewed Aerial Vehicle (UAV) photogrammetry combined with Acoustic Doppler Current Profiler (ADCP) bathymetry and 2D hydrodynamic simulations in large river reaches, or ii) mobile mapping technique through the MapStream QGIS plugin in wadable river reaches. Macroinvertebrates were sampled with Surber nets (0.05 m², 500 µm mesh) following a stratified random approach across mesohabitats. The Flow-T index was calculated using trait affinity to current velocity (Tachet et al., 2010) as described in Laini et al. (2022). A Random Forest (RF, Breiman, 2001) regression model was implemented in R environment, incorporating variable selection assessed using Mean Decrease in Accuracy (MDA), and collinearity minimization with a correlation matrix. Model testing, re-training, and validation used R^2, RMSE, and Pearson correlation (ρ) as performance metrics. Partial Dependence Plots (PDPs) visualized relationships between predictors and the Flow-T index.

The RF model was integrated into the SimStream-Web platform, provided by ISPRA, to extend the MesoHABSIM methodology for macroinvertebrate communities. This web service allows users to input hydromorphological data, and generates geo-referenced habitat maps, habitat-flow rating curves, and time series for the Habitat Integrity Index (IH) calculation. Adapted for the Flow-T index, SimStream-Web enables two analyses: (i) creating Flow-T maps in GIS format to visualize index values at the mesohabitat scale and (ii) generating Flow-T rating curves, showing Flow-T variation with discharge and wetted area at the reach scale.

3. Results

Field surveys produced more than 1000 macroinvertebrate samples and over 10,000 hydrodynamic measurements across more than 200 mesohabitats. The photogrammetric surveys provided high-resolution orthomosaics and Digital Terrain Models (DTMs), with bathymetric data. Hydrodynamic simulations were performed with a mesh size of 1 m, and provided raster maps of flow velocity and water depth with a ground resolution of 10 cm. The MapStream plugin provided GIS shapefiles containing the physical habitat description performed in the field. The training dataset of the Flow-T model was expanded, and the model re-trained. After re-training with the expanded dataset, the model's predictive accuracy improved with respect to the previous version (R^2 = 0.79 calibration; R^2 = 0.68 validation; RMSE = 0.065, Figure 1). RF identified 12 most influential predictors among surface gradient, flow velocity, water depth, substrate type, and longitudinal connectivity. Gradient showed a strong positive relationship with Flow-T, while fine substrates (i.e., pelal) negatively affected predictions. The model successfully distinguished lentic and lotic mesohabitats and captured macroinvertebrate responses across diverse river morphologies. The SimStream-Web platform supports macroinvertebrate community modeling using the Flow-T index. Users can obtain Flow-T maps and Flow-T rating curves as results of the application.

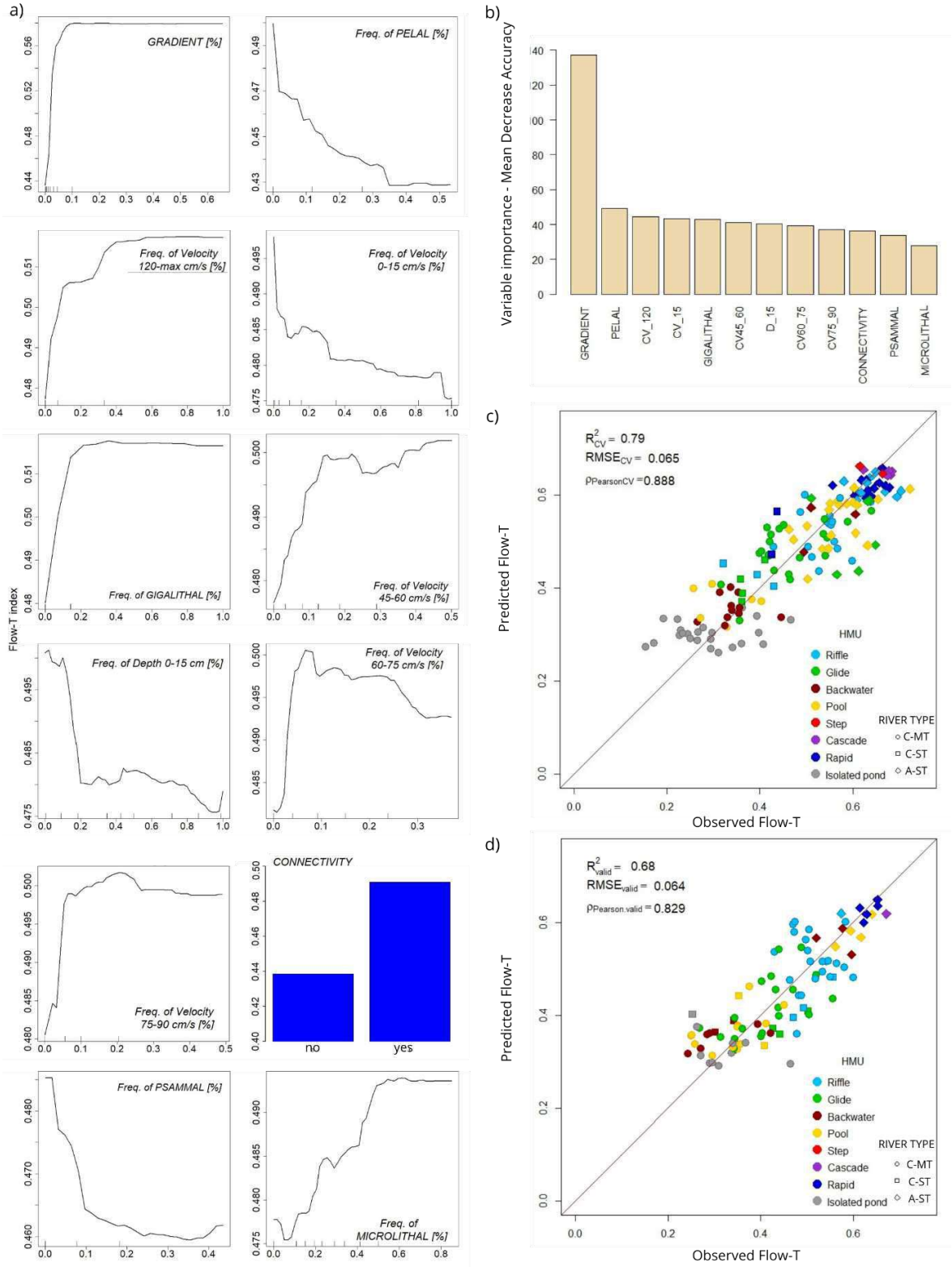

Figure 1. a) RF Partial Dependence Plots of the most important mesohabitat descriptors, b) variable importance ranking, c) scatter-plot of observed vs predicted Flow-T in cross-validation, and d) in pure validation.

4. Discussion and Conclusions

This study refines the macroinvertebrate community model based on the Flow-T index (Laini et al., 2022; Pinna et al., 2024), enhancing its predictive power and applicability across diverse river morphologies. The updated model, trained on a broader dataset of channel types and mesohabitats, identifies water surface gradient as the most influential predictor, alongside flow velocity and substrate composition. Fine substrates (e.g., pelal, psammal) are linked to low Flow-T values and lentic taxa, whereas coarse substrates (e.g., microlithal, gigalithal) correspond to higher Flow-T values and lotic communities. Flow velocity remains a dominant driver, and longitudinal connectivity continues to play an important ecological role. The model demonstrates high transferability and robustness across multiple river typologies, offering a valuable tool for ecological flow assessment and habitat management. Future research should explore its application in diverse seasons, bioperiods, and degrees of flow intermittence to provide an even more robust and transferable tool. The findings may have relevance for an ecologically integrated forecasting methodology applicable for ecological flows design based on different ecological targets (fish and macroinvertebrates), in perennial and non-perennial rivers.

References

Breiman, L. (2001). Random forests. Machine Learning, 45(1), 5–32.

Burgazzi, G., Vezza, P., Negro, G., Astegiano, L., Pellicanò, R., Pinna, B., Viaroli, P., Laini, A. (2021). Effect of microhabitats, mesohabitats and spatial position on macroinvertebrate communities of a braided river. Journal of Ecohydraulics, 6(2) https://doi. org/10.1080/24705357.2021.1938254.

Laini, A., Burgazzi, G., Chadd, R., England, J., Tziortzis, I., Ventrucci, M., Vezza, P., Wood, P.J., Viaroli, P., Guareschi, S. (2022b). Using invertebrate functional traits to improve flow variability assessment within European rivers. Science of the Total Environment, 832, 155047 https://doi.org/10.1016/j.scitotenv.2022.155047

Parasiewicz, P. (2007). The MesoHABSIM model revisited. River Research and Applications, 23(8), 893–903.

Pinna, B., Laini, A. , Negro, G., Burgazzi, G., Viaroli, P., and Vezza, P. (2024). Physical Habitat Modeling for River Macroinvertebrate Communities. Journal of Environmental Management 358: 120919. https://doi.org/10.1016/j.jenvman.2024.120919.

Tachet, H., Richoux, P., Bournaud, M., Usseglio-Polatera, P. (2010). Invertebrates Traits for Ecological Assessment. Freshwater Biology.

Vezza, P., Ghia, D., Fea, G., 2016. Quantitative habitat models for the conservation of the endangered European crayfish Austropotamobius pallipes complex (Astacoidea: astacidae). In: A Global Overview of the Conservation of Freshwater Decapod Crustaceans. https://doi.org/10.1007/978-3-319-42527-6_12.

Book of Abstracts of the *16th International Symposium on Ecohydraulics*
Challenges and solutions in the time of global changes
August 16–20, 2026, Lausanne, Switzerland
ISSN: 2790-2420 | ISBN: 978-90-837233-9-6 | doi:[10.64697/iahr.proc.ise2026.abs]
© 2026 IAHR. CC BY-NC-ND 4.0

ZOOPLANKTON MODULE INDICATES TOP-DOWN EFFECTS ON EUTROPHICATION: IMPLICATIONS FOR LAKE RESTORATION BY BIOMANIPULATION

Chen ZHANG[1], Ruolan YU[1]

[1] State Key Laboratory of Hydraulic Engineering Intelligent Construction and Operation, Tianjin University, Tianjin, China.
email: emil@tju.edu.cn
email: yuruolan@tju.edu.cn

ABSTRACT

Eutrophication drives algal blooms and loss of water clarity in shallow water ecosystems. Biomanipulation of fish and macrophytes is a practical restoration strategy, but quantitative evidence for zooplankton group-specific responses remains limited. We combined an in situ mesocosm experiment manipulating planktivorous fish and macrophytes with scenario-based simulations using a multi-species zooplankton module, which explicitly represents rotifers, cladocerans, and copepods. The model was calibrated and validated with observations from the temperate mesocosm system, including temperature, dissolved oxygen (DO), total nitrogen (TN), total phosphorus (TP), chlorophyll *a* (Chl*a*), macrophytes, zooplankton, and fish, and evaluated against mesocosm patterns. Model performance against the mesocosm observations was generally good to very good (NSE $\geq$ 0.71; $R^2 \geq 0.6$). Both observations and simulations showed strong seasonal effects with zooplankton group-specific responses. In spring and summer, reducing fish increased all three zooplankton groups, especially rotifers, and decreased phytoplankton. In autumn, rotifers increased, but cladocerans and copepods declined under fish removal, accompanied by higher phytoplankton. Increasing macrophyte coverage consistently promoted all zooplankton groups and suppressed phytoplankton across seasons, with particularly strong phytoplankton reductions in autumn. Overall, our results support a fish–zooplankton–macrophyte–phytoplankton cascade and suggest that macrophyte reestablishment and spring-summer removal of zooplanktivorous fish are effective methods to mitigate eutrophication in shallow water ecosystems.

Keywords: Eutrophication; trophic control; freshwater food web

1. Introduction

Eutrophication is a major and increasingly widespread threat to lakes, particularly for vulnerable shallow small water ecosystems (SWEs). Biomanipulation is widely used to suppress phytoplankton and improve water clarity by strengthening top-down control via zooplankton (Yin et al., 2022), while macrophyte reestablishment can further enhance zooplankton grazing by providing refuge from fish predation and by directly competing with phytoplankton for light and nutrients (Moss, 1990; Amorim and Moura, 2020). However, these effects can be difficult to sustain in the long term because top-down and bottom-up processes interact, and phytoplankton can resist grazing, especially when colonial or toxic cyanobacteria dominate (Zhang et al., 2022). Here, we assess the effects of fish biomanipulation and macrophyte reestablishment on eutrophication mitigation in SWEs by analyzing seasonal dynamics of rotifers, cladocerans, and copepods.

2. Materials & methods

Mesocosm experiments were conducted in the Lower Basin of a Sutla River backwater system in northwestern Croatia (45°54′51″ N, 15°41′48″ E) characterized by higher turbidity and no macrophytes cover (Zhang et al., 2023). Net enclosures were used to create three habitats: a macrophyte mesocosm with fish (MF, 40 mm mesh, allowing fish access), a macrophyte treatment without fish (MM, 10 mm mesh, excluding fish), and an external control with fish but no macrophytes (C). Sampling was conducted monthly from July to October 2013, with two sampling events in August. Zooplankton biomass (rotifers, cladocerans, copepods) and chlorophyll a (Chl*a*)

were measured along with temperature, DO, TN, and TP. Seasonal dynamics were simulated using the one-dimensional lake ecosystem model WET 1.0 (Schnedler-Meyer et al., 2022) with a multi-species zooplankton module. The model was forced with local meteorological data and observed nutrient conditions, calibrated with MF data and validated against MM and C. Biomanipulation scenarios were generated by scaling zooplanktivorous fish biomass (25%, 50%, 100%, 200%, 300% of the observed mean) and macrophyte coverage (0%, 25%, 50%, 75%, 100%), and scenario outputs were used to quantify effects on phytoplankton and group-specific zooplankton dynamics.

3. Results

3.1. The effects of biomanipulation on zooplankton in the mesocosm experiment

In the mesocosm, zooplankton biomass showed a clear seasonal pattern across treatments. Fish-present treatments (MF and C) generally had lower crustacean zooplankton than the macrophyte-only treatment (MM), while rotifers were most sensitive to the presence of fish and macrophytes. Differences among MF, MM, and C were most pronounced toward the late-summer to autumn transition, indicating group-specific responses to fish and macrophyte presence.

3.2. Seasonal effects of fish manipulation on zooplankton

The model simulations showed clear seasonal, group-specific responses of zooplankton and phytoplankton to fish manipulation (Fig.1). Reducing fish biomass increased cladocerans, copepods, and especially rotifers in spring and summer, with a decline in phytoplankton, whereas in autumn, rotifers increased but cladocerans and copepods declined, and phytoplankton increased. Across the fish-manipulation scenarios, rotifers exhibited the strongest overall increases, phytoplankton decreased in spring and slightly in summer but rose in autumn, and crustacean zooplankton shifted from positive responses in spring–summer to negative responses in autumn. Fish manipulation also altered phenology by delaying the timing of zooplankton and phytoplankton peaks, and the model indicated instability when fish biomass exceeded roughly three times the reference level.

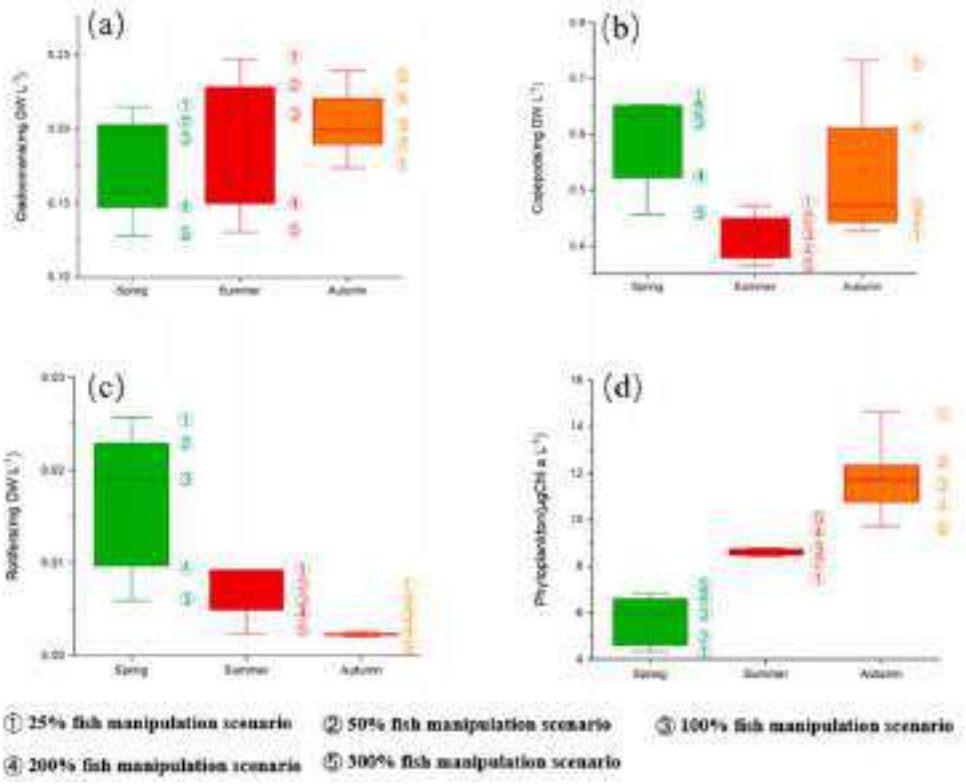

Fig. 1. Responses of modeled zooplankton (rotifers, cladocerans, copepods; a–c) and phytoplankton (d) to fish-biomass scenarios.

3.3. Seasonal effects of macrophyte manipulation on zooplankton

The model simulations indicated that increasing macrophyte coverage consistently increased the biomass of all three zooplankton groups across spring, summer, and autumn, while reducing phytoplankton in all seasons (Fig.2). Rotifers showed the strongest positive response to macrophyte increases, and under the no-macrophyte scenario, they were nearly absent in summer and autumn. Macrophyte manipulation also shifted plankton phenology by delaying seasonal biomass peaks, with phytoplankton peaks delayed slightly more than

zooplankton, while elevating zooplankton peaks and suppressing phytoplankton peaks. Overall, macrophyte coverage was a strong driver of seasonal plankton dynamics, broadly consistent with observed patterns.

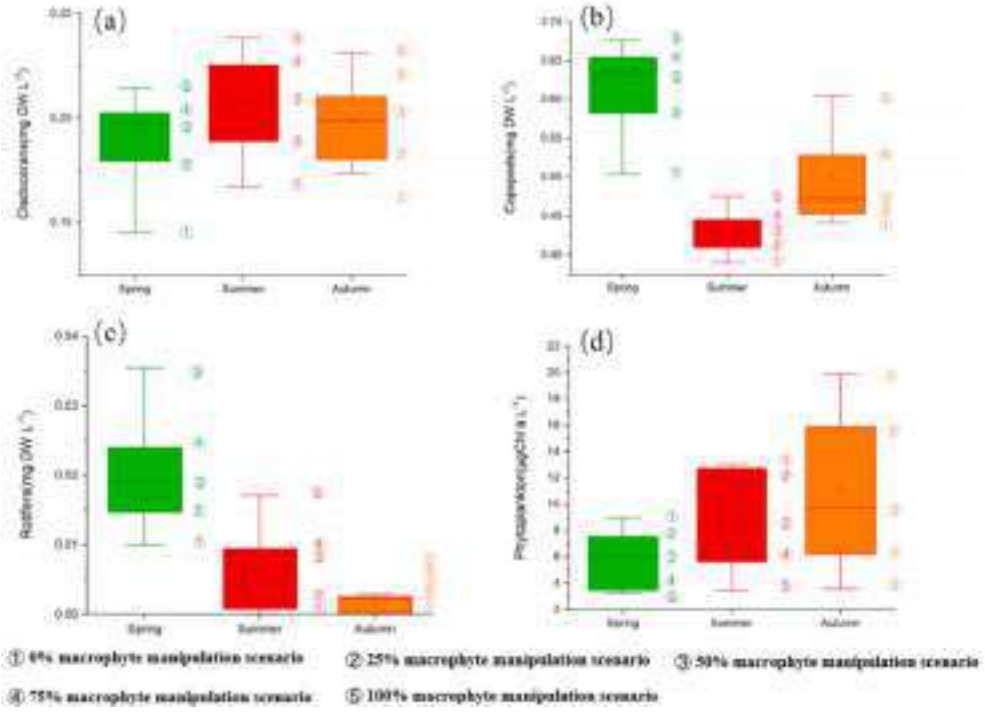

Fig. 2. Responses of modeled zooplankton (cladocerans, copepods, rotifers; a–c) and phytoplankton (d) to macrophyte-coverage scenarios.

3.4. Trophic cascade induced by top-down and bottom-up manipulation

The mesocosm and modeling results showed that both top-down and bottom-up manipulations can trigger trophic cascades that indirectly regulate phytoplankton (Fig.3). Increasing fish biomass generally decreased zooplankton and increased phytoplankton in spring and summer, while autumn responses became group-specific, with cladocerans and copepods increasing but rotifers and phytoplankton decreasing. In contrast, increasing macrophyte coverage consistently enhanced zooplankton and reduced phytoplankton across seasons, with the strongest phytoplankton suppression in autumn, driven by both indirect cascade effects and direct inhibition by macrophytes. Overall, biomanipulating top predators or primary producers induced a trophic cascade along the fish–zooplankton–macrophyte–phytoplankton pathway, reflected in changes in zooplankton biomass and Chl*a*.

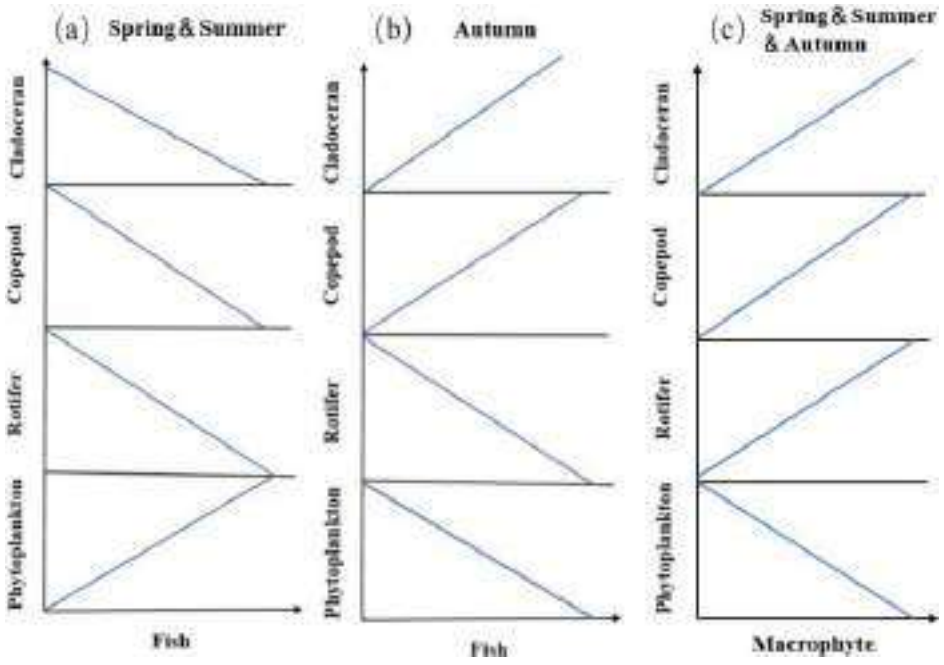

Fig. 3. Trophic cascade under fish manipulation in spring and summer (a) and in autumn (b), and under macrophyte manipulation (c).

4. Discussion

Our results link mesocosm observations with scenario-based simulations using a multi-species zooplankton module to demonstrate that both top-down fish manipulation and bottom-up macrophyte reestablishment can propagate through a fish–zooplankton–macrophyte–phytoplankton cascade. Across seasons, macrophytes consistently increased zooplankton and suppressed phytoplankton, while fish reduction lowered phytoplankton in spring and summer. However, the modeled autumn responses deviated from classic trophic-cascade expectations (Carpenter et al., 1985). Fish reduction increased phytoplankton, and rotifers did not appear to exert effective grazing control in autumn, despite their small size being assumed to reduce vulnerability to fish predation (Špoljar et al., 2018). Overall, macrophytes emerged as a strong lever because they can increase zooplankton refuge and reduce fish predation, while suppressing phytoplankton directly and indirectly through nutrient competition, allelopathy, and trophic cascades (Scheffer et al., 1997). This aligns with evidence that macrophyte reestablishment can drive phytoplankton reduction by limiting nutrient availability. Consequently, fish manipulation alone may be less suitable for small temperate waterbodies in autumn. Building on our results, we hypothesize that stage-structured fish management, introducing juvenile fish in late summer but harvesting adults in the following spring, may help suppress eutrophication while avoiding long-term top-down pressure on zooplankton.

Acknowledgements

We thank the WET 1.0 development team of Nicolas Azaña Schnedler-Meyer, Tobias Kuhlmann Andersen, Fenjuan Rose Schmidt Hu, Karsten Bolding, Anders Nielsen, and Dennis Trolle.

References

Amorim CA, Moura AN (2020) Effects of the manipulation of submerged macrophytes, large zooplankton, and nutrients on a cyanobacterial bloom: a mesocosm study in a tropical shallow reservoir. Environmental Pollution, 265, 114997
Carpenter SR, Kitchell JF, Hodgson JR (1985). Cascading trophic interactions and lake productivity. BioScience, 35, pp. 634-639
Hansson A, Nicolle A, Brodersen J, Romare P, Anders Nilsson P, Brönmark C, Skov C (2007). Consequences of fish predation, migration, and juvenile ontogeny on zooplankton spring dynamics. Limnology and Oceanography, 52, 696-706
Moss B (1990). Engineering and biological approaches to the restoration from eutrophication of shallow lakes in which aquatic plant communities are important components. Hydrobiologia, 200 (201), 367-377
Schnedler-Meyer NA, Andersen TK, Hu FRS, Bolding K, Nielsen A, Trolle D (2022). Water Ecosystems Tool (WET) 1.0 – a new generation of flexible aquatic ecosystem model. Geoscience Model Development, 15, 3861-3878
Scheffer M, Rinaldi S, Gragnani A, Mur LR, Nes EH (1997). On the dominance of filamentous cyanobacteria in shallow, turbid lakes. Ecology, 78, 272-282
Špoljar M, Dražina T, Lajtner J, Duić Sertić J, Radanović I, Wallace RL, Matulić D, Tomljanović T (2018). Zooplankton assemblage in four temperate shallow waterbodies in association with habitat heterogeneity and alternative states. Limnologica, 71, 51-61
Yin C, He W, Guo L, Gong L, Yang Y, Yang J, Ni L, Chen Y, Jeppesen E (2022). Can top-down effects of planktivorous fish removal be used to mitigate cyanobacterial blooms in large subtropical highland lakes? Water Research, 218, 118483
Zhang C, Brett MT, Nielsen JM, Arhonditsis GB, Ballantyne AP, Carter JL, Kann J, Müller-Navarra DC, Schindler DE, Stockwell JD, Winder M, Beauchamp DA (2022). Physiological and nutritional constraints on zooplankton productivity due to eutrophication and climate change predicted using a resource-based modeling approach. Canadian Journal of Fisheries and Aquatic Sciences, 79, 472-486
Zhang C., Zhou Y., Špoljar M, et al. (2023). How can top-down and bottom-up manipulation be used to mitigate eutrophication? Mesocosm experiment driven modeling zooplankton seasonal dynamic approach in the trophic cascade. Water Research, 243, 120364.

Book of Abstracts of the *16th International Symposium on Ecohydraulics*
Challenges and solutions in the time of global changes
August 16–20, 2026, Lausanne, Switzerland
ISSN: 2790-2420 | ISBN: 978-90-837233-9-6 | doi:[10.64697/iahr.proc.ise2026.abs]
© 2026 IAHR. CC BY-NC-ND 4.0

IDENTIFYING FISH MACROHABITATS IN EUROPEAN RIVERS

Geetika CHAUHAN[1], Kamila BELKA[1] Piotr PARASIEWICZ[1]

[1] National Inland Fisheries Institute, Poland.
email: gchauhan@infish.com.pl

ABSTRACT

This study aims to develop an improved Fish Community Macrohabitats model by clustering catchment characteristics with observed fish data. The model is then extrapolated across Europe using the river network derived from the Catchment Characterization Model.

Keywords: European rivers; fish macrohabitats; fish guilds; clustering

1. Introduction

Worldwide, river flow has been regulated through hydrotechnical structures, which are constructed, among other purposes, to protect society from extreme hydrological events (Wantzen et al. 2023). In Europe, rivers are fragmented by more than 1 million man-made barriers that physically limit the migration of aquatic species and modify freshwater habitats (Belletti et al. 2020). These habitats shape the biodiversity, biomass, and bioproductivity of rivers, facilitating the creation of ecological processes that strongly regulate river ecosystems. The habitat mosaics are formed by the interaction of catchment topography, rainfall and runoff patterns, valley slope and confinement, sediment transport, channel boundary conditions and vegetation (Parasiewicz et al. 2023). Fish assemblages are sensitive indicators of habitat quality in rivers because they respond significantly to almost all types of anthropogenic disturbances to river flow regimes (Acreman et al. 2014). Parasiewicz et al. (2023) identified fish macrohabitat types across Europe using environmental settings derived from the Catchment Characterization Model (CCM2). However, the abiotic parameters extracted from CCM2 are limited in resolution and accuracy compared to field-measured data.

In contrast, the present study identifies 17 fish community macrohabitat types across Europe using high-quality, field-measured catchment environmental settings (i.e., abiotic data) and observed fish community structures (i.e., biotic data). We applied a two-step clustering approach to the abiotic and biotic datasets collected from 992 river sites across Europe to develop a fish macrohabitat classification. Finally, we analyzed how these macrohabitat types relate to broad-scale environmental attributes to define a riverine macrohabitat typology for the entire European river network. This work sets a foundation for a macrohabitat model investigating impact of Cormorant predation on fish communities across the continent.

2. Method

2.1. Data

The data used in the study is the European intercalibrated database measured between 2006 and 2011 through the European commission Joint Research Center to support the implementation of Water Framework Directive. From this database abiotic parameters from 992 sites spread across 18 European countries were extracted. The abiotic parameters included the Strahler order, catchment size, slope, geology and altitude. The environmental zones were extracted from the Environmental Stratification of Europe (EnSv, v.8) datasets. The biotic parameters consisted of Habitat Use Guilds formed by calculating the relative abundance of fish species from the database.

2.2. Clustering

The data was clustered in two steps. The first step involved non-hierarchical clustering of the abiotic parameters. The data was clustered into clusters with similar habitat characteristics. The data was standardized using the grower distance matrix and the number of clusters were determined using scree and silhouette plots. A partitioning around medoids clustering model was applied to the data. The clusters obtained were added as an additional variable to the biotic data to produce a mixed datasets of guilds with physical clusters. This second dataset was then clustered in the similar manner as the abiotic data however the dataset was standardized using the Manhattan distance. The clustering of the mixed dataset resulted in 17 fish macrohabitat classes (FCMacHT). Finally, the FCMacHT class was added to the physical attributes for Classification and Regression Trees (CART) analysis. The decision tree generated by CART analysis was applied to rivers of Europe to determine their FCMacHT class.

3. Result

The guild compositions and broad environmental characteristics, such as river slope, stream order, catchment size, altitude, catchment geology, and climatic zones, were grouped into 17 clusters, see Fig.1.

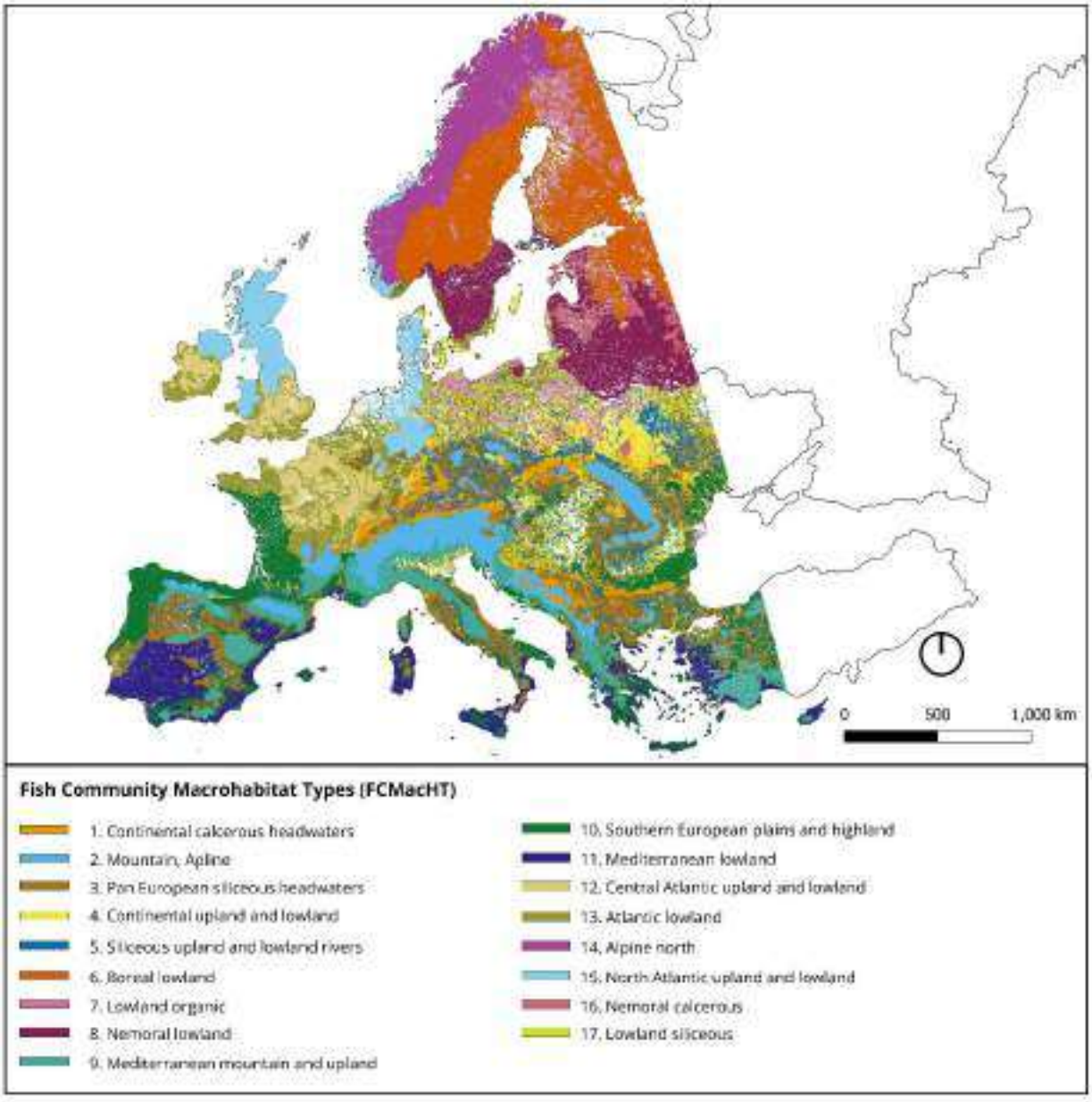

Fig. 1. Identified 17 clusters of the Fish Community Macrohabitat Types in European rivers.

Discussion

This study aims to develop an improved fish macrohabitat classification for Europe, by using high quality filed measured data. Our results demonstrate that incorporating field measured abiotic data does not fundamentally alter the classification elaborated in previous study, however, further validation is required. It lays the groundwork for many rivers management tasks as it provides a general reference for assessment of habitat and fish community alteration. In our case it will also allow to investigate how predator pressure (e.g., cormorants) affects fish communities in different geographical locations.

Acknowledgement

The further project activities are made possible thanks to the project funding from the European Union's Horizon Europe research and innovation programme under grant agreement nr. 101134976 for the project Protecting threatened river fish against predation (ProtectFish). Funding was also provided from Polish Ministry of Agriculture and Rural Development for the Direct Subsidy for 2025 and the National Inland Fisheries Research Institute (statutory work Z-018).

References

Acreman MC, Overton IC, et al. (2014) The changing role of ecohydrological science in guiding environmental flows, Hydrological Sciences Journal, 59:3-4, 433-450

Belletti B, Garcia de Leaniz C, et al. (2020) More than one million barriers fragment Europe's rivers. Nature 588, 436–441

Parasiewicz P, Belka K, et al. (2023) Over 200,000 kilometers of free-flowing river habitat in Europe is altered due to impoundments. Nature Communications 14, 6289

JRC (2011) WFD Intercalibration Report. Phase 2: Milestone report.

Wantzen KM, Tharme RE, Pypaert P (2023) Life as a Dance to the Rhythm of the Waters: An Analysis of Current Trends and Suggestions to Restore River Culture. In: Wantzen, K.M. (ed.): River Culture – Life as a Dance to the Rhythm of the Waters. Pp. 1–22. UNESCO Publishing, Paris.

Book of Abstracts of the *16th International Symposium on Ecohydraulics*
Challenges and solutions in the time of global changes
August 16–20, 2026, Lausanne, Switzerland
ISSN: 2790-2420 | ISBN: 978-90-837233-9-6 | doi:[10.64697/iahr.proc.ise2026.abs]
© 2026 IAHR. CC BY-NC-ND 4.0

INTEGRATED FUNCTIONAL HABITAT AND FISH POPULATION DYNAMICS MODELLING FOR IMPROVED RIVER RESTORATION

David FARÒ[1], Christian WOLTER[1]

[1] Leibniz Institute of Freshwater Ecology and Inland Fisheries (IGB), Berlin, Germany
email: david.faro@igb-berlin.com
email: christian.wolter@igb-berlin.com

ABSTRACT

In-stream habitat enhancement is widely used to improve ecological conditions, often targeting key fish life stages like spawning and juvenile development. Despite widely applied revitalization, there is nearly no quantitative target setting or benchmarking, nor standardised approaches to predict measure effects on recruitment and population dynamics.

We applied a spatially-explicit population dynamics model that integrates habitat availability, quality and functional connectivity to assess the recruitment potential for four rheophilic and lithophilic fish species (grayling, nase, barbel, and chub) in a section of the Inn River (Germany). The impacts of two restoration measures (a bypass channel and an island side-channel system) were evaluated. Model results suggest that the improved habitat conditions increased fish population densities on average by 14.9 ind./ha. However, limited accessibility of suitable nurseries was identified as key recruitment bottleneck. We also examined an alternative spatial configuration of implemented measures, which increased nursery habitat availability from 33.2% to 95.3%. Enhanced functional connectivity substantially increased recruitment potential, although species responses varied due to differing sensitivities to spawning-to-nursery habitat ratios. This study demonstrates the applicability of the integrated modelling approach and underscores the need to consider habitat ratios and connectivity to effectively enhance fish recruitment.

Keywords: habitat suitability; functional connectivity; larval drift; population dynamics modelling

1. Introduction

Many fish species, especially rheophilic (i.e. those preferring fast-flowing environments) and lithophilic ones (i.e. requiring coarse substrates to spawn), depend on a range of habitat types throughout their life. Because these habitat types differ markedly in their hydraulic conditions and occur in separate parts of the river, individuals must be able to reach the appropriate habitat at the right life stage. This requirement is particularly critical during early ontogeny, since larvae and age-0 juveniles have constrained swimming abilities due to their small body sizes. For example, larvae that hatch within gravel beds must be able to drift downstream to reach suitable nursery areas (Lechner et al., 2016).

A variety of tools exist to assist with planning and evaluating river restoration, and particularly in-stream habitat suitability models are now widely applied. However, these models typically do not capture the mechanistic links between habitat quantity, its spatial and temporal connectivity, and the ecological responses that may result, such as increases in the abundance of target fish species. To address this gap, spatially-explicit fish population models can be employed (Farò et al., 2021).

In this study, we combine functional habitat modelling between spawning and nursery areas with an age-structured, spatially explicit population dynamics model. This framework is used to assess how two river restoration scenarios (one already implemented and a hypothetical one) influence the recruitment potential of four potamodromous, rheophilic, and lithophilic fish species in a hydropower-impacted reach of the lower Inn River (SE Germany).

2. Materials and Methods

1.1. Study area and target fish species

The study area covers the impounded section of the Inn River located between the Ering-Frauenstein and the Egglfing-Obernberg hydro-power plants (HPPs) in SE Germany. Between 2017 and 2019, two restoration measures were implemented: construction of a bypass channel around the upstream Ering-Frauenstein HPP and creation of an island side-channel system downstream of it (Fig. 1).

The analysis focuses on four fish species: grayling (*Thymallus thymallus*), nase (*Chondrostoma nasus*), barbel (*Barbus barbus*), and chub (*Squalius cephalus*). These species were chosen based on reference community composition for the modelled river reach.



Fig. 1. Study reach between hydro-power plants Ering-Frauenstein and Egglfing-Obernberg, including two rehabilitation measures: an island side-channel system in the main river channel, downstream of the HPP Ering-Frauenstein; and a bypass channel around it.

1.2. Integrated functional habitat and population dynamics modelling

Potential recruitment is assessed using an integrated functional habitat and population dynamics modelling approach (Fig. 2).

Habitat availability was evaluated by modelling habitat suitability for both spawning areas and larval nursery zones, using literature-derived criteria for water depth, flow velocity, and substrate composition (Farò and Wolter, 2024a).

To examine usability of habitats, functional connectivity between spawning grounds and nursery habitats was analysed with a larval drift model (Farò and Wolter, 2024a). The drift simulation, based on a Lagrangian particle tracking approach (McDonald and Nelson, 2020), accounted for both passive and active drifting behaviour.

A spatially explicit, age-structured population model was applied, representing five major life stages: eggs, post-emergence larvae, 0+ juveniles, older juveniles (≥1+), and adults (Farò and Wolter, 2024b). Habitat-related mortality was included for the spawning phase and the early post-emergence period, since these are viewed as key bottlenecks in recruitment. Model parameter values were taken from the literature, with remaining gaps filled through expert judgment.

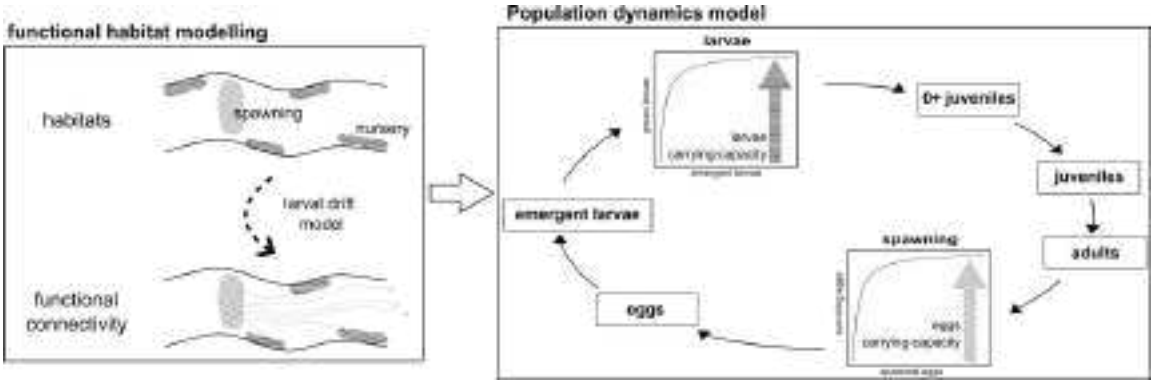

Fig. 2. Integrated functional habitats and population dynamics modelling approach. Modified from Farò and Wolter (2025).

1.3. Restoration scenario and bottleneck analysis

Two restoration scenarios were evaluated (Farò and Wolter, 2024a). One represents the present restored condition (scenario A), and the other reflects an alternative restoration layout (scenario B). In scenario A, spawning habitats are located in the newly built bypass channel and within the restored island area, both located on the left-hand side of the reach. In scenario B, an alternative bypass channel is positioned on the right side of the Inn, opposite the existing one.

To help identify potential habitat bottlenecks, fish densities were calculated across a broad range of spawning and nursery habitat sizes, spanning from 0.01% to 5% of the total channel wetted area.

3. Results

Habitat availability and habitat usability differed between the two modelled scenarios. Although the total amount of habitat available is the same in both cases, the share of nursery habitat that is actually usable (i.e. functionally connected to spawning areas) increases from 33.2% in scenario A to 95.3% in scenario B.

Overall recruitment potential is lower in scenario A, which shows a mean density of 14.9 ind./ha across all species. Scenario B reaches a higher mean density of 25.8 ind./ha. Species-level patterns however vary, since each species is affected differently by developmental bottlenecks linked to limited usable habitat (Fig. 3).

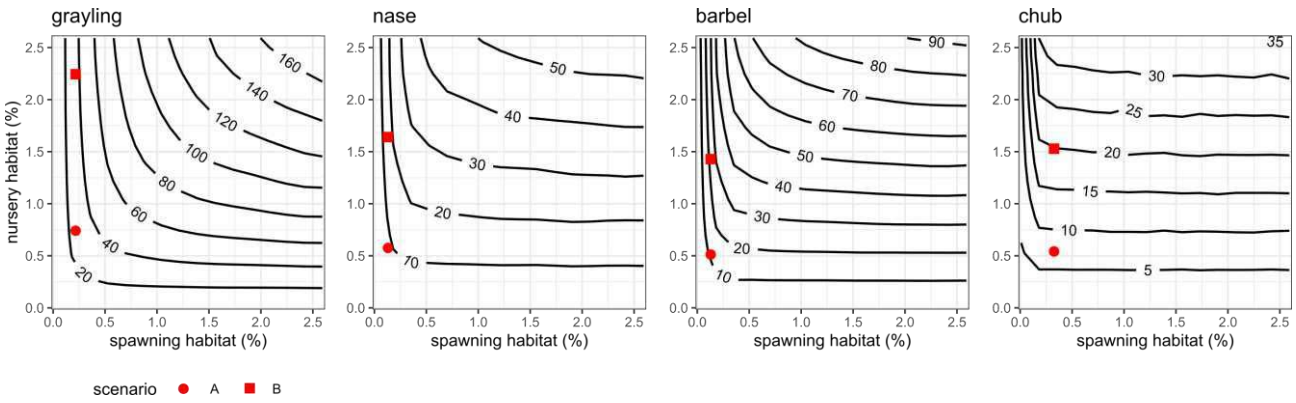

Fig. 3. Comparison of grayling, nase, barbel and chub median densities (in ind./ha) at equilibrium depending on potential spawning and nursery habitat availabilities. The red shapes represent current usable spawning and nursery habitats for scenarios A and B.

4. Discussion

The study indicates that the implemented restoration actions were effective compared to pre-restoration conditions. Newly created spawning areas and improved nursery access supplied key habitats (previously missing in the reach) that support recruitment in the impounded reach, likely strengthening population structure and increasing abundances.

Testing an alternative design that improved spawning-to-nursery functional connectivity showed that limited usability of nurseries was a major habitat bottleneck. Greater connectivity in this scenario (B) resulted in higher

at-equilibrium abundances. The habitat bottleneck assessment also showed that habitat ratios, and not only total habitat amounts, drive species-specific recruitment outcomes.

These insights offer guidance for further restoration. All species would benefit from additional nursery habitat, but grayling, nase, and barbel would also require more spawning areas. For chub, limited functionally-connected nurseries were the only constraint.

Overall, the results stress the need to consider both habitat quantity and quality (i.e. availability), but also the ratio of functionally connected habitats (i.e. usability). Ignoring connectivity would have severely overestimated nursery usability and resulting recruitment potential. Applying a habitat bottleneck analysis during planning or evaluation can help target species-specific restoration measures to increase population status.

Future research could account for short- and long-term habitat variability, expand spatial scales to include fish migration/dispersal and barrier-induced effects on such processes, and reduce modelling uncertainties through the development of the model into an integrated population model calibrated with empirical data (Schaub and Abadi, 2011).

Acknowledgements

This study was funded by the VERBUND Innkraftwerke GmbH.

References

Farò, D., & Wolter, C. (2024a). Integrating habitat suitability and larval drift modelling for spawning-to-nursery functional habitat connectivity analysis in rivers. Water Resources Research, 60(9), e2023WR036827. https://doi.org/10.1029/2023WR036827

Farò, D., & Wolter, C. (2024b). Linking functional habitat and fish population dynamics modelling to improve river rehabilitation planning and assessment. Journal of Environmental Management, 370, 122331. https://doi.org/10.1016/j.jenvman.2024.122331

Farò, D., & Wolter, C. (2025). Fisch-Populationsmodelle zur Abschätzung der Wirkung von Renaturierungsmaßnahmen am Unteren Inn. WasserWirtschaft, 115, 54–59. https://doi.org/10.1007/s35147-025-2555-5

Farò, D., Zolezzi, G., & Wolter, C. (2021). How much habitat does a river need? A spatially-explicit population dynamics model to assess ratios of ontogenetical habitat needs. Journal of Environmental Management, 286, 112100. https://doi.org/10.1016/j.jenvman.2021.112100

Kamler, E., & Keckeis, H. (2000). Reproduction and early life history of Chondrostoma nasus: Implications for recruitment (A review). Polskie Archiwum Hydrobiologii, 47(1), 73–85.

Lechner, A., Keckeis, H., & Humphries, P. (2016). Patterns and processes in the drift of early developmental stages of fish in rivers: a review. Reviews in Fish Biology and Fisheries, 26(3), 471–489. https://doi.org/10.1007/S11160-016-9437-Y

McDonald, R. R., & Nelson, J. M. (2020). A Lagrangian particle-tracking approach to modelling larval drift in rivers. Journal of Ecohydraulics, 6(1), 17–35. https://doi.org/10.1080/24705357.2019.1709102

Schaub, M., & Abadi, F. (2011). Integrated population models: A novel analysis framework for deeper insights into population dynamics. Journal of Ornithology, 152, S227–S237. https://doi.org/10.1007/s10336-010-0632-7

Book of Abstracts of the *16th International Symposium on Ecohydraulics*
Challenges and solutions in the time of global changes
August 16–20, 2026, Lausanne, Switzerland
ISSN: 2790-2420 | ISBN: 978-90-837233-9-6 | doi:[10.64697/iahr.proc.ise2026.abs]
© 2026 IAHR. CC BY-NC-ND 4.0

APPLICATION OF INSTREAM FLOW INCREMENTAL METHODOLOGY TO CHECK THE IMPACT OF FLOOD PROTECT MEASURES ON FISH MICROHABITATS

Meng-Chi HUNG[1], Chuan-Yi HUANG[2], and Chang-An HSU[3]

[1] Taiwan Biodiversity Research Institute, Taiwan
email: alberthung@tbri.gov.tw
[2] Sinotech Engineering Consultant, Inc., Taiwan
email: cyhuang@sinotech.org.tw
[3] Sinotech Engineering Consultant, Inc., Taiwan (retired)
email: cahsu0692@gmail.com

ABSTRACT

This study attempts to employ instream flow incremental methodology (IFIM) for evaluating the impact of flood protect measures on fish microhabitats instead of determining the instream flow needs (IFN). The downstream reach of Fengshan River Bridge in Northwest Taiwan was used as a case study. The swimming-type fish *Acrossocheilus paradoxus* and benthos fish *Rhinogobius candidianus* were selected as indicator species. A two-dimensional hydraulic model (SEC-HY21) with fine-resolution grids (10 m²) is used to simulate flow fields. Following instream flow incremental methodology (IFIM) procedures, index species habitat suitability curves for velocity and depth are incorporated into flow field simulations to derive spatial weighted usable area (WUA) distributions. The flow fields were simulated with flow discharge starting from zero and increasing step by step until the WUA reaching its maximum value. Comparing the WUA of scenarios with or without spurdikes installed to analyze their effects on fish habitat quality. Additionally, the swimming fish *A. paradoxus* is used as index species to assess the protection effect of refuge ponds and floodplain excavation during floods by analyzing differences in velocity suitability distributions within a river contraction.

Keywords: instream flow incremental methodology (IFIM); instream flow needs (IFN); Weighted Usable Area (WUA); spurdike; refuge pond; floodplain excavation.

1. Introduction

The habitat of riverine fish is influenced by microhabitat characteristics shaped by changes in flow conditions, including water temperature, velocity, depth, and substrate. These factors directly or indirectly affect fish community composition and population dynamics, and may even lead to invasions by non-native species. (Poff et al., 1997)(Bunn et al., 2002) The Instream Flow Incremental Methodology (IFIM) evaluates the quality of physical habitat by calculating the Weighted Usable Area (WUA) across a series of flow rates and is used to determine the instream flow needs (IFN) required to support riverine ecological functions. (Milhous et. al., 1989; Maddock, 1999)

However, several issues persist when using habitat models to estimate IFN. These include uncertainties in habitat suitability curves, the inability to capture hydrologic signals that trigger different life-history stages, and the difficulty of representing the needs of entire fish assemblages using suitability curves developed for single species. In Taiwan, the greatest challenge lies in the extreme contrast between wet and dry seasons. IFN values derived from IFIM often exceed the median of the flow duration curve, making them difficult to apply in practical ecological flow management. As a result, despite significant investment of manpower, funding, and time in establishing velocity and depth suitability curves for many species, these data often remain unused.

Since 2005, Taiwan has invested over US$ 7 billion in flood mitigation and aquatic environment enhancement. Large-scale river engineering projects have raised public concerns about degradation and potential irrecoverability of aquatic and riparian ecosystems. The International Union for Conservation of Nature (IUCN) has advocated for Nature-based Solutions (NbS), which aim to simultaneously improve biodiversity, climate resilience, and human well-being. NbS represent a strategic shift toward holistic thinking; however, existing large numbers of single-purpose hydraulic structures were originally designed with flood control as the primary consideration. Whether these designs can adapt to natural geomorphic processes—or whether they inadvertently create conditions unfavorable for aquatic habitat or species migration—remains an open question.

This study applies IFIM to evaluate the impacts of flood protection measures on fish microhabitats rather than to determine the IFN. The downstream reach of Fengshan River Bridge in Northwest Taiwan was selected as a case study. A swimming-type fish, *Acrossocheilus paradoxus* and a benthic fish *Rhinogobius candidianus*, were chosen as indicator species. A two-dimensional hydraulic model, SEC-HY21, with fine-resolution grids (10 m²) was used to simulate flow fields. Following IFIM procedures, habitat suitability curves for velocity and depth for the indicator species were incorporated into the hydraulic simulations to derive the spatial distribution of WUA. Flow fields were simulated under gradually increasing discharge conditions, starting from zero and increasing stepwise until WUA reaching its maximum value. The WUA results from scenarios with and without spurdike installations were than compared to analyze their effects on fish habitat quality. In addition, the swimming fish, *A. paradoxus* was used as the indicator species to evaluate the protective effects of refuge ponds and floodplain excavation during flood conditions by analyzing differences in velocity suitability distributions within a river contraction.

2. Materials and Methods

2.1. Study site

The Fengshan River is located in northwestern Taiwan within Hsinchu County and Taoyuan City. The river originates at an elevation of 1,320 m and joins the Touqian River before flowing into the Taiwan Strait. The watershed covers an area of 250.1 km², with channel slopes ranging from 1/360 to 1/155. In the river reach around Highway T-01, the main thalweg swings toward the right bank, and the channel then turns so that the flow core runs adjacent to the left-bank levee. Immediately downstream of Highway T-01, the flow directly impinges on the left bank, raising concerns about potential scouring of levee, as shown in the upper-right panel of Figure 1. To protect the levee, the River Bureau constructed spurdikes to reduce flow velocity and redirect the current. As shown in the lower-right panel of Figure 1, sediment deposition has already formed along the concave left bank following the installation of the spurdikes.



Fig. 1. The Fengshan River reach around Highway T-01 located in northwestern Taiwan.

2.2. Two-dimensional hydraulic model

SEC-HY21 (Hsu, 2010) is a two-dimensional general-purpose model developed by Sinotech Engineering Consultants, Inc. It can be applied to a wide range of surface-water problems, including two-dimensional hydraulics, pollutant transport, sediment transport and mobile-bed processes, landslide-generated waves, tsunamis, debris flows, and turbidity currents.

2.3. Design of improvement scenarios

Spurdikes are frequently used to protect levees along river contraction or outer bank at meandering. Several studies also show that spurdikes can improve fish habitat suitability at low flow conditions. (Shih et al., 2008;

Chang et al., 2013) In this study, a total of 15 spurdikes were planned along the left-bank toe downstream of the Fengshan River Bridge. The design of the spurdikes is with a spacing of 30 m, length of 15 m, height of 1.5 m, head height of 1 m, and root width of 5 m. The study includes two components: high-flow fish refuge assessment and low-flow microhabitat quality evaluation. For microhabitat evaluation, the IFIM framework was adopted, starting from a discharge of 1 cms and increasing the flow in increments of 1 cms until the maximum WUA was reached. Based on the hydraulic characteristics of the constricted channel, four improvement scenarios were developed to enhance habitat quality, described as follows: (1) Original channel condition; (2) Installation of spurdikes; (3) Installation of spurdikes with an ecological refuge pond; (4) Installation of spurdikes with floodplain excavation. The design of improvement scenarios is shown in Figure 2.

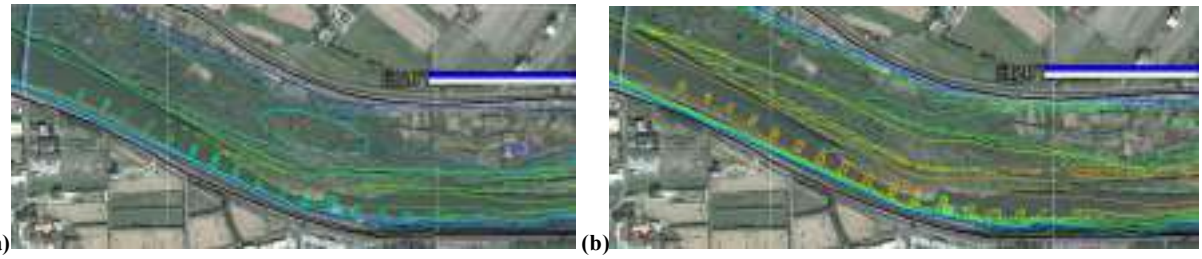

Fig. 2. Schematic of the improvement scenarios: (a) Installation of spurdikes with an ecological refuge pond; (b) Installation of spurdikes with floodplain excavation.

3. Results

3.1. High-flow fish refuge assessment

Differences among the scenarios in terms of fish refuge conditions can be identified, combining the velocity suitability distribution for *Acrossocheilus paradoxus* was plotted for comparison, as shown in Figure 3. Comparing Figures 3(a) and 3(b), it can be observed that although the spudikes reduce the flow velocity along the left bank and create refuge areas suitable for *A. paradoxus*, the velocity suitability on the right-bank floodplain decreases. Figures 3(c) and 3(d) show the velocity suitability comparisons under the conditions with spurdikes, incorporating either a refuge detention pond or floodplain excavation on the right bank.

Relative to Figures 3(a) and 3(b), Figure 3(c) shows that although adding a refuge detention pond on the right-bank floodplain does not reduce the velocity in the constricted bend section, the lower velocities within the pond itself create areas with higher suitability. In Figure 3(d), floodplain excavation on the right bank effectively reduces the velocity around the spurdikes. The widening of the deep channel lowers the average channel velocity and mitigates the local acceleration induced by the spurdikes. Although excavation reduces the overall floodplain area, the habitat quality of the floodplain improves substantially. The velocity suitability index (VSI) across the entire floodplain in the bend section exceeds 0.7, and Scenario (d)—installation of spurdikes combined with floodplain excavation—yields the largest area with VSI greater than 0.8

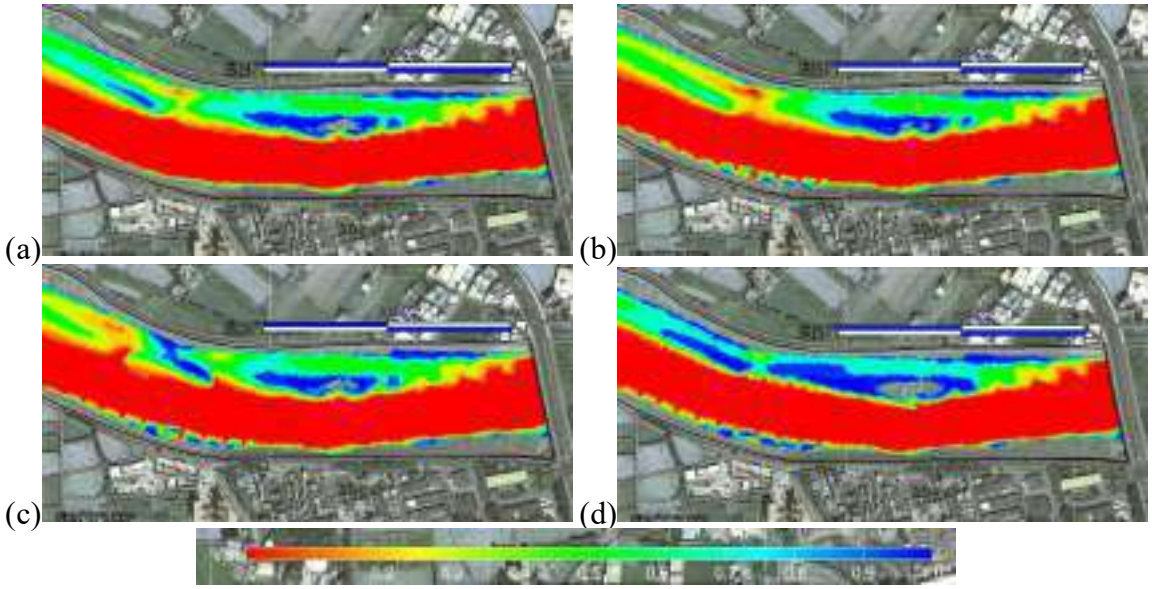

Fig. 3. Spatial distribution of the velocity suitability under improvement scenarios: (a)Original channel condition; (b)Installation of spurdikes; (c)Installation of spurdikes with an ecological refuge pond; (d)Installation of spurdikes with floodplain excavation.

3.2. Low-flow microhabitat quality evaluation

The evaluation of the impacts of spurdikes installation on riverine microhabitats focuses primarily on non-flood seasons, particularly for estimating ecological or environmental flows during low-flow periods. In this section, the IFIM framework is applied to calculate the microhabitat area of *R. candidianus* under low-flow conditions in the reach downstream of the Fengshan River Bridge, and to analyze how the quantity and quality of microhabitats change with increasing discharge.

Figure 4(a) shows the variation in wetted area with discharge. When the discharge is below 5 cms, the presence of spurdikes results in a larger wetted area, likely due to the spurdikes impounding water and creating pool-like zones. However, the wetted area with spurdikes above 5 cms becomes smaller because spurdikes are intended to protect the levee toe during high flows and thus reduce the wetted area by more than 1,000 m².

Figure 4(b) presents the Weighted Usable Area (WUA) for *R. candidianus* in this reach. Although the wetted area is smaller with spurdikes installed when discharge is below 6 cms, the WUA is more than 1,000 m² greater than in the no-spurdike condition. When discharge exceeds 7 cms, the increase in WUA with flow becomes limited under the spurdike condition, whereas without spurdikes, WUA continues to increase until reaching its maximum at about 16 cms.

These results indicate that although the no-spurdike scenario provides a higher overall WUA, the spurdike scenario offers higher WUA when discharge is below 7 cms, meaning habitat quality is better during the dry season when spurdikes are present. According to flow duration curve, the median flows (Q_{50}) of the Fengshan River in spring, summer, autumn, and winter are only 4.28 cms, 5.28 cms, 1.66 cms, and 1.74 cms, respectively. Therefore, in a watershed with pronounced wet–dry season variability, spurdike installation can provide adequate habitat quality under relatively low ecological base flows.

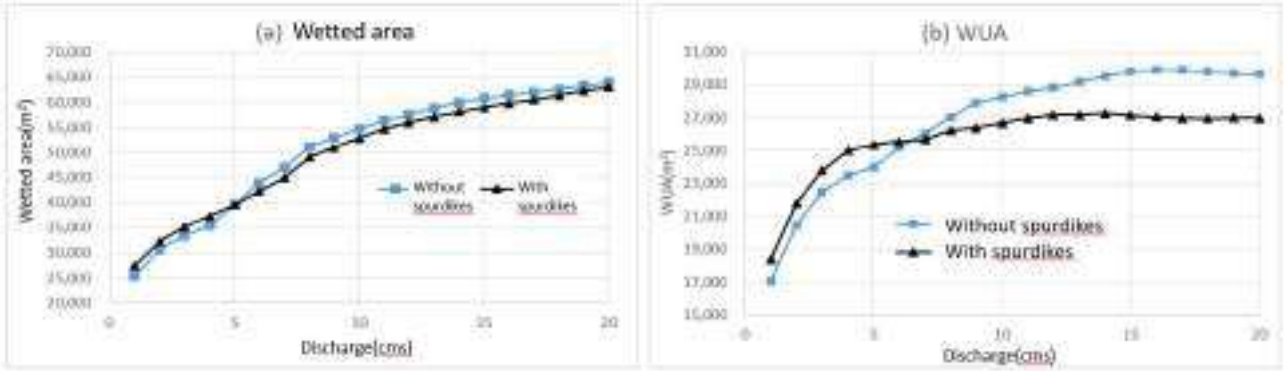

Fig. 4. Comparison of wetted area and weighted usable area of improvement scenarios with and without spurdikes.

4. Summary

The results indicate that spurdikes can improve habitat quality during the dry season and maintain a certain level with lower flow discharges. In contrast, installations that combine spurdikes with a refuge detention pond under extreme flood conditions can reduce flow velocity along the left bank and create refuge spaces suitable for *A. Paradoxus*, compared with installations that include only spurdikes. The VSI increases due to the lower velocities created by the pond's topography; however, habitat quality on the floodplain remains poor for both benthic species and swimming species.

References

Bunn SE, Arthington AH (2002) Basic Principles and Ecological Consequences of Altered Flow Regimes for Aquatic Biodiversity. Environmental Management, 30(4), 492–507.
Chang YL, Hsieh TY, Chen CH, Yang JC (2013). Two-Dimensional Numerical Investigation for Short- and Long-Term Effects of Spur Dikes on Weighted Usable Area of *Rhinogobius candidianus* (Goby), Journal of Hydraulic Engineering, 139, 1297–1303.
Hsu CA (2010). Development of a Generalized Two-Dimensional Hydraulic Model SEC-HY21 and its Application in Hydraulic Engineering, Journal of Civil and Hydraulic Engineering, 37(6), 27–38. (in Traditional Chinese)
Maddock I. (1999) The Importance of Physical Habitat Assessment for Evaluating River Health, Freshwater Biology, 41(2), 373–391.
Milhous RT, Updike M, Schneider D (1989) User's Guide to the Physical Habitat Simulation (PHABSIM)-Version II, U.S. Fish and Wildlife Service Biological Report.
Poff NL, Alan JD, Bain MD, Jarr JR, Prestegaard KL, Richter BD, Sparks RE, Stromberg JC (1997) The Natural Flow Regime – A Paradigm for River Conservation and Restoration. BioScience, 47(11), 769–784.
Shih SS, Lee HY, ChenCC (2008) Model-Based Evaluations of Spur Dikes for Fish Habitat Improvement: A Case Study of Endemic Species *Varicorhinus barbatulus* (Cyprinidae) and *Hemimyzon formosanun* (Homalopteridae) in Lanyang River, Taiwan, Ecological Engineering, 34, 127–136.

Book of Abstracts of the *16th International Symposium on Ecohydraulics*
Challenges and solutions in the time of global changes
August 16–20, 2026, Lausanne, Switzerland
ISSN: 2790-2420 | ISBN: 978-90-837233-9-6 | doi:[10.64697/iahr.proc.ise2026.abs]
© 2026 IAHR. CC BY-NC-ND 4.0

EFFECTS OF RELATIVE FLOODPLAIN WIDTH ON HYDRAULIC VARIABILITY AND AQUATIC HABITAT

Rohan BENJANKAR[1], Daniele TONINA[2]

[1] *Department of Civil Engineering, Southern Illinois University Edwardsville, Edwardsville, 62026, Illinois, USA*

Email: rbenjan@siue.edu

[2] *Center for Ecohydraulics Research, University of Idaho, Boise, 83702, Idaho, USA*

Email: dtonina@uidaho.edu

ABSTRACT

We developed two-dimensional (2D) hydrodynamic and aquatic habitat models to evaluate the impacts of channel confinement on hydraulic variability and fish habitat across four different discharges. Our results show that relative floodplain width does not influence aquatic habitat between moderately confined and confined reaches for flows below bankfull. For overbank flows, hydraulic variability and habitat availability increased with relative floodplain width. This study provides quantitative relations among floodplain width, hydraulic variability and habitat that inform river restoration design.

Keywords: Hydraulic variability; floodplain width; channel confinement; ecohydraulics; river restoration

1. Introduction

Aquatic habitats vary spatially and temporally based on channel-floodplain morphology and flow hydraulics (Bellmore and Baxter 2014; Wohl 2016). Diverse channel and floodplain morphology supports a better riverine aquatic habitat and ecosystem because it yields higher hydraulic variability for the given discharge (Bovee 1982; Gostner et al. 2013). In managed river systems, hydraulic variability is generally the primary limiting factor for aquatic and riparian habitat quality (Anim et al. 2018; Ward et al. 1999; Naiman et al. 2005).

Aquatic species respond directly to flow hydraulic conditions and their variability such as velocity (V), depth (D), and shear stress (SS) and the hydromorphological index of diversity (HMID) but it is unclear if a single variable can explain the habitat conditions (Wohl et al. 2005; Nilsson et al. 2003; Gostner et al. 2013). In general unconfined streams support a diverse riverine habitats relative to confined streams (Stanford and Ward 1993; Baxter and Hauer 2000; Isaak and Thurow 2006), but quantitative information is lacking on how floodplain width influences hydraulic variability and habitats for different discharge conditions. This research focuses on analyzing the role of floodplain width on hydraulic variability (e.g., HMID), aquatic habitats i.e., suitability index (SI) and weighted usable area (WUA) for a range of discharge conditions for a managed, semi-confined gravel-bed river.

2. Methodology

We simulated water depths and velocity using a combination of one-dimensional (1D) and two-dimensional (2D) hydraulic models in the South Fork Boise River (SFBR). The SFBR is located between Anderson Ranch and Arrowrock reservoirs in Southern Idaho (USA). The study reach is 22 km-long, which has variable channel and floodplain widths (30 m to 250 m) (Fig. 1) (Tranmer et al. 2023; Benjankar et al. 2019; Benjankar et al. 2025). The river has an average channel bankfull width of 41 m (68 m^3/s). The management of Anderson Ranch Dam for irrigation, flood control and energy production alters the

discharges downstream. Anderson Ranch Dam releases a minimum baseflow of 8.5 m^3/s from October to March, between 17 and 51 m^3/s during the irrigation period (IWRB, 1990). The peak discharge for the period 1946 to 2013 was 227 m^3/s.

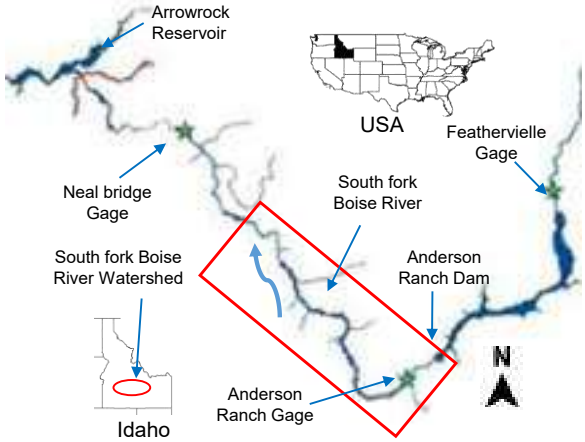

Fig. 1. Study area.

The calibrated 2D hydraulic model was used to simulate water depth and velocity for discharges of 8.5, 17, 28, and 143 m^3/s, which represent baseflow, low-flow, high-flow, and overbank-flow, respectively (Benjankar et al. 2019; Benjankar et al. 2018; Benjankar et al. 2025). The simulated hydraulic variables, depth (D) and velocity (V), and bull trout habitat preference criteria were used as inputs for the aquatic habitat model to simulate juvenile bull trout rearing habitat (SI and WUA). Furthermore, HMID is calculated based on coefficients of variation of D and V (Gostner et al. 2013). To evaluate the role of floodplain width in controlling hydraulic variability as well as aquatic habitat quality, we divided the study reach into 22 reaches of 1 km length. Relative floodplain width (W^*) was defined as: $W^* = W_f/W_b$, where W_f is the average floodplain width in each reach and W_b is the average bankfull channel width over the entire study site.

3. Results and discussion

Overall *HMID, SI and WUA* were all significantly higher in the moderately-confined ($W^* > 2$) reaches than in the confined ($W^* \leq 2$) (Mann-Whitney test, $p < 0.05$) for all discharges as observed in previous studies (e.g., Gostner et al. 2013) (Fig. 2). Median *SI* values were lower in the moderately-confined reaches than in confined reaches during the baseflow and low-flow conditions (MW test, $p < 0.05$). As discharge further increased, *SI* values increased during the high-flow and overbank-flow conditions in the moderately-confined reach than in the confined. Therefore, the hydraulic variability may increase with higher discharge, which may not translate to better habitat in laterally constrained river systems (Anim et al. 2019a; Anim et al. 2019b). This indicates that channel confinement becomes an important factor for habitat quality specifically during high-flow events. Aquatic habitat responded differently from hydraulic variability with respect to change in discharges and W^* because habitat quality is not solely a function of spatial and temporal hydraulic variability but must include specific hydraulic conditions preferred by a target species (e.g., juvenile bull trout). Nevertheless, higher hydraulic variability supports biodiversity and ecosystem function in the river systems (Naiman et al. 2005; Rood et al. 2010; Poff et al. 2011; Ward et al. 1999). The ecohydraulic modeling framework shows that hydraulic variability and riverine habitat depend on both discharge and W^*, which can be used to evaluate river management and restoration scenarios. Our approach can help managers prioritize different river reaches for restoration activities, optimize levee setback distances to improve aquatic habitat quality (Kondolf et al. 2006; Wohl et al. 2024; Pasternack et al. 2004; Phillips et al. 2025).

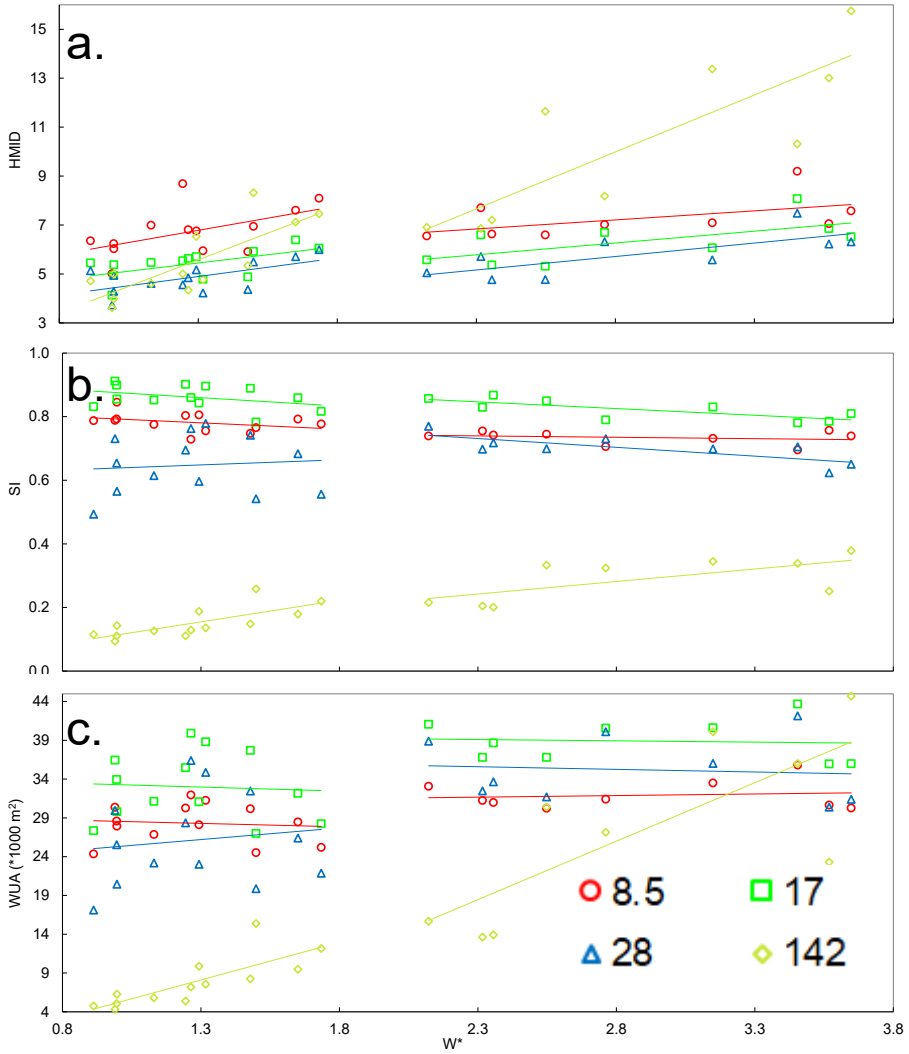

Fig. 2. a. Hydromorphological index of diversity (HMID), b. suitability index (SI), c. weighted usable area (WUA) distribution as a function of relative floodplain width (W*) for different flow scenarios.

4. Conclusion

We found that floodplain width affected the hydraulic variability as well as the availability of aquatic habitats over a range of discharges. For discharges above bankfull, hydraulic variability increased substantially in the moderately-confined reaches, whereas hydraulic variability was limited in the confined reaches. Aquatic habitat quality was generally higher in moderately confined reaches than in confined reaches particularly for overbank-flows. Hydraulic variability increased with relative floodplain width (*W**) in both confined and moderately confined reaches, but it did not directly translate to greater aquatic habitat quality owing to species-specific habitat requirements.

Acknowledgements

This work was financially supported by U.S. Reclamation (Grant# R12APJ1025; R18AP00094). We would like to acknowledge the Danish Hydraulic Institute (DHI) for providing MIKE software.

References

Anim DO, Fletcher TD, Pasternack GB, Vietz GJ, Duncan HP, Burns MJ (2019a) Can catchment-scale urban stormwater management measures benefit the stream hydraulic environment? J Environ Manage 233:1-11

Anim DO, Fletcher TD, Vietz GJ, Burns MJ, Pasternack GB (2019b) How alternative urban stream channel designs influence ecohydraulic conditions. J Environ Manage 247:242–252

Anim DO, Fletcher TD, Vietz GJ, Pasternack GB, Burns MJ (2018) Restoring in-stream habitat in urban catchments: modify flow or the channel? Ecohydrology 12 (1). doi:https://doi.org/10.1002/eco.2050

Baxter CV, Hauer FR (2000) Geomorphology, hyporheic exchange, and selection of spawning habitat by bull trout (Salvelinus confluentus). Can J Fish Aquat Sci 57:1470-1481

Bellmore JR, Baxter CV (2014) Effects of Geomorphic Process Domains on River Ecosystems: a Comparison of Floodplain and Confined Valley Segments. River Res Appl 30:617-630. doi:DOI: 10.1002/rra.2672

Benjankar R, Tonina D, Mckean JA, Sohrabi MM, Chen Q, Vidergar D (2018) Dam operations may improve aquatic habitat and offset negative effects of climate change. J Environ Manage 213:126-134

Benjankar R, Tonina D, McKean JA, Sohrabi MM, Chen Q, Vidergar D (2019) An ecohydraulics virtual watershed: Integrating physical and biological variables to quantify aquatic habitat quality. Ecohydrology 12 (2). doi:https://doi.org/10.1002/eco.2062

Benjankar R, Tonina D, Tranmer AW, Paudel S, Shrestha A (2025) The importance of floodplain width on hydraulic variability and aquatic-riparian habitat in semi-confined, regulated river systems. Ecol Eng 216:1-12. doi:https://doi.org/10.1016/j.ecoleng.2025.107637

Bovee KD (1982) A guide to stream habitat analysis using the instream flow incremental methodology. Instream Flow Information US Fish and Wildlife Service, Fort Collins, Colorado

Gostner W, Alp M, Schleiss AJ, Robinson CT (2013) The hydro-morphological index of diversity: a tool for describing habitat heterogeneity in river engineering projects. Hydrobiologia 712 (1):43-60

Idaho Water Resource Board (IWRB) (1990) Comprehensive State Water Plan: South Fork Boise River Sub-Basin.

Isaak DJ, Thurow RF (2006) Network-scale spatial and temporal variation in Chinook salmon (Oncorhynchus tshawytscha) redd distributions: patterns inferred from spatially continuous replicate surveys. Can J Fish Aquat Sci 63 (2):285-296

Kondolf GM, Boulton AJ, O'Daniel S, Poole GC, Rahel FJ, Stanley EH, Wohl E, Bång A, Carlstrom J, Cristoni C, Huber H, Koljonen S, Louhi P, Nakamura K (2006) Process-Based Ecological River Restoration: Visualizing Three-Dimensional Connectivity and Dynamic Vectors to Recover Lost Linkages. Ecology and Society 11 (2):1-17

Naiman RJ, Decamps H, McClain ME (2005) Riparia: Ecology, conservation and management of streamside communities. Elsevier Academic Press, San Diego, Ca

Nilsson C, Pizzuto JE, Moglen GE, Palmer MA, Stanley EH, Bockstael NE, Thompson LC (2003) Ecological Forecasting and the Urbanization of Stream Ecosystems: Challenges for Economists, Hydrologists, Geomorphologists, and Ecologists. Ecosystems 6:659-674

Pasternack GB, Wang CL, Merz JE (2004) Application of a 2D hydrodynamic model to design of reach-scale spawning gravel replenishment on the Mokelumne river, California. River Res Appl 20 (2):205-225

Phillips SJ, Pasternack GB, Larrieu K (2025) Development and testing of a mechanistic potential niche model of riparian tree seedling recruitment. Ecol Model 51:1-18. doi:https://doi.org/10.1016/j.ecolmodel.2024.110986

Poff B, Koestner KA, Neary DG, Henderson V (2011) Threats to Riparian Ecosystems in Western North America: An Analysis of Existing Literature. Journal of the American Water Resources Association (JAWRA) 47 (6):1-14

Rood SB, Braatne JH, Goate LA (2010) Favorable fragmentation: river reservoirs can impede downstream expansion of riparian weeds. Ecological Applications : 20:1664-1677

Stanford JA, Ward JV (1993) An ecosystem perspective of alluvial rivers: connectivity and the hyporheic corridor. J N Am Benthol Soc 12 (1):48-60

Tranmer AW, Benjankar R, Vidergar D, Tonina D (2023) Identifying failure mechanisms of native riparian forest regeneration in a variable-width floodplain using a spatially-distributed riparian forest recruitment model Ecological Engineering () 106865 187:1-11

Ward JV, Tockner K, Schiemer F (1999) Biodiversity of floodplain river ecosystems: ecotones and connectivity. River Res Appl 15:125-139

Wohl E (2016) Spatial heterogeneity as a component of river geomorphic complexity. Progress in Physical Geography 40 (4): 598–615

Wohl E, Angermeier PL, Bledsoe B, Kondolf GM, MacDonnell L, Merritt DM, Palmer MA, Poff NL, Tarboton D (2005) River restoration. Water Resour Res 41:1–12

Wohl E, Rathburn S, Dunn S, Iskin E, Katz A, Marshall A, Means-Brous M, Scamardo J, Triantafillou S, Uno H (2024) Geomorphic context in process-based river restoration. River Res Appl 40 (3):322-340. doi:https://doi.org/10.1002/rra.4236

Book of Abstracts of the *16th International Symposium on Ecohydraulics*
Challenges and solutions in the time of global changes
August 16–20, 2026, Lausanne, Switzerland
ISSN: 2790-2420 | ISBN: 978-90-837233-9-6 | doi:[10.64697/iahr.proc.ise2026.abs]
© 2026 IAHR. CC BY-NC-ND 4.0

HOW ECOHYDRAULIC PRINCIPLES AND TOOLS CONTRIBUTES TO SUSTAINABLE HYDROPOWER REFURBISHMENT

Atle HARBY[1], Mauro CAROLLI[1], Markus FOERST[1], Corinna KÖPKE[1], Sahra N. SABIL[1,2] and Håkon SUNDT[1]

[1] SINTEF Energy Research, Norway
email: atle.harby@sintef.no

[2] Norwegian University for Science and Technology, Norway

email: mauro.carolli@sintef.no
email: markus.foerst@sintef.no
email: corinna.koepke@sintef.no
email: sahra.n.sabil@ntnu.no
email: hakon.sundt@sintef.no

ABSTRACT

To meet targets for climate change, energy transition towards renewable electricity generation is urgently needed. Most of the remaining feasible renewable energy potential is found in variable resources from wind and solar power. Hydropower with storage capacity is crucial to meet the need for integrating this variable renewable power generation into the grid, and there is a strong need for modernization of the European hydropower fleet to meet this challenge. At the same time, freshwater biodiversity and ecosystem services from rivers and lakes have seen a rapid decline in the last decades, where impacts from hydropower are one of the key drivers. Modernization of hydropower must therefore combine the needs for increased energy services and improving the ecological status of affected rivers and lakes. Modernization includes both increasing flexibility and storage options to meet new demands in the energy system as well as adapting to modern requirements to meet ecological targets as well as societal needs such as flood control and water management. We focus on some guiding principles and methods to achieve more sustainable hydropower generation, giving also some examples of how research and innovation are contributing to real cases of improving both hydropower generation and ecological status using ecohydraulics principles and tools. Examples from new developments in Norway for retrofitting existing hydropower infrastructure with pumped storage and capacity expansions in the EnviPump project will be given as well as examples from the EU-funded innovation and demonstration project ReHydro about sustainable refurbishment of hydropower.

Keywords: Ecohydraulics; hydropower; modernization; ecology; sustainability

1. Introduction

To meet targets for climate change, energy transition towards renewable electricity generation is urgently needed. Most of the remaining feasible renewable energy potential is found in variable resources from wind and solar power. Hydropower with storage capacity is crucial to meet the need for integrating this variable renewable power generation into the grid, and there is a strong need for modernization of the European hydropower fleet to meet this challenge (IHA 2023; Quaranta et al. 2021). At the same time, freshwater biodiversity and ecosystem services from rivers and lakes have seen a rapid decline in the last decades, where impacts from hydropower are one of the key drivers. Modernization of hydropower must therefore combine the needs for increased energy services and improving the ecological status of affected rivers and lakes. Modernization includes both increasing flexibility and storage options to meet new demands in the energy system as well as adapting to modern requirements to meet ecological targets (Arthington et al. 2018) as well as societal needs such as flood control and water management.

2. Research projects

The main objective of the EnviPump project is to analyze the effects on physical and biological conditions from developing pumped storage hydropower in existing reservoirs, as well as to find effective mitigation measures. EnviPump will use hydro-physical modelling to explore impacts on water temperature, ice cover and flow. Further, key ecological impacts on fish populations of hydro-physical variations will be investigated.

The ReHydro project will demonstrate how biodiversity can be improved with new fish-friendly turbines, re-establishment of environmental flows, improving the thermal regime in downstream rivers and monitored using new tools such as eDNA and remote sensing. Smarter use of water resources will also be implemented, so that more services can be delivered to the power markets, while multi-purpose use of the water resources for navigation and recreation can be expanded and the ability to mitigate flooding and draughts are strengthened.

3. Ecohydraulics principles and tools

The main principles of Ecohydraulics are the combination and interaction of hydraulic conditions and effect on the ecosystem, including assessments of hydro-morphological conditions and biological requirements. Ecohydraulic principles must incorporate the effects of man-made infrastructures and river regulation such as alterations in hydrology, disturbance of morphological processes and the introduction of dams, weirs, barriers and other structures. When modernizing and retrofitting hydropower, there is an opportunity to improve also the ecological status of hydropower-affected rivers and lakes (reservoirs). Classic and modern ecohydraulics tools are therefore needed to understand how hydropower has impacted rivers and lakes historically, as well as to model and predict how modernization and retrofitting actually can improve the status.

4. Results

The first steps in designing more eel-friendly turbines show a potential to improve survival of downstream eel migration at the Belver power plant on the Tagus River in Portugal with a potential for application at several power plants in the Rhône River in France.

In the Ain River in France, a pumped storge plant will be built between the lower Coiselet reservoir and the Saut-Mortier reservoir upstream. As the small Saut-Mortier reservoir already has a pumping facility to pump water to the larger upper Vouglans reservoir, it is possible to pump water in two steps from Coiselet to Vouglans reservoirs. The main reason for introducing the new pumped storage plant is to better manage the inflow and reduce the need for hydropeaking. In addition, studies to investigate how releases from the upper Vouglans reservoir can contribute to decrease water temperature in the Ain River in periods with environmentally harmful high temperatures.

Across all scenarios, pump storage clearly modifies the thermal profile (Figure 1). In Dry conditions, pump storage leads to a noticeably cooler surface layer and a more uniform vertical temperature distribution, indicating enhanced mixing. Under Normal conditions, the effect remains significant, with reduced surface temperatures and a shallower thermocline compared to the non-pump scenario. In Wet conditions, the differences are subtler, but pump storage still contributes to slightly lower surface temperatures and diminished stratification. Overall, the figure demonstrates that pump storage operations play a key role in mitigating thermal stratification, especially during drier periods, thereby enhancing the reservoir's thermal resilience and supporting more adaptive water management strategies.

In two rivers that are bypassed by power plants in the Røldal-Suldal hydropower schemes in Norway, environmental flow for the survival of a special population of large brown trout will be provided by a small hydropower plant in the Roalkvamsåna River, and by pumping water from the downstream Suldalsvatn lake to the Brattlandsdalsåna River. If the pump for Brattlandsdalsåna had been installed over the last 20 years, it would have been necessary to run the pump for 62-165 days per year to guarantee at least 1 m^3/s in the lower part of the river (Figure 2).

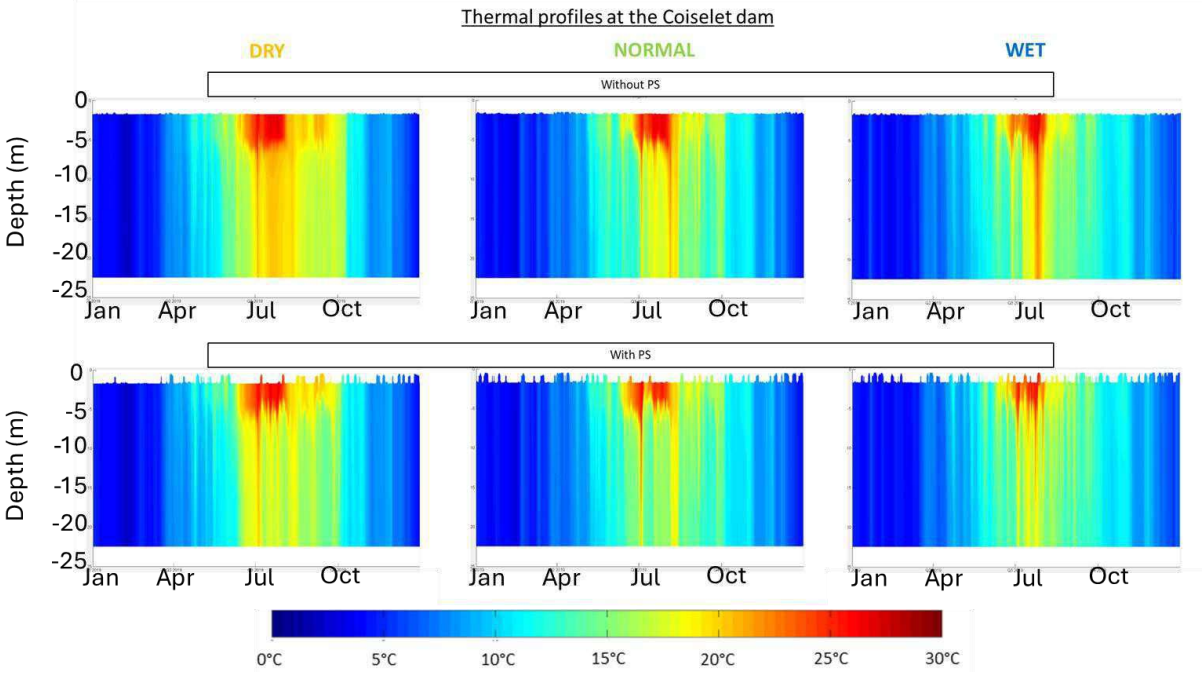

Figure 1. Thermal profiles of the Coiselet dam without pumped storage (above) and with pumped storage (below) in a dry (left), normal (middle) and wet (right) year.

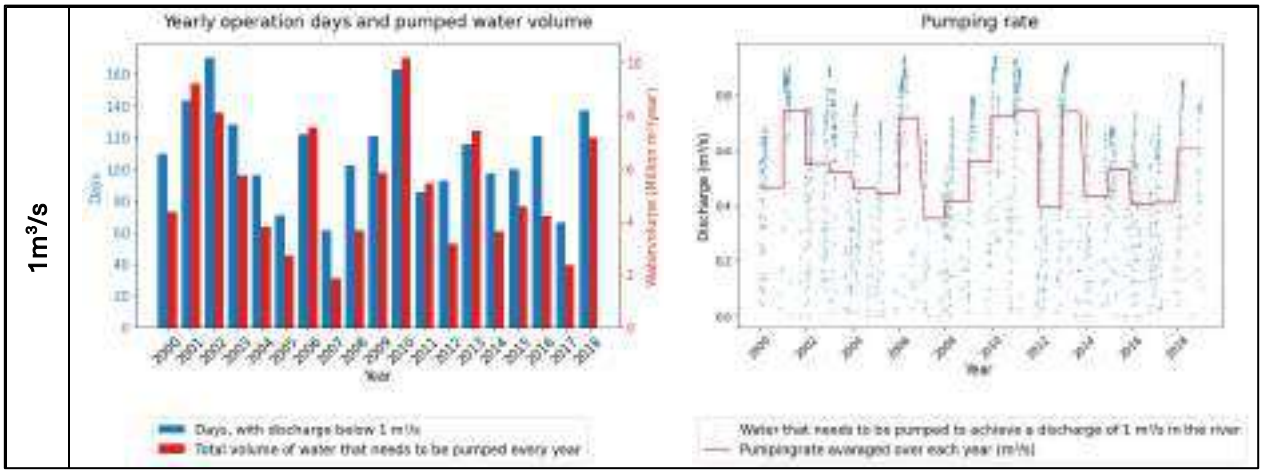

Figure 2. Left: Yearly operation days (in blue bars), yearly pumping volume in Mm³ (red bars). Right: Pumping rate averaged over operation days/year for 1 m³/s

Retrofitting reservoir hydropower to pumped storage hydropower will enhance the flexibility and storage capacity in power systems but introduces also some new environmental challenges (Harby et al. 2013). Pumped storage hydropower systems affect the environment primarily through two mechanisms. First, by transferring water between reservoirs, these systems mix water masses with different physio-chemical properties. Secondly, the operation of these systems results in fluctuations of water levels within the reservoir, which can influence shoreline erosion, habitat availability, and ecosystem structure. These fluctuations can disrupt natural thermal stratification by modifying the thermocline, affecting temperature profiles, and mixing processes. These processes increase turbidity and alter nutrient dynamics, leading to subsequent ecological changes.

We have analyzed expected water level fluctuations in the Holmavatn reservoir in a future power system using Holmavatn reservoir as the upper reservoir in retrofitting conventional hydropower with pumped storage capacity. Reservoir levels were derived from a power system model using future power price estimates combined with inflow and weather data from weather years 1989-2010. Figure 3 shows large variations between years as some years have quite stable and high-water levels for several months in early winter, whereas other years have very low water levels in early winter. Advanced hydro-dynamic modelling tools must be used to assess the impacts on hydro-physical conditions such as water temperature, stratification,

currens and ice cover, in order to understand the biological and ecosystem impacts of changes in hydro-physical conditions.

5. Conclusion

The European hydropower fleet will have to go through a process of modernization to increase flexibility and adapt to future power system needs, as well as meeting sustainability goals and improving both the geomorphological and ecological status of hydropower rivers and reservoirs. To meet this challenge, it is crucial to include ecohydraulic tools and knowledge in the early stages of planning modernization and retrofitting. This presentation will show more results and examples of how ecohydraulics tools have contributed to ensure that modern hydropower can meet both power system and sustainability requirements,

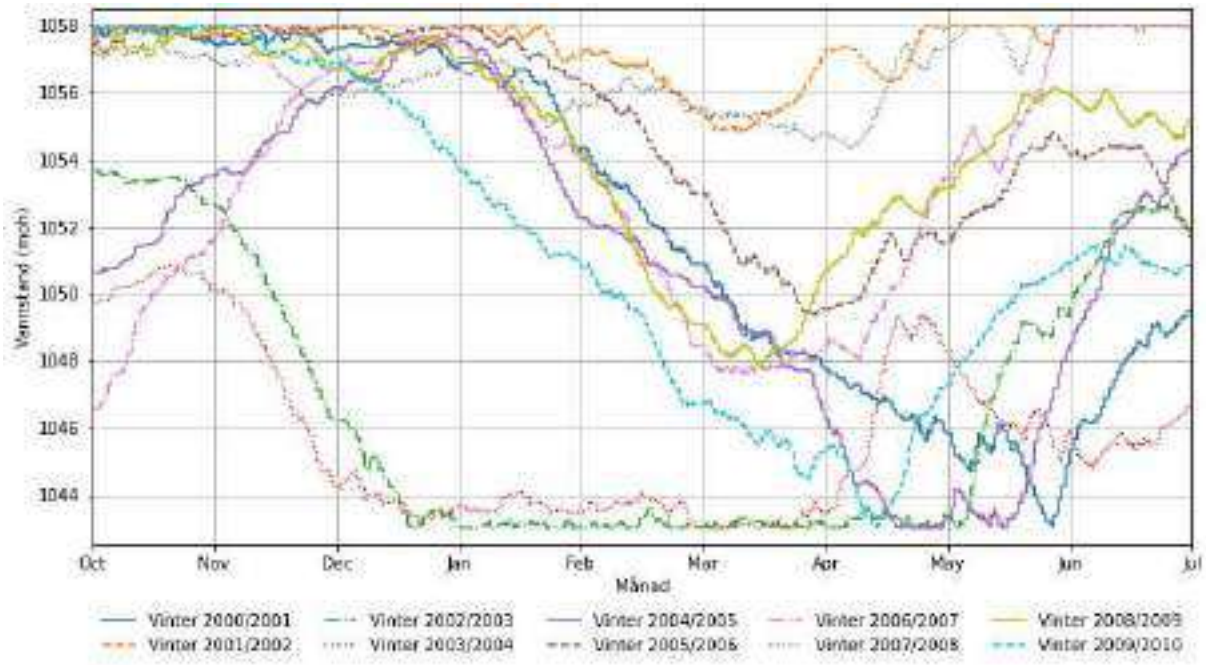

Figure 3. Water levels in Holmavatn reservoir with modelled pumped storage system for the months October-July for weather years 2001-2010.

6. Acknowledgements

The ReHydro project is funded by the EU under the Grant Agreement 101147310. The EnviPump project is funded by the Research Council of Norway under the Contract 358659.

7. References

Arthington AH, Bhaduri A, Bunn SE, Jackson SE, Tharme RE, Tickner D, Young B, Acreman M, Baker N, Capon S, Horne AC, Kendy E, McClain ME, Poff NL, Richter BD and Ward S (2018). The Brisbane Declaration and Global Action Agenda on Environmental Flows (2018). Front. Environ. Sci. 6:45. https://doi.org/10.3389/fenvs.2018.00045

Harby, A., Sauterleute, J., Korpås, M., Killingtveit, Å., Solvang, E. and Nielsen, T. 2013. Pumped storage hydropower. In Stolten, D. and Sherer, V. (eds) (2013). Transition to Renewable Energy Systems. Wiley-VCH. Pp 597-618. https://doi.org/10.1002/9783527673872.ch29

IHA (2025). World Hydropower Outlook. Sector trends and insight. https://www.hydropower.org/publications/2025-world-hydropower-outlook

Quaranta, E., Aggidis, G., Boes, R.M., Comoglio, C., De Michele, C., Patro, E.R., Georgievskaia, E., Harby, A., Kougias, I., Muntean, S., Pérez-Díaz, J.I., Romero-Gomez, P. Rosa-Clot, M., Schleiss, A.J., Vagnoni, E., Wirth, M. and Pistocchi, A. 2021.Assessing the energy potential of modernizing the European hydropower fleet. *Energy Conversion and Management*, Volume 246. https://doi.org/10.1016/j.enconman.2021.114655

Book of Abstracts of the *16th International Symposium on Ecohydraulics*
Challenges and solutions in the time of global changes
August 16–20, 2026, Lausanne, Switzerland
ISSN: 2790-2420 | ISBN: 978-90-837233-9-6 | doi:[10.64697/iahr.proc.ise2026.abs]
© 2026 IAHR. CC BY-NC-ND 4.0

MESOHYDRAULICS: MODELLING HABITAT SUITABILITY ON THE ODER RIVER AT THE MESOSCALE

Piotr PARASIEWICZ[1], Jura SABOLEK[2], Adam KICZKO[3], Dorota MIROSŁAW-ŚWIĄTEK[3], Jan WÓJTOWICZ[4]

[1]National Inland Fisheries Research Institute, ul Oczapowskiego 10, 10-719 Olsztyn, Poland
email: p.parasiewicz@infish.com.pl

[2]Department of Geography, Faculty of Science, University of Zagreb, Trg Marka Marulića 19/II, 10000 Zagreb, Croatia

email: jsabolek@geog.pmf.hr

[3]Institute of Environmental Engineering, Warsaw University of Life Sciences WULS-SGGW, ul. Nowoursynowska 159 02-776 Warsaw, Poland

email: adam_kiczko@sggw.edu.pl

email: dorota_miroslaw-swiatek@sggw.edu.pl

[4]IPIX S.C., ul. Warowna 3/1, 02-654 Warszawa, Poland

email: jan.wojtowicz@ipix.eu

This study evaluates the ecohydraulic relevance of the statistical mesoscale hydraulic model approach (MesoHydraulics) by analysing its influence on habitat suitability in a large regulated river system. The method represents flow-dependent hydraulic conditions using frequency distributions of depth, velocity, and hydromorphological unit (HMU) areas derived from a single field survey and transferred between hydromorphologically comparable river reaches. Habitat rating curves for functional fish guilds derived from simplified hydraulic inputs closely matched those obtained from a two-dimensional hydrodynamic model (R^2=0.98). The similarity of hydraulic distributions between the two modelling approaches, quantified using an affinity index, averaged 90%, with larger deviations observed at extreme flows. The results indicate that mesoscale habitat modelling in large regulated rivers is robust to simplified hydraulic representations and supports efficient ecohydraulic assessments at broader spatial scales.

Keywords: mesohabitat modelling; rating curves; statistical hydraulic model; Oder River

1. Introduction

The mesohabitat (MesoHABSIM) model has been widely used as a powerful tool for analysing relationships between hydrological conditions and biological responses in river systems (Parasiewicz, 2007). Its application in large regulated rivers, however, is often limited by the need for extensive field surveys and the development of complex hydrodynamic models that provide hydraulic inputs for habitat suitability analyses. As an alternative, the statistical hydraulic model MesoHydraulics was developed (Parasiewicz et al., 2025). This approach describes and transfers hydraulic conditions using frequency distributions of depth, velocity, and the relative areas of hydromorphological units (HMUs) between morphologically comparable river reaches, requiring only minimal field data collection.

The objective of this study was to quantify the effect of simplified hydraulic representations derived from the MesoHydraulics model on habitat modelling results, with particular emphasis on habitat rating curves for functional fish guilds in the Oder River, Poland.

2. Methods

The study was conducted on two one-kilometre-long reaches on the Oder River with similar hydromorphological characteristics shaped by equally spaced groynes. Both reaches were mapped as mosaics of hydromorphological units (HMUs), and hydrometric measurements were conducted in 2022 using an ADCP at reference discharges of 185 m^3/s for the Osiecznica reach and 162 m^3/s for the Szydłów reach.

Hydraulic conditions at three additional discharges necessary for habitat rating curve analysis were described using two approaches:

(1) Two-dimensional River2D hydrodynamic model (Steffler and Blackburn, 2002), used to generate a high-resolution hydraulic dataset serving as a reference for evaluating simplified hydraulic representations, and

(2) MesoHydraulics model, which assumes that flow-driven changes in hydraulic distributions observed at one reach (source) can be transferred to morphologically comparable target reaches. Frequency increments of depth, velocity, and HMU areas between discharges, derived from R2D-modelled distributions at the source reach, were applied to the hydraulic distributions measured at the target reach to reconstruct hydraulic conditions under different discharges.

Water depths were classified from <25 cm to >125 cm, and flow velocities from <15 cm/s to >105 cm/s, and the resulting classes were subsequently assigned to the corresponding HMUs. Both hydraulic approaches were used as input variables to the MesoHABSIM model, implemented in SimStream software, to assess habitat availability for functional fish guilds.

Model outputs were compared by analysing habitat rating curves from both models and applying the affinity index (Ia) Eq. (1), which represents the percentage similarity between two distributions (Novak & Bode, 1992), to quantify differences in hydraulic distributions between the two modelling approaches:

$$I_a = 100 - 0.5 \sum_{i=1}^{n} |a_i - b_i| \quad (1)$$

3. Results

The results demonstrated a high degree of similarity between habitat rating curves derived from the two hydraulic inputs, Fig.1. Habitat rating curves for fish guilds (Coghlan et al., 2020) exhibited almost identical shapes, with a correlation of $R^2 = 0.98$ between the two hydraulic inputs across the entire analysed discharge range and with an inflection point at ~1 l/s¹/km².

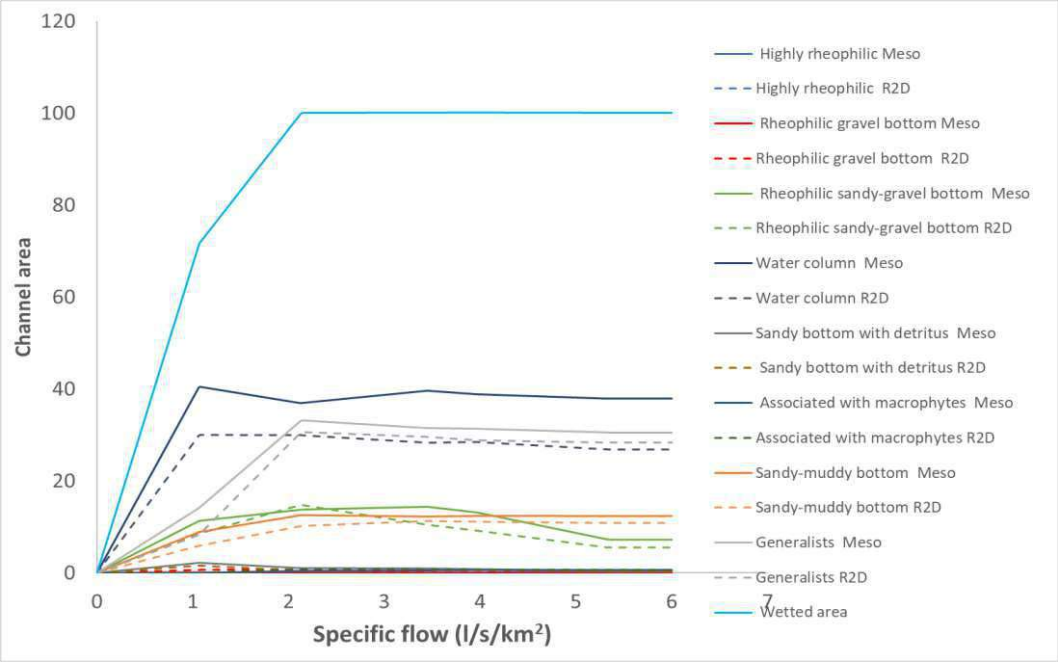

Fig. 1. Habitat rating curves for fish guilds calculated with both models, MesoHydraulic (Meso) and River2D (R2D)

The mean affinity index for hydraulic distributions between the MesoHydraulics and River2D models across four analysed discharges was 90%. The highest affinity was observed at the reference discharge (Ia = 99%), at which the hydrometric survey was conducted. More significant deviations were observed at lower and higher discharges, with mean Ia values of 86 % at 1.07 l/s¹/km² and 85 % at 5.36 l/s¹/km², Table 1. Variability in affinity indices was also observed among individual depth and velocity classes across different HMU types. Despite these deviations in hydraulic distributions, the overall habitat structure for the analysed fish guilds remained stable.

Table 1. Average affinity indices of depth and velocity classes aggregated across HMUs derived from both sites.

Flow	HMU	Depth (cm)						Velocity (cm/s)								Average
(l/s/km²)	Area	<25	25–50	50–75	75–100	100–125	>125	<15	15–30	30–45	45–60	60–75	75–90	90–105	>105	Ia
1.07	92%	94%	90%	67%	94%	81%	91%	98%	90%	91%	95%	97%	81%	87%	44%	86%
2.14	91%	97%	95%	65%	85%	93%	84%	99%	94%	87%	92%	95%	97%	87%	70%	89%
3.97/3.47	99%	99%	99%	99%	98%	98%	100%	100%	98%	97%	99%	99%	100%	100%	100%	99%
5.36	96%	50%	75%	73%	83%	67%	94%	97%	95%	89%	88%	94%	82%	94%	99%	85%

4. Discussion

The results indicate that mesohabitat modelling in large, regulated rivers is robust to simplifications in hydraulic input, provided that hydromorphological structure and statistical hydraulic patterns are adequately represented across the analysed reaches. Although the MesoHydraulics approach achieved an average affinity of 90% with the R2D hydrodynamic model, the resulting habitat rating curves for functional fish guilds remained almost identical. Analysis of hydraulic distributions suggests that model deviations follow consistent patterns across specific hydromorphological unit (HMU) types. In particular, the model tends to overshoot hydraulic distributions (depth and velocity) in the Run unit, which acts as a functional hydraulic default in the model output. In contrast, Backwater, Riffle, and Ruffle units were statistically smoothed during the transfer process, with Backwaters being underestimated in depth and Riffles and Ruffles in velocity. These patterns suggest that the model's statistical performance is influenced not only by hydraulic conditions but also by the morphological complexity of individual HMU types. Units characterized by relatively stable hydraulic conditions, such as Pools, showed consistently high affinity between the hydrodynamic and MesoHydraulics models. In contrast, more dynamic or transitional units, such as Runs and Backwaters, exhibited larger deviations, reflecting their sensitivity to flow variability and local morphological features. Despite systematic deviations, the habitat modelling results remained highly consistent. This indicates that the mesoscale (MesoHABSIM) habitat assessment approach is relatively robust and insensitive to moderate differences in hydraulic representations, particularly when evaluating guild-level habitat suitability.

5. Conclusions

From a practical perspective, the statistical hydraulic model (MesoHydraulics) substantially reduces field efforts and the time required for hydrodynamic model development, thereby facilitating habitat modelling at larger spatial scales, particularly in regulated and hydromorphologically homogeneous river systems. Future research should focus on applying, calibrating and validating the approach in smaller, more heterogeneous, and morphologically dynamic river systems

Acknowledgements

We thank the Rushing Rivers Institute and the Polish Ministry of Agriculture and Rural Development for support. We thank Wiktoria Cudna and Roshan de Zoysha for their valuable contributions to habitat data analysis

References

Coghlan B, Morrissey B, Ruiz CR, Fleming C, Bubb D, De Oliveira E, Verspoor E, Bowditch E, Garcia-Vasquez E, Dopico E, et al., (2020) D4.2 Report of Case Studies Demonstrating the Effects of Barrier Removal, Mitigation and Installation; AMBER Project-H2020-Grant Agreement #689682; Amber: London, UK, 2020; pp. 330. D4.2-Report-of-Case-Studies-Demonstrating-the-Effects-of-Barrier-Removal-Mitigation-and-Installation.pdf

Novak MA, Bode RW (1992) Percent model affinity: A new measure of macroinvertebrate community composition, Journal of The North American Benthological Society 11, 80–85.

Parasiewicz P (2007) The MesoHABSIM model revisited, River Research and Application 23 (8), 893–903.

Parasiewicz P, Sabolek J, Kiczko A, Mirosław-Świątek D, Wójtowicz J (2025) MesoHydraulics: Modelling Spatiotemporal Hydraulic Distributions at the Mesoscale, Water 17 (24), 3570 1-23.

Steffler B, Blackburn J (2002) River-2D: Two dimensional depth averaged model of river, hydrodynamics and fish habitat. In Introduction to Depth-Averaged Modeling and User's Manual; University of Alberta: Edmonton, AB, Canada.

Book of Abstracts of the *16th International Symposium on Ecohydraulics*
Challenges and solutions in the time of global changes
August 16–20, 2026, Lausanne, Switzerland
ISSN: 2790-2420 | ISBN: 978-90-837233-9-6 | doi:[10.64697/iahr.proc.ise2026.abs]
© 2026 IAHR. CC BY-NC-ND 4.0

PHYSICAL HABITAT SIMULATION OF SCHIZOTHORAX PRENANTI SPAWNING GROUNDS BASED ON INDOOR FLUME EXPERIMENTS

Min CHEN[1], Xianting He[1], Ruidong AN[1], Jia LI[1], Fanxu HU[2], Wei JIANG[2]

[1] State Key Laboratory of Hydraulics and Mountain River Engineering, Sichuan University, Chengdu, China
email: mchen@scu.edu.cn (for author1)
email: 2024223060049@stu.scu.edu.cn (for author2)
email: anruidong@scu.edu.cn (for author3)
email: lijia@scu.edu.cn (for author4)
[2] National Engineering Research Center of Eco-Environment in the Yangtze River Economic Belt, China Three Gorges Corporation
email: hu_fanxu@ctg.com.cn (for author 5)
email: jiang_wei6@ctg.com.cn (for author 6)

ABSTRACT

Quantifying suitable physical habitat parameters for *Schizothorax prenanti* spawning grounds is critical for their habitat restoration. This study developed an indoor recirculating flume system (10m×3m) combining four substrate configurations (sand:gravel:cobble ratios) with four velocity gradients (<0.15, 0.30-0.45, 0.60-0.80, 1.00-1.20 m/s). During over 270 hours of observation with 27 adult specimens, reproductive behaviors were quantified through video analysis. Mixed-grain substrates (2:5:3 ratio) at moderate velocities (0.30-0.45 m/s) maximized companion swimming (57.75 times/h) and patrolling (121.70 times/h), significantly higher than other combinations. Statistical analysis revealed substrate composition exerts stronger control than velocity on habitat selection. These findings provide quantitative parameters for optimizing habitat restoration and endemic fish conservation in the upper Yangtze River.

Keywords: *Schizothorax prenanti*; spawning habitat; flume experiment; substrate composition; reproductive behavior.

Introduction

Cascade reservoir construction in the lower Jinsha River has reduced natural habitats essential for endemic fish reproduction[1]. The Heishui River was designated as a tributary habitat conservation demonstration for endemic fish such as *Schizothorax prenanti*, but despite Phase I restoration measures (dam removal, ecological flow releases, fishway construction) successfully achieving fish diversity recovery, yet natural spawning remains difficult to ensure, indicating that altered hydraulic conditions may fail to trigger reproductive behaviors in rheophilic cyprinids preferring riffle-pool sequences for oviposition. Spawning behavior of *Schizothorax* is primarily regulated by water temperature, hydraulic characteristics, and substrate conditions. While temperature thresholds are addressed through basin-scale ecological dispatching, creating suitable hydraulic-substrate combinations remains the critical engineering target for habitat restoration. However, quantitative standards for spawning ground hydraulic parameters and substrate characteristics remain undefined, and the coupling mechanisms between substrate properties and hydraulic conditions on reproductive behavior remain unclear. This knowledge gap hinders quantitative habitat restoration design, which requires specific parameters for substrate placement and flow manipulation rather than qualitative descriptions.

Methodology

A self-designed recirculating flume (10m length × 3m width × 0.4m depth) with transparent acrylic walls was constructed, comprising flow straightening grids, substrate test sections, and propeller-driven circulation (three 60W motors, 0-50Hz). Four overhead cameras (30 fps) captured behaviors while four underwater cameras

were deployed in respective substrate zones for continuous recording of spawning behaviors. Environmental sensors monitored temperature (11-15°C), DO (8-12 mg/L), pH (7.0-8.5), and conductivity (300-500 μS/cm) at 2-hour intervals. Velocity was controlled through frequency modulation and validated using propeller velocimeters at 0.20m×0.30m grid resolution. Substrate zones were installed per **Error! Reference source not found.** configurations, with bare corridors and artificial vegetation buffer strips enabling fish autonomous habitat selection while maintaining flow continuity.

Field surveys of a river section with high-habitat heterogeneity, featuring deep pools and shallow shoals, showed that the surface flow velocity at natural spawning sites was 0.26-0.42 m/s and that the substrate was dominated by 70% gravels and 30% cobbles[2]. Thus, four velocity levels were designed: <0.15 m/s (resting), 0.30-0.45 m/s (core spawning), 0.60-0.80 m/s (high-flow), and 1.00-1.20 m/s (extreme-flow). Specifically, the 0-0.15 m/s conditon simulates the nearshore slow-flow habitat in mountainous rivers, 0.3-0.45 m/s simulates the typical habitat of the *Schizothorax prenanti*, 0.6-0.8 m/s simulates an environment that stimulates fish reproduction, and 1.0-1.2 m/s simulates the extreme habitat of steep river environments. Fourteen scenarios were established after eliminating unreasonable combinations. Twenty-seven sexually mature specimens obtained from aquaculture facilities (female-to-male ratio of 1:3; mean total length: 48 cm for males and 57 cm for females; body weight: 1500 ± 100 g; age: 3 years) were acclimated before the experiments conducted in April 2025, totaling over 270 observation hours.

Table 1. Experimental substrate configurations and velocity gradients

Substrate Type	Sand:Gravel:Cobble Ratio	Particle Size (mm)	Velocity Gradients (m/s)
Type I	2:5:3	0.5-2 / 6-60 / 60-120	All four gradients
Type II	0:0:1	60-120	Excluded <0.15
Type III	2:8:0	0.5-2 / 2-6	Excluded 1.0-1.2
Type IV	0:7:3	6-60 / 60-120	All four gradients

Reproductive behaviors were classified as companion swimming, patrolling, tail-diving, and resting[3]. Behavioral frequencies (occurrences/hour) were calculated per substrate zone. One-way ANOVA tested differences across substrates within each velocity and across velocities within each substrate, followed by Tukey HSD tests (α=0.05). Hierarchical clustering using Ward's method constructed difference trees visualizing habitat preferences.

Results and Discussion

Fish occurrence frequencies demonstrated strong substrate-velocity coupling effects (Fig. 1). Under core Companion swimming frequency in Type I zones (57.75 times/h) was 226% higher than Type II and 164% higher than Type III at equivalent velocity ($p<0.001$). Patrolling behavior peaked at 121.70 times/h in Type I substrate under 0.30-0.45 m/s velocity ($p=0.0036$ vs. other substrates), reflecting enhanced territorial defense enabled by stable micro-hydraulic fields. Tail-diving events, while less frequent overall (maximum 6.00 times/h), concentrated exclusively in Type I zones across middle velocity ranges (0.30-0.80 m/s), with occurrence dropping to near-zero in Type III (high sand content) across all velocities ($p=0.063$). Resting behavior exhibited inverse correlation with reproductive activities: Type I zones showed minimum resting frequency (17.00 times/h) at core spawning velocity but maximum (58.88 times/h) at high velocity (0.60-0.80 m/s), suggesting energy conservation trade-offs.

ANOVA confirmed extremely significant differences ($p<0.001$).) among substrate types across all velocities except <0.15 m/s ($p<0.001$).). Hierarchical clustering (Fig. 2) revealed substrate exerts stronger control than velocity. The difference tree for companion swimming (Ward distance=95.62) segregated extreme velocities at top level, with secondary bifurcations separating Type I from others. Tukey HSD identified Type I substrate at 0.30-0.45 m/s as optimal, with all behavioral metrics significantly exceeding alternatives ($p<0.01$). This configuration's heterogeneous structure (20% sand filling interstices, 50% gravel, 30% cobble) generated stable near-bed profiles (surface 0.32-0.42 m/s, bottom 0.08-0.12 m/s, measured in flume) matching field measurements.

Indoor experiments quantified optimal *Schizothorax prenanti* spawning habitat as mixed-grain substrate (sand:gravel:cobble=2:5:3) with moderate velocity (0.30-0.45 m/s), significantly outperforming single-grain substrates. Substrate heterogeneity exerts primary control by creating stable micro-hydraulic fields reducing energy expenditure, while velocity acts as secondary modulator.

Conclusion and Future Perspectives

This study identified optimal spawning habitat parameters for *Schizothorax prenanti* through indoor flume experiments. Results show that a mixed-grain substrate (sand:gravel:cobble = 2:5:3) combined with moderate flow velocity (0.30–0.45 m/s) significantly outperforms other configurations. Substrate heterogeneity creates stable micro-hydraulic environments that reduce fish energy expenditure and facilitate reproductive behaviors, with flow velocity serving as a secondary modulator. These quantified parameters address knowledge gaps in spawning ground standards, supporting habitat restoration in the Heishui River and endemic fish conservation in the upper Yangtze. Future work will integrate CFD modeling and field monitoring to establish a comprehensive conservation framework for regulated river systems.

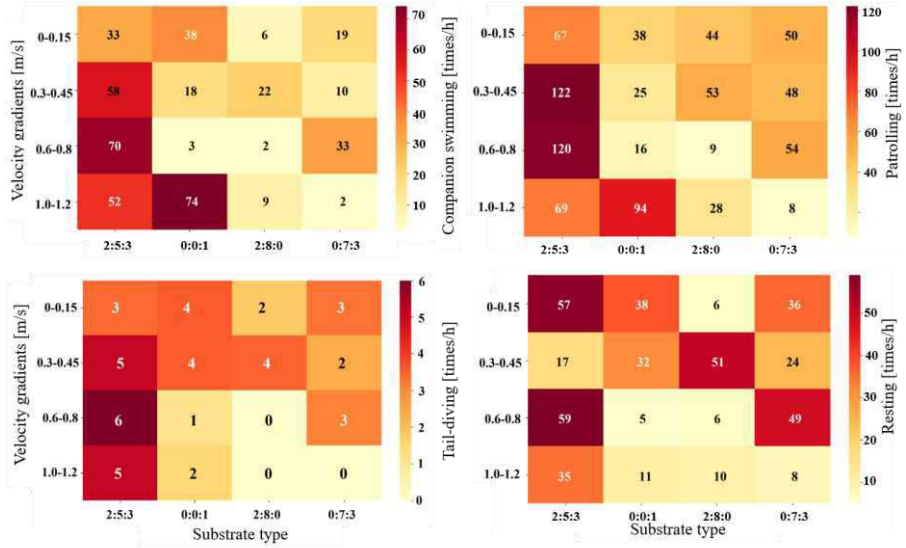

Fig. 1. Reproductive behavioral frequencies of *Schizothorax prenanti* across substrate types under different flow velocity gradients

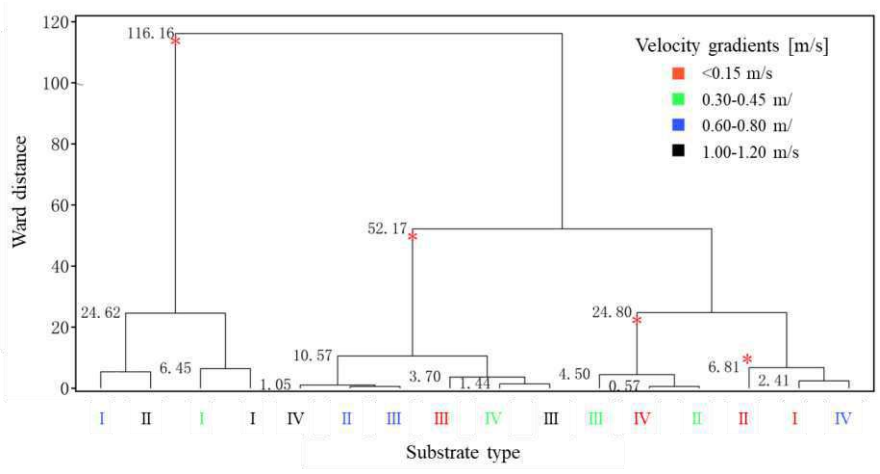

Fig. 2. Hierarchical clustering dendrogram of spawning habitat selection patterns based on companion swimming frequencies across substrate-velocity combinations,*indicates a significant difference between the two working conditions,The colors of numbers Ⅰ-Ⅳ represent different flow rate conditions

Acknowledgements

This work was supported by the National Natural Science Foundation of China (Grant No. U25B20220) and the Research project of China Three Gorges Corporation (NBZZ20220230).

References

[1] Chen Q., Li Q., Lin Y., Zhang J., Xia J., Ni J., et al. (2023) River damming impacts on fish habitat and associated conse rvation measures, Reviews of Geophysics, 61, e2023RG000819.
[2] Li B, Hu F, Li W, Su W, Zhu J, Jiang W (2025) Spawning habitat selection in Schizothorax wangchiachii using acoustic tagging and tracking, Frontiers in Ecology and Evolution, 13:1615081.
[3] Li B, Hu F, Li W, Su W, Zhu J, Jiang W (2025) Study on the Reproductive Group Behavior of Schizothorax wangchiachii Based on Acoustic Telemetry, Fishes, 10(7), 362.

Session A5

Global change impact, biogeochemical cycles, biodiversity losses, and ecosystem resilience

Book of Abstracts of the *16th International Symposium on Ecohydraulics*
Challenges and solutions in the time of global changes
August 16–20, 2026, Lausanne, Switzerland
ISSN: 2790-2420 | ISBN: 978-90-837233-9-6 | doi:[10.64697/iahr.proc.ise2026.abs]
© 2026 IAHR. CC BY-NC-ND 4.0

INFLUENCE OF GLOBAL WARMING ON URBAN STORMWATER QUALITY: IMPLICATION FOR EFFECTIVE MANAGEMENT

An LIU[1], Buddhi WIJESIRI[2], Ashantha GOONETILLEKE[3]

[1] Shenzhen University, P.R.China
email: liuan@szu.edu.cn

[2,3] Queensland University of Technology, Australia
email: b.mahappukankanamalage@qut.edu.au
email: a.goonetilleke@qut.edu.au

ABSTRACT

Stormwater represents a largely untapped resource that could help mitigate water shortages in urban areas. However, it requires treatment prior to use. Furthermore, projected shifts in rainfall patterns due to global warming are expected to alter stormwater quality characteristics. This study forecasts potential changes in the main source of stormwater degradation—particulates that carry the largest proportion of toxic pollutants, such as heavy metals. Findings reveal that global warming of 1.5 °C and 2 °C could lead to an increase in toxic pollutant loads by over 90% on urban surfaces and by nearly 50% in stormwater runoff. Under the upper-range projections for extended dry periods and intensified precipitation within the Representative Concentration Pathway (RCP) 8.5 scenario, stormwater quality is anticipated to further deteriorate. Compared to current conditions, the results suggest that cities will encounter greater challenges in designing effective measures to manage increasingly complex stormwater quality dynamics influenced by varying dry and wet weather conditions. Consequently, this study highlights that to protect stormwater reuse and reduce ecological risks, adaptive design must explicitly account for particle-specific responses to climate change and strengthen linkages between urban hydrological dynamics and ecohydraulic integrity.

Keywords: Global warming; Stormwater management; Urbanization; Alternative water resources

1. Introduction

Water scarcity threatens human well-being, highlighting the need for evidence-based tools to manage alternative water resources. As the last major untapped water source in urban areas, stormwater reuse depends on hydrological and ecohydraulic modelling to quantify climate-driven changes in water quality and maintain the ecohydraulic integrity of receiving waters (Liu et al., 2025). Climate change alters dry-wet patterns and thus pollutant build-up and wash-off dynamics, a core theoretical basis for such modelling (Fereshtehpour and Najafi, 2025). Longer dry periods increase urban surface pollutants, while intense storms generate concentrated runoff that disrupts key ecohydraulic processes including sediment transport, contaminant bioavailability, and near-bed flow conditions (Kumar et al., 2024). These changes increase pollution risks and reduce stormwater usability, showing that modelling frameworks linking urban hydrology and ecohydraulic responses are essential for long-term urban sustainability.

2. Methods and materials

1.1. Background to the research design

Stormwater quality varies significantly spatially and temporally, driven mainly by pollutant build-up and wash-off. While fine and coarse particles differ in accumulation, their wash-off patterns are similar, transferring variability to runoff. Predicting stormwater quality requires addressing two key uncertainties: process modelling (unreliable data, flawed structures) and inherent process variability (natural fluctuations in build-up/wash-off). Inaccurate predictions risk treatment failure, pollutant discharge, and public health issues, underscoring the need for improved modelling approaches.

1.2 *Research design*

Based on extensive fieldwork in northern Australia and stormwater pollution modeling, this study assesses future stormwater quality under 1.5 °C and 2 °C global warming scenarios, with 2007 (0.77 °C) as the baseline. All scenarios—including projected changes in dry periods and precipitation—were derived from IPCC (2018) projections. A MATLAB-based modeling approach was developed to account for pollutant build-up and wash-off under these future warming scenarios.

Firstly, the primary replication models of pollutant build-up and wash-off defined in Equations (1) and (2) and Equation (3) were utilised, corresponding to the reference scenario of global warming (denoted by subscript 'r').

Build-up of fine particles (< 150 µm, Eq.(1)) and coarse particles (> 150 µm, Eq.(2))

$$\boldsymbol{B_r = aD_r^{-b}} \quad (1) \qquad \boldsymbol{B_r = aD_r^{b}} \quad (2)$$

Wash-off of fine particles (< 150 µm) and coarse particles (< 150 µm)

$$\boldsymbol{W_r = (W_0)_r\left(1 - e^{-kI_rt}\right)} \quad (3)$$

Where B – build-up (g/m^2), W – wash-off (g) , W_0 – initially available build-up (g), D – antecedent dry period (day) , I – rainfall intensity (mm/hr) , t – rainfall duration (hour), a – build-up rate (g/m^2/day), b – build-up coefficient (determines the shape of build-up curve and the time to reach equilibrium), k – wash-off coefficient (1/mm)

Secondly, using above Equations (1) – (3), replication models (Equations (4) – (6)) were derived corresponding to the future scenarios of global warming (denoted by subscript 'f').

Build-up of fine particles (< 150 µm, Eq.(4)) and coarse particles (> 150 µm, Eq. (5))

$$\boldsymbol{B_f = a(D_r + \Delta CDD)^{-b}} \quad (4) \qquad \boldsymbol{B_f = a(D_r + \Delta CDD)^{b}} \quad (5)$$

Wash-off of fine particles (< 150 µm) and coarse particles (> 150 µm)

$$\boldsymbol{W_f = (W_0)_f\left\{1 - e^{-k\left(I_r + \frac{\Delta Rx5day}{120}\right)t}\right\}} \quad (6)$$

Where ΔCDD – projected change in consecutive dry days (day) between reference scenario and future scenarios of global warming, ΔRx5day – projected change in annual 5-day maximum precipitation (mm) between reference scenario and future scenarios of global warming

Then, build-up and wash-off were projected in the future scenarios, relative to the reference scenario. As such, Equations (7) and (8) define ratios between build-up loads in the future scenarios and build-up load in the reference scenario. Equations (9) – (14) define ratios between wash-off loads in the future scenarios and wash-off load in the reference scenario.

Build-up ratio for fine particles (< 150 µm)

$$\boldsymbol{\left(\frac{B_f}{B_r}\right)_{<150} = \left(1 + \frac{\Delta CDD}{D_r}\right)^{-b}} \quad (7)$$

Build-up ratio for coarse particles (> 150 µm)

$$\boldsymbol{\left(\frac{B_f}{B_r}\right)_{>150} = \left(1 + \frac{\Delta CDD}{D_r}\right)^{b}} \quad (8)$$

By combining Equations (1) and (3) and Equations (4) and (6) for fine particles (< 150 µm)

$$\boldsymbol{W_r = \left(aD_r^{-b}\right)\left(1 - e^{-kI_rt}\right)} \quad (9)$$

$$\boldsymbol{W_f = \left\{a(D_r + \Delta CDD)^{-b}\right\}\left\{1 - e^{-k\left(I_r + \frac{\Delta Rx5day}{120}\right)t}\right\}} \quad (10)$$

Wash-off ratio for fine particles (< 150 µm)

$$\boldsymbol{\left(\frac{W_f}{W_r}\right)_{<150} = \left(1 + \frac{\Delta CDD}{D_r}\right)^{-b}\left\{\frac{1 - e^{-k\left(I_r + \frac{\Delta Rx5day}{120}\right)t}}{1 - e^{-kI_rt}}\right\}} \quad (11)$$

By combining Equations (2) and (3) and Equations (5) and (6) for coarse particles (> 150 μm)

$$\boldsymbol{W_r = \left(aD_r{}^b\right)\left(1 - e^{-kI_r t}\right)} \tag{12}$$

$$\boldsymbol{W_f = \left\{a(D_r + \Delta CDD)^b\right\}\left\{1 - e^{-k\left(I_r + \frac{\Delta Rx5day}{120}\right)t}\right\}} \tag{13}$$

Wash-off ratio for coarse particles (> 150 μm)

$$\boldsymbol{\left(\frac{W_f}{W_r}\right)_{>150} = \left(1 + \frac{\Delta CDD}{D_r}\right)^b \left\{\frac{1 - e^{-k\left(I_r + \frac{\Delta Rx5day}{120}\right)t}}{1 - e^{-kI_r t}}\right\}} \tag{14}$$

3. Results and discussions

3.1 Influence of long dry periods on pollutant build-up

Under 1.5 °C and 2 °C global warming scenarios, dry periods in North Australia are projected to extend by 3.67–11.93 and 5.11–17.96 days, respectively, compared to the reference scenario. This leads to altered pollutant accumulation patterns, with fine and coarse particles exhibiting contrasting behaviours.

For fine particles, build-up decreases under both warming scenarios—by approximately 10–25% within the first 7 dry days under the 1.5 °C scenario, and further reductions occur with longer dry periods. Build-up does not reach reference levels even after 23 days. In contrast, coarse particle build-up increases significantly: under the 1.5 °C scenario, it reaches 2.5 times reference levels under median dry-period extensions (ΔCDDe), and nearly 4 times under upper limits (ΔCDDu). Under 2 °C warming, these values rise to 3 and nearly 5 times, respectively.

Uncertainty in predictions decreases as dry periods lengthen for both particle types, indicating higher variability during shorter dry intervals. These findings highlight that simply enlarging treatment capacity is insufficient. Effective mitigation requires targeted strategies tailored to specific particle fractions and dry-period phases, especially in regions facing shorter dry periods and higher predictive uncertainty.

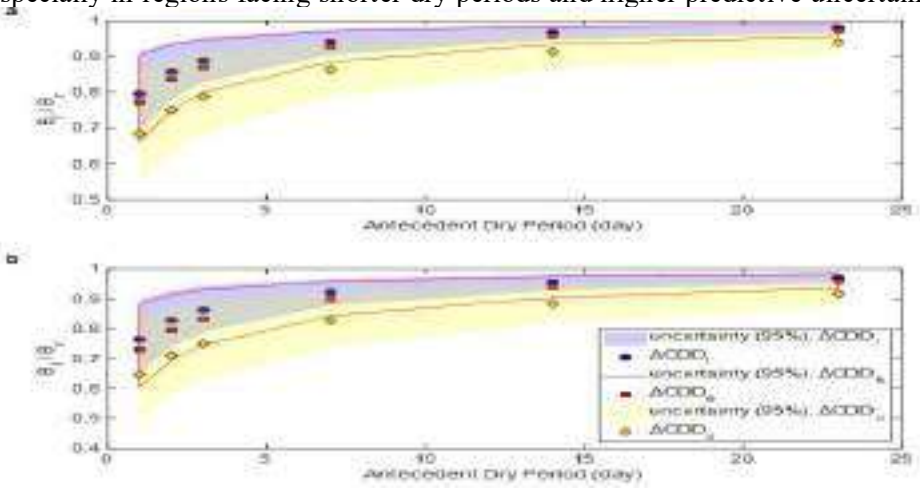

Fig.1. Variation of build-up ratio (B_f/ B_r) of fine particles (< 150 μm) (a: 1.5 °C; b: 2.0 °C)

3.2 Influence of storms on pollutant wash-off

Under 1.5 °C and 2 °C global warming scenarios, North Australia is projected to experience increased rainfall (Rx5day) of 0–4.5 mm and 0–5.58 mm, respectively. While more stormwater may be available, its quality is expected to decline significantly.

Wash-off behaviour diverges by particle size: fine particle wash-off decreases by about 5% under 1.5 °C warming and by 10% under 2 °C, even under the highest precipitation increase. In contrast, coarse particle wash-off rises to 1.25–1.75 times reference levels under 1.5 °C and increases further under 2 °C. These changes are less pronounced than those observed in build-up processes. Unlike build-up, wash-off does not vary significantly during rainfall events or with intensity.

Uncertainty is highest under maximum precipitation change (ΔRx5dayu), indicating greater variability in particulate loads under extreme rainfall. Previous studies also projected increases in runoff pollutants but often relied on lumped models or overlooked key factors like particle size and build-up-wash-off relationships, underscoring the need for more nuanced modelling approaches.

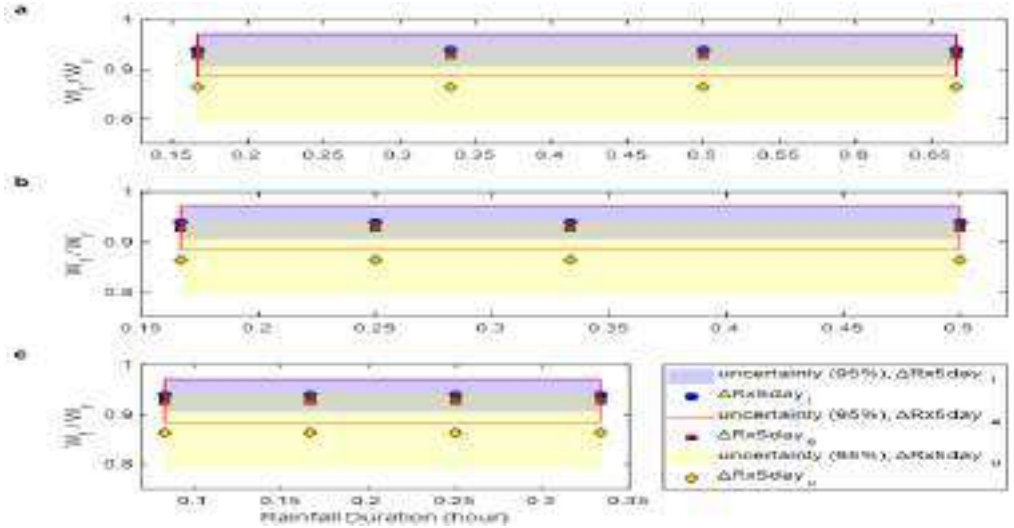

Fig.2. Variation of wash-off ratio (W_f / W_r) of fine particles (< 150 μm) in relation to 1.5 °C global warming scenario (a: 20 mm/h; b: 65 mm/h; c: 115 mm/h)

3.3 Influence of change in stormwater quality on ecohydraulic processes

Under global warming of 1.5–2 °C, fine and coarse particles on urban surfaces exhibit contrasting behaviors: coarse particles accumulate 2.5–5 times more after short dry spells, while fine particles decline beyond 7-day droughts. This increases first-flush effects and uncertainty, raising particle-bound heavy metal loads by 42–94% on surfaces and 21–47% in runoff.

These particle- and contaminant-driven shifts directly modify critical ecohydraulic processes in receiving waters, including flow turbulence, sediment deposition and resuspension regimes, near-bed shear stress, and the transport and mixing of particle-associated pollutants. Altered sediment dynamics and contaminant bioavailability further disrupt habitat structure, nutrient cycling, and the hydraulic suitability of aquatic ecosystems, impairing ecological structure and function. Conventional capture strategies will therefore be inadequate. To protect stormwater reuse and reduce ecological risks, adaptive design must explicitly account for particle-specific responses to climate change and strengthen linkages between urban hydrological dynamics and ecohydraulic integrity.

4. Conclusions

This study reveals that cities will face increasingly complex stormwater quality challenges as global warming progresses. Under 1.5 °C and 2 °C scenarios, fine particle accumulation may decrease by up to 40% after shorter dry periods (<7 days), yet coarse particles—which become significantly more dominant—can increase build-up and wash-off impacts by 2.5 and 1.25 times, respectively. This shift could raise toxic pollutant loads by over 90% in build-up and nearly 50% in runoff.

Current strategies focusing on fine particles and first-flush capture, such as nature-based solutions, will be insufficient under future climate conditions. The research emphasizes that to protect stormwater reuse and reduce ecological risks, adaptive design must explicitly account for particle-specific responses to climate change and strengthen linkages between urban hydrological dynamics and ecohydraulic integrity.

Acknowledgements

This work was supported by Guangdong Basic and Applied Basic Research Foundation (2024A1515010371) and Shenzhen Science and Technology Program (JCYJ20240813141507010 and ZDCYKCX20250901093359008).

References

Fereshtehpour M, Najafi MR (2025) Urban stormwater resilience: Global insights and strategies for climate adaptation, Urban Climate, 59, 102290.

Kumar S, Vishwakarma RK, Tyagi VK, Kumar V, Kazmi AA, Ghosh NC, Sasidharan S, Nayak NS, Hasan R, Joshi H (2024) Stormwater runoff characterization and adaptation of best management practices under urbanization and climate change scenarios, Journal of Hydrology, 635, 131231.

Liu M, Wang Z, Wang M, Li XF, Zhang Y, Yang B, Lai CG (2025) A framework for optimization and assessment of long-term urban stormwater management scenarios under climate change and performance challenges, Journal of Environmental Management, 390, 126298.

Book of Abstracts of the *16th International Symposium on Ecohydraulics*
Challenges and solutions in the time of global changes
August 16–20, 2026, Lausanne, Switzerland
ISSN: 2790-2420 | ISBN: 978-90-837233-9-6 | doi:[10.64697/iahr.proc.ise2026.abs]
© 2026 IAHR. CC BY-NC-ND 4.0

A STUDY OF POTENTIAL MITIGATION MEASURES FOR STORÅNE, A HYDROPEAKED RIVER IN NORWAY

Magnus Simon GRAF[1], Knut Tore ALFREDSEN[2], Noé BOCQUILLON[3], Bjørn Otto DØNNUM[4]

[1,2] Norwegian University of Science and Technology (NTNU) – Department of Civil and Environmental Engineering
email: magnus.graf@ntnu.no
email: knut.alfredsen@ntnu.no

[3] École nationale supérieure de techniques avancées (ENSTA)
email: noe.bocquillon@ensta.fr

[4] Hafslund Eco Vannkraft AS
email: bjornotto.donnum@hafslund.no

ABSTRACT

This study investigates a measure to mitigate ecological impacts of hydropeaking in the Storåne River, Norway. Using a 2D HEC-RAS model derived from bathymetric LiDAR data, the reconnection of a frequently drying side channel was simulated by introducing a small trench to sustain flow during low-discharge conditions. Results indicate that diverting a minor share of residual flow into the side channel improves hydraulic connectivity, increases wetted area, enhances habitat diversity, and reduces stranding risk, while having considerably minor effects on the main channel. The findings suggest that targeted in-stream measures can locally mitigate hydropeaking impacts without substantially limiting hydropower operation.

Keywords: hydropeaking; mitigation; hydraulic modeling; HEC-RAS; bathymetric LiDAR

1. Background

The growing share of wind and solar energy in the energy mix, both of which are intermittent energy sources, highlights the increasing need for balancing energy sources (Gaudard and Romerio, 2014; Hafslund AS, 2025). In this context, a more flexible energy market—driven by a larger share of wind and solar generation, expanded inter-country cable connections, and higher prices for services that stabilize the electricity grid—makes optimizing power production more important than ever. Hydropower, thanks to the ability to store water in reservoirs as potential energy and to rapidly respond to grid fluctuations on demand, is well suited to provide these services and therefore represents an attractive source of revenue. Reflecting this trend, energy companies already have concrete plans of upgrading the maximum capacity of several hydropower facilities in the comingyears, increasing electricity generation during peak periods and thereby further boost revenues (Hafslund AS, 2025; Statkraft, n.d.).

As flexible hydropower operation increases, the negative impacts of frequent ramping events (hydropeaking) in rivers have become more pronounced. Given the extensive literature on the adverse effects of hydropeaking, there is no doubt that organisms and habitats are generally negatively affected. This includes, among other things, the stranding and trapping of fish in drying areas or in confined pools or channels, causing direct mortality or exposure to potential freezing or predators (Saltveit et al., 2001). Other sources report drift, i.e., the physical washing away of benthic organisms, plants, and even finer sediments (Bejarano et al., 2020; Tonolla et al., 2022; Vericat et al., 2020). In the long term, this amplifies the risk of species selection, leading to a less diverse flora and fauna within ecosystems affected by hydropeaking, raising conflicts between economic interests and ecological consequences. Due to favorable topographic and hydrological conditions, the potential for hydropower generation and consequently the exposure to related challenges, is particularly high in Norway (Alfredsen et al., 2022).

2. Material

2.1. Case study

A prominent example for the described operational issues is Storåne, a strongly hydropeaked river in the Buskerud County in Norway (see Fig. 1). Here the hydropower plant Hol 1 releases discharges into the river, ranging between 0 $m^3 s^{-1}$ and 60 $m^3 s^{-1}$. Given a residual flow of 6 $m^3 s^{-1}$ and at times only 2 $m^3 s^{-1}$, the peaking amplitude corresponds to a ratio of 11 or 33. The rapid changes in flow cause vertical drawdowns and drying of smaller side channels with rates that in certain places are above 20 cm h^{-1}, clearly exceeding the proposed maximum drawdown rates of 10-13 cm h^{-1} (Halleraker et al., 2003; Juárez et al., 2019).

The natural river part, located downstream of the first 400 channelized meters of the stream, is particularly affected. Effects manifested mainly in stranding of fish (Saltveit et al., 2020). Further, Saltveit et al., (2020) showed that the amount of hydropeaking events increased in fall and winter, clashing with the critical reproduction periods and early life stages of several fish species.

Another area severely affected by rapid drawdown rates is the northern side channel around Gjerdeøyne, an island in Storåne located approximately 1.2 km downstream of the Hol 1 power plant outlet (see Fig. 1). While the channel conveys water during higher flows around the island, it dries out completely and becomes disconnected under low-flow conditions.

2.2. Data

Storåne benefits from the availability of bathymetric LiDAR data, providing a high-quality basis for analysis. Parts of this bathymetric terrain scan are shown in Fig. 1. The figure highlights an elevated section in the upstream part of the side channel bathymetry, which causes the channel to dry out under low-flow conditions.

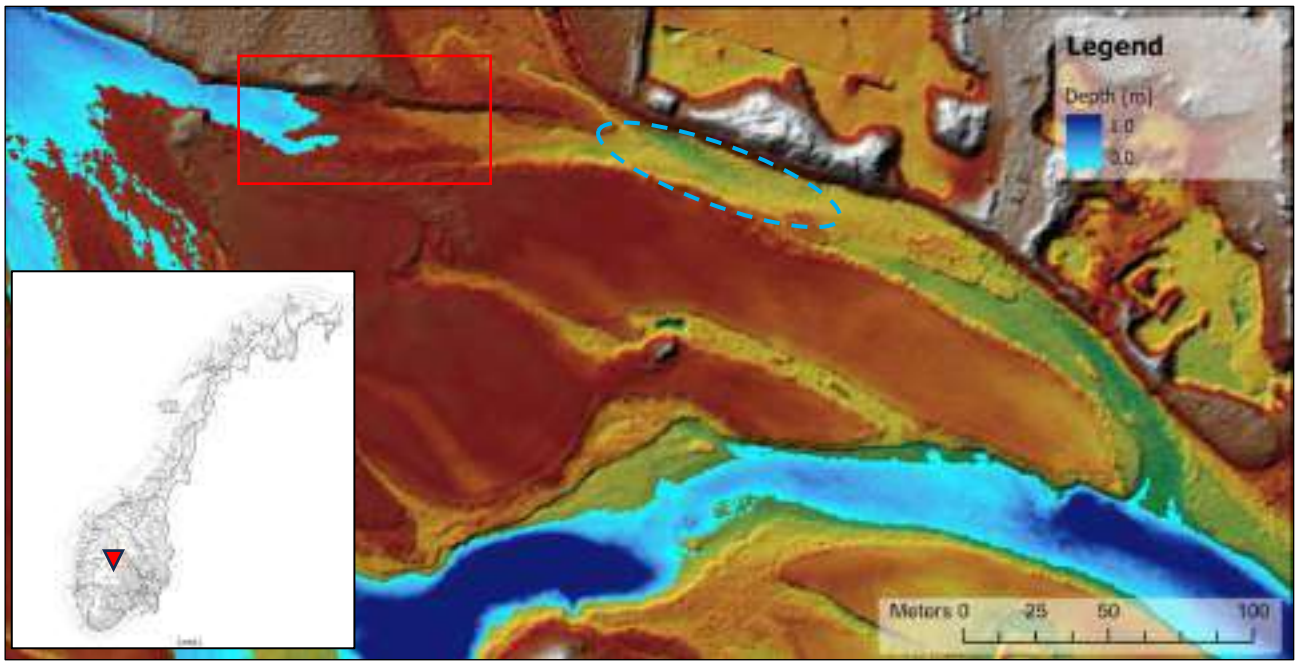

Fig. 1 Study site's location in Norway (lower corner left) (Kartverket, Norwegian mapping authority) and water depths during minimal flow of 2 $m^3 s^{-1}$ around the disconnected side channel (disconnection marked with red area). The channel shows eventually a smaller pool after down ramping (indicated by the dashed blue oval). The pool is however disconnected and rather shallow providing therefore no shelter.

3. Methodology

3.1. Mitigation measure - reconnecting side channel

Efforts of previous studies developed a mitigation through regulation, forcing the last turbine in production to slowly ramp from maximum capacity down to full stop (Juárez et al., 2019). Although this mitigation measure was effective, its applicability is limited by technical turbine constraints, as an instantaneous shutdown becomes necessary below a certain operating level.

Alternative mitigation measures are now to be explored, determining whether ecological improvements are possible without restricting the operation and therefore the economic potential of the power plant. Different

in-stream mitigations measures were studied, offering an alternative or combination possibility to the suggested ramping adaptations. Closing side channels with weirs to avoid water inflow and consequently prevent stranding, the connection of isolated pools, and trees creating shelter spaces were some of the tested mitigation measures. Even a retention or compensation basin was considered. The example presented is one of the most promising measures and aims for reconnecting the in Fig. 1 presented side channel, that gets disconnected during low flow periods.

By excavating a small trench on the channels upstream end (see Fig. 2) and linking it to the main river channel, a continuous water supply of the side channel should be maintained, even under minimum flow conditions. This, in turn, would reduce the extent of stranding areas and potentially decrease the risks of freezing and predation significantly.

3.2. Hydraulic model

To assess the effectiveness of potential mitigation measures, a two-dimensional, hydraulic modeling approach was applied using HEC-RAS. The model utilizes the bathymetric LiDAR scan, which was transformed into a 0.5 m x 0.5 m raster file and has proven to be a sound basis in previous studies. Calibrated, the model then enabled different mitigation approaches to be tested.

In the model, the reconnection of the side channel was represented by lowering the terrain elevation at the side channel intake. The trenches elevation was chosen to be similar to the ground upstream of the plateau and then sloping steadily downwards. The excavated channel was placed where the terrain started sloping upwards and ended with the bed elevation being level with the excavation again. Then, a simulation representing a down-ramping scenario from full production (66 $m^3 s^{-1}$) to minimum residual flow (2 $m^3 s^{-1}$) was performed to study the effects of the mitigation measure.

4. Results

Results, visualized in Fig. 2, show that an artificial trench, connecting stranding exposed areas in a side channel to the main river branch, can mitigate negative effects of down-ramping. The diversion of a minor fraction of the residual flow (0.1 $m^3 s^{-1}$, approximately 5 % of total flow) into the side channel maintains a continuous flow through the channel, thereby reconnecting the deeper pools that are otherwise isolated and are prone to drying.

After implementation of the measure, water depths in the side channel increased.. Enhanced flow velocities were locally observed, particularly in the narrower sections. The wetted area within the newly connected channel network increased compared to the unmodified scenario, while hydraulic conditions in the main channel remained largely unchanged.

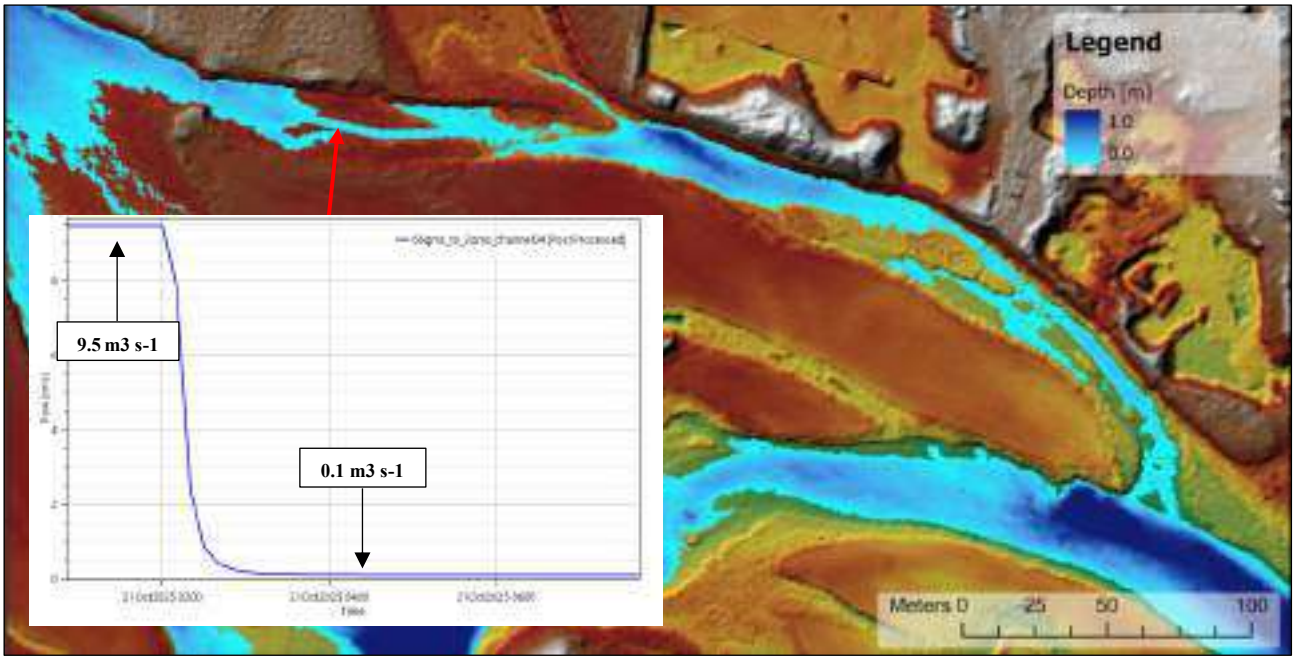

Fig. 2 Water depth (after removal of numeric fragments) at a flow of 2 $m^3 s^{-1}$ in northern side channel. Flow into side channel during the ramping event is shown in lower left corner (extraction location marked by red arrow).

5. Discussion

The large ramping amplitudes and short down-ramping intervals place considerable pressure on the river system and the organisms inhabiting it. Diverting further discharge from the already stressed main channel into a side channel could potentially shift, rather than solve, the problem. The results show, however, that the trench excavation increased the connected wetted area locally by 16 % (from 19,870 m² to 22,980 m²), while only about 5 % of the discharge was diverted from the main channel. Consequently, changes in the main channel remained minor, whereas the side channel became fully passable and hydraulically connected.

As this study focused on conceptual hydraulic effects, no detailed assessment of the construction phase was undertaken. In practice, excavation would represent a physical intervention in the river environment and may cause temporary ecological disturbance. Minimizing this impact would require limiting construction activities to the smallest necessary extent and avoiding permanent damage. Equally important is the long-term stability of the measure, particularly with respect to sedimentation and erosion processes. Appropriate stone placement and bed stabilization would therefore need to be designed in accordance with the identified flow velocities.

The observed hydraulic changes are likely to provide ecological benefits. Increased water depth and maintained connectivity reduce the risk of pool isolation and drying, while deeper zones can improve shelter availability and a more heterogeneous velocity field may enhance habitat diversity and ecosystem resilience during low-flow conditions. Higher velocities in narrow sections could further act as guiding currents for fish movement. As these effects were achieved by diverting only a small fraction of the discharge, such targeted measures may help mitigate hydropeaking impacts without significantly restricting hydropower operation or substantially altering the natural ecosystem. Long-term effectiveness, however, will depend on the morphological stability of the modification and its interaction with sediment processes. More broadly, combining several small-scale mitigation measures may contribute to preserving important habitats and shelter areas, even during unconstrained hydropower operation. This approach requires first identifying hotspot areas with the strongest ecological impacts, followed by the selection of suitable measures and a careful evaluation of their hydraulic and morphological consequences.

References

Alfredsen, K., Amundsen, P.-A., Hahn, L., Harrison, P.M., Helland, I.P., Martins, E.G., Twardek, W.M., Power, M., 2022. A synoptic history of the development, production and environmental oversight of hydropower in Brazil, Canada, and Norway. Hydrobiologia 849, 269–280. https://doi.org/10.1007/s10750-021-04709-4

Bejarano, M.D., Sordo-Ward, Á., Alonso, C., Jansson, R., Nilsson, C., 2020. Hydropeaking affects germination and establishment of riverbank vegetation. Ecological Applications 30, e02076. https://doi.org/10.1002/eap.2076

Gaudard, L., Romerio, F., 2014. The future of hydropower in Europe: Interconnecting climate, markets and policies. Environmental Science & Policy 37, 172–181. https://doi.org/10.1016/j.envsci.2013.09.008

Hafslund AS, 2025. Årsrapport 2024 (Årsrapport). Oslo.

Halleraker, J.H., Saltveit, S.J., Harby, A., Arnekleiv, J.V., Fjeldstad, H. -P., Kohler, B., 2003. Factors influencing stranding of wild juvenile brown trout (Salmo trutta) during rapid and frequent flow decreases in an artificial stream. River Research & Apps 19, 589–603. https://doi.org/10.1002/rra.752

Juárez, A., Adeva-Bustos, A., Alfredsen, K., Dønnum, B.O., 2019. Performance of A Two-Dimensional Hydraulic Model for the Evaluation of Stranding Areas and Characterization of Rapid Fluctuations in Hydropeaking Rivers. Water 11, 201. https://doi.org/10.3390/w11020201

Kartverket, n.d. Norgeskart [WWW Document]. URL https://norgeskart.no/#!?project=norgeskart&layers=1001&zoom=13&lat=6739501.93&lon=128202.13&markerLat=6739501.92578 1052&markerLon=128202.13482122343&p=searchOptionsPanel&sok=hol (accessed 10.27.25).

Saltveit, S.J., Brabrand, Å., Juárez, A., Stickler, M., Dønnum, B.O., 2020. The Impact of Hydropeaking on Juvenile Brown Trout (Salmo trutta) in a Norwegian Regulated River. Sustainability 12, 8670. https://doi.org/10.3390/su12208670

Saltveit, S.J., Halleraker, J.H., Arnekleiv, J.V., Harby, A., 2001. Field experiments on stranding in juvenile atlantic salmon (Salmo salar) and brown trout (Salmo trutta) during rapid flow decreases caused by hydropeaking. Regul. Rivers: Res. Mgmt. 17, 609–622. https://doi.org/10.1002/rrr.652

Statkraft, n.d. Slik oppgraderer vi norsk vannkraft [WWW Document]. URL https://www.statkraft.com/var-virksomhet/vannkraft/vannkraftprosjekter/ (accessed 10.17.25).

Tonolla, D., Dossi, F., Kastenhofer, O., Doering, M., Hauer, C., Graf, W., Schülting, L., 2022. Effects of hydropeaking on drift, stranding and community composition of macroinvertebrates: A field experimental approach in three regulated Swiss rivers. River Research & Apps 39, 427–443. https://doi.org/10.1002/rra.4019

Vericat, D., Ville, F., Palau-Ibars, A., Batalla, R.J., 2020. Effects of Hydropeaking on Bed Mobility: Evidence from a Pyrenean River. Water 12, 178. https://doi.org/10.3390/w12010178

Book of Abstracts of the *16th International Symposium on Ecohydraulics*
Challenges and solutions in the time of global changes
August 16–20, 2026, Lausanne, Switzerland
ISSN: 2790-2420 | ISBN: 978-90-837233-9-6 | doi:[10.64697/iahr.proc.ise2026.abs]
© 2026 IAHR. CC BY-NC-ND 4.0

THE IMPACT OF CLIMATE CHANGE ON RIPARIAN VEGETATION IN BOREAL CONDITIONS

J. Bastian HÖLLER[1], Anders G. ANDERSSON[2], J. Gunnar I. HELLSTRÖM[3]

[1,2,3] Division of Fluid and Experimental Mechanics, Department of Engineering Sciences and Mathematics, Luleå University of Technology, Sweden
email: bastian.holler@ltu.se
email: anders.g.andersson@ltu.se
email: gunnar.hellstrom@ltu.se

ABSTRACT

Riparian zones are among the most species-rich ecosystems and function as important links between the aquatic and terrestrial systems. Among other anthropogenic pressures on the river systems, climate change will further alter river discharges and challenge the water-dependent riparian zones. This study shows how climate change will influence the riparian vegetation in a boreal river. Hydrological and climate data are combined with an ecohydraulic approach to model the potential riparian area and different vegetation belts. The results show how the riparian zone will decrease as a result of the changed flow characteristics. Furthermore, the composition of the riparian vegetation will transform. The work marks the importance of management of riparian zones and the need for suitable mitigation measures.

Keywords: riparian vegetation, climate change, ecohydraulics, boreal rivers

1. Introduction

The temporarily inundated riparian zone is the transition zone between aquatic and terrestrial ecosystems along freshwater bodies. Riparian zones provide habitat and food for numerous species and act as buffer zones for the waterbody. In their natural state, riparian zones support biodiversity and ecosystem resilience. The plant communities established in riparian zones are adapted to the local flow characteristics and temporal inundation. A change in flow characteristics will thereby necessarily affect riparian vegetation. In the future, climate change will alter river flow globally. In the boreal region, higher air temperatures will lead to changed precipitation patterns and earlier snowmelt in spring.

In the 5th Assessment Report (IPCC 2014), the Intergovernmental Panel on Climate Change (IPCC) defined different climate scenarios as Representative Concentration Pathways (RCP). These scenarios describe different pathways of emissions until 2100, with the RCP8.5 describing a high-emission scenario with continued dependence on fossil fuels. Based on these pathways, climate models enable projections of the future precipitation and river flows. In this study, the effect of climate change-induced discharge alteration on the riparian vegetation in a boreal river reach is investigated.

2. Study Site

The study site Sikselet is located in river Juktån in Northern Sweden directly downstream of the Storjuktan reservoir and dam. The hydrology in Sikselet is naturally characterised by a mean annual discharge of 30 m^3/s and a strong seasonal variation. The snow melt causes a peak flood in May or June, before the discharge decreases over summer and fall and reaches a minimum in winter. The construction of the Storjuktan dam and a diversion hydropower plant with outlet directly into the river Umeälven in 1978, led to a reduction of the annual discharge into the Juktån riverbed by almost 90 %. This minimum discharge was seasonally redistributed during a restoration project in 2021 to qualitatively agree with the natural flow pattern and benefit the river ecosystem. In previous work, the potential riparian vegetation for the regulated and natural states was compared. In this work, the potential riparian vegetation under unregulated conditions for a climate scenario is compared to a historic reference scenario.

3. Methods

3.1. Hydrographs

For the investigations, a historic reference hydrograph and a projected hydrograph for 2071-2100 were used. The historic hydrograph is an average hydrograph for the river subbasin based on a hydrologic model of the Swedish Meteorological and Hydrological Institute (SMHI 2025a) for the years 1991 to 2000. Based on this average reference hydrograph and climate data from the SMHI (SMHI 2025b), a hydrograph for the period 2071-2100 considering climate scenario RCP8.5 was calculated (see Fig. 1). The data by SMHI were monthly averages of projected change of discharge until 2071-2100 based on the reference period 1971-2000. These monthly values were interpolated to obtain daily factors. The projected hydrographs were, in a last step, adjusted to fit the monthly averages.

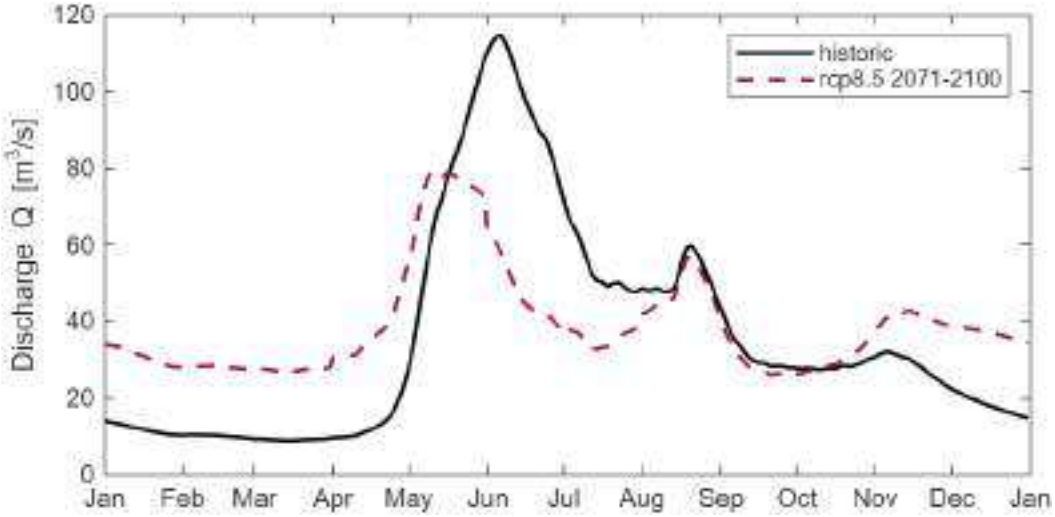

Fig. 1. Discharge hydrographs for the reference period 1991-2000 (black) and the climate change scenario RCP8.5 for the years 2071-2100 (red)

3.2. Hydraulic Model

The significant discharges from Figure 1 were simulated in the 2D-model of Sikselet already used in previous work (Höller et al. 2025a; Höller et al. 2025b). The model of the river reach was generated using the Delft3D FM suite, based on the unsteady shallow water equations. The model contains 115,202 rectangular and triangular cells. The bathymetry was interpolated from Acoustic Doppler Current Profiler (ADCP) cross-sections and complemented with elevation data in the floodplains. The relevant discharges were defined as the upstream boundary condition with a corresponding water level as the downstream boundary.

3.3. Ecohydraulic Approach

Data on inundation tolerance of riparian vegetation belts from Ström et al. (2012) was used to model the riparian area and vegetation belts based on the hydraulic simulations. They defined four vegetation belts in boreal riparian zones and inundation thresholds for these. The most flood-tolerant amphibious belt is located adjacent to the aquatic zone. On higher elevations in the riparian zone, graminoids and willow shrubs can be found with an inundation tolerance of maximum 120 and 62 days, respectively. The riparian forest containing trees tolerating up to 23 days of inundation separates the riparian zone from the upland vegetation defined by a 5-day inundation threshold. Based on the hydrographs, the discharges that exceeded on these numbers of days were identified and are displayed in Table 1.

Table 1. Relevant discharge values Q [m^3/s] defining the upper borders of the different riparian vegetation belts

	Border riparian forest	Border willow shrubs	Border graminoids	Border amphibious	Minimum Discharge
Historic Hydrograph	113	96.1	60.2	48.1	8.9
Climate Scenario RCP 8.5	78.5	73.7	47.6	38.5	26.1

4. Results & Conclusion

In the boreal region, climate change and the induced global warming will cause an in time extended spring flood with a decreased peak and significantly increased discharges in winter. This leads to a more constant

flow over the year. The simulations of relevant discharges resulted in lower water levels for the peak flows of the climate scenario but higher levels for the minimum discharge compared to the historic scenario. As a result, the potential total riparian area decreased by more than 60% (see Fig. 2). With regard to the different vegetation belts, especially the willow shrubs and the amphibious zone would decrease significantly while the area of the graminoid belt remains similar (see Table 2).

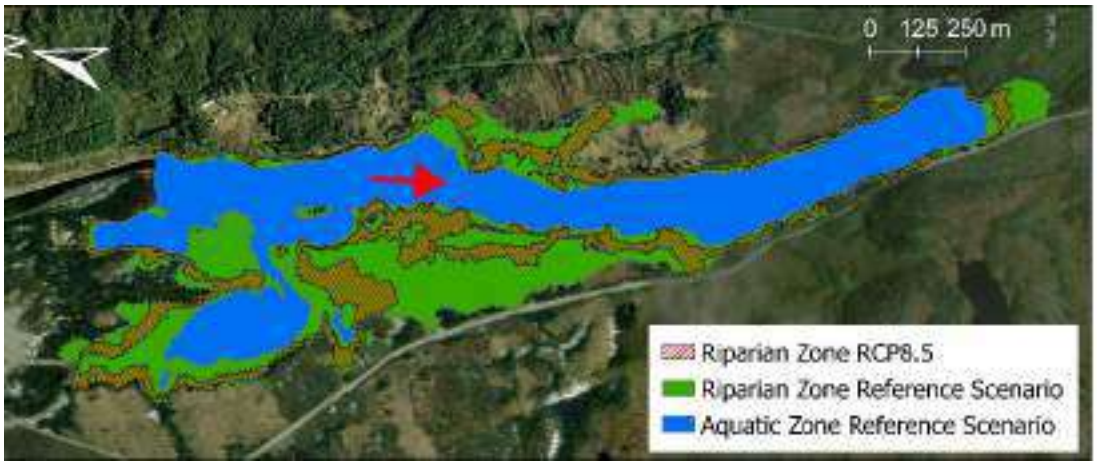

Fig. 2. Extent of the riparian area for historic discharge and the climate change scenario RCP8.5

Table 2. Area [m²] of the riparian vegetation belts and the riparian zone for the historic and the climate scenario

	Riparian forest	Willow shrubs	Graminoids	Amphibious zone	Total riparian area
Historic	56,423	193,621	25,651	212,857	488,551
Climate Scenario RCP 8.5	37,388	71,593	20,814	51,417	181,212

The model predicts only the potential area of the different vegetation belts. A positive relationship between riparian area and plant species richness can be assumed. The results of this study show how climate change will increase the pressure on riparian zones and vegetation in unregulated boreal rivers and emphasise the importance of managing these important ecosystems. Future research should also investigate how river regulation, e.g. for hydropower, and altered discharge due to climate change interrelate.

Acknowledgements

This work is part of the Re-Hydro project funded by the EU programme Interreg Aurora (Grant number 20358005). The work has also partially been funded by the Swedish Energy Agency within the program for Sustainable Hydropower, which aims to contribute to the transition to a sustainable and renewable energy system through research on and development of technologies, systems, methods and issues related to hydropower.

References

Höller JB, Andersson AG, Hellström JGI (2025a) Effects of Flow Restoration on the Hydraulic Conditions in River Juktån. In: Mendonça A, Matos J, editors. 8th IAHR Europe Congress: Water - Across Boundaries. p. 93–103. 8th IAHR Europe Congress; June 4-7, 2024; Lisbon, Portugal: LNEC

Höller JB, Jansson R, Malm-Renöfält B, Widén Å, Hellström JGI, Andersson AG (2025b). Ecological benefits of reintroducing seasonal flow variation for riparian vegetation, Journal of Ecohydraulics, doi: 10.1080/24705357.2025.2584774

IPCC (2014) Climate Change 2014: Synthesis Report. Contribution of Working Groups I, II and III to the Fifth Assessment Report of the Intergovernmental Panel on Climate Change [Core Writing Team, R.K. Pachauri and L.A. Meyer (eds.)]. IPCC, Geneva, Switzerland.

SMHI (2025a). Nedladdning av S-HYPE-data [Download of S-HYPE-data]. Swedish Meteorological and Hydrological Institute, Stockholm. Retrieved September 15, 2025, from https://vattenwebb.smhi.se/modelarea/

SMHI (2025b) Klimatscenariotjänsten [Climate Change Scenario Tool]. Swedish Meteorological and Hydrological Institute, Stockholm. Available from https://www.smhi.se/klimat/framtidens-klimat/klimatscenariotjansten/klimatscenariotjansten

Ström L, Jansson R, Nilsson C (2012) Projected Changes in Plant Species Richness and Extent of Riparian Vegetation Belts as a Result of Climate-Driven Hydrological Change along the Vindel River in Sweden, Freshwater Biology, 57(1), 49–60

Book of Abstracts of the *16th International Symposium on Ecohydraulics*
Challenges and solutions in the time of global changes
August 16–20, 2026, Lausanne, Switzerland
ISSN: 2790-2420 | ISBN: 978-90-837233-9-6 | doi:[10.64697/iahr.proc.ise2026.abs]
© 2026 IAHR. CC BY-NC-ND 4.0

TOTAL DISSOLVED GAS IN NEOTROPICAL SYSTEMS AND ITS EFFECTS ON THE FISH FAUNA

Lorena B. NOGUEIRA[1], Higor A. G. VIEIRA[1] , Breno A. MAGALHÃES[1] , Dieimys S. RIBEIRO[2], Liandro ROSA[3] , Juliano MAFRA[3] , Guilherme FERRAZ[4] , Andrey L. F. de CASTRO[1] , Carlos B. MARTINEZ[2] , Luiz G. M. SILVA[5]

[1] Federal University of São João del-Rei, UFSJ, Brazil
email: lorenanogueira@ufsj.edu.br
email: higorvieira1703@gmail.com
email:brenoa904@gmail.com
email:andreycastro@ufsj.edu.br

[2] Federal University of Itajubá, UNIFEI, Brazil
email: dieimys@unifei.edu.br
email: cmartinez@unifei.edu.br

[3]SINOP Energia, Brazil
email:liandro.rosa@sinopenergia.com.br
email: juliano.mafra@sinopenergia.com.br

[4]HVEX, Brazil
email: ferraz@hvex.com.br

[5]ETH Zürich, Switzerland
email:lumartins@ethz.ch

ABSTRACT

Fish mortality near hydropower facilities is increasingly linked to total dissolved gas (TDG) supersaturation, which can cause gas bubble disease (GBD) in aquatic organisms. While TDG thresholds are documented for temperate species, data for Neotropical fish remain unknown. This study introduces a mobile TDG laboratory designed to expose fish to controlled supersaturation levels and reports preliminary findings for *Prochilodus nigricans*. Acute exposure experiments were conducted under four TDG treatments (control, 115%, 125%, and 130%). All exposed individuals exhibited GBD-related injuries, including emboli in fins, gills, and internal organs. Mortality occurred within 2–4 hours at 125% and 130%, while fish at 115% did not die within the 24h exposure, but showed chronic lesions. These results suggest Neotropical species may be more sensitive to TDG than previously thought, highlighting the need for region-specific thresholds in environmental regulation and hydropower planning.

Keywords: *Total Dissolved Gas*; *Gas Bubble Disease*; *Neotropical fish; Experiments*

1. Introduction

Reports of fish mortality near hydropower facilities are increasing worldwide, drawing global attention of management authorities, scientists and operators (Silva et al., 2021). One contributing factor associated with mortality events is total dissolved gas (TDG) supersaturation, which can lead to gas bubble disease (GBD) in aquatic organisms (Geist et al., 2013; Velle et al., 2024). TDG supersaturation occurs when air mixes with water under pressure - a process often linked to dam operation, especially during spill events (Wan et al., 2020).

When water is supersaturated with TDG, fish tissues also become supersaturated, leading to bubble formation and tissue damage. Gas bubble disease (GBD) causes bubbles in the gills, skin, and other tissues (Cao et al., 2019), and may result in swim bladder over-inflation (Shrimpton, 1990). These effects can lead to haemorrhaging, infections, impaired development, behavioural changes, and ultimately mortality (Stroud, 1975; Xue, 2019).

The TDG supersaturation levels that can lead to injuries or mortality in fish are, apparently, variable amongst different taxonomic groups. For example, the U.S. Environmental Protection Agency (EPA) sets a threshold for water quality limiting TDG to supersaturation up to 110%, considering that levels above 125% are widely lethal (Fidler & Miller, 1994; Deng et al., 2020). On the other hand, laboratory studies suggest that 120% is generally non-lethal for cyprinids in China (Cao et al., 2016).

Thus, determining threshold values of TDG leading to injuries and mortality in fish remains a topic of debate. Most empirical data come from temperate regions (Pleizier et al., 2020), and information on Neotropical species remains limited, hindering the planning and establishment of mitigation solutions. This study introduces a custom-built mobile TDG laboratory designed to expose fish to controlled gas supersaturation, enabling the first empirical evaluation of TDG effects on Neotropical species. Furthermore, it presents preliminary results of experiments conducted with a target species.

2. Methods

Experiments on acute exposure of fish to TDG levels were carried out in a mobile laboratory installed within a maritime container. The system comprises of a TDG supersaturator collumm and a pressurised tank to generate controlled TDG levels (machinery room), a wet lab containing nine independent experimental tanks, and an analytical room (Figure 1). A custom-built interface delivered precise TDG concentrations, ranging from 110% to 145%, to the experimental tanks. This setup ensured consistent, reproducible exposure conditions across all experimental units. During the experiments, TDG levels and water temperature were continuously monitored using an OxyGuard Handy Polaris TGP® probe.

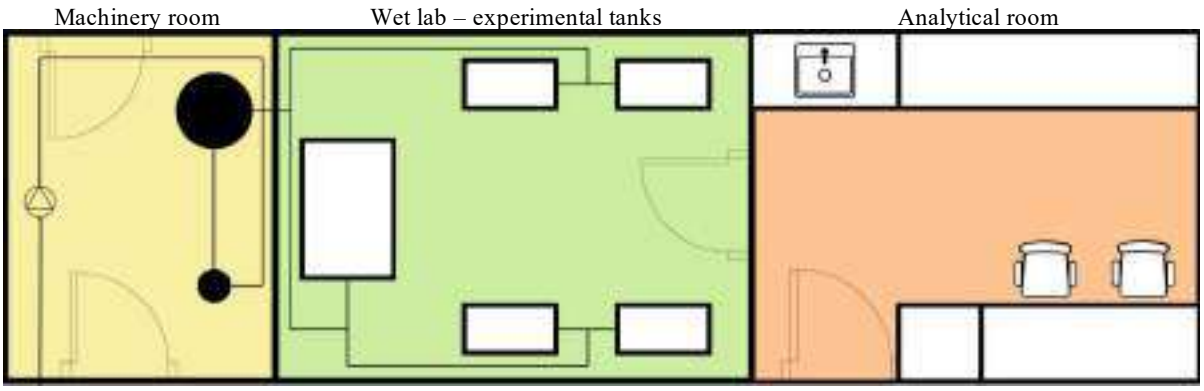

Figure 1. Scheme of the mobile laboratory in container.

Pilot experiments were performed using the Amazonian species curimba (*Prochilodus nigricans*). For the experimental trials, individual fish were placed in a experimental tank. Four TDG saturation treatments were applied (Table 1), representing different exposure scenarios. Fish behavior was continuously monitored and recorded on video throughout the trials. Experiments were terminated immediately upon observation of clear stress indicators, such as abrupt movements or difficulty maintaining position in the water column. Following termination, fish were euthanised using a lethal eugenol solution (1,000 mg/L) in accordance with ethical guidelines. Necropsies were then performed to identify injuries representative of gas bubble disease.

All experiments were conducted in accordance with the regulations established by the Animal Use Ethics Committee of the Federal University of São João del-Rei (CEUA/UFSJ), approved under protocol number 3265040425 (ID 000625).

Table 1. Total dissolved gas (TDG) treatments used for acute exposure experiments, standard length (SL) of the tested individuals, and water temperature during the experiments.

Treatment	TDG level	SL (cm)	T °C
Control	100%	39.9 ± 2.0	28
Group 1	115%	39.5 ± 1.9	28.8 ± 0.4
Group 2	125%	43.0 ± 11.3	28.7 ± 1.1
Group 3	130%	39.5 ± 2.3	28.3 ± 1.1

3. Preliminary results and outlook

All individuals tested exhibited injuries consistent with gas bubble disease (Figure 2) when exposed to supersaturated water, including extensive emboli in fins, gills, eyes, and extended gas bladder. Emboli were also observed in internal structures such as blood vessels, liver, and heart. Behavioral responses were also observed, such as positive buoyance and lack of balance. Mortality occurred within 2 to 4 hours under the lethal TDG levels (125% and 130% TDG, respectively). In Group 1 (TDG = 115%), no mortality was recorded, and exposure lasted 24 hours characterizing a chronic condition (Figure 3). However, post-euthanasia assessments confirmed the presence of GBD-related injuries. The individuals from Control group were not submitted to supersaturated water, however the same handling procedures from the other groups were maintained, not showing any GBD-related injury upon necropsy.

These preliminary findings suggest that Neotropical species may be more sensitive to TDG than previously recognized to non-Neotropical fish, underscoring the need for region-specific thresholds in environmental regulations and hydropower planning.

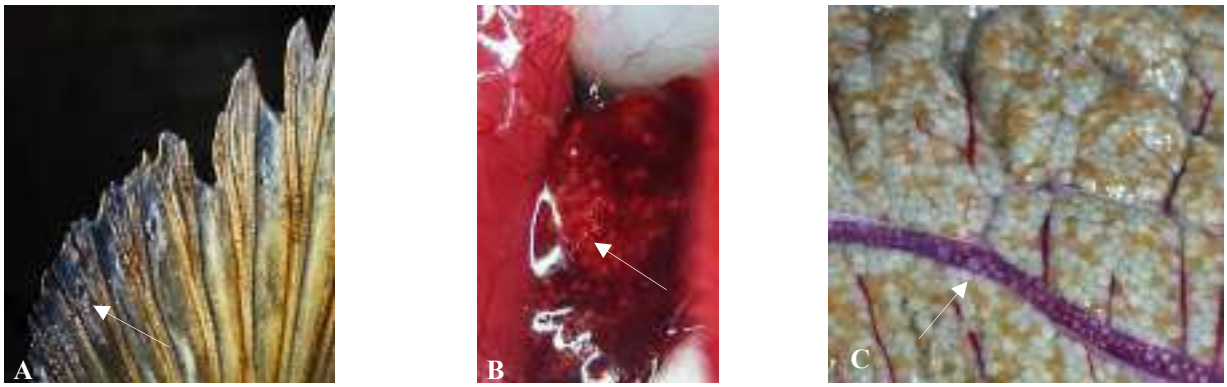

Figure 2. Emboli identified in the dorsal fin (A), heart (B), and blood vessels (C) of *Prochilodus lineatus* esposed to supersaturated water.

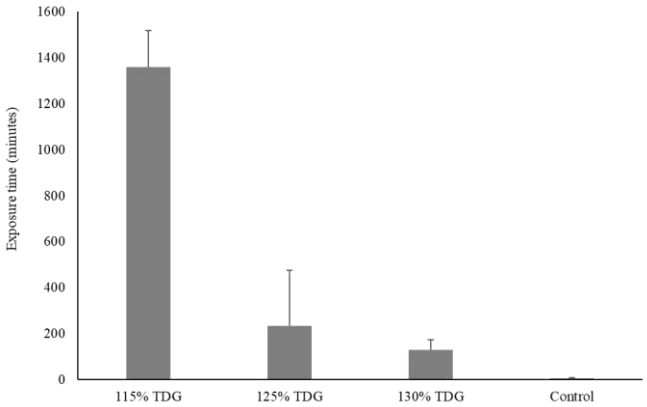

Figure 3. Exposure time (min) of individuals from *Prochilodus nigricans* submitted to different concentrations of total dissolved gase (TDG).

3.1. Outlook

The experimental phase will continue until December 2026 and aims to test up to 12 Amazonian fish species. Target species were selected based on their frequency and abundance in mortality events reported in the Amazon region. Additionally, the study will evaluate TDG levels exceeding 130%.

Acknowledgements

We would like to thank Dr. Robert Naudascher and Lisa Moor for their valuable contribution during the pilot study. We also thank Hvex for their support with the design and construction of the mobile laboratory. This study is funded under the Cooperation Agreement between Sinop Energia, the Federal University of Itajubá and the Federal University of São João del-Rei (AP 23088.012191/2023-30).

References

Cao, L., Li, Y., An, R., Wang, Y., Li, K., Buchmann, K. (2019). Effects of water depth on GBD associated with total dissolved gas supersaturation in Chinese sucker (*Myxocyprinus asiaticus*) in upper Yangtze River. Scientific Reports, 9(6828), 1–08. https://doi.org/10.1038/s41598-019-42971-8

Cao, L., Li, K., Liang, R., Chen, S., Jiang, W., Li, R. (2016). The tolerance threshold of Chinese sucker to total dissolved gas supersaturation. Aquactic Researcg, 47(9),2804–13. https://doi.org/10.1111/ are.12730

Deng, Y., Cao, C., Liu, X., Yuan, Q., Feng, C., Shi, H., Yang, Y., Wu, Y. (2020). Effect of total dissolved gas supersaturation on the survival of bighead carp (*Hypophthalmichthys nobilis*). Animals, 10 (166), 1–14. https://doi. org/10.3390/ani10010166

Fidler, L. E., Miller, S. B. (1994). Britsh Columbia water quality guidelines for dissolved gas supersaturation. Canada: BC Ministry of Environment Canada Department of Fisheries and Oceans Environment.

Geist, D. R., Linley, T. J., Cullinan, V., Deng, Z. (2013). The Effects of Total Dissolved Gas on Chum Salmon Fry Survival, Growth, Gas Bubble Disease, and Seawater Tolerance. North American Journal of Fisheries Management 33(1):200–215 doi:10.1080/02755947.2012.750634.

Pleizier, N. K., Algera, D., Cooke, S. J., Brauner, C. J. (2020). A meta-analysis of gas bubble trauma in fish. Fish and Fisheries, 21(6), 1175–94. https://doi.org/10.1111/faf.12496

Silva, Luiz G. M., Castro, A. L. F., Kemp, P. (2021). Fish mortality at hydropower plants: identifying problems and co-creating solutions. São João del-Rei, Federal University of São João del-Rei, Brasil and University of Southampton, United Kingdom.

Shrimpton, J. M., Randall, D. J., & Fidler, L. E. (1990). Factors affecting swim bladder volume in rainbow trout (Oncorhynchus mykiss) held in gas supersaturated water. Canadian Journal of Zoology, 68, 962–968.

Stroud, R. K., Bouck, G. R., & Nebeker, A. V. (1975). Pathology of acute and chronic exposure of salmonid fishes to supersaturated water. In Chemistry and Physics of Aqueous Gas Solutions (pp. 435–449). Electrothermics and Metallurgy and Industrial Electrolytic Divisions, Electrochemical Society.

Velle, G., Isaksen, T. E., Lennox, R. J., Pulg, U. (2024). Bubbling trouble: Effects of supersaturated water on benthic macroinvertebrates. Ecohydrology doi:10.1002/eco.2665.

Xue, S., Kefeng, L., Liang, R., Cao, L., Wang, Y., Li, Y., Feng, J. (2019). In situ study on the impact of total dissolved gas supersaturation on endemic fish in the Upper Yangtze River. River Research and Applications, 35(9),1511–19. https://doi.org/10.1002/rra.3503

Wang Y, Liang R, Li K, Li R. (2020). Tolerance and avoidance mechanisms of the rare and endemic fish of the upper Yangtze River to total dissolved gas supersaturation by hydropower stations. River Research and Applications, 36(7), 993–1003. https://doi.org/10.1002/ rra.3677

Book of Abstracts of the *16th International Symposium on Ecohydraulics*
Challenges and solutions in the time of global changes
August 16–20, 2026, Lausanne, Switzerland
ISSN: 2790-2420 | ISBN: 978-90-837233-9-6 | doi:[10.64697/iahr.proc.ise2026.abs]
© 2026 IAHR. CC BY-NC-ND 4.0

ASSESSMENT OF ECOSYSTEM REGULATION ON WATERSHED ECOHYDRAULIC VARIABLES UNDER CLIMATE AND LAND USE CHANGE IN SOUTHERN CHINA

Jianxiang XIONG[1,2], Lingqiao KONG[1,*], Zhiyun OUYANG[1,2]

[1] State Key Laboratory of Regional and Urban Ecology, Research Center for Eco-Environmental Sciences, Chinese Academy of Sciences, Beijing, China
[2] University of Chinese Academy of Sciences, Beijing, China
email: jxxiong_st@rcees.ac.cn (for Jianxiang XIONG)

email: lqkong@rcees.ac.cn (for Lingqiao KONG)

email: zyouyang@rcees.ac.cn (for Zhiyun OUYANG)

ABSTRACT

Forests, wetlands, and grasslands regulate the hydrological cycle by intercepting precipitation, conserving water, and modulating runoff, thereby mitigating extreme hydrological events. This study examines the Xiangjiang River Basin in southern China, a subtropical monsoon region with abundant but unevenly distributed precipitation and frequent floods and droughts. We quantify the hydrological regulation capacity of different ecosystems and their roles in water balance. Using the VIC model and machine learning approaches, we analyzed temporal variations of hydrological variables, including precipitation, surface runoff, and vegetation water retention, and characterized their seasonal dynamics. We further quantified how ecosystems partition precipitation into evapotranspiration, runoff, and storage. Grid-scale regression analyses of runoff coefficients against land cover proportions, performed with OLS, Random Forest, and XGBoost, reveal a pronounced nonlinear response of runoff to land-use patterns. These findings highlight the critical influence of ecosystem composition on basin-scale hydrology, and provide policy-relevant guidance for setting scientifically informed ecological restoration targets to enhance ecosystem resilience under future climate scenarios.

Keywords: *water retention; climate change; land cover pattern; VIC model; ecosystem; watershed*

1. Introduction

Ecosystems such as forests, wetlands, and grasslands play a pivotal role in regulating the hydrological cycle by intercepting precipitation, retaining water, and modulating runoff, thereby mitigating the impacts of extreme hydrological events. In the context of global climate change, the frequency and intensity of floods and droughts are projected to increase, posing significant challenges to water resource management and ecosystem sustainability.

The Xiangjiang River Basin in southern China, located within a subtropical monsoon climate zone, experiences abundant but highly unevenly distributed precipitation and is frequently affected by both floods and droughts. Despite extensive research on hydrological processes in this region, the quantitative understanding of how different ecosystem types contribute to water regulation and their seasonal dynamics remains limited. Furthermore, the influence of land-use patterns on runoff generation and water partitioning has not been fully explored at fine spatial scales.

To address these gaps, this study integrates the Variable Infiltration Capacity (VIC) hydrological model with machine learning techniques to evaluate temporal variations of key hydrological variables, including precipitation, surface runoff, and vegetation water retention. Additionally, we examine the conversion of

precipitation into evapotranspiration, runoff, and storage across different ecosystems, and conduct grid-scale regression analyses using OLS, Random Forest, and XGBoost to investigate the nonlinear response of runoff coefficients to land-use patterns. The findings aim to enhance the understanding of ecosystem-based water regulation and provide scientifically grounded guidance for ecological restoration and climate adaptation strategies in the basin.

2. Study area and methods

2.1. Study area

The Xiangjiang River Basin covers a total area of 94,660 km². The basin exhibits complex and diverse topography, being surrounded by mountains on the east, west, and south, while connecting to the Dongting Lake Plain in the north, with terrain gradually flattening from south to north. The Xiangjiang River Basin lies within a subtropical monsoon climate zone, characterized by abundant water and thermal resources. However, precipitation is unevenly distributed throughout the year, primarily concentrated from March to August, resulting in a distinct wet-dry seasonal cycle.



Fig. 1. Study area

2.2. Data

The data used in this study primarily include model input data and observed data for model calibration and evaluation. The model input data consist of meteorological data and land surface characteristics. Meteorological data, such as precipitation, temperature, and wind speed, are used to drive hydrological processes, while land surface data—including digital elevation models, soil properties, and land use—are employed to characterize the basin, extract runoff information, and set model parameters. For model calibration, observed daily streamflow data at the basin outlet, represented by the Xiangtan Hydrological Station, are used to assess the accuracy of the simulated results..

2.3. Methods

The Variable Infiltration Capacity (VIC) model, developed collaboratively by the University of California, Berkeley, the University of Washington, and Princeton University, is a grid-based, large-scale distributed hydrological model [1]. The VIC model comprehensively accounts for the physical processes among soil, vegetation, and atmosphere, providing an integrated representation of changes and transfers of water and energy across these components. It is capable of simultaneously simulating water and energy balances throughout the hydrological cycle. One of the model's key strengths lies in its consideration of the spatial heterogeneity of soil, topography, and vegetation cover, enabling the grid-based simulation of infiltration, evapotranspiration, and runoff processes, and thereby more accurately reflecting actual evapotranspiration and runoff under different vegetation conditions. The calculation of water conservation capacity using the VIC model is expressed as [2–4]:

$$WR = P - ET - Rs$$

where WR represents water conservation, P is precipitation, ET is actual evapotranspiration, and Rs denotes surface runoff.

To ensure the accuracy of model calibration and computational efficiency, the Rosenbrock optimization method was employed for automatic parameter optimization and calibration of the VIC model [5–7]. Model performance was evaluated using the Nash–Sutcliffe efficiency coefficient (NSE) and the coefficient of determination (R^2), which were jointly applied to assess the accuracy of runoff simulations [8–9].

Absolute hydrological variables, such as runoff, evapotranspiration, and water conservation, are driven by interannual meteorological fluctuations and often exhibit pronounced temporal variability. Under specific land surface conditions, however, the proportion of precipitation allocated by ecosystems to different hydrological components tends to remain relatively stable. To quantify this allocation capacity, this study introduces hydrological proportion coefficients, including the evapotranspiration coefficient ($ET_{(C)}$), runoff coefficient ($Rs_{(C)}$), and water conservation coefficient ($WR_{(C)}$), which represent the fraction of precipitation converted into each hydrological component. These coefficients are calculated as follows:

$$C_{ET} = \frac{ET}{P}, C_{Rs} = \frac{\mathrm{Rs}}{P}, C_{WR} = \frac{WR}{P}$$

whereC_{ET}, C_{Rs} , and C_{WR} denote the evapotranspiration coefficient, runoff coefficient, and water retention coefficient, respectively.

Using the hydrological flux datasets derived from the VIC model, an intercept-free, area-weighted response equation was constructed with the runoff coefficient as the intermediary variable. By integrating traditional regression and machine learning algorithms, localized empirical parameters are extracted to rapidly assess the impact of land-use changes on water retention capacity.

3. Results

3.1. Parameter calibration

According to the model configuration, the main parameters calibrated in this study include the variable infiltration curve parameter (B), the nonlinear baseflow parameter (Ds), the maximum baseflow rate (Dm), and the soil thickness parameters (d2 and d3), totaling six parameters [6–10]. The search ranges and calibration values for these parameters are listed in Table 2.

Table 1 Search Range and Optimal Values of Soil Parameters

Parameters	Search Range	Optimal Value
B	[0.1:0.5]	0.05
Ds	[0.05:0.1]	0.7
Dm	[1:1.5]	1.3
Ws	[5:30]	5
d2	[4.5:5.5]	5
d3	[2.5:3.5]	3

3.2. Model performance

Runoff simulations for the Xiangjiang River Basin were conducted using the optimized parameters, and the results indicate that the model performs well at both daily and monthly scales. As shown in Table 3, during the calibration period from 2009 to 2011, the NSE values at daily and monthly scales were 0.77 and 0.883, respectively; during the validation period from 2012 to 2014, the NSE values were 0.631 and 0.85, respectively. Overall, the simulation accuracy at the monthly scale was higher than at the daily scale (monthly NSE = 0.872, R^2 = 0.906). The simulated results are consistent with observed basin conditions, demonstrating the good applicability of the model.

Table 2 Evaluation of Runoff Simulation Results

Simulation stage	Time span	Daily scale		Monthly scale	
		NSE	R^2	NSE	R^2
Calibration period	2009 - 2011	0.77	0.77	0.883	0.93

Probation period	2012 - 2014	0.631	0.657	0.85	0.879
Simulation period	2009 - 2014	0.713	0.718	0.872	0.906

3.3. Spatiotemporal variations of hydrological variables

Trend regression analysis was performed on grid-scale hydrological variables to identify areas with significant changes at $q<0.1$. Across the entire basin, only evapotranspiration exhibited significant changes, occurring in 5.3% of the basin area.

Analysis of the spatiotemporal patterns of seasonal hydrological component allocation indicates that the hydrological elements in the Xiangjiang River Basin exhibit pronounced wet-dry alternation within a year. Precipitation peaks in spring (536.5 mm), followed by summer (454.6 mm), and declines to 198.5 mm and 195.3 mm in autumn and winter, respectively. Driven by the uneven intra-annual distribution of precipitation, water retention in the basin shows an alternating "storage-consumption" pattern: the system experiences positive water surplus in spring and winter (156.6 mm and 64.2 mm, respectively), whereas summer and autumn are characterized by significant water deficits (-23.6 mm and -73.5 mm, respectively).

3.4. Response of runoff coefficient to land cover types

Using the first five years of the simulation period as the training set and the final year as the test set, regression predictions of the runoff coefficient were performed based on the area proportions of different land cover types within each grid using Ordinary Least Squares (OLS), Random Forest (RF), and XGBoost algorithms. The introduction of machine learning algorithms significantly improved predictive performance, suggesting a highly nonlinear response of the runoff coefficient to land-use patterns.

4. Conclusion and implications

During the study period, evapotranspiration showed significant increases in 5.3% of the basin. Seasonally, spring and winter were the main water retention periods, while summer and autumn were characterized by water deficits. The mean values of the evapotranspiration coefficient, runoff coefficient, and water retention coefficient during the study period were 0.16, 0.78, and 0.06, respectively. The result of the regression analysis showed a nonlinear response of runoff coefficients to land-use patterns. This study provides a framework for assessing the impact of land cover changes on runoff coefficients and ecosystem water retention service at the watershed scale, as well as their future changes under climate change scenarios.

Acknowledgements

This work is supported by the National Key Research and Development Program of China (Grant No. 2024YFF1306103).

References

Hamman J., et al.(2018).The Variable Infiltration Capacity model version 5 (VIC-5): infrastructure improvements for new applications and reproducibility.Geoscientific Model Development,11(8),3481-3496.
Wang Y., et al. (2021). A review of the connotation and estimation methods of water conservation. South-to-North Water Transfers and Water Science & Technology (Chinese and English), 19(06), 1041–1071.
Stoyan N., et al.(2022).Modeling water regulation ecosystem services: A review in the context of ecosystem accounting.Ecosystem Services,56.
Zhang C., et al.(2021).Application of ecosystem service flows model in water security assessment: A case study in Weihe River Basin, China.Ecological Indicators,120,106974.
Zhang X. (2006). Application of the VIC model in humid regions of China (Master's thesis, Hohai University).
Adeyeri O.E., et al.(2020).Conceptual hydrological model calibration using multi-objective optimization techniques over the transboundary Komadugu-Yobe basin, Lake Chad Area, West Africa.Journal of Hydrology: Regional Studies,27,100655-100655.
Liu Z., et al. (2025). Hydrological simulation and application of the VIC model in the Daqing River Basin. Journal of Wuhan University (Engineering Edition), 58(10), 1541–1548.
Qiu Y., et al.(2025).Combined application of variable infiltration capacity model and Budyko hypothesis for identification of runoff evolution in the Yellow River Basin, China.Journal of Arid Land,17(8),1048-1063.
Li M., et al. (2024). Variations in water conservation function and attributions in the Three-River Source Region of the Qinghai–Tibet Plateau based on the SWAT model. Agricultural and Forest Meteorology, 349, 109956.
Liu Y., et al.(2024).A holistic approach to projecting streamflow and analyzing changes in ecologically relevant hydrological indicators under climate and land use/cover change.Journal of Hydrology,632,130863.

Book of Abstracts of the *16th International Symposium on Ecohydraulics*
Challenges and solutions in the time of global changes
August 16–20, 2026, Lausanne, Switzerland
ISSN: 2790-2420 | ISBN: 978-90-837233-9-6 | doi:[10.64697/iahr.proc.ise2026.abs]
© 2026 IAHR. CC BY-NC-ND 4.0

HABITAT MODELLING OF FISH COMMUNITIES IN THE ODER RIVER: APPLICATION OF THE MESOHABSIM MODEL UNDER ENVRIOMENTAL STRESS CONDITIONS

Wiktoria CUDNA[1,2], Katarzyna SUSKA[1,2], Piotr PARASIEWICZ[1,2]

[1] Warsaw University of Life Sciences, Poland

[2] National Inland Fisheries Research Institute, Poland
email: w.cudna@infish.com.pl

ABSTRACT

Using the MesoHABSIM simulation model, we analyse the status and dynamics of fish habitats in the Oder River in relation to threats associated with the spread of Prymnesium parvum. The MesoHABSIM model is used to analyse habitat availability by identifying and evaluating hydromorphological units under different flow conditions. It provides a framework for assessing how changes in hydrology affect the spatial structure and suitability of aquatic habitats. When combined with high-resolution imaging data, this modelling allows for the delineation of hydromorphological units that form the basis for subsequent habitat analysis. The habitat model for fish guilds and community structures was calculated with the help of SimStream 8.0 software (Rushing Rivers Institute), which integrating measured habitat parameters, water quality, and fish occurrence. The resulting habitat suitability map for Oder was overlaid with the probability distribution of P. parvum occurrence, allowing identification of vulnerable habitats for each species and target group. Preliminary analyses indicate that the river provides habitats used by fish for both spawning and rearing, although these conditions are not always optimal. Slow-flowing habitats such as backwaters and shallow areas appear particularly susceptible to algal blooms, despite frequently scoring favorably in habitat suitability models for fish spawning and rearing. This highlights the complex nature of these habitat types and the environmental pressures affecting overall fish community condition. The model is applied to simulate and optimise management and restoration scenarios for the Oder River. Habitat suitability analysis is an essential instrument for conservation planning, biodiversity assessment, and environmental management.

Keywords: MesoHABSIM; fish habitat modelling; Oder River; ecohydraulics; *Prymnesium parvum*; envriomental management.

1. Introduction

The Oder River experienced a major ecological crisis in 2022, driven by a bloom of the toxic alga *Prymnesium parvum*. This event highlighted the need for advanced ecohydraulic tools to assess habitat dynamics and inform management decisions. The current study integrates field data, hydrodynamic simulations, and habitat modeling using MesoHABSIM to provide insights into the resilience of fish communities. In addition, the risk of *P. parvum* occurrence model was applied on representative river reaches of the Oder, allowing spatial assessment of algal threats in relation to habitat conditions.

2. Methods

This study used the MesoHABSIM system to assess habitat availability and suitability for riverine fish under varying hydrological conditions. Representative river reaches were surveyed to delineate hydromorphological units (HMUs), such as riffles and pools, characterized by flow velocity, depth, substrate, and shelter. A two-dimensional hydrodynamic model of the Oder River, calibrated for multiple flow regimes, was integrated with habitat mapping and ecological modeling. SubDisMo estimated substrate composition, while SIM-Stream 8.0 calculated habitat suitability for fish guilds, which were identified from the GIS-based habitat mapping enabled spatial quantification of available habitats under different flows. The P. parvum probability model was

developed using hyperspectral and field data, and logistic regression based on key water quality parameters such as pH, sodium, and total phosphorus. The model estimated the likelihood of *P. parvum* presence and density, and its predictive performance was evaluated using standard metrics.

3. Results

Preliminary results indicate that although the modeled reaches of the Oder River contain habitats used by key fish species, their conditions are not always optimal, as can be observed for one of the studied sites – Osiecznica, see Fig. 1. Overlaying the *P. parvum* risk model provided a predictive map of potential algal blooms along the river, see Fig. 3. Many habitats identified as suitable for fish were simultaneously at elevated risk of *P. parvum* proliferation, particularly during low-flow conditions and within backwaters, slow-flowing sections, and other reduced-velocity areas, see Fig. 1. and Fig. 2. Despite the generally limited condition of fish communities, the Oder River still offers numerous rearing habitats for various species, see Fig. 2, highlighting the coexistence of valuable fish habitats with areas susceptible to harmful algal blooms.

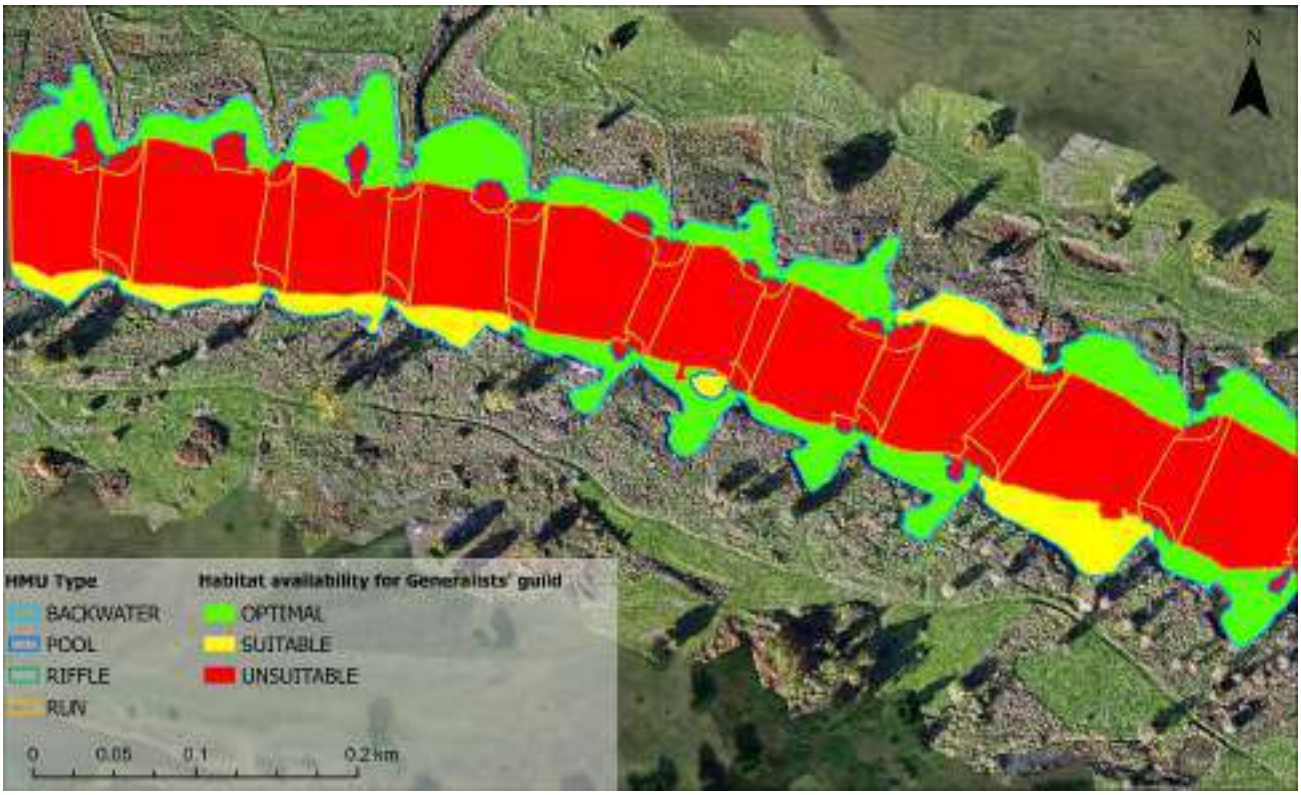

Fig. 1. Map of distribution of habitat availability for Generalists' - rearing guild across the Odra River at Osiecznica site, modeled for a flow rate of Q = 100 m³/s. This river section contains four types of hydromorphological units: backwater, pool, riffle and run. Habitat availability was assessed using a three-level scale: 0 – unsuitable, 1 – suitable, 2 – optimal. Orthomosaic of the Odra River acquired by drone, by Katarzyna Suska Basemap: Orthophotomap geoportal.gov.pl

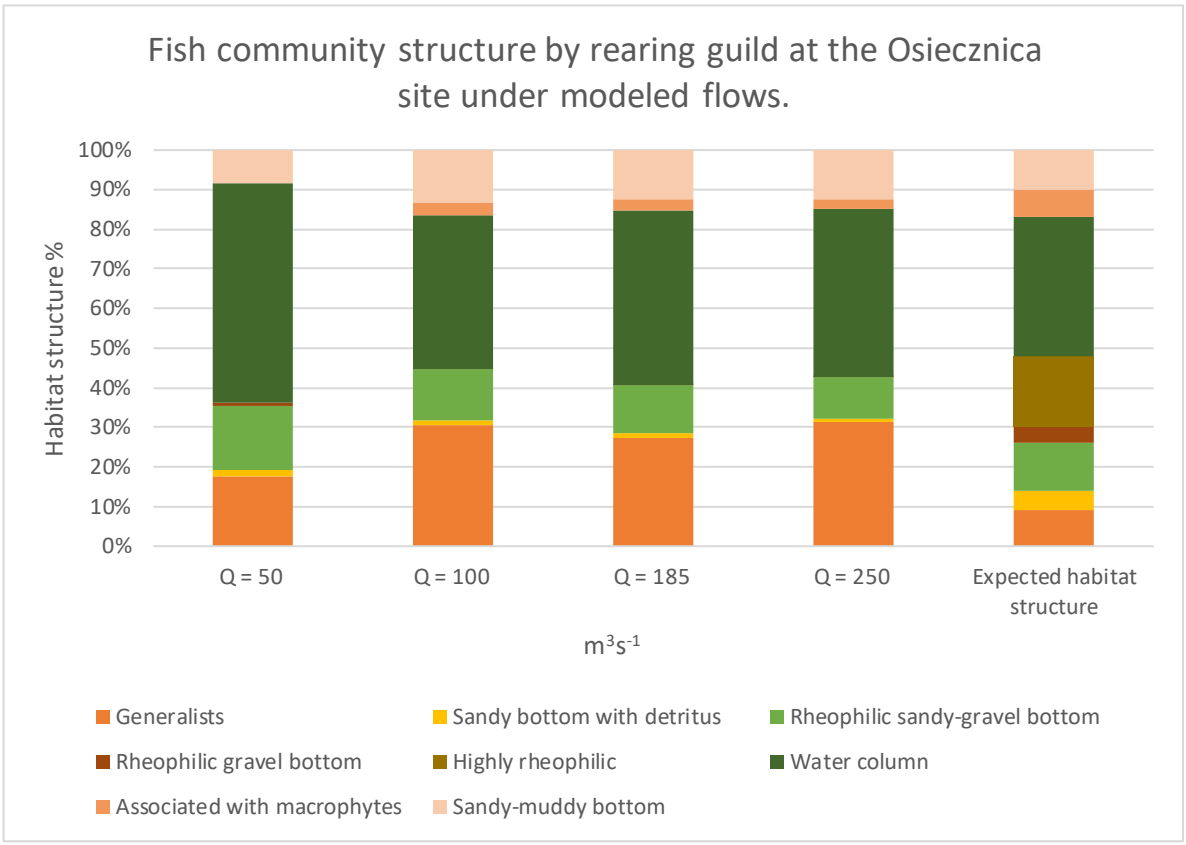

Fig. 2. Fish community structure by rearing guild at the Osiecznica site under modelled flows. The example shows how community composition shifts with river flow values and how these shifts compare with expected models.

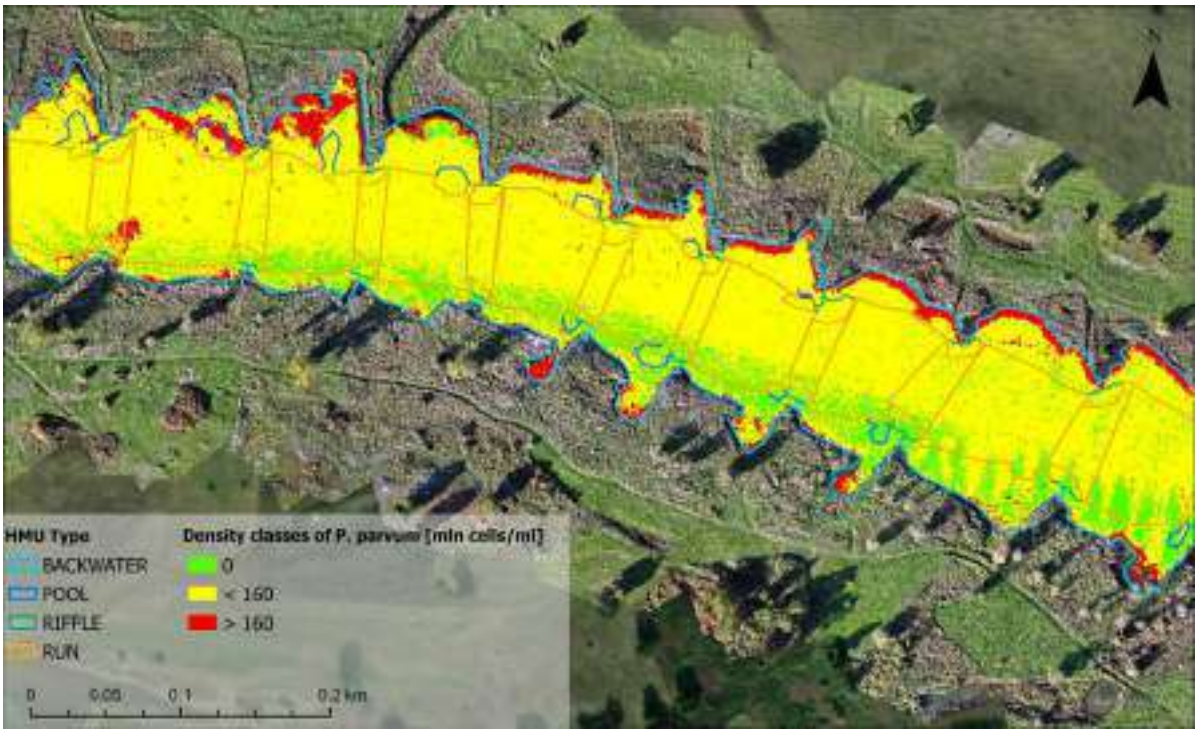

Fig. 3. Map of distribution of *Prymnesium parvum* across habitats along the Odra River at Osiecznica site, modeled for a flow rate of Q = 100 m³/s. This river section contains four types of hydromorphological units: backwater, pool, riffle and run. The probability estimated from the logistic regression was calculated as a weighted sum of 0.25 for algal presence and 0.75 for algal density, with algal presence assessed on a three-level scale: 0 – no occurrence, 1 – below 160 million cells per millilitre, and 2 – above 160 million cells per millilitre Hyperscpectral data: MGGP Aero Sp. Z o. o. Model *P. parvum* by: Katarzyna Suska and Piotr Parasiewicz Orthomosaic of the Odra River acquired by drone, by Katarzyna Suska.. Basemap: Orthophotomap geoportal.gov.pl.

4. Conclusion

The MesoHABSIM-based analysis of the Oder River provides valuable insights into the effects of hydromorphological and environmental changes on fish habitats. The framework offers a robust tool for adaptive river management and restoration planning. Subsequent work will focus on monitoring habitat changes after the bloom and assessing appropriate management or mitigation strategies. Complementary findings regarding of application of hyperspectral data is presented in the accompanying abstract "Spatial distribution of the probability of *Prymnesium parvum* occurrence in the Oder River." by Katarzyna Suska and others.

Acknowledgements

The further project activities are made possible thanks to the project Odra Together: Joint Analyses and Solutions for Transboundary Management of Water Quality, Biodiversity, Fisheries, and Other Ecosystem Services, carried out with support from Interreg VI A Brandenburg–Poland 2021–2027 and co-funded by the European Regional Development Fund. Partners: Potsdam Institute of Inland Fisheries (DE ,lead partner), Federal Institute of Hydrology (DE), Leibniz Institute of Freshwater Ecology and Inland Fisheries (DE), Warsaw University of Life Sciences Institute of Information Technology and Institute of Environmental Engineering (PL), Wrocław University of Environmental and Life Sciences Institute of Environmental Engineering (PL).). The project was funded by: The Ministry of Climate and Environment of the Republic of Poland, The Ministry of Agriculture and Rural Development of the Republic of Poland and The National Inland Fisheries Research Institute (statutory work Z-018). Thanks to MGGP Aero Sp.z o. o. for delivering and analysis hyperspectral data.

References

Parasiewicz, P. (2007). The MesoHABSIM model revisited. River Res. Appl., 23, 893–903.
Parasiewicz, P., Prus, P., Suska, K., & Marcinkowski, P. (2018). "E = mc2" of Environmental Flows: A Conceptual Framework for Establishing a Fish-Biological Foundation for a Regionally Applicable Environmental Low-Flow Formula. Water, 10(11), 1501.
Rushing Rivers Institute. 2014. SimStream: A MesoHABSIM Simulation Software. Available online: https://rushingrivers.org/ (accessed on 25 November 2025)
Badania parametrów jakościowych wody rzeki Odry na bazie lotniczych danych hiperspektralnych zebranych na wybranych odcinkach poniżej kanału Gliwickiego w trakcie masowego spływu śniętych ryb i mięczaków, National Inland Fisheries Research Institute Olsztyn, Poland. Prepared for The Institute of Environmental Protection – National Research Institute in Poland. Not published.
Yang H., Kong J., Hu H., Du Y., Gao M., Chen F. (2022). A Review of Remote Sensing for Water Quality Retrieval: Progress and Challenges. Remote Sensing. 14(8):1770. doi: 10.3390/RS14081770.

Book of Abstracts of the *16th International Symposium on Ecohydraulics*
Challenges and solutions in the time of global changes
August 16–20, 2026, Lausanne, Switzerland
ISSN: 2790-2420 | ISBN: 978-90-837233-9-6 | doi:[10.64697/iahr.proc.ise2026.abs]
© 2026 IAHR. CC BY-NC-ND 4.0

WHEN THE RIVER MEETS ENERGY DEMAND: BALANCING ENERGY, CLIMATE, AND NATURE

Markus FOERST[1], Atle HARBY[2]

[1,2] SINTEF Energy Research, Norway
email: markus.foerst@sintef.no
email: atle.harby@sintef.no

ABSTRACT

The growing share of wind and solar power increases the need for flexible hydropower and energy storage. Pumped-storage hydropower can address these challenges by enhancing operational flexibility and storing surplus energy. This study evaluates the feasibility of upgrading the Nedre Driva hydropower system by pumping water to an expanded Gjevilvatnet reservoir and constructing a new high-capacity station discharging into the fjord. Habitat mapping shows that the river has very good mesohabitat conditions for salmon, but a bottleneck occurs at flows below 5 m³/s. Hydrological analysis of historical discharge data combined with habitat mapping indicates that maintaining summer flows of approximately 20 m³/s and winter flows of at least 5 m³/s is essential for habitat quality and fish survival. The concept shows potential for balancing energy flexibility with ecological integrity, while supporting climate adaptation and renewable integration.

Keywords: Ecohydraulics; hydrology; habitat; pumped storage hydropower

1. Background

TrønderEnergi is assessing potential upgrades and expansions to the Driva power plant and its associated waterways. One option under consideration is to pump water from the Driva River at Festa to the existing reservoir Gjevilvatnet to be used in the existing Driva power plant with outlet directly in the Driva River further downstream. Another alternative involves constructing a new Driva power plant with an outlet directly into the Sunndalsfjord. These developments could deliver several environmental benefits, while also increasing power production and enabling more flexible energy generation. Since the water to be pumped would consist of surplus flow during high-water and flood events in the Driva River, the environmental impacts may not be a barrier. This approach would provide an additional 400 meters of head and more inflow for electricity generation. Currently, there is no infrastructure for releasing water from the Gjevilvatnet reservoir, as it is a so-called *drawdown reservoir* (storage volume is only below natural water level). A pump system will install waterways that can allow water to be released back into the Driva River. If found economic feasible, it is also possible to install a turbine or a pump-turbine to generate electricity while releasing water to the river.

2. Methods and Results

2.1. Mesohabitat

The mesohabitat and river type has been mapped during normal summer flows around 20-30 m^3/s by Foldvik et al. (2023) following the method from Forseth and Harby (2014) described in table 1 and 2.

Table 1: A classification of mesohabitats based on physical criteria. „Smooth" water surfaces are defined as exhibiting wave heights of 5 cm or less (smooth or small wavelets). „Turbulent" surfaces exhibit wave heights greater than 5 cm (lager wavelets/broken surface). Gradients in excess for 4% are defined as „steep", or „moderate" if the gradien is less than 4%. Water flow in excess of 0.5 m/s is defined as „fast", or „slow" if flow is less than 0.5 m/s. Water depths greater than 70 cm are defined as „deep", or „shallow" if they are less than 70 cm. Source: Forseth and Harby (2014).

Criteria	Water surface	Gradient	Water velocity	Water depth	Class
Classification	Smooth (small wavelets)	Steep	Fast	Deep	A
				Shallow	
			Slow	Deep	
				Shallow	
		Moderate	Fast	Deep	B1
				Shallow	B2
			Slow	Deep	C
				Shallow	D
	Turbulent (Large wavelets, broken surface, standing waves)	Steep	Fast	Deep	E
				Shallow	F
			Slow	Deep	
				Shallow	
		Moderate	Fast	Deep	G1
				Shallow	G2
			Slow	Deep	
				Shallow	H

Table 2: Classification of river classes based on physicla critiera and obtained by the pooling of mesohabitats (table 1).

				velocity	
Glide	A+B1+B2	Smooth	Moderate	Fast	Shallow/Deep
Pools	C	Smooth	Moderate	Slow	Deep
Shallows	D	Smooth	Moderate	Slow	Shallow
Whitewater	E+F	Turbulent	Steep	Fast	Deep/Shallow
Rapids	H+G1+G2	Turbulent	Moderate	Fast	Shallow/Deep

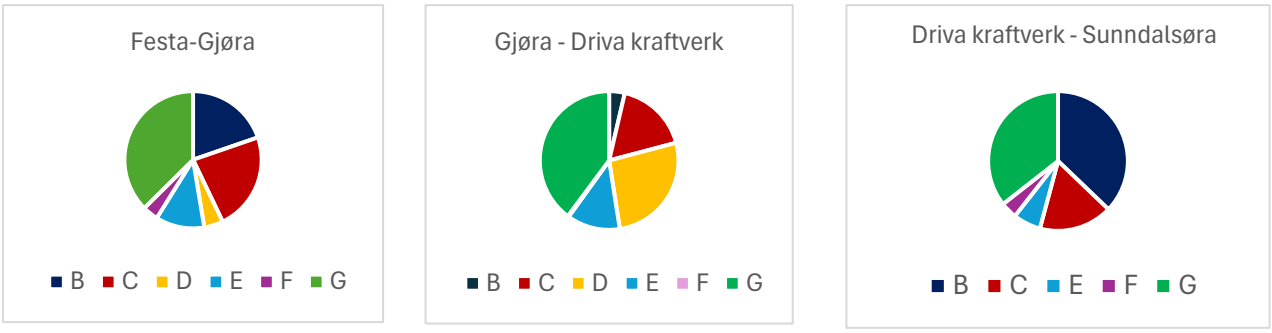

Fig. 1. Distribution of river types across three sub-reaches in the Driva River, calculated based on the area of each river type from Foldvik et al. 2023.

Figure 1 visualizes the results from the mapping. It shows very good mesohabitat conditions during flow conditions between 20 and 35 m^3/s. Calculations of diversity and contagion indices derived from landscape ecology (Shannon 1948, Ricotta et al. 2002) show a good diversity of different habitat types spread across the river reach. Based on the maps at 20 m^3/s, we estimated how the habitat will change at lower flows.

We expect there will be a bottleneck for fish survival at low flows in winter below 5 m^3/s. In figure 2 we estimated the distribution of habitat types during this discharge. The habitat around 5 m^3/s shows a large

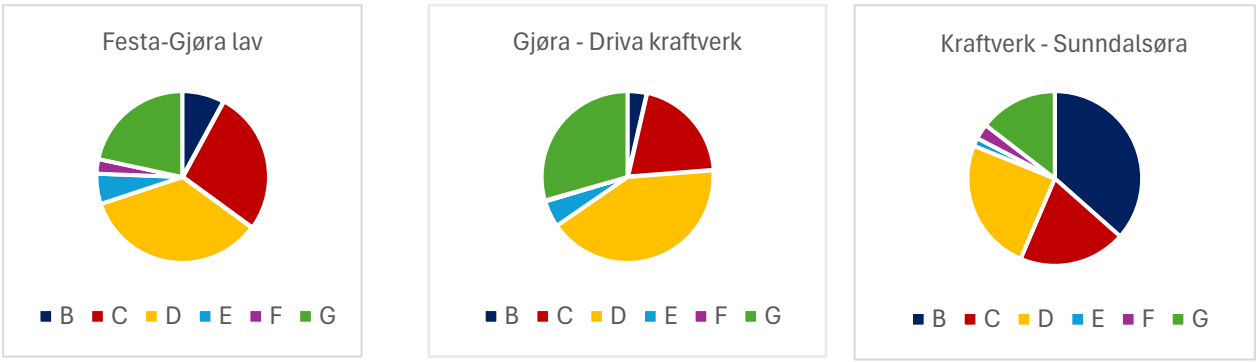

Fig. 2. Estimated distribution of river types across three sub-reaches in the Driva River at 5 m³/s, based on an approximate adjustment of river type.

2.2. Hydrology

The Driva catchment is located in Mid-Norway. Lake Gjevilvatnet is used as a drawdown reservoir (storage volume is only below natural water level), blocking the outlet of the lake to Festa River, a tributary to Driva River. Some tributaries to Driva River are diverted into Gjevilvatnet. A pump transfer water from the nearby Ångårsvatnet lake to Gjevilvatnet, reducing the flow in the Vinndøla River, a tributary to Driva River. The current Driva hydropower plant has its outlet into the Driva River about 20 km from the mouth in the Sunndalsfjord. The catchment has normally a distinct snow smelting period in spring and some autumn storms later in the year. Based on the requirements to fill up the reservoir by 20th June and the assumption of an environmental flow of 20 m^3/s during summer and 5 m^3/s during winter, we evaluated different scenarios for pumping. Here we present the scenario with a maximum pumping capacity of 30 m^3/s.

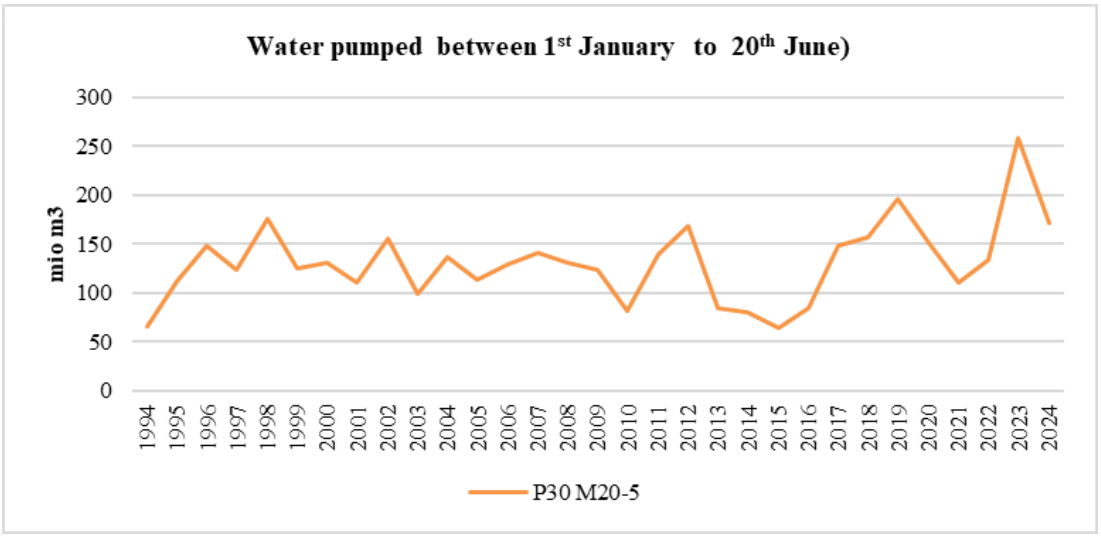

Fig. 3. Possible pumped water into Gjevilvatnet reservoir, based on historical values. The requirement to be able to pump 68 mio m^3 has been met most of the years.

2.3. Climate change

In both graphs, shown in figure 3 and 4, the trend to a wetter wintertime seems visible. Figure 3 shows the amount of water which would be used for pumping has been increasing during the last years. Figure 4 shows that the natural flow during wintertime has increased. At the same time, it is expected that other periods during the year will be drier. This will affect both the economy of hydropower development and the environmental aspects of the project.

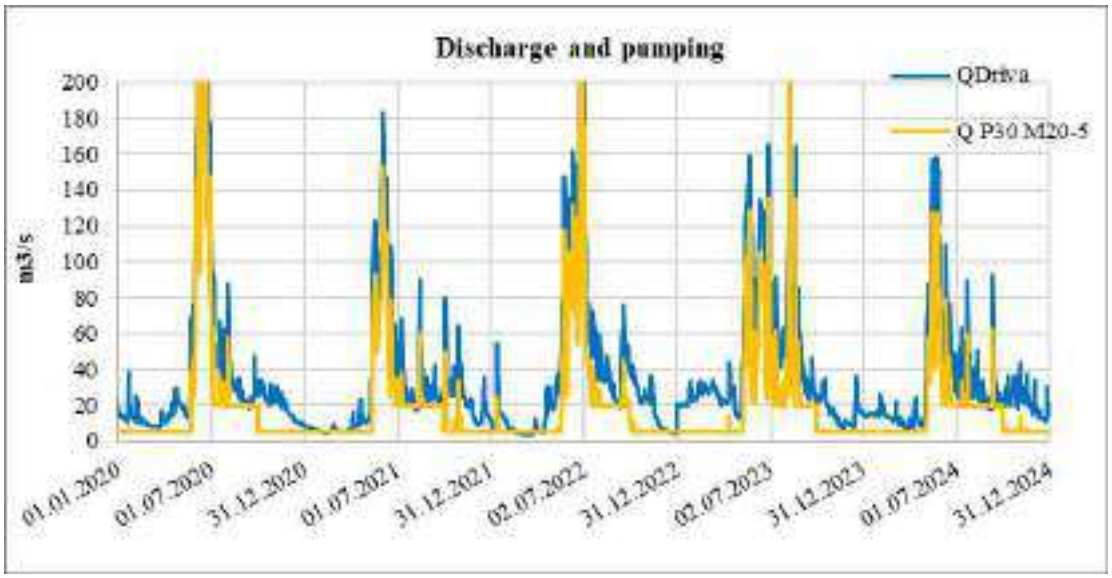

Fig. 4. Comparison between natural flow for the years 2020 to 2024.

2.4. Challenges

There are several challenges that need to be addressed. The first is that transferring water from the Driva River to the Gjevilvatnet lake in opposite direction of natural flow, introduces the risk of unintentionally spreading of invasive species.

Another knowledge gap concerns how the stability of the ice cover in the reservoir will be affected by pumping and power generation leading to fluctuating water levels during the winter period, and which areas around the intake will be influenced by the inflow of warmer water (Asvall, 2007).

The first analysis of pumping water from Driva River shows stable flows of around 20 m^3/s over a longer period in the river. It will be necessary to secure a variety of flow conditions during summertime.

3. Conclusion and further work

This preliminary study indicates that pumped-storage hydropower in the Driva catchment could enhance energy flexibility while preserving ecological objectives. Maintaining a minimum winter flow of 5 m^3/s and summer flows around 20 m^3/s is essential to preserve habitat quality and fish survival. The proposed concept shows potential for balancing surplus water transfer with environmental flow requirements, but further analysis is needed.

Future work will focus on:

- Detailed habitat assessments under low-flow conditions, particularly below 10 m^3/s, to validate and improve current estimates.
- Comprehensive calculations of pumping capacity and operational strategies for water release to optimize both energy production and ecological integrity.
- Evaluating how this pumped storage needs to develop to meet climate change challenges, ensuring both economic feasibility and adaptive river management.

Acknowledgements

I would like to thank TrønderEnergi, which gave us the possibility and permission to publish the data and this project.

References

Asvall, R. P. (2007). Selective withdrawel to reduce regulation effects on ice cover downstream outlet of Alta power plant. NVE.

Foldvik, A., Sundt-Hansen, L., Hindar, K. & Solem, Ø. 2023. Kartlegging av gyteområder og ungfiskhabitat i anadrom del av Drivavassdraget. NINA Rapport 2352. Norsk institutt for naturforskning.

Forseth, T and Harby, A. 2014. Handbook for environmental design in regulated salmon rivers. NINA Special Report 53, Trondheim, Norway.

Book of Abstracts of the *16th International Symposium on Ecohydraulics*
Challenges and solutions in the time of global changes
August 16–20, 2026, Lausanne, Switzerland
ISSN: 2790-2420 | ISBN: 978-90-837233-9-6 | doi:[10.64697/iahr.proc.ise2026.abs]
© 2026 IAHR. CC BY-NC-ND 4.0

CLASSIFYING HYDROMORPHOLOGICAL CONDITIONS FOR IMPACT ASSESSMENTS IN PROTECTED WATERCOURSES IN NORWAY USING A REMOTE SENSING APPROACH

Håkon SUNDT[1], Mauro CAROLLI[1], Atle HARBY[1]

[1] SINTEF Energi AS, Norway
email: info@sintef.no

ABSTRACT

Currently, there is an ever increasing need to facilitate the successful transition to sustainable and renewable energy production in a changing climate while also meeting global commitments on biodiversity. In Norway, watercourses protected from hydropower development only are now reconsidered for new hydropower development, but the public discussion is often based on a limited base of knowledge and facts. The *Biodiversity-energy nexus* project will seek to increase the knowledge base to induce an informed debate about priorities of societal objectives. More specifically, the project aims to develop a toolbox to evaluate protected watercourses regarding 1) existing anthropogenic impacts without hydropower, and 2) potential impacts of new hydropower development. In addition to biodiversity hotspot mapping (species richness, turnover and connectivity), a hydromorphological (HyMo) classification system was developed to assess potential anthropogenic impacts. A selection of HyMo indicators for classification were tested for compatibility with existing remote sensing (RS) data sources. As a first step towards a toolbox on watercourse HyMo classification, we set up a HyMo classification framework to 1) access relevant RS data sources, 2) delimit data to first order streams/reach scale, 3) calculate HyMo indicator levels, and 4) classify HyMo on reach scale. In the second step, we assessed the HyMo classification function of the original tool in a control reach by ground truthing using a combination of UAV-based multispectral imagery, LIDAR data and relevant national databases. Preliminary results indicate that certain HyMo indicators can be classified on reach scale using RS data, but securing significance in indicator levels requires additional field data for verification.

Keywords: Hydromorphology; Protected Watercourses; Remote Sensing; Anthropogenic Impacts; Classification

1. Defining the research questions

In Norway, the technical-economical feasible yearly potential for hydropower production is 216 TWh, while the current annual production amounts to 137 TWh (in 2024). Through five updates from 1973 through 2018, a Protection Plan for River Systems was implemented and included 387 watercourses to be protected from hydropower development. No other major anthropogenic impacts were included in the plans, and many of today's protected watercourses have been altered due to other human interferences. Currently, discussions are ongoing as to open protected rivers for hydropower production. The *Biodiversity-energy nexus* project aims to close the knowledge gap and provide facts to the debate on whether society should allow for development of new hydropower in protected watercourses. In addition to issues related to biodiversity and user interests (energy production, flood protection,

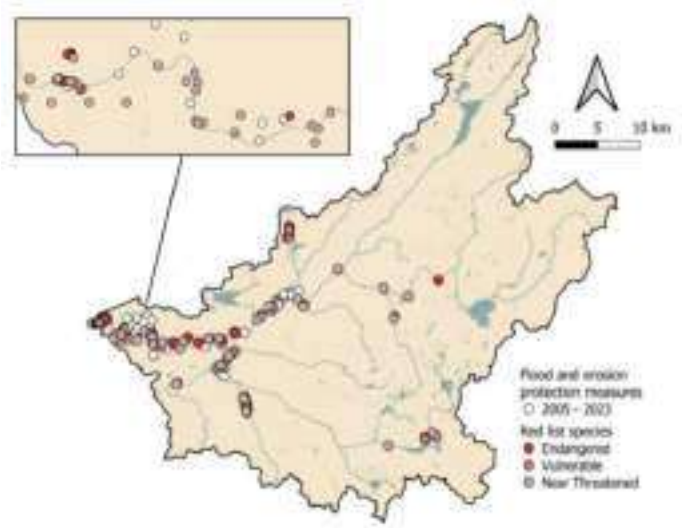

Figure 1: Hydromorphological impacts in a protected watercourse in Norway since the implementation of the Protection Plan.

recreational use, indigenous people), *a major research question deals with the assessment of the status of hydromorphological alterations in protected watercourses*.

2. Methodology

The research question was addressed by providing a tool to classify hydromorphological impacts in watercourses through a two-step approach: 1) Setting up a HyMo classification framework, and 2) Refining the framework using field data for HyMo ground truthing.

2.1. Using existing HyMo work to select indicators

The Water Framework Directive (WFD) is implemented as part of the Common Implementation Strategy. Currently in Norway, environmental conditions that comply with the WFD are only defined by ecological and chemical status. Hydromorphological status is yet to be implemented in environmental condition assessments of water bodies, but recently national consensus on relevant HyMo indicators that should be used has been reached.

There are three elements to consider when classifying hydromorphological conditions: 1) the hydrological system (quantity, variation and dynamics of discharge), b) river continuity (free passages for animals, plants, nutrients, water and sediments), and c) morphological conditions (physical properties of the river, riverbed substrate and structure). In the Norwegian method for HyMo classification proposed by Harby and Bakken (2023), the three above elements are described through four impact categories and their respective indicators as shown in Table 1.

Table 1: Norwegian system for hydromorphological classification sorted by impact category

Impact category	HyMo indicator	Indicator for change	Ecological impact strength / scientific evidence
Along the river (lateral)	Lateral connectivity	Running length of river impacted	Strong / High
	Embankments	Running length of river impacted	Strong / High
	Riparian vegetation	Running length of river with higher vegetation	Medium / High
	Channelization	Changes in sinuosity	Weak / Medium
	Incision	Average incision of the river	Medium / Medium
Across the river (longitudinal)	Instream barriers	Number of barriers (absolute / partly)	Strong / High
	Instream backwater effects	Running length of river impacted	Medium / Medium
	Barriers in upstream catchment/water bodies	Distance to upstream barrier	Strong / High
Instream	Removal/adding sand and gravel	Running meters of impacted river	Strong / Low
	Structures in the river	Running meters of impacted river	Medium / Medium
	Mesohabitats/river types	Changes in Shannon & Li and Reynolds indices	Strong / Medium
	Substrate size, roughness and porosity	Changes in shelter class	Medium / Low
Hydrology	Total flow	Changes in mean annual flow	Strong / High
	Summer low flow	Change in weekly low flow Jun-Sep	Medium / Medium
	Winter low flow	Change in weekly low flow Nov-Mar	Strong / Medium
	Annual floods	New return period for natural annual flood	Medium / High
	10-year floods	New return period for natural 10-year flood	Strong / Medium
	Short-term flow changes	Ratio between high and low flow	Medium / Low
	Ramping rates of flow changes	Dewatering ramping rate	Strong / High
	Dewatered riverbed	Reduction in wetted area	Medium / Medium

2.2. Setting up a HyMo classification framework tool

Five of the HyMo indicators were selected to be suited for inclusion in the classification framework tool. These were lateral connectivity, embankments, riparian vegetation, instream barriers and instream backwater effects. The indicators were selected based on 1) ecological impact strength and scientific evidence, 2) RS data compatibility on reach scale, and 3) relevance for large scale anthropogenic impact assessments in protected rivers.

Using *Jupyter Notebook* (based on *Python*) as a framework we programmed the tool to do a stepwise classification of the selected indicators on reach scale. The resulting indicator vectors and rasters were set up to be compiled in a SQL database including connections to biodiversity data using national river network identifiers.

2.3. Spatial and temporal resolution of datasets and indicators

Indicator classification was done using the highest available spatial resolution datasets available. Figure 2 shows the combination of riparian vegetation classification based on height calculated using DEM of difference from national terrain datasets and wetted area vector outline from Sentinel-2 NDWI classification. The DEM of difference classes are given on a 1x1m spatial scale while the Sentinel-2 derived wetted area are on a 10x10m spatial scale. Figure 2 also shows barriers (i.e., bridges and pillars, waterfalls) as discontinuities in wetted area polygons along the river (given as light blue coloring).

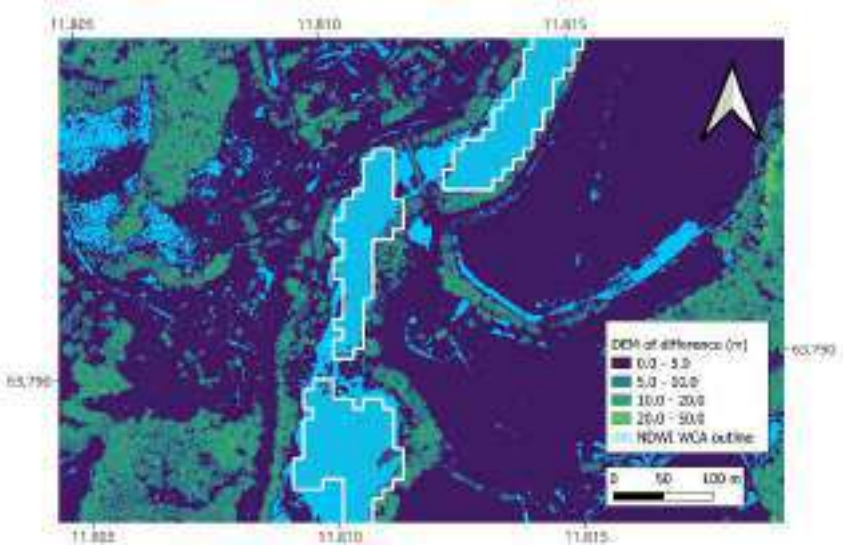

Figure 2: Riparian vegetation classification based on height calculated using DEM of difference from national terrain datasets and wetted area vector outline from Sentinel-2 NDWI classification in Verdalselva, Norway.

2.4. Refining the framework

In river Verdalselva, verification of tool classification of indicators was conducted using a combination of information derived from local UAV-based multispectral images and manual mapping of embankments, barriers and backwater effects, see Figure 3 for an example of a UAV image used to verify riparian vegetation zones along the riverbank. Additional information on instream mesoscale habitat types was also mapped on reach scale and used for connecting HyMo indicators to biodiversity data.

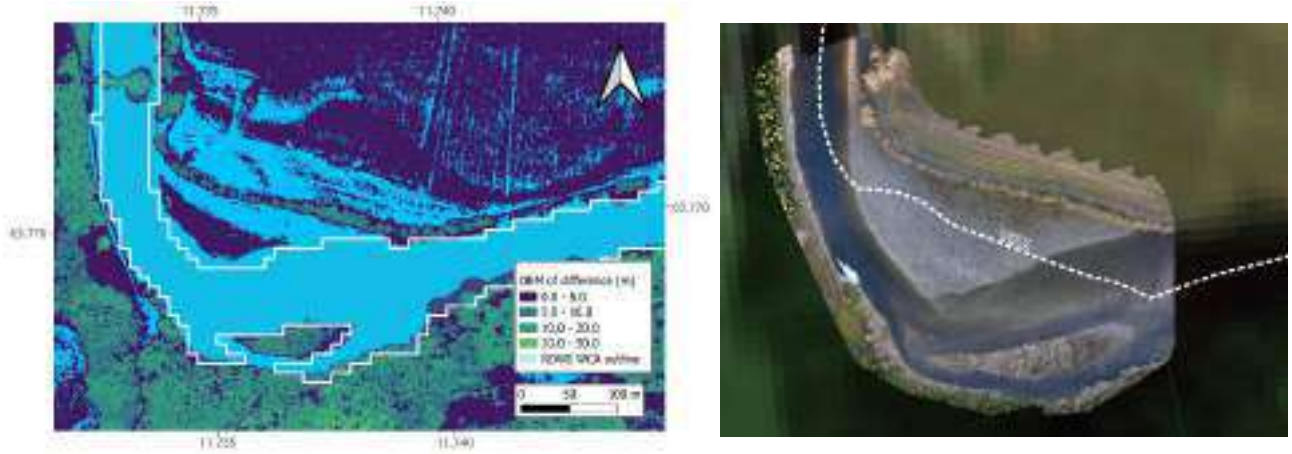

Figure 3: Riparian vegetation classification and wetted area outline (left) and UAV-image of the same river reach (right). Drone images are used for semiautomatic refinement classification of e.g., riparian vegetation and verification of additional indicator

3. Initial results and planned analysis

3.1. First steps

The first iteration of the Framework tool was tested in river Verdalselva. API access to national databases provided spatial vector and metadata on catchment and river networks. These data were coupled with cloud free Sentinel-2 data. Delimitation of data to only include main water courses was done through buffering based on stream order classification in the national river network database. In a final step before the final reach classification of the five HyMo indicators was calculating the wetted area from the Sentinel-2 data using NDWI classification.

3.2. Planned work for first half of 2026

Further plans for the development and refinement of the Framework tool are presented in Table 2, including algorithms to be implemented and possible national remote sensing data sources.

Table 2: Suggested approaches for reach scale HyMo indicator classification using remote sensing data sourcing

Indicator	Suggested approach for classification algorithm	Suggested approach for classification refinement/verification	RS data sources
Lateral connectivity	Combining national DTM and DOM for DOD along riparian zones, NDWI classification on Sentinel-2 images and national databases on erosion and flood mitigation measures	UAV image analysis through SfM, aerial photos	UAV images, national image databases
Embankments	Using national DTM and DOM for DOD along riparian zones (wetted area vector outline) and national databases on erosion and flood mitigation measures		
Riparian vegetation	Using national DTM and DOM for DOD along riparian zones (wetted area vector outline) and Sentinel-2 derived NDVI data		
Instream barriers	Combining national river network data, Sentinel-2 derived wetted area, national DTM in disruption analysis	UAV image analysis through SfM, aerial photos, green LIDAR, Supervised classification/Machine learning	UAV images, national image databases, LIDAR/DTM
Instream backwater effects.	Based on instream barrier algorithms with additional data on wetted area shape upstream potential barriers		

References

Harby A & Bakken TH (2023) HyMo 1.0 - Hydromorfologisk klassifisering av vannforekomster i elver og innsjøer (English: Hydromorphological classification of water bodies in rivers and lakes), Norwegian Environment Agency, 55 pp. HyMo 1.0 - Hydromorfologisk klassifisering av vannforekomster i elver og innsjøer - miljodirektoratet.no

Book of Abstracts of the *16th International Symposium on Ecohydraulics*
Challenges and solutions in the time of global changes
August 16–20, 2026, Lausanne, Switzerland
ISSN: 2790-2420 | ISBN: 978-90-837233-9-6 | doi:[10.64697/iahr.proc.ise2026.abs]
© 2026 IAHR. CC BY-NC-ND 4.0

ADVANCING LIMNOLOGICAL RESEARCH IN CENTRAL ASIA: CONTRIBUTIONS TO FRESHWATER BIODIVERSITY AND ECOLOGY FROM THE HYDRO4U PROJECT

Daniel S. HAYES[1], Erkin KARIMOV[2], Pieterjan VERHELST[3], Otabek OMONOV[2], Andrea FUNK[1], Ianina KOPECKI[4], Johan COECK[3], Bakhtiyor K. KARIMOV[2], Jan DE KEYSER[5], Fazliddin MUHAMMADIYEV[2], Matthias SCHNEIDER[4], Bernhard ZEIRINGER[1], Bertalan ALAPFY[6], Justine CAREY[1], Carina SELIGER[1], Falko WAGNER[7], Tom ROESSGER[8], Martin SCHLETTERER[1]

[1] BOKU University, Institute of Hydrobiology and Aquatic Ecosystem Management, Austria
email: daniel.hayes@boku.ac.at
[2] Tashkent Institute of Irrigation and Agricultural Mechanization Engineers, National Research University, Uzbekistan
[3] Research Institute for Nature and Forest (INBO), Belgium
[4] SJE Ecohydraulic Engineering GmbH, Germany
[5] BOKU University, Institute of Hydraulic Engineering and River Research, Austria
[6] Technical University Munich, Chair of Hydraulic Engineering, Germany
[7] Institute of Aquatic Ecology and Fish Biology Jena, Germany
[8] Dresden University of Technology, Institute of Hydraulic Engineering and Technical Hydromechanics, Germany

ABSTRACT

Central Asian freshwater ecosystems face increasing pressure from anthropogenic activities, including the expansion of water infrastructure for irrigation and hydropower. In addition to these challenges, knowledge of the biogeography and ecology of aquatic organisms in the region remains limited. This study, conducted as part of the "Hydro4U" project, aims to address these knowledge gaps by investigating regional freshwater biodiversity as well as habitat use and seasonal migration patterns of a key fish species in Central Asia. We conducted fish surveys across >100 sites in over 80 rivers, complemented by environmental DNA sampling at a subset of sites, to assess large-scale biodiversity patterns. Additionally, we studied longitudinal zonation of benthic macroinvertebrate communities in the Shakhimardan River Basin. The key fish species, *Schizothorax eurycephalus*, was studied in detail to understand its migration patterns and seasonal habitat preferences. We employed radio telemetry to track the seasonal movements of tagged individuals over a two-year period between the Shakhimardan River and its headwaters, the Koksu and Aksu Rivers. Our results reveal significant spatial and altitudinal variability in aquatic biodiversity. Macroinvertebrate communities showed clear longitudinal zonation, with abundance and composition varying along the altitudinal gradient. Seasonal migration patterns of tagged fish indicate that *S. eurycephalus* use tributaries like the Koksu River as winter refugia, likely due to warmer water temperatures. These findings provide valuable insights into the ecology of Central Asian river systems and a baseline for biomonitoring, ecohydraulic studies, and Red List assessments.

Keywords: *snowtrout; snow barbel; Schizothoracinae; macroinvertebrates; water management; e-flow; fish protection facilities; Syr Darya River Basin*

1. Introduction

Freshwater ecosystems in Central Asia face increasing pressure from anthropogenic impacts, including land use changes and water infrastructure development. However, knowledge of biogeography and ecology of aquatic organisms remains limited. Most studies on freshwater biota were conducted some decades ago, particularly when Central Asia was still part of the Soviet Union (1918-1991), and focused primarily on geomorphological river dynamics, fish species systematics, and distribution patterns at the broad river catchment level (e.g., Berg, 1948; Nikolsky, 1938). Water regulation infrastructure in Central Asia is expanding. Agriculture and irrigation have traditionally been prioritized; now hydropower development is increasingly in focus (De Keyser et al., 2026). Most dams and weirs, however, are without adequate environmental flow releases, fish protection measures, and fish migration corridors (Alapfy et al., 2025). There

is, therefore, a pressing need to advance research on biogeography, ecology, and ecohydraulics to guide river management and aquatic conservation efforts.

One of the aims of the EU Horizon 2020 project "Hydro4U" is to fill this knowledge gap by (i) studying the current distribution of freshwater biota, classifying species assemblages according to natural abiotic characteristics and anthropogenic impacts at a large-scale (fish) and along a longitudinal gradient (macroinvertebrates), and (ii) studying migration patterns and seasonal habitat use of *Schizothorax eurycephalus* (Berg, 1932), a target fish species in the Syr Darya River basin.

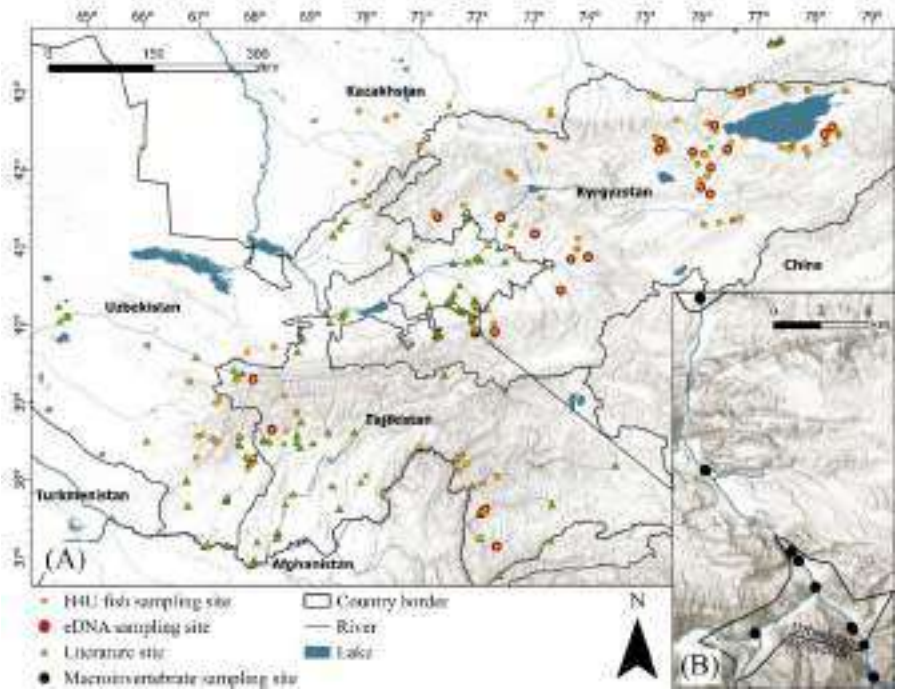

Fig. 1. Study area, showing (a) the distribution of sampling sites in high-mountain Central Asia (some sites [from the literature] are not shown as they are outside the range of panel a), and (b) the transboundary Shakhimardan River basin, the case study for assessments on fish ecology and macroinvertebrate community zonation.

2. Methods

2.1. Freshwater biodiversity assessments

Fish presence/absence surveys were conducted in rivers throughout Central Asia (**Fig. 1a**). Sites were sampled via electrofishing or (where electrofishing permission was not granted) using nets or angling. In addition, we complemented our field efforts with data from recent literature. In total, our dataset spans >100 sites from over 80 rivers. Moreover, at 23 sites, we collected environmental DNA (eDNA) samples (n=131). River water was filtered manually through Whatman® glass microfiber filters (grade GF/F, 25 mm) using sterile 50 mL syringes. The number of replicates depended on turbidity (range: 4-10, including control sample of distilled water). The filters were stored in Longmire lysis buffer for DNA preservation. They were analyzed in the laboratory for fish using 12S metabarcoding, next-generation sequencing (NGS) (Funk et al., in prep).

We also conducted quantitative sampling of benthic macroinvertebrate communities in the Shakhimardan River basin, located in the Alay Mountain range. In March 2025, we collected samples from ten sites (**Fig. 1b**) along an altitudinal gradient from 1,581 to 964 m, using a standard kick-net method with a 500 µm mesh. Sampling of macroinvertebrates was carried out in the dominant microhabitats. At each site, at least five microhabitats were sampled and stored separately. The collected samples were preserved in 96% ethanol and transported to the laboratory. Macroinvertebrates were identified at the family level; species-level identification was performed when possible.

2.2. Snow trout ecology: fish migration, seasonal habitats, and hydraulic cues

We studied the movement ecology of snow trout (*S. eurycephalus*), a socio-economically important fish species, and an ecological indicator, in the Shakhimardan basin (**Fig. 1b**). For the first time, snow trout migration and seasonal habitat use were assessed in detail using radio telemetry and recording habitat characteristics of detected fish via a QField Mapper application. In October 2022, 27 snow trout were tagged

with radio transmitters (Advanced Telemetry Systems) and tracked until July 2024 (i.e., 21 months). The fish were positioned manually via a hand-held receiver (ATS R2000 radio receiver) every one to two weeks.

Moreover, in collaboration with the OptiPass project (Kopecki et al., 2026), we experimentally tested snow trout responses to hydraulic cues when migrating downstream. Better understanding of how spatial velocity gradients influence migration can help to identify optimal bypass designs tailored to local fish species.

3. Results and Discussion

3.1. Large-scale fish biodiversity

Field surveys recorded 50 fish taxa. Integration of literature data increased this to 99 taxa across 131 rivers; 24 of them are endemic. Richness was highest at sites <750 m altitude (83 taxa), with communities dominated by *Pseudorasbora parva*, *Triplophysa strauchii*, *Carassius gibelio*, *Abbottina rivularis*, *S. eurycephalus*. Conversely, the high alpine zone (>3,000 m) exhibited the lowest richness with only 10 taxa, particularly *T. stoliczkai* and *Schizopygopsis sewerzowi*. In our dataset, *T. stoliczkai* exhibited the broadest altitude range from around 370 to 3,750 m, followed by *S. gobioides* (380-3,530 m). The most frequent species was *S. eurycephalus*, recorded in 35 distinct river systems, followed by *P. parva* and *S. gobioides*. In contrast, around one third of all taxa were caught only in one river system.

For the first time, environmental DNA metabarcoding using the 12S gene marker was applied to assess fish biodiversity in Central Asian rivers. After stringent bioinformatic filtering and taxonomic assignment, e.g. ≥99% reference sequence for species assignment (Hänfling et al., 2016), a diverse regional fish assemblage was revealed, with *Schizothorax* sp. and *Triplophysa* sp. being the most frequent taxa. The data also revealed signals from anthropogenic activities, including stocked *Salmo ischchan*. Preliminary community composition analysis showed clear gradients along hydrogeomorphic variables (e.g., slope, altitude, minimum discharge) (**Fig. 2a**). These results highlight the structuring role of river geomorphology on fish assemblages in Central Asian mountain streams (Funk et al., in prep.).

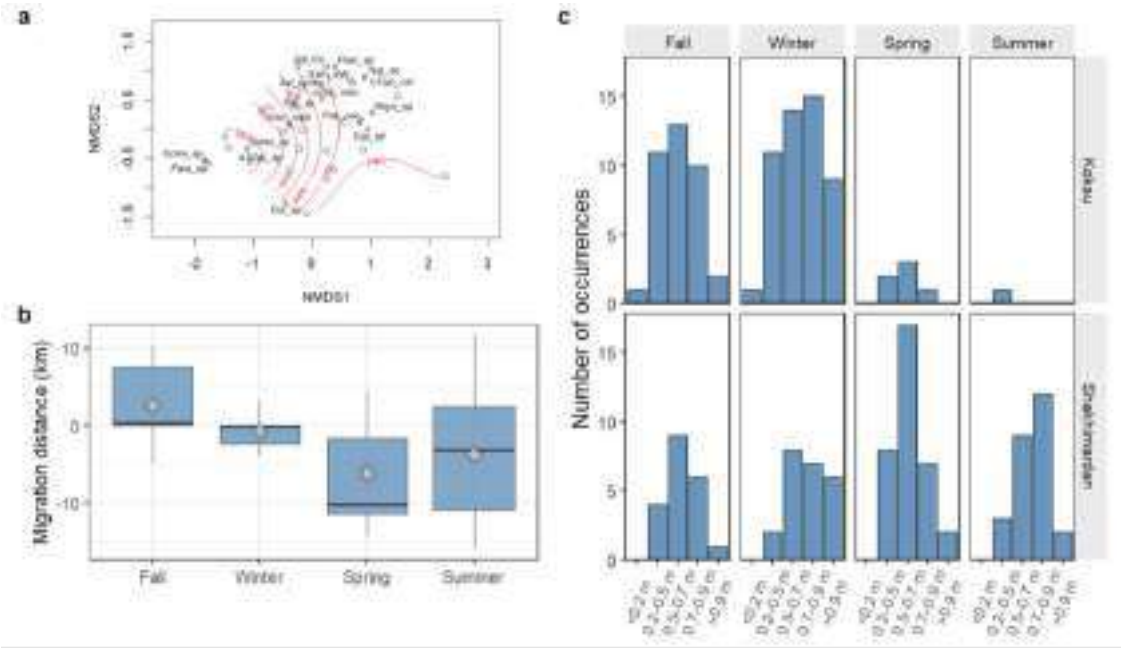

Fig. 2. (a) Non-metric multidimensional scaling (NMDS) plot of the altitudinal gradient and fish taxa (eDNA samples); seasonal patterns of radio-tagged *S. eurycephalus*: (b) migration distances (median=black line; mean=grey diamond) and (c) habitat use (water depth) in Koksu and Shakhimardan Rivers.

3.1. Longitudinal zonation of macroinvertebrates in the Shakhimardan Basin

Mean macroinvertebrate density was 665±368 ind./m². It was lowest near the river source (469 ind./m²), increasing downstream. Maximum abundance occurred in the Aksu River (1,415 ind./m²), decreasing further downstream. Communities were dominated by EPT-Taxa (65.4±6.3%) and Diptera (28.2±10.0%). Oligochaeta were scarce (4.7±7.5%) (Muhammadiyev et al., 2025).

3.2. Migration patterns, seasonal habitat shifts, and hydraulic thresholds

Of the 27 tagged snow trout, 19 individuals yielded high-quality data over two years (Oct 2022-July 2024). Nearly all fish used both the Shakhimardan mainstem and the groundwater-fed Koksu tributary. Clear seasonal

migration occurred (**Fig. 2b**): downstream movement peaked in spring/early summer, while upstream migration into the Koksu River dominated in fall (Sept–Oct). Many fish overwintered in the Koksu River (Sept–Mar), likely using its warmer, thermally stable waters as a refuge, with minimal movement during winter. Seasonal habitat use varied markedly. In fall and winter, fish occupied depths of 0.5–0.9 m in both rivers, plus shallow (0.2–0.5 m) and deep (>0.9 m) zones, especially in Koksu River. Spring depths remained at 0.5–0.7 m, but individuals largely vacated Koksu River. In summer, fish concentrated in the Shakhimardan River, predominantly at depths ranging from 0.5 to 0.9 m (**Fig. 2c**). Across all seasons, snow trout strongly selected flow velocities of 0.4–1.5 m/s, underscoring the need to maintain fast-flowing, structurally diverse habitats (Omonov et al., submitted).

As part of Hydro4U's demonstration activities, a 2 MW diversion hydropower plant, using the Francis Container Power Solution, was constructed at Koksu River (Alapfy et al., 2025). Based on our ecological assessments, an environmental flow (Hayes et al., 2025) as well as a vertical slot fishway for upstream and a bypass system for downstream migration were implemented.

An assessment of downstream bypass acceptance at the Koksu hydropower plant showed that, under natural conditions, *S. eurycephalus* exhibit avoidance reactions to flow acceleration comparable to those documented for *Barbus barbus*. In detail, *S. eurycephalus* specimens delayed downstream passage in zones with a spatial velocity gradient >0.23 m s^{-1} m^{-1}.

3.3. Conclusions and outlook

Central Asia's hydropower potential offers a pathway to carbon-neutral energy, yet its sustainable development hinges on robust ecological understanding of the region's rivers. The Hydro4U project delivers critical baseline data on freshwater biodiversity, altitudinal and longitudinal community gradients, and the ecology of *S. eurycephalus*, a potamodromous species sensitive to longitudinal habitat fragmentation. This kind of knowledge is essential for safeguarding freshwater ecosystems, guiding environmentally sound development, and aligning hydropower operations with ecological requirements (Hayes et al., 2025). Large-scale results will be integrated into online decision-support systems and used to update global assessments, such as the IUCN Red List of Threatened Species.

Future work should prioritize long-term biomonitoring programs built on the baselines established in Hydro4U, expand eDNA surveillance across additional catchments and organism groups (such as macroinvertebrates), and test fish passage and downstream-migration facilities under real-world Central Asian settings. Such efforts will help ensure that the region's transition to renewable energy strengthens, rather than compromises, its unique and still poorly known freshwater biodiversity.

Acknowledgements

The Hydro4U project has received funding from the European Union's Horizon 2020 research and innovation programme under grant agreement No 101022905. Sampling equipment for eDNA was funded by a Microgrant from the eDNA Collaborative in January 2023 (to Erkin Karimov). We thank the Verein für Ökologie und Umweltforschung (VÖU) and Kleinwasserkraft Österreich for funding eDNA laboratory analysis. The OptiPass project is funded by the German Federal Environmental Foundation (DBU).

References

Alapfy B, Hayes DS, De Keyser J, Jorde K, Karimov B, Kopecki I, Verhelst P (2025) Progress in the implementation of sustainable small hydro in Central Asia. *The International Journal on Hydropower & Dams*, 32(1), 35-40.

Berg LS (1948) Fishes of Fresh Waters of the USSR and Adjacent Countries. Akad. Nauk SSSR, Moscow, 496 pp.

De Keyser J, Fuentes PO, Hayes DS, Habersack H (2026) A review of hydropower in Central Asia: past, present, and future. *Renewable and Sustainable Energy Reviews*, 226 (Part A), 116239. https://doi.org/10.1016/j.rser.2025.116239

Funk A, Hayes DS, Karimov E, Karimov B, Omonov O, Wallinger C, Traugott M, Schletterer M (in prep.) Assessing Central Asia's river fish community using environmental DNA.

Hänfling B, Handley LL, Read DS, Hahn C, Li J, Nichols P, Blackman RC, Oliver, A, Winfield IJ (2016). Environmental DNA metabarcoding of lake fish communities reflects long-term data from established survey methods. *Molecular Ecology*, 25, 3101-3119.

Hayes DS, Hägele T, Kopecki I, Zeiringer B, Karimov E, Karimov BK, Coeck J, Verhelst P, De Keyser J, Omonov O, Schneider M (2025) Environmental flows assessment integrating snow trout habitat requirements in the Shakhimardan basin, Central Asia. *International Journal of Environmental Science and Technology*, 22, 16935–16946. https://doi.org/10.1007/s13762-025-06761-2

Kopecki I, Roessger T, Wagner F (2026) Optimization of fish bypass entrances: The Optipass Approach. *Proceedings of the 16th International Symposium on Ecohydraulics*, Lausanne, Switzerland.

Muhammadiyev F, Hayes DS, Karimov B, Schletterer M (2025) Quantitative assessment of macroinvertebrates in the Shakhimardan River Basin. *Proceedings of the XVth All-Russian Trichopterological and Xth All-Russian with International Participation Symposium on Amphibiotic and Aquatic Insects*, 18-23 May 2025, Vladikavkaz, Russia 249-257. ISBN 978-5-00081-718-6

Nikolsky GV (1938). Fishes of Tadjikistan. Acad. Sci. USSR, Moscow, Leningrad.

Omonov O, Verhelst P, Coeck J, Dockx R, Goethals P, Karimov B, Karimov E, Kopecki I, Oldoni D, Schletterer M, Hayes DS (submitted) Migration patterns and seasonal habitat shifts of snow trout in a Central Asian mountain river.

Book of Abstracts of the *16th International Symposium on Ecohydraulics*
Challenges and solutions in the time of global changes
August 16–20, 2026, Lausanne, Switzerland
ISSN: 2790-2420 | ISBN: 978-90-837233-9-6 | doi:[10.64697/iahr.proc.ise2026.abs]
© 2026 IAHR. CC BY-NC-ND 4.0

FROM PHOSPHORUS CONTROL TO HABITAT RESPONSE: WATER COLUMN RECOVERY AND LEGACY SEDIMENT EFFECTS IN A CHALK STREAM

Giuditta TRINCI[1], Kate HEPPELL[1,2], Thomas KELLY[1], Geraldene WHARTON[1]

[1] Department of Geography and Environmental Science, Queen Mary University of London, UK
email: giuditta.trinci@qmul.ac.uk
email: g.wharton@qmul.ac.uk
email: t.kelly@qmul.ac.uk
[2] Chiltern National Landscape, UK
email: kheppell@chilterns.org.uk

ABSTRACT

This study evaluates the effects of phosphorus stripping at Chesham Sewage Treatment Works (CSTW) on water quality and habitat recovery in the River Chess, a globally rare UK chalk stream. Chalk streams support ecologically distinctive habitats sustained by clear, mineral-rich groundwater and aquatic macrophyte communities, but they are highly vulnerable to nutrient enrichment and urban pressures. High-frequency monitoring data from the Chess Watch citizen science programme, together with Modular River Surveys (https://docs.modularriversurvey.org/) and laboratory analyses of water and sediment quality, are providing a framework for assessing changes in physicochemical characteristics and soluble reactive phosphorus (SRP) concentrations. Preliminary results show that SRP concentrations downstream of CSTW declined by 74.6% following phosphorus stripping, with partial improvement in Water Framework Directive (EC, 2000) compliance. However, compliance remained below target, and sediment analyses identified elevated legacy phosphorus stores downstream, likely constraining recovery. Findings suggest that phosphorus stripping alone may be insufficient for rapid ecological restoration, highlighting the need for sustained integrated catchment management and long-term monitoring of both sediment-bound and dissolved phosphorus.

Keywords: chalk streams; soluble reactive phosphorus; sewage treatment; bed sediment; monitoring

1. Introduction

The River Chess is one of the 256 chalk streams in the UK that provide unique, ecologically significant and distinctive habitats for aquatic biota (English Nature and Environment Agency, 1999; Robinson et al., 2022). Chalk streams are groundwater-fed, resulting in baseflow dominance, clear water rich in minerals, thermal stability, and fine-scale hydraulic heterogeneity (Bowes et al., 2005), all of which support ecological distinctiveness (Mainstone and Parr, 2022). These hydrological conditions sustain dense communities of aquatic macrophytes, principally Ranunculus spp., whose submerged patches are not only ecological indicators but structural elements of the hydraulic habitat (Cotton et al., 2006), generating the velocity gradients and near-bed turbulence on which brown trout and diverse invertebrate communities depend (Wharton et al., 2006). This unique environment makes chalk streams particularly vulnerable to anthropogenic pressures such as abstraction, nutrient enrichment, fine sediment, and urbanisation (Salter and Singleton-White, 2019). Abstraction for water supply can modify chalk stream hydrology and reduce stream discharge (Rameshwaran et al., 2021) and climate change may further influence hydrological regimes through an increased occurrence of extreme weather events such as droughts and intense rainfall (Stubbington et al., 2022; Bolan et al., 2024). Reduced river flows can decrease pollutant dilution capacity and contribute to higher water temperatures (UKCEH, 2022). Although rainfall events may increase dilution temporarily, they can also elevate pollutant inputs via surface runoff and Combined Sewer Overflow (CSO) discharges when wastewater treatment infrastructure exceeds operational capacity. Together, these pressures can adversely affect the ecological condition and functioning of chalk stream systems. On the River Chess, one of the dominant threats is point-source pollution from the Chesham Sewage Treatment Works (CSTW), which discharges a mixture of

untreated combined sewer overflows and treated effluent into the river (Thames Water, 2021), contributing to catchment-wide phosphorus non-compliance with WFD. Nutrient enrichment alters stream ecology by modifying dissolved oxygen dynamics and accelerating eutrophication (Bowen et al., 2005). These impacts frequently result in excessive algal growth, reductions in dissolved oxygen, the formation of hypoxic "dead zones," and declines in biodiversity, all of which damage ecosystem functioning (Wurtsbaugh et al., 2019). For instance, fish mortality incidents in England, including deaths of brown trout, increased tenfold between 2020 and 2024 and were associated with a 54% rise in sewage discharges (Wild Trout Trust, 2024). Understanding how changes in treatment practices at STWs that deliver point-source nutrient management translate into habitat recovery remains a critical and poorly evidenced challenge for river science and environmental policy. This study examined how the intervention of phosphorus-stripping at Chesham Sewage Treatment Works changed the downstream water and sediment quality in the River Chess, and highlighted how nutrient-rich legacy sediments are influencing the trajectory of chemical and ecological recovery in this chalk stream system.

2. Methodology

The study design takes advantage of a natural experiment created by the installation of phosphorus-stripping infrastructure at Chesham Sewage Treatment Works (CSTW) on 12 February 2025. Four main sites (two upstream control sites and two downstream impact sites) were selected based on their hydrological position, accessibility, and integration within ongoing monitoring programmes. This intervention and the four sites enable a Before–After–Control–Impact (BACI) framework to assess spatial and temporal changes in physicochemical conditions associated with wastewater management.

The study employed a multi-method approach integrating field sampling, laboratory analysis, and secondary data from Citizen Science programmes (Chess Watch and MoRPh Rivers). The Chess Watch citizen science monitoring scheme (Heppell et al., 2021), co-developed by the River Chess Association, Chilterns Chalk Streams Project, and Queen Mary University of London, has maintained continuous, high-frequency water quality monitoring across four sites on the River Chess and Little Chess tributary since 2018.

Continuous water quality sondes deployed at all four sites (Sites A (Blackwell Hall: 51°41.292' N, 0°35.069' W), B (Willow Cottage: 51°41.04' N, 0°35.23 W); Sites C (Restore Hope:51°40.702' N, 0°33.773' W) and D (Sarratt: 51°40.804' N, 0°30.997' W) record temperature, dissolved oxygen, electrical conductivity, pH, and turbidity at 15-minute intervals. Furthermore, water samples for laboratory analysis of soluble reactive phosphorus (SRP) and nitrate have been collected at regular intervals since 2023, providing a continuous pre- and post-intervention record. SRP compliance is assessed against the WFD Good ecological status threshold of 0.06 mg P L^{-1}.

A total of 36-bed sediment surface samples were also collected and analysed using sequential phosphorus fractionation to identify bioavailable phosphorus stores and evaluate the potential influence of legacy sediment phosphorus on river recovery.

Finally, MoRPh Rivers (Shuker et al., 2017) has been used to monitor physical habitat characteristics and human pressures over short reaches of the River Chess and in this study and in this study MoRPh surveys assessed changes in physical habitat conditions before and after the intervention.

3. Preliminary results

Preliminary analysis indicates that pre-intervention, mean soluble reactive phosphorus (SRP) at the primary impact site (Site C, immediately downstream of CSTW) was approximately 2.4 times the WFD Good Ecological Status threshold, with 0% compliance. Following phosphorus stripping, mean SRP at Site C fell by approximately 74.6%, with WFD compliance rising to 23.5%. This is an encouraging improvement, though the river remains non-compliant. Bed sediment analysis reveals elevated bioavailable phosphorus downstream of CSTW, identifying legacy sediment stores as a persistent internal loading mechanism likely to constrain full recovery of the water column. Sequential phosphorus fractionation of bed sediments at three of the sites (A, C and D) reveals substantially elevated bioavailable phosphorus fractions downstream of CSTW, identifying legacy sediment stores as an internal loading mechanism likely to constrain water column recovery independently of further reductions in effluent quality. Legacy sediment stores, combined with continuing population growth and rising diffuse inputs, suggest the phosphorus-stripping upgrade alone may not deliver

rapid ecological recovery. Sustained, integrated sediment and water quality monitoring is recommended to evaluate longer-term improvements in this globally rare habitat, in combination with ongoing MoRPh Rivers and Riverfly monitoring.

Acknowledgements

Thank you to QMUL laboratory technician, Megan Dougherty, and students, Millie Stears, Simone Swaby, Chiara Buquicchio, Lewis Ingham, who helped with fieldwork and laboratory analysis.

References

Bolan, S., Padhye, L.P., Jasemizad, T., Govarthanan, M., Karmegam, N., Wijesekara, H., Amarasiri, D., Hou, D., Zhou, P., Biswal, B.K., Balasubramanian, R., Wang, H., Siddique, K.H.M., Rinklebe, J., Kirkham, M.B. and Bolan, N. (2024). Impacts of climate change on the fate of contaminants through extreme weather events. Science of the Total Environment, 909, p.168388. doi: https://doi.org/10.1016/j.scitotenv.2023.168388

Bowes, M.J., Leach, D.V. and House, W.A. (2005). Seasonal Nutrient Dynamics in a Chalk stream: the River Frome, Dorset, UK. Science of the Total Environment, 336(1-3), pp.225–241. doi: https://doi.org/10.1016/j.scitotenv.2004.05.026

Cotton J.A., Wharton G., Bass J.A.B., Heppell C.M. & Wotton R.S. (2006) The effects of seasonal changes to in-stream vegetation cover on patterns of flow and accumulation of sediment. Geomorphology, 77, 320–334.

[EC] European Commission 2000. Directive 2000/60/EC of the European Parliament and of the Council of 23rd October 2000 establishing a framework for Community action in the field of water policy. Official Journal of the European Communities, L32 7/1. European Commission, Brussels.

English Nature and Environment Agency (1999) Chalk Rivers: Nature Conservation and Management. English Nature, Peterborough, UK, 184 pp.

Heppell, C., Bartlett, A., Beechley, A., Jennings, P. and Soteriou, H. (2021). Observations on a Citizen Science approach to catchment management. [online] London: QMUL. Available at: https://www.qmul.ac.uk/media/qmul/about/sustainability/documents/ChessWatch.pdf.

Mainstone C.P. & Parr W. (2002) Phosphorus in rivers – ecology and management. Science of the Total Environment, 282, 25–47. DOI: https://10.1016/s0048-9697(01)00937-8

Rameshwaran, P., Bell, V.A., Brown, M.J., Davies, H.N., Kay, A.L., Rudd, A.C. and Sefton, C. (2021). Use of Abstraction and Discharge Data to Improve the Performance of a National-Scale Hydrological Model. Water Resources Research, 58(1). doi: https://doi.org/10.1029/2021wr029787

Robinson, R.F.A., Mills, G.A., Gravell, A., Schumacher, M. and Fones, G.R. (2022). Occurrence of organic pollutants in the River Itchen and River Test—two chalk streams in Southern England, UK. Environmental Science and Pollution Research, 30(7). doi: https://doi.org/10.1007/s11356-022-23476-w.

Salter, M. and Singleton-White, S. (2019). Chalk Streams in Crisis: a Call for Drought Action Now. [online] Chilterns Chalk Stream Project . Available at: https://www.chilternstreams.org/chalk-streams-in-crisis/ [Accessed 22 May 2026].

Shuker, L.J., Gurnell, A.M., Wharton, G., Gurnell, D.J., England, J., Finn Leeming, B.F. and Beach, E., 2017. MoRPh: a citizen science tool for monitoring and appraising physical habitat changes in rivers. Water and Environment Journal, 31(3), pp.418-424.

Stubbington, R., Dimon, J., England, J. and Watts, G., 2022. Chalk streams of the future: the effects of climate change on biodiversity in England's iconic river ecosystems. Available at: https://dynamicstreams.wixsite.com/website/publications [Accessed: 26.05.2026]

Thames Water (2021). Groundwater Impacted System Management Plan Chesham, River Chess. [online] Available at: https://www.thameswater.co.uk/media-library/home/about-us/regulation/drainage-reports/groundwater-infiltration-management-plans/chesham-groundwater-infiltration-management-plan.pdf [Accessed 22 May2026].

UKCEH (2022). The Impacts of Drought on Water Quality and Wildlife . [online] www.ceh.ac.uk. Available at: https://www.ceh.ac.uk/news-and-media/blogs/impacts-drought-water-quality-and-wildlife [Accessed 22 May 2026].

Wharton G., Cotton J.A., Wotton R. S., Bass J.A.B., Heppell C.M., Trimmer M., Sanders I.A. & Warren L.L. (2006) Macrophytes and suspension-feeding invertebrates modify flows and fine sediments in the Frome and Piddle catchments, Dorset (UK). Journal of Hydrology, 330, 171–184. 10.1016/j.jhydrol.2006.04.034

Wild Trout Trust (2024). Sewage in Rivers: What you Need to Know in 2024 | Wild Trout Trust. [online] Wild Trout Trust. Available at: https://www.wildtrout.org/wttblog/sewage-in-rivers [Accessed 22 May 2026].

Wurtsbaugh, W.A., Paerl, H.W. and Dodds, W.K. (2019). Nutrients, eutrophication and harmful algal blooms along the freshwater to marine continuum. Wiley Interdisciplinary Reviews: Water, 6(5). doi: https://doi.org/10.1002/wat2.1373

Session B1

Urban, suburban, and periurban streams

Book of Abstracts of the *16th International Symposium on Ecohydraulics*
Challenges and solutions in the time of global changes
August 16–20, 2026, Lausanne, Switzerland
ISSN: 2790-2420 | ISBN: 978-90-837233-9-6 | doi:[10.64697/iahr.proc.ise2026.abs]
© 2026 IAHR. CC BY-NC-ND 4.0

PREDICTING EUTROPHICATION POTENTIAL OF AN URBAN WETLAND IN BRAHMAPUTRA VALLEY, INDIA: APPLICATION OF A 1D-2D HYDRODYNAMIC AND WATER QUALITY MODEL

Daisy KOCH[a], Dhrubajyoti SEN[b], Ashok Kumar GUPTA[c]

[a]School of Water Resources, Indian Institute of Technology Kharagpur, Kharagpur, 721302, India

Email: daisykoch@gmail.com

[b,c]Department of Civil Engineering, Indian Institute of Technology Kharagpur, Kharagpur, 721302, India

E-mail addresses: djsen@civil.iitkgp.ac.in (D. Sen), agupta@civil.iitkgp.ac.in (A.K. Gupta)

ABSTRACT

Eutrophication is a major threat to the urban wetland Deepor Beel, situated in northeast India, adjacent to the city of Guwahati in the Brahmaputra River valley, northeast India. The influx of water into it from the city having a poor quality, and spatial shrinkage due to urbanization have plagued the wetland, a Ramsar site and a resting place for migratory birds and home to a number of endangered floral and faunal species. The wetland's major source of inflow, the Basistha channel, drains the nearby urban catchments, and this study models the combined urban catchment-inlet channel-wetland system using a coupled 1D-2D hydrodynamic and water quality model using the modelling software, MIKE. This approach bridges the gap in traditional water quality assessment techniques, through its ability of predictive, scenario-based simulations. In this study, two key water quality indicators, dissolved oxygen (DO) and biological oxygen demand (BOD), are taken as representative of water quality indicators and the Trophic State Index (TSI) was taken as an indicator of eutrophication in the wetland. The results establish the significance of dilution and reaeration for maintaining good water quality in a small channel like Basistha, and its impact on the variation of DO and BOD across the spatial extent of Deepor Beel. Areas showing high BOD and low DO are identified as locations having poor water quality, and with a potential for eutrophication observed from the TSI levels. The key findings of this study highlight the usefulness of the modelling approach for identifying potential eutrophication zones in urban wetlands, thereby contributing to its conservation and management. This innovative methodological framework will be proficient for eutrophication studies of urban wetlands, especially in the South and Southeast Asia regions.

Keywords: Water quality; urban wetland; eutrophication; hydrodynamic and water quality model

1. Introduction

Deepor Beel, a freshwater wetland located in northeast India, on the southern bank of the Brahmaputra River, is chosen as a representative urban wetland undergoing stresses of urbanization, encroachment and pollution. The water quality and ecosystem health of this wetland has seen a steady decline over the last few decades along with shrinkage of its spatial area. This study makes use of the hydrological and hydraulic capabilities of the MIKE software package to model the connectivity of the wetland to its peri-urban catchment through the major inlet channel, Basistha. The environmental modelling tool of the package is then used to model the water quality variations within the wetland, with the untreated wastewater and stormwater runoff from the surrounding urban catchment of Guwahati city acting as the main source of contamination. The rainfall runoff model of the catchment is integrated with the 1D-2D coupled hydrodynamic and water quality models of the inlet channel and the wetland, considering the latter as a shallow water body. The two primary water quality parameters, dissolved oxygen (DO) and

biological oxygen demand (BOD), which are modelled across the length of the Basistha channel and within the expanse of the wetland, are used as indicators to predict the potential eutrophication zones in the wetland. The results are correlated with the standard Trophic State Index (TSI) used for classification of eutrophication zones in surface water bodies. The TSI values, determined at the different locations in the wetland by considering observed and simulated chlorophyll-a (Chl-a) levels, are plotted in the form of spatial maps for highlighting the eutrophic zones in the wetland.

2. Methodology

2.1 Study area

The Deepor Beel freshwater wetland is located on a former channel of the Brahmaputra River, spanning over a spatial extent of 400 ha (Fig.1). The inflows to the wetland is through the Basistha channel, which drains a part of the Guwahati city catchment; while excess flows are routed through the outlet channel, Khanajan, that connects the wetland to the Brahmaputra River. The wetland is bordered by the Rani reserve-forest on the south and by agricultural lands on the east, west and northern peripheries. A solid waste landfill is located on the south-eastern edge of the wetland close to the Basistha rivulet, right before it enters the wetland. It is feared that leachate from the landfill may be affecting the water quality in both the channel and the wetland. The wetland is also renowned for its rich biodiversity, providing a natural habitat to more than 200 species of birds, several species of mammals and fish, and around 70 species of migratory birds, among others (Saikia, 2005). Recognizing its ecological significance, Deepor Beel was designated as a Ramsar site in 2002 (Ramsar Site no: 1207; Source: https://rsis.ramsar.org/ris/1207).

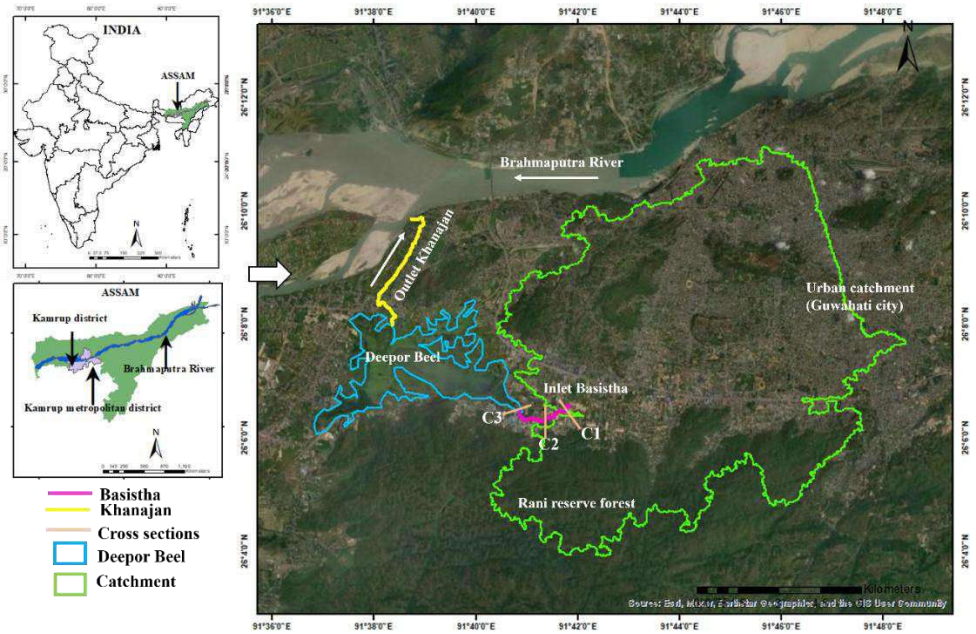

Fig.1. Study area map of Deepor Beel, its inlet and outlet channels and the urban catchment of Guwahati city (Reproduced with permission from Koch et al., (2025))

2.2 Model description and data requirement

The coupled 1D-2D model setup was built using the MIKE+ integrated modelling platform. The rainfall-runoff module in MIKE+ was used for determining the catchment discharge to the wetland. The catchment delineation was carried out using ArcGIS and imported to MIKE+. The final two-kilometre stretch of the Basistha channel was modelled for 1D hydrodynamics and water quality simulation, with the discharge hydrograph generated from the rainfall-runoff module being used as the upstream boundary condition. The 2D hydrodynamic and water quality model of the wetland was done using the MIKE21 module and integrated into MIKE+ by coupling the downstream end of the Basistha channel 1D model boundary with the 2D hydrodynamic and water quality model of the wetland. The water level recorded at the terminal end of the wetland near its junction with the Khanajan outlet channel was taken

as the downstream boundary condition for the model. The runoff from the rainfall-runoff module was validated with field measured catchment discharge during the August 2022 monsoon season, and the pre-monsoon season of February 2023. Water quality parameters, DO, BOD and Chl-a, measured across different cross sections of the Basistha channel and in different grid locations of the wetland for this same period are used for the calibration and validation of the coupled model. The data collection process was designed to cover six seasons from 2021 to 2023, as the wetland is located on a monsoon dependent sub-tropical climate. A 500m by 500m square grid was followed for collecting water samples within the Deepor Beel's spatial extent for evaluating water quality of the wetland. Water samples were also collected from the different cross sections of the Basistha channel as well.

3. Results and discussion

3.1 Water quality variation in Basistha inlet channel

Of the six seasons between 2021 and 2023 that the study was conducted, the results for the pre-monsoon season of 2023 are presented here, when continuous monitoring was carried out for ten days. The model results show R^2 values for BOD and DO at 0.78 and 0.72 respectively, for the different cross sections of the channel, and may be considered reasonably acceptable. From Fig. 2, it may be observed that the variation in the water quality parameters, DO and BOD along the channel is governed by the changing runoff in the channel. In fact, both the parameters adhere to the hydrologically consistent trend of increasing discharge leading to decrease in BOD levels and increasing DO levels, implying natural mixing and reaeration. This implies that reduced dilution capacity and sustained organic load inputs during the dry seasons, which is consistent with observed field conditions, are responsible for degrading water quality of the channel. When this inflow enters the wetland, it naturally becomes a major source of nutrients, pollutants, organic loads, etc., forming a eutrophication-prone environment and influencing adversely the overall ecosystem health of the wetland.

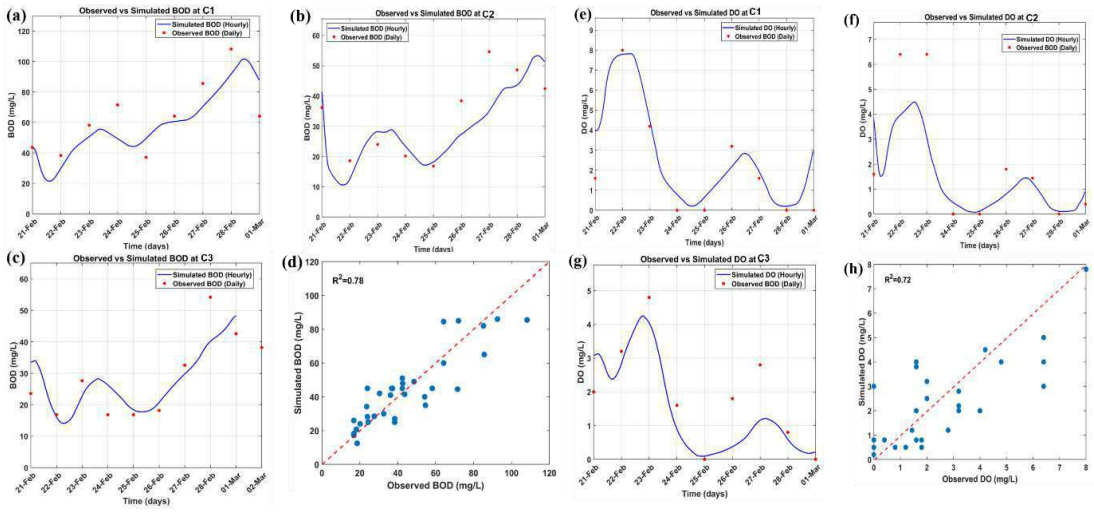

Fig. 2. (a) to (c) Observed BOD vs Simulated BOD at different cross sections of Basistha (d) Overall Observed BOD vs Simulated BOD (e) to (g) Observed DO vs Simulated DO at different cross sections of Basistha (h) Overall Observed DO vs Simulated DO

3.2 Eutrophication in the Deepor Beel wetland

Eutrophication is mainly guided by nutrient dynamics and aquatic biogeochemistry governed by oxygen demand and organic matter decomposition. It has already been established earlier from this study the role of flow hydrodynamics in contributing to wetland eutrophication. The spatial variation of BOD, simulated by the coupled model, in the pre-monsoon season of 2023 is shown in Fig. 3. From the spatial maps, it is evident that certain locations of the wetland, due to reduced flow circulation, have minimal levels of DO and high BOD. Physical sampling and observations during field visits also confirmed these zones as nutrient rich and prone to eutrophication. The spatial maps of the observed TSI shows that the regions with higher BOD levels are also the regions more susceptible to eutrophication. The simulated TSI values also correlate well with the observed TSI maps with Chl-a levels predicted by the model with R^2 value of 0.70.

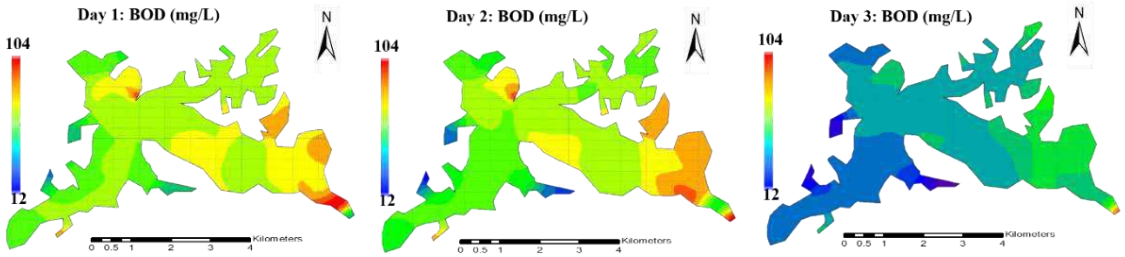

Fig. 3. Spatio-temporal variation of BOD (mg/L) in the wetland from simulated results for pre-monsoon season of 2023

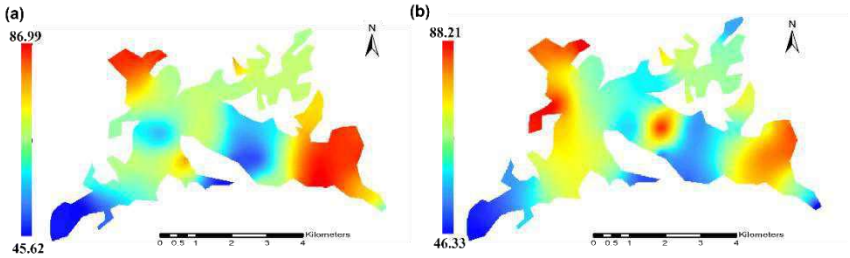

Fig. 4. Spatial maps of (a) Observed TSI vs (b) Simulated TSI for pre-monsoon season of 2023

4. Conclusions

This study attempts to throw light on the impact of anthropogenic stresses, such as wastewater influxes from urbanization in bringing about changes to the natural ecohydraulic characteristics of an urban wetland in different seasons. Since the environmental health of a wetland ecosystem is deeply governed by its hydrobiogeochemical processes, it is often difficult to model these due to their interrelationships and complexity. The study explores the prediction of the spatio-temporal variation of two key indicators that govern wetland health: the dissolved oxygen (DO) and biological oxygen demand (BOD). The investigations, carried out through mathematical modelling using the software package MIKE, and supported by field data, reveal that elevated BOD concentrations during dry periods reduce DO levels help promote anaerobic conditions and consequent internal nutrient release in the Deepor Beel wetland, thus enhancing eutrophication symptoms. The study also highlights the important role of the nutrient rich urban-catchment runoff and wetland hydrodynamics in eutrophication-prone wetlands. It is hoped that this coupled model, validated against observed data, may be employed for developing sustainable solutions for eutrophication management in this and similar urban wetlands.

Acknowledgement

The authors are grateful to Department of Science and Technology, Ministry of Science and Technology, Government of India and Indian Institute of Technology Kharagpur, India, for financial support (Project code: DST/TMD/EWO/WTI/2K19/EWFH/2019/225(G)) and to the Department of Chemistry, Assam Don Bosco University, Guwahati, Assam for providing laboratory facilities. The authors are also grateful to DHI for providing student license for using the MIKE software.

References

Bassi, N., Kumar, M.D., Sharma, A., Pardha-Saradhi, P., 2014. Status of wetlands in India: A review of extent, ecosystem benefits, threats and management strategies. J. Hydrol. Reg. Stud. 2, 1–19. https://doi.org/10.1016/j.ejrh.2014.07.001.

Koch, D., Sen, D., Uddameri, V., Gupta, A.K., 2025. A multi-method approach to assess long-term urbanization impacts on an ecologically sensitive urban wetland in Northeast India. Sci. Total Environ. 966, 178681. https://doi.org/10.1016/j.scitotenv.2025.178681.

Mitra, S., Wassmann, R., Vlek, P.L.G., 2003. Global inventory of wetlands and their role in the carbon cycle, ZEF Discusson Paper on Development Policy, Bonn.

Saikia, P.K., 2005. Qualitative and Quantitative Study of Lower and Higher Organisms and Their Functional Role in the Deepor Beel Ecosystem [WWW Document]. URL https://ftti.indiabiodiversity.org/.

Sánchez-espinosa, A., Schröder, C., 2019. Land use and land cover mapping in wetlands one step closer to the ground : Sentinel-2 versus landsat 8. J. Environ. Manage. 247, 484–498. https://doi.org/10.1016/j.jenvman.2019.06.084.

Verhoeven, J.T.A., Arheimer, B., Yin, C., Hefting, M.M., 2006. Regional and global concerns over wetlands and water quality. Trends Ecol. Evol. 21, 96–103. https://doi.org/10.1016/j.tree.2005.11.015.

Book of Abstracts of the *16th International Symposium on Ecohydraulics*
Challenges and solutions in the time of global changes
August 16–20, 2026, Lausanne, Switzerland
ISSN: 2790-2420 | ISBN: 978-90-837233-9-6 | doi:[10.64697/iahr.proc.ise2026.abs]
© 2026 IAHR. CC BY-NC-ND 4.0

HYDRO-ECOLOGICAL PERFORMANCE OF THE ARVE–DRIZE FISHWAY: ASSESSING SEDIMENT CLOGGING AND SELF-SCOURING PROCESSES

Nicolas DUPARC[1], Anthony GARCIA[1], Nicolas ANDREINI[1], Davide CERESETTI[1]

[1] University of Applied Sciences and Arts of Western Switzerland, HES-SO, HEPIA Geneva
email: davide.ceresetti@hesge.ch

ABSTRACT

The reopening of the Drize River and its reconnection to the Arve River requires a fishway capable of enabling upstream fish migration while remaining operational under the highly variable sediment loads of the Arve River. To address potential clogging risks and ensure long-term functionality, we implemented a multi-scale methodology combining (i) a 1:1 in-situ prototype to characterise real sediment inputs, (ii) numerical modelling to assess hydraulic performance, and (iii) a 1:3 physical model to investigate coupled hydraulics and sediment transport. Sediments collected in the field were analysed for grain-size distribution and cohesive fraction; the mixture used in the 1:3 model was slightly modified by removing the largest particles to satisfy particle Reynolds and Shields similarity, while maintaining the natural cohesive fraction, which is critical for clearing behaviour. The 1:3 model is then used to test the effectiveness of a jet-based flushing system designed to enhance self-scouring capacity. Various jet configurations, discharge scenarios, and geometric adaptations are evaluated to determine whether such a system can efficiently mobilise and evacuate deposited sediments while preserving favourable conditions for fish passage. This integrated multi-scale approach provides a robust basis for designing a self-clearing fishway capable of functioning more than 300 days per year as requested by the Federal Office for the Environment.

Keywords: Fishway; Sediment flushing; Self-Scouring; Physical Model; scale similarity.

1. Introduction

The reopening of the Drize River represents one of the most ambitious ecological restoration projects currently underway in Switzerland. For several decades, the Drize flow has been conveyed through underground channels before discharging into the Arve River, disrupting ecological continuity and preventing fish from accessing upstream habitats. As part of a broader river renaturation strategy, the future open-air Drize requires a structure that restores longitudinal connectivity while overcoming a significant hydraulic drop between the two rivers. To meet this challenge, a technical fishway composed of 21 consecutive pools and a lateral discharge ramp has been proposed (cf. Figure 1).



Figure 1 – 3D printing of the future fishpass at the confluence of Drize and Arve rivers.

The fishway must remain operational under the highly variable hydrological (30-300 l/s) and sedimentary conditions of the Arve. This river, strongly influenced by an alpine–glacial regime, exhibits pronounced intra-seasonal fluctuations in discharge, turbidity, and suspended sediment concentration. During high-flow events, the Arve can transport substantial quantities of suspended particles creating a significant risk of clogging within engineered structures. The total amount of suspended particles is estimated to be approximately 400,000–600,000 tonnes per year (Launay, 2019). Ensuring the long-term functionality of the future fishway therefore requires not only an appropriate hydraulic design that supports fish passage, but also a robust understanding of sediment transport, deposition mechanisms, and the potential for sediment accumulation within the structure.

2. Project objectives

The objective of the study is to design a fishway that meets ecological continuity requirements while remaining operational for at least 300 days per year under typical Arve sediment loads, as recommended by the Federal Office for the Environment. More specifically, the study aims to:

- Characterise the real sediment load -grain-size distribution, cohesive fraction, accumulation patterns.
- Investigate sediment deposition and potential clogging mechanisms.
- Assess hydraulic performance -velocity fields, water levels, energy dissipation- ensuring suitable passage conditions for the target fish species.
- Evaluate the effectiveness of a jet-based flushing system integrated into the fishway to promote sediment mobilisation and evacuation.
- Identify design improvements that enhance self-clearing capacity while maintaining ecological and hydraulic requirements.

This combination of field measurements, numerical modelling, and physical modelling allows us to address both hydraulic and sediment dynamics, which are rarely investigated concurrently in fishway studies but are critical in sediment-rich environments such as the Arve.

3. Methodology

Our approach relies on the principle that understanding sediment behaviour across different spatial and temporal scales significantly improves predictive capability. Each scale plays a distinct role:

3.1. In-situ prototype: sediment accumulation and grain distribution

We constructed a simplified full-scale prototype consisting of two pools with geometry equivalent to that of the future fishway, installed at different altimetric levels (Figure 2.a). Its purpose is not to evaluate fish passage hydraulics but rather to capture real-world sediment deposition processes. The prototype was installed directly in the Arve River bank, as close as possible to the future fishway site.

During high-flow events, sediment samples deposited in the prototype pools are collected. Laboratory analyses provide detailed grain-size distribution. Sediment accumulation patterns within the pools are quantified through image analysis combined with manual measurements on a 10 × 10 cm grid. These observations are essential for reproducing realistic boundary conditions in the scale model and for identifying which sediment fractions are most likely to accumulate and potentially obstruct the fishway.

3.2. Numerical modelling: hydraulic conditions for target fish species

In parallel, 2D and 3D numerical simulations (Hec-Ras 2D and Flow3D-HYDRO respectively) are performed to assess hydraulic conditions in the fishway under various discharge scenarios. The numerical models focused on water surface profiles, flow distribution within the pools, discharge between successive pools, the location and extent of recirculation zones, bottom shear stress patterns, and overall energy dissipation.

These results provide an initial assessment of whether the proposed geometry is suitable for fish migration and help refine design choices prior to constructing the physical model.

3.3. Reduced scale physical model: sediment behaviour and self-scouring capabilities

The core of the project lies in the reduced-scale physical model constructed in our laboratory's hydraulic hall. The scale ratio was defined as the best compromise between obtaining measurable parameters (e.g., flow velocity, water depth), maintaining an affordable size that fits within the laboratory hall, and ensuring that the boundary conditions (water levels, minimum and maximum flows) could be reproduced in the facility. This

resulted in a 1:3 model of a limited section of the fishway, specifically, the portion that is frequently submerged, approximately twice per year.

The model serves multiple purposes: investigating hydraulic behaviour with high spatial resolution; visualising flow patterns, recirculation zones, and bottom shear stress; reproducing high-flow conditions in the Arve that promote sediment deposition; and simulating the flushing capacity of the Drize during flood events.

A key challenge (Fuentes-Pérez, 2024) is that the model must accurately reproduce a wide range of hydraulic conditions, from the low flows that characterise the Drize for most of the year ($Q_{5\%}$: 20 l/s, Q_{median}: 160 l/s) to Drize 1-year flood discharges (7 m^3/s) and elevated water levels in the Arve. The facility enables controlled experimentation and systematic testing of design alternatives, including geometric adjustments and flushing strategies. Sediment deposition and flushing processes are assessed using a scaled sediment mixture derived from field samples, as described in the following section.

4. Sediment scaling strategy

Preliminary analyses of Arve River sediments deposited near the future fishway location indicate that the material is predominantly composed of fine sand. Approximately 10% of the sediment consists of silt-sized particles (< 63 µm), with a median grain size (d50) of about 200 µm and a d90 close to 1 mm. The clay fraction represents less than 1% of the total mass, while the cohesive fraction (< 20 µm) is estimated at around 5–7%.

Sediments collected in the field cannot be used directly in the 1:3 physical model because their grain-size distribution would violate similitude requirements (Yalin, 1971). Instead, we adopted a scaling strategy that satisfies two key criteria: i) Particle Reynolds similarity, ensuring that particle motion in the reduced-scale model remains dynamically comparable to that observed in the prototype; ii) Shields similarity, guaranteeing that the threshold for sediment entrainment occurs under equivalent dimensionless shear stress.

To meet these conditions, we adjusted the grain-size distribution of the Arve sediments in order to preserve the dominant grain-size fractions relevant for deposition in the fishway, ensuring compliance with similarity laws. Importantly, we maintained the natural cohesive fraction, which plays a central role in clogging behaviour (Van Rijn, 2025).

Even though the behavior of cohesive materials at reduced scale is not fully understood, maintaining the natural proportion of cohesive sediment ensures that the flushing tests realistically reproduce the behavior of the most problematic fractions observed in the Arve, providing a conservative and safe design approach.

5. Experimental testing in the 1:3 model

In our laboratory, we built a reduced-scale model consisting of 11 fishway pools (Figure 2.b). The setup includes a supply basin and a reception basin, which can function under fixed-stage conditions. The system is contained within a 6-meter-diameter tank, which normally remains dry but allows simulation of Drize River floods (2.4 m^3/s, corresponding to 150 l/s at the model scale) under controlled conditions.



Figure 2 – a) Full-scale fishway pool realized on site. b) Construction of the 1:3 reduced-scale model of the fishway Drize-Arve.

The initial experiments without sediment focus on hydraulic performance: flow distribution across pools, subcritical/supercritical flow, maximum and minimum velocities in fish passage zones, identification of low-velocity recirculation areas, influence of structural roughness on shear stress distribution.

Video recordings and velocity probe measurements are used to quantify flow and water depth. These measurements provide a baseline for assessing whether the fishway geometry supports adequate fish passage.

Since sediment clogging appears during Arve floods with specific flood-levels and discharge, sediments are manually located on the pools following the actual deposition pattern observed in the full-scale prototype. Then, we apply constant discharge on the fishway and we measured the turbidity profile at the outfall. The test is stopped when 95% of the sediments have been flushed. Once the test stopped, we let the fishway dry and analyze, by video and stereoscopic camera, the sediment distribution in the pools.

This allows us to evaluate self-scouring capacity of the fishpass depending on the Drize discharge. The model allows us to observe where sediments naturally settle and where shear stress remains too low to mobilise fine particles.

A key innovation of this study is the integration of a jet-based flushing system (Lui, 2025) designed to improve self-scouring capacity (Pellegrini, 2020). The system consists of jets placed at strategic locations to create high-velocity pulses aimed at mobilising sediments that accumulate on pool bottoms. This operation is still ongoing. We will evaluate jet orientation, jet diameter, discharge and pressure, activation frequency, interaction with natural flow patterns, ability to remobilise cohesive layers (Figure 3).



Figure 3 – Preliminary sediment flushing by hydraulic jets.

The aim is to implement an environmental-friendly solution consisting in creating a automatic flush by using Drize river water, taken in small quantity directly from the river, to flush the sediments downstream.

6. Results and implications for design

Though the study is ongoing, preliminary results already reveal several key insights:

1. Sediment deposition occurs predominantly in low-velocity recirculation zones, confirming the need to modify geometry or enhance shear stress.
2. Cohesive fractions pose the greatest risk of long-term clogging, as predicted. Their presence justifies the focus on maintaining natural cohesion in the scaled mixture.
3. Jet-based flushing shows promising initial results, particularly when combined with geometric adjustments that guide sediment towards evacuation paths.
4. Numerical modelling effectively identifies potential problem zones and supports iterative optimization.
5. The multi-scale approach enhances confidence that the final fishway will meet year-round operational requirements.

Acknowledgements

The authors gratefully acknowledge the support of the Geneva Cantonal Office of Water and the collaboration of the engineering consultancies Gruner SA and Biotec SA.

References

Fuentes-Pérez, J. B.-C.-V.-R. (2024). The effect of hydrological variability on stepped fishways. Journal of Hydrology(643).
Launay, M. ,. (2019). Réévaluation des apports moyens de matières en suspension del'Arve au Rhône. La Houille Blanche, 89-100.
Lui, J. L. (2025). Experimental study on submerged stationary jet in stiff cohesive soil. Ocean Engineering(330).
Pellegrini, M. P. (2020). Application of an Innovative Jet Pump System for the Sediment Management in a Port Channel: Techno-Economic Assessment based on Experimental Measurements. Journal of Marine Science and Engineering.
Van Rijn, L. P. (2025). Particle size and settling velocity of bed and suspended sediments for mud-sand beds. International Journal of Sediment Research, 369-382.
Yalin, M. S. (1971). Similarity in Sediment Transport. Theory of Hydraulic Models (pp. 145-186). London: Red Globe Press London.

Book of Abstracts of the *16th International Symposium on Ecohydraulics*
Challenges and solutions in the time of global changes
August 16–20, 2026, Lausanne, Switzerland
ISSN: 2790-2420 | ISBN: 978-90-837233-9-6 | doi:[10.64697/iahr.proc.ise2026.abs]
© 2026 IAHR. CC BY-NC-ND 4.0

THE SHIFTING SANDS OF GRAVEL STREAMBEDS: CYCLIC TRENDS IN EMBEDDEDNESS FLUCTUATION IN AN URBANZIED STREAM

Justus HARGETT[1], Jonathan CZUBA[2]

[1,2] Virginia Tech, United States
justush@vt.edu
jczuba@vt.edu

ABSTRACT

Globally, excess fine sediment (< 2 mm diameter) is recognized as a leading pollutant to freshwater systems. In the United States alone over 250,000 stream kilometers are indicated as impaired by sediment. Furthermore, habitat protections are under threat in the United States that if enacted would be further damaging to endangered and threatened species (Czuba, 2025). Excess fine sediment accumulation can degrade aquatic habitat by filling interstitial space between coarser substrates, causing decreases in surface area, porosity, oxygenation, and habitat reduction for benthic fish, salmonids, and macroinvertebrates (Dubuis and De Cesare, 2023; Wharton et al., 2017; Jones et al. 2011; Kemp et al., 2011). To quantify this degree of fine sediment accumulation around coarser particles in streambeds, ecologists and engineers use a metric often referred to as embeddedness.

Physical techniques for measuring embeddedness can be labor intensive and spatially limited. Recent studies by Czuba et al. (2022) have established a relationship between bankfull shear velocity and embeddedness. Building on this concept, Smith et al. (rev) incorporated geospatial data to develop models that remotely estimate embeddedness for the conterminous United States. However, physical measurements are limited to conditions at a single point in time and remote estimates are limited to the average stream embeddedness. Fluvial systems are incredibly dynamic, with stream flow and environmental factors constantly changing. Thus, embeddedness can be expected to fluctuate temporally. In altered watersheds, such as those affected by urbanization and agriculture, these fluctuations can be exacerbated.

The goal of this study was to discern how environmental factors contribute to temporal fluctuations in embeddedness and benthic habitat quality in an urbanized watershed. Additionally, we wanted to assess the accuracy of the embeddedness model by Smith et al. (rev) in the face of large temporal variability. Our study area was a heavily monitored stream restoration site located on Stroubles Creek in Blacksburg, Virginia in the United States. The lower extent of this second order stream is typical of those in the Ridge and Valley ecoregion defined by the US Environmental Protection Agency (USEPA). However, the upstream watershed of our site drains much of the Blacksburg area with a resulting drainage composed of 80% urbanized area with the remainder being mostly agricultural pasture and crop land. In the Virginia Ridge and Valley alone, over 2,600 streams of similar size have watersheds comprised of over 75% urban-agriculture combination. With global trends of urbanization and a growing need to supply food, this number is expected to grow.

We completed intensive embeddedness surveys every 2-3 weeks from April 2022 to November 2024 to develop a detailed time series of incremental changes in embeddedness, flow regime, and temperature to examine how these factors influenced embeddedness fluctuations. We found that embeddedness displayed substantial patterns in temporal variability with fluctuations between 20 and 80% embeddedness. Embeddedness reached peak values in late Winter/early Spring and minimum values in Summer (Fig. 1). The strongest factors contributing to temporal variation were the average air temperature, freeze thaw cycling, and maximum stage between sampling events. In the presence of these fluctuations, the Ridge and Valley model by Smith et al. (rev) produced a reliable estimate of the average condition with a mean absolute error between 9 and 16%.

To our knowledge, no other studies have examined temporal variability of streambed sediment at this fine temporal scale. Our results indicate that it is possible to predict how and when embeddedness fluctuates to some extent and highlights the importance of multiple measurements. Few studies consider the temporal aspect

of streambed sediment. Accounting for seasonal fluctuations, especially where freeze thaw cycling occurs, may prove to be a useful tool for stream ecologists and engineers to determine if or when suitable habitat could become unsuitable habitat.

Keywords: *Sediment; embeddedness; gravel bed streams; freeze thaw cycling; urbanization; temporal variation*

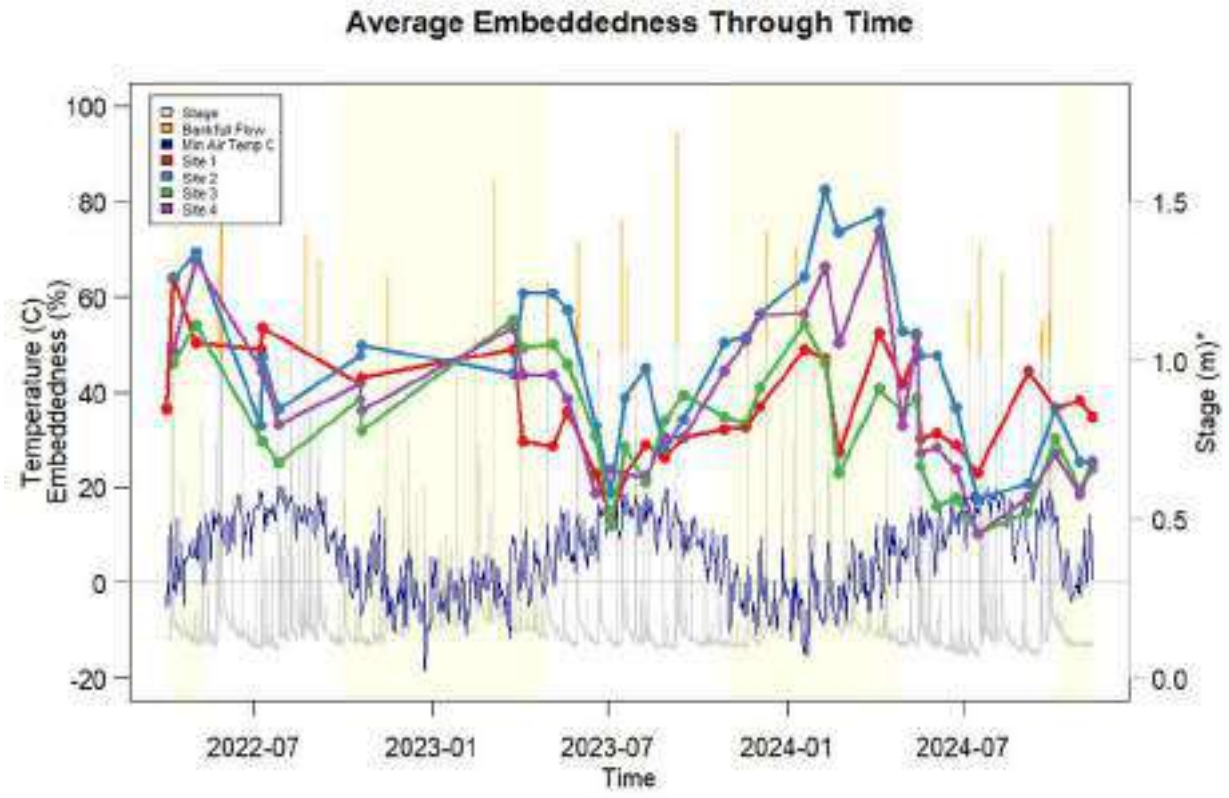

Fig. 1. *Average embeddedness over sample years 2022-2024. Light gray represents water stage with orange regions representing bankfull flows over 1 meter. Dark blue is the daily minimum temperature with yellow highlighted rectangles showing times where temperature was frequently below or crossing 0°C.*

Acknowledgements

This work was partially supported by NSF grant 2243003, USDA NIFA HATCH project 7006589, Virginia Agricultural Experiment Station, and the Global Change Center at Virginia Tech

References

Czuba JA (2025) 'Harm' must not be redefined by US conservation agencies, Nature, 642(8069), 867

Czuba J A, Hirschler M, Pratt EA, Villamagna A, Angermeier PL (2022) Bankfull shear velocity predicts embeddedness and silt c over in gravel streambeds, River Research and Applications, 38(1), 59–68

Dubuis, R., De Cesare, G. (2023). The clogging of riverbeds: A review of the physical processes. Earth-Science Reviews, *239*, 104374

Jones JI, Murphy JF, Collins AL, Sear DA, Naden PS, Armitage PD (2011) The Impact Of Fine Sediment On Macro-Invertebrates, River Research and Applications, 28(8), 1055–1071

Kemp P, Sear D, Collins A, Naden P, Jones I (2011) The impacts of fine sediment on riverine fish, Hydrological Processes, 25(11), 1800–1821

Smith SL, Hargett JM, Czuba JA, Angermeier PL, Entrekin S (2025) Predicting streambed embeddedness across the continental U.S., [Submitted for publication]. Biological Systems Engineering, Virginia Tech

Wharton G, Mohajeri SH, Righetti M (2017) The pernicious problem of streambed colmation: a multi-disciplinary reflection on the mechanisms, causes, impacts, and management challenges, WIREs Water, 4, e1231

Book of Abstracts of the *16th International Symposium on Ecohydraulics*
Challenges and solutions in the time of global changes
August 16–20, 2026, Lausanne, Switzerland
ISSN: 2790-2420 | ISBN: 978-90-837233-9-6 | doi:[10.64697/iahr.proc.ise2026.abs]
© 2026 IAHR. CC BY-NC-ND 4.0

SOIL AND WATER BIOENGINEERING AS RIVER HEAT PERIOD MITIGATION IN AN URBAN STREAM

Helene MUELLER[1], Anna LUDWICZEK [1], Magdalena VON DER THANNEN [1], Hans Peter RAUCH [1]

[1] BOKU University, Department of Landscape, Water and Infrastructure, Institute of Soil Bioengineering and Landscape Construction, Peter-Jordan-Strasse 82|III – 1190 Vienna, Austria

email: helene.mueller@boku.ac.at
email: anna.ludwiczek@students.boku.ac.at
email: magdalena.von-der-thannen@boku.ac.at
email: hp.rauch@boku.ac.at

ABSTRACT

Urban streams are highly modified and hydraulically constrained yet increasingly affected by thermal stress during low-flow conditions. Restoration measures often slow flow and raise thermal sensitivity, while shading from riparian vegetation can mitigate heat inputs - but this vegetation frequently conflicts with hydraulic capacity requirements. This study quantifies the cooling effect of riparian vegetation during a the median river heat period (RHP) in 2015-2024 in the semi-urban Liesingbach (Vienna, Austria). Vegetation shading was derived from hemispherical photography, and water temperature was simulated for an 8.3 km reach using the HEC-RAS water quality module. Model calibration and validation against two RHPs showed good agreement. Removing riparian vegetation increased daily peak water temperatures by 1.3°C, demonstrating that even sparse tree lines or shrubby vegetation implemented trough soil and water bioengineering techniques provide meaningful thermal buffering. The results underscore the importance of integrating thermal considerations into urban river restoration, as shading can substantially reduce heat stress during critical low-flow periods while supporting ecological resilience.

Keywords:. urban stream; water temperature; soil and water bioengineering; riparian vegetation; ecological low flow; slow hydrology;

1. Introduction

Urban streams are strongly pressured. They have often been heavily modified, hardly embanked, straightened and show a higher slope. Especially in urban areas hydraulic capacity and requirements on flood control are driving factors for channel geometry and morphology, leaving strongly limited lateral space availability (Müller et al., 2022). Nevertheless, there are efforts to restore them. Within this process hydraulic conditions change, roughness is getting higher, slope might be reduced. These morphological changes are impacting hydraulic characteristics. Often the existence of riparian vegetation and hydraulic capacity are in concurrence, as the hydraulic capacity is highest in absence of woody vegetation on the riverbanks or adjacent areas.
But these urban streams have to face both hydroclimatic extremes: floods and low flows. Low flow situations are strongly connected to thermal stress, as water temperature is a key driver in the ecological functioning of river systems (Ficklin et al. 2023; Kail et al. 2021; Kalny et al., 2017, Beschta 1997). In urban stream systems thermal energy input during low flow situations is mainly connected to short wave radiation and to air temperature. Restoration works slow down the system, increasing hydraulic residence time. In consequence slower systems exhibit a higher energy input, which makes them more sensitive to heat stress. Slow flowing water therefore has more demand on shading (LeBlanc and Brown 2000). Additionally, stream flow during hot periods is widely assumed to decline, which will impact stream temperature indirectly (Wondzell et al. 2019).

Riparian vegetation can buffer energy input via shading effects (Kalny et al., 2017). When addressing the trade-off between the services provided by riparian vegetation and hydraulic capacity, linking hydraulic and thermal aspects could provide valuable insights.

This extended abstract dedicates the impact of riparian vegetation on water temperature during low flow conditions at small to medium size urban rivers. Based on a water temperature model the effects on water temperature trough shade during a river heat period (RHP) are quantified and compared to different a scenarios of riparian vegetation.

2. Study area

Study area is the INTERLAYER Living Lab Liesingbach. It is a semi urban stream with a catchment area of 117 km² in the south of Vienna. The river inundates into the river Schwechat and is part of the bigger Danube catchment between Enns and March. In the urban river section a sealed trapezoidal riverbed was installed in the 1970s. Since the year 2000 river stretches have been restored and are now well accepted as urban recreational areas and steppingstone biotopes. Restoration works are still going on. The area of observation in this study is a river segment of 8.3 km within the urban setting. On average the yearly flood shows 14.40 m³/s, while Q95 shows 0.16 m³/s. Riparian vegetation is limited in its lateral extent. On the upper slopes single old trees prevail. Within the restored section we can find mostly shrubby vegetation implemented by soil and water bioengineering techniques. The model is set up between two gauging stations in the urban area of the catchment. The profile was idealized following the geometry of the trapezoidal riverbed, with 4 m width and embankment slope of 18.4°. It shows an average longitudinal slope of 0.5 %.

3. Methods

3.1. River heat periods (RHP)

For the years 2015-2024 river heat periods (RHP) were detected. Based on 30 min meteorological data a yearly seven-day period with the highest combination of mean air temperature, global radiation, and sunshine duration, while requiring minimal precipitation to ensure stable hydraulic conditions, was detected. All variables were standardized and combined into a River Heat Period Index (RHPI), and the period with the maximum RHPI was selected for each year. Additional hydroclimatic parameters were extracted for further modeling. Ten years data was summarized via its median values.

3.2. Vegetation characteristics

To characterize riparian vegetation hemispherical photographs were taken every 500 m along the river, with additional images added at locations where vegetation changed significantly. 95 images were processed in HEMIVIEW to calculate solar radiation below the vegetation cover and canopy indices for a day in July. Threshold-based classification and a simplified atmospheric radiation model were chosen. Based on calculated radiation below canopy vegetation configurations were generated, representing P10, P25, P50, P75 and P90 percentile of radiation transmission.

3.3. Water temperature model

The study modelled water temperature using the HEC-RAS water quality module, based on a uniform trapezoidal channel geometry and steady-flow hydraulics solved with the standard-step method. Heat dynamics were simulated with the full energy-budget approach, incorporating advection–dispersion, atmospheric exchanges, streambed interactions, and adjusted shortwave radiation to account for shading from vegetation derived from hemispherical photos. The hydroclimatic inputs were gained from the detected RHP. Groundwater influence was assumed negligible due to a sealed riverbed. Discharge was set to 0.11 m³/s, representing the median discharge of the RHP.

4. Results

The prevailing vegetation leads to daily radiation sums below canopy of 148 – 866 MJ/m². The mean daily sum over all river sections was calculated with 482 MJ/m². Removing the current vegetation leads to a daily radiation input over the whole river stretch of 881 MJ/m². The buffering effect of moderately dense vegetation (P50 radiation transmissivity) can reduce peak incoming radiation by up to 600 W/m² on a July day compared to conditions without vegetation. Under very dense vegetation (P10), peak radiation is reduced to below 100 W/m².

The water temperature model was calibrated with RHP 2022 The validation was carried out for RHP 2021. Modell performance was good, after a warming time of 6 hours, NSE of 0.75 – 0.81 were reached. RMSE shows values from 1.0 – 1.1. Under prevailing vegetation cover in the RHP 2015-2024 water temperature maxima reach values between 21.0 – 24.6°C, while minima cover the range of 13.8-18.4°C. Mean daily temperature amplitude covers 6.2°C.
Over the period 2015–2024, the range of maximum water temperatures depending on vegetation density is on average 4.4°C. Reducing the shading effects of vegetation to P90 radiation transmission would lead to an average increase in peak temperatures of 1.3°C. An increase in vegetation density to P50 or P25 radiation transmission results in a reduction of daily maximum water temperatures of -1.3°C (P50) and -2.6°C (P25). A vegetational impact on daily water temperature minima was not detected.

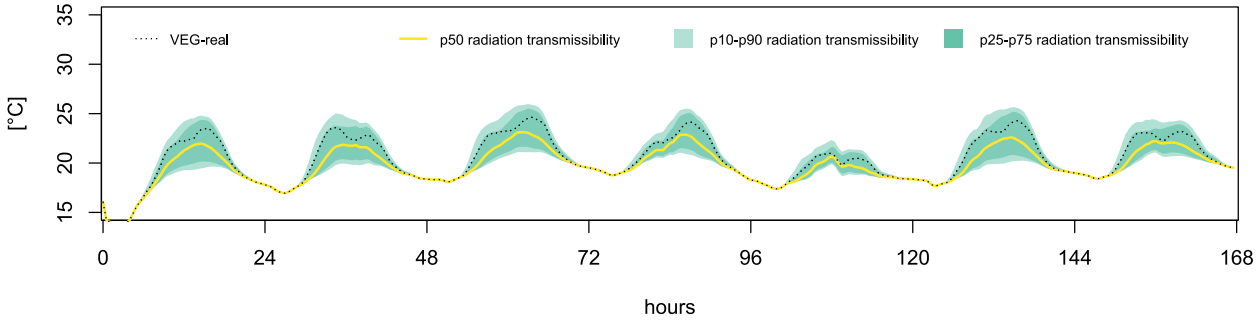

Fig. 1. Water temperature model for RHP median [2015-2024]. One scenario was carried out with real vegetation cover. Additional vegetation configurations were tested based on their radiation transmissivity. For daily maxima an average buffering of 1.3°C by the prevailing vegetation cover was detected.

5. Discussion

The results clearly state the influence of shading riparian vegetation on water temperature. The observed tendencies are in line with other studies (Davies-Colley and Payne 2023, Wondzell et al. 2019), although the dimension at river Liesingbach is lower. Which can be attributed to differences in vegetation density, flow lengths and the setting in an urban area.
The thermal regime acts as a regulator of biotic processes in riparian systems and is strongly impacting the self-purification ability of riparian systems (LeBlanc and Brown 2000). If restoration efforts in urban river systems concentrate exclusively on hydraulic capacity, the shading functions of riparian vegetation may be underestimated. This is particularly critical in heavily stressed urban environments, where rising water temperatures pose a significant concern.
The importance of vegetation in moderating peak water temperatures has been clearly demonstrated for river Liesingbach. Its ecological value for maintaining water quality is immense, it strongly supports the ecological flow during low flow situations. Differences of ±1.3 °C in peak water temperatures can have major ecological consequences for riparian systems. In the critical range of temperatures above 20°C, even small temperature changes can alter habitat suitability for fish, as many species exhibit narrow thermal tolerance zones (Niedrist 2023; Trimmel et al. 2018; Melcher et al. 2013) .
Based on our results vegetation effects are not limited to dense riparian forests. Even single tree lines, or shrubby vegetation implemented through soil and water bioengineering techniques have remarkable influence on water temperature. Vegetation can clearly support ecological aspects during low flows. With the prevailing water temperature model, we created a tool to quantify the impacts and predict potential changes. Building on this integration of hydraulic and vegetation modelling will enable us to improve ecological outcomes during low-flow periods.

Acknowledgements

The authors would like to thank the European Commission and the Austrian Science Found (FWF) for funding in the frame of the collaborative international consortium INTERLAYER financed under the 2022 Joint call of the European Partnership 101060874 — Water4All. Water4All reference: Water4All-2022-00261. This research was funded by the Austrian Science Found (FWF) [grant DOI 10.55776/16894].

References

Beschta R.L. (1997) Riparian shade and stream temperature; an alternative perspective. Rangelands Archives 19, 25–28.

Davies-Colley R.J., Payne G.W. (2023) Cooling streams with riparian trees: Thermal regime depends on total solar radiation penetrating the canopy. Austral Ecology 48, 1064–1073. https://doi.org/10.1111/aec.13345

Ficklin D.L., Hannah D.M., Wanders N., Dugdale S.J., England J., Klaus J., Kelleher C., Khamis K., Charlton M.B. (2023) Rethinking river water temperature in a changing, human-dominated world. Nat Water 1, 125–128. https://doi.org/10.1038/s44221-023-00027-2

Kail J., Palt M., Lorenz A., Hering D. (2021) Woody buffer effects on water temperature: The role of spatial configuration and daily temperature fluctuations. Hydrological Processes 35, e14008. https://doi.org/10.1002/hyp.14008

Kalny G., Laaha G., Melcher A., Trimmel H., Weihs P., Rauch H.P. (2017) The influence of riparian vegetation shading on water temperature during low flow conditions in a medium sized river. Knowl. Manag. Aquat. Ecosyst. 5. https://doi.org/10.1051/kmae/2016037

LeBlanc R.T., Brown R.D. (2000) The Use of Riparian Vegetation in Stream-Temperature Modification. Water & Environment J 14, 297–303. https://doi.org/10.1111/j.1747-6593.2000.tb00264.x

Melcher A., Pletterbauer F., Kremser H., Schmutz S. (2013). "Temperaturansprüche und Auswirkungen des Klimawandels auf die Fischfauna in Flüssen und unterhalb von Seen." Österreichische Wasser- und Abfallwirtschaft 65 (11–12): 408–17. https://doi.org/10.1007/s00506-013-0118-y.

Müller H., Hörbinger S., Franta F., Mendes A., Li J., Cao P., Baoligao B., Xu F., Rauch H.P., (2022). Hydromorphological Assessment as the Basis for Ecosystem Restoration in the Nanxi River Basin (China). Land 11, 193. https://doi.org/10.3390/land11020193

Niedrist G.H. (2023). "Substantial Warming of Central European Mountain Rivers under Climate Change." Regional Environmental Change 23 (1): 43. https://doi.org/10.1007/s10113-023-02037-y.

Trimmel H., Weihs P., Leidinger D., Formayer H., Kalny G., and Melcher A. (2018). "Can Riparian Vegetation Shade Mitigate the Expected Rise in Stream Temperatures Due to Climate Change during Heat Waves in a Human-Impacted Pre-Alpine River?" Hydrology and Earth System Sciences 22 (1): 437–61. https://doi.org/10.5194/hess-22-437-2018.

Wondzell S.M., Diabat M., Haggerty R. (2019) What Matters Most: Are Future Stream Temperatures More Sensitive to Changing Air Temperatures, Discharge, or Riparian Vegetation? J American Water Resour Assoc 55, 116–132. https://doi.org/10.1111/1752-1688.12707

Book of Abstracts of the *16th International Symposium on Ecohydraulics*
Challenges and solutions in the time of global changes
August 16–20, 2026, Lausanne, Switzerland
ISSN: 2790-2420 | ISBN: 978-90-837233-9-6 | doi:[10.64697/iahr.proc.ise2026.abs]
© 2026 IAHR. CC BY-NC-ND 4.0

SOLUTIONS TO FLOODING OF THE ESTEPONA RIVER IN THE URBAN CENTER OF BAKIO (BIZKAIA, SPAIN)

Paola SANGALLI [1], Sergio SANGALLI [1] ,Guillermo TARDIO [2]

[1] Sangalli Coronel y Asociados SL ,Spain
email: sangalli@sangallipaisaje.com
email: sergio.sangalli@sangallipaisaje.com
[2] UPM, Spain
email: guillermo.tardio.cerrillo@upm.es

ABSTRACT

1. Introduction

The town of Bakio, located on the Cantabrian coast (North of Spain), is subject to significant flooding, which is attributable to the confluence of two factors: the flooding of the Estepona River and the equinoctial tides. These phenomena have a substantial impact on a considerable portion of the town's urban area. To mitigate the adverse effects and enhance the area's resilience to climate emergencies, the following project has been undertaken. This consists of de-channelizing a section of the river and enabling the current floodplain (4 hectares) to mitigate the floods and remove part of the homes in the vicinity from risk. The project also involves integrating the floodplain as a park in the town center.

Bakio is a small municipality located on the Cantabrian coast, with a population of approximately 2,600 inhabitants. The town is situated in a valley through which the Estepona River flows and is surrounded by mountains that reach a height of approximately 500 meters. The Estepona River is 14 km long and has a catchment area of 24.7 km². The river is characterised by its steep gradient, short concentration time, and torrential nature, attributable to the high levels of rainfall in the region. The river has been significantly altered within the urban area, mainly through canalization, a process that has extended to the mouth of the river. In addition to the morphological alterations observed, the river has undergone a significant change in the vegetation on its banks, with a notable presence of invasive plant species. The rainfall regime in the area, the abundance of tributaries, the presence of tides, and the limited space of the river cause the flow rates to increase very rapidly and tend to overflow (Smith et al., 2022).

The project has been developed in several phases.

-Firstly, a hydraulic study of the Estepona River in Bakio was conducted by the UPV and UPC in 2018. The present study analyzed flood risk areas and potential solutions.

Our company then drafted the preliminary project for the implementation of an inland marsh in Bakio. This occurred between 2018 and 2019, during which period the solutions were prospected, and the subsequent hydraulic operation was analysed using a two-dimensional programme. -

The executive project was conducted in collaboration with an engineering and geotechnical enterprise (Ikerlur SL), during the period from 2021 to 2022. The executive project creates a new topography which, while improving the flooding scenarios for the return period considered (100 years), proposes a frequent functioning of the system, a recovery of the ecosystems and their services, and an integration into the urban area through the creation of a flood park. All the proposed solutions are based on Soil and Water bioengineering techniques and Landscape architecture as the coordinator of the different disciplines

- The project is part of the LIFE 18 IPC/ES/000001 LIFE-IP URBAN KLIMA 2050 project and is currently under construction by the Basque Water Agency (URA) with the target completion date set for May 2026.



Fig. 1. Flooding of the Estepona River in the town of Bakio. Infographic. Planning. Progress document

2. Analysis

During the implementation phase of the project, a comprehensive analysis was carried out of the specific issues affecting this section of the River Estepona.

During this phase, a detailed topographical and bathymetric survey of the area in question was conducted. In addition, a geotechnical survey was carried out, which included various test pits and boreholes. The current hydrology and hydraulics were analysed using 2D models (Iber), with the aim of identifying flood-prone areas for different return periods.

A comprehensive analysis of the existing vegetation was carried out, paying particular attention to the presence of invasive species. Furthermore, all trees in the project area were measured and their volumes calculated. An analysis of the local fauna was carried out in collaboration with a specialist from the Society of Sciences Aranzadi.

We work with the relevant authorities, including the Coastal Authority (Ministry of Miteco), the Basque Water Agency, the Provincial Council of Bizkaia and the local council itself.

Urban planning, the homes affected by the river, the existing network of green spaces, the presence of archaeological remains and the cultural elements of Bakio were studied.

Finally, various workshops and presentations were held with the residents of Bakio, with the aim of promoting community participation and understanding of the issues related to the river.

3. Proposal

Therefore, the objectives that we pursued in this project are

1- Improvement of flooding conditions

2- Improvement of the environmental conditions of the Estepona river.

3- Construction strategy using Nature-Based Solutions

4- Urban integration of the intervention

1.1. Improvement of flooding conditions

In general, these actions aim to improve the flooding conditions in the urban area.

The proposed solutions are adapted both to the current morphodynamics of the river and to the influence of the tide in accordance with the following zones:

A- Floodable Forest in which the riverbed is split: this second riverbed will carry water from the river, being designed to be activated at a certain frequency throughout the year.

B- Transition zone where the river moves away from the houses.

C- Marshland. This is the area of tidal influence, which is expected to be flooded daily at high tide.

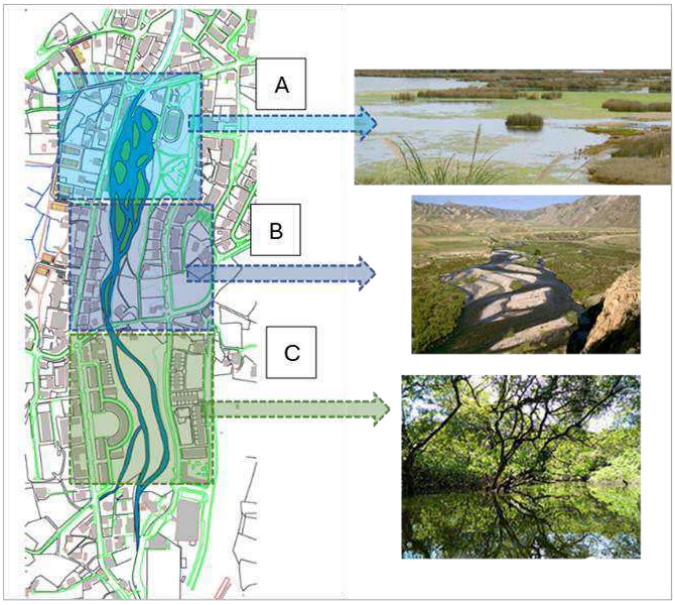

Fig. 2. Proposal: zonification of the interventions SCIA SL

The following hydrological and hydraulic studies were carried out to inform the design of the configuration and functioning of the floodable forest and inland marsh systems:

- A study of the first overflow points in the Estepona River and its tributaries.
- Determination of a reference flow for activating the systems.
- Determination of the activation depth of the floodable forest and inland marsh systems.
- Identification of flood spots for different return periods (Generator flow, T10, T100, and T500).

The hydraulic analysis was carried out in parallel with the definition of the earthwork's strategy.

1.2. Improvement of the environmental conditions of the Estepona river.

Earth balance:

As mentioned above, in addition to the previously considered hydraulic objectives, the aim is to reuse and relocate a considerable proportion of the excavated earth on the plots in order to minimize the amount of earth taken to landfill. Around 40,000 m³ of the 55,000 m³ of excavated earth can be reused on the same plot to create a new topography in the park. The remainder will be reused for other purposes, such as the restoration of forest tracks near the area.

Measures for fauna

-Search for structural diversity within the fluvial system: presence of deeper waters, shallower waters, areas with calmer waters, areas with alternating rapids and pools, etc.

-Creation of refuge areas through wood and vegetation elements.

-Creation of areas designed for the European mink, the long-legged frog and the black-green lizard, three of the catalogued species present in the area.

-Alternation of open and shaded areas along the riverbank.

Planting strategy:

All actions are planned to recreate a mosaic of vegetation, consisting of shaded areas and open spaces. This will create a wide variety of conditions and, consequently, habitats.

The vegetation included in the projects will be native to the area. The salinity gradient between the marsh area and the riparian forest, as well as the hydrological gradient in the riparian forest cross-section, has been taken into account.

The project will include the eradication of the currently abundant invasive flora (Phyllostachys sp., Arundo donax, Acacia dealbata, and Acacia melanoxylon), as well as other exotic flora.



Fig.3. Infographic of the inland marshland SCIA SL

1.3. Construction strategy: use of soil and water bioengineering

According to the European Federation of Bioengineering (EFIB), Soil and Water Bioengineering is a specific biologically oriented engineering discipline, in which native plants and plant fragments are used as living construction material to solve erosion and soil conservation problems, contributing to the regeneration of ecosystems degraded by natural or anthropogenic causes, to the dynamics of ecological and geomorphological processes and to the recovery of Biodiversity.

Depending on the hydraulic parameters of velocities and tension obtained during the simulation, we choose the different techniques to be used, which in the project are the following: Kreiner crib wall, Fluvial simple crib wall, brush matters, halophytes/ helophytes fascines, willow fascines…

Priority will be given to soil and water bioengineering techniques in the projects, as these can be categorised as Nature-Based Solutions (NBSs) and contribute to the regeneration of riparian vegetation.

1.4. Urban integration of the intervention

One of the key features of the planned intervention is the incorporation of urban integration, enabling people to enjoy a new landscape through the design of a public park inspired by the area's history and other local features. The following have been prioritised in the park's design:

- improving connectivity and walkways.

- Using sustainable drainage techniques that make use of runoff water and encourage infiltration and percolation.

- Using plant species native to the area and designing areas with a strong landscape focus.

- The creation of new recreational areas for public use and enjoyment.

The project has also incorporated suggestions made by the public during workshops organised for its presentation.

CONCLUSIONS

Expected results.

- Significant reduction in flooding in the floodable forest and marsh systems. The Preferential Flow Zone (PFE) within the municipality has been significantly reduced, and the proposed earthworks are well-balanced.

-The floodable forest and inland marsh systems have an inter-annual functioning that allows the associated plant communities to develop well. A greater variability of hydrodynamic conditions is achieved (richness of the mosaic of vegetation and habitats associated with the systems).

- The green and blue infrastructure of Bakio is developed, as well as the ecosystem services generated for the public, resulting in a suitable transition between the systems proposed and the urban area of the municipality

Keywords: Soil and Water Bioengineering; Climatic mitigation; Nature-Based Solution; Landscape architecture.

Book of Abstracts of the *16th International Symposium on Ecohydraulics*
Challenges and solutions in the time of global changes
August 16–20, 2026, Lausanne, Switzerland
ISSN: 2790-2420 | ISBN: 978-90-837233-9-6 | doi:[10.64697/iahr.proc.ise2026.abs]
© 2026 IAHR. CC BY-NC-ND 4.0

WATER QUALITY DYNAMICS IN COMBINED WASTEWATER–STORMWATER CHANNELS AND A TIDAL RECEIVING RIVER: A 1D-2D MODELLING STUDY OF KOLKATA, INDIA

Ronak Prakash DAS[1], Manas Kumar DAS[2], Bibhas Chandra BARMAN[3], Dhrubajyoti SEN[4]

[1] Ph.D. Candidate, Dept. of Civil Engineering, Indian Institute of Technology Kharagpur, West Bengal, India
email: ronak1311@kgpian.iitkgp.ac.in

[2] Deputy Director (retired), Hydraulic Study Department, Syama Prasad Mookerjee Port, Kolkata, India
email: emailofmanasdas@gmail.com

[3] Director, River Research Institute, Irrigation and Waterways Directorate, Nadia, West Bengal, India
email: bcbrri@gmail.com

[3] Professor, Dept. of Civil Engineering, Indian Institute of Technology Kharagpur, West Bengal, India
email: djsen@civil.iitkgp.ac.in

ABSTRACT

Urban drainage canals in many deltaic cities discharge partially treated wastewater into tidal rivers, where the hydrodynamic conditions strongly influence the transport and transformation of pollutants. The city of Kolkata, located in eastern India on river Hooghly, disposes a large fraction of its wastewater through three major drainage canals – Bagjola, Kestopur, and the Storm Weather Flow (SWF) channels – which convey combined wastewater and storm runoff to a smaller tidal creek Bidyadhari. Although observational studies have reported poor water quality in these canals and in the receiving river, the influence of tidal hydrodynamics and gate operations on the downstream transport and partial self-purification of pollutants has not been systematically investigated. The present study examines the dynamic variation of two key water-quality indicators, dissolved oxygen (DO) and biochemical oxygen demand (BOD_5), in the drainage canals and the receiving river using a coupled hydrodynamic–water-quality modelling framework. The canals are represented using a one-dimensional model, while the tidal Bidyadhari River is simulated using a depth-averaged two-dimensional model implemented in the MIKE+ hydrology-hydraulics computation platform. The numerical simulations show that tidal reversals and the opening and closing of flap gates at the canal outfalls strongly influence the spatial distribution of DO and BOD_5 in the receiving waters. During rising tides, enhanced mixing and natural reaeration contribute to partial oxygen recovery in the river, whereas during falling tides the release of accumulated polluted canal water produces localized deterioration of water quality near the outfalls. The results highlight the important role of tidal flushing and gate operation in governing the self-purification capacity of tidal receiving waters and provide insights that may assist in the management of urban drainage discharges in deltaic environments.

1. Introduction to Kolkata: settlement, topography and drainage

Kolkata, formerly known as Calcutta and the erstwhile seat of British colonial India, grew up along the eastern bank of river Hooghly – around 100 km inward from its mouth where it meets the Bay of Bengal. The land gradient of Kolkata is eastward and thus the canals for disposing waste water and runoff flow from the city to the tidal creek Bidyadhari, further to the east (Murmu et al. 2022). The central part of Kolkata is drained by the Storm Weather Flow (SWF, 26 km) channel, the settlement "Salt Lake" by the Kestopur (34 km) channel, and the north Kolkata and "New Town" areas by the Bagjola (38 km) channel (Figure 1) – each of which convey a combined load of waste water, mostly municipal, and storm runoffs to the Bidyadhari.

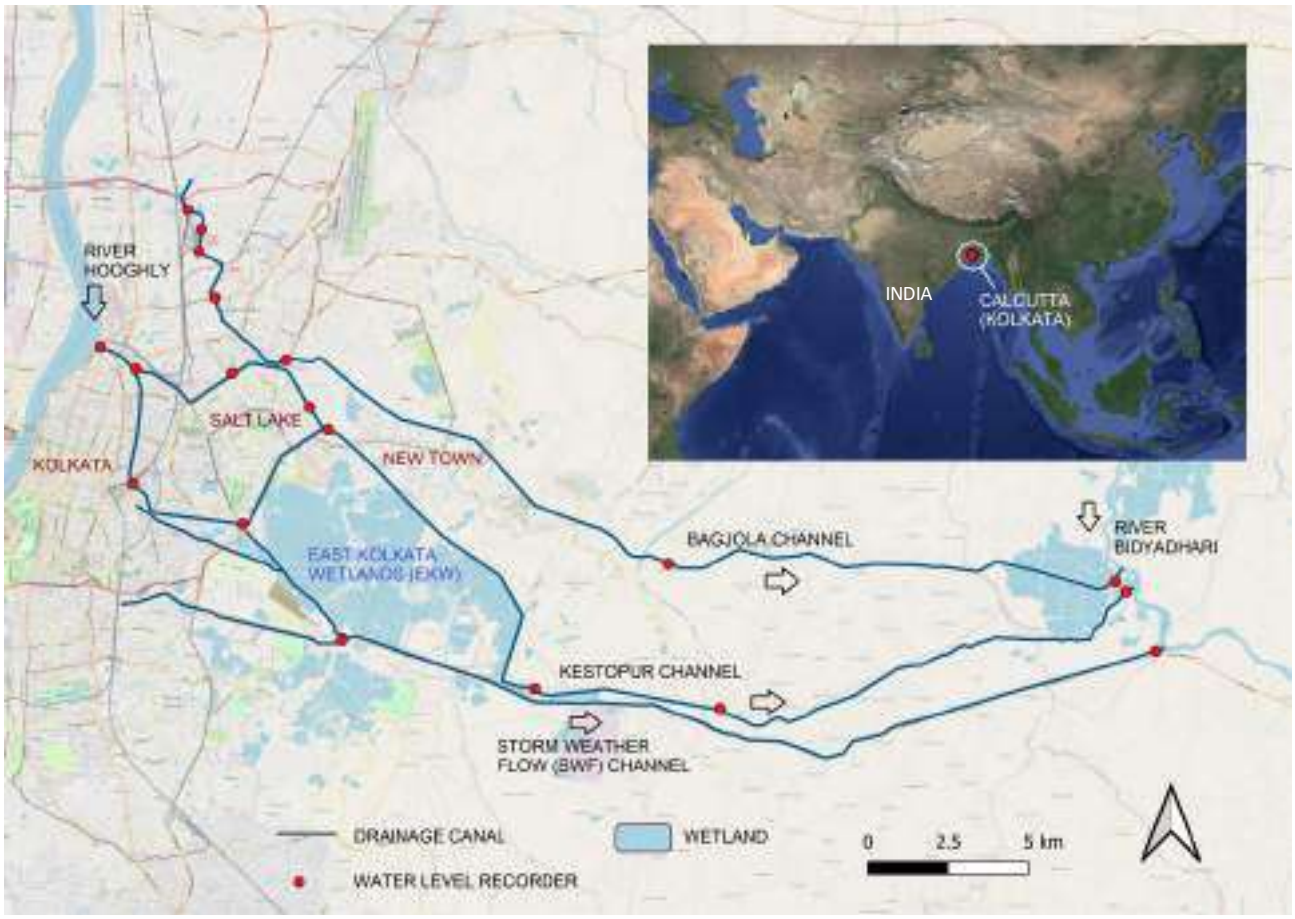

Fig. 1. City of Kolkata, flanked by river Hooghly on its west and river Bidyadhari on its east, discharges its combined waste and storm discharges through drainage channels to the latter. The three major drainage canals – Bagjola, Kestopur, and the Storm Weather Flow or SWF channels – are shown. The water level monitoring stations are used for management of flooding in the canals during the monsoons. Inset: location of the city of Kolkata, India. (Maps courtesy: Open Street Maps and Google Map).

2. Water quality issues in the receiving waters

As per the report NMCG (2019), average dry weather flows from the Bagjola, Kestopur, and SWF channels are around 127, 29, and 31 m^3s^{-1} respectively, with Biochemical Oxygen Demand (BOD_5) in the order of 25 $mg \cdot L^{-1}$. Nadella and Sen (2022) investigated the water quality of the SWF channel, including the water quality parameters Dissolved Oxygen (DO) and BOD_5 (Table 1). The figures indicate that at the upstream end of the SWF channel, both the DO and BOD_5 qualities are very poor, but improve as the flow moves downstream. The Bagjola channel, according to a slightly older reference (Saha et al., 2000), indicates that the BOD_5 generally remains as high as between 50 to 90 $mg \cdot L^{-1}$ in the canal towards the city end. However, during the monsoons, the water in the canal gets diluted and its quality improves to some extent.

The three channels discharge to the tidal river Bidyadhari (Figure 1), the water quality of which is consequently affected, thus raising a concern for the sustenance of aquatic life. Data accessed from WBPCB (2025) shows that at 5 km upstream of the outfalls, at Haroa, BOD_5 in the river is around 22 $mg \cdot L^{-1}$ during the dry weather, but reduces to less than 15 $mg \cdot L^{-1}$ during the monsoons. At 5 km downstream, at Malancha, the corresponding value of BOD_5 is about 18 $mg \cdot L^{-1}$ (dry weather), reducing to within 10 $mg \cdot L^{-1}$ (monsoon). Another 25 km downstream, more towards the ocean, the water quality improves (DO > 6, and BOD_5 < 3).

Table 1. Typical water quality parameter values along the Storm Weather Flow channel (adapted from Nadella and Sen, 2022).

Parameter/ Location	Dissolved Oxygen (DO, $mg \cdot L^{-1}$)	Biochemical Oxygen Demand (BOD_5, $mg \cdot L^{-1}$)	Ammonia (NH_3-N, $mg \cdot L^{-1}$)	Total Coliform / Fecal coliform (MPN/100 mL)
Typical values at city (upstream) end	~1.0 – 3.0 (often very low in dry-weather)	~40 – 100 (very high at some city-end locations)	Peaks near mid-upper reaches (e.g. ~1–8)	Very high (often >>10^4 – 10^6 MPN/100 mL)
Typical values near outfall (downstream) end	~3.5 – 6.0	~5 – 30	Decreses downstream (microbial trans-formation, dilution)	Markedly lower but still elevated (decreases in orders of magnitude)

3. Application of numerical simulation to assess DO and BOD_5 dynamics

This study addresses the question of how tidal hydrodynamics and canal-outfall gate operations influence pollutant transport and the self-purification capacity of the Bidyadhari River, given the effluent pouring into it through the three major discharge channels. In order to prevent back flow of water during high tides, the drainage channels are connected to the Bidyadhari through one-way flap gates near their respective outfalls. As a consequence, flow through the gates varies with time in accordance with the tidal level variation in the river. At times of high tide in the river, the water in the channels stop temporarily flowing out and this period is designated as the gate closure or tidal-lockage time. Subsequently, the canals start releasing the locked-in water along with further inflows when the gates gradually open during the following low tide. Similarly, during rising tide the water moves up along river Bidyadhari while during falling tide, the accumulated flow migrates downstream towards the ocean. This alternating movement of water in the river due to tides plays a role in improving its DO by turbulence which is investigated in this using the computation platform MIKE+ (DHI, 2025). Figure 2 (a) shows the plan layout of the three canals, with cross section locations marked with red ticks. The flow and water quality in the canals are simulated with one-dimensional (1D) models, while the river flow is done so with a two-dimensional (2D) model. The connection of the 1D model of the canals to the 2D model of receiving river is defined a few meters downstream of the tidal lock gates of each canal. Figure 2 (b) shows a magnified view of the two dimensional unstructured computation mesh of the river. The general flow directions are shown in either figure although, being tidal, the river flow moves both ways.

Initialization of the simulation requires specifying the initial and boundary conditions for the channels, and that for the river. In each case, the upstream most boundaries are imposed with known discharges and water quality values. At the lowermost boundary of the Bidyadhari River, the observed time-dependent water level record measured at the gauging station and measured water quality parameter values are imposed. The ambient DO and BOD_5 values, as measured from samples collected from the channels during field data collection campaigns, are used as initial conditions. For the river, reported DO and BOD_5 values obtained from the water-quality portal of state environmental monitoring department, West Bengal Pollution Control Board (WBPCB, http://emis.wbpcb.gov.in/waterquality/viewsampledatacitizen.do), are used.

4. Results and discussion

The variation in DO and BOD_5 levels in the Bidyadhari River vary with rising and falling tides, and also with the opening or closing of the flap gates. During the rising tide, initially when the river water level is low and the gates are open (Figure3a), DO is seen to be good on the downstream. While the river is rising, and the gates are closed after some time (Figure 3b), DO rises in the river. During the falling phase, when the gates are initially closed (Figure 3c) and the river starts flowing down, the influx of poor water from the upstream causes the DO to drop towards the upstream. At later stages of falling tide, when the gates open and influxes poor water from the canals into the river (Figure 3d), the DO in the river starts falling.

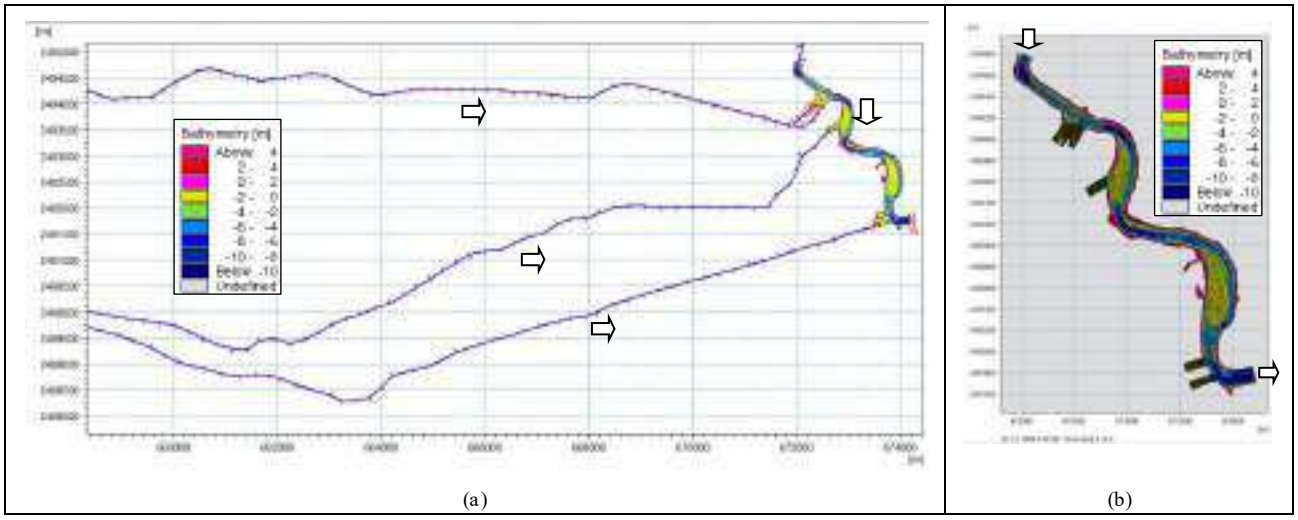

Fig. 2. MIKE modelling framework: (a) One-dimensional hydrodynamic and water quality setup showing the model layout with cross section locations marked for the Bagjola, Kestopur, and the Storm Weather Flow channels. The channels are connected to the two-dimensional model of the Bidyadhari river; (b) Bidyadhari river two-dimensional computational mesh (detail).

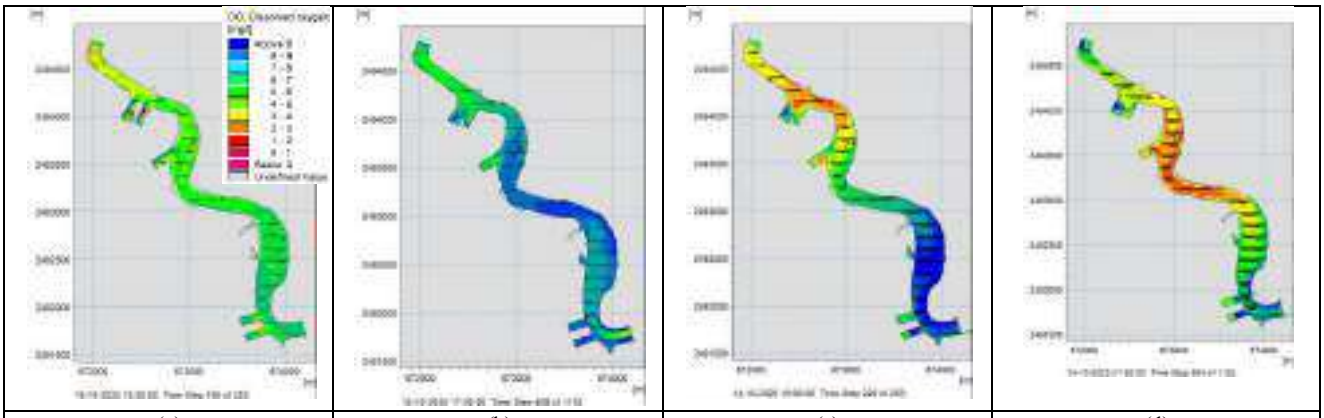

(a) (b) (c) (d)

Fig. 3. Variation of DO in river Bidyadhari with tide and gate condition: (a) rising-closed (b) rising-open; (a) falling-closed; (b) falling-open.

During the rising tide phases (Figures 4a and 4b), the BOD_5 levels, which are high on the downstream, gradually improve in the river but still remain very high near the canal outfalls. During falling tide (Figures 4c and 4d), the locked up poor quality canal waters initially lower the BOD_5 levels, but eventually improve.

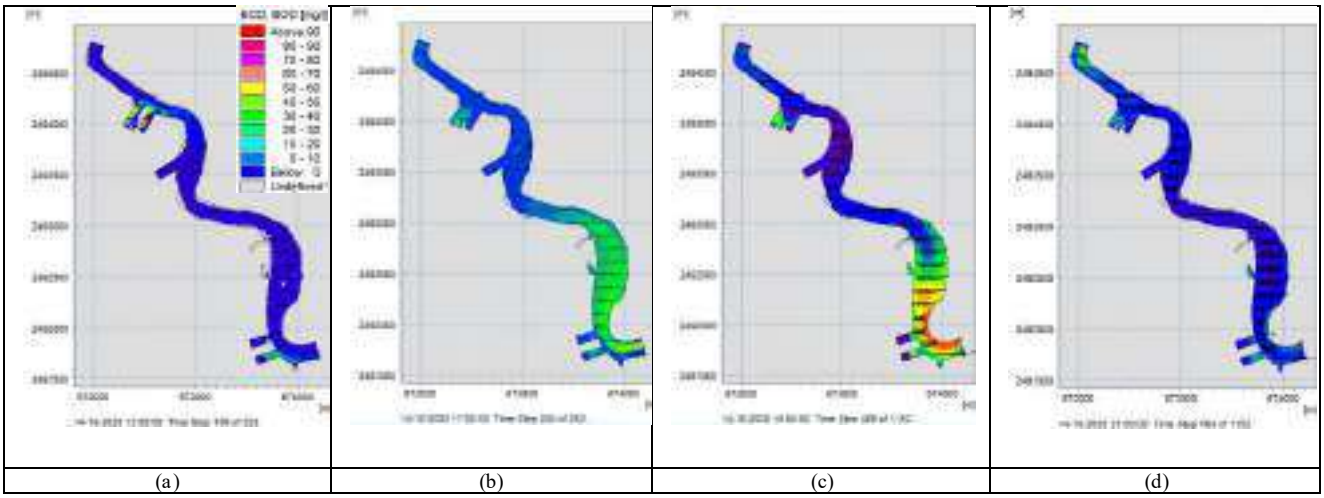

(a) (b) (c) (d)

Fig. 4. Variation of BOD_5 in Bidyadhari with tide and gate condition: (a) rising-closed (b) rising-open; (a) falling-closed; (b) falling-open.

5. Conclusions

This study investigates the hydrodynamic and water-quality interactions between the wastewater-carrying drainage canals of Kolkata and their tidal receiving river, the Bidyadhari, using a coupled one- and two-dimensional modelling framework. The simulations demonstrate that the temporal and spatial variations of dissolved oxygen (DO) and biochemical oxygen demand (BOD_5) in the receiving river are strongly influenced by tidal dynamics and the operational state of the outfall flap gates. Indeed, the results indicate that during rising tides, cleaner tidal water entering the river promotes mixing and natural reaeration, resulting in partial recovery of dissolved oxygen levels. In contrast, during falling tides the opening of the gates allows accumulated polluted water from the canals to enter the river, producing localized increases in BOD_5 and corresponding reductions in DO near the discharge points. The tidal cycle is thus seen to create alternating phases of water-quality degradation and recovery, indicating that the natural self-purification capacity of the river is closely linked to tidal flushing processes. The modelling framework too demonstrates an opportunity for future decision-making for improving water-quality management in a drainage network.

References

Nadella, A., and Sen, D. (2022). Application of wastewater quality index (WWQI) as an evaluation tool: A case of stormwater flow channel (SWF) of Kolkata, India. *Environmental Monitoring and Assessment*, *194*(2), 80.

National Mission for Clean Ganga. (NMCG, 2019). *Proposed action plan for rejuvenation of river Vidyadhari*. Ministry of Jal Shakti, Government of India.

DHI (2025). *MIKE+ 2025 documentation index* [Web page].

Murmu, S. K., Islam, N., and Sen, D. (2022). The heritage sewer networks of Kolkata (Calcutta) and ascertaining their coping potential under growing urban pressures. *ISH Journal of Hydraulic Engineering*, *28*(3), 325-335.

Saha, T., Ghosh, P. B., Mandal, C. C., & Bandyopadhyay, T. S. (2000). Quality assessment of Bagjola canal waste water, Calcutta. *Journal of the Inland Fisheries Society of India (India).*, *32*(1&2).

Session B3

Ecohydraulics meets landscape architecture

Book of Abstracts of the *16th International Symposium on Ecohydraulics*
Challenges and solutions in the time of global changes
August 16–20, 2026, Lausanne, Switzerland
ISSN: 2790-2420 | ISBN: 978-90-837233-9-6 | doi:[10.64697/iahr.proc.ise2026.abs]
© 2026 IAHR. CC BY-NC-ND 4.0

Mapping 360° Transitional Landscapes: Hydraulics for Ecological Ecosystem Connectivity in the Orbe–Chavornay Region

Ben GITAI[1], Chiara LOMBARDI DELLAMONICA,[1] Beate JESSEL[1]

[1] LAND Laboratory, EPFL, Switzerland
email: ben.gitai@epfl.ch
email : chiara.lombardi-dellamonica@epfl.ch

ABSTRACT

Water infrastructure marks both space and time in evolving landscapes. Canals, dams, and drainage systems show where decades of human intervention meet millennia of geological formation. Traditional water management, however, relies on static maps that often fail to show how water systems, ecosystems, and human activities change with climate and land use. The Orbe-Chavornay region in Switzerland demonstrates this gap for over a century; complex water systems have coexisted with intensive agriculture, roads, railways, and industry in a small area, creating flood risks that conventional ecological maps fail to represent.

This research challenges how we perceive and manage hydraulic corridors that no longer fit traditional urban-rural categories. We attempt to transcend the traditional city-countryside and urban-rural divide. As such, the project challenges the current socio-ecological frameworks through which landscapes are perceived and shaped. What were once rural landscapes are now often transitional landscapes, a connective in-between tissue with a metabolic function for urban landscapes. We developed a 360° Moving Map methodology integrating ecohydraulics, different landscape features, mapping water monitoring, governance systems, and water age across landscapes. It examines interactions among blue (hydraulic), green (ecological), and grey (built) infrastructures, highlighting conflicts, synergies, and socio-environmental impacts. Seasonal and daily dynamics reveal critical points where agriculture, liveability, and urban planning problems emerge. Hydrological operations fragment ecological corridors, agricultural drainage alters hydrological conditions, and infrastructure conflicts intensify under climate hazards. Winter and summer variations in water flow create seasonal shifts in availability, affecting irrigation, water quality, energy, and ecological processes. By observing these dynamics across multiple timescales, our method illustrates and makes visible the interconnectedness between these systems. This framework helps communities manage transitional landscapes for productive, ecological, and hydrological functions simultaneously under climate stress in climate-vulnerable regions.

1. Introduction and context

Every perceived space is a landscape and deserves attention as such (European Landscape Convention, Florence, 2000). In the complex fabric of landscape today, infrastructures serve as spatio-temporal markers where event-driven history dovetails with long-term geological processes. In other words, infrastructures interact and interface with evolving geomorphological and hydrological formations. Infrastructures crystallize and illustrate moments of collision and synthesis between the short temporalities of politics and the longer temporalities of environmental and hydrological systems in transitional landscapes. Transitional landscapes are in-between spaces that connect and support surrounding urban areas while remaining ecological, productive, and social places. More specifically, transitional landscapes can be described as both connecting spaces that combine a variety of land uses and places defined by their own aesthetic, social, cultural, and ecological characteristics. They challenge the current socio-ecological frameworks through which landscapes are perceived and shaped. What were once rural landscapes are now often transitional landscapes, a connective in-between tissue with a metabolic function for urban landscapes. The Orbe plain, historically known as a vast marshland, underwent significant drainage works in the 19th century. The two Jura water correction campaigns, followed later by the Wahlen Plan (1940–1945), played a decisive role in reshaping the region's

watercourses. (BAFU, 2017). However, these operations also profoundly altered the area's ecological functioning. The soil's permeability, but above all its retention capacity, has been severely impacted by its conversion to arable land and the decades of intensive farming that followed. Added to this is the continuous expansion of grey infrastructure, which has fragmented the landscape and severely constrained other types of infrastructure. The plain is now highly vulnerable to severe flooding, threatening agricultural production and endangering the region's overall ecosystem.

Climate change further reshapes the movement of water through the landscape, and traditional water management, built on static maps and fixed infrastructure plans, cannot capture these evolving dynamics or the ways water systems interact with ecosystems and human activities. (Lwasa et al., 2022, Cerin et al. 2022). The Swiss region of Orbe-Chavornay is a good example of these socio-ecological and hydrological transitions. For over a century, a complex hydrological system has coexisted with a dense industrial and agricultural landscape. Complex interdependencies have gradually emerged, along with a series of risks that are difficult to represent using traditional mapping tools. Analytical tools capable of apprehending the multiple layers of its landscape have become more necessary than ever.

2. Mapping 360° Transitional Landscapes

The region is characterised by a dense network of infrastructure. Grey infrastructure includes, for example, the historic Moulins Rod, the Nestlé and TERCO industrial sites, and the Orbe–Chavornay railway line, which is being modernised (TRAVYS, 2022), as well as agricultural operations. Blue infrastructure includes the Orbe, Talent and Nozon rivers, the Entreroches canal, and six hydroelectric plants producing 204,000 MWh per year (Historical Dictionary of Switzerland, 2012), (Torpille.ch, 2022). Finally, green infrastructure includes the Gorges de l'Orbe nature reserve, the Creux-de-Terre wetlands and riverside corridors.

This study introduces a 360° Moving Map methodology at the intersection of ecohydraulics and landscape architecture, focusing on the connectivity of the ecological, infrastructural and governance systems (see Fig.1). The approach develops analytical tools to map and understand water age distribution across landscapes for sustainable management strategies, showcasing innovative mapping that integrate hydraulic systems with territorial planning for sustainable, multifunctional spaces and the creation of new habitats for innovative, integrated urban and ecological development. Through an analysis of blue (hydraulic), green (ecological) and grey (built and productive) infrastructure in the landscape, the methodology developed observes the interactions between governance systems, socio-environmental benefits, and conflicts that emerge at the points where these infrastructures intersect (Hansen & Pauleit, 2014). The research aims to produce, based on an analysis of water interactions in different urban ecosystems (Salliou et al., 2025), a comprehensive map of water interactions in the transitional landscape of Orbe-Chavornay (Huang et al., 2025).



1) 2) 3)

Fig. 1,2,3. ***360° Digital Mapping Model of the Orbe River, November 2025, 14h00.*** **LAND EPFL, PL-MTI EPFL, 2025.**

The 360° Moving Map is developed by integrating multiple open datasets obtained through Swiss federal and cantonal open data portals, including for example the federal geoportal map.geo.admin.ch (swisstopo), the national hydrological monitoring network hydrodaten.admin.ch (BAFU), and cantonal spatial data infrastructures such as the Vaud GIS platform. Hydrological data, including water levels and flow records, are sourced from the Federal Office for the Environment (BAFU, 2025). Hydrological monitoring data: stations and data, Station 2378, Swiss Confederation) The national hydrography monitoring network, which provides continuous station-based measurements for rivers and lakes across Switzerland, specifically at the water monitoring station in Orbe. Land use and cadastral data are obtained from the Swiss Federal Office of Topography (swisstopo), while infrastructure records are compiled from regional planning authorities, expert testimonies, and local farmers. These datasets and conducted interviews are georeferenced, layered, and processed within a Unity-based 3D visualization engine, enabling dynamic, time-sensitive rendering of blue, green, and grey infrastructure interactions across seasonal and diurnal cycles. The integration workflow involves aligning spatial datasets at a common resolution before embedding them into the simulation

environment, where flow parameters and temporal variables can be animated and observed simultaneously. While the current implementation is grounded in the Orbe-Chavornay case study, the methodology is designed to be transferable to other landscapes, waterscapes, and climate-vulnerable regions where open hydrological and land-use datasets are available.

3. Temporal Dynamics: Capturing Seasonal and Diurnal Variations

The method developed is based on a monitoring cycle that combines two-time scales. The first focuses on seasonal dynamics, while the second is more precise and focuses on daily variations. Indeed, the daily cycle highlights the functional and spatial relationships that may exist between water, soil, vegetation and human activities. During the day, the use of agricultural land and infrastructure is much more important, which puts pressure on groundwater reserves and surface dynamics and has a direct influence on the speed, temperature and biochemical composition of water flows.

Conversely, at night, another cycle takes place. With human activity significantly reduced, natural cycles are under less pressure. Lower night-time temperatures reduce evapotranspiration, allowing groundwater to recharge and soils to rebalance their moisture levels. Understanding changes in day-night cycles is essential for landscape analysis (Burns et al., 2012). It allows us to observe the interactions that may exist between the hydrological cycle and land use. Only considering these elements, is it possible to develop strategies that reconcile natural ecological cycles with anthropogenic water management systems. The day and night moving maps function as paired temporal layers that reveal differential water dynamics between diurnal and nocturnal periods. These visualizations trace variations in flow velocity, temperature gradients, and moisture levels throughout the twenty-four-hour cycle and across seasons. The 360° digital mapping model (see fig. 01,03) exposes a systematic temporal pattern, eg, irrigation-driven flows generate pronounced diurnal peaks during morning, midday, and evening hours that frequently exceed the landscape's natural drainage capacity. Nocturnal flows recede to baseflow conditions, establishing alternating zones of accumulation and depletion across the daily cycle.

Comparing these temporal patterns identifies critical intervention points. By examining velocity maps and flow streamline moving images across multiple time scales, and by drawing on transcripts from expert interviews conducted on site, specific management emerges in the model. Field research of interviews and recorded conversations with local farmers and cantonal water management officers reveals the entrenched tensions structuring this landscape in time: corrected waterways were historically engineered to drain agricultural land as rapidly as possible toward the lake, yet today the same infrastructure generates the flood peaks the mapping tool captures. From the farmers' perspective, these shifting hydrological conditions directly threaten crop viability and agricultural planning. Rising groundwater tables, increasingly intense and rapid flood events, and the growing unpredictability of seasonal water availability make it difficult to maintain stable cropping cycles. As interview transcripts reveal, farmers generally perceive water management problems only when they are directly affected by flooding, at which point drainage infrastructure is blamed for failing to perform. This reactive relationship with water risk reflects a broader challenge: the absence of accessible, real-time tools that would allow farming communities to anticipate hydrological stress, adjust irrigation schedules, and plan crop rotations in response to seasonal and diurnal flow dynamics. As one senior water manager of the Canton of Vaud noted, the paradigm is shifting, where the priority was once to evacuate water as fast as possible; the aim is now to give water back its space and restore more natural flow regimes. Among the most actionable findings emerging from this temporal analysis is the potential for irrigation peak redistribution as a low-cost adaptive strategy.

The 360° moving maps reveal that morning and midday irrigation cycles generate flow peaks that exceed local drainage capacity, creating predictable accumulation zones that correlate with documented flood risk areas of the plain of Orbe. This aligns with the expert water manager of the Canton of Vaud observations that flood events are becoming more extreme and faster, and that raising dikes indefinitely is no longer a viable long-term response. As illustrated in Figure 3, these accumulation and depletion zones are spatially explicit and seasonally consistent, suggesting that targeted, time-based management interventions can be identified and communicated directly to farmer partners and local water governance bodies using the annotated map outputs while looking at this moving transitional landscape. Interviewees also highlighted that land ownership remains the principal obstacle to giving rivers more space, and that successful interventions depend on securing stakeholder buy-in at the municipal and agricultural level. While showing this intervention and looking in the landscape, the mapping tool can directly support by making complex hydrological dynamics legible to specialist and non-specialist audiences. To support community-level application, a dedicated annotated figure could accompany this analysis, showing how local stakeholders, including farmer partners and water

governance bodies, can read accumulation and depletion zones within their own landscape and identify priority areas for intervention. This demonstrates the tool's capacity not only to diagnose landscape vulnerability, but to generate spatially grounded, community-readable recommendations for adaptive water management that are accessible to a broad range of stakeholders, from regional planners to farming communities in climate-vulnerable regions worldwide.

In this way, the mapping serves as a diagnostic tool that identifies long-term flood risk and inundation cycles in relation to annual hydrological patterns, revealing where and when water flows diverge from desired ecological or governance objectives. This temporal analysis connects immediate operational concerns with longer-term resilience planning, enabling interventions that address both daily infrastructure stress and seasonal flood vulnerability. For its part, seasonal motion image captures the dialogue that takes place between natural hydrological processes and landscape productive practices. Reading the transitional landscape through these various time scales provides a subtle moving-mapping that correlates ecological and human development. This approach does more than simply document change; it identifies strategic moments when relationships between infrastructures shift from synergy to conflict. This makes it possible to imagine adaptive management of hydraulics, ecosystems, and urban water cycles and establish visual models that reinforce ecological functions, address governance issues, and consolidate environmental resilience in this transitional landscape that is vulnerable to climate change.

Acknowledgements

Fig. 1,2,3. 360° Drone video image: Platform MTI team (Laurent Deschamps, Matthias Loup, Alejandro Santa Cruz Paz); Mapping model: LAND team (Ben Gitai, Chiara Lombardi Dellamonica); Technical information: Gestion intégrée de la Plaine de l'Orbe (Gesorbe); Chef du Service des eaux, sols et assainissement du Canton de Vaud, Valentin 10, Lausanne, 15.09.2005. The beta version of the interactive interface incorporates the superimposition of a 19th-century drawing sourced from the Cantonal Archives of Vaud, highlighting the temporal layers and landscape transformation systems represented in the map. LAND-EPFL, PL-MTI EPFL, 2026.

References

BAFU (2017). 150 ans de la correction des eaux du Jura. Swiss Federal Office for the Environment.

BAFU (Federal Office for the Environment). (2025). Hydrological monitoring data: stations and data, Station 2378. Swiss Confederation. https://www.hydrodaten.admin.ch/fr/seen-et-fluesse/stationen-und-daten/2378#waterlevel-annual

Burns, M.J., Fletcher, T.D., Walsh, C.J., Ladson, A.R., & Hatt, B.E. (2012). Hydrologic shortcomings of conventional urban stormwater management and opportunities for reform. Landscape and Urban Planning, 105(3), 230–240.

Council of Europe (2000). European Landscape Convention. Florence, 20.X.2000. ETS No. 176.

Dictionnaire Historique de la Suisse (2012). Orbe (rivière). Retrieved from https://hls-dhs-dss.ch/fr/articles/008759/

Fletcher, T.D., Shuster, W., Hunt, W.F., Ashley, R., Butler, D., Arthur, S., ... & Viklander, M. (2014). SUDS, LID, BMPs, WSUD and more — The evolution and application of terminology surrounding urban drainage. Urban Water Journal, 12(7), 525–542.

Folke, C., Carpenter, S.R., Walker, B., Scheffer, M., Chapin, T., & Rockström, J. (2010). Resilience thinking: Integrating resilience, adaptability and transformability. Ecology and Society, 15(4), 20.

Hansen, R., & Pauleit, S. (2014). From multifunctionality to multiple ecosystem services? A conceptual framework for multifunctionality in green infrastructure planning for urban areas. AMBIO, 43(4), 516–529.

Huang, J., Bibri, S. E., & Keel, P. (2025). Generative spatial artificial intelligence for sustainable smart cities: A pioneering large flow model for urban digital twin. Environmental Science and Ecotechnology.

Huang, W. T. K., Masselot, P., Bou-Zeid, E., Fatichi, S., Paschalis, A., Sun, T., ... & Manoli, G. (2023). Economic valuation of temperature-related mortality attributed to urban heat islands in European cities. Nature Communications, 14(1), 7438.

Lwasa, S., Seto, K. C., Bai, X., Blanco, H., Gurney, K. R., Kilkiş, S., ... & Yamagata, Y. (2022). Urban systems and other settlements. Climate Change 2022: Mitigation of Climate Change. Contribution of Working Group III to the Sixth Assessment Report of the Intergovernmental Panel on Climate Change.

Pahl-Wostl, C. (2007). Transitions towards adaptive management of water facing climate and global change. Water Resources Management, 21(1), 49–62.

Salliou, N., Urech, P., Leitão, J.P., & Grêt-Regamey, A. (2025). Urban water projects must consider landscape architecture. Nature Water, 3, 260–270.

Torpille.ch (2022). Patrimoine au Fil de l'Eau - Orbe. July 22.

Vörösmarty, C.J., McIntyre, P.B., Gessner, M.O., Dudgeon, D., Prusevich, A., Green, P., ... & Davies, P.M. (2010). Global threats to human water security and river biodiversity. Nature, 467, 555–561.

Book of Abstracts of the *16th International Symposium on Ecohydraulics*
Challenges and solutions in the time of global changes
August 16–20, 2026, Lausanne, Switzerland
ISSN: 2790-2420 | ISBN: 978-90-837233-9-6 | doi:[10.64697/iahr.proc.ise2026.abs]
© 2026 IAHR. CC BY-NC-ND 4.0

LA MARJAL AND GRØNNINGEN BISPEPARKEN FLOODABLE PARKS, TWO DIFFERENT DESIGNS, ONE SINGLE AIM

Silvia MARTÍN MUÑOZ

[1] University of Antwerp (Belgium)

Silvia.MartinMunoz@uantwerpen.be

ABSTRACT

Keywords: Climate change; floods; multifunctional urban design; nature based solutions; floodable parks; water retention; biodiversity; ecosystem services; co-benefits.

1. Societal, social, economic, environmental or technological problems and challenges

It is projected that by 2050 more than two-thirds of the world's population will live in urban areas (Oertli & Parris, 2019). Built-up space is also expected to triple in surface (Matos Silva & Costa, 2016). Urbanization creates a diversity of ecological problems including air and water pollution, the degradation and fragmentation of habitats and biodiversity loss, which are exacerbated by an increasingly altered climate and intensified natural disasters. Floods are currently the most common natural disaster in cities globally (Guerrero et al., 2018). The frequency of flooding has risen a 48% compared to historic levels (Vörösmarty et al., 2010), with climate change being the main driver of this increase (Lourenço et al., 2020). The anthropogenic activities related to city expansion, such as deforestation and river plain modification, as well as increased imperviousness, inevitably cause the intensification of flood hazards' impacts (Cremades et al., 2021). Consequently, urban development on low-lying areas that were previously considered safe from flooding are now being exposed as highly vulnerable. Extreme droughts are also associated to the alteration of the atmospheric dynamics, which have raised the urban water demand leading to severe water use restrictions on the most vulnerable regions (Pinho et al., 2023).

Traditionally, hard engineering measures have been used to address water hazards, but evidence suggests that they are unlikely to meet the future demand of stormwater management (Lourenço et al., 2020). Nature-based Solutions (NbSs) can be used as a tool to create greener and more sustainable cities and help tackle the aforementioned challenges (Fluhrer et al., 2021). NbSs are measures which use natural processes to provide environmental, social and economic benefits and to increase resilience to climate-change hazards. NbS have been promoted across Europe, the USA, and Australia through guidelines and policies which encourage water-sensitive urban design (WSUD), low-impact developments (LID) practices and best management practices (BMPs) .

Aquatic NbSs (aNbSs) address, among others, water-related problems such as droughts and floods. aNbS deliver as well other ecosystem services (ESs) such as recreation, the attenuation of the Urban Heat Island (UHI) effect, and other benefits such as the enhancement of biodiversity. The most recent guidelines for the

implementation of NbS highlight biodiversity conservation not only as an objective but as a pre-requisite(European Comission, 2021; Pettorelli et al., 2021; Seddon et al., 2021; Xie et al., 2022). However, a research by Xie et al. (2022) found that only 351 out of 976 of NbS projects in European cities had defined explicit biodiversity goals, hindering the deceleration of the rate of biodiversity loss and ecosystem degradation (Brondizio et al., 2019; Secretariat of the Convention on Biological Biodiversity, 2020). Emphasis should be given to the preservation and enhancement of biodiversity in future urban development plans.

2. Integrated urban and ecological development of future cities

One emerging aNbS is floodable urban parks. They can be defined as recreational spaces to which runoff water is conveyed for its retention and drainage and which can be temporarily flooded as a result of the infiltration occurring in the surrounding aNbSs (e.g., rain gardens, bioswales, dry infiltration basins) (Martín Muñoz et al., 2024) (**Figure 1**). Therefore, unlike a normal park, this aNbS is designed for its complete or partial inundation to attenuate surface runoff during extreme precipitation events. The role of the vegetation biodiversity of the surrounding aNbSs in this aNbS is crucial for the gradual filling of the park, since it supports the water regulating ESs by promoting water infiltration, retention, interception and evaporation. Other benefits intimately linked with plant biodiversity are recreation, air purification and microclimate regulation. An additional benefit of this type of solution is that it can potentially be connected with treatment plants for the post-rainfall treatment of the stored water, such as in "La Marjal" floodable park (Alicante, Spain), a model example of a circular water system (Sánchez-Almodóvar et al., 2022, 2023). This aNbS allows for a paradigm shift in urban water management strategies towards resilience and circularity, helping mitigate water scarcity, improving water quality and enhancing urban ecosystems' health.

However, the inundation of the park might negatively impact the delivery of other benefits (namely recreation and biodiversity). On the other hand, biodiversity also affects ESs such as water infiltration (Leimer et al., 2021) but the magnitude of these effects is poorly known, especially for built ecosystems. Thus, to plan a floodable park which minimizes trade-offs and maximizes benefits, it is necessary to study the impact of inundation on the delivery of the ESs. ESs have proven to be effective for communicating to non-scientists the value of natural and artificial ecosystems.

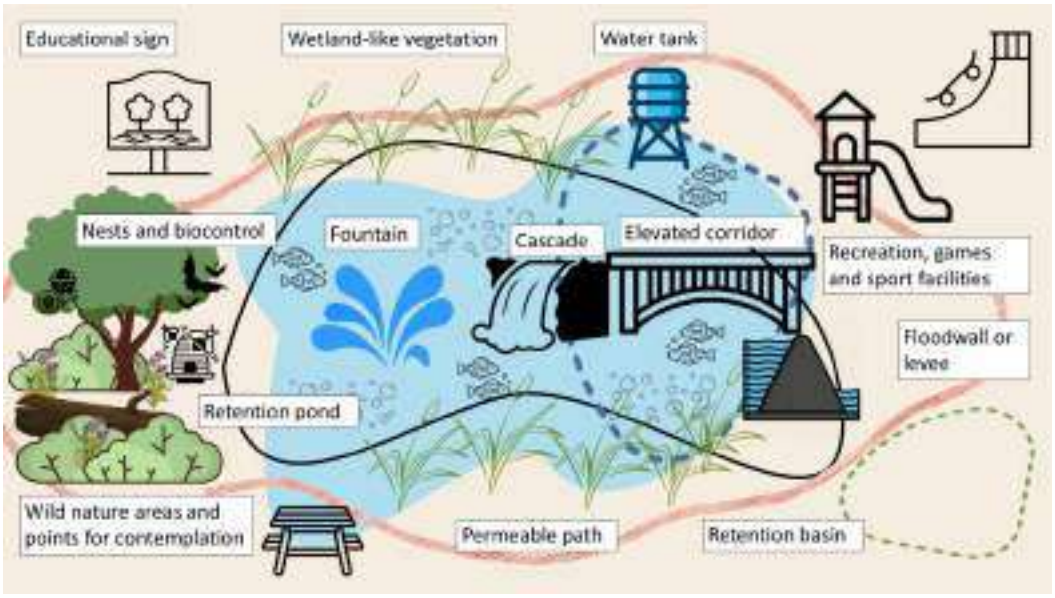

Fig. 1. Graphical scheme of floodable park design features.

3. Innovative design that integrate water systems with urban planning for sustainable, multifunctional spaces and the creation of new habitats

The ES supply after a complete inundation will likely be largely determined by the design of the floodable park. However, to present, scarce research has been done on the implications of different designs of floodable parks. Two existing floodable parks were selected for the study of their design. The first, La Marjal, is located in Alicante (Spain). La Marjal is located in a zone where natural ravines had been replaced by urban

development, thus creating flooding problems in the surroundings. Thus, a floodable park was created in 2015 which could tackle the observed issues while having additional co-benefits. The second park is Grønningen Bispeparken (Copenhagen, Denmark). This park is part of a Cloudburst program which was developed to decrease the flooding downstream and finished on 2024. The park was designed through co-creation processes. All two parks focused on the water retention, recreation and biodiversity features.

In order to elucidate the main design features and management strategies which dictated the planning of the parks, interviews and surveys were performed with the different organizations and experts that took part in the phases of the floodable park's development/implementation process of the selected case studies. They were asked for a group interview, prioritizing the representation of each phase of the process and mixing different professional backgrounds. At least one group interview (from 4-8 actors per group) was conducted (online). The aim of the interview study was to gain more understanding on the1) drivers for the implementation of the parks, 2) prior landscape and geophysical evaluation made, 3) design and management strategies objectives, 4) cost and maintenance of the parks, 5) barriers and lessons learnt (e.g., success of the design and management to deal with the trade-offs between water mitigation and other benefits of the park in prior flood events, i.e., presence of mosquitoes in the parks' surroundings, eutrophication, vegetation loss). Open discussions were guided, ensuring that each participant gives their insight. To complete the interview, a survey was conducted on Qualtrics XM software.

A thematic map was created where the main themes and codes extracted from the interviews were associated, creating a general narrative common to both case studies and applicable to future floodable parks. Differences between both case studies were distinguished, especially regarding the location (downstream vs upstream) and the design (La Marjal is a wet floodable park while Grønningen is a dry floodable park). However, the maintenance principles and the success stories regarding water mitigation performance, public acceptance and habitat creation for biodiversity were alike.

La Marjal, opted for a wet floodable park design with a permanent water sheet. Additional aeration systems were implemented when oxygen was observed to cross the ecological thresholds. Management of pond targets specifically eutrophication and mosquito biocontrol was enhanced by building nests for insectivorous birds and promoting bats and fish colonization. On the other hand, Grønningen was designed as a dry floodable park with a cascade of retention basins. This park is a retrofit of an unused grass lawn. As in La Marjal, native vegetation was planted according to the different flooding zones, taking care that invasive species are eradicated. In this case, co-creation was a main component of the planning process since social unsafety was one of the main drivers for its construction.

The lessons learned in the interviews can be summarized as follows:

- To construct a floodable park, three main requisites need to be fulfilled:
  1) have current flooding problems
  2) have availability of space close to the problem and treatment plant and
  3) reduce land changes (via synergies with existing infrastructure and rainwater separation in separate sewage systems).
- Interdisciplinary and multi-governance enhance the chances of success (for example, via co-creation, art and education)
- Regular monitoring is required (especially of the water quality and vegetation), but extensive and adaptive management tackles better the uncertainties posed by climate change
- A multifunctional flexible design can successfully address diverse challenges that cities are facing, from water hazards and habitat fragmentation to lack of green and the urban heat island effect.

On the other hand, limitations and barriers for the initial planning of floodable parks were identified in the survey, including 1) Fear/doubts about this new nature-based solution, 2) Lack of public acceptance (also chosen as not important for 1 person), 3) Lack of (non-economic) resources to begin and sustain adaptation efforts, 4) Lack of political leadership and 5) Lack of areas where to implement floodable parks.

Overall, the results show that, despite the differences driven by their socio-cultural and climatic context, the parks were both constructed following similar design goals and, regardless of the final design, both claim the success of all three main design goals: creating a space both for humans and biodiversity, and effective runoff water mitigation.

Acknowledgements

This work was supported by the University of Antwerp through a BOF (Bijzonder Onderzoeksfonds) grant. Additional funding was provided by the Biodiversa+ programme, part of the European co-funded biodiversity partnerships. We also gratefully acknowledge support from the DUT (Driving Urban Transitions) initiative, which will contribute to continue this research in the 2026-2029 period.

References

Brondizio, E., Diaz, S., Settele, J., & Ngo, H. T. (2019). *Global assessment report on biodiversity and ecosystem services of the Intergovernmental Science-Policy Platform on Biodiversity and Ecosystem Services*.

Cremades, R., Sanchez-Plaza, A., Hewitt, R. J., Mitter, H., Baggio, J. A., Olazabal, M., Broekman, A., Kropf, B., & Tudose, N. C. (2021). Guiding cities under increased droughts: The limits to sustainable urban futures. *Ecological Economics*, *189*, 107140. https://doi.org/10.1016/j.ecolecon.2021.107140

European Comission. (2021). *Directorate-General for Research and Innovation, Evaluating the impact of nature-based solutions – A handbook for practitioners*.

Fluhrer, T., Chapa, F., & Hack, J. (2021). A Methodology for Assessing the Implementation Potential for Retrofitted and Multifunctional Urban Green Infrastructure in Public Areas of the Global South. *Sustainability*, *13*(1), 384. https://doi.org/10.3390/su13010384

Guerrero, P., Haase, D., & Albert, C. (2018). Locating Spatial Opportunities for Nature-Based Solutions: A River Landscape Application. *Water*, *10*(12), 1869. https://doi.org/10.3390/w10121869

Leimer, S., Berner, D., Birkhofer, K., Boeddinghaus, R. S., Fischer, M., Kandeler, E., Kuka, K., Marhan, S., Prati, D., Schäfer, D., Schöning, I., Solly, E. F., Wolters, V., & Wilcke, W. (2021). Land-use intensity and biodiversity effects on infiltration capacity and hydraulic conductivity of grassland soils in southern Germany. *Ecohydrology*, *14*(6). https://doi.org/10.1002/eco.2301

Lourenço, I. B., Beleño de Oliveira, A. K., Marques, L. S., Quintanilha Barbosa, A. A., Veról, A. P., Magalhães, P. C., & Miguez, M. G. (2020). A framework to support flood prevention and mitigation in the landscape and urban planning process regarding water dynamics. *Journal of Cleaner Production*, *277*, 122983. https://doi.org/10.1016/j.jclepro.2020.122983

Martín Muñoz, S., Elliott, S., Schoelynck, J., & Staes, J. (2024). Urban Stormwater Management Using Nature-Based Solutions: A Review and Conceptual Model of Floodable Parks. *Land*, *13*(11), 1858. https://doi.org/10.3390/land13111858

Matos Silva, M., & Costa, J. (2016). Flood Adaptation Measures Applicable in the Design of Urban Public Spaces: Proposal for a Conceptual Framework. *Water*, *8*(7), 284. https://doi.org/10.3390/w8070284

Oertli, B., & Parris, K. M. (2019). Review: Toward management of urban ponds for freshwater biodiversity. *Ecosphere*, *10*(7). https://doi.org/10.1002/ecs2.2810

Pettorelli, N., Graham, N. A. J., Seddon, N., Maria da Cunha Bustamante, M., Lowton, M. J., Sutherland, W. J., Koldewey, H. J., Prentice, H. C., & Barlow, J. (2021). Time to integrate global climate change and biodiversity science-policy agendas. *Journal of Applied Ecology*, *58*(11), 2384–2393. https://doi.org/10.1111/1365-2664.13985

Pinho, P., Haase, D., Gebler, D., Staes, J., Martelo, J., Schoelynck, J., Szoszkiewicz, K., Monaghan, M. T., & Vierikko, K. (2023). *Urban Aquatic Nature-Based Solutions in the Context of Global Change: Uncovering the Social-ecological-technological Framework* (pp. 139–157). https://doi.org/10.1007/978-3-031-34378-0_8

Sánchez-Almodóvar, E., Olcina-Cantos, J., & Martí-Talavera, J. (2022). Adaptation Strategies for Flooding Risk from Rainfall Events in Southeast Spain: Case Studies from the Bajo Segura, Alicante. *Water*, *14*(2), 146. https://doi.org/10.3390/w14020146

Sánchez-Almodóvar, E., Olcina-Cantos, J., Martí-Talavera, J., Prieto-Cerdán, A., & Padilla-Blanco, A. (2023). Floods and Adaptation to Climate Change in Tourist Areas: Management Experiences on the Coast of the Province of Alicante (Spain). *Water*, *15*(4), 807. https://doi.org/10.3390/w15040807

Secretariat of the Convention on Biological Biodiversity. (2020). *The Global Biodiversity Outlook 5 (GBO-5)*. https://www.cbd.int/gbo/gbo5/publication/gbo-5-en.pdf

Seddon, N., Smith, A., Smith, P., Key, I., Chausson, A., Girardin, C., House, J., Srivastava, S., & Turner, B. (2021). Getting the message right on nature-based solutions to climate change. *Global Change Biology*, *27*(8), 1518–1546. https://doi.org/10.1111/gcb.15513

Vörösmarty, C. J., McIntyre, P. B., Gessner, M. O., Dudgeon, D., Prusevich, A., Green, P., Glidden, S., Bunn, S. E., Sullivan, C. A., Liermann, C. R., & Davies, P. M. (2010). Global threats to human water security and river biodiversity. *Nature*, *467*(7315), 555–561. https://doi.org/10.1038/nature09440

Xie, L., Bulkeley, H., & Tozer, L. (2022). Mainstreaming sustainable innovation: unlocking the potential of nature-based solutions for climate change and biodiversity. *Environmental Science & Policy*, *132*, 119–130. https://doi.org/10.1016/j.envsci.2022.02.017

Book of Abstracts of the *16th International Symposium on Ecohydraulics*
Challenges and solutions in the time of global changes
August 16–20, 2026, Lausanne, Switzerland
ISSN: 2790-2420 | ISBN: 978-90-837233-9-6 | doi:[10.64697/iahr.proc.ise2026.abs]
© 2026 IAHR. CC BY-NC-ND 4.0

ECOHYDRAULIC ASSESSMENT OF WATERSHED HYDROLOGICAL SERVICES USING THE VIC MODEL: A CASE STUDY OF THE LUAN RIVER BASIN, NORTH CHINA

Yuze YANG[1,2], Ruonan LI[1,*], Hua ZHENG[1]

[1] Research Center for Eco-Environmental Sciences, Chinese Academy of Sciences, Shuangqing Road 18, Beijing China

2 Institute of International Rivers and Eco-Security, Yunnan University, No.2 North Road of the Green Lake, Kunming,Yunnan, China
email: lnjzyangyz@163.com (for Yuze YANG)
email: rnli@rcees.ac.cn (for Ruonan LI)
email: huazheng@rcees.ac.cn (for Hua Zheng)

ABSTRACT

Using the VIC distributed hydrological model, this study quantitatively evaluates the spatio-temporal dynamics of hydrological ecosystem services, including water-supply (WS) and water-retention (WR), in the Luan River Basin from 1980 to 2018, and examines the joint influences of climate change and vegetation restoration. Here, WR is defined as a hydrological regulation index derived from soil water storage and baseflow, representing the capacity of ecosystems to retain precipitation and sustain delayed release. The results show decreasing precipitation, increasing air temperature and evapotranspiration, and significantly rising NDVI. Over the study period, WS decreased by 16.81%, whereas WR increased by 5.66%, revealing a clear trade-off between enhanced regulation and reduced water yield in this water-scarce basin. The spatially explicit results provide useful evidence for ecological restoration, blue–green infrastructure planning and water management under stringent water-resource constraints in northern China.

Keywords: Luan River Basin; Hydrological ecosystem services; VIC hydrological model; vegetation restoration.

1. Introduction

Quantifying watershed hydrological ecosystem services (HES) and understanding how ecosystem change alters these services are essential for sustainable basin management in water-limited regions (Ha et al., 2023; Harrison-Atlas et al., 2016; Decsi et al., 2022). In northern China, large-scale ecological restoration and rapid land-use transitions have substantially modified ecohydrological processes, raising concerns about trade-offs between vegetation restoration, water availability and riverine ecosystem functioning (Bai et al., 2020; Feng et al., 2016; Yue et al., 2023).

The Luan River Basin, located in the semi-arid–semi-humid transition zone of North China, is a typical water-scarce basin that supplies water to cities, agriculture and ecological projects. Over the past four decades, the basin has experienced climate warming, decreasing precipitation, vegetation greening, afforestation and rapid urban expansion (Yue et al., 2023). These changes likely reshaped the partitioning of precipitation into evapotranspiration, runoff and subsurface storage, with direct implications for ecohydraulic conditions and landscape planning along river corridors.

This study aims to: (1) characterise long-term climate and ecosystem changes in the Luan River Basin (1980–2020); (2) set up and localise a Variable Infiltration Capacity (VIC) distributed hydrological model; (3) quantify water-supply (WS) and water-retention (WR) services across main ecosystem types; and (4) explore the relative roles of climate change and vegetation restoration in shaping these services.

2. Study area and methods

2.1. Study area

The Luan River Basin extends from mountainous headwaters in the north-west to middle and lower reaches draining to the Bohai Sea. The monsoonal climate features concentrated summer rainfall and strong interannual variability. Recent decades show a warming and relatively drying tendency.

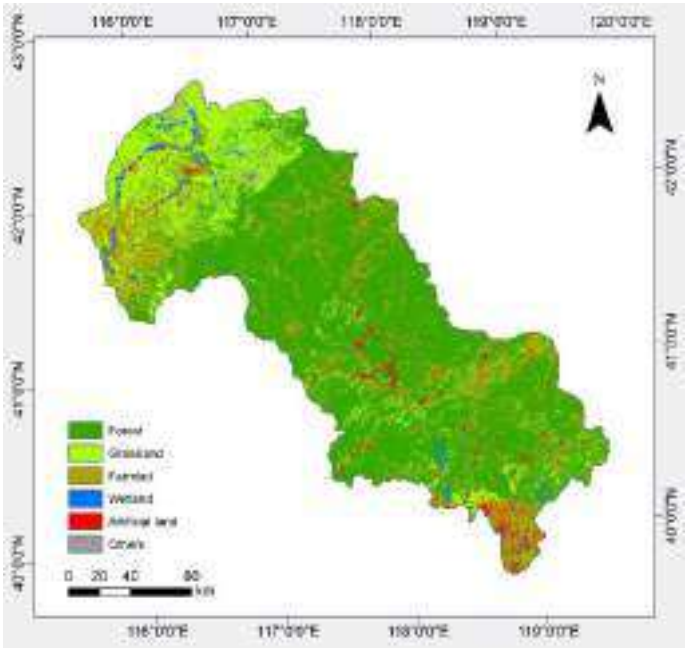

Fig. 1. Location of the Luan River Basin and main ecosystem types

2.2. Data

The upper basin is dominated by forest and grassland; the middle and lower reaches are a mosaic of cropland, urban land and remaining natural vegetation. A multi-source dataset for 1980–2020 was compiled, including daily meteorological data, discharge at key gauges, land-use/land-cover maps and remotely sensed NDVI. Field surveys supported land-cover verification and parameter localisation.

2.3. Methods

A distributed VIC hydrological model was implemented on a gridded domain covering the basin. The model represents sub-grid variability in soil moisture through a variable infiltration scheme and simulates evapotranspiration, surface runoff and baseflow driven by meteorological forcings, soil and vegetation parameters. Soil hydraulic and depth parameters were derived from regional data and refined; vegetation parameters (leaf area, rooting depth, canopy resistance, albedo) were assigned by land-cover type.

Model calibration and validation used multi-year discharge records at representative outlets with a split-sample strategy. Performance was evaluated using Nash–Sutcliffe efficiency (NSE), the ratio of RMSE to the standard deviation of observations (RSR), and percent bias (PBIAS). Thresholds for "good" performance were NSE > 0.75, RSR < 0.50 and |PBIAS| < 10 %. Trend significance was evaluated by linear regression at $p < 0.05$.

On the basis of the calibrated model, long-term simulations (1980–2018) were conducted. Two HES indicators were quantified annually at grid scale and then summarised by ecosystem type and sub-basin. To support attribution, interannual variations in WS and WR were further compared with changes in forest NDVI and forest area in the upper, middle and lower reaches, so that the relative influence of climate background and vegetation restoration could be interpreted more explicitly within the distributed modelling framework.

(1) Water-supply service (WS): annual surface runoff + baseflow in $mm \cdot yr^{-1}$;

(2) Water-retention service (WR): a regulation index derived from annual soil water storage and baseflow, expressed in equivalent water depth ($mm \cdot yr^{-1}$), reflecting the capacity of ecosystems to retain water and sustain delayed release.

WS and WR were aggregated by ecosystem type (forest, grassland, cropland, urban and others) and by sub-basin. Linear regression was used to detect trends, and grid-based outputs were used to identify areas with the strongest changes in hydrological services and their correspondence with major vegetation restoration zones.

3. Results

3.1. Climate and ecosystem change

From 1980 to 2020, basin-averaged annual precipitation decreased, while mean annual temperature and actual evapotranspiration increased significantly ($p < 0.05$), indicating a warming and relatively drying climate. NDVI also showed a significant upward trend ($p < 0.05$), especially in the middle and lower reaches, where ecological restoration has been intensive. Over the same period, forest and urban areas expanded by 24.08 % and 192.55 %, respectively, whereas grassland and cropland areas declined by 22.01 % and 21.40 %, substantially modifying the basin's ecohydrological setting.

3.2. Model performance

The localised VIC model reproduced observed runoff well. At main gauging stations, NSE was greater than 0.75, RSR less than 0.50 and PBIAS within ±10 % in both calibration and validation periods, indicating "good" or better performance. The model captures seasonal flow regimes and low- and high-flow conditions sufficiently for subsequent HES assessment.

3.3. Spatial patterns and trends of hydrological services

Hydrological services exhibit clear differences among ecosystem types and along the river continuum. Forest ecosystems provide the highest mean WS and WR (33.42 mm and 240.59 mm), followed by cropland (31.42 mm and 231.20 mm) and grassland (23.75 mm and 190.61 mm). Both WS and WR generally increase from the north-western upper basin towards the south-eastern lower basin, reflecting combined climatic and land-cover gradients. Grid-based results indicate that the strongest WR increases occurred mainly in vegetation-restored areas of the middle and lower basin, whereas WS declined more broadly in reforested and greening zones, highlighting marked spatial heterogeneity.

At the basin scale, WS and WR show contrasting long-term trends during 1980–2018. Basin-averaged WS displays a marked decreasing trend, with a cumulative reduction of about 16.81 %, indicating reduced water yield. In contrast, WR increases by about 5.66 %, suggesting enhanced water-retention and regulation capacity under joint climate change and ecosystem adjustment. Correlation-based attribution further suggests that vegetation restoration, reflected by increasing forest NDVI and forest area, is more strongly associated with WR enhancement, while declining precipitation and increasing evapotranspiration contributed substantially to WS reduction. These results indicate that climate drying and vegetation greening acted together, but with different dominant effects on the two services.

Table1 Average water resource supply services of each ecosystem in 1980 and 2018

Year	Ecosystem	Water-supply service (mm)	Water-retention service (mm)
1980	Forest	37.79	242.79
	Grassland	25.34	177.49
	Farmland	34.59	226.78
2018	Forest	29.05	238.28
	Grassland	22.15	230.72
	Farmland	28.25	235.62

4. Conclusion and implications

Using a localised VIC distributed hydrological model and long-term multi-source data, this study: (1) quantifies WS and WR and their spatial and temporal changes in the Luan River Basin from 1980 to 2018; (2) demonstrates that the VIC model performs well and is suitable for ecohydraulic assessment in a semi-arid–semi-humid transition basin; (3) shows that forest ecosystems provide the highest hydrological services, followed by cropland and grassland, with both WS and WR generally increasing from the upper to the lower basin; and (4) reveals a basin-wide trade-off in which WS decreased substantially (by about 16.81 %), while WR increased (by about 5.66 %), indicating stronger retention and regulation but reduced water yield under

combined climate change and vegetation restoration. Although uncertainty remains due to forcing data, parameterisation and the simplified attribution approach, the overall direction of change is robust.

For ecohydraulic management and landscape architecture, the results emphasise that ecological restoration and blue–green infrastructure should be designed within the limits of regional water-resource carrying capacity. In practical terms, upper-basin forest and grassland areas should prioritise conservation of existing regulating functions, whereas in the middle and lower basin, where restoration has been intensive and water demand is high, vegetation configuration, restoration intensity and river-corridor blue–green space should be optimised to balance enhanced retention with sufficient downstream water supply. Spatially explicit HES maps derived from VIC simulations can therefore support priority-area identification, differentiated restoration zoning and multifunctional landscape design in northern China.

Acknowledgements

This research was funded and supported by National Natural Science Foundation of China, Grant/Award Number: 42361144872 and 42171099.

References

Bai P, Liu X, Zhang Y, et al. Assessing the impacts of vegetation greenness change on evapotranspiration and water yield in China[J]. Water Resources Research, 2020, 56(10): e2019WR027019.

Decsi, B., Ács, T., Jolánkai, Z., Kardos, M. K., Koncsos, L., Vári, Á., & Kozma, Z. (2022). From simple to complex–comparing four modelling tools for quantifying hydrologic ecosystem services. Ecological Indicators, 141, 109143.

Feng, X., Fu, B., Piao, S., Wang, S., Ciais, P., Zeng, Z., ... & Wu, B. (2016). Revegetation in China's Loess Plateau is approaching sustainable water resource limits. Nature Climate Change, 6(11), 1019-1022.

Ha, L. T., Bastiaanssen, W. G., Simons, G. W., & Poortinga, A. (2023). A new framework of 17 hydrological ecosystem services (HESS17) for supporting River Basin planning and environmental monitoring. Sustainability, 15(7), 6182.

Harrison-Atlas, D., Theobald, D. M., & Goldstein, J. H. (2016). A systematic review of approaches to quantify hydrologic ecosystem services to inform decision-making. International Journal of Biodiversity Science, Ecosystem Services & Management, 12(3), 160-171.

Yue, S., Huang, J. C., & Zhang, Y. L. (2023). Quantitative evaluation of the impact of vegetation restoration and climate variation on runoff attenuation in the Luan River Basin based on the extended Budyko model. Land 12, 1626.

Book of Abstracts of the *16th International Symposium on Ecohydraulics*
Challenges and solutions in the time of global changes
August 16–20, 2026, Lausanne, Switzerland
ISSN: 2790-2420 | ISBN: 978-90-837233-9-6 | doi:[10.64697/iahr.proc.ise2026.abs]
© 2026 IAHR. CC BY-NC-ND 4.0

DESIGNING THE WATER MACHINE: INTERDISCIPLINARY APPROACHES TO THE DENDER VALLEY

Qinyi ZHANG[1], Nathan FREDRICK[2]

[1] Studio Paola Viganò, Italy
email: q.zhang@studiopaolavigano.eu

[2] Studio Paola Viganò, Italy
email: studiobrussels@studiopaolavigano.eu

ABSTRACT

In the context of climate change and environmental crisis, technological solutions and disciplines, including Ecohydraulics, are increasingly engaged in urban projects and planning. Urban designers and landscape architects now work closely with engineers to maintain, repair, and even generate ecologies through tightly interwoven natural and technological systems. While achieved notable successes, the increasing engagement of engineering risks reducing the need for an integrated design which serves the interest of human and non-human communities to a need for technological solutions. The project of ecology, when treated as an apolitical domain, loses its capacity to integrate social-environmental benefits and respond to more complex urban questions.

This paper examines this risk through the case of Geraardsbergen aan Boord, a masterplan for creating a safe, ecological, and socially inclusive public space along the Dender River. The case shows how ecohydraulic principles can be used as a "band-aid" providing technical fixes that obscure deeper ecological questions. It highlights the need for interdisciplinary design to play a stronger role in mediating diverse stakeholder agendas and coordinating a rational use of technology.

Keywords: climate change, Eco hydraulics, interdisciplinarity, political ecology, Dender river, social-environmental benefits, human and non-human communities

1. Flanders: The Limits of Technocratic Eco-Solutions

From Ian McHarg's 'Design with nature' in the 1960s, the understandings of natural processes are introduced in the urban practice. Since then, the entanglement of ecology, water systems and the landscape project has been amplified. From the 1986 'Plan Ooievaar', favoring the extension of ecological space for the river opposed to heightening and strengthening the dikes, to a gradual move to more engineered approaches such as the 2007 'Ruimte voor de Rivier' in the Netherlands, or 'Ruimte voor Water' in Flanders.

The risk exists when landscapes are reductively treated as 'things' (P. Viganò et al. 2023. p.129), objects rather than subjects, isolated from their context, instead of "dynamic constructs, complex systems and networks of simultaneous, multidirectional environmental, ecological, and social exchanges" (De Block et al. 2019). The project of ecology, when treated as an apolitical domain, loses its capacity to integrate and respond to more complex urban and social questions.

This risk is clearly visible in Flanders, where water bodies are managed in a horizontally fragmented manner by multiple authorities and stakeholders: navigable waterways by De Vlaamse Waterweg, unnavigable waterways by the provincial governments, run-off systems by the municipalities, and wastewater infrastructure by Aquafin. Confronted with climate change and environmental crises—including increasing risks of flooding and drought, and the loss of valuable ecological spaces—such fragmentation hampers an integrated and systemic approach. Instead of forming a coherent landscape that serves both ecological and social purposes,

responses tend to devolve into a segregated set of technological fixes—fish passages, raised dikes, locks, pumps—applied in isolation rather than as part of a meaningful and interconnected spatial strategy.

2. Case study: Dender river at Geraardsbergen

The river of Dender is a river in Belgium, sources in Wallonia and enters Scheldt. The Dender river is rainwater river, with heavily fluctuating water regimes. To control these fluctuations, for centuries the river has been infrastructuralised and artificialized, contributing to the growth and productivity of the city. This artificial landscape originates from the canalisation between the 12th and 15th century and the placement of sluices to keep a navigable water level along its course. Today, its entire course is divided by locks into seven "linear lakes", the flows and height of each is fully controlled. Geraardsbergen is the first Flemish city which Dender runs through, where the "sluis" is being renovated as due to recent severe flooding events.

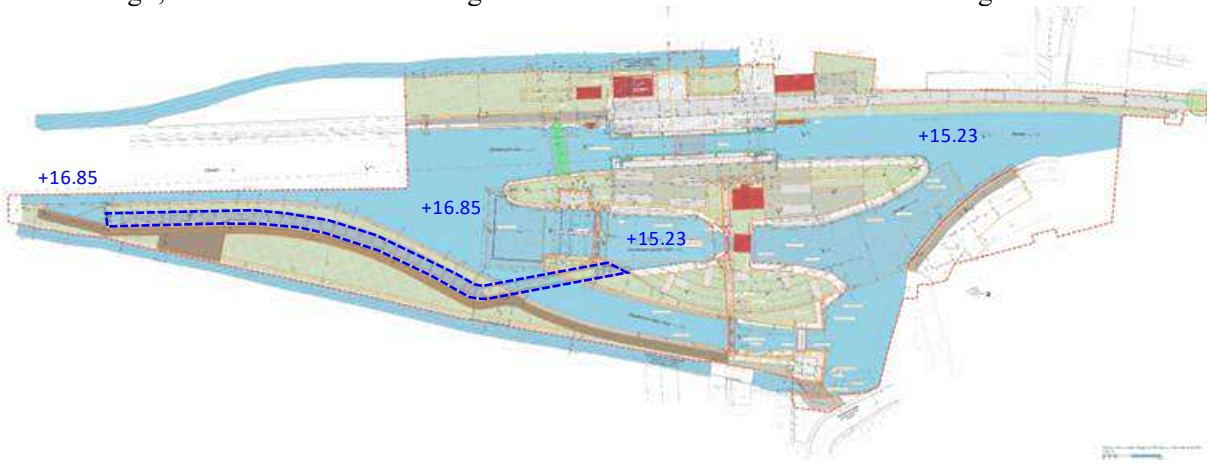

Fig. 1. *Building permit: plan of the sluice and fish passage in Geraardsbergen (De Vlaamse Waterweg)*

A complex situation involving a manifold of stakeholders with ambitions ranging from complete renaturalisation of the river without sluices and embankments (ecological activists), the protection of the city against increased flood with climate change (Region, city and The Flemish Waterway/owners), the demand to keep a navigable river (The Flemish Waterway), to a pragmatism to keep the river as it is. The compromise is a navigable and sluiced river, mainly embanked, with upgraded sluices (read technologically more advanced) and as compensation a highly engineered fish passage, an ecohydraulic solution which can function properly but at the same time a disruptive element in the landscape, just enough to be permitted, yet leaving the issue of ecological river dynamics unaddressed. Ironically the fish passage, meant as a connection for river species, is placed between sections of the river that are today closer to ponds than to a river ecology.

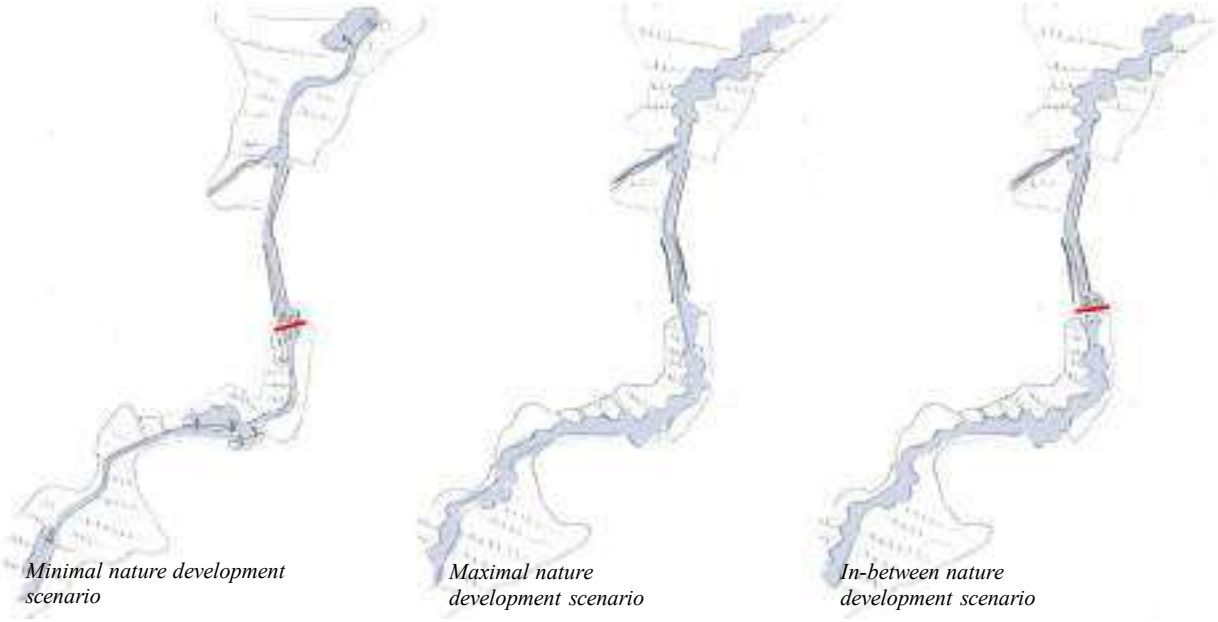

Fig. 2. *Different ambitions on the renaturalisation of the Dender river (elaborated by author)*

Therefore, the engineered Ecohydraulic solution in this way is used to avoid addressing the true complexity of urban environments and ecological processes, resulting in a continuous addition of infrastructure to accommodate a problem of political pragmatism rather than ecology.

3. The role of design with interdisciplinarity

The man-made landscape of the Dender's complex water system has evolved over time and is now inseparable from the development of the city and its valley ecosystem. Once embedded in a wet, marshy valley, the Dender was progressively elevated, straightened, and drained to enable cultivation and economic exploitation—at the cost of significant portions of its aquatic ecology. Continuous drainage has gradually transformed the *meersen*—wet landscapes with a fine-grained network of streams, ditches, and canals, shaped by periodic flooding and supporting a rich assemblage of plants and animals—into forest. These new woodlands are not only comparatively low in ecological value but also often too dense and closed to function as parks or support everyday human use.

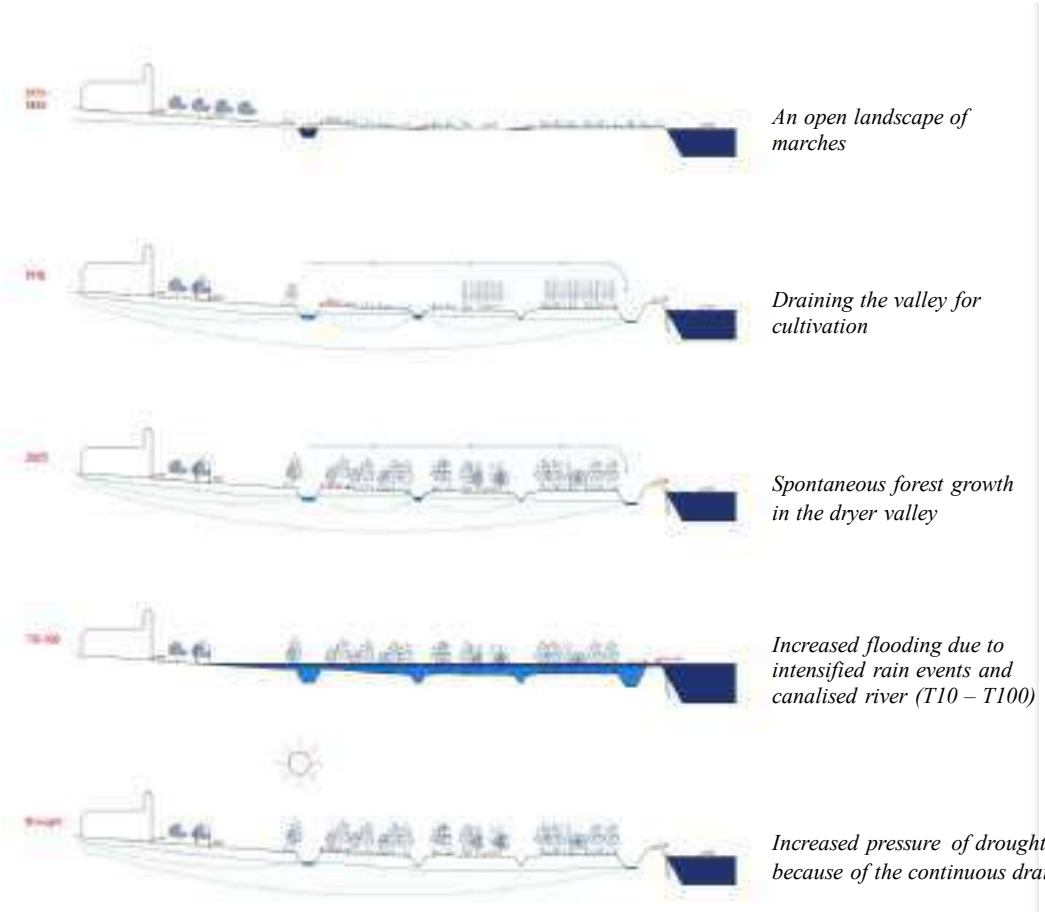

Fig. 3. *The evolution toward an artificial and drained water system. Pressure on the landscape - flooding and drought. (elaborated by author). Geraardsbergen aan Boord, Studio Paola Viganò + CLUSTER.*

Designing with interdisciplinarity, a close collaboration between urbanists, landscape architects, ecologists, engineers and participation experts, enables the re-imagining of a new water machine for the Dender Valley—one that slows drainage, restores the groundwater table, and revives the meersen ecology. This forms the basis for redefining the landscape and public-space system of Geraardsbergen. Such an integrated framework can align and rationalize ecological measures and technologies, overcome fragmentation, and coordinate stakeholders around a unified design vision. It can also help reactivate political responsibility toward the valley's real challenges: flood risk, accessibility, water pollution, and the river's role in economy and navigation.

This approach enables a more critical and discerning use of technology—integrated where necessary and avoided where it merely compensates for sectoral complexity—ensuring that interventions serve the broader landscape and societal goals rather than isolated technical agendas.

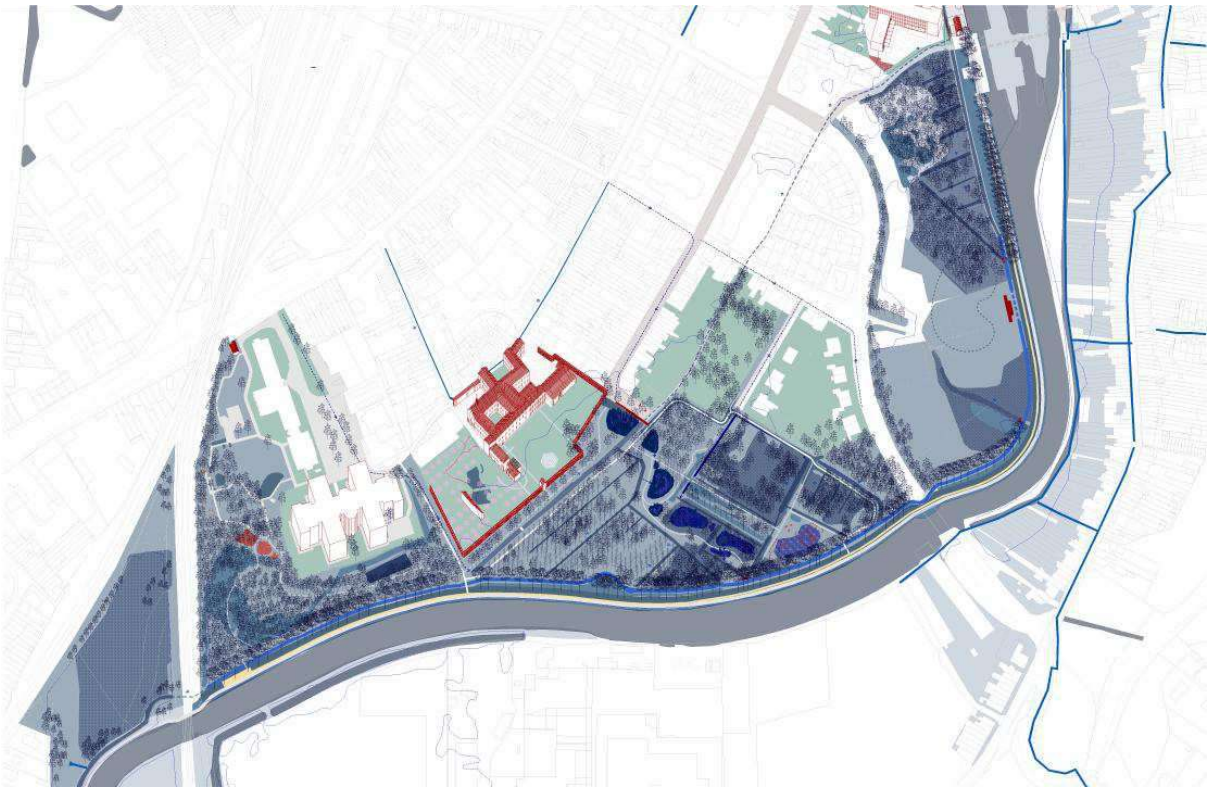

Fig. 4. *Towards an integrated and liveable water landscape (elaborated by author). Geraardsbergen aan Boord, Studio Paola Viganò + CLUSTER.*

References

Viganò P, Nguyen ST, Zhang Q (2023) Territory Subject: Designing Human-Environment Interactions in Cities and Territories, Introduction to Designing Environments. In: Hensel MU, Hensel DS, Binder CR, Ludwig F (eds) Introduction to Designing Environments. Springer Cham, pp113-137.

De Block G, Vicenzotti V, Diedrich L, Notteboom B (2019) For whom? Exploring landscape design as a political project. J Landsc Archit 14(3):4–7. https://doi.org/10.1080/18626033.2019.1705568

Book of Abstracts of the *16th International Symposium on Ecohydraulics*
Challenges and solutions in the time of global changes
August 16–20, 2026, Lausanne, Switzerland
ISSN: 2790-2420 | ISBN: 978-90-837233-9-6 | doi:[10.64697/iahr.proc.ise2026.abs]
© 2026 IAHR. CC BY-NC-ND 4.0

DESIGNING A TECHNONATURE: INTEGREATED WATER SYSTEM IN THE FUTURE RINGPARKS IN ANTWERP

Qinyi ZHANG[1], Nathan FREDRICK[2]

[1] Studio Paola Viganò, Italy
email: q.zhang@studiopaolavigano.eu

[2] Studio Paola Viganò, Italy
email: studiobrussels@studiopaolavigano.eu

ABSTRACT

In the era of climate change and escalating ecological crises, the theme of techno-natural hybridity has become increasingly central to urban and landscape design across all scales. As scientific and technological fields—including ecohydraulics—advance to maintain, repair, and generate ecosystems, the very meanings of *nature* and *ecology* and their relation with technology continue to evolve and expand. Among others, Escobar's concept of *technonature* captures this shift: organic nature is increasingly monitored, intervened in, and even produced through technological systems, rendering the biological a matter of design (Escobar 1999:12).

Working within technonature opens new possibilities for designers—not only in terms of applying science and technology, but also in shaping new everyday experiences and creating hybrid typologies that respond to ecological, social, and political challenges. Such an approach reconfigures how the relationship between humans and their environment can be conceptualized and practiced.

This paper explores these new possibilities through the case of the Ringparks projects in Antwerp—a future large-scale green and public-space system built atop the capped highway ring. Here, an integrated and hybrid water system that combines natural and artificial water sources, with varying rhythms, quantities, and qualities, serves as a framework for designing diverse ecologies and rich public-space experiences within the dense urban fabric of Antwerp.

Keywords: climate change, technonature, interdisciplinarity, integrated water system, hybridity

1. Flanders: The Limits of Technocratic Eco-Solutions

Humans now live within inseparable natural–artificial hybrids. As Escobar notes, echoing Latour, all natures are hybrid. Ellis similarly describes today's woodlands—symbols of "wilderness"—as anthro-ecological palimpsests: ecosystems reshaped by human activity, fragmented by infrastructure, altered by climate change, and transformed by species movement. Nature is already changing with us, making a return to "pure nature" impossible. We are moving instead toward planetary urbanization.

Recognizing and designing with techno-nature is therefore not optional but necessary. Designers have long exposed the deep entanglement of technology, infrastructure, and landscape—from Banham's Architecture of Four Ecologies to the "Urban Metabolism" agenda of IABR 2014. These perspectives show that separating society from nature is no longer productive; nature must be understood as embedded within urban life, redefining the "second nature" we inhabit.

Engaging with techno-nature opens new design possibilities. The pursuit of scientific and technical solutions—such as those developed within ecohydraulics—can be extended beyond serving specific ecologies or species to generate hybrid ecological–social typologies, new everyday experiences, and alternative relationships between humans and their environments. It also supports a broader, less prescriptive aesthetic—one that responds to ecological and societal transitions rather than reproducing idealized visions of nature.

2. Case study: Ringparks in Over De Ring, Antwerp

The Ringparks project within Over De Ring serves as a case study to explore new techno-natural typologies as inclusive ecological and social spaces in a society in transition.

Antwerp's northern landscape historically formed where the sandy plateau meets the peat polders along the Scheldt. The Schijn—fed by the Klein and Groot Schijn—shaped two distinct valleys whose pedology, hydrology, and ecology defined the area. This territory is a palimpsest of major artificial interventions: the Brialmont fortifications, the expansion of rail infrastructure, the early-20th-century harbor embankments that erased much of the Oosterweelpolders, the construction of the Albert Canal, and later the E17 highway. The forthcoming Oosterweel project represents a sixth transformation, completing and tunnelling large segments of the ring road. Over De Ring proposes "Ringparks" atop these tunnels, creating a new city-scale green and public-space system.

Such interventions will profoundly reshape water systems and ecologies: groundwater flows sustaining existing wet ecologies will be interrupted, and deep, biodiverse soils will be replaced by shallow soils above the tunnel. They will also reconfigure key social spaces and connections and significantly impact on the city's infrastructural networks—often overlooked in political and participatory debates.

Lobroekdok is a highly symbolic urban place in Antwerp. As a large open water as the remnants of the historical fortification belt and the industrial Dam neighborhood, and at the convergence of the Schijn valleys and surrounded by big infrastructures, it has always been one of the most isolated places in Antwerp, known as Tweemont, "the end of the world". The design of Ringpark Lobroekdok bring together larger territorial systems into an open metropolitan figure, a metropolitan water landscape, that reconnects Antwerp to its territory, to the neighbourhoods and the ecological areas.



Fig. 1. Pre-design: Masterplan Ringpark Lobroekdok (Studio Paola Viganò – Maarch – Sweco Belgium)

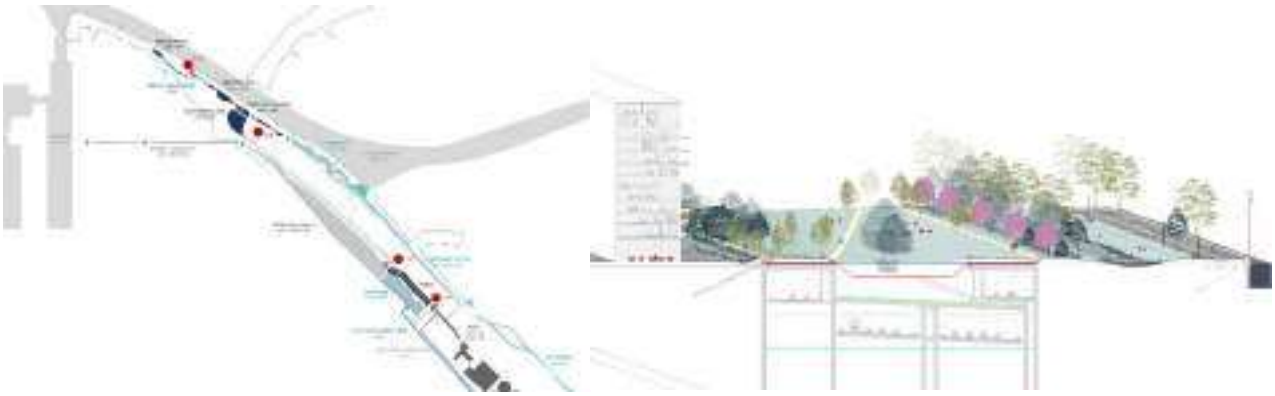

Fig. 2. Left: Pre-design: scheme of a hybrid water system for Ringpark Lobroekdok (Studio Paola Viganò – Maarch – Sweco Belgium)
Fig. 3. right: Pre-design: landscapes of hybrid water system at Ringpark Lobroekdok (Studio Paola Viganò – Maarch – Sweco Belgium)

The design of Ringpark Lobroekdok proposes an integrated water system that brings together multiple sources: natural groundwater from the sandy plateau, continuously pumped "leakage water" used to keep the tunnel dry, surface and tunnel runoff, the reopened and naturalized Grote Schijn River, and the brackish water of the Albert Canal. Through a combination of natural processes and engineered infrastructures, these waters structure a sequence of interconnected ecologies within a dense, infrastructure-dominated urban landscape.

The system supports diverse habitats, ranging from dry prairie vegetation on the capping to canal foreshores with wetlands and fish-breeding areas, as well as ecological corridors nourished by leakage water beneath the railway bridges. Beyond the creation of new forms of urban "wilderness," the project also introduces inclusive public spaces, including water playgrounds, swimming docks, open park landscapes, sports facilities, and a variety of spatial experiences and viewpoints.

Such a system relies on a carefully calibrated technical design that accommodates water sources of varying qualities and seasonal availability. It requires not only the engineering of connections and flows between the different water bodies of the park, but also the careful design of their bottoms and edges. Permeable bases allow groundwater seepage in selected locations, while impermeable layers prevent water loss toward the pumping systems that maintain the dry conditions of the tunnel infrastructure.

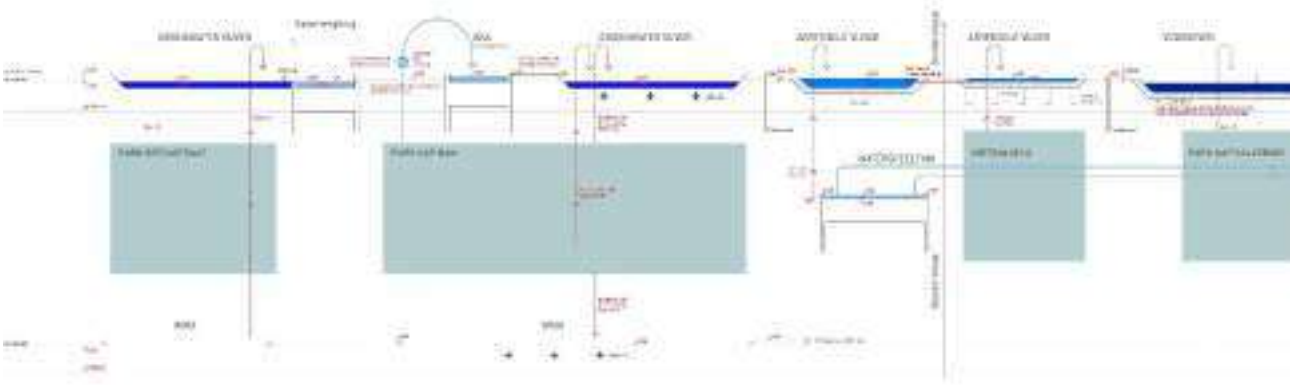

Fig. 4. Pre-design: scheme of waterflows and the water bodies, Ringpark Lobroekdok (Studio Paola Viganò – Maarch – Sweco Belgium)

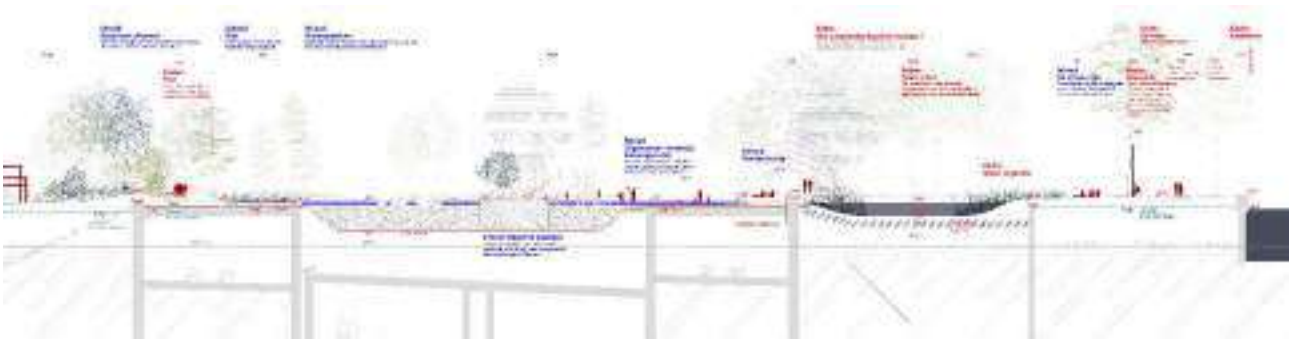

Fig. 5. Pre-design: section of water playgournd and its overflow, Ringpark Lobroekdok (Studio Paola Viganò – Maarch – Sweco Belgium)

The future tunnel will be constructed within an artificial polder, enclosed by deep concrete "polder walls" extending down to the impermeable clay layer known as *Boomse klei*. Inside this enclosure, groundwater levels are maintained below the tunnel through continuous pumping—a system already used to keep the existing highway, also located below the city's groundwater table, dry. This pumping produces a constant discharge of leakage water, with a minimum flow of approximately 5 l/s. Rather than releasing this relatively clean water directly into the canal, the project proposes to reuse part of it to supply a 300-metre-long open swimming dock and a children's water playground. In increasingly dry summer periods, this flow provides a reliable source of water suitable for recreational use.

Overflow from this system feeds other water bodies and vegetated areas within the park before ultimately reaching the vooroever, an artificial foreshore along the Albert Canal. This linear water body, located behind the canal's quay wall, brings together several water sources: the slightly brackish canal water (maintained at approximately 4.25 m above sea level), the freshwater of the Grote Schijn River, and the clean overflow of the leakage system. Their interaction will produce a dynamic landscape that supports rich biodiversity, creating favorable habitats and breeding grounds for fish species from both the river and the canal.





Fig. 6. Left: Pre-design: impression of a "vooroever", an artificial water and "wilderness" in the dense city of Antwerp, Ringpark Lobroekdok (Studio Paola Viganò – Maarch – Sweco Belgium)

Fig. 7. Right: Pre-design: impression of the water playground, Ringpark Lobroekdok (Studio Paola Viganò – Maarch – Sweco Belgium)

3. From a technonature to a new common

In Ringpark Lobroekdok, the concept of techno-nature is conceived to generate new forms of urban commons: accessible and varied public spaces that reconnect fragmented territories, recover historically significant sites, and introduce an aesthetic of wild, robust, and dynamic nature in contrast to conventional manicured parks. This framework supports metropolitan cohesion while responding to societal and climatic transitions.

The co-creation process of the ringpark encourages stakeholders and citizens to move beyond local concerns and engage with broader systemic questions. Yet the creation of techno-nature remains contested, shaped by technical, economic, and political tensions. Rather than depoliticizing nature and technology, Ringpark Lobroekdok's approach opens possibilities for new "social-technical or social-ecological commons" (De Block, 2016).

References

Escobar A (1999) After nature: steps to an anti-essentialist political ecology. Curr Anthropol 40(1):1–30. https://www.journals.uchicago.edu/doi/10.1086/515799

De Block G (2016) Ecological infrastructure in a critical-historical perspective: from engineering 'social' territory to encoding 'natural' topography. Environ Plan A 48(2):367–390. https://doi.org/10.1177/0308518X15600719

Book of Abstracts of the *16th International Symposium on Ecohydraulics*
Challenges and solutions in the time of global changes
August 16–20, 2026, Lausanne, Switzerland
ISSN: 2790-2420 | ISBN: 978-90-837233-9-6 | doi:[10.64697/iahr.proc.ise2026.abs]
© 2026 IAHR. CC BY-NC-ND 4.0

RENATURATION OF THE DRIZE AND AIRE RIVERS IN GENEVA'S PAV DISTRICT: AN INTEGRATED APPROACH TO URBAN ECOHYDRAULICS AND LANDSCAPE ARCHITECTURE

Pierre BOURQUI[1], Marina LAUNAY[1], Marco RAMPINI[2], Yves BACH[3], François GERBER[4], Kim EHRENSPERGER[5]

[1] Gruner SA, Switzerland
email: pierre.bourqui@gruner.ch
email: marina.launay@gruner.ch

[2] Atelier adr, Switzerland
email: marco.rampini@atelier-adr.ch

[3] EDMS, Switzerland
email: yves.bach@edms.ch

[4] Biotec Biologie appliquée, Switzerland
email: francois.gerber@biotec.ch

[5] République et Canton de Genève - Office cantonal de l'eau (OCEau), Switzerland
email: kim.ehrensperger@etat.ge.ch

ABSTRACT

The PAV Aire-Drize project represents the latest evolution in Geneva's 25-year waterway renaturation programme, addressing the challenge of integrating functional river systems into dense metropolitan development. Over 20 years, 2.5 kilometers of the buried Drize and Aire rivers will be brought to the surface to form the structural spine of nine new neighborhoods. Unlike earlier projects such as the award-winning upper Aire renaturation in a rural valley context, the Drize confronts severe urban constraints requiring innovative ecohydraulic solutions that balance flood conveyance, stormwater management, habitat creation, and climate adaptation within narrow corridors bounded by underground infrastructure. The design integrates multi-stage hydraulic configurations, controlled morphological processes, and multifunctional public spaces providing urban cooling, biodiversity connectivity, and social programming. This interdisciplinary collaboration between hydraulic engineers, landscape architects, ecologists, geo- and hydrogeologists, and urban planners exemplifies Geneva's sustained political commitment to visionary approaches, demonstrating that contemporary urban renaturation must design novel ecosystems capable of delivering multiple services under extreme anthropogenic pressures rather than restoring historical conditions. The first 450-meter phase inaugurated in November 2025 establishes design principles and monitoring frameworks informing subsequent stages, generating transferable knowledge for urban river projects globally while testing whether ambitious ecological integration can be sustained through decades of metropolitan transformation.

Keywords: Urban river renaturation; Climate adaptation; Biodiversity corridors; Multifunctional infrastructure; Interdisciplinary collaboration

1. Introduction: 25 years of vision in Geneva

The Praille-Acacias-Vernets (PAV) Aire-Drize project emerges from a quarter-century of ambitious waterway renaturation in the Canton of Geneva. Since the programme's launch in 2000, Geneva has restored several thousand meters of buried waterways to the open air and renatured nearly forty kilometers of riverbanks, with new water access points along the lake and flood protection secured across almost the entire canton. This sustained commitment reflects a political vision that has evolved from addressing historical degradation to confronting contemporary urban challenges. As Geneva becomes increasingly densely populated within its constrained territory, and as heatwaves since 2015 confirm accelerating climate change, the renaturation programme has adapted its ambitions accordingly.

The PAV Aire-Drize project represents the next frontier in this evolution: opening urban waterways to create cooling corridors within new high-density neighborhoods. Where earlier projects often addressed peri-urban or rural contexts, this initiative tackles the challenge of integrating functional river systems into the heart of metropolitan development. Over 20 years, 2.5-km of the Drize and Aire rivers will be brought back to the surface to serve as the structural spine for nine new neighborhoods accommodating housing units, with a goal of carbon neutrality by 2050. The first phase, inaugurated in November 2025, brought 450 m of the Drize back to the surface in the Étoile and Boissonnas sectors (see Fig.1), demonstrating principles that will guide subsequent phases.



Fig. 1. Open-air section of the Drize in the Boissonnas area, inaugurated on 25 November 2025

2. The Ecohydraulic Challenge

The Drize, a 9-km tributary of the Aire, has been confined to underground galleries since the 1930s for the industrial zone of la Praille and its infrastructure. These galleries remain the sole water conveyance through the PAV perimeter during floods. Unlike the upper Aire renaturation in a rural valley where the river received extensive lateral space, the Drize must operate within severe spatial constraints imposed by dense urban infrastructure. The biological context also differs fundamentally: where the upper Aire reconnected with relatively intact upstream habitats, the Drize emerges into a heavily modified urban matrix with fragmented ecological connectivity and novel assemblages of urban-adapted species.

These constraints demand innovative ecohydraulic solutions. The design must simultaneously provide routine flow conveyance, accommodate flood events, manage stormwater from the intensifying catchment, and create habitat diversity within a narrow corridor bounded by underground parking, utilities, and buildings. The approach incorporates natural riverbanks with variable hydraulic roughness, stone walls providing structural support and habitat complexity, and overflow zones attenuating peak flows while allowing controlled morphological adjustment within defined boundaries.

The reopening creates diverse natural habitats in the city center. By reconstructing gravel beds, creating floodable terraces, and shaping gently sloping banks, the design shown in Fig.2 establishes varied habitats

from very wet to very dry, supporting insects, small mammals, birds, dragonflies, and butterflies. The planting strategy, based on natural models and climate change projections, ensures trees, hedges, and meadows offer shelter, food, and breeding sites while withstanding high summer temperatures, drought, heavy rainfall, and flooding.

The hydraulic design integrates engineering precision with ecological function through multi-stage channel configurations, strategic vegetation and stone placement managing velocities while enhancing habitat, and sediment transport corridors enabling limited geomorphic processes. Hydraulic modeling incorporated climate change projections for precipitation intensification and urban runoff increases, ensuring performance under future uncertainty. This represents a distinct ecohydraulic challenge: designing novel urban ecosystems capable of providing services under extreme anthropogenic pressures rather than restoring historical reference conditions.

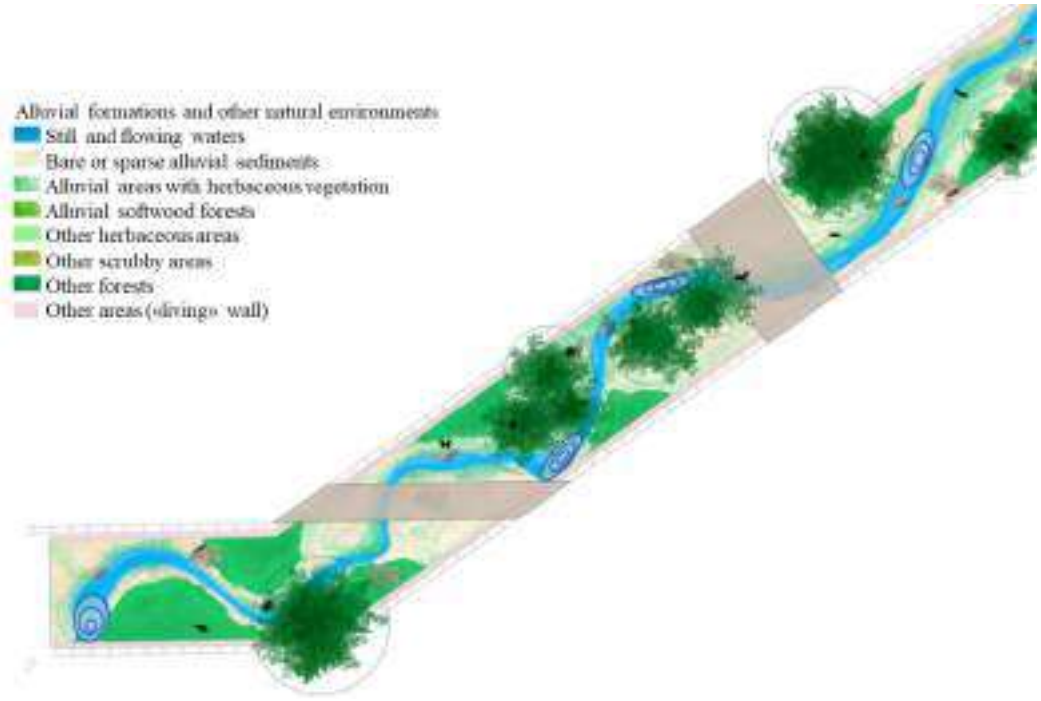

Fig. 2. Snapshot of the alluvial formations expected in the early years of the Drize reopening project. Subsequently, the desired dynamics of the watercourse will change their distribution.

3. Landscape Architecture Vision and Interdisciplinary Innovation

The Canton of Geneva's renaturation programme has consistently supported innovative approaches to waterway restoration. The upper Aire renaturation, which received the Council of Europe's Landscape Award in 2019, exemplified this through conceptual boldness: rather than erasing the historical canal, the design team created a deliberate juxtaposition, preserving the former canal as a linear garden while establishing a new, morphologically dynamic channel alongside it. The design employed a geometric grid as an initial structure the river would progressively transform, recognizing that clearly defined starting conditions paradoxically enable authentic emergence of complexity.

The PAV Aire-Drize project applies visionary approaches to fundamentally different challenges. Where the upper Aire addressed restoration in a rural valley with available agricultural land, the Drize confronts dense urbanism where every square meter serves multiple functions. The innovation lies in designing systems that integrate dynamic natural processes within rigid urban constraints while delivering multiple services. The 2.5-km Drize corridor with 120,000 m² of public space forms the organizational framework for the entire PAV development, inverting conventional planning by structuring the urban fabric around the river. The corridor integrates thermal comfort zones, biodiversity corridors, mobility infrastructure, social spaces, and stormwater management, reflecting urban necessity where renaturation must simultaneously address climate adaptation, public health, social equity, and infrastructure performance.

The project exemplifies integrated design with ecohydraulic expertise embedded throughout. The collaborative team includes landscape architects, hydraulic engineers, ecologists, civil engineers, geo- and hydrogeologists,

and urban planners working together from inception. Unlike the upper Aire where disciplines could work somewhat sequentially, the Drize's constraints demand constant negotiation. Hydraulic requirements must accommodate structural engineers' foundation loads over underground parking while ecologists' habitat specifications align with construction phasing and social programming. This intensive collaboration generates new knowledge about multifunctional urban infrastructure where conventional separation of concerns proves impossible. The project treats each phase as an experiment, with monitoring informing subsequent stages and generating transferable knowledge for urban river projects globally.

4. Climate adaptation and implementation

The project addresses multiple climate pressures simultaneously. For heat mitigation, the river corridor provides cooling through evaporative surfaces, vegetation transpiration, shade, and cool air drainage corridors, with early monitoring showing significant temperature reductions. For flood management, the renatured channel provides increased conveyance capacity, overflow zones accommodating extreme events, upstream retention, and permeable surfaces reducing runoff. The visible river restores public flood risk awareness, enhancing community preparedness. The corridor creates stepping-stone habitat for aquatic and riparian species, supporting urban-adapted assemblages that provide water quality improvement, microclimate regulation, pollination services, and psychological benefits.

Realizing the project requires resolving unprecedented technical challenges. The river's design must ensure its functionality within a changing urban environment over several decades. Planning incorporates these transitional phases while guaranteeing the required objectives and desired quality. Integrating a dynamic channel with underground parking, utilities, and building foundations demands specialized foundations, cantilevered bridges, and flexible interfaces allowing soil settlement. Constructing incrementally while maintaining flood protection requires temporary conduits and modular design. In connection with the new river, extensive public spaces will serve future residents and users. The unique presence of a living river in this increasingly dense urban area creates a distinctive environment offering residents direct daily contact with ecological processes, fostering environmental awareness and social cohesion. The river corridor becomes not merely infrastructure but a defining feature of neighborhood identity and quality of life.

The project represents substantial public investment justified by flood risk reduction, climate adaptation, public health benefits, biodiversity gains, and property value appreciation. While specific to Geneva, it offers transferable principles: designing dynamic processes, embedding ecohydraulic function within social and urban systems, making natural processes legible, building flexibility for uncertainty, and fostering genuine interdisciplinary integration.

Conclusion

The PAV Aire-Drize project demonstrates a new paradigm for urban river renaturation, showing that cities can integrate flood risk and runoff water management, functional ecological systems and social goal within dense metropolitan development. By treating ecohydraulics and landscape architecture as complementary rather than competing disciplines, the project achieves outcomes impossible through conventional sectoral approaches.

As cities globally confront simultaneous pressures of densification, climate change, and biodiversity loss, Geneva's quarter-century trajectory offers instructive lessons. Sustained political vision enables ambitious projects to evolve across changing contexts. Institutional learning allows each project to build on predecessors' experiences while innovating for new challenges. Willingness to support unproven approaches, accept complexity, and commit resources commensurate with ambitions proves essential for transformative urban renaturation. The coming decades, as the PAV project unfolds and matures, will test whether this vision can be sustained, making Geneva's experiment a critical case study for 21st-century sustainable urbanism.

Session B4

Governance, socio-environmental benefits, and areas of conflict

Book of Abstracts of the *16th International Symposium on Ecohydraulics*
Challenges and solutions in the time of global changes
August 16–20, 2026, Lausanne, Switzerland
ISSN: 2790-2420 | ISBN: 978-90-837233-9-6 | doi:[10.64697/iahr.proc.ise2026.abs]
© 2026 IAHR. CC BY-NC-ND 4.0

A LIGHTWEIGHT THERMAL MODELLING APPROACH FOR EMBEDDING WATER QUALITY IN MULTI-OBJECTIVE RESERVOIR OPERATION

Maria Elena ALFANO[1,3], Marta ZANIOLO[2] , Roberto BOSIO[1] , Laura SAVOLDI[3] , Davide POGGI[1]

[1] Department of Environment, Land and Infrastructure Engineering, Politecnico di Torino, Corso Duca degli Abruzzi, 24, 10129 Torino, Italy

[2] Department of Civil and Environmental Engineering, Duke University, 121 Hudson Hall, Durham, NC 27708, USA

[3] MAHTEP Group, Department of Energy "Galileo Ferraris", Politecnico di Torino, Corso Duca degli Abruzzi, 24, 10129 Torino, Italy
email: mariaelena.alfano@polito.it

email: marta.zaniolo@duke.edu

email: roberto.bosio@polito.it

email : laura.savoldi@polito.it

email : davide.poggi@polito.it

ABSTRACT

In alpine water-resource systems, advancing reservoir management hinges on incorporating ecological dynamics into operational models, with water-temperature regimes playing a central role. In this study, we integrate a lightweight 1D energy-balance thermal model directly into a multi-objective optimisation framework for multi-purpose reservoir management. Applied to the Orco basin in the Italian Alps, the approach quantifies trade-offs among hydropower production, hydropeaking mitigation, irrigation supply, and ecological thermal integrity, revealing the dominant influence of withdrawal release timing on downstream conditions. Embedding temperature as an operational variable produces Pareto-optimal strategies that attenuate thermal exceedances while preserving essential water uses. The resulting Pareto strategies reveal substantial trade-offs between ecological thermal protection and hydropower production, with thermally optimal operations reducing hydropower revenue by up to 40% relative to purely economic policies. This framework advances toward dynamically eco-informed reservoir operations consistent with emerging environmental management goals.

Keywords: Water quality modeling; Thermal regime alteration; Multi-purpose reservoir operation; Integrated Water Resources Management (IWRM); Mountain basins

1. Motivation and summary

Multi-purpose reservoirs substantially reorganize downstream ecohydrological regimes by reshaping flow pulses, trapping suspended sediments and nutrients, and creating depth-dependent thermal heterogeneity. Hydropower-driven operational modes, such as hydropeaking and pumped-storage, further amplify thermal discontinuities and short-term fluctuations in discharge and temperature, which in turn modify mixing processes, reaeration dynamics, and biogeochemical reaction rates (Wüest, 2009; Kobler et al., 2018.). Such alterations are particularly consequential in mountain basins, where cold-water taxa exhibit narrow thermal and oxygen tolerances. Even moderate deviations in water temperature (T) and dissolved oxygen (DO) can thus trigger pronounced ecological responses. Numerous empirical studies demonstrate that regulated rivers frequently decouple the natural air–water temperature relationship (Mohseni et al., 1999; Erickson et al., 2000), and that depth-selective withdrawals generate downstream thermal signals that cannot be captured by static thresholds or simplistic post-hoc assessments.

Despite this evidence, water quality remains weakly integrated into contemporary reservoir – management optimization frameworks. Operational analyses typically prioritize hydropower or irrigation, relegating ecological integrity to external constraints rather than embedding it as an explicit dynamic objective. Regulatory frameworks reinforce this gap: although the EU Water Framework Directive and national legislation (e.g., D.Lgs. 152/2006; DM 56/2009) mandate ecological status evaluations using DO and nutrient criteria, they do not prescribe time-resolved thermal metrics or operational guidance for mitigating high-frequency thermal disturbances. Moreover, the concept of "reference conditions" is increasingly questioned, as recent studies show that many nominally pristine sites display elevated anthropogenic disturbance (Erba et al., 2022).

These gaps motivate the central research question of this work: How can water quality be operationally embedded within the management of multi-purpose reservoir systems to preserve downstream ecological states and habitats?

2. Case study

Our study focuses on the Orco Valley in Piemonte, a heavily regulated Alpine catchment featuring six major reservoirs and multiple hydropower plants. This system provides a highly relevant case study for reservoir-driven thermal alterations, as underlined by a 2023 report from ARPA Piemonte - the regional environmental protection agency responsible for monitoring water quality, atmospheric conditions, and ecological status in the Piedmont region. ARPA Piemonte's assessment classified the ecological status of the river downstream of these impoundments as "not good," highlighting the urgent need to address thermal and water quality impacts linked to reservoir operations in this basin.

3. Methodology

Given the oligotrophic Alpine context - where nutrient limitation is rarely the primary ecological stressor - we select **water temperature** as the principal operational water-quality variable. Temperature exerts first-order control on DO dynamics, metabolic rates, gas solubility, and habitat suitability, making it the most actionable indicator for integration into optimisation. ARPA datasets allow rigorous empirical justification of this modelling choice: correlation analyses at multiple stations confirm the expected inverse temperature–oxygen relationship and reveal stable coupling patterns in minimally impacted reaches.

To balance physical realism with computational efficiency, we adopt a one-dimensional, density-stratified Lagrangian thermal model consistent with the DYRESM family (Imberger et al., 1981). The model discretises the water column into evolving layers whose temperature follows a vertically resolved energy-balance equation , Eq. (1):

$$\frac{dT_i}{dt} = \frac{1}{\rho c_p A_i h_i}(Q_{SW} + Q_{LW} + Q_{sens} + Q_{lat} + Q_{rain} + Q_{\mathrm{mix},i}) \quad (1)$$

where terms represent short-wave radiation (J s^{-1}), net long-wave radiation (J s^{-1}), sensible and latent heat fluxes (J s^{-1}), precipitation heat input (J s^{-1}), and internal mixing processes (J s^{-1}); density ρ(kg m^{-3}); specific heat capacity c_p(J kg^{-1} K^{-1}); area A_i(m^2); layer thickness h_i(m); temperature derivative $\frac{dT_i}{dt}$(K s^{-1}).

The thermal model was implemented in Python to enable hard-coupling with the multi-objective optimisation framework. The physics-based formulation allows application in data-scarce systems (Hamilton et al., 1997), such as the Orco Valley reservoirs, where temperature profile observations are unavailable. To ensure the robustness of the results, model performance was assessed through two complementary approaches: comparison against analogous case studies reported in the literature, and systematic benchmarking against the well-established GLM model (Hipsey et al., 2019). The benchmarking yielded a linear correlation, demonstrating that the thermal model accurately reproduces physically consistent conditions and provides a reliable basis for integration into the optimisation framework.

This thermal module is embedded within a multi-objective optimisation framework jointly addressing hydropower generation, irrigation supply, and ecological performance (hydropeaking reduction). Specifically, the study adopts the Evolutionary Multi-Objective Direct Policy Search (EMODPS) approach proposed by Giuliani et al., 2016: a simulation-based optimisation framework in which closed-loop operating policies are parameterised through nonlinear function approximators and refined via NSGA-II to generate Pareto-approximate solutions. The lightweight structure of the thermal model makes it suitable for iterative evaluation within this simulation-optimisation loop.

Four objective functions are simultaneously optimised: minimisation of the irrigation deficit, weighted by a squared penalty term to reflect the nonlinear relationship between water shortfalls and agricultural yield losses; maximisation of hydropower economic revenue; minimisation of hydropeaking, quantified as high-frequency fluctuations in release discharge; and minimisation of the thermal alteration index, defined as the difference between reservoir inflow and downstream release temperature.

The two model components operate at different temporal resolutions reflecting their distinct physical requirements: the mass balance model runs at an intra-daily (hourly) time step, necessary to capture sub-daily dynamics such as hydropeaking events and short-term variations in hydropower revenue, while the thermal model is solved at a daily resolution, at which scale the objective function values are also aggregated. This dual-resolution structure balances the need for process accuracy with computational tractability within the iterative optimisation loop.

4. Results and Limitations

Integrating temperature dynamics within reservoir optimisation reveals the key operational drivers responsible for downstream ecosystem alterations, disentangling the relative influence of withdrawal depth, storage fluctuations, and hydropower release timing on water quality. The results focus on the main reservoir of the Orco Valley hydraulic system, the Ceresole reservoir, over the period 2012–2022 at a daily time scale.

The approach produces Pareto-optimal reservoir management strategies (Fig. 1) that explicitly quantify the inherent trade-offs among irrigation reliability (J1), ecological objectives - thermal alteration (J2) and hydropeaking (J3) - and hydropower economic revenue (J4). Figure 1 presents the full set of non-dominated policies as a parallel coordinate plot, where each line represents the performance of a single policy across all four objective functions. The axes correspond to the extreme values of each objective within the Pareto-optimal solution space, with units specific to each objective formulation. The figure makes explicit the conflict between environmental objectives and both agricultural and energy production goals. Agriculture and energy production are themselves in conflict, while J2 and J3 exhibit a broadly consistent behaviour, suggesting that managing thermal alteration and hydropeaking tends to impose similar operational constraints.

Quantitatively, the results indicate that under the current operational configuration, with a withdrawal depth of approximately 8 metres above the reservoir bottom, prioritising thermal integrity by minimising the difference between inflow and release temperature (J2) entails a hydropower revenue reduction of approximately 40% relative to the purely revenue-maximising policy (J4). This trade-off highlights the significant but not insurmountable ecological cost of thermally informed operations, and underscores the value of the Pareto framework in making such conflicts explicit and navigable for decision-makers.

These dynamics become considerably clearer in Fig. 2, which reports the storage trajectories corresponding to the policy optimising each individual objective. These trajectories allow direct appreciation of how the system responds differently depending on which objective is prioritised, making the conflicts among competing water uses both intuitive and operationally interpretable.

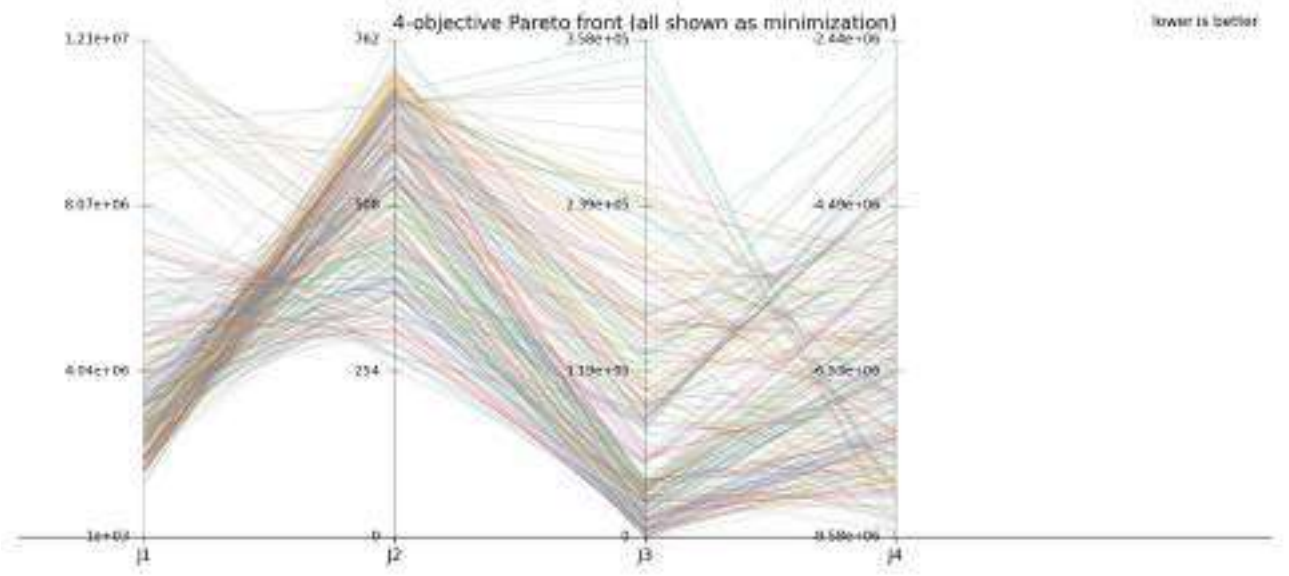

Fig. 1. Pareto-optimal reservoir management strategies (Lower is better). Four objective function (J1-irrigation deficit , J2- water temperature disturbance, J3- minimizing the hydropeaking, J4- hydropower income).

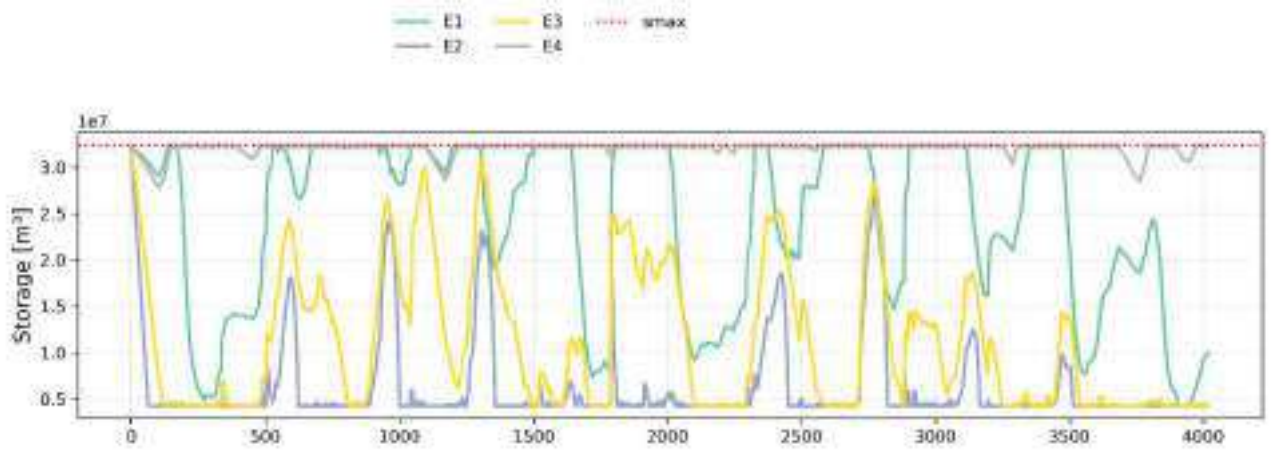

Fig. 2. Daily evolution of reservoir storage under the four single-objective optimal policies over the 2012-2022 period. Each trajectory corresponds to the operating strategy minimising one objective function: irrigation deficit (J1), thermal alteration (J2), hydropeaking (J3), and -hydropower revenue (-J4).

This framework facilitates the translation of static regulatory thresholds, such as those imposed by the EU Water Framework Directive and national legislation, into dynamic operational decisions that better preserve water habitats and maintain thermally stable ecological conditions characteristic of Alpine rivers.

While the one-dimensional thermal model ensures computational efficiency and physical consistency, it cannot capture all complex three-dimensional processes affecting thermal stratification and mixing. Similarly, the nonlinear interactions between temperature, dissolved oxygen, and nutrient dynamics are simplified by focusing on temperature as the primary indicator. While dissolved oxygen ultimately represents the most direct ecological indicator of habitat suitability, its explicit computation was not included in the current optimisation loop. Verifying that optimised thermal regimes translate into acceptable oxygen conditions through post-processing temperature–oxygen relationships remains an important step for future work.

The proposed lightweight thermal modelling approach offers a computationally efficient, physically coherent tool for integrating temperature-driven water-quality constraints into multi-objective reservoir operation. By embedding water quality directly into the optimization loop, the framework advances operational ecohydraulics toward more integrated and ecologically informed reservoir management.

References

Erba S, Buffagni A, Cazzola M et al (2022) Italian reference rivers under the Water Framework Directive umbrella: do natural factors actually depict the observed nutrient conditions? Environmental Sciences Europe, 34, 63.
Erickson TR, Stefan HG (2000) Linear Air/Water Temperature Correlations for Streams during Open Water Periods. Journal of Hydrologic Engineering, 5, 317-321.
Giuliani, M., Castelletti, A., Pianosi, F., Mason, E., & Reed, P. M. (2016). Curses, tradeoffs, and scalable management: Advancing evolutionary multiobjective direct policy search to improve water reservoir operations. Journal of Water Resources Planning and Management, 142(2), 04015050.
Hamilton DP, Schladow SG (1997) Prediction of water quality in lakes and reservoirs. Part I — Model description. Ecological Modelling, 96(1–3), 91-110.
Hipsey, M. R., Bruce, L. C., Boon, C., Busch, B., Carey, C. C., Hamilton, D. P., & Winslow, L. A. (2019). A General Lake Model (GLM 3.0) for linking with high-frequency sensor data from the Global Lake Ecological Observatory Network (GLEON). *Geoscientific Model Development*, *12*(1), 473-523.
Imberger, J., & Patterson, J. C. (1981). A dynamic reservoir simulation model—DYRESM: 5. *Transport models for inland and coastal waters*, 310-361.
Kobler UG, Wüest A, Schmid M (2018) Effects of Lake–Reservoir Pumped-Storage Operations on Temperature and Water Quality. Sustainability, 10, 1968.
Mohseni O, Stefan HG, Erickson TR (1999) A nonlinear regression model for weekly stream temperatures. Water Resources Research, 35(12), 3723-3733.
Wüest A (2009) Downstream relevance of reservoir management. In: Alpine Waters. Springer Berlin Heidelberg, Berlin, Heidelberg, pp 235-246.

Book of Abstracts of the *16th International Symposium on Ecohydraulics*
Challenges and solutions in the time of global changes
August 16–20, 2026, Lausanne, Switzerland
ISSN: 2790-2420 | ISBN: 978-90-837233-9-6 | doi:[10.64697/iahr.proc.ise2026.abs]
© 2026 IAHR. CC BY-NC-ND 4.0

THE FUTURE OF ECOHYDRAULICS: A COMMUNITY PERSPECTIVE

Monica BASILIO HAZAS[1], Joël WITTMANN[2], Davide Vanzo[3], Jan DE KEYSER[4], Melina SATTELMEIER[5], Hannah SCHWEDHELM[6], Kevin MERL[7], Francesca PADOAN[8], Ana ADEVA-BUSTOS[9], Davide VETTORI[10], Mathias CHABAL[11], Sahra N. SABIL[12], Daniele TONINA[13], Daniel S. HAYES[14]

[1] Friedrich-Alexander-Universität Erlangen-Nürnberg (FAU), Germany
email: monica.basilio@fau.de

[2] ETH Zurich, Switzerland
email: joelw@ethz.ch

[3] Karlsruhe Institute of Technology, Germany
email: davide.vanzo@kit.edu

[4,7,14] BOKU University, Austria
email: jan.de-keyser@boku.ac.at
email: kevin.merl@boku.ac.at
email: daniel.hayes@boku.ac.at

[5] Luleå University of Technology, Sweden
email: melina.sattelmeier@ltu.se

[6] Technical University of Munich, Munich, Germany
email: hannah.schwedhelm@tum.de

[8] École Polytechnique Fédérale de Lausanne (EPFL), Switzerland
email: francesca.padoan@epfl.ch

[9] SINTEF Energy Research, Norway

[10] University of Glasgow, UK
email: davide.vettori@glasgow.ac.uk

[11] Institut national de la recherche scientifique, Canada
email: mathias.chabal@inrs.ca

[12] NTNU, Norway
email: sahra.n.sabil@ntnu.no

[13] University of Idaho, USA
email: dtonina@uidaho.edu

[14] LimnoSolve – Team for Applied Limnology, Austria
email: daniel.hayes@limnosolve.eu

ABSTRACT

At the 15th International Symposium on Ecohydraulics and Fish Passage (ISE-FP 2024) in Québec, Canada, the Early Careers on Ecohydraulics Network prepared and conducted a community survey. Here, we present key outcomes, encompassing the demographic landscape in the ecohydraulics community, the skills and training needed, and the emerging technologies that are shaping the direction of the research. Our results show that the community calls for better training in the use of emerging technologies, interdisciplinary collaboration and the development of soft skills. Improving such training will help the entire community for innovation, collaboration and cross-disciplinary engagement.

Keywords: Interdisciplinarity; education and training; AI; ECoENet.

1. Introduction

Ecohydraulics combines disciplines such as hydraulic engineering, aquatic ecology and environmental sciences to study interactions between hydrodynamics, morphodynamics, and biota. Thus, it covers a wide spectrum of applied research themes, namely, freshwater habitat degradation, climate change, mitigation and restoration, and integrated water resource management, among others (Casas-Mulet et al., 2016; Boavida et al., 2020). Given the interdisciplinary nature of ecohydraulics, collaboration with researchers from different backgrounds is key. In this sense, Early Career Researchers (ECRs) – typically doctoral and postdoctoral researchers – can play a pivotal role driving interdisciplinary research. However, their potential may be hindered by challenges such as poor training, unclear career pathways, restricted professional networks and low acceptance or limited recognition in the established scientific community, or in non-interdisciplinary communities (Wierenga et al., 2025; Salmela et al., 2025).

Here, we present findings from the survey developed by the Early Career on Ecohydraulics Network (ECoENet) at the 15th International Symposium on Ecohydraulics and Fish Passage (ISE-FP 2024). The survey allowed us to characterize the demographics of the ecohydraulics community, identify the relevant skills and emergent technologies shaping current and future research, and provide insights into education and training needs, in particular from the perspective of early career researchers.

2. Survey

The survey was developed during the ECoENet pre-conference workshop at ISE-FP 2024, held in Québec City, Canada, from 5-9 May 2024, and was based on previous surveys and workshops run by ECoENet in 2016 (Wilkes et al., 2016) and 2018 (Casas-Mulet et al., 2023). It consisted of four sections with a total of 42 questions. The sections were related to 1) demography, educational background, and professional development, 2) challenges on ecohydraulics, 3) self-rated skills, and 4) open questions for additional challenges, emergent technologies in ecohydraulics, and skills needed to excel in the research area, as well as preferred seminar topics that people would like to attend. The survey was distributed before the ISE-FP 2024 conference in May and further distributed online via social media, newsletters and emails until October 2024. This work covers demography (section 1) and the open questions (section 4). For the analysis of the open questions, we disaggregated complex answers into individual entries, such that the answer of a single participant could have multiple entries.

3. Results and discussion

3.1. *Demographics in ecohydraulics*

A total of 105 people participated in the survey, of whom only 21% were female. Although all continents were represented, most participants were based in Europe (Fig. 1a). Despite the increase of participation from the Global South (28% in 2024 compared to 10% in the 2018 survey; Casas-Mulet et al. 2023), we recognize that these regions can face challenges that difficult research, such as data scarcity, safety in the field-work, funding, and political and economical stability. In general, the underrepresentation of certain groups (women, Global South) suggests that although the scientific community continues fostering inclusivity and diversity in science, external social issues may still hinder or discourage some individuals from pursuing a career in ecohydraulics. Regarding career stage, 49% of the participants were ECRs (graduate student, PhD candidate and temporary researcher) and 51% senior scientists. The amount of permanent researchers and the ones coming from the private sector increased compared to the previous survey (42% in 2018, Casas-Mulet et al. 2023) (Fig. 1b), which could also reflect the transition of some community members to more established positions.

The disciplinary background was dominated by Engineering, followed by Biological Sciences, Interdisciplinary background, and Earth Sciences (Fig. 1c). The participants mainly research macrotopics related to hydraulic modeling, hydrology, and fish and flow responses, while only less than 5% working on social aspects (Fig. 1d). Therefore, even though ecohydraulics is attracting more professionals from engineering fields (58% in 2024 vs 37% in 2018, Casas-Mulet et al. 2023), a better integration of social, economic, legal and humanistic aspects is still missing. We believe that a stronger collaboration between STEM (Science, Technology, Engineering, and Mathematics) and social-humanistic sciences can foster the engagement of society and policy-makers in ecohydraulics applications.

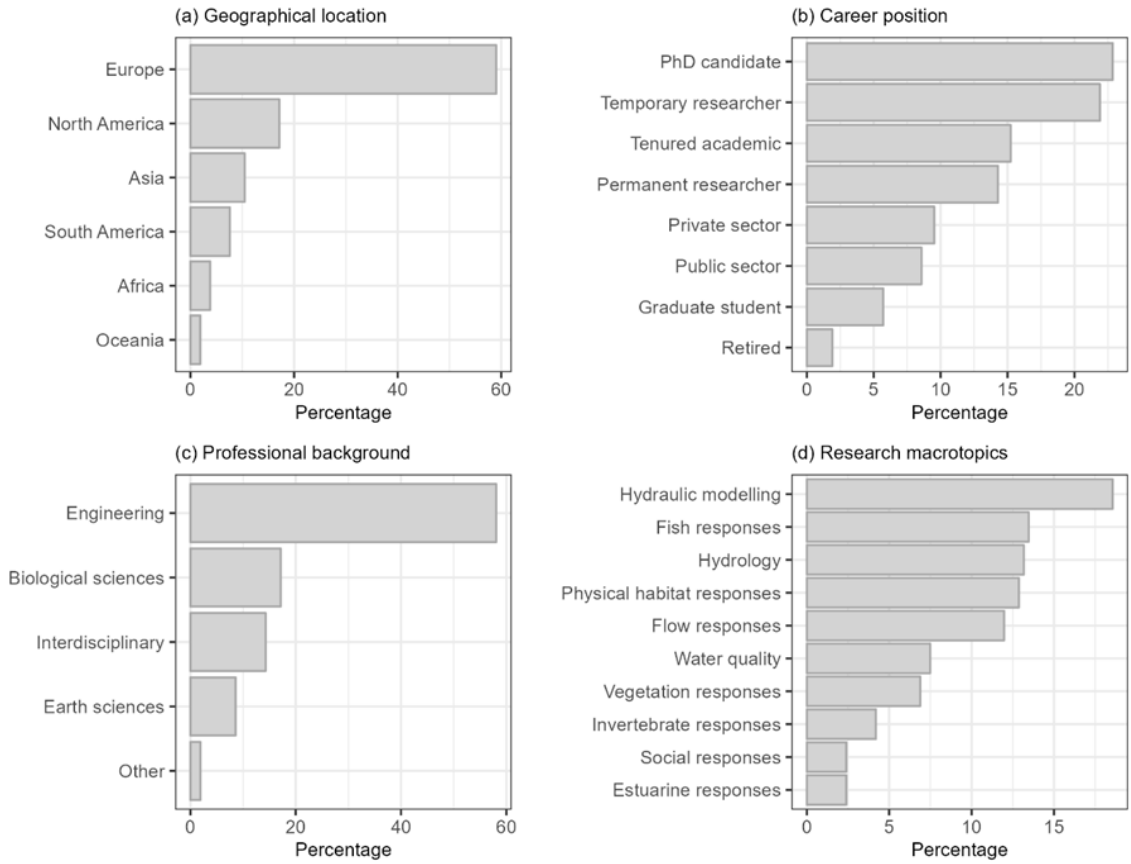

Fig. 1. Demographics by geographical location, professional background, career position and research macrotopics.

3.2. *Skills and emergent technologies*

We collected a total of 186 entries on the topic of skills relevant in ecohydraulic research. After assigning each entry to a specific topic, we identified three groups: (1) Modeling, Analysis and Data Science, (2) Personal and Professional Skills, and (3) Data collection. The skills related to modeling, analysis and data science were mentioned most frequently (47%). Surprisingly, personal and professional skills were the second most mentioned (38%). Interdisciplinarity (20 entries) was as frequently mentioned as programming and statistics/data analysis (20 and 19 entries, respectively). Table 1 (left) shows a summary of the most frequent entries.

Table 1. Most frequent skills and emerging technologies in ecohydraulics mentioned in the open questions.

Skills needed to excel in ecohydraulics		**Emerging technologies in ecohydraulics**	
Group 1: Modeling, Analysis and Data Science		**Group 1: Data Collection and Monitoring Technologies**	
computer programming	20	remote sensing	19
statistics / data analysis	19	biotelemetry	15
hydro-numerical modeling	12	UAVs (drones)	15
spatial analysis (e.g., GIS)	11	sensors	15
other	25	other	38
Group 2: Personal and Professional Skills		**Group 2: Data Analysis and Modeling**	
interdisciplinary	20	artificial intelligence (AI)	23
social skills	10	1D/2D hydrodynamic	8
Critical thinking (problem solving, creatiĵvity, critical analysis, etc.)	7	real-time controls	7
other	41	other	35
Group 3: Data Collection		**Group 3: Technological/Innovative End-User Applications**	
field work	12	nature-based solutions	5
experimental work	6	internet of things	5
other	10	other	4

Regarding the answers on emerging technologies relevant to ecohydraulic research, we collected 196 entries, identified 35 different technologies and grouped them into: (1) Data Collection and Monitoring Technologies, (2) Data Analysis and Modeling, and (3) Technological/Innovative End-User Applications. In contrast to the skills, 53% of the technologies mentioned were related to data collection and monitoring (in particular remote sensing, biotelemetry and UAVs), followed by data analysis and modeling (40%), with special emphasis on artificial intelligence (AI) (23 mentions). The most frequent entries are listed in Table 1 (right).

Overall, the survey results highlighted that the community has a clear preference towards advanced methods for data acquisition, automation, data analysis, (data-driven) modeling, and behavioral observations, which is observed in both the skills and emerging technologies that scientists consider relevant. Finally, even though "hard scientific skills" remain dominant in the field, the community recognizes the importance of integrating social aspects and developing an interdisciplinary scientific profile.

3.3. *Identified topics for seminars, education, and training*

Participants mentioned a total of 78 distinct topics. While most responses belonged to disciplinary and technical topics (e.g., remote sensing, sensors, field measurements, statistics as well as biophysical modeling and relationships), the interest extended to other non-disciplinary topics, such as science communication, in particular to policy makers, as well as methods for working and collaborating in an interdisciplinary environment. In this regard, we consider that interdisciplinarity and collaboration plays a big role not only in the development of ecohydraulics. As such, the scientific community is called to increase the recognition of ECRs engaged in interdisciplinary work.

Many ECRs wish a stronger preparation to meet the knowledge and skills needed for working in such an interdisciplinary research field as ecohydraulics (Casas-Mulet et al., 2023; Wilkes et al., 2016). This is also reflected in the interest in seminars on practical skills and emerging tools and technologies, as well as broader topics. Training for researchers in ecohydraulics, including ECRs, should consider hands-on training with new technologies for data acquisition and analysis, but also aim for stronger connection with the real world. At the same time, new developments in AI and language-based tools can support research and training, and assist ECRs in applying traditional skills such as science communication, knowledge synthesis and writing. However, implementation of such tools still requires paying attention to human oversight, collaboration, and ethical use.

4. Conclusion

The ecohydraulics community is present in all continents, with members from multiple backgrounds and engaged in a variety of research macrotopics. As a discipline, ecohydraulics is evolving to more data-intensive approaches, which are also bonded to emerging technologies in aquatic science. Thus, the community needs to engage in gaining skills and training of its researchers, in particular ECRs. While technical and traditional skills remain essential for the research, interdisciplinarity and collaboration skills will likely also play a more relevant role.We welcome IAHR initiatives for the integration of ECRs, such as IAHR Young Professionals Hydro-Environment Challenge and the Young Professionals Congress, both of which have included challenges and sessions dedicated to ecohydraulics. At the same time, we call for a continuous investment and support for ECRs in order to sustain and advance the field.

Acknowledgements

We thank the Local Organizing Committee of ISE-FP 2024, who provided support for the ECoENet workshop, as well as the anonymous survey respondents and workshop participants.

References

Boavida I, Fuentes Pérez JF, Hayes DS, Jesus J, Moreira M, Belmar O, et al. (2020) Ecohydraulics of river flow alterations and impacts on freshwater fish, Limnetica, *39*(1), 213–232.
Casas-Mulet R, King E, Hoogeveen D, Duong L, Lakhanpal G, Baldwin T, et al. (2016) Two decades of ecohydraulics: trends of an emerging interdiscipline, Journal of Ecohydraulics, *1*(1-2), 16–30.
Casas-Mulet R, Vanzo D, Adeva-Bustos A, Macnaughton CJ, Stewardson MJ, Pasternack GB, et al. (2023) How to strengthen interdisciplinarity in ecohydraulics? Outcomes from ISE 2018, Journal of Ecohydraulics, *8*(1), 1–12.
Salmela M, Vienni-Baptista B, Cheas K (2025) Towards the Recognition of Interdisciplinary and Transdisciplinary Researchers, Minerva. Advance online publication.
Wierenga M, Heucher K, Chen S, Grewatsch S, Montgomery AW (2025) Communities for impact: Empowering early-career researchers in the pursuit of impact, Strategic Organization, *23*(1), 19–30.
Wilkes MA, Neverman AJ, Casas-Mulet R, Adeva-Bustos A, McCluskey AH, Ouellet V, et al. (2016) Early careers on ecohydraulics: challenges, opportunities and future directions, Journal of Ecohydraulics, *1*(1-2), 102–107.

Book of Abstracts of the *16th International Symposium on Ecohydraulics*
Challenges and solutions in the time of global changes
August 16–20, 2026, Lausanne, Switzerland
ISSN: 2790-2420 | ISBN: 978-90-837233-9-6 | doi:[10.64697/iahr.proc.ise2026.abs]
© 2026 IAHR. CC BY-NC-ND 4.0

BUILDING POLISH DATABASE OF FREE-FLOWING RIVERS TOWARDS PRIORITIZATION OF RESTORATION EFFORTS

Kamila BELKA[1], Michał BRACH[2], Geetika CHAUHAN[1], Mariusz GĄSIOR[3], Szymon JUSIK[4], Krzysztof KARPIO[2], Paweł KONECKI[5], Adam NADOLNY[5], Włodzimierz NATORF[6], Przemysław NAWROCKI[3], Sławomir BURY[5], Piotr PARASIEWICZ[1]

[1] National Inland Fisheries Research Institute, Poland
email: k.belka@infish.com.pl, p.parasiewicz@infish.com.pl

[2] Warsaw University of Life Sciences, Poland
email: michal_brach@sggw.edu.pl, krzysztof_karpio@sggw.edu.pl

[3] WWF Poland Foundation, Poland
e-mail: mgsior04@gmail.com, pnawrocki@wwf.pl

[4] Poznań University of Life Sciences, Poland
e-mail: szymon.jusik@up.poznan.pl

[5] Wroclaw Institute of Spatial Information and Artificial Intelligence Applications (WIZIPISI), Poland
e-mail: pawel.konecki@wizipisi.ai, adam.nadolny@wizipisi.ai, slawomir.bury@wizipisi.ai,

[6] Ipix s.c., Poland
e-mail: wnatorf@ipix.eu

ABSTRACT

Free-flowing rivers play a critical role in maintaining ecological connectivity, supporting biodiversity, and sustaining ecosystem services, yet their extent in Europe has been drastically reduced by centuries of hydromorphological alteration. In Poland, the lack of a standardized, nationwide inventory of river fragmentation has hindered effective planning and prioritization of restoration actions. This study presents the development of the first Polish database of free-flowing rivers, designed in accordance with the EU-endorsed Guidance on criteria for identifying free-flowing river stretches and aligned with the objectives of the Nature Restoration Regulation and the EU Biodiversity Strategy for 2030. The database integrates hydrological, hydromorphological, and infrastructural datasets, including barrier inventories, river typology, slope, catchment characteristics, and fish macrohabitats. Statistical modelling addresses data gaps in barrier distribution and passability, guiding targeted field verification. The resulting assessment framework will support prioritization of restoration measures and enable multi-scale evaluation of river continuity. A web-based interface will facilitate stakeholder engagement and decision-making. This work provides a fundamental tool for evidence-based river management in Poland and contributes to broader European efforts to restore free-flowing rivers and enhance freshwater ecological integrity.

Keywords: free-flowing rivers; river connectivity; restoration; hydromorphology; GIS; barrier inventory.

1. Introduction

Free-flowing rivers are among the most ecologically valuable yet increasingly scarce freshwater ecosystems worldwide. Their uninterrupted hydrological connectivity, morphological diversity, and natural ecohydrological cycles support essential ecological functions, enable the migration of fish and other aquatic and semi-aquatic species, and sustain a wide range of socio-economic benefits. These qualities make free-flowing rivers biodiversity hotspots within an increasingly human-modified landscape. In Europe river continuity has been profoundly altered by centuries of hydraulic engineering, channelization, dam

construction, and land-use change reducing productivity and diversity of ecosystems, thus hampering ecosystem services.

Momentum for restoring river continuity has grown significantly at the European level, the key development being the adoption of the Nature Restoration Regulation (EU) 2024/1991, which entered into force in 2024. This regulation obliges Member States to implement restoration actions targeting degraded ecosystems, including rivers, and sets the ambitious goal of restoring at least 25,000 km of free-flowing rivers by 2030. To support these objectives, the EU has issued the Guidance on criteria for identifying free-flowing river stretches, endorsed by the Water Directors (European Commission, 2025). This document provides a harmonized methodological framework for assessing river continuity, identifying barriers, and evaluating hydromorphological conditions required to maintain or restore ecological processes.

In Poland, as in many European countries, the absence of a standardized and comprehensive national inventory of free-flowing rivers has long hindered evidence-based decision-making and the strategic allocation of restoration resources. Addressing this gap is essential for effective implementation of the Water Framework Directive, the EU Biodiversity Strategy for 2030, and the Nature Restoration Regulation. This on-going study responds to these needs by developing the first nationwide database of free-flowing rivers in Poland.

2. Methods

2.1. Database

The source database integrates national data sources of river network, barriers to longitudinal, transversal, and vertical connectivity (including dams, sluices, weirs, ramps, fords, culverts, embankments, and dikes); as well as hydromorphological river types, channel slope, catchment size, and fish macrohabitats. The database of hydrotechnical structures across and along rivers, prepared under the initiative of "The most valuable rivers and streams of Poland" led since 2014 by WWF Poland Foundation and Poznań University of Life Sciences, was used and the barriers therein assigned to one of the above barrier types. This comprehensive database product was also used to prepare a custom made classification of Polish rivers into hydromorphological types (straight, sinuous, meandering, transitional, braided, anabranching, and anthropogenically straightened), and to calculate slopes and altitudes of river reaches. Catchment size has been calculated based on the Polish river network (MPHP10v16), and fish macrohabitats reclassified onto the national river network following the procedure developed by Parasiewicz et al. (2023).

Recognizing the incompleteness of the national barrier inventory—a critical limitation for assessing river continuity—the project applies machine learning algorithm (Random Forest) to estimate the probability of barrier presence based on environmental and socio-economic predictors. These estimates were integrated into the final assessment and will guide targeted field verification in selected rivers.

2.2. Assessment rules and algorithms

All datasets are imported into a PostgreSQL and PostGIS database and processed using Python and Python-based libraries. The assessment follows the EU-endorsed Guidance on criteria for identifying free-flowing river stretches (European Commission, 2025), adapted to Polish conditions and the available data. Certain assumptions had to be made in order to compromise between data availability and the expected outcome.

In order to segment river network into homogenous reaches (HR) the following data are taken into consideration: WFD waterbodies delimitation, hydromorphological types, major tributaries, river corridor confinement, and fish macrohabitat types.

Longitudinal connectivity is assessed positively in a HR provided there are no dams, weirs, sluices or culverts (along small streams). Lateral connectivity is assessed in a river corridor which extent depends on the river width and hydromorphological type. Vertical connectivity is assessed as impacted from information on artificial reaches contained in the MPHP10. The probability of barriers presence was used to derive the assessment for those reaches where presence of barriers in a database was not confirmed.

Minimum length of a HR was assessed following to the Guidance Document.

Large-scale assessment of river continuity for fish and sediments is performed with the following main assumptions. No migration barrier for fish downstream of the reach up to the sea must be present when migratory species are expected. A barrier is considered here a structure of either of the following types: dam, weir, sluice gate, culvert, and other if their height and construction would prevent fish from passing freely. Three migratory fish species are considered, i.e. sea trout, eel and lamprey. Heights significant for them are:

0,5 m for the former, and none for the others. Construction settings include presence of fishpass. On the other hand, when migratory fish are not expected the length of the barrier-free section is determined in relation to fish macrohabitat functional unit (FMFU) length, and could not be shorter than 20% of that. FMFU is defined as a fish macrohabitat present in a river of certain Strahler stream order. Sediment significant barriers are considered dams that block more than 30% of catchment of the HR. When barrier probability data are considered the assessment score is given in relation to a given probability class (high, medium, low).

Final assessment is given to a reach based on those partial assessments. The assessment options are: free-flowing river, free-flowing river – hight probability, free-flowing river – medium probability, free-flowing river – low probability, not a free flowing river, and not assessed.

2.3. Stackeholders

Stakeholder engagement involves consultations and cooperation with public authorities engaged in the process of implementing the European Nature Restoration Regulation and the Water Framework Directive. Their involvement ensures alignment with national policy needs and enhances the practical implementation of the outputs.

3. Results

The project produces an integrated GIS database and a web-based portal of the Polish free-flowing rivers (available at http://rzeki.infish.com.pl), and integrates national river network, available database of hydrotechnical structures that restrict fish migration and sediment transport, together with river reaches classification into hydromorphological types and fish macrohabitat types. Database incompleteness is proactively handled by probability estimating model (Fig. 1).

A web-based interface will serve as an interactive platform for stakeholders, enabling visualization of assessment results, supporting the design of restoration strategies, and facilitating compliance with EU obligations. The project has the ambition to integrate with national barrier database when it is ready and further provide simulation platform for prioritization of restoration strategies.



Fig. 1. The Polish Free-flowing Rivers portal. The assessment panel on the right-hand side shows the assessment scores and the final result of the highlighted river reach visible on the map. Here longitudinal connectivity is passed for sediment and hydrology, and passed with medium probability for fish criteria; lateral connectivity is not passed; vertical connectivity is passed; minimum length criterion is not passed and large-scale assessment is not passed for fish criteria. On the left hand side the user can switch between the source layers used for the assessment.

Acknowledgements

This project has been financed by the Ministry of Agriculture and Rural Development direct subsidy.

References

Belletti, B., et al. (2020) More than one million barriers fragment rivers across Europe, Science, 369, 117–119.

European Commission: Directorate-General for Environment, Criteria for identifying free-flowing river stretches – Common Implementation Strategy for European Union Water Law. Guidance document no. 41, 2025, https://data.europa.eu/doi/10.2779/6009587

European Parliament and Council (2024) Regulation (EU) 2024/1991 of the European Parliament and of the Council of 24 June 2024 on nature restoration, Official Journal of the European Union, EU, L 1991.

Grill, G., et al. (2019) Mapping the world's free-flowing rivers, Nature, 569, 215–221.

Parasiewicz, P., Belka, K., Łapińska, M., et al. Over 200,000 kilometers of free-flowing river habitat in Europe is altered due to impoundments. Nature Communications 14, 6289 (2023). https://rdcu.be/dn6hb

Tickner, D., et al. (2020) Bending the curve of global freshwater biodiversity loss: An emergency recovery plan, BioScience, 70, 330–342.

Book of Abstracts of the *16th International Symposium on Ecohydraulics*
Challenges and solutions in the time of global changes
August 16–20, 2026, Lausanne, Switzerland
ISSN: 2790-2420 | ISBN: 978-90-837233-9-6 | doi:[10.64697/iahr.proc.ise2026.abs]
© 2026 IAHR. CC BY-NC-ND 4.0

WHO GETS ROOM FOR THE RIVER? NEGOTIATING THE FRONTIER OF FLOOD RISK IN KATHMANDU'S ECOLOGICAL URBAN RENEWAL

Alejandro GÓMEZ TEJERA[1, 2]

[1] Laboratory of Landscape Development, IA, ENAC, Ecole Polytechnique Fédéral de Lausanne, Switzerland.

[2] Laboratory for Human-Environment Relations in Urban Systems, IIE, ENAC, Ecole Polytechnique Fédéral de Lausanne, Switzerland.

https://orcid.org/0009-0004-6512-6197
email: alejandro.gomeztejera@epfl.ch

ABSTRACT

1. Introduction

Across many cities worldwide, rivers have been straightened, embanked and converted into open sewers. Rapid, weakly regulated urbanisation has increased paved surfaces and wastewater loads while concentrating low-income residents in marginal land along river corridors (Castaldo et al., 2025). Climate projections point to rising urban flood exposure, particularly in Asian cities where dense settlement patterns intersect with intense monsoon regimes (Zhang et al., 2025). In Kathmandu, decades of urban expansion have reconfigured a river system once structured through the hiti-pokhari regime, a vernacular water management system attuned to seasonal hydrology (Gautam et al., 2018).

The Bagmati basin is now heavily polluted and hydraulically constrained by embankment works. Infrastructure development and land reclamation have altered topography and drainage patterns across the basin (Shrestha et al., 2025). These transformations increase flood hazard by reducing conveyance and obstructing flow paths, while urbanisation expands into low-lying areas.

Within this floodplain, informal settlements occupy some of the city's most exposed river margins. Their presence reflects long-term economic, political and social processes: migration into a speculative land market, rising prices and planning regimes that offer no affordable alternatives. In the urban core, at least 33 such settlements host around 18,000 residents exposed to recurrent monsoon flooding (Table 1; Fig. 1).

Against this background, the Kathmandu Ecological Urban Renewal Project Preparation Study (KEUR-PPS), launched by ADB and CDIA in 2024, presents ecological urban renewal as a response to river degradation and flood risk. It combines green-blue corridors, wetland restoration, wastewater interception and river setback enforcement. Yet the land targeted for corridor restoration is already occupied by long-established riverside settlements. The project therefore confronts a socio-ecological dilemma: flood-risk reduction may require reclaiming inhabited space, while relocation can dismantle livelihoods, social networks and urban belonging.

Within this projectual context, beyond the question of whether relocation is justified, this study examines how flood risk becomes a category of action in ecological urban renewal. It analyses the devices through which risk is translated into intervention thresholds, the rationalities through which these thresholds are defined, and the ways riverside residents contest and negotiate them in practice.

Table 1. Exposed population of informal settlements by flood frequency. Source: custom survey results

Flood Frequency	Exposed Population of Informal Settlements
Once every year	11,741
Once every two to five years	3,142
Once every > ten years	2,572
Once every five to ten years	214
Never	4,441

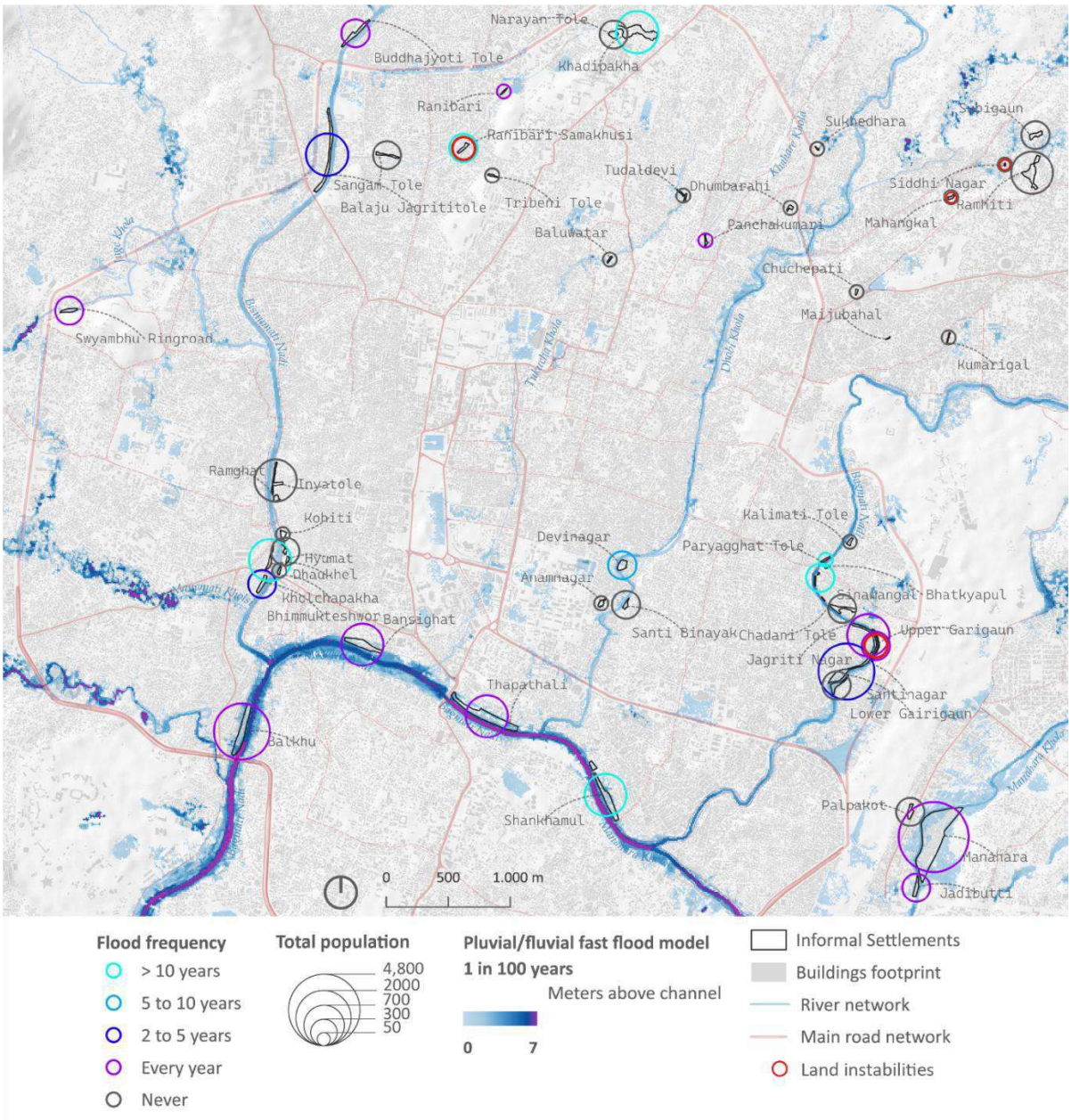

Fig. 1. Flood frequency, landslide susceptibility and exposed population of informal settlements in Kathmandu. Data: OSM, Alos Palsar, Watson et al., 2024, KEUR custom survey, author's elaboration.

2. Methods

This study draws on material produced within the KEUR Project Preparation Study, to which the author contributed as part of the Groupe Huit consulting team, and further develops it through an independent master's thesis at the University of Geneva (Gomez Tejera, 2026). A nested, multi-scalar design was adopted because flood-risk dynamics operate across basin, corridor and settlement levels. At the valley scale, flood exposure was assessed by combining hazard outputs from a simplified 2D steady-state hydrodynamic model at 10 m resolution (Watson et al., 2024) with a spatially validated geodatabase of informal settlements compiled through KEUR field surveys. This established a basin-wide baseline of how hazard, exposure and vulnerability intersect across riverbank settlements.

At institutional and settlement scales, document analysis was combined with qualitative field material to examine how risk is defined, translated and contested in practice. The corpus includes a federal-level stakeholder workshop, 15 semi-structured interviews with residents, NGOs, public officials, experts and neighbouring residents (25 participants, 24% women), a focus group in Thapathali informal settlement (23 residents and four consultants), and a five-day ethnographic immersion in Thapathali informal settlement. Thematic coding and critical discourse analysis were used to identify recurring problem framings and rationalities across documents, interviews, workshops and field observations. Cross-reading these materials relates basin-scale risk configuration to institutional thresholds and community counter-framings.

3. Key Findings

The findings first confirm that flood hazard along the Bagmati is acute, spatially concentrated and materially amplified by decades of urban transformation. Exposure mapping shows that many informal settlements occupy low-lying river margins where reduced conveyance, obstructed flow paths and recurrent monsoon flooding converge. In this sense, the danger is not merely perceived or discursively produced; it is rooted in a degraded and hydraulically constrained floodplain where vulnerable households are disproportionately exposed.

Yet the analysis also shows that this hazard does not translate mechanically into intervention. Within KEUR, flood risk becomes actionable through planning devices that abstract socio-ecological complexity into operational categories, including corridor envelopes, setback rules, pilot projects and eligibility filters. These devices do not simply describe danger. They stabilise it into spatial templates and intervention lists that can be defended within planning, legal and financing procedures. In this process, the urgency of flood risk helps legitimise a wider corridor agenda in which ecological restoration, urban image and modernisation become mutually reinforcing.

The resulting thresholds are therefore not set by hydraulic criteria alone. The findings identify different rationality bundles shaping intervention choices in distinct ways (Fig. 2). One institutional coalition links flood risk, ecological continuity and beautification, framing the corridor as a space that must be cleared, ordered and remade as legible ecological infrastructure. A second coalition links legality, administrative legibility and financial packaging, turning a metropolitan housing problem and a basin-scale hydrological dynamic into bounded, auditable and investable pilot interventions. On the community side, residents evaluate flood risk through a different calculus: recurrent losses are weighed against the costs of losing centrality, livelihood access, social support networks and protection from debt or speculative capture. What appears institutionally as ecological necessity may therefore be experienced locally as a narrowing of rights and options.

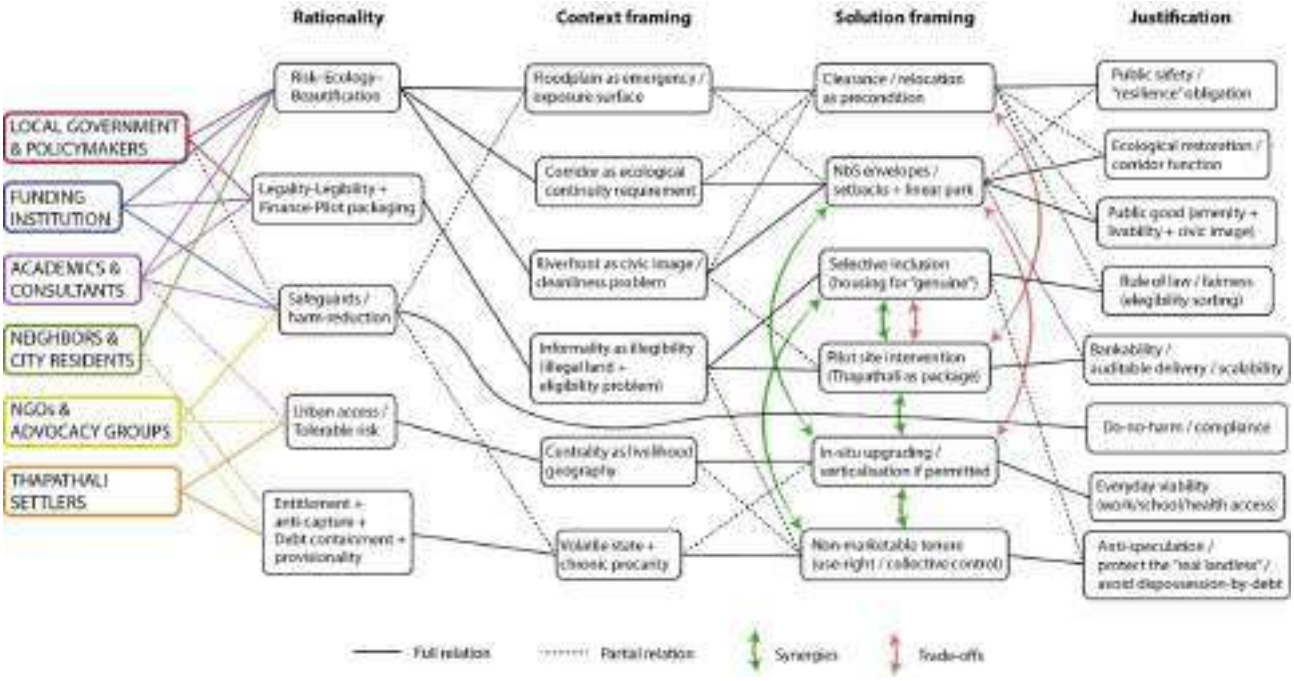

Fig 2. Actor coalitions, rationality bundles and negotiation spaces shaping the flood-risk frontier. Solid lines indicate alignment, dashed lines partial or contested alignment; green arcs mark potential synergies, pink arcs key trade-offs. Author's elaboration.

The analysis also shows that each rationality leaves key dimensions partially invisible. Institutional framings tend to undercount the social costs of displacement and to treat informality as a spatial obstacle rather than as a form of urban inhabitation produced by wider political and economic conditions. Community perspectives, in turn, foreground immediate habitability and access to the city but cannot fully address basin-scale drivers of hazard or corridor-wide sequencing effects that shift pressure from one settlement to another. The flood-risk frontier therefore becomes visible where trade-offs concentrate, between clearance and in-situ upgrading, ecological corridor width and habitable upgrading, and selective eligibility and inclusive access to secure housing. At the same time, the findings point to conditional synergies. Nature-based interventions can be coupled with socio-environmental justice when ecological functions are integrated with existing uses, while

non-marketable tenure, phased relocation and safeguards used as negotiation infrastructure can help make burdens, guarantees and sequencing rules explicit. The frontier of risk is thus not a fixed line derived from hazard alone, but a negotiated boundary where environmental exposure is translated into legitimacy, intervention and exclusion.

4. Implications for Ecological Urban Renewal

These findings suggest that restoring floodplain function in densely settled basins cannot be approached as a purely technical adjustment of biophysical form and process. In inhabited floodplains such as the Bagmati, measures designed to improve conveyance or ecological continuity also redistribute access to housing and the right to the city. Adaptive capacity, tenure security and everyday social infrastructures must therefore be treated as part of the design problem.

The findings do not support a simple choice between wholesale relocation and static in-situ upgrading. Instead, they point toward hybrid configurations that combine, for instance, selective retreat, targeted drainage improvement, flood-adapted upgrading and basin-wide phased implementation. Such approaches do not eliminate conflict, but they make it possible to reduce flood hazard while limiting the detrimental effects of displacement and loss of livelihood access.

More broadly, the Kathmandu case shows how river restoration projects shaped by global adaptation finance often circulate design models and nature-based solutions across contexts with very different socio-ecological histories. These frameworks may carry strong ecological and hydraulic rationales, yet they are implemented in urban contexts marked by specific land regimes, institutional arrangements and long-standing practices of inhabiting the river corridor. Following Watson's (2003) notion of *conflicting rationalities*, the challenge is not simply to improve coordination among actors, but to recognise that different stakeholders are working with different understandings of what the river corridor is for, what counts as a legitimate intervention, and what forms of urban future are worth sustaining.

From this perspective, the central planning question is how the boundary between environmental hazard and social exclusion is drawn and operationalised. Co-designing strategies along this negotiated frontier becomes essential if ecological restoration is to proceed without reproducing dispossession. In this sense, “room for the river” is also a distributive question within contemporary urban river restoration.

Keywords: Urban river restoration, Flood risk, Informal settlements, Nature-based solutions, Kathmandu

References

Castaldo, A. G., Nocentini, M. G., Lemes De Oliveira, F., & Mahmoud, I. H. (2025). Nature-based solutions and urban planning in the Global South: Challenge orientations, typologies, and viability for cities. *Land Use Policy*, *150*, 107439. https://doi.org/10.1016/j.landusepol.2024.107439

Gautam, D., Thapa, B. R., & Prajapati, R. N. (2018). Indigenous water management system in Nepal: Cultural dimensions of water distribution, cascaded reuse and harvesting in Bhaktapur City. *Environment, Development and Sustainability*, *20*(4), 1889–1900. https://doi.org/10.1007/s10668-017-9964-2

Gomez Tejera A (2026) Who gets room for the river? Negotiating the frontier of flood risk in Kathmandu’s ecological urban renewal. Master, University of Geneva. PID: unige:192157 URL: https://archive-ouverte.unige.ch/unige:192157

Shrestha, S., Chapagain, P. S., Dahal, K., Adhikari, N., Shrestha, P., & Manandhar, L. (2025). Urban Growth and River Course Dynamics: Disconnected Floodplain and Urban Flood Risk in Manohara Watershed, Nepal. *Water*, *17*(16), 2391. https://doi.org/10.3390/w17162391

Watson, C. S., Gyawali, J., Creed, M., & Elliott, J. R. (2024). City-scale high-resolution flood models and the role of topographic data: A case study of Kathmandu, Nepal. *Geocarto International*, *39*(1), 2387073. https://doi.org/10.1080/10106049.2024.2387073

Watson, V. (2003). Conflicting rationalities: Implications for planning theory and ethics. *Planning Theory & Practice*, *4*(4), 395–407. https://doi.org/10.1080/1464935032000146318

Zhang, Q., Li, C., Wen, D., Kang, J., Chen, T., Zhang, B., Hu, Y., & Yin, J. (2025). Global South shows higher urban flood exposures than the Global North under current and future scenarios. *Communications Earth & Environment*, *6*(1), 594. https://doi.org/10.1038/s43247-025-02585-7

Book of Abstracts of the *16th International Symposium on Ecohydraulics*
Challenges and solutions in the time of global changes
August 16–20, 2026, Lausanne, Switzerland
ISSN: 2790-2420 | ISBN: 978-90-837233-9-6 | doi:[10.64697/iahr.proc.ise2026.abs]
© 2026 IAHR. CC BY-NC-ND 4.0

PROCESSES & INTERNATIONAL COLLABORATION ON SEDIMENT MANAGEMENT IN THE RHÔNE: TOWARDS SUSTAINABLE SEDIMENT CONTINUITY

Charlotte GIRARD[1], Franck PRESSIAT[2], Marion CHERRAK[1], Seydina DIOUF[1], Laurent PINET[2]

[1] Service Industriels de Genève (SIG), Switzerland
email: marion.cherrak@sig-ge.ch
email: charlotte.girard@sig-ge.ch
email: seydina.diouf@sig-ge.ch
[2] Compagnie Nationale du Rhône (CNR), France
email: f.pressiat@cnr.tm.fr
email: l.pinet@cnr.tm.fr

ABSTRACT

The Rhône River, from its glacial source to the Mediterranean, has undergone extensive anthropogenic modifications since the 19th century, notably through hydroelectric developments that have significantly modified its hydraulic regime. In the Geneva section, more than a century of river engineering—gravel pits, dams, and other interventions—has compounded the impact of substantial sediment inputs from the Arve River: between 10,000 and 200,000 m³/year of bedload depending on hydrological conditions, and approximately 700,000 m³/year in suspension. These deposits result in an average accumulation of 360,000 m³/year in the Verbois reservoir, located 14 km downstream from Lake Geneva and 12 km from the Rhône–Arve confluence. This sedimentation can raise water levels and groundwater tables, posing flood risks for lower Geneva's district.

Historically, sediment management relied on flushing operations (1945–2012). However, growing environmental awareness prompted a paradigm shift, leading to the establishment of a Franco–Swiss working group tasked with developing alternative strategies. In 2014, this collaboration resulted in a management scenario comprising the following components:

- **Partial drawdowns of the Verbois (CH) and Génissiat (FR) reservoirs,** combined with a full drawdown of the intermediate Chancy–Pougny reservoir (CH & FR), conducted in May/June under strict monitoring to maintain suspended sediment concentrations below ecological thresholds defined by French authorities—classified as Controlled Sediment Flushing Operations (CSFO).
- **Flood support from the Arve,** involving increased discharge at Verbois through releases from Lake Geneva to dilute suspended sediments and enhance transport.
- **Targeted dredging** to ensure flood safety for Geneva**.**
- **Annual biodiversity monitoring** (fish, birds, macroinvertebrates, mammals, insects).

This approach was formalized in an action plan authorized by Swiss and French authorities for 2016–2026 following a comprehensive environmental impact assessment. As this authorization nears its end, a new permit must be secured. This marks the beginning of a renewed phase of Franco–Swiss collaboration aimed at refining existing transboundary management methods and exploring innovative solutions.

Current challenges include the gradual return of Arve gravel to the Rhône in Geneva, the need for improved sediment transparency in Upper Rhône structures, heightened safety concerns in social and political spheres, hydrological and sedimentary shifts driven by climate change, and the ongoing decline of alluvial biodiversity.

This paper outlines the methodological framework guiding operators in addressing these challenges through a participatory, transboundary approach designed to foster stakeholder acceptance of technical solutions.

Research Question:

Through which processes is sediment management in the Rhône implemented and continuously improved to meet technical, environmental, and societal challenges?

Paper structure :

1. Historical overview of sediment management in the Geneva Rhône and collaboration with the Upper Rhône

Annecy sessions [1968 & 1989], Espoo Convention [1991], questioning of management approach [1997–2000], creation of the flushing working group [2002–2008], operations in 2012, implementation of an international sediment management authorization for 2016–2026.

2. Proposed strategy:

2.1. Three-phase vision:

- Transitional (2027–2028): Maintain safe operation of structures, allowing emergency sediment management if needed.
- Authorization period (2029–2041): Select a realistic management mode meeting Swiss and French safety needs, reducing environmental impacts while remaining economically viable and proportionate.
- Long-term vision (post-2041): Establish a working group of authorities and operators to validate a long-term scenario, potentially including major structures for sediment management or flood protection.

2.2. International collaboration among decision-making bodies:

- COPILs (DREAL-OCEAU + CNR-SIG)

2.3. International collaboration among operators:

- COPRO (CNR-SIG)
- Collaborative sessions

3. Methodological process:

3.1. Sediment monitoring in the Geneva's Rhône and Arve catchment

3.2. Exploration of alternatives & optimization of existing management methods:

- Scientific state of the art
- SIG workshops
- Hydraulic and sediments expert roundtables
- CNR-SIG roundtables

3.3. Qualification of management modes:

- Feasibility studies (short, medium, long term)
- Hydraulic and sedimentary studies
- Environmental expert roundtables
- Stakeholder roundtables: industry
- Stakeholder roundtables: NGOs
- Regulatory authorities (CH & FR)

3.4. Franco-Swiss multi-criteria analysis

3.5. Reporting & communication with stakeholders

Keywords: International governance, sediment management, participative process

Session C1

Peaking regimes and environmental flows

Book of Abstracts of the *16th International Symposium on Ecohydraulics*
Challenges and solutions in the time of global changes
August 16–20, 2026, Lausanne, Switzerland
ISSN: 2790-2420 | ISBN: 978-90-837233-9-6 | doi:[10.64697/iahr.proc.ise2026.abs]
© 2026 IAHR. CC BY-NC-ND 4.0

ECOLOGICAL CONSEQUENCES OF FLOW REGIME ALTERATION FROM HYDROPOWER REGULATION: A COMPARATİVE ASSESSMENT OF THE RHÔNE AND ÇORUH RIVERS

Ibrahim Halil DEMIREL[1], Giovanni DE CESARE[2]

[1] Kozluk Vocational High School, Department of Construction, Batman University, Batman, Türkiye
email: ihalil.demirel@batman.edu.tr

[2] Platform of Hydraulic Constructions (PL-LCH), ENAC - IIC, École Polytechnique Fédérale de Lausanne (EPFL), Lausanne, Switzerland
email: giovanni.decesare@epfl.ch

ABSTRACT

This study investigates flow regime alteration from hydropower regulation in two contrasting hydroclimatic systems: the Rhône River (Switzerland) and the Çoruh River (Türkiye). Change-point, trend, and ecological deficit analyses using daily flow data (2000–2024) reveal that regulation primarily alters temporal rather than volumetric components of flow. Increased rise–fall rates in the Rhône indicate intensified hydropeaking, whereas regulation in the Çoruh basin, including upper-basin cascade developments, is associated with smoother short-term variability patterns. Despite stable baseflows, both rivers show seasonal eco-phase shifts and artificial timing patterns, reflecting anthropogenic control over natural regimes. The findings demonstrate that regulation produces "artificial seasonality" and emphasize the need to integrate ecohydrological indicators such as Richards–Baker Flashiness Index, Baseflow Index, and Eco-Deficit into hydropower management and water policy frameworks to ensure ecological resilience.

Keywords: Flow regime alteration; Hydropower regulation; Ecohydrology; Hydropeaking; Eco-deficit.

Introduction

The natural flow regime is a multidimensional concept encompassing seasonal patterns, flood and drought frequency, daily variability, and rates of change (Zuo et al., 2015). Alterations in these components can cause ecological disturbances for aquatic organisms, including fish, macroinvertebrates, and riparian vegetation, leading to reproductive failure, habitat loss, and reduced biodiversity (Shi et al., 2019). Human interventions, particularly dam construction and flow regulation, have globally modified river integrity (Sakaris, 2013; Sabater et al., 2018; Park et al., 2024). These impacts extend beyond discharge magnitude to the timing of flows and sediment regimes. Environmental flow assessment should therefore consider all ecological components of the flow regime, not only minimum discharge (Bizzi et al., 2012; Peres & Cancelliere, 2016).

In rivers regulated for hydropower (e.g., Rhône and Çoruh), distinguishing natural and operational flow components is challenging (Alaoui et al., 2014). This study analyses flow regime changes and their ecological implications by comparing pre- and post-regulation periods at the Rhône–Porte du Scex (Switzerland) and Çoruh–Laleli (Türkiye) streamflow gauging stations. Although based on daily data that do not capture sub-daily hydropeaking, the analysis highlights the ecological relevance of such fluctuations (Courret et al., 2021; Meile, 2011). The study tests the Natural Flow Regime Hypothesis (Richter et al., 1996) under regulated conditions and, considering the limited integration of hydromorphological alteration metrics within the current implementation framework of the Water Framework Directive (Mentzafou et al., 2023), and provides a methodological example applicable to HPPs in data-limited regions such as Türkiye. The two case studies were selected to represent contrasting hydroclimatic and hydropower operation conditions (Alpine peaking vs. Turkish cascade), offering a meaningful comparative basis for ecohydrological evaluation.

Materials and methods

1.1. Study area

This study covers two Streamflow Gauging Stations (SGS) representing different hydroclimatic conditions and hydropower operation types: the Rhône-Porte du Scex in Switzerland (FOEN ID: 2009), affected by peaking hydropower regulation, and the Çoruh-Laleli in Türkiye (DSI ID: E23A020), characterized by cascade-type regulation. The Rhône SGS (5238 km² drainage area, 182 m³/s average flow rate) has a nivo-glacial character, data for the period 2000-2024 were used. Çoruh-Laleli SGS (4759 km² drainage area, 29 m³/s average flow rate) shows nival regime characteristics and is characterized by cascade-type regulation, i.e., multiple hydropower plants arranged sequentially along the main channel, where outflow from one becomes inflow to the next. The period 2000–2020 was analysed.



Fig. 1. The two study areas, left the Rhône in Switzerland and right the Çoruh-Laleli in Türkiye

1.2. Methods

The hydrometric indicators used, their formulas and ecological meanings are summarized in Table 1. Regime breaks were identified using the Pettitt test, after which indicators were computed for pre- and post-break periods (P0–P1) and evaluated using Mann–Kendall and Sen's slope methods. In the last stage, seasonal ecological imbalances were evaluated with Eco-Deficit and Eco-Surplus analyses. This integrated approach enabled the interpretation of flow regime changes together with hydrological and ecological indicators.

Table 1. Hydrometric indicators used, formulas and ecological interpretations

No	Indicator / Test	Formula	Ecological meaning / Reason for use
1	Richards–Baker Flashiness Index (RB) (Baker et. al, 2004)	$RB = \frac{\sum\lvert Q_i - Q_{i-1}\rvert}{\sum Q_i}$ (1)	Reflects the hydropeaking effect and habitat instability by measuring the daily volatility in stream flow.
2	Rise and Fall Rates (Olden & Poff, 2003)	$\text{Rise} = \frac{Q_{t+1} - Q_t}{\Delta t}$ $\text{Fall} = \frac{Q_t - Q_{t+1}}{\Delta t}$ (2)	Measures daily rates of increase and decrease. 95% values represent extreme fluctuations.
3	Baseflow Index (BFI) (Smakhtin, 2001)	$BFI = \frac{Q_{\text{base}}}{Q_{\text{total}}}$ (3)	Represents groundwater contribution during periods of low flow. High BFI means stable base flow.
4	Mean Discharge (Q_mean) (Vogel et al., 2007)	$Q_{\text{mean}} = \frac{1}{n}\sum Q_i$ (4)	Shows the average annual flow rate. Summarizes general trends in flow volume.
5	Eco-Deficit / Eco-Surplus (Vogel et al., 2007)	$\text{EcoDeficit} = \int_0^1 [Q_{\text{nat}}(p) - Q_{\text{obs}}(p)]dp$ (5) $\text{EcoSurplus} = \int_0^1 [Q_{\text{obs}}(p) - Q_{\text{nat}}(p)]dp$ (6)	Quantifies the relative difference between natural and observed Flow Duration Curves (FDC), indicating ecological deficit or surplus.
6	Pettitt Test (Pettitt, 1979)	$U_t = 2\sum_{i=1}^{t}\sum_{j=t+1}^{n} \text{sgn}(x_i - x_j)$ (7)	Identifies the single break point (year of regime change) in the time series.
7	Periodic Difference Analysis (Box et. al. 1976)	$Z = \frac{P1_{\text{median}} - P0_{\text{median}}}{IQR_{P0}}$ (8)	Measures the difference between the period before (P0) and after (P1) regulation.
8	Mann-Kendall Trend Test (Mann, 1945; Kendall, 1975)	$S = \sum_{i=1}^{n-1}\sum_{j=i+1}^{n} \text{sgn}(x_j - x_i)$ (9) $\text{Var}(S) = \frac{n(n-1)(2n+5)}{18}$ (10)	Tests for monotonic upward/downward trends in current indicators.
9	Sen's Slope Coefficient (Sen, 1968)	$Q_i = \frac{x_j - x_k}{j - k}$ (11)	Determines the direction and magnitude of the trend; quantitatively expresses the rate of change.

Results and discussion

In this section, the changes of the flow regime indicators obtained during the study periods are evaluated and the results are interpreted from an ecological point of view. The findings of the analysis are summarized in Table 2, while the related graphs are presented in Fig. 2 for Rhône-Porte du Scex and Çoruh-Laleli SGSs.

Major hydropower development in the Çoruh basin intensified after the early 2000s, including both cascade-type and run-of-river plants, particularly between 2002 and 2020. In Switzerland, environmental flow regulations were strengthened in the early 2010s, which may have influenced operational strategies. These contextual developments provide background for interpreting the detected regime shifts without implying direct causal attribution.

Table 2. Summarizes the main hydrological indicators and their ecological interpretation

No	Indicators / Features	Rhône (2000–2024)	Çoruh (2000–2020)	Comment / Comparison
1	Regime break year	2018	2004	Change began earlier in the Çoruh.
2	RB (Flashiness)	Small increase (+0.3 σ)	Decrease (p=0.007)	While fluctuations increased in the Rhône, they decreased in the Çoruh due to a regulating effect.
3	Rise/Fall	+0.7–1.3 σ (distinct ↑)	+2–24 σ (very strong ↑)	Sudden releases and closures are much more pronounced in the Çoruh than in the Rhône.
4	BFI (Base flow rate)	Steady	Steady	Base flow (e.g. groundwater) contribution is maintained in both systems.
5	Q_mean (Mean flow)	Light ↑	Light ↑	Flow volume remains generally unchanged, but the timing has changed.
6	Eco-surplus season	Summer (JJA ≈ 47)	Spring (MAM ≈ 22)	The Rhône experiences overflow in summer, while the Çoruh experiences overflow in spring.
7	Eco-deficit	Low (1–2 unit)	No	Overflow is dominant in both systems, rather than underflow.
8	Ecological impact	Increased rise–fall rates during summer suggest potential benthic stress due to rapid water level fluctuations.	Early spring discharge, habitat instability	Hydropeaking pressure is evident in both rivers; the timing is different.

The 2018 break at the Rhône SGS corresponds to increased rise–fall rates consistent with hydropeaking patterns (Courret et al., 2021). Baseflow remained stable, indicating operational rather than volumetric change (Peres & Cancelliere, 2016). In contrast, the Çoruh showed a significant decreasing RB trend (p = 0.007), suggesting smoothing of daily variability despite intensified rise–fall rates, likely reflecting operational adjustments associated with the upper-basin cascade segment and ongoing downstream cascade development.. Overall, regime alteration primarily affected timing and fluctuation rates rather than total discharge.

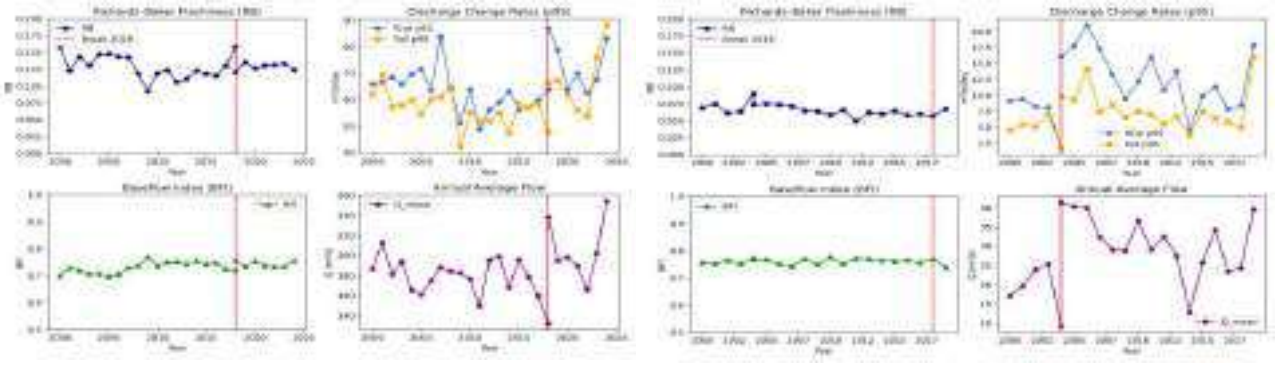

a) Rhône-Porte du Scex b) Çoruh-Laleli

Fig. 2. RB, DCR, BFI and Q_mean graph of the SGSs

For the Rhône River, the RB index increased after 2018, indicating intensified short-term flow fluctuations associated with hydropeaking. In contrast, the Çoruh River exhibited a decreasing RB trend (p = 0.007), suggesting regulation-induced smoothing of daily variability. Decreasing RB values reflect that the operational flow has stabilized, even though the continuous rate of increase/decrease is excessive (Fig. 2). According to

the Mann–Kendall test, only the RB indicator showed a significant decreasing trend ($p = 0.007$) for 2000–2020, indicating reduced flow flashiness and partial regulation. Other indicators (rise_mean, fall_mean, BFI, Q_mean) showed no significant trend ($p > 0.05$), suggesting that operational fluctuations dominate over long-term variability in the Çoruh. This reduction may be associated with coordinated upstream regulation within the basin. Although flashiness (RB) decreased, the rise and fall rates increased, implying that regulation has become more structured but also more intense. This may reflect short, intense turbine oscillations followed by longer steady phases, as inferred from daily discharge data.

Contrasting operational logics explain system differences: the Rhône is influenced by peaking energy demand, considerable high Alpine non-cascading storage volumes and large-scale hydropeaking, whereas the Çoruh is affected by upstream controls distributing flow pulses over shorter intervals. In both rivers, regime alteration mainly concerns timing and rate of change rather than flow volume. These deviations, linked to seasonal energy demand and snowmelt timing, cause ecological fragmentation and stress, reducing overall river resilience.

Conclusion

Analyses at the Rhône–Porte du Scex and Çoruh–Laleli SGSs revealed that hydropower regulation primarily alters the temporal, not volumetric, components of the flow regime. Regime breaks detected in 2018 (Rhône) and 2004 (Çoruh) indicate distinct operational shifts. Increased rise–fall rates and eco-surplus patterns indicate operational timing disturbances rather than volumetric or climatic change. Although based on daily data, the results indirectly highlight the influence of turbine operations on ecosystem stability. The contrasting Alpine and Turkish systems show that regulation under different climatic contexts can drive convergent hydrological patterns that potentially reduce ecological heterogeneity. These findings emphasize the need to integrate ecohydrological metrics such as RB, BFI, and eco-deficit into hydropower licensing and monitoring to better capture ecological impacts and to guide sustainable flow management.

References

Alaoui, A., Willimann, E., Jasper, K., Felder, G., Herger, F., Magnusson, J. and Weingartner, R., 2014. Modelling the effects of land use and climate changes on hydrology in the Ursern Valley, Switzerland. Hydrological Processes, 28(10), pp.3602–3614.
Baker, D.B., Richards, R.P., Loftus, T.T. and Kramer, J.W., 2004. A new flashiness index: Characteristics and applications to midwestern rivers and streams. Journal of the American Water Resources Association (JAWRA), 40(2), pp.503–522.
Bizzi, S., Pianosi, F. and Soncini-Sessa, R., 2012. Valuing hydrological alteration in multi-objective water resources management. Journal of Hydrology, 472, pp.277–286.
Box, G.E.P., Jenkins, G.M. and Reinsel, G.C., 1976. Time Series Analysis: Forecasting and Control. San Francisco: Holden-Day.
Courret, D., Baran, P. and Larinier, M., 2021. An indicator to characterize hydrological alteration due to hydropeaking. Journal of Ecohydraulics, 6(2), pp.139–156.
Kendall, M.G., 1975. Rank Correlation Methods. 4th ed. London: Griffin.
Mann, H.B., 1945. Nonparametric tests against trend. Econometrica, 13(3), pp.245–259.
Meile, T., Boillat, J.L. and Schleiss, A.J., 2011. Hydropeaking indicators for characterization of the Upper-Rhone River in Switzerland. Aquatic Sciences, 73(1), pp.171–182.
Mentzafou, A., Katsafados, P., Papadopoulos, A. and Dimitriou, E., 2023. Hydrological regime alteration assessment in the context of WFD 2000/60: A European and global review. Sustainability, 15(22), 15704.
Olden, J.D. and Poff, N.L., 2003. Redundancy and the choice of hydrologic indices for characterizing streamflow regimes. River Research and Applications, 19(2), pp.101–121.
Park, J., Jang, S., Lee, H., Gou, J. and Song, I., 2024. Evaluation of fish habitat suitability based on stream hydrodynamics and water quality using SWAT and HEC-RAS linked simulation. Scientific Reports, 14(1), 19236.
Peres, D.J. and Cancelliere, A., 2016. Environmental flow assessment based on different metrics of hydrological alteration. Water Resources Management, 30(15), pp.5799–5817.
Pettitt, A.N., 1979. A non-parametric approach to the change-point problem. Applied Statistics, 28(2), pp.126–135.
Richter, B.D., Baumgartner, J.V., Powell, J. and Braun, D.P., 1996. A method for assessing hydrologic alteration within ecosystems. Conservation Biology, 10(4), pp.1163–1174.
Sabater, S., Bregoli, F., Acuña, V., Barceló, D., Elosegi, A., Ginebreda, A. and Ferreira, V., 2018. Effects of human-driven water stress on river ecosystems: a meta-analysis. Scientific Reports, 8(1), 11462.
Sakaris, P.C., 2013. A review of the effects of hydrologic alteration on fisheries and biodiversity and the management and conservation of natural resources in regulated river systems. In: Current Perspectives in Contaminant Hydrology and Water Resources Sustainability, pp.273–297.
Sen, P.K., 1968. Estimates of the regression coefficient based on Kendall's tau. Journal of the American Statistical Association, 63(324), pp.1379–1389.
Shi, P., Liu, J., Yang, T., Xu, C.Y., Feng, J., Yong, B. and Li, S., 2019. New methods for the assessment of flow regime alteration under climate change and human disturbance. Water, 11(12), 2435.
Smakhtin, V.U., 2001. Low flow hydrology: A review. Journal of Hydrology, 240(3–4), pp.147–186.
Vogel, R.M., Sieber, J., Archfield, S.A., Smith, M.P., Apse, C.D. and Huber-Lee, A., 2007. Relations among storage, yield, and instream flow. Water Resources Research, 43, W05403.
Zuo, Q. and Liang, S., 2015. Effects of dams on river flow regime based on IHA/RVA. Proceedings of the International Association of Hydrological Sciences, 368, pp.275–280.

Book of Abstracts of the *16th International Symposium on Ecohydraulics*
Challenges and solutions in the time of global changes
August 16–20, 2026, Lausanne, Switzerland
ISSN: 2790-2420 | ISBN: 978-90-837233-9-6 | doi:[10.64697/iahr.proc.ise2026.abs]
© 2026 IAHR. CC BY-NC-ND 4.0

ECOLOGICAL PORTRAIT OF THE KIPAWA RIVER IN LIGHT OF A POTENTIAL HYDROELECTRIC DEVELOPMENT

William JACQUES, Etienne FOULON, André St-Hilaire, Eva C. ENDERS,

Institut national de la recherche scientifique, Centre Eau Terre Environnement, Canada
email: william.jacques@inrs.ca
email: etienne.foulon@inrs.ca
email: andre.st-hilaire@inrs.ca
email: eva.enders@inrs.ca

ABSTRACT

Small-scale hydropower can increase our capacity to produce renewable energy cost-effectively. Over the past four decades, to reduce carbon emissions, Canada has seen an increase in small-scale hydropower developments located in small rivers or streams. While small-scale hydropower is a promising option for producing sustainable and inexpensive energy in remote areas, environmental impacts on wildlife and aquatic ecosystems must be considered. Here, we modeled the potential impacts of a small-scale hydropower project on fish habitat in the Kipawa River located in western Quebec, Canada. Research activities included monitoring of water levels and environmental conditions, assessing fish habitat, and applying hydrological models to simulate flow variations and fish habitat availability before impacts and under various hydroelectric scenarios. The research was conducted in partnership with the *Société des établissements de plein air du Québec* (Sépaq). The data collected will inform management decisions on small-scale hydroelectric development on the Kipawa River in particular and provide a framework for impact assessments of small-scale hydroelectric developments in general.

Keywords: environmental flow, fish habitat assessment

1. Introduction

Fish are recognized as indicators of the ecological integrity of aquatic ecosystems (Bunn & Arthington, 2002; Poff & Zimmerman, 2010). Indeed, they are frequently used as biological indicators because of their sensitivity to habitat alterations and their key role in food webs. In a context of widespread and accelerating degradation of aquatic ecosystems worldwide (Dudgeon et al., 2019), monitoring fish communities is an essential tool for guiding conservation, sustainable management, and land use planning (Karr 1991; Schiemer 2000).

Here, we are presenting a research project on the Kipawa River situated in Quebec, Canada. Its objective was to model the impacts of flow modification on fish habitat in the portion of this river that flows through Opémican National Park. This nearly 16-km long river stretch was targeted because of its location in a national park and its importance to recreational users of the area, particularly water sports enthusiasts, fishermen, and outdoor enthusiasts (Cloutier et al., 2011). This area is also of particular interest because an envisioned hydroelectric project that proposes to divert part of the river's flow (OBVT, 2017). Current knowledge of the fish community in this section was limited and the potential impacts on fish habitat unknown (Cloutier et al., 2011), which reinforced the relevance of an in-depth ecological characterization. The research project was composed of several components including a description of the fish community, the available aquatic habitat, and hydrological modeling efforts for the Kipawa River.

2. Materials and Methods

The section of the Kipawa River of interest flows westward for 16 km between the Kipawa Reservoir and Lake Timiskaming. This section features a marked alternation between narrow, fast-flowing stretches and wider,

slower-flowing stretches. It also has a 90 m drop, including an impressive waterfall nearly 20 m high called *Grande Chute*. To effectively document the fish community in a diverse habitat, we caught fish using electro-fishing, seining, and angling. In addition, we collected environmental DNA (eDNA) samples. Habitat use by several fish species in the river was assessed through microhabitat-level data collection. To characterize aquatic habitats, substrate, river width, water depth, velocity, and type of aquatic vegetation were recorded. In addition, a cartographic interpretation was carried out using recent aerial and satellite images to document the spatial distribution of geomorphological features across the studied river sections. Field validation was carried out to confirm assignments. We modelled the flow using HEC-RAS and developed two-dimensional (2D) models of two rivers sections to capture complex hydraulic features, such as eddies and velocity gradients, that influence fish habitat use. Subsequently, we imported the simulated flow scenarios into CASiMiR to model habitat availability across a range of discharge conditions, allowing us to assess how proposed changes in flow would influence the spatial distribution of suitable fish habitat.

3. Results

3.1. Fish community

Sampling efforts in the summer of 2024 resulted in the capture of 1,400 fish and the detection of 22 fish species in the Kipawa River. Of these species, 20 were captured, while two were detected only through eDNA. We related these findings to previous studies (Tab. 1).

The comparison of fish sampling data collected over time highlights changes in the ichthyological community of the Kipawa River. The species detected between 1998 and 2024 are grouped according to their thermal guild (Tab. 1). These guilds are defined based on the preferred summer water temperatures of each species (Coker et al., 2001). Three main classes are distinguished: cold-water (<19 °C), cool-water (19–25 °C), and warm-water (>25 °C). Intermediate classes (cold-cool and cool-warm) are assigned to species whose preferred temperature range overlaps two main categories.

Tab. 1. Species categorised by thermal guild that were detected in given sampling year.

Thermal guild	Species	1998[1]	2011[2]	2022[2]	2024[3]
Cold	Mottled Sculpin	■			■
	Lake Cisco	■	■	■	■
	Ninespine Stickleback	■			■
	Lake Whitefish	■			■
	Lake Chub	■	■	■	■
	Longnose Sucker	■	■	■	■
Cold-Cool	Burbot	■	■	■	■
	Spottail Shiner	■			■
Cool	Rock Bass	■	■	■	■
	Iowa Darter	■			■
	Walleye	■	■	■	■
	Northern Pike	■	■	■	■
	White Sucker	■	■	■	■
	Longnose Dace	■			■
	Fallfish	■			■
	Yellow Perch	■	■	■	■
	Johnny Darter	■			■
Cool-Warm	Logperch	■	■	■	■
	Northern Redbelly Dace	■	■	■	■
Warm	Smallmouth Bass	■		■	■
	Brown Bullhead	■			■
	Pumpkinseed	■			■

The 1998 data come from a study conducted by Génivar[1] on behalf of Hydro-Québec. The 2011 and 2022 data are based on general observations provided by the MELCCFP[2], while the 2024 data were collected during the sampling campaign carried out for the present project[3].

3.2. Fish habitat assessment

The section upstream from the *Grande Chute* has a moderate average slope of 0.3% but includes highly variable slopes ranging from less than 0.1% to more than 2%. In contrast, the section between the top of the *Grande Chute* and the mouth of the river has a much steeper average slope of around 1.7% (Génivar, 1998). These significant variations in slope values contribute directly to the diversity of morphologies observed along the river. As a result, a multitude of flow facies follow one another along the studied section, enriching the ecological and geomorphological diversity of the area (Figure 1). Weighted usable area for three life-stages of Walleye in relation to discharge are presented in Figure 2.

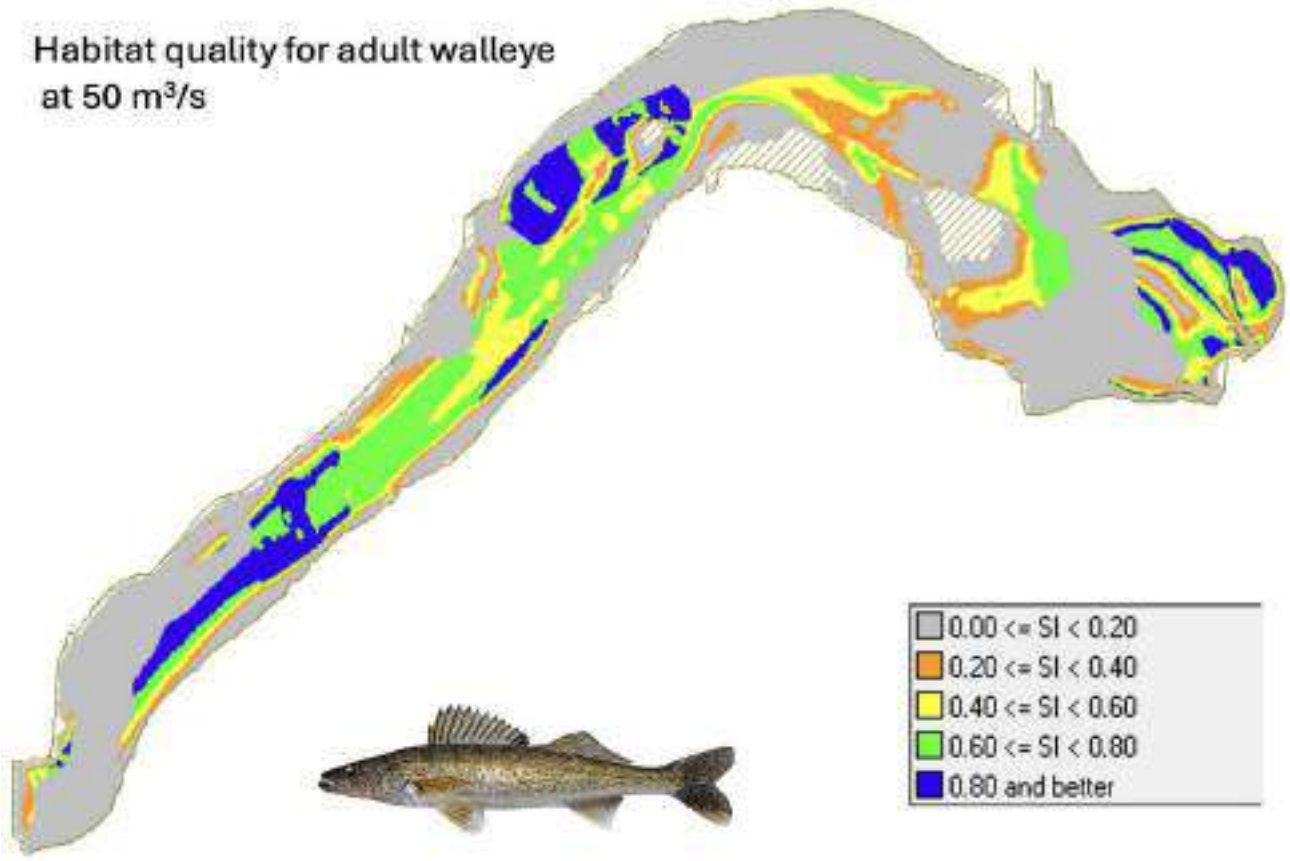

Fig. 1. Simulated habitat suitability for adult Walleye rearing habitat at the discharge of 50 m^3 s^{-1}.

4. Conclusion

When examining the thermal preferences of the species present in the river, we observed that in 1998, 45% of the species detected (5/11) belonged to cold or cold-temperate thermal guilds. By 2024, this proportion had fallen to 33% (7/21), suggesting a certain transformation of the community over time to warming climate. The available data suggest that this change occurred gradually. For example, Northern Pike were first observed in 2011, while Smallmouth Bass were not detected until 2022. Along with the appearance of these thermophilic species, the apparent disappearance of Lake Whitefish, a species strongly associated with cold waters (Jacobson et al., 2010), from this portion of the river reinforces the idea of a transition to a community more adapted to warmer waters.

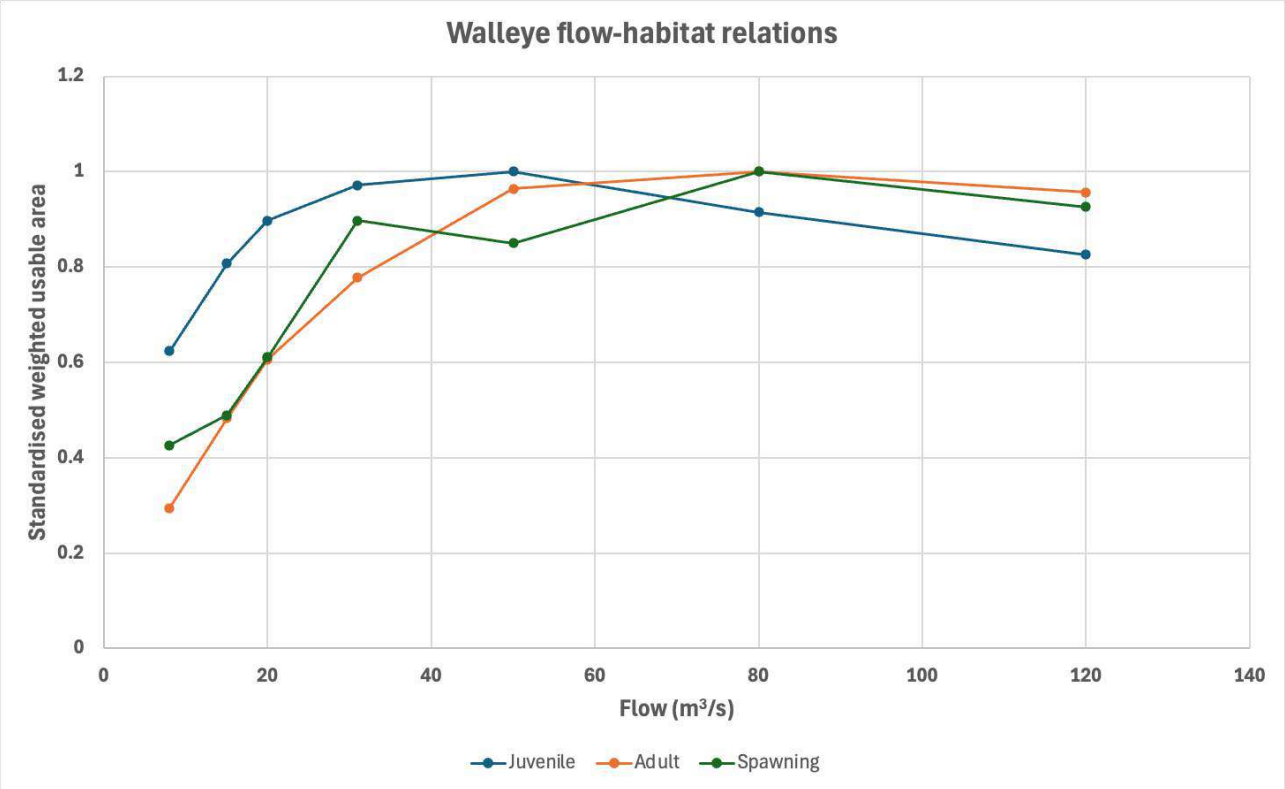

Fig. 2. Relationships between standardized weighted usable area and discharge for three life-stages, juvenile rearing habitat in blue, adult rearing habitat in red, and spawning habitat in green, of Walleye.

Acknowledgements

The authors would like to thank the Opémican National Park team for their support during the field campaigns and to several collaborators for their valuable contributions in the field: Habiba Ferchichi, Rafael Forteza, Jules Bartial, Aglaé Lambert, Joël Tremblay, Jérémie Montlevier, Lily Veyres, and Nicolas Vachon. Special thanks go to Valérie Langlois' lab for their expertise and support with the eDNA analysis. Finally, the authors would like to thank Mitacs and the Sépaq for their financial support.

References

Bunn, S. E. et Arthington, A. H. (2002). Basic principles and ecological consequences of altered flow regimes for aquatic biodiversity. Environmental Management, 30, 492507.

Centre de données sur le patrimoine naturel du Québec (CDPNQ). (2024). Extractions du système de données pour des occurrences fauniques sensibles à la diffusion pour le projet d'établissement d'un portrait écologique de la rivière Kipawa. Ministère de l'Environnement, de la Lutte contre les changements climatiques, de la Faune et des Parcs (MELCCFP), Québec.

Coker, G. A., Portt, C. B., & Minns, C. K. (2001). Morphological and ecological characteristics of Canadian freshwater fishes . Canadian Manuscript Report of Fisheries and Aquatic Sciences No. 2554, iv + 89 p.

Cloutier, M., J. Boisclair, N. Dignard, R. Pomerleau, I. Tessier et A. Thibault. (2011). État des connaissances : Projet de parc national d'Opémican. Consulté 27 janvier 2024,

Dudgeon, D. (2019). Multiple threats imperil freshwater biodiversity in the Anthropocene. Current Biology, 29(19), R960-R967.

Génivar (1998). Projet de centrale Tabaret – Étude d'impact sur l'environnement. Tome 1 : Description des éléments d'inventaire. Rapport préparé pour Hydro-Québec.

Jacobson, P. C., Stefan, H. G., & Pereira, D. L. (2010). Coldwater fish oxythermal habitat in Minnesota lakes: influence of total phosphorus, July air temperature, and relative depth. Canadian Journal of Fisheries and Aquatic Sciences, 67(12), 2002 -2013.

Karr, J.R., 1991. Biological integrity: A long-neglected aspect of water resource management. Ecological Applications 1, 66- 84.

Organisme de bassin versant du Témiscamingue (OBVT). (2017). Évaluation préliminaire des impacts environnementaux et sociaux – Projet hydroélectrique Onimiki Rapport Final Version révisée août 2018, 87 pages.

Poff, N. L., et Zimmerman, J. K. (2010). Ecological responses to altered flow regimes: a literature review to inform the science and management of environmental flows. Freshwater Biology, 55(1), 194-205.

Schiemer, F., 2000. Fish as indicators for the assessment of the ecological integrity of large rivers. Hydrobiologia 422/423, 271- 278.

Book of Abstracts of the *16th International Symposium on Ecohydraulics*
Challenges and solutions in the time of global changes
August 16–20, 2026, Lausanne, Switzerland
ISSN: 2790-2420 | ISBN: 978-90-837233-9-6 | doi:[10.64697/iahr.proc.ise2026.abs]
© 2026 IAHR. CC BY-NC-ND 4.0

IMAGING ORGANISM DRIFT CONTINUOUSLY AT 1-SECOND RESOLUTION: A 10 WEEK CASE STUDY

Joël R. WITTMANN[1], Levi GRAF[1], Vittorio FERRERO[1], Lea KUSTER[1], Anaïs WIGGER[1], Giulia ZAMBOTTO[1], Frédéric DE SCHAETZEN[2], Sandro GIACOMUZZI[1], Roman STOCKER[1], Luiz G. M. SILVA[1]

[1] ETH Zürich, Switzerland
joelw@ethz.ch
lumartins@ethz.ch

[2] Kraftwerke Oberhasli AG, Switzerland
frederic.deschaetzen@kwo.ch

ABSTRACT

Drift net studies are essential to understand the dispersal of early life-stages of fish and macroinvertebrates in rivers, but they are limited by a trade-off between temporal resolution and sampling effort. The Riverine Organism Drift Imager (RODI) overcomes this limitation by continuously recording drifting organisms, effectively decoupling the temporal resolution from the sampling effort. In this study, nine RODIs were deployed in a hydropeaking Swiss alpine River for 10 weeks to evaluate their technical reliability and demonstrate the detection of drifting organisms with a temporal resolution of one second. The RODIs recorded 77.6% of the deployment period. Sixteen classes of drifting objects were identified, including fish and insects, with a strong class imbalance. Ongoing work is refining and automating the classification process. Significantly more brown trout fry (*Salmo trutta*) drifted at night during a 72-hour case study, illustrating how high-resolution data obtained with RODI can improve our understanding of drift.

Keywords: fish larvae, macroinvertebrates, hydropeaking, artificial intelligence.

1. Introduction

There are major knowledge gaps in understanding the dispersal of the early life-stages of fish and macroinvertebrates in riverine ecosystems (Lechner et al., 2016; Naman et al., 2016). They mainly disperse by drift, a process which is predominantly studied using drift nets. However, sampling with drift nets comes with a trade-off between temporal resolution and sampling effort from net deployments, since they aggregate organisms over their deployment period in a downstream collection container (Schnack, 1974). The sampling resolution in drift studies typically varies from a few minutes to several hours, repeated at intervals of a few hours to several days (Braaten et al., 2012; Grimardias et al., 2012; Randall, 1982). Furthermore, post-processing the samples is a laborious task involving manual identification of collected organisms, which usually must be euthanized during preservation. The Riverine Organism Drift Imager (RODI) was developed to overcome the limitations of drift-net sampling and to enhance drift studies (de Schaetzen et al., 2023). With RODI, drifting organisms are guided through a flow-through imaging tube, where a camera records them before they return to the river. Subsequently, the recorded videos are analyzed for drifting organisms, and their time of drift is calculated, effectively decoupling the temporal resolution of the collected data from the sampling effort: High temporal resolution no longer requires collecting samples at high frequency. This study i) evaluates the reliability of RODI for continuous recording of drifting organisms, ii) demonstrates the detection of drifting organisms in the recorded video data, and iii) illustrates how the obtained data can be analyzed in a case study comparing day and night drift of brown trout fry (*Salmo trutta*).

2. Methodology

2.1. RODI setup and data collection

Nine RODIs were deployed continuously from April 25th to July 8th, 2025, across four sampling sites in the Poschiavino river, Valposchiavo, Switzerland. Two sites were located in the residual flow reach upstream of

the Hydropower Plant Robbia (HPR), separated by 56 m along the river (namely RFUP and RFDO, see **Fig. 1**). Another two sites, HYUP and HYDO, were located downstream of HPR, separated by ca. 50 m, in the hydropeaking reach. Due to safety concerns for personnel accessing HYUP during peak flow, the site was moved 42 m downstream of HYDO and renamed to HYDODO on May 16th. The residual flow reach of the Poschiavino river has an annual average discharge of 1.35 m^3/s, into which up to 7.3 m^3/s are released intermittently by the HPR.

At RFUP, RFDO, HYUP, and HYDODO, two RODIs were deployed side by side on the left shore. Each RODI was secured to the riverbed and attached to a drift net with a 50 cm by 100 cm opening and 1 mm by 2 mm mesh size (**Fig. 2**). The upstream ends of adjacent drift nets were laterally connected, jointly sampling a two-meter segment of the river cross-section. At HYDO, the same setup was deployed but with three RODIs sampling a three-meter cross-section to account for the locally increased river width. Each RODI was connected to a land station, which housed the necessary electrical equipment. A computer stored the video recordings on an external 4TB hard drive, allowing uninterrupted data collection until the drive filled up (up to 9.8 days). Once full, the hard drives were replaced, which took 3.4 minutes on average.

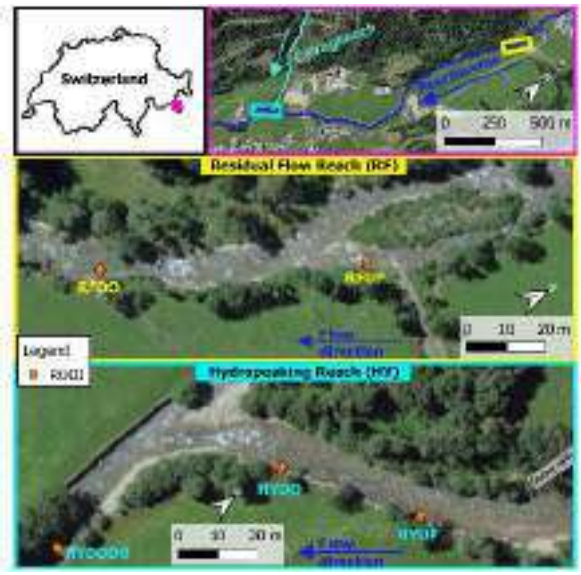

Fig. 1. The sampling sites upstream (HY) and downstream (RF) of the hydropower plant Robbia in southeastern Switzerland. At each sampling site two or three RODIs were deployed. Background by Bundesamt für Landestopografie swisstopo.

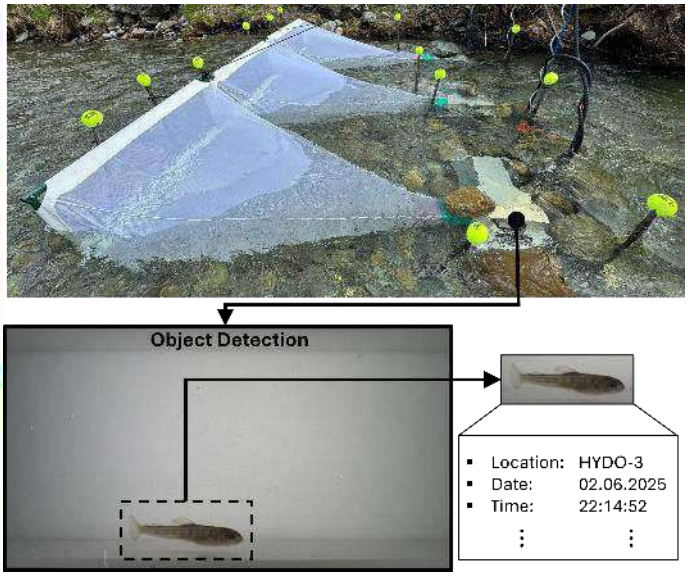

Fig. 2. Drifting organisms are guided into RODI by a rectangular drift net where they are recorded before returning to the river. A custom-made script extracts drifting objects and stores a cropped Region of Interest (RoI) together with associated metadata.

The drift nets filtered drifting organisms into RODI's 50 mm by 50 mm imaging tube. To reduce the effects of net clogging on the volume of filtered water, the drift nets were cleaned every six hours by detaching their downstream end from RODI, flushing collected debris through, and reattaching the net. Discharges through the upstream net opening were documented before and after cleaning by measuring water depth and flow velocity in the net opening. During cleaning, the nets were checked for damage and either repaired on site or replaced with an undamaged net. To avoid excessive damage to nets, they were removed from the river if the public weather forecast predicted intense rainfall. The RODIs remained operational in the river without the nets, thus sampling a lower water volume. The Relative Operational Time (ROT) of RODI was calculated as the ratio between the cumulative recorded video length and the cumulative intended deployment duration.

2.2. Post-processing of RODI recordings

Drifting objects were extracted from the recorded videos using a custom-made Python script that followed the approach from de Schaetzen et al. (2023). Detection of drifting objects uses a combination of background subtraction and thresholding. Each detected object is saved as a Region of Interest (RoI), a cropped JPG image of the corresponding video frame showing the detected object (**Fig. 2**). Corresponding metadata for each RoI was stored in a CSV file, including timestamp, location, and object area, among others. A data sample of six hours and 22 minutes was assessed to demonstrate detection of drifting organisms in the video data (*detection sample*, site RFUP, May 13th, 17:33 – 23:55). This sample was selected because of a high probability to contain fry, since it was taken during the second half of the fry emergence window in the study area. The 79,852 RoIs extracted from the *detection sample* were manually reviewed and the detected objects classified. A larger *case study sample* was extracted from the videos recorded at RFUP and HYDO over 72 hours between May 26th and 28th. The obtained 843,574 RoIs were filtered by RoI size and manually checked for fry.

3. Results & Discussion

3.1. Reliability of RODI

Across all study sites, a cumulative 10,828 hours of videos were recorded by RODIs (**Fig. 3**), corresponding to an overall ROT of 77.6%. RODIs became operational between April 27th and April 30th (except HYDODO on May 16th). Recording was stopped on July 4th, except for HYUP (May 16th) and the second RODI at HYDODO (June 16th) due to safety concerns at high flows. Interruption of recording mainly happened due to memory overflow at locations with larger numbers of drifting objects (RFDO-2, HYDO-3), which was improved with adjustments to the software. Hardware failure was mainly caused by damaged underwater data cables, which was addressed by changing the cable type. One RODI flooded throughout the deployment (RFDO-2, May 26th) likely due to water moving through a damaged underwater data cable.

The discharge sampled per net, thus per RODI, was on average 142 l/s before cleaning (median 126 l/s, maximum 516 l/s) and 206 l/s after cleaning (median 196 l/s, maximum 532 l/s). Drift nets were continuously deployed and cleaned except during the three floods of May 6th – 11th, May 21st – 24th, and June 1st – 12th. Redeployment of the nets after a flood was site-dependent due to varying flow conditions. Shorter interruptions were due to repairs of severely damaged nets before redeployment. No nets were deployed at HYUP.

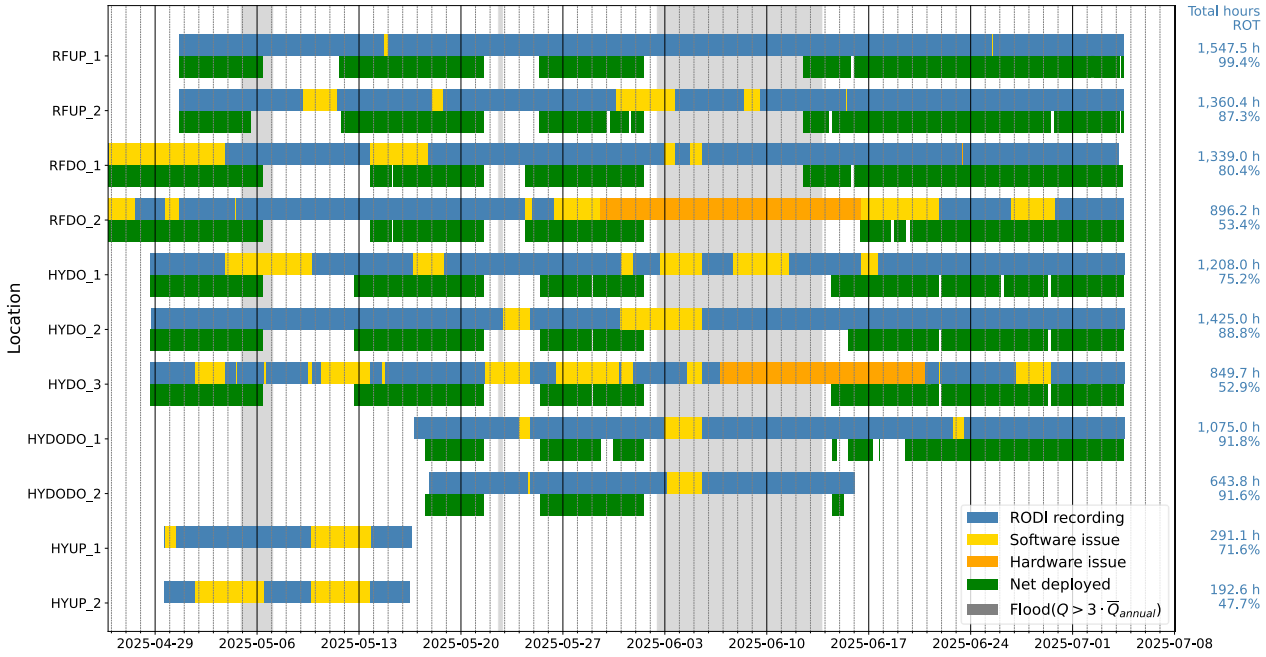

Fig. 3. A total of 10,828 hours of drift was recorded across all RODIs (blue). Gaps in recording were caused from issues with software (yellow) or hardware (orange) resulting in an overall relative operational time of 77.6% (ROT, ratio between the cumulative recorded video length and the cumulative intended deployment duration). Issues with hardware were rare but resulted in longer interruptions. Drift nets were connected to the RODIs for most of the time (green), except at HYUP and during floods (grey background). A flood is defined for discharges larger than three times the annual average. Each RODI is identified by its sampling site and counting from the shore into the river.

The RODI system proved resilient for continuous long-term deployment, with interruptions mainly caused by software issues and damaged data cables, for which solutions and improvements were developed during this study. Thus, RODI can be deployed continuously for extended periods exceeding previous drift studies in both temporal resolution and extent (e.g., Braaten et al., 2012: 8 nets, ca. 31 hours each, 5min resolution). In combination with drift nets a single RODI can sample several hundred liters per second for drifting organisms.

3.2. Demonstration of ROI extraction from video data

A total of 16 preliminary classes of RoIs were identified in the *detection sample* **(Fig. 4**), which will be refined in the future. Classes were defined based on the identified object (*fish*, *insects*, *leaves dry*, *leaves green*, *bubbles*, *worm-shaped*), the shape of unidentified objects (*rounded*, *variable*, *elongated*), or the general state of the RoI if no single full object could be selected (*empty*, *turbid*, *dark*, *reflection*, *side visual*, *partial object*, *overlapping objects*). The classes were highly imbalanced, ranging from 10 RoIs showing fish to 27,766 RoIs with objects of variable shape. The number and definition of classes will likely change as more RoIs from this and future RODI deployments are classified. For each detected object, the time of passage through RODI was derived successfully and rounded to the closest second. Manual inspection of the 79,852 RoIs from the

detection sample demonstrated the ability for automated extraction of drifting objects and their passage time from the RODI video recordings.

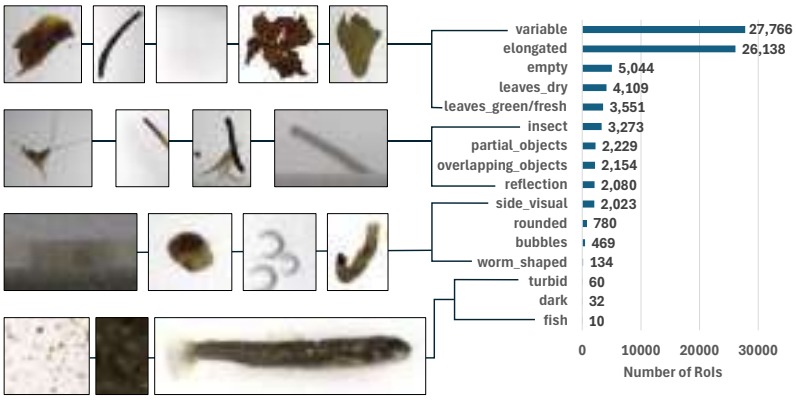

Fig. 4. Distribution and examples of the RoIs extracted from 6 hours 22 minutes of RODI recording at RFUP, on May 13th (17:33 – 23:55). The 79,852 RoIs were manually classified into 16 classes with 10 to 27,766 RoIs each.

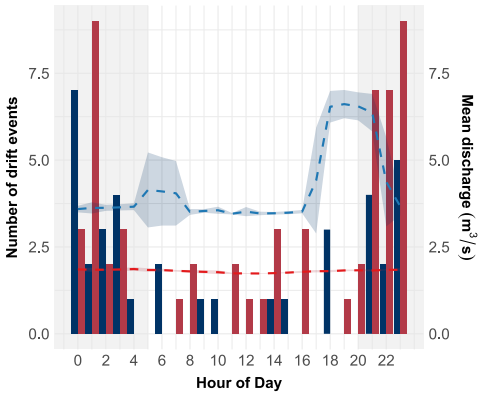

Fig. 5. Number of drifting fry detected at HYDO (blue) and RFUP (red) for each hour in the circadian cycle on May 26th – 28th. Grey areas are considered night (8pm – 5am). At HYDO the discharge fluctuated while it was more constant at RFDO (dashed lines).

3.3. Case Study: Fry Drift at Day vs. Night

In the 843,574 RoIs obtained from the *case study sample*, 433 RoIs contained brown trout fry, corresponding to 93 fry drifting through a RODI (4.66 RoIs per drift event on average). The distribution of fry drift throughout the day is shown in **Fig. 5**, using the timestamp of the extracted RoIs. Drift of fry is significantly higher at night (8pm – 5am) for the analyzed 72-hour period (binomial test, $p = 0.003$ at HYDO, $p = 0.002$ at RFUP), which is in accordance with Lechner et al. (2016). The example of day and night drift of brown trout fry at two sites illustrates how the detailed data on riverine drift obtained with RODI can be analyzed.

4. Conclusion

RODI overcomes the limitations of drift-net sampling by providing high temporal resolution over several weeks of deployment. The relative operational time of 77.6% provides comprehensive drift data so far unavailable during extended deployments and improvements identified in this study will increase the reliability further. Drifting objects were extracted automatically from the recorded data and identified manually. Ongoing work will improve the class definition and automate object identification by training a machine learning classifier. Automating the post-processing of RODI data enables us to considerably extend the temporal scope and resolution of drift monitoring. The potential of drift data collected with RODI to investigate ecological questions was demonstrated by identifying significant differences of brown trout fry drift at day and at night. The full dataset will be investigated to identify impacts on hydropeaking on brown trout fry dispersal.

Acknowledgements

The authors thank the Swiss National Science Foundation for funding this study (grant IC00I0-232304), the Amt für Jagd und Fischerei Graubünden, Repower AG, and AquaPlus AG for their valuable cooperation, and Michael Arnold and Martin Huber for their technical support. A special thank you to the numerous helpers in the field without whom the field campaign would not have been possible.

References

Braaten, P. J., Fuller, D. B., Lott, R. D., Ruggles, M. P., Brandt, T. F., Legare, R. G., & Holm, R. J. (2012). An experimental test and models of drift and dispersal processes of pallid sturgeon (Scaphirhynchus albus) free embryos in the Missouri River. *Environmental Biology of Fishes*, *93*(3), 377–392. https://doi.org/10.1007/s10641-011-9925-9

de Schaetzen, F., Impiö, M., Wagner, B., Nienaltowski, P., Arnold, M., Huber, M., Meyer, M., Raitoharju, J., Silva, L. G. M., & Stocker, R. (2023). The Riverine Organism Drift Imager: A new technology to study organism drift in rivers and streams. *Methods in Ecology and Evolution*. https://doi.org/10.1111/2041-210X.14130

Grimardias, D., Faivre, L., & Cattaneo, F. (2012). Postemergence downstream movement of European grayling (Thymallus thymallus L.) alevins and the effect of flow. *Ecology of Freshwater Fish*, *21*(4), 495–498. https://doi.org/10.1111/j.1600-0633.2012.00572.x

Lechner, A., Keckeis, H., & Humphries, P. (2016). Patterns and processes in the drift of early developmental stages of fish in rivers: A review. *Reviews in Fish Biology and Fisheries*, *26*(3), 471–489. https://doi.org/10.1007/s11160-016-9437-y

Naman, S. M., Rosenfeld, J. S., & Richardson, J. S. (2016). Causes and consequences of invertebrate drift in running waters: From individuals to populations and trophic fluxes. *Canadian Journal of Fisheries and Aquatic Sciences*, *73*(8), 1292–1305. https://doi.org/10.1139/cjfas-2015-0363

Randall, R. G. (1982). Emergence, population densities, and growth of salmon and trout fry in two New Brunswick streams. *Canadian Journal of Zoology*, *60*(10), 2239–2244. https://doi.org/10.1139/z82-288

Schnack, D. (1974). On the Reliability of Methods for Quantitative Surveys of Fish Larvae. In J. H. S. Blaxter (Ed.), *The Early Life History of Fish* (pp. 201–212). Springer. https://doi.org/10.1007/978-3-642-65852-5_16

Book of Abstracts of the *16th International Symposium on Ecohydraulics*
Challenges and solutions in the time of global changes
August 16–20, 2026, Lausanne, Switzerland
ISSN: 2790-2420 | ISBN: 978-90-837233-9-6 | doi:[10.64697/iahr.proc.ise2026.abs]
© 2026 IAHR. CC BY-NC-ND 4.0

DISCHARGE MODIFICATIONS BY FLOOD DAMPENING FROM HYDROPOWER RESERVOIRS: SURNA CASE STUDY

Sahra SABIL[1], Keilly BULLE ARIAS[2], Tor Haakon BAKKEN[3], Knut ALFREDSEN[4]

[1,3,4,] Norwegian University of Science and Technology, Norway
[2] École Nationale du Génie de l'Eau et de l'Environnement de Strasbourg, France

email: sahra.n.sabil@ntnu.no
email: keilly.bullearias@tractebel.engie.com
email: tor.h.bakken@ntnu.no
email: knut.alfredsen@ntnu.no

ABSTRACT

The flood peak dampening due to hydropower reservoirs in the Surna river basin in Norway was studied by simulating unregulated floods with an HBV model and routing them through a Level-Pool Reservoir Routing python script. Four scenarios with future runoff data and spatial and temporal runoff variations were simulated to investigate limiting factors of flood dampening and environmental impacts by looking at flood-reoccurrence intervals. The study found that the reservoirs had a peak reduction of 50-96% under median reservoir filling levels. The minimum pre-release period to prevent spilling amounts 5.3-35.8 days. Limiting factors for flood peak reduction are reservoir storage capacities, transfer intake capacities within the basin, regulation rate of the basin, and hydrograph shapes. To target an outflow corresponding to a 10-year flood (Q10) during the flood event, additional discharge regulation is necessary, involving either increasing the outflow by up to 210 m^3/s or reducing it by up to 51 m^3/s.

Keywords: 10-year floods; climate change; hydropower reservoirs; flood dampening;

1. Introduction

Floods constitute one of the most damaging natural hazards in Norway and are expected to intensify under climate change (Dyrrdal et al., 2025). Hydropower reservoirs play a critical role in Norwegian water management by regulating flows and reducing downstream flood peaks. Reservoir regulation can substantially reduce damaging flood events through controlled storage and release of water during high-inflow periods, although such management requires careful balancing between flood mitigation and hydropower production under uncertain inflow forecasts (Killingtveit et al., 2021). This study investigates the flood dampening effect of multiple reservoirs with brooklet intakes in a cold-climate, hydropower-regulated basin characterized by a nival hydrological regime. Using hydrological and reservoir operation models, it examines how initial filling levels, pre-releases, tunnel transfer capacities, hydrograph shapes, regulation rate of the catchment and pre-release capacities influence the flood dampening capacity in the future. The work provides new insights into flood control under future climate conditions for complex hydropower systems and investigates environmental impacts from flood dampening in a simplified way.

2. Study site and data

The Surna catchment is the study site, located in Central Norway and spans an area of 1203 km^2. River Surna origins in the Trollheim mountains and is 45 km long. It flows to the Surnadalsfjorden (62.9°N, 8.7°E). Over 3000 people live along the river. An overview of the study site is given by Figure 1.

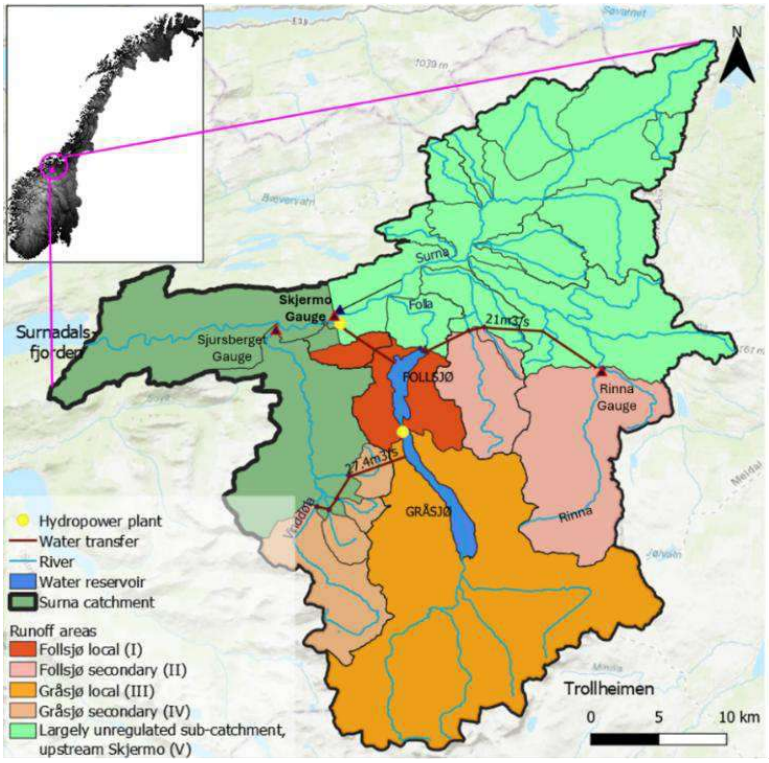

Figure 1. Overview of the Surna catchment, including the local and secondary runoff areas, reservoirs, streamflow gauges, and transfers.

Hydropower operations in the basin are supported by two regulated reservoirs, Follsjø and Gråsjø. The production flow amounts to 38m^3/s in the lowermost power plant Trollheim. The study focuses on flood dampening effect at Skjermo gauge, where all important regulation effects are captured. The simulated area's elevation ranges from 278 to 1669 m.a.s.l., with an average discharge of 57 m^3/s at the river mouth.

Data for the study were compiled from several national sources. Catchment characteristics were obtained from NEVINA (NVE, 2025a). Spatially interpolated precipitation and temperature data for 1971-2000 were sourced from the Norwegian Meteorological Institute's *SeNorge2* dataset (Lussana et al., 2018). Hydrological data and GIS shapefiles were collected from NVE databases (NVE, 2025b; NVE, 2025c; NVE, 2025d). Information on the hydropower system was based on data from NVE Atlas (NVE, 2025b) and the system operator Statkraft. The temperature and precipitation data for the investigations of the future scenarios and ecological impact of drawdown are taken from the EURO-CORDEX and bias-corrected.

3. Methodology

To assess flood dampening in the Surna River basin, both unregulated and regulated conditions were simulated using HBV (Bergström, 1992) and Level Pool Routing (Zoppou, 1999). Flood events in the past and in the future were selected for this study. Different filling conditions were elaborated during the chosen scenarios. For reservoir routing, hourly hydrographs are derived by scaling the daily values from HBV simulations using two observed hydrographs from an unregulated river within the catchment.

Flood dampening effect was calculated by:

$$Reduction\ of\ Q_{max} = \frac{Qmax,uc - Q,max,rc}{Qmax,uc} * 100 \quad (1)$$

Where Q_{max} is the maximum discharge and the subscripts *uc* and *rc* refer to the unregulated and regulated condition, respectively. To calculate the amount of time needed to empty the reservoir to avoid spilling during the flood event, following equations were used:

$$S_{available} = S_{full,G}\text{-}S_{used,G} + S_{full,F}\text{-}S_{used,F} \quad (2)$$

$$t_{Pre\text{-}release} = \max(0, (V_{inn}\text{-}S_{available}))/Q\ /86400 \quad (3)$$

Where V_{inn} is the water volume flowing into the reservoir [m^3], $S_{available}$ is the available storage in the reservoir [m^3], S_{full} is the full storage capacity [m^3], S_{used} is the used storage capacity [m^3], the indices $_G$ and $_F$ represent Gråsjø and Follsjø, $t_{Pre\text{-}release}$ is the emptying time [d], and Q is the pre-release discharge [m^3/s].

Flood dampening can prevent damage to downstream habitat, but the absence of floods has impacts on substrate composition. This will eliminate habitat maintenance and potentially lead to greater embedding and less shelter. Therefore, additional discharge adjustments required to achieve a Q10 flood during the flood event were calculated. This was done by subtracting the unregulated runoff at Skjermo gauge and any reservoir spill contribution from the target Q10 discharge of 342 m^3/s.

4. Results

HBV calibration (1974–1979) and validation (1979–1984) were performed against observations at Sjursberget gauge and then applied to the full basin via parameter transfer. In general, the R^2 value for the simulated flow at Sjursberget was 0.64 for the calibration and 0.65 for the validation periods. Different individual flood events show R^2 values of 0.85 to 0.97.

The reservoir did not spill during the median filling condition, spilled in 2 out of 4 scenarios during the maximum filling condition and spilled for all four scenarios when the reservoirs were full. The flood peak reduction varies from 5% to 96%. The results are presented in Table 2.

Table 1. Results for the 4 future flood event, prerelease-time are in days, discharges in m^3/s, and reoccurrence intervals are taken from Drageset (2004).

Scenarios	Hydro-graph	Reservoir filling	Undampened flood discharge incl. peak factor& interpolated recurrence interval of flow		Dampened flood discharge & interpolated recurrence interval of flow		Reduction of Q_{max} [%]	Spilling event	Pre-release time via production flow to avoid spilling	Discharge to aim for Q10 during flood event
1	Delayed peak-scaled	median	433	Q37	132	<Q5	69	No	-	210
		max			332	Q9	23	Yes	7.5	10
		full			337	Q9	22	Yes	13.3	5
	Rapid peak-scaled	median	433	Q37	132	<Q5	69	No	-	210
		max			283	<Q5	35	Yes	7.6	59
		full			370	Q15	14	Yes	13.4	-28
2	Delayed peak-scaled	median	191	<Q5	9	<Q5	96	No	-	-
		max			9	<Q5	96	No	-	-
		full			178	<Q5	7	Yes	35.8	-
	Rapid peak-scaled	median	191	<Q5	9	<Q5	96	No	-	-
		max			9	<Q5	96	No	-	-
		full			181	<Q5	5	Yes	35.8	-
3	Delayed peak-scaled	median	460	Q55	145	<Q5	68	No	-	197
		max			324	Q8	30	Yes	5.3	18
		full			356	Q12	23	Yes	13.5	-14
	Rapid peak-scaled	median	460	Q55	145	<Q5	68	No	-	197
		max			253	<Q5	45	Yes	5.5	89
		full			394	Q21	14	Yes	13.6	-52
4	Delayed peak-scaled	median	439	Q40	219	<Q5	50	No	-	123
		max			219	<Q5	50	No	-	123
		full			373	Q16	15	Yes	11.4	-31
	Rapid peak-scaled	median	439	Q40	219	<Q5	50	No	-	123
		max			219	<Q5	50	No	-	123
		full			393	Q21	10	Yes	11.5	-51

5. Discussion and Conclusion

Uncertainties remain throughout the analysis: (1) SeNorge climate data may underestimate peak runoff due to spatial and temporal smoothing; (2) future climate projections remain uncertain despite bias correction and may not capture more severe future events; (3) HBV calibration is reasonably good but still reveals uncertainty in the model's capability to represent future floods. In addition, it relies on parameter transfer from a neighboring catchment, introducing especially uncertainty in snow and runoff simulation; (4) scaling daily to hourly hydrographs may both under- and overestimate flood peaks; and (5) the simplified reservoir routing excludes hydropower production and dynamic operations, although different reservoir filling levels were evaluated to address this limitation.

Simulations showed that the flood peaks at Skjermo can be notably reduced due to the hydropower system. The median filling initial reservoir scenarios never filled completely during floods, while the reduction of discharge peaks were varying between 50-96%, meaning the available storage is not the only limiting factor. Variations in flood reduction were additionally due to transfer capacities, differences in how much of each flood originated from regulated vs. unregulated sub catchments, and hydrograph shapes.

Pre-release times range between 11.4-35.8 days in order to completely avoid spilling and are consistent with the range reported for forecast-informed reservoir operations, where pre-release decisions commonly rely on forecasts from several hours up to several weeks (Lu and Merwade, 2025; Nohara, 2022; Timberlake et al., 2025). There are no steerable gates, so the planned release needs to be conducted only through hydropower production.

However, from an environmentally perspective, the flood dampening through the reservoirs might look too effective. To keep a 10-year flood of 342m^3/s at Skjermo gauge would need an increased outflow during flood event up to 210m^3/s. Maintaining pre-release flows near Q_{10} would have ecological benefits for the Surna River, which is an important habitat for Atlantic salmon (*Salmo salar*) and sea trout (*Salmo trutta*). Discharges of this magnitude support channel morphology and habitat conditions (Rood et al., 2005; Trush et al., 2000). Consequently, it is important to have a regulatable outflow during the flood event. This is within the current hydropower system not possible and would need major infrastructure upgrade.

Although the model included uncertainties and simplifications (e.g., no energy production analysis) these did not compromise the comparison between regulated and unregulated flows. Future research should include uncertainty handling, habitat modelling under different flow conditions, scenarios for increased release capacities and analyzing flood duration in addition to peak flow.

References

Bergström, S. (1992). THE HBV MODEL - its structure and applications.
Dyrrdal, A.V., Bakke, S.J., Hanssen-Bauer, I., Mayer, S., Nilsen, I.B., Nilsen, J.E.Ø., Paasche, Ø., Saloranta, T., Årthun, M. [redaktører] (2025) Klima i Norge – kunnskapsgrunnlag for klimatilpasning oppdatert i 2025, NCCS-rapport 1/2025, doi:10.60839/4rgq-nn84
Drageset, T.-A. (2002). Flomberegning for Orkla ved Meldal og Orkanger. www.nve.no
Eikenaes, O., Njøs, A., Østdahl, T., & Taugbøl, T. (2000). Flommen kommer ... Sluttrapport fra HYDRA-et forskningsprogram om flom Redaktører.
Killingtveit, Å., Alfredsen, K., Rinde, T., Østhus, N., & Røhr, P. C. (2021). Flood-forecasting and flood management in Skienselva river system in Norway. *The International Journal on Hydropower & Dams*, *28*(2), 67–73.
Lu, M., & Merwade, V. (2025). Transitioning to Multi-Purpose Reservoirs: Advancing Performance With Forecast-Based Pre-Release Operations. *JAWRA Journal of the American Water Resources Association, 61*(2), e70005.
Lussana, C., Saloranta, T., Skaugen, T., Magnusson, J., Tveito, O. E., & Andersen, J. (2018). seNorge2 daily precipitation, an observational gridded dataset over Norway from 1957 to the present day. *Earth System Science Data*, *10*(1), 235–249. https://doi.org/10.5194/essd-10-235-2018
Nohara, D. (2022). Optimized reservoir prior release operation for flood control considering operational weekly ensemble hydrological forecast. In *Advances in Hydroinformatics: Models for Complex and Global Water Issues—Practices and Expectations* (pp. 369–382). Singapore: Springer Nature Singapore.
NVE. (2025a). NEVINA. Nedbørfelt og vannføringsindeksanalyse. Http://Nevina.Nve.No.
NVE. (2025b). *NVE Atlas. Version 3.0*. Http://Atlas.Nve.No.
NVE. (2025c). *NVE Reservoir filling statistics*. Https://Www.Nve.No/Energi/Analyser-Og-Statistikk/Magasinstatistikk/.
NVE. (2025d, March). *NVE Sildre*. Https://Sildre.Nve.No/.
Rood, S.B., Samuelson, G.M., Braatne, J.H., Gourley, C.R., Hughes, F.M., Mahoney, J.M. (2005). Managing river flows to restore floodplain forests. *Frontiers in Ecology and the Environment, 3*(4), 193–201.
Timberlake, T. W., Ramirez-Avila, J., Grigg, N. S., & Curtis, D. C. (2025). Forecast-Informed Prerelease Reservoir Operations for Flood Risk Management. *Journal of Water Resources Planning and Management, 151*(9), 03125002.
Trush, W. J., McBain, S. M., Leopold, L. B. (2000). Attributes of an alluvial river and their relation to water policy and management. *Proceedings of the National Academy of Sciences, 97*(22), 11858–11863.
Zoppou, C. (1999). Reverse routing of flood hydrographs using level pool routing. Journal of hydrologic engineering, 4(2), 184-18.

Book of Abstracts of the *16th International Symposium on Ecohydraulics*
Challenges and solutions in the time of global changes
August 16–20, 2026, Lausanne, Switzerland
ISSN: 2790-2420 | ISBN: 978-90-837233-9-6 | doi:[10.64697/iahr.proc.ise2026.abs]
© 2026 IAHR. CC BY-NC-ND 4.0

ASSESSING HYDROPEAKING IMPLICATIONS ON BROWN TROUT (SALMO TRUTTA) POPULATIONS ON THE NORTH BRANCH OF THE POTOMAC RIVER

Benjamin DYE[1], Jonathan CZUBA[1]

[1] Virginia Tech, United States of America
benjamindye@vt.edu
jczuba@vt.edu

ABSTRACT

Dam releases can result in hydropeaking events, most noticeable during the low-flow summer months of July and August. These events can disrupt low flow periods that are critical to the life cycles of benthic species (Shacheri et al., 2025). The various life stages of brown trout (*Salmo trutta)* are impacted by hydropeaking events. They require low flow periods to spawn and nest. If dam releases are too rapid, this could result in negative impacts on brown trout populations.

Negative impacts primarily affect reproductive phases in the trout life cycle. Eggs are deposited in a redd that is buried in a gravel stream bed for months until they hatch. While they are buried, rapid flow increases can scour the redd and wash away the eggs. Additionally, rapid rises and decreases in the flow can injure trout in the fry or juvenile stage (Maryland Department of Natural Resources). Controlling dam releases to reduce hydropeaking events reduces the risk young stages of trout face in river systems.

The Sustainable Rivers Program is a partnership between the U.S. Army Corps of Engineers (USACE) and The Nature Conservancy (TNC) to improve downstream river ecosystem health by adjusting dam operations (Bahabib et al., 2025). The USACE and TNC are interested in determining if the controlled dam releases at Jennings Randolph Dam are too rapid and are negatively affecting recruitment of brown trout in the North Branch Potomac River on the border of Maryland and West Virginia, USA. It is hypothesized that flow changes due to the release of the dam are much more rapid than natural flow changes. The extension of the hypothesis is that the unnatural increases in flow rate influence the biota of the North Branch Potomac River. The purpose of this study is to compare the flow recorded at the USGS gage downstream of Jennings Randolph Dam with other gages on the North Branch of the Potomac River with natural flows will give insight into whether Jennings Randolph Dam causes hydropeaking events that could influence trout populations.

Releases from this dam can be identified by comparing data from U.S. Geological Survey (USGS) 15-minute streamflow data from several nearby gages. Gage 01595500 Kitzmiller, is upstream of Jennings Randolph Dam and is not affected by hydropeaking, and gage 01595800 Barnum, is downstream of the dam; both on the North Branch Potomac River. Additionally, gage 01596500 Barton, is upstream of Savage Dam on the Savage River, a tributary to the North Branch Potomac River. Barton is also not affected by hydropeaking.

The 15-minute instantaneous streamflow data were analyzed for all three gages. RStudio was utilized to download the data from the USGS servers, and organize, analyze, and plot the data. First, the change in flow between subsequent 15-minute intervals was calculated, and we refer to this as the change in flow or flow difference. This indicates how much the flow changed every 15 minutes. The change in flow was plotted with the instantenous flow as a scatter plot (Fig. 1). The data was filtered for periods where a greater than 10%

change in flow occurred in a 15-minute time interval to isolate the likely signature of an hydropeaking event (rapid increases in flow).

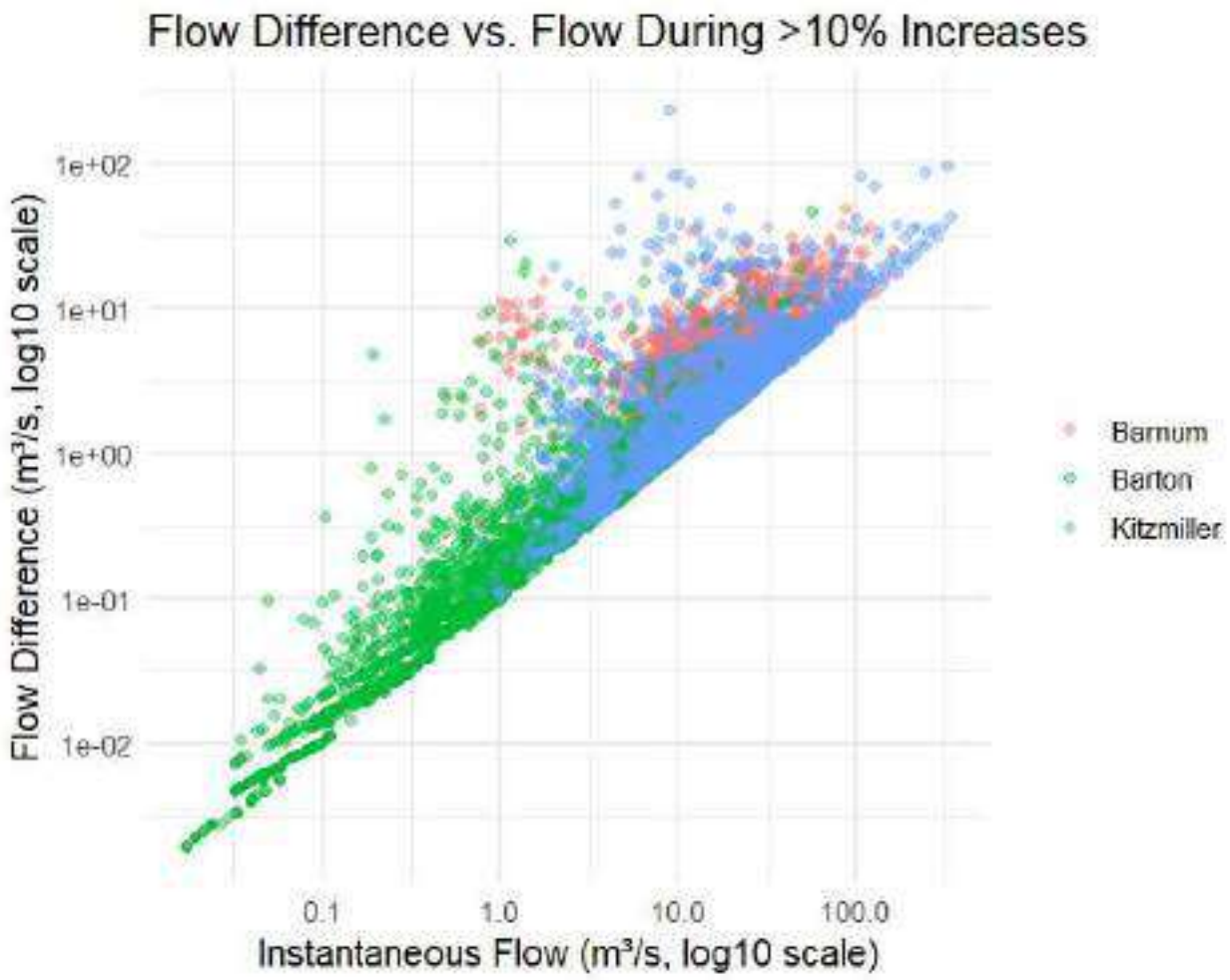

Fig 1. Scatter plot of instantaneous flow vs flow difference for values ≥10% increases at USGS gages at Kitzmiller, Barton, and Barnum

Next, the flow difference was normalized by the instantaneous flow, so that these flow changes could be quantified as an increase relative to the current flow value. That is, was the increase a 10% increase or 50% increase in flow, etc. The kernel density plots and cumulative density plots were generated for each dataset to visualize the shape of the distribution (Fig. 2). At both Kitzmiller and Barton, upstream of dams, the flows above a 10% increase, 75 and 83% of these values, respectively, were less than a 25% increase. However, at Barnum, downstream of Jennings Randolph Dam, of the flows above a 10% increase, only 50% of the values were less than a 25% increase. While there were some much higher increases at both Kitzmiller and Barton, these were rare. The flow at Barnum exhibited more rapid increases across the 25 to 100% increase range compared to the other locations (Fig. 2). This suggests that flow increases should more often be limited to <25% increase from the dam to be comparable to locations unaffected by dam releases.

This method and further investigation into these data following this approach provides a quantitative basis for assessing the degree to which hydropeaking events are affecting the rate of rise of the hydrograph. Ultimately, this knowledge will be used by the USACE to improve downstream ecosystem health by limiting the rate of flow increases, to the extent possible, for brown trout populations.

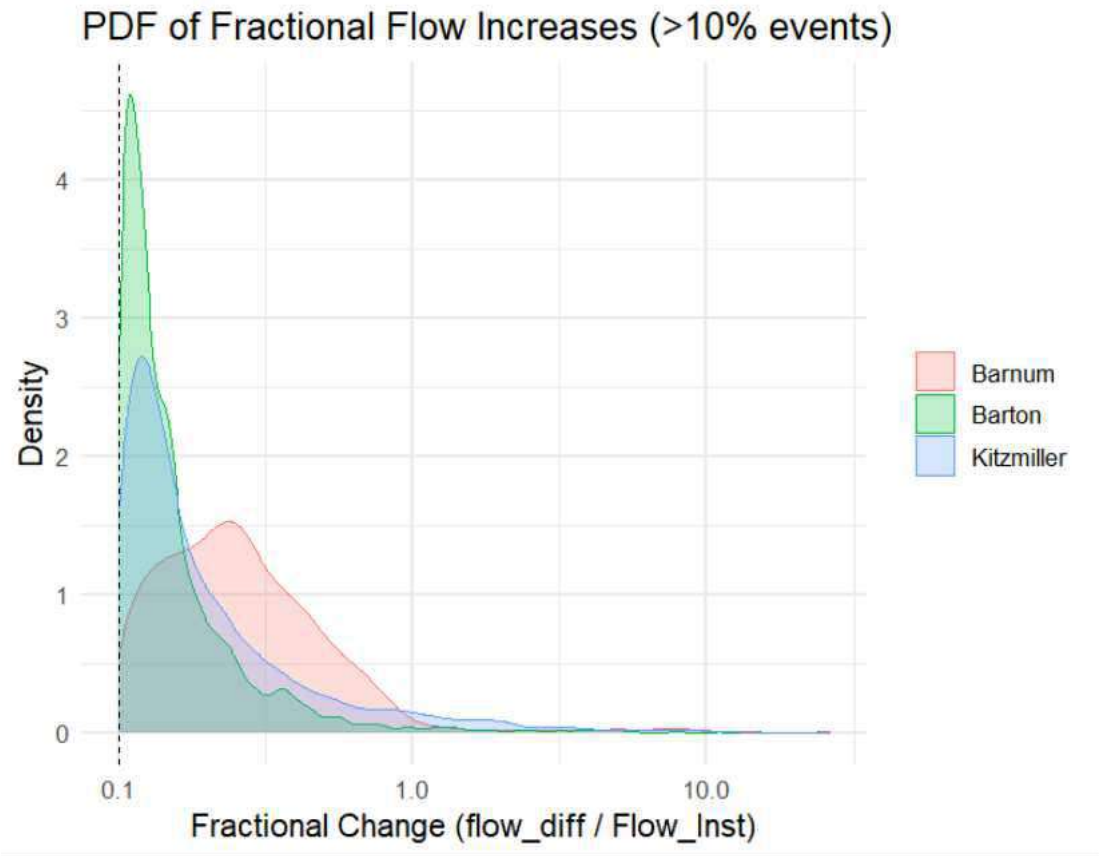

Fig 2. Kernal density plot of fractional change in flow for USGS gages at Kitzmiller, Barton, and Barnum

Keywords: brown trout; dam release; hydropeaking; North Branch Potomac River; sustainable rivers program

Acknowledgements

This work was conceived at the Sustainable River Program workshop for Jennings Randolph Dam and North Branch Potomac River during August 2025.

References

Bahabib F, Ciaramellano Campbell V, Felter L, Fritz J, Montgomery F, Roach A, Spindler M (2025) Sustainable Rivers Program, Jennings Randolph Lake & North Branch Potomac River Environmental Flows, State of the Science Report. U.S. Army Corps of Engineers, 105 p.

Maryland Department of Natural Resources (2025) USACE Environmental Flows Workshop, North Branch of the Potomac River Tailwater Trout Fisheries

Shacheri, F, Czuba JA, Perkins MA (2025) Isolating the compounding effects of dam hydropeaking and climate change on freshwater mussel recruitment. Science of The Total Environment, 977, 179390.

Book of Abstracts of the *16th International Symposium on Ecohydraulics*
Challenges and solutions in the time of global changes
August 16–20, 2026, Lausanne, Switzerland
ISSN: 2790-2420 | ISBN: 978-90-837233-9-6 | doi:[10.64697/iahr.proc.ise2026.abs]
© 2026 IAHR. CC BY-NC-ND 4.0

USING GENETIC TOOLS TO ASSESS FISH POPULATION ABUNDANCE AND CONNECTIVITY IN A REGULATED RIVER

Julien DI PANE[1], Jérôme PRUNIER[2], Vincent DUBUT[2], Olivier LEPAIS[3], Véronique GOURAUD[1], Laurence TISSOT[1], Jeremy PIFFADY[4], Pierre BOMPARD[5]

[1] EDF R&D, LNHE, Chatou, France
julien.di-pane@edf.fr, laurence.tissot@edf.fr, veronique.gouraud@edf.fr
[2] ADENEKO, Saint-Girons, France
jerome.prunier@adeneko.fr, vincent.dubut@adeneko.fr
[3] Univ. Bordeaux, INRAE, BIOGECO, Cestas, France
olivier.lepais@inrae.fr
[4] INRAE, UR RiverLy, EcoFlowS, Villeurbanne, France
jeremy.piffady@inrae.fr
[5] FDPPMA 01, Viriat, France
Bompard@federation-peche-ain.com

ABSTRACT

To better understand the effects of hydropower management on aquatic populations, it is essential to first assess their ecological status. However, estimating fish abundance in large river systems remains challenging using conventional methods such as electrofishing, which are often limited by depth, flow conditions, or restricted accessibility. Genetic approaches for population assessment, particularly the concept of "effective population size" (*Ne*), offer a promising alternative. Effective population size represents the average number of individuals contributing genes to the next generation. Neutral genetic markers, such as microsatellites, are commonly used to estimate *Ne* based on genetic diversity.

The Lower Ain River and its tributaries represent an area of major importance for both hydropower production and fisheries resources. Within a cascade of six dams currently operating along the river, a pumped-storage facility is in the planning phase and is expected to mitigate the impacts of hydropeaking and improve temperature conditions of the downstream river, beneficial for aquatic life. This work is being carried out as part of the European Horizon ReHydro project, which aims to develop methods and tools for assessing the environmental benefits of refurbishment projects.

To assess the ecological status of brown trout (*Salmo trutta fario*), a genetic study was initiated in 2024 to establish a three-year pre-operational baseline prior to the commissioning of the pumped-storage facility. Its objectives are to 1) quantify genetic diversity and inbreeding levels, 2) evaluate functional connectivity across the river network, and 3) estimate effective population size. Repeated measurements after commissioning will then allow evaluation potential benefits of the hydropower–pumped storage project on the trout population.

Results presented here are from the first sampling year (2024). Small fin clips were collected at multiple locations along the Ain and its tributaries. Fish samples were genotyped, for 18 microsatellites developed by SSRseq, and various genetic metrics were calculated. Genetic analyses revealed high allelic diversity across all sampled sites and no detectable signal of inbreeding in wild populations. Patterns of genetic structure indicated strong connectivity throughout the river network, with no major barriers to gene flow, supporting the existence of a well-connected system downstream the Ain dam cascade. Estimates of effective population size (*Ne*) were in the range of several tens of individuals per site, with a metapopulation estimate exceeding 400 individuals. Based on commonly reported *Ne/Nc* ratios, this translates into a census size on the order of a few thousand individuals at the scale of the study area.

These findings establish a robust genetic reference state and illustrate the relevance of population genetics as a complementary tool for ecological assessment in large, regulated rivers.

Keywords: Hydropower; Ecological assessment; Fish; Effective population size; Genetic connectivity

Introduction

Understanding how the presence and operation of hydroelectric facilities influence fish populations is crucial for adapting management practices and thereby preserving biodiversity in regulated river systems (Bozeman *et al.*, 2025). In reservoir-influenced reaches or in large rivers such as the Lower Ain River (France), conventional fish sampling methods, including electrofishing, are often constrained by depth, discharge, and limited accessibility. As a result, indirect approaches are needed. Population genetic tools provide robust indicators of demographic status and functional connectivity by enabling the estimation of effective population size (*Ne*), genetic diversity, and gene flow among habitats (Frankham, 2010; Palstra & Fraser, 2012).

The Lower Ain River is currently regulated by a cascade of six hydropower dams, and a pumped-storage project is planned in its upstream section. This project of public interest involves the installation of a new turbine–pump unit at the Saut-Mortier dam. The new equipment will allow water to be pumped (pump mode) from Lake Coiselet to Lake Saut-Mortier, and then to Lake Vouglans using the existing Vouglans pump-turbine system; or released downstream (turbine mode) to generate electricity.

Beyond improving flexibility in energy demand management, the planned pumped-storage scheme is expected to improve downstream flow regulation and thermal condition below the Allement dam, the lowermost structure in the cascade. Such modifications may generate ecological benefits for fish populations, particularly salmonids. Establishing a quantitative genetic baseline prior to these operational changes is therefore essential to evaluate future ecological responses. Within this framework, a research collaboration between EDF (Electricité de France), the Ain Departmental Federation for Fishing (FDPPMA 01), the French National Research Institute for Agriculture, Food and Environment (INRAE), and a consulting firm specialized in population genetics (ADENEKO) was initiated to assess the relevance of DNA-based approaches for monitoring brown trout (*Salmo trutta fario*) in the Lower Ain River.

The first phase of the study, presented here, focuses on establishing a pre-operational baseline over a three-year period. Specifically, it aims to 1) quantify genetic diversity and inbreeding levels, 2) evaluate functional connectivity across the river network, and 3) estimate effective population size. Together, these complementary metrics will provide a robust reference framework for detecting and quantifying potential ecological changes following the implementation of the pumped-storage scheme through repeated post-commissioning assessments.

Materials and methods

The first field sampling campaign was conducted during the summer of 2024 at eight sites located along the Ain River and its tributaries (Veyron, Suran, Riez, Oiselon, and Albarine), all situated downstream of the dam cascade. Approximately 30 individuals per site were sampled, mostly juveniles of the year, along with several mature adults. Additional samples were also taken from 32 individuals from a fish farm to account for potential stocking effect. Small fin clips were collected non-invasively from each fish, and fish DNA was analyzed using 18 microsatellite markers genotyped by SSRseq (Lepais *et al.*, 2020). Genetic metrics, including allelic richness, expected heterozygosity, and inbreeding coefficients, were computed using standard population genetics software. Effective population size (*Ne*) and metapopulation size (meta-*Ne*) were estimated using a Bayesian inference framework (Wang, 2016) to ultimately calculate total abundance (*Nc*).

Results and discussion

Genetic analyses revealed high allelic diversity across all sampled sites (Fig 1-A), with no evidence of loss of heterozygosity (Fig 1-B) or inbreeding (Fig 1-C). The high genetic admixtur observed among tributaries and the main river suggests that trout movement and gene flow remain largely functional, even across areas with hydraulic structures exceeding two meters in height. The Albarine population, despite its geographical isolation, displayed clear genetic connectivity with other sampled groups, indicating ongoing exchange within the system. Other results, not illustrated here, revealed a genetic signature of farmed fish in the Oiselon River, stemming from a past stocking event. This signature gradually diluted with distance to this Ain tributary. The event locally increased allelic richness in the subpopulation due to admixture between wild and farmed trout.

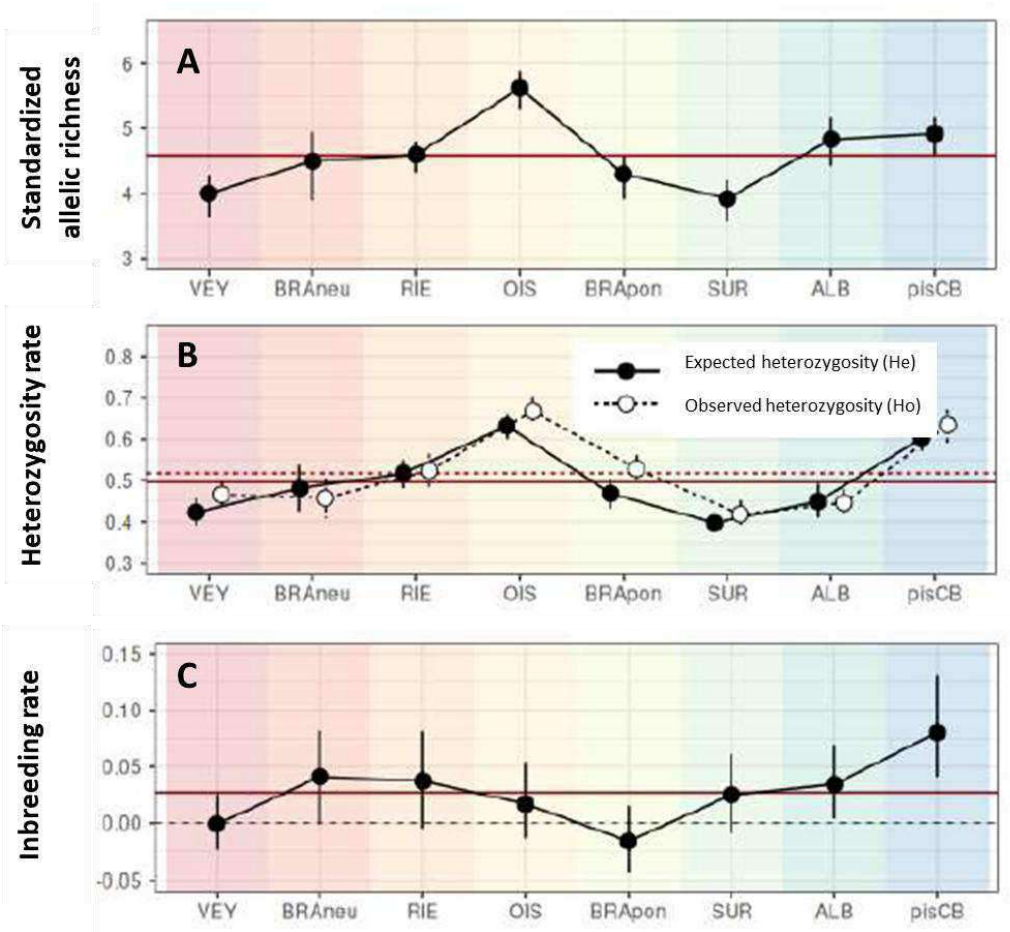

Fig. 1. Brown trout allelic richness (A) expected and observed heterozygosity (B) and mean individual inbreeding coefficient (C) per population. Error bars represent 95% confidence intervals around the mean (dot). Red lines indicate the mean value of the parameter across all populations.

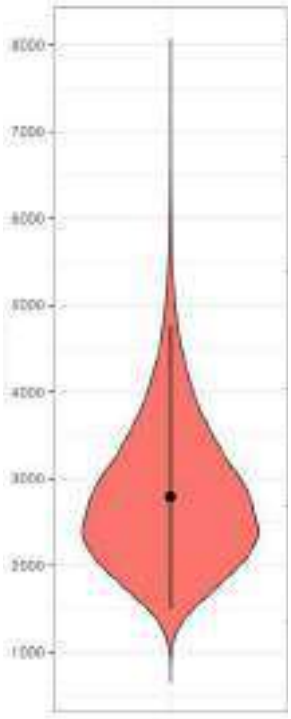

Estimates of effective population size suggested a stable and self-sustaining metapopulation. While the precise numerical estimates are associated with some uncertainty due to methodological constraints (indirect estimation, assumed *Ne/Nc* ratio, spatial coverage), the results remain consistent with previous independent assessments. The observed patterns support the hypothesis of a single, well-connected population with sufficient genetic diversity to ensure long-term viability. Effective population size *Ne* was estimated to range from 40 to 80 individuals within individual sites of the Ain River and its tributaries, with an overall meta-*Ne* of approximately 430 individuals. This corresponds to an estimated total abundance of roughly 2,800 individuals (Fig. 2), or about 10 individuals per hectare.

.

Fig. 2. Distribution of abundance estimates (meta-*Nc*) of brown trout in the Ain River, including the uncertainty associated with the estimation of the metapopulation size (meta-*Ne*) and the uncertainty linked to the species-specific ratio (*Ne/Nc*). The mean and the 95% confidence interval are shown in black.

Conclusion

Despite multiple anthropogenic pressures, brown trout populations in the Lower Ain River maintain high levels of genetic diversity and strong connectivity across the river network. These findings indicate a currently resilient and functionally connected metapopulation.

This study highlights also and mainly the value of genetic approaches as complementary tools to conventional monitoring methods, particularly in large and regulated rivers where direct abundance estimates are challenging. By providing quantitative metrics of diversity, connectivity, and effective population size, population genetics offers a robust framework to support adaptive management of hydroelectric infrastructures.

Future work will extend this baseline through temporal monitoring, incorporating additional reference years and post-implementation sampling following the commissioning of the pumped-storage hydropower project. This before–after design will allow detection of potential genetic and demographic changes associated with modified hydrological operations.

Acknowledgements

We thank all partners involved in this study: the Fédération de l'Ain pour la Pêche et la Protection du Milieu Aquatique, EDF Hydro Alpes as the main funder of the study, the local fishing associations, and all the volunteers for their valuable contribution in the field.

References

Bozeman, B. B., Pracheil, B. M., & Matson, P. G. (2025). The environmental impact of hydropower : A systematic review of the ecological effects of sub-daily flow variability on riverine fish. *Reviews in Fish Biology and Fisheries*, *35*(1), 45-76.

Frankham, R. (2010). Challenges and opportunities of genetic approaches to biological conservation. *Biological Conservation*, *143*(9), 1919-1927.

Lepais, O., Chancerel, E., Boury, C., Salin, F., Manicki, A., Taillebois, L., ... & Guichoux, E. (2020). Fast sequence-based microsatellite genotyping development workflow. *PeerJ*, *8*, e9085.

Palstra, F. P., & Fraser, D. J. (2012). Effective/census population size ratio estimation : A compendium and appraisal. *Ecology and Evolution*, *2*(9), 2357-2365.

Wang, J. (2016). A comparison of single-sample estimators of effective population sizes from genetic marker data. *Molecular* Ecology, *25*(19), 4692-4711.

Book of Abstracts of the *16th International Symposium on Ecohydraulics*
Challenges and solutions in the time of global changes
August 16–20, 2026, Lausanne, Switzerland
ISSN: 2790-2420 | ISBN: 978-90-837233-9-6 | doi:[10.64697/iahr.proc.ise2026.abs]
© 2026 IAHR. CC BY-NC-ND 4.0

ECOLOGICAL FLOWS AS A DRIVER FOR FUTURE HYDROPOWER DEVELOPMENT

Giovanni NEGRO[1], Sara VIALE[1], Alessandro GUGLIELMETTO[1], Paolo VEZZA[1,2]

[1] Department of Environment, Land and Infrastructure Engineering (DIATI), Polytechnic of Turin, Italy
email: giovanni.negro@polito.it, sara.viale@polito.it, alessandro.guglielmetto@polito.it

[2] INGENIO, Universitat Politècnica de València, Spain
emails: paolo.vezza@polito.it, paovez@upvnet.upv.es

ABSTRACT

At the intersection of environmental protection and energy transition, Italy is called to find new approaches to safeguard river ecosystems while modernizing its hydropower infrastructure. Achieving this balance under the new Ecological Flow (EF) framework requires integrated strategies that reconcile ecological integrity with energy efficiency. This study evaluates the eco-hydrological and operational implications of redefining EFs for run-of-river (RoR) plants, exploring synergies between new EF regimes and potential plant re-powering through increased maximum water abstraction capacity. Focusing on three Alpine rivers (Ayasse, Brenve, and Savara), EF design was based on the mesohabitat simulation model (MesoHABSIM) and on the Habitat Integrity Index (IH), an ecologically meaningful indicator composed of five quality classes. Hydropower performance was assessed by computing the corresponding total volume of water diverted to turbines. Results showed that improving habitat quality from "Bad" to "High" required base flow (BF) increases of 1.6-9.4 times current rates, reducing diverted water volumes by 8-28%. However, coupling higher BF with expanded water abstraction capacity enhanced hydropower production by 124-169% while preserving river ecological integrity. This framework supports the design of RoR configurations that harmonize ecological sustainability, economic feasibility, and climate resilience.

Keywords: *Ecological Flows, Hydropower repowering, Habitat Integrity Index, MesoHABSIM, Alpine rivers.*

1. Introduction

As countries intensify efforts to reduce greenhouse gas emissions, the global demand for renewable energy continues to rise. Within this transition, hydropower remains a key contributor to renewable electricity generation, offering a unique combination of reliability, operational flexibility, and a near-zero carbon footprint (Zarfl et al., 2015). Its economic competitiveness and stable performance make it a key driver in the shift toward a fully decarbonized energy system (Aubin et al., 2025).

However, diverting or storing water for hydropower can substantially affect river ecosystems (He et al., 2024). Dams and weirs modify hydrological and sediment regimes, and alter the organic material supply in the downstream reaches, compromising habitats and diminishing aquatic biodiversity (Poff & Zimmerman., 2010). To mitigate these impacts, the concept of Environmental Flows (EF) has been developed since the 1970s. Italy introduced Minimum Flow (MF) requirements in 1989, but static MF releases often failed to provide meaningful ecological protection. More recently, the European Union promoted a broader EF framework, considering temporal variability, seasonality, sediment transport, and species' habitat requirements. In 2017, the Italian Ministry of Environment and Energy Security formalized this approach through the Decree DD 30/STA 2017, which aimed to mimic natural flow variation by establishing base flows (BF) and controlled high-flow events to support river ecosystems.

Constructed primarily between the 1920s and 1970s, most of Italy's large and medium hydropower plants now face challenges related to aging infrastructure and limited operational flexibility (Stucchi et al., 2023). Originally designed for stable, and predictable energy demand, many plants lack the adaptive capacity needed for integration with variable renewable sources and modern energy markets. Enhancing hydropower flexibility through re-powering, control system upgrades, and operational improvements has become a strategic priority to support both renewable energy targets and grid stability. This study evaluates how newly established EF regimes influence both river habitats and hydropower production, while exploring opportunities for future re-powering. Using three Alpine streams in the Aosta Valley as case studies, it integrates ecological and operational analyses across multiple EF release scenarios and plant configurations. River ecological integrity was assessed using the MesoHABitat SImulation Model (MesoHABSIM; Parasiewicz, 2007) in combination with the Habitat Integrity Index (IH; Vezza et al., 2017). The results provide practical insights into sustainable hydropower strategies that align renewable energy production with the conservation of mountain river ecosystems.

2. Materials and Methods

2.1. Study area

The study was conducted considering three Alpine streams, Ayasse, Brenve, and Savara, located in the Aosta Valley, Northwestern Italy. These short, steep watercourses (3.7-27 km; 7-15% slope) exhibit step-pool or cascade morphologies and coarse gravel-boulder substrates, with minimal anthropogenic disturbance. All sites host run-of-river (RoR) systems with small weirs and negligible storage, representative of most Italian hydropower installations (Galletti et al., 2025). The area has an Alpine-Continental climate, with winter low-flow conditions driven by freezing, snow accumulation, and glacier influence.

2.2. Habitat description and analysis

Habitat assessment was performed using the MesoHABSIM, a physical habitat modeling framework that quantifies spatio-temporal variations in fish distribution as a function of in-stream flow and channel morphology (Vezza et al., 2017). The approach involves detailed mapping and characterization of hydro-morphological units (HMUs; e.g., pools, riffles, rapids; Belletti et al., 2017) to evaluate habitat availability for target species under different discharge conditions. For each surveyed discharge, available habitat is then estimated using species-specific habitat suitability criteria (HSC) that incorporate local physical attributes of HMUs, including depth, velocity, substrate, and cover (Vezza et al., 2017). Brown trout (*Salmo trutta*) and marble trout (*Salmo marmoratus*), the only fish species inhabiting the investigated streams, were selected as ecological targets. Habitat availability was assessed for the rearing and growth bioperiods (adults and juveniles; Vezza et al., 2012) and for the critical spawning period (adult only).

Habitat simulations were performed using SimStream-Web, an online platform that supports the MesoHABSIM methodology (https://mesohabsim.isprambiente.it/app/home/). The platform generates habitat-flow rating curves, which allow streamflow time series to be expressed in terms of habitat availability. By comparing a reference eco-hydrological scenario (without hydropower operation) with an altered one (reflecting hydropower plant activity), the platform computes the Habitat Integrity Index (IH). This index quantifies the deviation between reference and altered conditions through two sub-indices: The Index of Spatial Habitat availability (ISH) – representing the mean loss of habitat; and the Index of Temporal Habitat availability (ITH) – analyzing the duration and frequency of habitat stress events (i.e., periods when habitat availability falls below the 97th percentile of the reference series; see Vezza et al., 2017; Vassoney et al., 2019 for details). Both ISH and ITH range from 0 to 1, with lower values indicating stronger degradation. The overall IH is defined as the minimum of the two sub-indices among all target species. According to the Vezza et al. (2017) and consistent with the European Water Framework Directive, IH values are divided into five habitat quality classes (High, Good, Moderate, Poor, and Bad) using 0.2 incremental thresholds.

2.3. Ecological flows and hydropower re-powering

To evaluate the effects of EF on hydropower production and re-powering potential, both base flow and maximum water abstraction capacity (Max Flow) were varied to defined specific altered time series (scenario). Two scenario groups were defined: Group A considered BF changes only (6 scenarios; **Fig. 1A**), while Group B combined BF variations with increased water abstraction capacity (6 scenarios; **Fig. 1B**). For **Fig. 1A** and **1B**, Scenario 1 represented the current conditions (constant minimum flow and existing turbine capacity), whereas Scenarios 2-6 incorporated monthly variable BF (Group A) and, for Group B, combined with increased turbine capacity, assumed up to 250% higher than current levels. Each scenario aimed to achieve a

specific habitat quality class (Bad to High) based on the IH index. Hydropower production was estimated from the total volume of water diverted to turbines, based on the difference between the reference (natural flow regime) and the altered scenarios. Reference streamflow was generated using the Continuum distributed hydrological model (Silvestro et al., 2012), producing a 13-year daily record (2008-2021).

3. Results

Three to four river surveys were conducted at each site, covering a range of discharges from low-flow conditions (99th percentile of the reference time series) to medium flows (up to 15th percentile of the reference time series). Habitat-flow rating curves were generated using SimStream-Web for all sites, species, and bioperiods. In the Ayasse Stream, adult trout habitat increased monotonically with discharge, whereas juvenile and spawning habitats exhibited non-monotonic patterns, peaking at lower flows (~0.5 m³/s). The Brenve Stream, the smallest of the three, exhibited monotonically increasing curves for all bioperiods, indicating consistent habitat availability gains with flow. In contrast, habitat availability for all targets in the Savara Stream peaked between 1 and 2.5 m³/s, with higher flows leading to a decline in suitability due to excessive velocities.

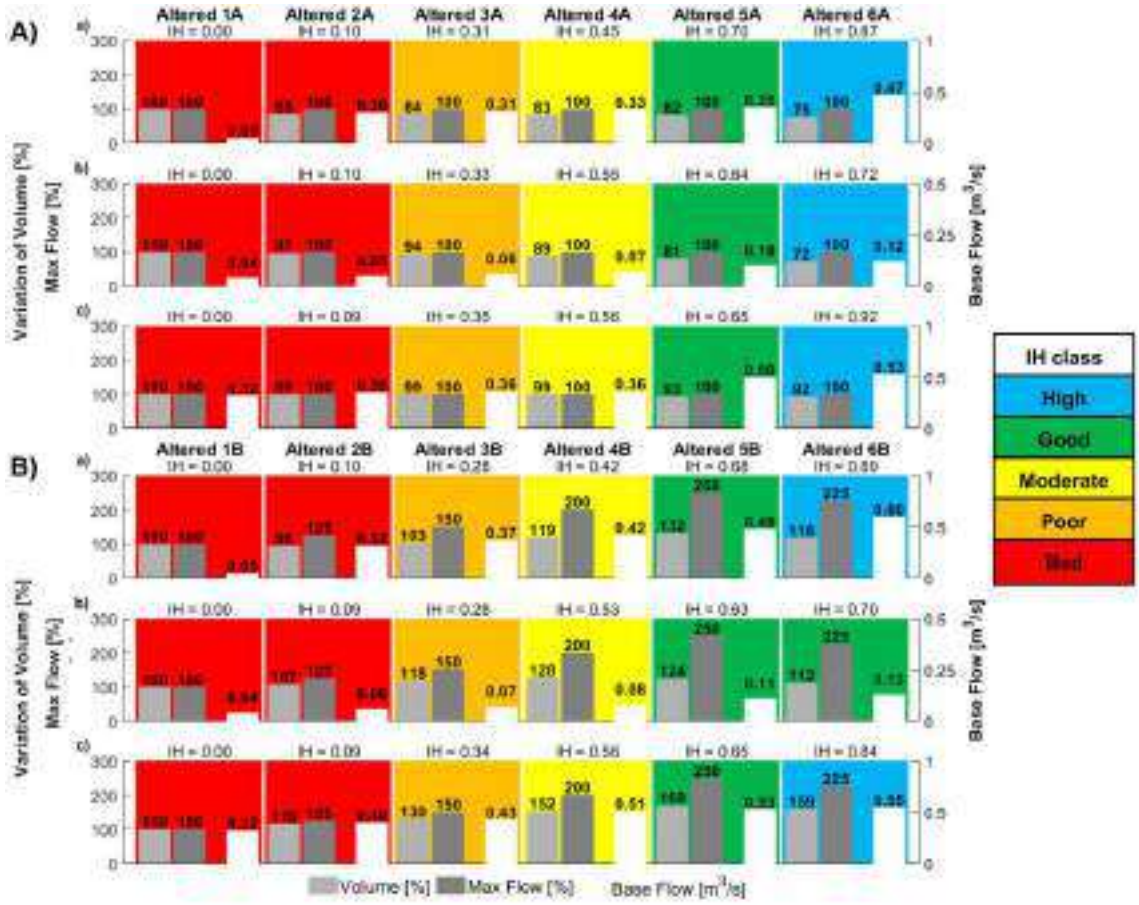

Fig. 1. Results of the scenario analysis for the three study sites: a) Ayasse, b) Brenve, and c) Savara streams. Group A) scenarios (top panels) explore variations in base flow (BF) under the current maximum water abstraction capacity, while Group B) scenarios (bottom panels) combine changes in BF with increased water abstraction capacity to assess re-powering potential. For Figures 1A and 1B, Scenario 1 represented the current conditions (constant minimum flow and existing turbine capacity). The grey bars (left y-axis) illustrate the percentage change in total diverted volume (light grey) and maximum water abstraction capacity (dark grey). The white bar (right y-axis) shows the mean BF released to the river when diversion operates below its maximum capacity. Background colours indicate habitat quality classes based on the Habitat Integrity Index (IH).

Based on the resulting habitat-flow rating curves and considering the reference flow time series, 12 altered series were defined for each site. Altered scenario analyses evaluated the effects of BF and maximum water abstraction capacity on habitat quality and hydropower production. Group A (varying BF only) showed that achieving a "High" IH class required increasing BF from 1.6× (Savara) to 9.4× (Ayasse) current values, reducing turbine-diverted volumes by 8-28% (**Fig. 1**A). Group B (combining varying BF and increased maximum water abstraction capacity) enabled hydropower production gains of 124-169% for "Good" habitat quality (**Fig. 1**B). Concentrating withdrawals during high-flow periods, impacts on fish habitat were reduced. Interestingly, trade-offs emerged for high maximum water abstraction values: further IH improvements required reducing turbine withdrawals, particularly in Ayasse and Savara Streams (ALTERED 6B; **Fig. 1**B).

4. Discussion and Conclusions

Our study shows that hydropower re-powering through increased maximum water abstraction capacity can be sustainable when combined with carefully designed EF regimes. EF releases which varied on seasonal or monthly scale are essential to maintain habitat availability for all fish species and bioperiods. Maximizing water abstraction capacity without considering ecological impacts can compromise river integrity, while EF strategies ignoring technical and economic constraints may be impractical. Sustainable hydropower depends on achieving a balance between energy generation, ecological preservation, and economic feasibility.

EF and maximum water abstraction thresholds should be adapted to local conditions, as each hydropower plant functions within a unique eco-hydro-morphological context. Increasing water abstraction capacity allows greater water withdrawals during high-flow periods, reducing ecological stress while boosting energy generation, whereas EF releases safeguard habitat integrity during low flows. Coupling increased turbine capacity with dynamic EF regimes creates synergies: river habitats benefit from ecologically meaningful flows and high-flow pulses, while hydropower operators can exploit periods of hydrological abundance. This alignment is particularly valuable in the Alpine context, where summer snowmelt generates peak hydropower production precisely when electricity demand for air conditioning reaches its highest levels. This integrated approach supports adaptive, sustainable hydropower where ecological restoration and energy objectives are mutually achievable.

The urgency of adaptive management is heightened under climate change, which alters Alpine hydrology through warming, glacier retreat, and shifting precipitation patterns, affecting both hydropower reliability and ecosystem resilience. Many aging RoR plants, often with limited storage, could better utilize short-term hydrological peaks and more variable summer/autumn flows via enhanced water abstraction capacity. Combined with climate-informed EF strategies, this approach ensures technically robust, ecologically sound, and economically viable hydropower operations. The future of hydropower in Italy, and similar regions with aging infrastructure, depends on adopting adaptive, ecologically informed management strategies that ensure both clean energy production and resilient river ecosystems.

References

Aubin V, Helseth A, Korpås M (2025) Do we have to choose between the ecosystems and the energy transition? Environmental trade-offs with operation of Norwegian hydropower. Renewable Energy, 244, 122595.

Belletti B, Rinaldi M, Bussettini M, Comiti F, Gurnell AM, Mao L, Nardi L, Vezza P (2017) Characterising physical habitats and fluvial hydromorphology: A new system for the survey and classification of river geomorphic units, Geomorphology, 283, 143-157.

Galletti A, Zarghami Dastjerdi S, Majone B (2025) Comprehensive inventory of large hydropower systems in the Italian Alpine Region, Earth System Science Data, 17, 3353–3373.

He F, Zarfl C, Tockner K, Olden JD, Campos Z, Muniz F, Svenning JC, Jähnig SC (2024) Hydropower impacts on riverine biodiversity. Nature Reviews Earth & Environment, 5(11), 755-772.

Parasiewicz P (2007) The MesoHABSIM model revisited, River Research and Applications, 23(8), 893-903.

Poff NL, Zimmerman JK (2010) Ecological responses to altered flow regimes: a literature review to inform the science and management of environmental flows. Freshwater biology, 55(1), 194-205.

Silvestro F, Gabellani S, Delogu F, Rudari R, Boni G (2012) Continuum: a distributed hydrological model for water management and flood forecasting, Hydrology & Earth System Sciences Discussions, 9(6).

Stucchi L, Bocchiola D, Simoni C, Ambrosini SR, Bianchi A, Rosso R (2023) Future hydropower production under the framework of NextGenerationEU: The case of Santa Giustina reservoir in Italian Alps. Renewable Energy, 215, 118980.

Vezza P, Parasiewicz P, Rosso M, Comoglio C (2012) Defining minimum environmental flows at regional scale: Application of mesoscale habitat models and catchments classification, River Research and Applications, 28, 717–730.

Vassoney E, Mammoliti Mochet A, Rocco R, Maddalena R, Vezza P, Comoglio C (2019). Integrating meso-scale habitat modelling in the multicriteria analysis (MCA) process for the assessment of hydropower sustainability. Water, 11(4), 640.

Vezza P, Zanin A, Parasiewicz P (2017) Manuale tecnico-operativo per la modellazione e la valutazione dell'integrità dell'habitat fluviale.

Zarfl C, Lumsdon AE, Berlekamp J, Tydecks L, Tockner K (2015) A global boom in hydropower dam construction. Aquatic sciences, 77(1), 161-170.

Book of Abstracts of the *16th International Symposium on Ecohydraulics*
Challenges and solutions in the time of global changes
August 16–20, 2026, Lausanne, Switzerland
ISSN: 2790-2420 | ISBN: 978-90-837233-9-6 | doi:[10.64697/iahr.proc.ise2026.abs]
© 2026 IAHR. CC BY-NC-ND 4.0

EVALUATING YOUNG-OF-THE-YEAR FISH RESPONSE TO A HYDROPEAKING MITIGATION MEASURE: THE GKI DIVERSION HYDROPOWER PLANT

Kevin MERL[1], Bernhard ZEIRINGER[2], Daniel S. HAYES[3], Patrick HOLZAPFEL[4], Christoph HAUER[5], Martin SCHLETTERER[6], Stefan SCHMUTZ[7], Franz GREIMEL[8]

[1, 2, 3, 6, 7, 8] BOKU University, Institute of Hydrobiology and Aquatic Ecosystem Management, Department of Ecosystem Management, Climate and Biodiversity, Gregor-Mendel-Straße 33, 1180 Vienna, Austria
email: kevin.merl@boku.ac.at
email: bernhard.zeiringer@boku.ac.at
email: daniel.hayes@boku.ac.at
email: martin.schletterer@boku.ac.at
mail: stefan.schmutz@boku.ac.at
email: franz.greimel@boku.ac.at

[4, 5] BOKU University, Institute of Hydraulic Engineering and River Research, Department of Landscape, Water and Infrastructure, Am Brigittenauer Sporn 3, 1200 Vienna, Austria

email: patrick.holzapfel@boku.ac.at

email: christoph.hauer@boku.ac.at

[6] Department of Hydropower Engineering, TIWAG -Tiroler Wasserkraft AG, Eduard-Wallnöfer-Platz 2, 6020 Innsbruck, Austria
email: martin.schletterer@boku.ac.at

ABSTRACT

Hydropeaking, caused by the rapid release of water from storage hydropower plants, disrupts riverine ecosystems and particularly impacts young-of-the-year (YOY) fish. These YOY fish are highly vulnerable to hydropeaking due to their dependence on shallow, slow-flowing near-bank habitats, which are frequently exposed to rapid dewatering. This study evaluates the effectiveness of the GKI hydropeaking diversion power plant on the Inn River, Austria, in mitigating fish ecological impacts. Pre- and post-implementation monitoring was conducted, focusing on YOY brown trout (*Salmo trutta*) and European grayling (*Thymallus thymallus*) two years before (2021–2022) and two years after (2024–2025) the plant began operations. Preliminary results show that amplitude was reduced, particularly during low-flow periods. YOY brown trout abundance increased in more heterogenous river sections with better structural habitat heterogeneity. In contrast, YOY grayling abundance remained unchanged following the implementation of the measure. The conditions could improve in the following years as the ecosystem might need more time to adapt to these changes. These preliminary findings emphasize the need to integrate hydropeaking management with habitat restoration measures, such as river widening, to achieve meaningful ecological improvements.

Keywords: *pulsed flow, juvenile fish, flow ramping, river widening, habitat restoration*

1. Introduction

The global effort to combat climate change has increased the reliance on renewable energy sources. Storage hydropower plants play a critical role in stabilizing the variability of energy production from other renewable sources, such as solar and wind, by functioning as large-scale batteries (Gaudard and Romerio, 2014). However, the rapid release of stored water to meet energy demands creates artificial flow fluctuations, a phenomenon known as hydropeaking (Greimel et al., 2016). These fluctuations can have significant negative impacts on river ecosystems, particularly on young-of-the-year (YOY) fish (Hayes et al., 2019; Moreira et al., 2019; Young et al., 2011).

YOY fish, are highly sensitive to hydropeaking due to their preference for slow-flowing, shallow habitats near riverbanks (Bardonnet et al., 2006; Heggenes and Traaen, 1988). Hydropeaking disrupts these habitats, forcing fish to either drift downstream due to increased flow velocities or become stranded when water levels recede rapidly, leaving large sections of the riverbank dry (Bipa et al., 2024; Hayes et al., 2019; Young et al., 2011).

Hydropeaking is primarily characterized by hydrological parameters such as ramping rate, amplitude, flow ratio, and event frequency (Greimel et al., 2016). However, hydrology interacts with river morphology to form the hydro-morphological / hydraulic response. While wider and more complex river geometries can lead to higher stranding rates, it can also increase habitat availability for YOY fish (Bätz et al., 2024; Hauer et al., 2014; Hayes et al., 2024; Person et al., 2014; Vanzo et al., 2016).

To mitigate these hydrological impacts, hydropeaking diversion power plants have been proposed as a solution. By diverting flow fluctuations away from the main river channel through a pressure tunnel to the following hydropower station, this mitigation scheme aims to reduce hydrological disturbances while generating additional electricity. The GKI hydropeaking diversion power plant on the Inn River in Austria was constructed to reduce the hydropeaking of the upstream storage power plant Martina. Up to 75 m^3/s of the 93 m^3/s hydropeaking wave coming from Martina can be diverted 23 km downstream, while the rest is assumed to be buffered in the impoundment, which has a usable storage volume of 416,000 m^3 (Moreira et al., 2020; Reindl et al., 2023).

This study investigates the effectiveness of the GKI hydropeaking diversion power plant in improving the abundance of YOY salmonids, specifically brown trout (*Salmo trutta*) and European grayling (*Thymallus thymallus*). Additionally, it explores the interactions between hydrology, river morphology, the influence of tributaries to better understand the ecological implications of diversion power plants as hydropeaking mitigation measures.

2. Methods

A pre- and post-monitoring design was used to assess the ecological impacts of the GKI hydropeaking diversion power plant. Data were collected over four years: two years before (2021–2022) and two years after the plant's implementation (2024–2025). Seven sampling sites were selected along the 23 km diversion stretch (Reindl et al., 2023) in order to capture the hydrological gradient downstream of the hydropeaking source. Additionally, tributaries and their confluences with the main channel were sampled to assess their potential role in mitigating hydropeaking impacts.

Preferred YOY habitats were sampled using a strip fishing method, which combined visual counts with electrofishing in spring (June) and in summer (August/September) (Zeiringer et al., 2024). This study focused on the river's characteristic salmonid species: brown trout (*Salmo trutta*) and European grayling (*Thymallus thymallus*). The captured fish were measured and counted. YOY abundance was standardized using a catch-per-unit-effort approach, with values recalculated as the number of individuals per 100 meters of fished length.

Hydrological data were recorded at 15-minute intervals using gauging stations operated by the hydropower company TIWAG and the Austrian Hydrographic Service. These data were analysed following the methodology of Greimel et al. (2016), which includes calculating key flow metrics such as event frequency, ramping rate, amplitude, and flow ratio.

Morphologic and hydraulic diversity was assessed using the parameter structural heterogeneity (Hauer and Holzapfel, 2024), a metric describing the lateral expansion of the wetted width with increasing discharge. For each cross-section, a flow spectrum (Q95PCT, 3×Q95PCT, 2×MQ, 5×MQ) was simulated using 1D hydraulic modelling, with hydrological inputs derived from a water-balance model, which estimates long-term average runoff BMLFUW (2007). Changes in discharge and wetted width were normalized to ensure comparability across and within rivers, and the structural heterogeneity was quantified as the slope of the linear relation

between normalized width and normalized discharge. General morphological parameters (channel slope, mean width, width variability, sinuosity) were derived via GIS analysis, and morphological status data describing departures from natural conditions were incorporated from national surveys of the River Basin Management Plan (RBMP; BMLRT, 2022).

3. Results

Preliminary hydrological data show a reduction of hydropeaking waves' amplitude, especially during low flow conditions. Further analysis will reveal the exact changes in ramping rate, event frequency and amplitude.

Regarding morphological characteristics, the sites within the investigated stretch can be broadly classified into four groups:

- Upper gorge – unaltered (RBMP) section with low width and low structural heterogeneity values
- Lower gorge – moderately altered (RBMP) section with low width and low structural heterogeneity values
- Heterogeneous stretches – moderately altered (RBMP) sections wider sections with higher structural heterogeneity values
- Altered stretches – heavily altered (RBMP) section narrower than heterogenous stretches, characterized by low structural heterogeneity values

Data from the pre-monitoring period revealed very low YOY fish abundances, with fewer than 5 brown trout per 100 meters and a complete absence of grayling. In the first post-implementation year, no clear changes were observed, as YOY fish abundances remained persistently low, with fewer than 6 brown trout per 100 meters.

By the second post-monitoring year, however, a positive response from brown trout was detected at some sites. In spring, the highest abundances were observed in a altered stretch, with 8 individuals per 100 meters, and a heterogeneous stretch with 21 individuals per 100 meters. In summer, two sites in heterogeneous stretches showed higher abundances, with 10 and 28 individuals per 100 meters, respectively. Notably, the highest values in both spring and summer corresponded to the same site.

4. Discussion

The preliminary findings of this study indicate that while hydropeaking seems to be successfully reduced, it is not fully gone. The low YOY fish abundances observed during the first post-implementation year may be attributed to prolonged high-flow conditions, which likely hindered recruitment and survival of brown trout. In the second year of post monitoring, the response of YOY brown trout was limited and site-specific. Positive responses were observed mainly in two heterogenous sections of the river. One of these sites is a restored stretch where the river was widened and groin fields create flow shelters, while the second site is a relatively wide section dominated by a large point bar. This highlights the critical interaction between hydrological mitigation of hydropeaking and morphological river restoration in enhancing ecological outcomes (Hauer et al., 2014; Person et al., 2014; Vanzo et al., 2016).

In contrast, YOY grayling showed no measurable response, suggesting that additional factors, such as species-specific habitat requirements or life-history traits, may influence their response to hydropeaking mitigation. These results furthermore underscore the need for an integrated approach to hydropeaking mitigation that combines hydrological management with targeted habitat restoration, such as river widening and the creation of refuge areas. It also shows the importance interannual variability in flow conditions when evaluating the effectiveness of hydropeaking mitigation measures, and, therefore, the need for multiple years of monitoring. This study only addresses the first response of the ecosystem shortly after implementation of the mitigation measure. More substantial changes are expected in the coming years as the ecosystem has more time to react.

This study contributes to the growing body of research on hydropeaking mitigation (e.g., Bruno et al., 2023) by demonstrating the importance of coupling a reduction of hydropeaking intensity with enhancing habitat conditions to support YOY fish populations. The findings also highlight the necessity of monitoring multiple years and conducting detailed hydro-morphological analyses to better understand the complex interactions between hydrology, morphology, and biological responses. Such analyses are essential for refining mitigation strategies in consideration of energy flexibility needs and promoting the sustainable management of rivers ecosystems impacted by hydropower operations (Boavida et al., 2025).

Acknowledgements

This research was funded by TIWAG (Tiroler Wasserkraft AG). Kevin Merl acknowledges the Doctoral School *Human River Systems in the 21st Century (HR21)* at BOKU University for supporting this research.

References

Bardonnet, A., Poncin, P., Roussel, J. -M., 2006. Brown trout fry move inshore at night: a choice of water depth or velocity? Ecol. Freshw. Fish 15, 309–314. https://doi.org/10.1111/j.1600-0633.2006.00160.x

Bätz, N., Judes, C., Vanzo, D., Lamouroux, N., Capra, H., Baumgartner, J., Berger, B., Weber, C., 2024. Patch-scale habitat dynamics: three metrics to assess ecological impacts of frequent hydropeaking. J. Ecohydraulics 0, 1–29. https://doi.org/10.1080/24705357.2024.2426790

Bipa, N.J., Stradiotti, G., Righetti, M., Pisaturo, G.R., 2024. Impacts of hydropeaking: A systematic review. Sci. Total Environ. 912, 169251. https://doi.org/10.1016/j.scitotenv.2023.169251

BMLFUW, 2007. Hydrologischer Atlas Österreichs. 1. Lieferung 2003. 2. Lieferung 2005. 3. Lieferung 2007. Bundesministerium für Land- und Forstwirtschaft, Umwelt und Wasserwirtschaft, Wien.

BMLRT, 2022. Nationaler Gewässerbewirtschaftungsplan 2021. Bundesministerium für Landwirtschaft, Reg. und Tour. 2021.

Boavida, I., Aarestrup, K., Abungba, J.A., Bor, A., Casas-Mulet, R., Chen, S.F., Franklin, P.A., Gouraud, V., Haas, J., Halleraker, J.H., Hayes, D., Hemakumara, S.P., Koehnken, L., Leturcq, G., Oladosu, G., Phiri, I., Pracheil, B., Quaranta, E., Rijal, N., Ruokamo, E., Salack, S., Schletterer, M., Smokorowski, K.E., Szabó-Mészáros, M., Tuhtan, J.A., Vanzo, D., Yangouliba, G.I., Alfredsen, K., Costa, M.J., Venus, T.E., Bakken, T.H., 2025. A Global Horizon Scan of Emerging Challenges and Opportunities for Sustainable Hydropower. https://doi.org/10.2139/ssrn.5377117

Bruno, M.C., Vallefuoco, F., Casari, A., Larsen, S., Dallafior, V., Zolezzi, G., 2023. Moving waters to mitigate hydropeaking: A case study from the Italian Alps, in: River Research and Applications. John Wiley and Sons Ltd, pp. 570–587. https://doi.org/10.1002/rra.4086

Gaudard, L., Romerio, F., 2014. The future of hydropower in Europe: Interconnecting climate, markets and policies. Environ. Sci. Policy 37, 172–181. https://doi.org/10.1016/j.envsci.2013.09.008

Greimel, F., Zeiringer, B., Höller, N., Grün, B., Godina, R., Schmutz, S., 2016. A method to detect and characterize sub-daily flow fluctuations. Hydrol. Process. 30, 2063–2078. https://doi.org/10.1002/hyp.10773

Hauer, C., Holzapfel, P., 2024. Teil C – Morphologisch/hydraulische Maßnahmen-Bewertung, Leitfaden zur Bewertung und Minderung von Schwallbelastungen - Entwurf. Inst. für Wasserbau, Hydraul. und Fließgewässerforsch.

Hauer, C., Unfer, G., Holzapfel, P., Haimann, M., Habersack, H., 2014. Impact of channel bar form and grain size variability on estimated stranding risk of juvenile brown trout during hydropeaking. Earth Surf. Process. Landforms 39, 1622–1641. https://doi.org/10.1002/esp.3552

Hayes, D.S., Hauer, C., Unfer, G., 2024. Fish stranding in relation to river bar morphology and baseflow magnitude: Combining field surveys and hydrodynamic–numerical modelling. Ecohydrology 17, e2616. https://doi.org/10.1002/ECO.2616

Hayes, D.S., Moreira, M., Boavida, I., Haslauer, M., Unfer, G., Zeiringer, B., Greimel, F., Auer, S., Ferreira, T., Schmutz, S., 2019. Life stage-specific hydropeaking flow rules. Sustain. 11, 1–17. https://doi.org/10.3390/su11061547

Heggenes, J., Traaen, T., 1988. Downstream migration and critical water velocities in stream channels for fry of four salmonid species. J. Fish Biol. 32, 717–727. https://doi.org/10.1111/j.1095-8649.1988.tb05412.x

Moreira, M., Hayes, D.S., Boavida, I., Schletterer, M., Schmutz, S., Pinheiro, A., 2019. Ecologically-based criteria for hydropeaking mitigation: A review. Sci. Total Environ. 657, 1508–1522. https://doi.org/10.1016/j.scitotenv.2018.12.107

Moreira, M., Schletterer, M., Quaresma, A., Boavida, I., Pinheiro, A., 2020. New insights into hydropeaking mitigation assessment from a diversion hydropower plant: The GKI project (Tyrol, Austria). Ecol. Eng. 158, 106035. https://doi.org/10.1016/J.ECOLENG.2020.106035

Person, E., Bieri, M., Peter, A., Schleiss, A.J., 2014. Mitigation measures for fish habitat improvement in Alpine rivers affected by hydropower operations. Ecohydrology 7, 580–599. https://doi.org/10.1002/eco.1380

Reindl, R., Neuner, J., Schletterer, M., 2023. Increased hydropower production and hydropeaking mitigation along the Upper Inn River (Tyrol, Austria) with a combination of buffer reservoirs, diversion hydropower plants and retention basins. River Res. Appl. 39, 602–609. https://doi.org/10.1002/rra.4052

Vanzo, D., Zolezzi, G., Siviglia, A., 2016. Eco-hydraulic modelling of the interactions between hydropeaking and river morphology. Ecohydrology 9, 421–437. https://doi.org/10.1002/eco.1647

Young, P.S., Cech, J.J., Thompson, L.C., 2011. Hydropower-related pulsed-flow impacts on stream fishes: A brief review, conceptual model, knowledge gaps, and research needs. Rev. Fish Biol. Fish. 21, 713–731. https://doi.org/10.1007/s11160-011-9211-0

Zeiringer, B., Merl, K., Auer, S., Führer, S., Greimel, F., Schmutz, S., 2024. Teil F – Methodik zur Durchführung des fischökologischen Prä- und Post-Monitorings in schwallbeeinflussten Gewässern, Leitfaden zur Bewertung und Minderung der Auswirkungen von Schwallbelastungen - Entwurf. Bundeministerium für Land- und Forstwirtschaft, Reg. und Wasserwirtschaft.

Book of Abstracts of the *16th International Symposium on Ecohydraulics*
Challenges and solutions in the time of global changes
August 16–20, 2026, Lausanne, Switzerland
ISSN: 2790-2420 | ISBN: 978-90-837233-9-6 | doi:[10.64697/iahr.proc.ise2026.abs]
© 2026 IAHR. CC BY-NC-ND 4.0

ASSESSING ECOLOGICAL GAINS OF HYDROPEAKING MITIGATION MEASURES IN A CLIMATE CHANGE CONTEXT

Veronique GOURAUD[1], Fabio TARENA[2], Agnès BARILLIER[3], Julien DI PANE[1], Marie LAMOUR[1], Atle HARBY[4], Hervé CAPRA[2], Leah BECHE[3], Nicolas LAMOUROUX[2]

[1] EDF R&D LNHE, France
veronique.gouraud@edf.fr, julien.di-pane@edf.fr, marie.lamour@edf.fr

[2] INRAE, RIVERLY, France
fabio.tarena@inrae.fr, herve.capra@inrae.fr, nicolas.lamouroux@inrae.fr

[3] EDF CIH, France
agnes.barillier@edf.fr, leah.beche@edf.fr

[4] SINTEF, Norway
atle.harby@sintef.no

ABSTRACT

Hydroelectric plants can generate rapid flow variations to meet peak electricity demand (hydropeaking), which may impact aquatic organisms (stranding, drift, etc.) and their habitats (dewatering, hydraulic instability). To mitigate these impacts, while preserving as much as possible energy flexibility, it's necessary to accurately diagnose the nature and magnitude of the ecological impacts of hydropeaking, combined with other human pressures on the river stretches. To facilitate such diagnostics, we developed a conceptual framework to characterize how mitigation measures improve habitat conditions and the state of biological communities. In order to build this framework, we have identified and selected a set of appropriate ecological indicators that can be transferred to any site. To test them, we used a demonstration site where a large amount of ecological data and different models can be gathered, the section of the Ain River (50 km), located downstream of a hydropower plants chain in France. At this study site, a pumped storage facility is currently under construction and will mitigate the impacts of hydropeaking and improve the temperature conditions. First, abiotic and biotic conditions were assessed using results from hydrological, thermal, hydraulic and habitat modelling and biological monitoring surveys conducted over the past two decades. Second, based on these assessments, the application and the critical review of several available standardized frameworks assessing the impacts of hydropeaking allowed us to identify and select reliable indicators to estimate ecological gains. These indicators were applied to the Ain River under different climate change scenarios and with/without the refurbishment with the new pumped-storage unit. The results have led to a new methodological framework for evaluating the environmental benefits of refurbishment projects.

Keywords: *ecological gains; hydropeaking, eco-hydrological indicator; eco-thermal indicators; habitat.*

1. Introduction

Faced with global change, the hydropower plant operations are a major issue for optimizing the management of water resources and preserving biodiversity. In this context, the European ReHydro project aims to demonstrate how European hydropower can be renovated and modernized to be adapted to the future energy system, respecting sustainability requirements and societal needs in a context of climate change. In order to ensure the sustainability of refurbishment measures, methods and tools should be proposed to assess the ecological gains induced by refurbishment taking into account climate change. Among the possible refurbishment measures, we focused on those that contribute to mitigating hydropeaking that can impact aquatic organisms due to rapid flow variations (generated to meet maximum electricity demand). Various

methods of assessing the ecological impact of hydropeaking have been proposed in the literature (Bruder et al., 2016; Harby et al. 2016; Tonolla et al., 2017; Harby et al. 2019; Godinho et al 2023; Tonolla et al., 2023; Baran et al., 2024). They must be compared and supplemented by a critical analysis of the assessments they provide on expected improvements in biotic status. This will provide a conceptual framework to characterize how mitigation measures improve habitat conditions and the state of biological communities. Our goal was to identify, select and test a set of appropriate ecological indicators to assess expected ecological gains with the implementation from these measures. These ecological indicators have to be transferable to any site. To test them, we used a demonstration site where many ecological data and models were available and hydropeaking mitigation measures will be implemented. Based on these assessments, we combined the application of a tool which allow to cross abiotic and biotic indicators with a literature review to identify and select robust ecological indicators. We bring all these elements together to propose a methodological framework for assessing the ecological gains resulting from mitigation measures of hydropeaking in a hydropower refurbishment context.

2. Material and methods

2.1. Study site

The 190 km long Ain River, located in France, originates at an altitude of 681 m and flows in a north-south direction before joining the Rhône River. The project focuses on the chain of hydroelectric schemes in the lower Ain valley, comprising 5 hydropower plants (Vouglans, Saut Mortier, Coiselet, Cize-Bolozon and Allement), and more specifically the Vouglans, Saut-Mortier and Coiselet schemes. That corresponds to a stretch of approximately 100 km between Vouglans and the confluence of Ain and Rhône Rivers. The building of the pumped storage between Vouglans and Saut Mortier is planned for the period 2024–2028. It will increase available reservoir storage capacity, thereby simultaneously improving generation flexibility and resilience to climate change. The project will also reduce ecological impacts by decreasing hydropeaking intensity downstream of the scheme, resulting in fewer rapid and frequent changes in discharge and improved habitat conditions on the entire downstream river reach up to the confluence with the Rhône River. In this study, we focused on this river section (about 50 km) located downstream of the last hydroelectric power station.

2.2. Collection of a wide set of data and models

Concerning hydrological and thermal conditions, we used the results of a digital twin of the whole catchment of the Ain River (Guénand, 2025) to analyse how flood control, drought management and other water services could be improved. The digital twin includes hydrological rainfall-runoff models to calculate inflow, and hydropower operation models to calculate storage volumes available or used. It provides the flow and temperature conditions downstream of the last hydropower plant (upstream section limit for the 50 km impacted reach). The results of the thermal model developed by Seyedhashemi (in press) was used to evaluate river temperatures based on flow and climatic conditions along the 50 km reach.

For hydraulic conditions, a 2D unsteady hydrodynamic model (mapping flow velocities averaged over the vertical; Rubar 2D; Bazin et al., 2017) was used to evaluate hydraulics indicators

Regarding habitat conditions, we used and compared different types of habitat models, ranging from "blind" statistical models that do not require any field data, to detailed numerical habitat models that link the 2D hydrodynamic model with biological models of microhabitat selection. The advantage of the "blind" approach is its potential easy application at any other study site.

On the basis of the numerous biological surveys undertaken over the last 20 years, the biotic state of the reach were assessed, in particular by characterizing the general state of the biotic communities (diatoms, macrophytes, macroinvertebrates, fish) and the potential alterations related to hydropeaking (fish and macro-invertebrate reproduction, larval development, drift, stranding-trapping, habitat use) (Barillier et al., 2021; Gouraud et al., 2024).

2.3. Assessment of ecological impacts due to hydropeaking

We focused on the available standardized frameworks allowing to assess the impacts of hydropeaking and guide the implementation of appropriate mitigation strategies. More precisely, we tested different approaches which allow to assess hydropeaking ecological impacts i) by crossing abiotic and biotic indicators ii) before and after the refurbishment of the facility and for different climate change scenarios. For that purpose, on the one hand, we applied available methodologies to assess hydrological alterations (Courret et al, 2021; Li & Pasternak, 2021) and hydraulic alterations (Moreira et al., 2019; Hayes et al., 2019) due to hydropeaking. On

the other hand, we applied some existing frameworks which typically rely on the cross-evaluation of a set of biotic and abiotic indicators, such as the Swiss technical guide (Tonolla et al., 2017, 2023), the Austrian guide (Zeiringer et al., 2025), the French water agency approach (Baran et al., 2024), and the Norwegian "FIThydro Hydropeaking tool" (Harby et al. 2016; Harby et al. 2019; Godinho et al 2023).Those methods are essentially based on coupling hydrological and biological indicators or the hydraulic modelling of study sites and the preferenda of various stages of fish life cycle. Those approaches were applied on the Ain River.

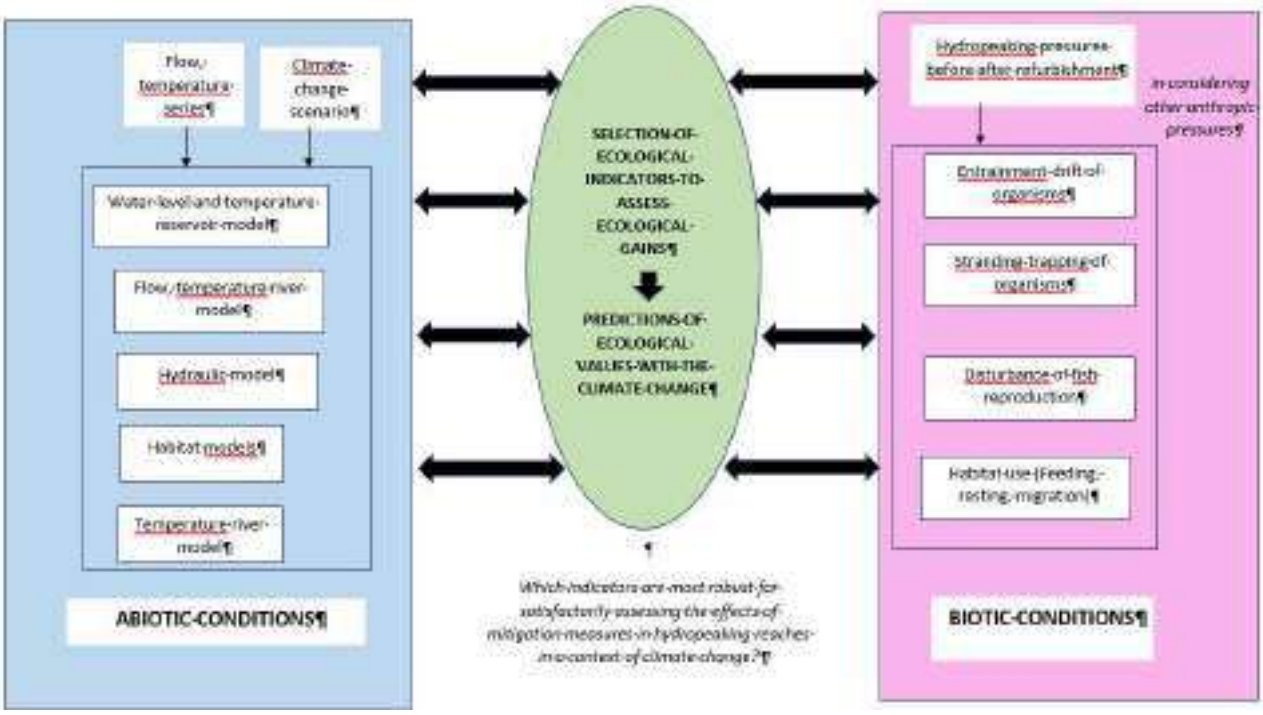

Fig. 1..Representation of the abiotic and biotic conditions used for the selection of ecological indicators to assess ecological gains of mitigation measures in the hydropeaking reach of the Ain river

2.4. Construction of a methodological framework

A critical review allowed us to question and complete the previous selection of indicators and how they are combined in the different approaches. These indicators are commonly assigned threshold values, which allow the classification of ecological conditions according to a qualitative ordinal scale (e.g., low, moderate, high impact). Their combination allows a relatively fast and communicable means of diagnosing the severity of ecological impairments. However, the scientific basis for these threshold values and their combination is not always clear. In many cases, it remains uncertain whether the limits were determined through empirical studies, expert consensus, or more arbitrary decisions. This ambiguity limits the transparency and reproducibility of hydropeaking impact assessments and complicates the implementation of robust, site-specific mitigation measures.

Our critical analysis will provide a review of the thresholds currently applied in various assessment frameworks to identify the indicators that have solidly grounded thresholds for inclusion in the methodological framework. Based in particular on Schmutz et al (2025)'s results, we will seek to prioritize indicators that reflect the key factors determining the impact of hydropeaking.

3. Results

We brought all these elements together to propose a methodological framework for assessing the ecological gains resulting from measures to mitigate hydropeaking. Based on their application on the demonstration site of the Ain River, a selection of pertinent ecological indicators was proposed to assess ecological gains induced by hydropeaking mitigation measures and a proposal was done to predict ecological values while accounting for climate change (Figure 1).

4. Conclusion and perspectives

The structured set of ecological indicators proposed in our methodological framework provide a robust assessment of the effects of mitigation measures in hydropeaking reaches in a context of climate change. Its

transferability should be enhanced by applying it to different types of study sites. In addition, our assessments have focused on the local impacts of operating modes of the facilities and have neglected the broader environmental footprint across the entire value chain of refurbishment and operation of the facilities. The link between local and global indicators which allow to quantify pressures on biodiversity also is being investigated in other work packages of the ReHydro project.

Acknowledgements

We gratefully acknowledge all the people who contributed to the fieldwork.

References

Baran P, Terrier B (2024) Assessing morphoecological impacts due to hydropeaking in the Rhone-Mediterranean and Corsica river basins. 15th International Symposium on Ecohydraulics and Fish Passage; Connectivity and processes across the riverscape, May 5-9, 2024 Québec City, Canada.

Barillier A, Beche L, Malavoi JR, Gouraud V (2021) Identification of effective hydropeaking mitigation measures: are hydraulic habitat models sufficient in a global approach?, Journal of Ecohydraulics, DOI: 10.1080/24705357.2020.1856008

Bazin PH, Mignot E, Paquier A (2017) Computing flooding of crossroads with obstacles using a 2D numerical model, Journal of Hydraulic Research, 55(1), 72-84.

Bruder A., Tonolla D., Schweizer SP., Vollenweider S., Langhans SD., Wüest A. A conceptual framework for hydropeaking mitigation, Science of The Total Environment, Volume 568, 2016, Pages 1204-1212, ISSN 0048-9697, https://doi.org/10.1016/j.scitotenv.2016.05.032.

Courret D., Baran P. & Larinier M. (2021): An indicator to characterize hydrological alteration due to hydropeaking, Journal of Ecohydraulics, DOI:10.1080/24705357.2020.1871307.

Godinho FN, Alexandre C, Almeida PR, Martínez-Capel F, Cortes RMV, Quintella BR, Sanz-Ronda J, Santos J., Palau A, Pinheiro AN, & Boavida I (2023), Hydropeaking impact assessment for Iberian cyprinids and leuciscids: An adaptation of the hydropeaking tool method. River Research and Applications, 39(3), 340–348. https://doi.org/10.1002/rra.3943.

Gouraud V, Beche L, Barillier A (2024) Identify effective hydropeaking mitigation measures: lessons learnt from site studies. 15th International Symposium on Ecohydraulics and Fish Passage; Connectivity and processes across the riverscape, May 5-9, 2024 Québec City, Canada.

Guénand Y (2025) Initial studies for retrofitting pumped storage, Deliverable D2.1 of ReHydro european project - Demonstration of Sustainable Hydropower Refurbishment.

Harby A, Forseth T, Ugedal O, Bakken TH, Sauterleute J (2016) A method to assess impacts from hydropeaking, Proceedings, 11th International Symposium on Ecohydraulics, Melbourne, Australia.

Harby A, Charmasson J, Boavida I, Pinheiro AN, Godinho F; Tuhtan J; Albayrak I; Detert M, Boes R, Schneider M, Pawels I (2019) Deliverable 3.2 Tools for fish behaviour assessment – FIThydro Fishfriendly Innovative Technologies for Hydropower.

Hayes, D. S., Moreira, M., Boavida, I., Haslauer, M., Unfer, G., Zeiringer, B., Greimel, F., Auer, S., Ferreira, T., & Schmutz, S. (2019). Life Stage-Specific Hydropeaking Flow Rules. Sustainability, 11(6), 1547. https://doi.org/10.3390/su11061547.

Li, T., Pasternack G. B. 2021. Revealing the diverse pattern of hydropeaking flow. Journal 6 of Hydrology 598: 126392. DOI. 10.1016/j.jhydrol.2021.126392.

Moreira, M., Hayes, D. S., Boavida, I., Schletterer, M., Schmutz, S., & Pinheiro, A. (2019). Ecologically-based criteria for hydropeaking mitigation : A review. Science of The Total Environment, 657, 1508-1522. https://doi.org/10.1016/j.scitotenv.2018.12.107

Schmutz S, Hayes D, Greimel F, Jungwirth M, Zeiringer B, Auer S (2025). How hydropower peaks impair fish: Disentangling multiple factors affecting young fish. In Hayes, D.S., Greimel, F. (2025). Solutions for Global Sustainability in Hydropower – Conference Proceedings. 3rd International Conference on Sustainability in Hydropower (SUSHP), BOKU University, Vienna, Austria. https://doi.org/10.5281/zenodo.16978242

Tonolla D, Bruder A, Schweizer S (2017) Evaluation of mitigation measures to reduce hydropeaking impacts on river ecosystems - a case study from the Swiss Alps, Sci Total Environ., 574, 594-604. doi: 10.1016/j.scitotenv.2016.09.101. Epub 2016 Oct 14. PMID: 27653558.

Tonolla, D. (2023). Élaboration et appréciation de mesures d'assainissement des éclusées – Nouvelles connaissances issues de la recherche et de la pratique. Rapport sur mandat de l'OFEV.Zeiringer B, Merl K, Auhser A, Hayes D, Leitner P, Graf W, Schmutz S, Greimel F (2025) Austrian hydropeaking assessment method, Proceedings, 3rd International Conference on Sustainability in Hydropower; Vienna, Austria.

Book of Abstracts of the *16th International Symposium on Ecohydraulics*
Challenges and solutions in the time of global changes
August 16–20, 2026, Lausanne, Switzerland
ISSN: 2790-2420 | ISBN: 978-90-837233-9-6 | doi:[10.64697/iahr.proc.ise2026.abs]
© 2026 IAHR. CC BY-NC-ND 4.0

HYDRAULIC AND ECOLOGICAL CHARACTERIZATION OF TWO ADJACENT RIVER REACHES WITH DIFFERENT REGULATED STREAMFLOW

Silvia QUADRONI[1], Livia SERVANZI[2], Paolo ESPA[2]

[1] Department of Theoretical and Applied Sciences, University of Insubria, Italy
email: silvia.quadroni@uninsubria.it

[2] Department of Science and High Technology, University of Insubria, Italy
email: lm.servanzi@uninsubria.it
email: paolo.espa@uninsubria.it

ABSTRACT

This study investigates the hydraulic characteristics and related ecological conditions of two reaches of the Mera River (Central Italian Alps), mainly differing in terms of streamflow regulation: a residual-flow reach with poorly variable discharges (R1) *vs.* a reach with larger runoff but subjected to hydropeaking fluctuation (R2). Contrary to the expectations, the considered hydraulic and ecological parameters did not strongly differ between the two reaches during the study year, which was preceded by a sediment pulse and was characterized by a prolonged drought. At both reaches, the ecological status did not achieve the good class, highlighting possible limitations in the current streamflow management.

Keywords: Alpine river; hydropeaking; minimum flow; channel-flow simulation; biomonitoring.

1. Introduction and study context

Alpine streams and rivers developed for hydropower are frequently affected by relevant hydrological alteration (Quadroni et al., 2017). Although current normative frameworks require the release of ecological flows (e-flows) below water intakes (WFD CIS, 2015), the effectiveness of adopted compensation measures is still under debate. As hydropower development of mountain catchments is commonly implemented by cascade systems, implying multiple intakes/power stations, hydrologic alteration may range from streamflow reduction (i.e., residual-flow reaches) to hydropeaking. This is the case of the catchment of the Mera River, the second main tributary of Lake Como in terms of length (50 km, 23 km in Italy and 27 km in Switzerland) and runoff (mean annual flow of 34.5 $m^3 s^{-1}$ in its final section). Here, two reaches (hereafter R1 and R2), located at short distance each other (3.5 km), are characterized by significantly different streamflow patterns. R1, the upstream one, is a residual-flow reach, characterized by generally low and poorly variable discharges (i.e., the sum of minimum flows released by the upstream intake structures plus the contribution of the unexploited catchment). Slightly downstream, at R2, streamflow is significantly larger, and it is subjected to hydropeaking fluctuation determined by intermittent operation of the most downstream power station of the hydropower cascade of the Mera catchment.
The Mera River was also affected by an extreme sedimentation event (August 2017 - Salmaso et al., 2020), impacting streambed substrate and the biological community composition and evolution at least in the short-medium term (Salmaso et al., 2021).
In this study, we compared both hydraulic and ecological conditions of the mentioned river reaches, focusing on the hydraulic parameters with major ecological relevance (i.e., water depth, water velocity and shear stress). Moreover, we quantified to what extent the ecological status, based on benthic macroinvertebrate community, differs from the good class required by the Water Framework Directive, which is the first assumption that allows defining an e-flow management scheme.

2. Methods

2.1. *Hydraulic dataset and channel-flow simulation*

Complete hydrographs from September 2021 to August 2022 were considered (Fig. 1), with daily and 0.5 hours resolution at R1 and R2, respectively. In this period, at R1, streamflow ranged from the Minimum Flow (MF) 1.5 $m^3 s^{-1}$ to about 90 $m^3 s^{-1}$, being Q 95% and Q 5% equal to MF and 9.6 $m^3 s^{-1}$, respectively. At R2, discharge ranged from 1.5 $m^3 s^{-1}$ to about 150 $m^3 s^{-1}$, being Q 95% and Q 5% equal to 2.1 $m^3 s^{-1}$ and 37 $m^3 s^{-1}$, respectively. A standard daily hydrograph at R2 is represented in Fig. 1, displaying typical hydropeaking fluctuations: it is characterized by two peaks, one in the mid-morning and one in the late afternoon, due to usual powerhouse schedule. Along the investigated year, maximum peak flow induced by hydropower operation was generally about 35-40 $m^3 s^{-1}$.
A sediment pulse event, causing the temporary increase of fine sediment content at both reaches, occurred in summer 2021; nevertheless, during the investigated period, similar events did not take place. It is worth mentioning that the study year was exceptionally dry, in the catchment of the Mera River as well as in all southern Europe.
1D channel-flow simulations were performed at both study reaches by HEC-RAS 6.0 Beta 2 (US Army Corps of Hydraulic Engineers – USACE, 2021). Detailed Digital Terrain Models (DTMs) were generated after riverbed surveys carried out in October 2021 for R1 and in March 2022 for R2 (Servanzi et al., 2024) and were used to set up geometry domains. DTMs had 0.25 x 0.25 m spatial resolution, and 49 and 56 cross sections were extracted and used as geometry input for R1 and R2, respectively.
For both reaches, steady-flow simulations were performed for Q 95, 75, 50, 25 and 5%. Moreover, only for R2, unsteady-flow simulation was performed for the daily flow hydrograph presented in Fig. 1. After calibration based on streamflow measurement and water surface elevations detected during the mentioned topographic surveys, a constant Manning coefficient of 0.04 s $m^{-1/3}$ was applied to both simulated reaches.

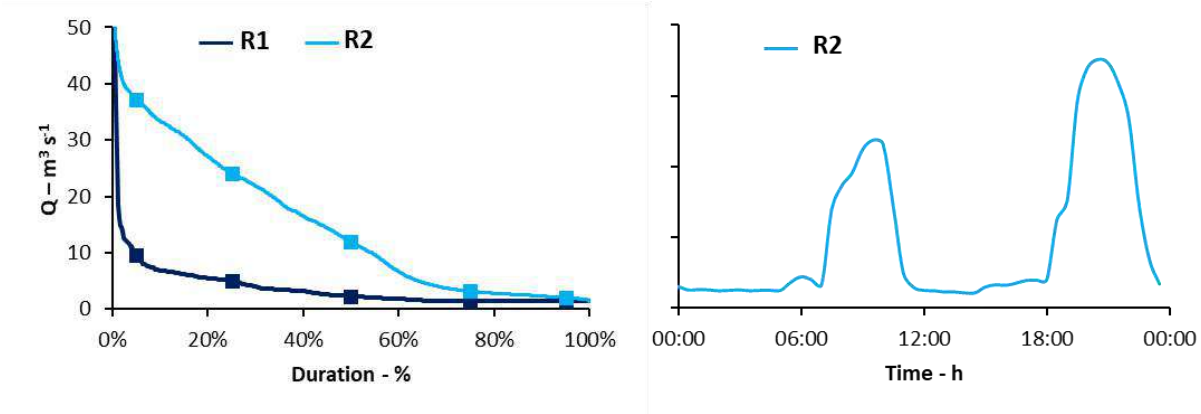

Fig. 1. Flow duration curves at R1 and R2 from September 1, 2021 to August 31, 2022 (left); typical daily flow hydrograph at R2 (April 28, 2022; right).

2.2. Biomonitoring

Benthic macroinvertebrate community was collected seasonally during the study year at R1 and R2, following a standard multihabitat approach. Samples were sorted and identified to genus (Plecoptera and Ephemeroptera) or family level. Total density was calculated along with total richness (i.e., total number of taxa) and diversity (i.e., Shannon-Wiener index). Moreover, the ecological status sensu WFD was defined through the calculation of the Italian official, multimetric STAR_ICM index. This index is based on ecological quality ratios between observed and reference conditions for each sub-metric, including richness and diversity. Finally, similarity of percentage (SIMPER) analysis was performed to detect differences of taxonomical composition between the two reaches.